



INTERNATIONAL CIVIL AVIATION ORGANIZATION
NATIONAL ACADEMY OF SCIENCES OF UKRAINE
MINISTRY OF EDUCATION AND SCIENCE OF UKRAINE
NATIONAL AVIATION UNIVERSITY

PROCEEDINGS

OF THE THIRD WORLD CONGRESS "AVIATION IN THE XXI-st CENTURY"

"SAFETY IN AVIATION AND SPACE TECHNOLOGY"



Volume 1

September 22-24, 2008
Kyiv, Ukraine

**INTERNATIONAL CIVIL AVIATION ORGANIZATION
MINISTRY OF EDUCATION AND SCIENCE OF UKRAINE
NATIONAL ACADEMY OF SCIENCES OF UKRAINE
NATIONAL AVIATION UNIVERSITY**

PROCEEDINGS

**OF THE THIRD WORLD CONGRESS
“AVIATION IN THE XXI-ST CENTURY”**

***“SAFETY IN AVIATION
AND SPACE TECHNOLOGY”***

September 22-24, 2008

Volume 1

**We wish to thank the following for their contribution to the success of this conference:
European Office of Aerospace Research and Development, Air Force Office of Scientific
Research, United States Air Force Research Laboratory <<http://www.london.af.mil>>.**

KYIV 2008

SYMPOSIA

Volume 1

SYMPOSIUM 1. FLIGHT SAFETY AND CONTINUED AIRWORTHINESS

- Session A. New methods of aircraft maintenance and retrofitting. Information support of aircraft in service life time*
- Session B. Parametric diagnostics and deferent condition monitoring*
- Session C. Aircraft and engines durable: to and life cycle*
- Session D. Surface engineering and aircraft parts repair*
- Session E. Automation of the energy complexes and management on transport.*

SYMPOSIUM 2. DIAGNOSTIC SYSTEMS IN AEROSPACE TECHNOLOGIES

Volume 2

SYMPOSIUM 3. AIR TRAFFIC MANAGEMENT SECURITY AND SAFETY

- Session A. Communication, navigation, surveillance /air traffic management (CNS/ATM)*
- Session B. Computer aided design*
- Session C. Navigation, control and flight management systems*

SYMPOSIUM 4. AVIATION CONGRESS SCHOOL OF YOUNG SCIENTISTS IN PROBLEMS OF ENVIRONMENT PROTECTION FROM CIVIL AVIATION IMPACT

- Session 1. Environment protection zoning of the airports*
- Session 2. Operational aircraft noise impact reduction*
- Session 3. Air/water/soil pollution in airports*
- Session 4. Environmental performances of the fuels, lubricants & technical liquids*
- Session 5. Green aviation industry*

SYMPOSIUM 5. ECONOMICS IN AVIATION

SYMPOSIUM 6. HUMAN FACTOR IN AVIATION

- Session A. Achievements and trends human factor optimization and psychological support in Aviation*
- Session B. English proficiency of pilots and air traffic controllers as a safety aspect*

CONTENTS

A.M. Grekhov, S.A. Dmytriyev, E.V. Shevtsova The method for an estimation of the aviation safety level on the basis of imitating modeling	11.1
V.S. Boutko, Ye.N. Syabryuk Investigation of hydraulic control systems regulators	11.6
Ju.N. Rukynich, A.E. Sitnikov, Ja.B. Fedoruchko, A.G. Kucher, G.J. Zajonchkovsky Forecasting operating changes of the technical state of electromagnetically driven valves at the stage of designing	11.10
A.A. Itskovich, I.A. Faynburg, V.S. Shapkin, A.S. Gromov, A.V. Semin, A. Grishin Application of effective programs of maintaining TU-154M aircraft airworthiness in the aircraft maintenance centers	11.14
N.N. Smirnov, Doctor of Technical Sciences, N.P. Smirnov Development of minimum equipment lists ensuring safe aircraft	11.22
A.I. Bogdanovych Comparison of the wear activation energy (E^p) “IIIX15” in fuel “TC-1” with analogous value “TC-1*” OF A long-term storage	11.25
V.I. Burlakov, PhD, D.V. Popov, O. I. Yurchenko, I.A. Slepuhina PhD, N.V. Korsunenko, Management processes of technical operation of aviation technics	11.28
L. Zhuravlova A concept of an aircraft engine health monitoring platform	11.32
V.G. Dokuchayev, A.S. Tugarinov, Yu.I. Kazarinov Influence of the neutral environment on thermal loading of structural members of brake wheels and their durability	11.37
A.A. Kuchaev Algorithm of building three dimensional magnetohydrodynamic model for submerged nozzle-liner electromagnetic stirrer system of continuous caster	11.41
E.A. Sapeliyk, Y.N. Chokha Features of realisation of a complex kontrol-calculated method in processes of diagnosing of composite dynamical objects aircraft technicians	11.46
A. Popov, I. Kinashchuk, V. Nechiporuk Algorithm of diagnosing jet engine at in combined damaged units of a flowing part	11.54
V. Ushakov, V. Gopeyenko, G. Filipsons, N. Sidenko Numerical analysis of periodic pulsation interactions of external flow on cylinder`s aerodynamics and heat-exchange	11.58
M.V. Karuskevich, E. Yu. Korchuk, T.P. Maslak Extrusion-intrusion pattern as an indicator of accumulated fatigue damage	12.1
S.R. Ignatovich, V.I. Zakiev, S.S. Yutskevych Metal fatigue process investigation by the interference nanoprofilometer	12.7
V. Astanin, M. Borodachov, S. Bogdan The stress-strain state of aviation thin-slab structure elements of under impact load	12.11
V. V. Astanin, G. O. Olefir Material impact strength researches in the context of civil aviation safety	12.20

V.V. Astanin, P. Vynogradskyy Multipurpose data acquisition system for investigation of mechanical properties of materials	12.29
Müge Armatlı Kayrak Non-destructive inspection of aircraft composite plates by using immersion ultrasonic method	12.37
M. Kupchyk Indirect thrust measurement during the ground tests of the	13.1
P.S. Abdullayev, A.S. Yakushenko, A. J. Mirzoyev, The complex approach to the decision forming of aviation gas turbine engine technical condition	13.5
Yury I.Belykh, Vladimir A. Naida, Anton S. Pozolotin Technological aspects of development of electronic trainer for acquisition of skills and abilities on a start and testing of aviation engine	13.7
V.Panin, L. Morozov, L.Volyanskaya Optimization of parameters of turbofan aft-fan engine	13.10
Y.M. Tereshchenko, Y.Y. Tereshchenko, I.M. Antonuk Crisis of viscous flow in airfoil cascade	13.15
Olexiy Kucher, Mustafa A.S. Mustafa Optimisation of processes of airline logistics	13.20
N.S.Kulyk, A.A.Tamargazin, I.I.Linik Air transport integration process management	13.28
Vsevolod Kharyton, Olexiy Kucher, Jean-Pierre Laine, Fabrice Thouverez Cracked blade presence influence on bladed disk dynamic response	13.32
Enis T. Turgut, Dr. T. Hikmet Karakoc, Arif Hepbasli Exergoeconomic assessment of aircraft turbofan engines	13.40
V.I. Dvoruk, M.V. Kindrachuk Metallophysics of wearing friction sliding in the presence of abrasive material	14.1
A.A. Kornienko, L.A. Lopata, M.V.Luchka Triboengineering of composite electrolytic gradient coatings	14.6
E.A. Kulkhavyi, A.S. Kryzanovskiy Tribological problems of aircraft safety	14.9
G.V. Tsybanov, V.E. Marchuk, V.V. Zhiginas Fretting-resistance of aircraft tribological assembly details in the conditions of alternating loads	14.14
M.N. Svirid, V.V. Lubyaniy, V.G. Paraschanov, S.N. Zanjko Monitoring of friction node tribological parameters in conditions of mass removing	14.18
I.Pavelko, V.Pavelko Fatigue crack growth in aircraft structural elements at real operation conditions	14.26
I.Pavelko, V.Pavelko, S.Kuznetsov, E.Ozolinsh, I.Ozolinsh Fatigue crack indication by lamb wave non-destructive testing	14.34
D.M. Krasnoshapka, A. Skalyga Features of calculation of the established modes of the cascade asynchronous machine	15.1
D. M. Krasnoshapka, T. Mazur Automatic control of process of design of the asynchronous muff with massive ferromagnetic cartridge case on the secondary rotor	15.5

E. Tachinina, E. Tachinin	
Development of algorithm of generation of advisory information for crew under evolution of abnormal condition in flight	15.10
V. Vorobyev, V. Zakharchenko, S. Enchev, V. Tikhonov	
Probabilistic dynamic model of estimation of fail-safe feature boothing ergatic interface	15.15
A. D. Kiselev, V.M. Vorob'ev	
Base complex of radio electronic equipment of an-148 airplane	15.19
A. Lysenko, P.I. Kirchu	
Computer certification of the robust control algorithm	15.23
V. Neret	
Method of evaluation of reliability and vitality of difficult electroenergy systems of air-ports	15.27
O.V. Samkov, V.I. Lytvynenko, I.E. Lomavatsky, J. Zaharchenko	
Optimization methodology of financing projects on the basis of immune algorithm clonal selection	15.34
O. Lysenko, E. Tachinia, V. Slobodianyuk	
Resource – constrained project scheduling task and their application for conflict scenarios modeling ...	15.38
A. Aslanyan, A. Belskaya	
Informational providing of technical operation “on condition”	15.41
Kazak V.N., Shevchuk D.O., Roman I.M.	
Aspects the application gas suppression assemblies at the compressor station	15.44
B.C. Martinyuk	
Statistical methods of control of technical state of equipment of channel of electric power system	15.48
O. Samkov, A. Visochansky	
Modernization methodology of Ukrainian civil aviation park	15.54
J. Cwiklak, A. Fellner, H. Jafernik	
Initial analysis of the ornithology situation concerning airfield in the aspect of bird strike to aircraft	15.58
J. Bialy, A. Fellner, J. Cwiklak, H. Jafernik, J. Kozuba	
A prediction of aircraft position in satellite navigation receiver for instrument landing system	15.65
Onder Turan, T.Hikmet Karakoc	
Experimental study of microturbine engine for man and unmanned aircraft	15.72
T.Hikmet Karakoc, Onder Turan	
Fuel consumption estimation of commercial turbofans	15.78
V. Ushakov, N. Sidenko	
Aerodynamic characteristics of an on the ground mounted vertical air jet behind the directing vanes of aerodynamic propeller	15.85
S.I. Martynenko, A.A. Markov, M.S. Sharov, L.S. Yanovskiy	
Development of numerical methods for solving navier-stokes equations in primitive variables formulation	15.92
F. Kirchu, O. Drach, N. Kachur	
Numerical investigations of transsonic axial compressor stage	15.96
S.F. Filonenko, V.M. Stadnychenko, A.P. Stakhova	
The modelling of acoustic emission radiation at normal wear	2.1

S.F. Filonenko	
Acousto-emission method in diagnostics of constructions' condition	2.9
V.O. Ignatov, S.O. Kudrenko	
Veracity of measurements in heterogeneous air & space complexes	2.17
V.I. Ignatov, Wu Zijuan	
Comparative analysis of modeling adequacy of the nonstationary traffic in telecommunication networks	2.24
O.P. Martynova	
Multicriterion routing in computer networks	2.30
V.P. Kvasnikov, A.L. Perederko, S.V. Uvarov	
Working out of the technique of definition of the lapse of parameters of vibrational diagnostic of gas-turbine plants	2.33
K. Yakovishin	
Designing local area networks that has a voice-video-text traffic	2.38
V.P. Kvasnikov, V.V. Osadchy	
The information-measuring monitoring system of water-black oil emulsions burning process	2.46
N.A. Vinogradov, I. A. Zhukov, N.N. Guziy	
Management of data flows and control of overload in aeronautical telecommunication networks	2.50
N. Shibitskaya, G. Timofeeva	
Pilot's skills predicting systems for flight safety	2.54
P. Pavlenko, V. Trejtyak	
Method of management of productivity of the equipment for the automated systems of industrial purpose	2.58
Cherednikov I., Borisov A.	
The synthesis of the measuring systems of deviations from cylinderstics	2.61
R. Lobus	
Methods of data processing by sensors of traffic monitoring	2.65

*A.M. Grekhov, PhD, Professor, S.A. Dmytriyev, PhD, Professor, E.V. Shevtsova
(National Aviation University, Ukraine)*

THE METHOD FOR AN ESTIMATION OF THE AVIATION SAFETY LEVEL ON THE BASIS OF IMITATING MODELING

The method of an estimation of the aviation safety level is proposed on the basis of imitating modeling. Calculations of aviation risks by Monte-Carlo method were carried out in view of technical factors, the human factor and organizational factors for definition of acceptable risk area.

The concept of aviation safety is given in ICAO document (Doc 9859): safety is the state in which the risk of harm to persons or property damage is reduced to, and maintained at or below, an acceptable level through a continuing process of hazard identification and risk management. Hazard is understood as a condition, object or the activity being the potential reason of personnel mutilations, damages of the equipment or designs, material losses, reduction of ability to execute the ordered functions.

The risk is treated as an opportunity of losses or mutilations, measured by a degree of aftereffect and probability. Areas of acceptable, tolerable and intolerable risks are distinguished.

Carrying out of real experiments for definition of aviation risks is unreasonable and hardly feasible in practice. Therefore we shall carry out imitating modeling - computer experiments - with the purpose of revealing properties and regularities of aviation safety. These experiments are carried out with models instead of the real systems. In the case of aviation safety an imitation is unique way of research without realization of real experiments.

Gathering the necessary information about aviation risks for decision-making is very complicated. But for an adequate estimation of risk it is necessary to have enough information for a formulation of plausible hypotheses about probable distributions of key parameters. With this purpose the absent data are replaced by values received in a result of imitating experiment (i.e. generated by a computer).

Quantitative estimations and probabilistic criteria of flight safety [1,2] have been developed and used for forecasting and flights management. However quantitative calculations of aviation risks with the help of Monte-Carlo method in view of technical factors, the human factor and organizational factors represent special interest now.

In this paper we use the stochastic models containing random variables, which can not be managed by decision-makers. Imitation allows drawing conclusions based on probabilistic distributions of random factors.

The purpose of this paper is:

- 1) To develop the information structure of model for the estimation of aviation risks;
- 2) To develop a model for an estimation of acceptable, tolerable and intolerable risks areas;
- 3) To determine the statistical characteristics used for formation of target functional;
- 4) To prove weight factors of outcomes in stochastic models of aviation safety;
- 5) To carry out imitating modelling (on the basis of Monte-Carlo method) and to estimate aviation risks for models;
- 6) To carry out forecasting dynamics of aviation safety parameters in view of internal and external factors.

Classification of factors influencing aviation safety

Under each separate factor it is necessary to understand any action, a case, a condition or circumstance, presence or absence of which increases probability of adverse end of flight. It is practically impossible to take into account all factors. The degree of their importance is determined by certain conditions and their influence on occurrence of potential dangers for flights. It is possible

to allocate the general groups of the factors influencing on functioning reliability and, hence, on aviation safety:

- 1) functional efficiency of a crew;
- 2) functional efficiency of an aircraft;
- 3) functional efficiency of air traffic management and air traffic control;
- 4) a management efficiency of flight operations;
- 5) an efficiency of the aviation technical operation;
- 6) factors of adverse external influence.

Definition of statistical characteristics and formation of target functional

The stochastic model functional based on a criterion of a mathematical expectation of some effect was chosen in the following form:

$$R = \sum_{i=1}^n \omega_i B_i = \sum_{i=1}^n \omega_i \sum_{j=1}^m \rho_{ij} B_{ij}$$

where R - the mathematical expectation of a total effect, which is accepted as a parameter of risk;
 i - a number of an outcome or occurrence of the adverse factors block,
 n - a number of outcomes for model casual parameters;

ω_i - a probability of an outcome or occurrence of a random variable B_i , $\sum_{i=1}^n \omega_i = 1$;

B_i - a discrete random variable, which describes the block of adverse factors i or the size of an effect in case of an outcome i .

In proposed model $i = 1 \div 6$:

B_1 - describes functional efficiency of a crew (the human factor),

B_2 - functional efficiency of an aircraft (technical factors),

B_3 - air traffic control (human, technical and organizational factors),

B_4 - flight operations management (organizational factors),

B_5 - system of technical operation (human, technical and organizational factors);

B_6 - factors of adverse external influence.

ρ_{ij} - a probability of the adverse factor B_{ij} ; $\sum_{j=1}^m \rho_{ij} = 1$;

B_{ij} - a value of the adverse factor j from the block i .

Table 1.

Characteristics of functional efficiency

№	Characteristic	Probability of adverse factor	Value of adverse factor (a.u.)
1	2	3	4
	Crew (B_1)	ρ_{1j}	B_{1j}
1	Insufficient professional training	ρ_{11}	B_{11}
2	Insufficient discipline and sense of duty	ρ_{12}	B_{12}
3	Insufficient functional efficiency of crew members (psychological and physiological conditions)	ρ_{13}	B_{13}
4	Absence of retraining, upgrading, improvement of professional skills	ρ_{14}	B_{14}
	Aircraft (B_2)	ρ_{2j}	B_{2j}

(Finish of the table)			
1	2	3	4
5	Insufficient design - constructive and ergonomic perfection, low operational adaptability; destruction of elements; difficulties in control.	ρ_{21}	B_{21}
6	Unsatisfactory operational condition; failures of units and systems.	ρ_{22}	B_{22}
7	Unsatisfactory maintenance; unsatisfactory repair, poor-quality modifications and upgrading.	ρ_{23}	B_{23}
	Air traffic control (B_3)	ρ_{3j}	B_{3j}
8	Imperfection of air traffic control system (accuracy, reliability, noise stability, fullness of the air space information, rate, amount of solved problems, degree of automation for collecting processes and information processing, display and the analysis of air conditions)	ρ_{31}	B_{31}
9	Low professional training of controllers and dispatchers	ρ_{32}	B_{32}
10	Low discipline and sense of duty of the air traffic control personnel	ρ_{33}	B_{33}
11	Low organization level of air traffic control service	ρ_{34}	B_{34}
	Flight operations management (B_4)	ρ_{4j}	B_{4j}
12	Existence of civil aviation administration authority and the national aviation legislation (compliance with ICAO Standards and Recommended Practices)	ρ_{41}	B_{41}
13	Absence of regulation: - Preparations and performance of flights; - Preparations and operation of aircrafts; Absence of norming: - Flight activity; - The admission to flights; - The admission to performance of aviation works.	ρ_{42}	B_{42}
14	Quality of officials, accountable managers activity in fields of: - Professional training and the flight personnel licensing; - Crew resource management, preliminary and preflight training; - Flights analysis.	ρ_{43}	B_{43}
15	Slow response of flight operations management	ρ_{44}	B_{44}
	System of technical operation (B_5)	ρ_{5j}	B_{5j}
16	Level of organization perfection; quality of the specifications and technical documentation.	ρ_{51}	B_{51}
17	Material resources	ρ_{52}	B_{52}
18	Level of professional training	ρ_{53}	B_{53}
19	Discipline and sense of duty of technical staff	ρ_{54}	B_{54}
	Adverse external influence (B_6)	ρ_{6j}	B_{6j}
20	Adverse weather conditions	ρ_{61}	B_{61}
21	Fire	ρ_{62}	B_{62}
22	Collisions of planes in air	ρ_{63}	B_{63}

All parameters B_{ij} are estimated with the help of a 100-mark scale in arbitrary units (a.u.). The bigger is value of these parameters, the higher probability of risk (for example, the value 100 a.u. - means "very bad", the value 1 a.u. - means "very good").

Probabilities ω_i and ρ_{ij} should must be determined on the basis of existing empirical statistics of aviation safety, and parameters B_{ij} - on the basis of normative documents of the state aviation administration.

In paper special interface for the input of parameters $\omega_i, \rho_{ij}, B_{ij}, \Delta B_{ij}$ was developed.

As an example the simplified model was considered. In this model only two characteristics of functional efficiency ("Crew" and "Plane") were included, and the script «Prevalence of the human factor importance» was considered. In this case

$$R = \omega_1 B_1 + \omega_2 B_2.$$

We choose

$$\omega_1 = 0,6 - \text{"crew"}$$

and $\omega_2 = 0,4 - \text{"airplane"}$.

For adverse factors from Table 1 we choose arbitrary but reasonable meanings:

$$\rho_{11} = 0,4 - \text{"experience"}$$

$$\rho_{12} = 0,2 - \text{"discipline"}$$

$$\rho_{13} = 0,3 - \text{"psychophysics"}$$

$$\rho_{14} = 0,1 - \text{"retraining"}$$

and $\rho_{21} = 0,5 - \text{"type, destruction, management"}$

$$\rho_{22} = 0,3 - \text{"an operational condition, refusals"}$$

$$\rho_{23} = 0,2 - \text{"servicing, repair"}$$

For these set parameters it was chosen two variants for values of parameters B_{ij} :

Case 1 : $B_{11} = B_{12} = B_{13} = B_{14} = 30$ a.u.; the range ΔB_{ij} of changes for parameters B_{ij} equals to 10 a.u.; values of parameters B_{ij} was randomly taken with equal probability from this range and substituted in the formula for R .

Case 2 : $B_{11} = B_{12} = B_{13} = B_{14} = 60$ a.u.; $\Delta B_{ij} = 10$ a.u.

An amount of experiments for modeling by Monte-Carlo method we set $N=110$. In Fig. 1, 2 dependences $R=f(N)$ for cases 1, 2 are shown. On diagrams three areas are allocated: I - a zone of acceptable risk, II - a zone of tolerable risk, III - a zone of intolerable risk.

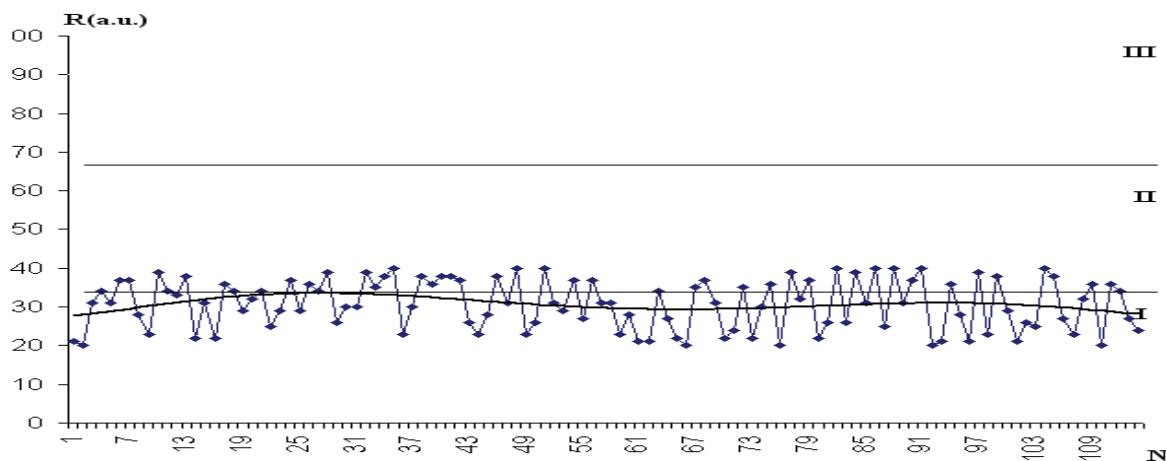


Fig. 1. Distribution of risk parameter R (case 1)

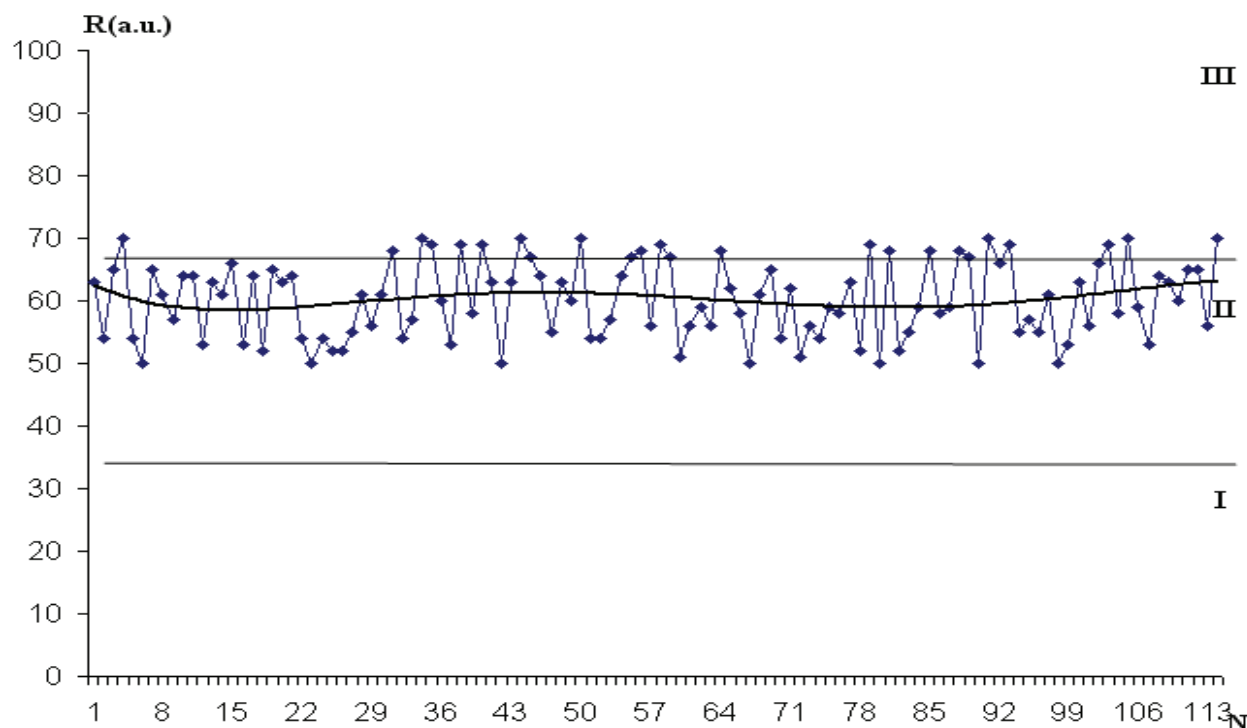


Fig. 2. Distribution of risk parameter R (case 2)

The solid line on diagrams shows the trend received in result of polynomial approximation.

In case 1: values of risk parameter are located mainly in a zone of accepted risk, the line of a trend is completely located in a zone of acceptable risk. However in substantial number of experiments the value of risk parameter is located in a zone of tolerable risk. It is possible to draw a conclusion that in this case a level of safety is high enough.

In case 2: values of risk parameter are mainly located in a zone of tolerable risk, the line of a trend is completely located in a zone of tolerable risk. But calculations have shown that in this case the significant share of experiments has values of risk parameter in a zone of intolerable risk. It is possible to draw a conclusion that in this case a level of safety is not so high.

The proposed method allows to carry out forecasting of aviation safety dynamics in view of internal and external factors, and also to find a series of the coordinated, logically interconnected events and sequence of steps, which with the certain probability lead to a predicted final state (to a preset value of acceptable risk).

References

1. Aviation Safety / V.P.Babak, V.P.Kharchenko, V.O.Maximov and others. – Kyiv: Tekhnika, 2004. – 584p.
2. Flight Safety: Textbook for Universities/ R.B.Sakach, B.V.Zubkov, M.F.Davydenko and others: -Moscow: Transport, 1989. – 239 p.

INVESTIGATION OF HYDRAULIC CONTROL SYSTEMS REGULATORS

The influence of evaluation of change of design parameters of two-stage automatic regulators on deviation from given work characteristic $Q=f(p)$ exactly on the area of regulating has been made on example of variable-flow pump of valve-slits type and differentially-throttle type. The conclusions have been made on received results.

Hydraulic systems provide functions of aircraft control on the ground and in the air, and are used whenever it is necessary to get significant forces and smooth speed adjustment. On modern aircrafts hydraulic systems together with electrical units of control commands transfer are the main systems for mechanization and automation of the control process.

As the source of power in hydraulic control systems the variable discharge pumps with two-stage automatic regulators are used lately. Such pumps allow unloading the pump on output, namely with increase of the load (of the pressure) regulators automatically switch the pump on the minimal output regime.

Research and analysis of static characteristic is made for variable discharge pumps with the regulators of indirect operation. As an example of such pumps the differentially-throttle pump (with nozzle-flap regulator) (fig. 1) and valve-slits pump (fig. 2) are considered.

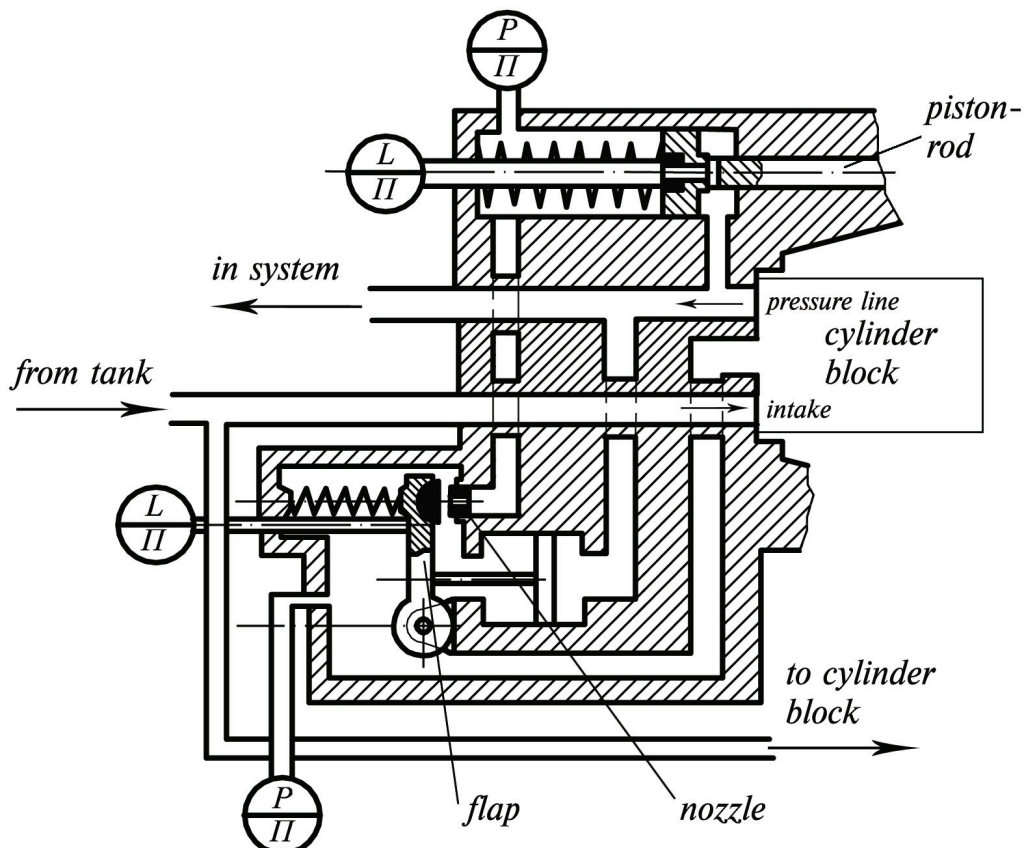


Fig. 1. Structural scheme of variable discharge pump with nozzle-flap regulator.

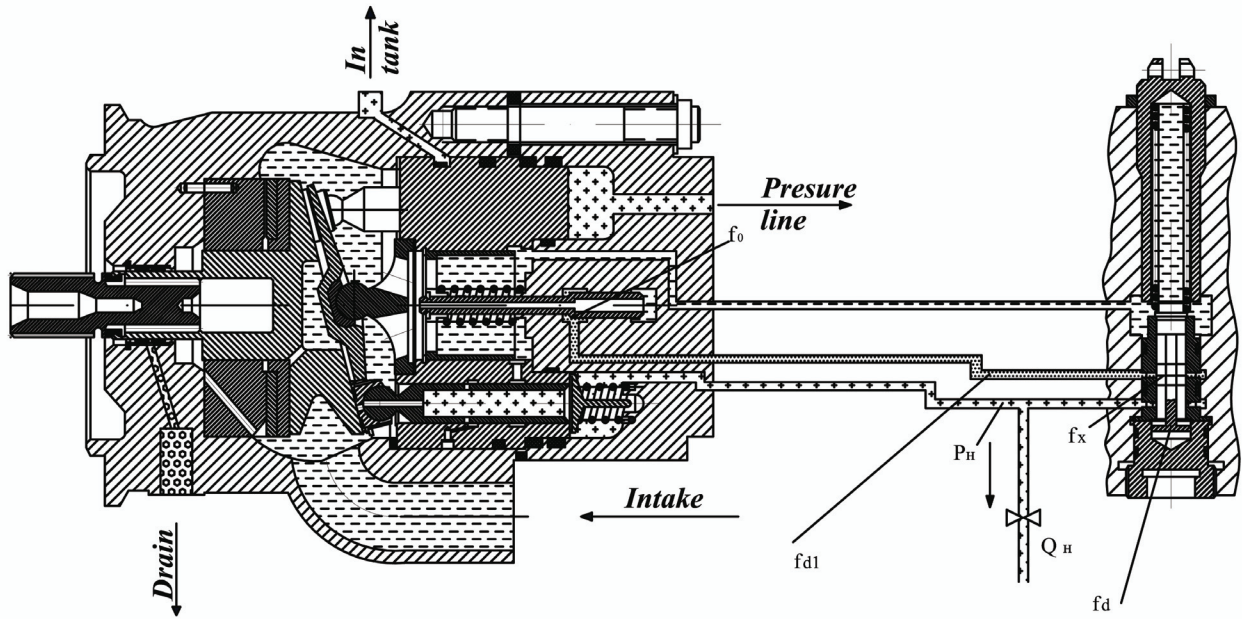


Fig. 2. Structural scheme of variable discharge pump of valve-slits type.

For each of these pumps corresponding equations of work characteristics have been compiled. Their final form:

- for the valve-slits variable discharge pump:

$$Q_H = \frac{1}{K_2} \frac{\partial Q_H}{\partial y} \left[G_2 - F_2 \frac{f_{d1}^2 \left(\frac{\partial f_x}{\partial x} \frac{P_H F_1 - G_1}{K_1} + f_0 \right)^2 P_H}{f_d^2 f_{d1}^2 + \left(f_d^2 + f_{d1}^2 \right) \left(\frac{\partial f_x}{\partial x} \frac{P_H F_1 - G_1}{K_1} + f_d \right)^2} \right]$$

- for the differentially-throttle variable discharge pump:

$$Q_{H.r.} = A \left\{ L_{\max} - \frac{1}{c_1} \left(\left[S - \frac{1}{1 + B(p - p^*)^2} S_0 \right] p - \left[S - \frac{1}{1 + B(p_p - p^*)^2} S_0 \right] p_p \right) \right\} - k_{\text{leak}} p$$

Using these characteristics the evaluation of influence on the work characteristic $Q=f(p)$ of design parameters change of two-stage automatic regulators has been made, exactly on the area of flow regulation. Because with the change of parameters there is change of shape of static characteristic curve and deviation of this shape from linear, that's why the evaluation of this deviation ε is made (fig. 3).

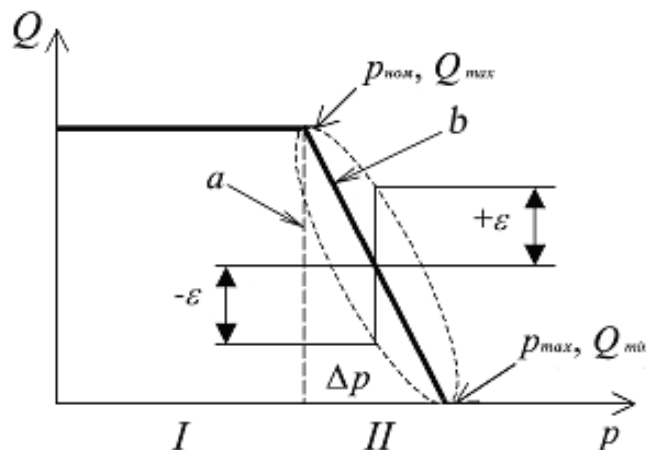


Fig. 3. Static characteristic of variable discharge pump: a - ideal; b - theoretical.

If static characteristic is a straight line, then its middle point in the regime of regulated flow has coordinates:

$$Q_{n.average} = \frac{Q_{max} + Q_{min}}{2} \text{ and } P_{n.average} = \frac{P_{max} + P_1}{2}.$$

With respect to change in parameter's values, Q_{max} and Q_{min} do not change, as well as $Q_{n.average}$, because these values are given and they are determined by invariable parameters of the pump – maximal piston stroke and promptness, and also the fluid consumption in the system of flow regulating.

Thus at linear static characteristic and value $P_{n.average}$ the output must be equal to the $Q_n = Q_{n.average}$. At the same time, while determining the $P_{n.average}$ it is necessary to measure P_{max} and P_1 , which were obtained at specific value of variable parameter.

If the static characteristics is non-linear, then at $P_{n.average}$ the value of output $Q'_{n.average} \neq Q_{n.average}$ will be received. Value $\varepsilon = \frac{Q'_{n.average} - Q_{n.average}}{Q_{average}} \cdot 100\%$ can characterize the deviation of the characteristic from linear shape.

Received graphics have next form:

- for variable discharge pump with nozzle-flap regulator (fig. 4):

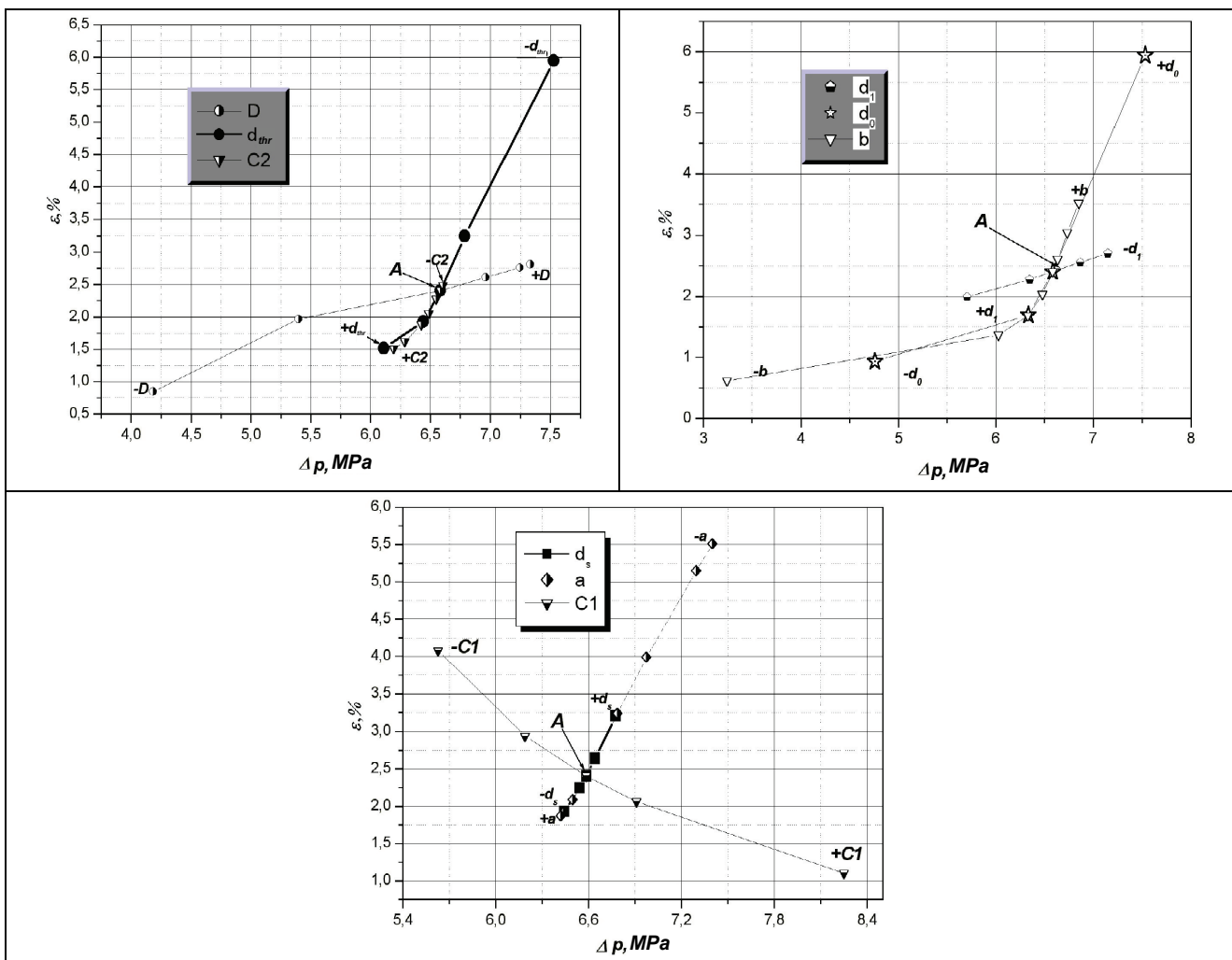


Fig. 4. Relative deviation ε of static characteristic from linear shape with the change of values of design parameters for the pump with the with nozzle-flap regulator. «A» – value of ε at chosen nominal parameters; «+» - increasing change of the parameter from its start value in point «A»; «-» - decreasing change of the parameter from its start value in point «A».

- for the variable discharge pump of valve-slits type (fig. 5):

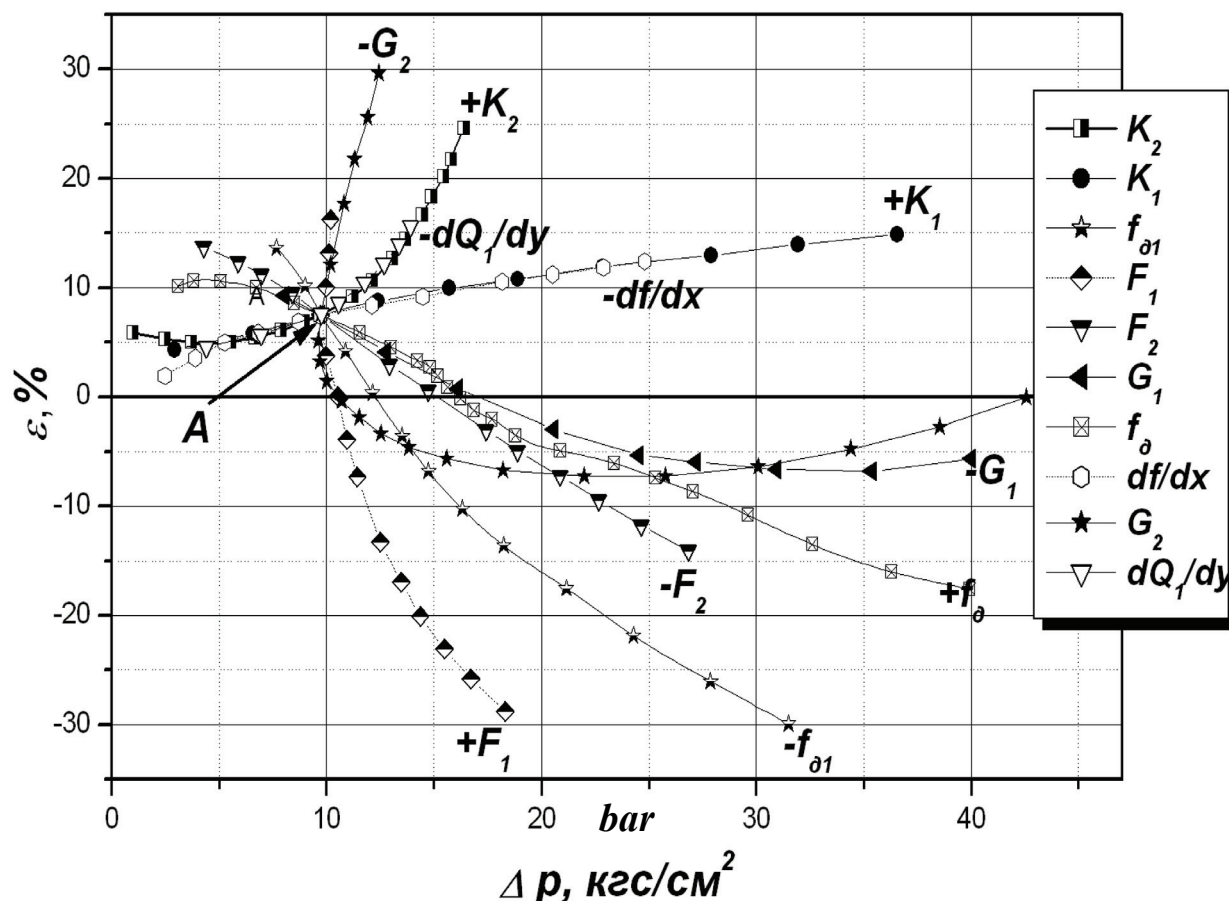


Fig. 5. Relative deviation ε of static characteristic from linear shape with the change of values of design parameters for the pump of valve-slits type. «A» – value of ε at chosen nominal parameters; «+» - increasing change of the parameter from its start value in point «A»; «-» - decreasing change of the parameter from its start value in point «A».

Conclusions. From graphical analysis on figures 4 and 5 there are following conclusions:

- 1) all relations have non-linear character;
- 2) for the pump with the with nozzle-flap regulator increase of values of construction parameters C_1 , C_2 and d_1 leads to the decrease of the value of relative deviation ε , while decrease of design parameters a , b , D , d_s , d_{thr} , d_0 promotes increase in ε ;
- 3) for the pump of valve-slits type the salience of static characteristic ($+\varepsilon$) is increased with increase the value of design K_1 , K_2 , f_{d1} , F_2 , G_1 and is decreased ($-\varepsilon$) with increase of design parameters F_1 , G_2 and f_d .

References

1. Т.М. Башта, И.З. Зайченко, В.В. Ермаков, Е.М. Хаймович Объемные гидравлические приводы. – М.: Машиностроение. – 1969, 492 с.
2. Попов Д.Н. Динамика и регулирование гидро- и пневмо систем. – М.: Машиностроение. – 1987. – 464 с.
3. Е.Н. Сябрюк Анализ статических характеристик автоматических регуляторов. // Вісник Сумського державного університету. Серія Технічні науки: науковий журнал. – 2003. – №13(59). – С. 95-102.

*Ju.N. Rukynich, A.E. Sitnikov, Ja.B. Fedoruchko
(Kiev Central Design Bureau of Valves),
A.G. Kucher, Doctor of Science (engineering),
G.J. Zajonchkovsky, Doctor of Science (engineering),
(National Aviation University)*

FORECASTING OPERATING CHANGES OF THE TECHNICAL STATE OF ELECTROMAGNETICALLY DRIVEN VALVES AT THE STAGE OF DESIGNING

The report is devoted to the development of scientific bases and practical recommendations on forecasting possible operating changes in the technical state of electromagnetic valves with an electromagnetic drive over resource completion.

Development of modern aviation and space technique requires substantial reduction of terms of design and introduction of new production. It can be provided due to reduction of terms and diminishing of expenses on implementation of experimental-design efforts. The requirement on providing of necessary level of reliability and faultlessness of new production remain unchanging. To a full degree these requirements belong to creation of new electromagnetic valves (EMV) of the aircraft systems.

However much the traditional ways of development of EMV remain it is not enough effective and already does not answer the requirements of time. It is needed introductions are new, more effective going near their development. One of such approaches is folded in using of methods of prognostication of possible operating changes of the technical state of EMV for planning. Such prognostication allows:

- to find out those operating influences on the capacity of valve, for determination of which at traditional approach, conducting of long duration and expense resource tests is needed;
- to find out possible violations of the capable of working state of valve, which show up rarely enough and can not be discovered the methods of resource tests through a small sample size;
- to find out operating factors and their levels which more substantial than all influence on an origin and development of degradation changes in elements and knots of valve;
- to determine elements constructions of valve, which limit his resource;
- in good time to develop concrete measures in relation to the improvement of construction of valve and providing of necessary level of his reliability and faultlessness.

As an object of researches was chosen two positions EMV with a pulling-pushing drive, which is used in the pneumatic block of serve of oxygen to the electrochemical generators of the power feed system of the space station (fig. 1). The principle chart of valve is resulted on a fig. 2.

It was found out those particular features of operating loads and basic degradation processes which result in substantial changes in the technical state of EMVs and determine their resource possibilities.

It is discovered that to the basic degradation processes it is possible to take in a valve:

- an accumulation of micro damages in the volume of construction material of details of valve;
- degradation of macro relief of contact surfaces; painting from the fatigue of contact surfaces;
- deformation of details in the area of contact of butt end surfaces;
- change of form of stop puck and of the rod head;
- change of relative position of details.

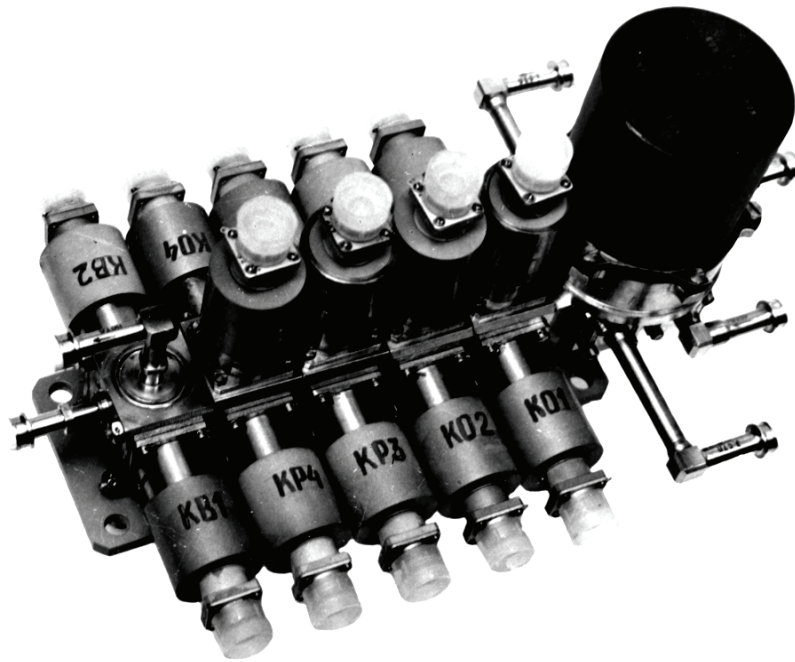


Fig. 1. Pneumatic block of serve of oxygen to the electrochemical generators of the of the power feed system of the space station

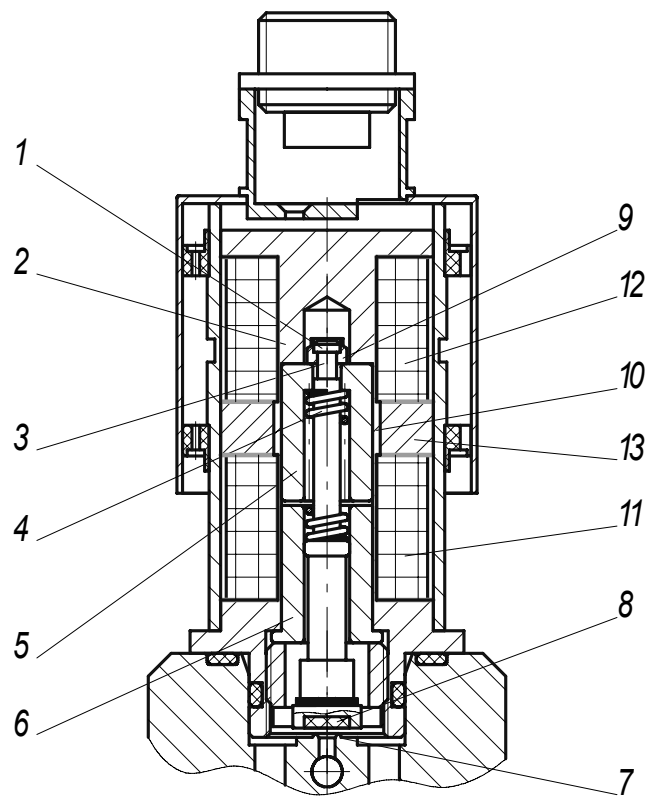


Fig. 2. Structural chart of valve:

1 – a rod head; 2 – a corps of electromagnet; 3 – ШТОК; 4 – a buffer spring; 5 – a slide-block (anchor); 6 – a lower feet; 7 – a saddle; 8 – a slide-valve; 9 – a stop puck; 10 – a distributive tube; 11 – a closing puttee; 12 – an opening puttee; 13 – a permanent magnet

Experimental a way certainly character and intensity of changes of basic structural and functional parameters of valves of the considered types from the amount of cycles of work.

Theoretical bases of design of operating changes of the technical state of EMV are developed with the use of probabilistic model of accumulation of damages in elements and knots of EMV.

From the physical point of view the process of accumulation of damages in material of details of valve is related to the accumulation of the irreversible one-sided plastic deformations, development of processes of fatigue, wear and by other irreversible changes of structure of material. On development of these processes, in same queue, external casual factors influence is a change of terms of work and change of parameters of loading of details in the process of exploitation. At every influence of loading (casual or regular) there is an elementary act of accumulation in material of the irreversible deformations (increase of damages), size and character of which is the casual function of mechanical descriptions of material, sizes of tensions, number of cycles and other factors. The process of accumulation of damages in this case is examined as a result of the statistical adding up of large number evenly small micro jump of elementary independent damages. Then at n cycles a size Π_n will be determined accumulated damaged Π_n by a sum, where Π_i is a size damaged in i -th elementary cycle. For some period of time, when n large enough, accumulated damageability Π_n aspires to normal distribution. Such process of accumulation of damages can be examined as a casual process with independent increases, built on the type of Markov sequence.

As a process of accumulation of damages it is possible to examine indirect parameters which reproduce character of change of basic physical processes of damageability material of details well enough, such as, for example, motion of slide-valve h of EMK of the examined type (rice 3). In this case descriptions of casual process of accumulation of damages can be certain, probed and forecast statistical methods.

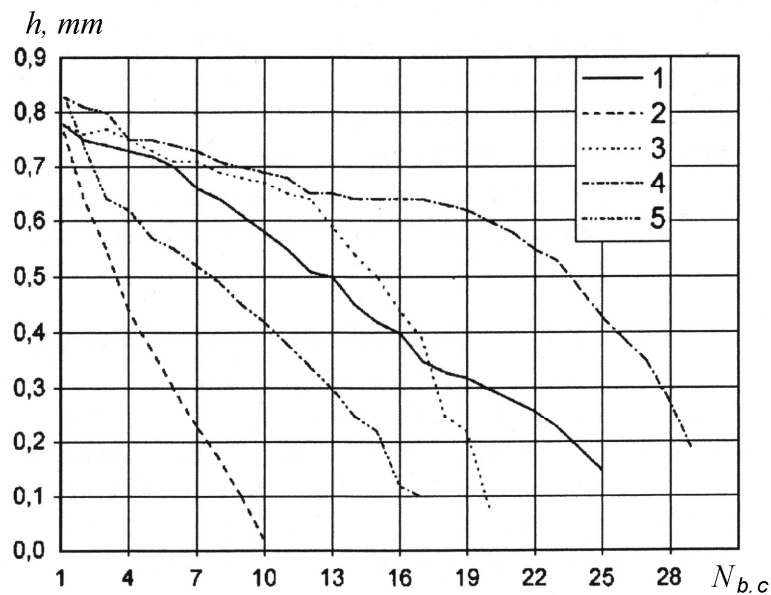


Fig. 3. Dependences of change of motion of slide-valve h of five experimental standards of valve on the amount of the block-cycles working $N_{b,c}$ (1 block-cycle = 50000 workings)

Two casual processes are probed (sequences): initial process of origin of damages $\Pi'(t_1), \Pi'(t_2), \dots, \Pi'(t_n)$ and generated by him process of accumulation of damages

$\Pi(t_1) = \Pi'(t_1), \Pi(t_2) = \Pi'(t_1) + \Pi'(t_2), \dots; \Pi(t_n) = \sum_{i=1}^n \Pi'(t_i)$. The first process at some

suppositions it is possible to examine as a homogeneous casual stationary process, and second – as a casual unsteady process.

Accepting supposition, that the law of distributing of the accumulated damages is near to normal, that then found the confirmation from data of processing of experimental data, the probabilistic models of adding up of both independent and dependent casual damages were developed in elements and knots of valve. With the use of these models mathematical dependences are got for determination of the expected value m_n and dispersion S_n^2 of the accumulated damages in elements and knots of valve, and also closeness $f_{\Pi_n}(\Pi_n)$ and function of distributing of the accumulated damages for the different possible values of coefficient of correlation r :

$$m_n = \sum_{i=1}^n m_i = nm;$$

$$S_n^2 = S_n^2(1 + (n-1)r);$$

$$f_{\Pi}(\Pi_n) = \frac{1}{\sqrt{2\pi S_n^2 n(1 + (n-1)r)}} \times \exp\left(-\frac{(\Pi_n - nm)^2}{2S_n^2 n(1 + (n-1)r)}\right);$$

$$F_{\Pi}(\Pi_n) = \Phi\left(\frac{\Pi_n - nm}{S\sqrt{n(1 + (n-1)r)}}\right).$$

Mathematical dependences are got also for determination of closeness of distributing f_p and function of distributing F_p of numbers of cycles to destruction of critical element of valve, which can be used for the estimation of probabilistic descriptions of reliability and longevity of EMV.

Mathematical models are developed also and on their basis the proper methods of prognostication of change of structural and functional parameters of EMV with the use of least-squares method, method of extrapolation and method of the directed selection [2, 3].

It is discovered that work of EMV of this type completely as a result of tireless destruction of neck of штока depends on specific kinetic energy of moving of the mobile system of occasion. On the basis of experimental researches the method of prognostication of indexes of faultlessness of EMK is developed with the use of power criteria[4].

The basic results of researches are inculcated in practice of planning of EMV in the Kiev Central Designer Bureau of Valves.

References

1. Хильчевский В.В., Ситников А.Е., Ананьевский В.А. Надежность трубопроводной пневмо-гидроарматуры. – М.: Машиностроение, 1989. – 208 с.
2. Ситніков О.Є., Кучер О.Г., Зайончковський Г.Й., Федоричко Я.Б. Оцінювання і прогнозування ресурсу пневматичних клапанів з електромагнітним приводом // Промислова гідравліка і пневматика. – 2003. – №2. – С. 7–23
3. Ситников А.Е., Федоричко Я.Б., Кучер А.Г., Зайончковский Г.И., Сухоруков А.Ю. Прогнозирование изменения функциональных параметров клапанов с электромагнитным приводом при выработке ресурса // Промислова гідравліка і пневматика. – 2004. – №3 (5). – С. 10–22.
4. Рыкунич Ю.Н., Ситников А.Е. Выбор запасов работоспособности проектируемых электромагнитных клапанов с использованием энергетических критериев // Промислова гідравліка і пневматика. – 2006. – № 1 (11). – С. 43–46.

*A.A. Itskovich, I.A. Faynburg, Moscow State University of CA, Russian Federation;
V.S. Shapkin, A.S. Gromov, A.V. Semin,
State Scientific and Research Institute of CA, Russian Federation;
A. Grishin, "Tupolev" Open Stock Company, Russian Federation*

APPLICATION OF EFFECTIVE PROGRAMS OF MAINTAINING TU-154M AIRCRAFT AIRWORTHINESS IN THE AIRCRAFT MAINTENANCE CENTERS

This article gives the description of the Program of maintaining Tu-154 aircraft airworthiness in the maintenance center on the basis of progressive technologies, develops model analysis of the effectiveness of the program of maintaining Tu-154 aircraft airworthiness, gives proposals to improve information support.

In international practice there is a tendency to reject general overhaul in aircraft operation. For the Russian manufactured aircraft, having a type certificate, maintenance programs also don't envisage general overhaul. In the last years this tendency began to spread on the aircraft, which don't have a type certificate and are on their final operation stage. In relation to the fleet of these aircraft there was accumulated an experience of their long-term operation under the conditions of a stage-by-stage prolongation of their service life and service time and performing general overhaul. In international practice, when the aircraft service time is over 14 years, these aircraft are regarded to be the aging aircraft fleet. For such types of aircraft Aging Aircraft Operation Programs, worked out by the Designer and approved by the Aviation Administration, begin to operate. Their implementation is obligatory for aircraft operators and the advisability of the further operation of the aircraft fleet is the economic component of such a program.

In accordance with the ICAO recommendations (Annex 8 to the Convention on International Civil Aviation) the State of Design should draw up a program of maintaining the integrity of the aircraft structure to ensure aircraft airworthiness. The ICAO Continuing Airworthiness Manual (Doc 9642) contains recommendations related to the contents of the Aircraft Structure Integrity Program, which should include: additional check-ups, measures to prevent corrosion, structure modifications. Structure integrity analysis should be confirmed by the results of the tests and operation with the estimation of the operational spectra of loads and their distribution in the structure, characteristics of the materials. Test modes should take into account the diversity of the periods before cracking and the spreading speed. The first check up period, the periodicity of checkups and, if necessary, the replacement periods are being established.

Taking into account the fact, that the average service time of the majority of the aircraft, making up the basis of the Russian aircraft fleet, is over 15 years, the analogous approach to the aging aircraft is also functioning in Russia. IAC normative documents (АП 25-571, МОР 25-571) envisage that ensuring aircraft structure safety in relation to the strength conditions in long-term operation is being achieved on the basis of the principles of damage permissibility, safe damage and safe service life (service time).

At present the Tu-154M aircraft fleet of the following airlines: "Aeroflot-RAL" Open Stock Company, "UTair" Open Stock Company, "Sibir" Open Stock Company, "ALROSA" Open Stock Company, "Kogalymavia" Open Stock Company, "Yakutia" Open Stock Company is being operated according to the Program of maintaining airworthiness on the basis of progressive technologies (without general overhaul) [1]. In accordance with the program, developed by the "Tupolev" Open Stock Company, State Scientific and Research Institute of Civil Aviation, State Scientific and Research Institute of Air Navigation and Central Aerogydrodynamic Institute, airworthiness monitoring of every Tu-154M aircraft sample is being carried out annually in the conditions of the following Aircraft Maintenance Centers: "Domodedovo Aircraft Maintenance Base" Closed Stock Company, "VARIS-400" Open Stock Company and "Sibir-technik" Ltd. Civil Aircraft Airworthiness Oversight Department of the Federal Authority for Transport Oversight determines by its decision conditions of establishing for the Tu-154M aircraft fleet of the airlines

the overhaul period 25000 flight hours, 10000 flights within the framework of the current overhaul time (prior to the 1st overhaul) 15 calendar years, specified life and service time 50000 flight hours, 20000 flights, 30 years.

The above-indicated conditions specify performing in the Aircraft Maintenance Centers a complex of works on monitoring and maintaining airworthiness of the Tu-154M aircraft, including the estimation of their operational status in the scope of the F-2 periodic maintenance, performing structure modifications according to the industry bulletins and airworthiness instructions, replacing airframe primary structural members and vendor items with replacement life, testing airframe critical members (corrosion damage, fatigue failure, mechanical damage), testing parameters and item trouble-free operation level, performing additional list of works.

For the purpose of increasing the efficiency of the Tu-154M aircraft operation in the airlines it is envisaged that the procedure of establishing the service life and service time is combined with the aircraft sample certification procedure.

Characteristics of the initial and the new programs of maintaining the Tu-154M airworthiness are given in Table 1. Both programs envisage rational distribution of the unit and vendor item nomenclature by methods of technical operation: by service life – 24%, by the condition in relation to the parameter test – 12%, by the condition till safe failure – 64%. Reliability level control is being carried out in all methods of technical operation.

There is a necessity to solve the problems of the comparative estimation of the new program of maintaining the Tu-154M aircraft airworthiness in the conditions of the Aircraft Maintenance Centers on the basis of the progressive technologies (without general overhaul) and the initial aircraft maintenance program in the conditions of the stage-by-stage prolongation of their service life and service time and performing general overhauls.

In order to solve these problems one should work out a model process of maintaining aircraft airworthiness, reflecting the peculiarities of the application of the indicated programs of maintaining the Tu-154M aircraft airworthiness, and submit the proposals on the improvement of the initial data presentation form.

The application of the mathematical apparatus of the semimarkov processes to describe the process of maintaining aircraft airworthiness for the period of their operation in accordance with the corresponding program of maintaining aircraft airworthiness requires to present the process of maintaining aircraft airworthiness as a whole complex of semimarkov processes $m_q \subset M, q = \overline{1, r}$, distinguished by the time intervals (operating time) of the aircraft in operation [2-4]. It is supported that the processes $m_q \subset M, q = \overline{1, r}$ are ergodic. It is also supported that within each time interval (stage of operation) process parameters remain invariable, and the duration of every $m_q \subset M, q = \overline{1, r}$ process functioning is long enough compared to the average time of being in each state, and this is why the time may be considered infinite while solving the problem of optimizing the program. Stages of the Tu-154M aircraft operation in the initial program of maintaining aircraft airworthiness may be interpreted as a calendar duration of serving out aircraft service life in operation to the 1st overhaul (L.B.O.). When applying the new program of maintaining the Tu-154M aircraft airworthiness, stages of operation are assumed to equal 1 year (periodicity of airworthiness monitoring in the Aircraft Maintenance Center). At each stage of operation the whole spectrum of the states of maintaining aircraft airworthiness is put in conformity with the state of the aircraft being in flight $K_i^j \in K, j = \overline{1, r}, i = \overline{1, m}$, which makes it possible to differentiate the scope of the aircraft maintenance works depending on the aircraft operational status and consider versions with the incomplete restoration of the objects' working condition.

The semimarkov model of the process of maintaining aircraft airworthiness may be presented as a graph of states and changes (Figure). The structure of the process of maintaining aircraft airworthiness is given in Table 2, which shows their compliance with the examined programs of maintaining the Tu-154M aircraft airworthiness and the statistical accounts form "Aircraft Calendar

Time Data” [4]. Bold type is used to show the states, which are suggested to be additionally introduced to analyze the efficiency of the process (programs) of maintaining aircraft airworthiness.

Table 1

Description of the initial (with general overhaul) and new (without general overhaul) programs of maintaining the Tu-154M aircraft airworthiness

№	Service life, service time, kinds of works	Initial program of maintaining aircraft airworthiness (with general overhaul)	Progressive program of maintaining aircraft airworthiness (without general overhaul)
1	Life limit to 1 st overhaul (life between overhauls – LBO), hours/landings	18000 flight hours 8000 landings	30000 flights hours 10000 landings
2	Time limit to 1 st overhaul (time between overhauls TBO), years	15 years	15 years
3	Assigned service life limit, hours/landings	50000 flight hours 20000 landings	50000 flight hours 20000 landings
4	Assigned service time, years	30 years	30 years
5	Individual extension of service life and service time	yes	no
6	Aircraft airworthiness certification	independently	combined
7	Overhaul	yes	no
8	Maintenance without overhaul (in the scope of F-2 inspection) at the Aircraft Maintenance Center	no	yes
9	Modifications according to the service bulletins (Annex 2)	yes	yes
10	Replacement of primary structures elements and parts with replacement life (Annex 3)	yes	yes
11	Periodic inspection of the airframe structural elements, units, components and systems (Annex 4)	yes	yes
12	Performing the list of additional works (Annex 5) at the Aircraft Maintenance Center	yes	yes
13	Reliability, parameter test and replacement of units and components according to the methods of maintenance: by life limitation, by limited condition, by condition till the safe failure	yes	yes
14	Performing scheduled maintenance according to the maintenance schedule of line and periodic maintenance (scheduled and unscheduled checks)	yes	yes

Indices of the efficiency of the process of aircraft airworthiness continuing are determined by the following formulas:

factor of being in the j state

$$K_j = \frac{p_j m_j}{\sum_{k=1}^N p_k m_k},$$

factor of use

$$K_{\text{H}} = \frac{p_i m_i H_c}{\sum_{k=1}^N p_k m_k 24}, i \in K^j_l.$$

Factor of specific idle (layup) period

$$K_{\Pi} = \frac{\sum p_l m_l 24}{p_i m_i H_c}, l \notin K^j_l, i \in K^j_l,$$

Labor content per unit output related to continuous air worthiness

$$\tau_{y\partial} = \frac{\sum p_l \tau_l}{p_i m_i H_c}, l \notin K^j_l, i \in K^j_l,$$

Material content per unit output related to continuous air worthiness

$$C_{m,y\partial} = \frac{\sum p_l c_{ml}}{p_i m_i H_c}, l \notin K^j_l, i \in K^j_l$$

Unit cost related to continuous air worthiness

$$C_{y\partial} = \frac{\sum p_l c_l}{p_i m_i H_c}, l \notin K^j_l, i \in K^j_l,$$

where π_l - stationary probability in i-condition of the continuous air worthiness process,

μ_l - average time of containment in i-condition, τ_l - average labor costs in i-condition, c_{ml} - average material costs in i-condition, c_l - average costs in i-condition, H_c - daily flight time, hours per day,

The model of the airworthiness process (see fig.) involves the hierarchy structure and contains multiplicity of the airworthiness process conditions conforming to the U1 cycle of operation of serviceable aircraft fleet, periodic U2 cycle of operation of operative aircraft fleet, and U3 maintenance cycle of the total registered aircraft fleet of the given type.

For the purpose of analyzing the effectiveness of basic and new programs, statistics related to periodicity, duration, labor intensity and cost of works should be submitted by the airlines to the Continuous Airworthiness Research Centre of the State Civil Aviation Scientific Research Institute together with an application to monitor airworthiness of each unit of TU-154M aircraft at the Maintenance Centre accompanied by an act of its technical evaluation

With a view of analyzing the results of TU-154M airworthiness monitoring at the Maintenance Centre on the basis of progressive technologies with use of the semi-Markov model, mentioned above, there have been suggested the forms of basic data concerning dwelling time, labor, material and financial costs related to airworthiness monitoring of each TU-154M at the airline and Maintenance Centre.

Analysis of operation of TU-154M aircraft on the basis of the new continuous airworthiness program showed a positive effect of its implementation. It also proved that factors of effective use, aircraft fleet serviceability had been improved and aircraft ground time reduced.

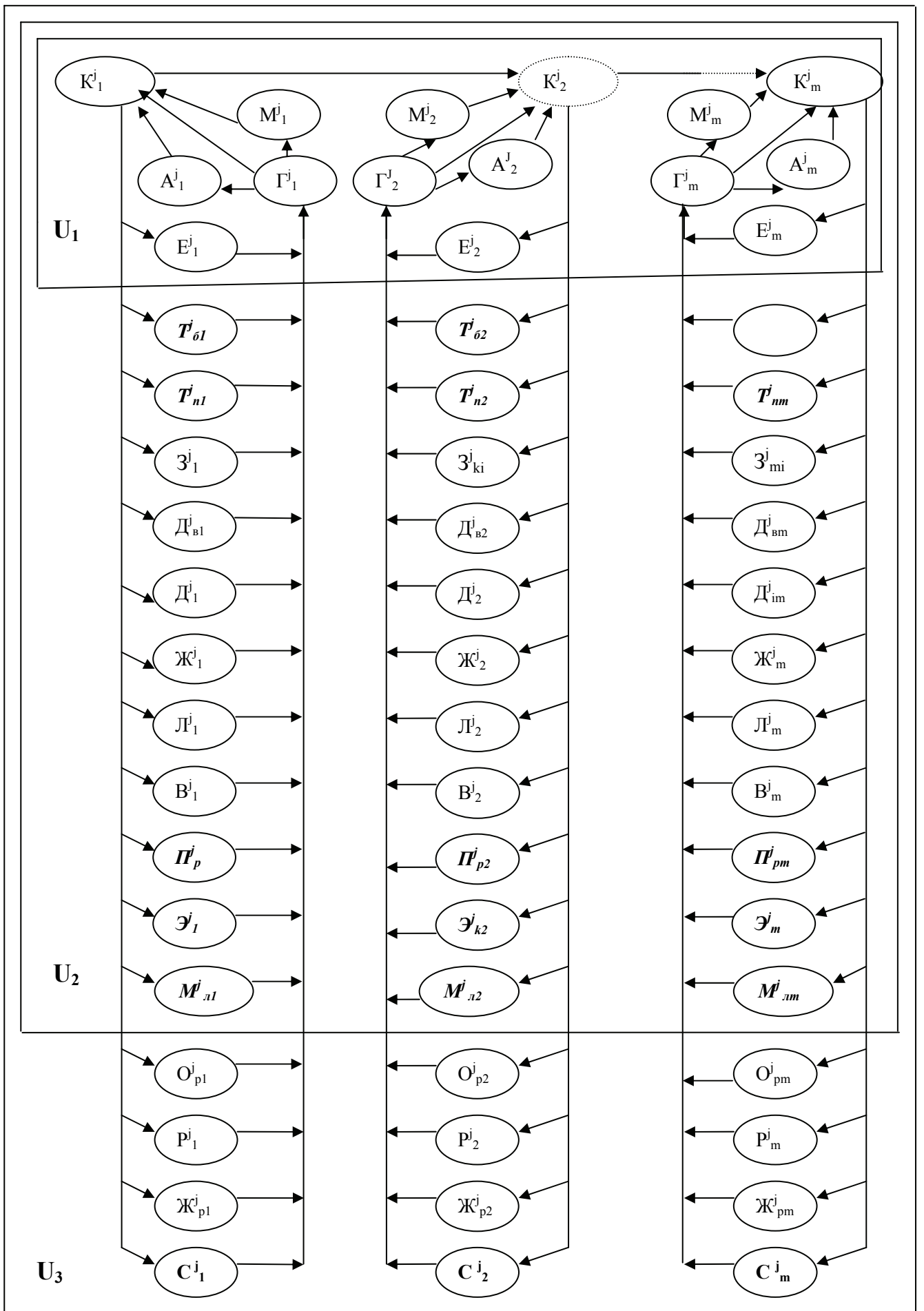


Fig. Graphic presentation of conditions and transitions in the semi-Markov TU-154M continuous airworthiness model

Table 2

Structure of the continuous airworthiness process

Subset of the airworthiness process conditions	State of the airworthiness process		Airworthiness program type		Content of the form “Information on calendar aircraft time”	
	Name	Symbol	Initial	New	Existing	Suggested
Serviceable and in operation	In operation	K	+	+	+	+
	<i>In flight</i>	<i>И</i>	+	+		+
	<i>Departure in operation</i>	<i>Ер</i>	+	+		+
Serviceable in the airline	Stand-by	Г	+	+	+	+
	Serviceable, not operated	A	+	+	+	+
	Grounded due to weather conditions	M	+	+	+	+
	Departures from the base airport	E	+	+	+	+
	Maintenance	ТО	+	+	+	
Unserviceable in the airline	<i>Type “B” operational maintenance</i>	<i>T_o</i>	+	+		+
	<i>Periodic maintenance</i>	<i>T_n</i>	+	+		+
	Lack of spare parts	З	+	+	+	+
	Отсутствие двигателей	Дв	+	+	+	+
	Bulletin service	Д	+	+	+	+
	Reclamation by the industry	Ж	+	+	+	+
	Accident investigation	Л	+	+	+	+
	Damage recovery	B	+	+	+	+
	<i>Renewal of the overhaul period and service life</i>	<i>И_p</i>	+			+
	<i>Certification of aircraft</i>	Э	+	+		+
	<i>Airworthiness monitoring</i>	<i>M_n</i>		+		+
	Aircraft retirement	C	+	+	+	+
	Maintenance expectation	O _p	+		+	+
	Under maintenance	P	+	+	+	+
Reclamation by the maintenance plant	Жр	+	+	+	+	
Unserviceable at the Maintenance Centre						

We also might speak about improvements in conditions of the planning process related to continuous airworthiness and reductions in uncertainty of the expected volumes of operations and ground time with relation to the individual prolongation of life span and service time, including problems of elimination of corrosive defects, replacement of load bearing elements of the airframe and service bulletin performance.

The process of planning for the next year showed how many aircraft went through maintenance procedure at the Maintenance Centre every month where airworthiness monitoring was combined with service bulletin performance and airworthiness directives.

It is well known that one of the principle factors influencing taking decisions on possibility of further operation of TU-154M aircraft is its corrosive condition.

During the first stage of new program application aircraft troubleshooting procedures are carried out on the basis of the current flight performance documentation. Nevertheless while acquiring experience of detecting corrosive defects it appeared necessary to widen the range of troubleshooting activity accompanied by dismounting of the galley, rear toilets, floorboards, receiving tank, air duct system in the area of the frames 37-41 and fully remove the anti-corrosive cover in the baggage compartments №1 and №2 . Only after performing necessary dismounting operations and quality troubleshooting activity a huge amount of additional corrosive defects were detected which very often could lead to full or partial replacement of the airframe elements. In its turn unavailability of the sufficient amount of required spare parts of category 1 resulted in prolongation of aircraft staying in the Maintenance Centre.

Based on the results of the analysis of the first stage of works in accordance with the new Continuous Airworthiness Program forecasting of a new volume of activity in troubleshooting and maintenance of electrical elements of the airframe for the second stage was carried out in 2005. Such an approach allowed to place orders for manufacturing required spare parts in advance and maintain a more exact time scheme of work planning.

After completion of a two-year period of corrosion control by the end of 2006 at the third stage of such activity in 2007 the average number of corrosive defects decreased twice as little. That proved the effectiveness of efforts taken during 2005-2007 period. Decrease in average number of corrosive defects per one aircraft, depending on the stage of work activity based on the new program, is characterized by the following data received during the process of observation seven TU-154M aircraft at the Maintenance Centre: 85 corrosive defects in 2005 (1st stage), 77 corrosive defects in 2006 (2nd stage), 37 corrosive defects in 2007 (3^d stage).

Quality of corrosion control became better. In comparison with previous years more than half (53%) of the detected defects were related to corrosion the amount of removal of which did not exceed maximum acceptable values. Such corrosive defects were eliminated by way removal of corrosion and restoration of paint coating on the spot.

According to the assessments by the specialists of “Tupolev”, Open Joint-Stock Company, along with insufficient corrosive endurance of B95N1 alloy, one of the causes of the corrosive defects of the aircraft, subjected to the overhaul procedure, is application, before airframe and power unit troubleshooting procedure, unauthorized solvents and cleaning fluids (645, 646, Cee Bee A-952) which remove from the surface of the airframe and power units not only preventive composition, but also paint coating. Besides the solvents get into slots and backlashes between stringers and trimmings. Taking into account that all these liquids are corrosively active and practically cannot be removed from inside, the causes of new corrosion seats and ways of their developments become apparent. That is why the manufacturer requires not to apply the solvents (except authorized ones, like white spirit, kerosene) for removal of preventive compositions from the assembled construction.

An important factor for organization of control and accounting of corrosive defects on the airframe is implementation of passports of corrosive conditions of the aircraft and registration of the technical conditions of the airframe.

Together with the State Civil Aviation Scientific-Research Institute and “Dalic” company, France, the manufacturer carried out implementation of the new technological process of local anodic treatment for restoration of defected aluminium parts by Zn-Ni coating.

An important activity of the manufacturer related to enhancing reliability of anti-corrosive protection of the outer surface of the aircraft and improving aircraft outward appearance is development and perfection of new methods of painting the outer surface.

On the basis of cooperation with the leading foreign manufacturers of paint and lacquer coating “AKZO-Nobel” (Netherlands) and PPG Aerospace PRC-De Soto (UK) and based on the results of joint tests and under-control operation of two Aeroflot-Russian Airlines’ aircraft during 15 months, it is recommended to use the following paints which are the best ones taking into account the complex of their bulk properties: Aviox Primer 37098 coating + Aviox Finish 77702 enamel + Aviox Advanced Mike Series decorative coating + Aviox Clearcoaf UVR lacquer.

The results of the under-control operation are approved by the appropriate acts of the manufacturer, representatives of the Aeroflot – Russian Airlines and developers of the paint and lacquer coating.

Application of the mathematic equipment for controlled semi-Markov processes used for modeling of Tu-154M continuous airworthiness during their entire lifecycle gives an opportunity to assess the effectiveness of various adaptations of the program. It is proved that providing the given level of flight safety and regularity the new TU-154M continuous airworthiness program (without overhaul repair) in conditions of the Maintenance Centre is more effective than the source continuous airworthiness program (with overhaul repair and stage-by-stage prolongation of overhaul-period renewal and operating life) on the basis of intensity of service and economy of technical operation of TU-154M aircraft. The results of the research carried out and experience of application of the effective TU-154M continuous airworthiness program (without overhaul repair) at the maintenance Centre could be used during the operation of the “aging” aircraft fleet of other types of aircraft.

References

1. *Butushin S.V., Diogenov S.V., Semin A.V., Shapkin V.S.* “Continuous Airworthiness in Conditions of Maintenance-free Operation of Tu-154M Aircraft Operated by Aeroflot – Russian Airlines”. Moscow State Civil Aviation University Scientific Bulletin, “Aeromechanics and Durability” series, №119, 2007, pp. 102-108.
2. *Itskovich A.A.* “Aircraft Technical Operation Process Management”, Part 2- “Methodology for Programmed Aircraft Technical Operation Process Management. Textbook. Moscow State University of Civil Aviation, 2002.
3. *Fineburg I.A.* “Modelling Semi-Markov Model of Continuous Airworthiness Process Management”. Moscow State Civil Aviation University Scientific Bulletin, “Air Transport Operation” series, №123, 2008.
4. *Shapkin V.S., Itskovich A.A., Semin A.V., Fineburg I.A.* “Analysis of the Efficiency of TU-154M Continuous Airworthiness Program at the Aircraft Maintenance Center on the Basis of the Progressive Technologies”. Moscow State Civil Aviation University Scientific Bulletin, “Aeromechanics and Strength” Series, № 130, 2008. pp. 102-108.

DEVELOPMENT OF MINIMUM EQUIPMENT LISTS ENSURING SAFE AIRCRAFT FLIGHTS.

This presentation provides general provisions and legal foundations for the establishment of the “Master Minimum Equipment List” (MMEL) and “Minimum Equipment List” (MEL). It also shows MMEL development procedures and economic aspect of its use.

General

Modern aircraft, built according to the “safe damage” principle, have a high level of operational structural redundancy.

Redundancy characteristics laid into the aircraft structure allow solving successfully the problems of ensuring regularity of operations and acceptable safety level.

Realization of the redundancy characteristics laid into the aircraft structure is being accomplished by means of using minimum equipment lists (MEL). Such MELs allow aircraft operators and flight crews to temporarily perform safe operations with the defective (unused) equipment, if necessary.

Master Minimum Equipment List (MMEL) is developed by the company for the aircraft type, Minimum Equipment List (MEL) is developed by the aircraft operator for each aircraft.

Both MEL and MMEL are normative and legal documents, which are approved or adopted by the airworthiness control body. They include enumeration of components and systems, which are being given the “Permissible”, “Permissible if” or “Not permissible” status depending on their influence on flight safety. Components having the “Permissible” or “Permissible if” status may stay in the defective condition in the course of a limited period of time. Availability of the components having the “Not permissible” status is the reason for the prohibition of operations.

Legal Foundation to Establish MEL and MMEL

Official definition of the Minimum Equipment List is given in “Annex 6 – Chapter 6: Aeroplane Instruments, Equipment and Flight Documents”:

“6.1.3 The operator shall include in the operations manual a minimum equipment list (MEL), approved by the State of the Operator which will enable the pilot-in-command to determine whether a flight may be commenced or continued from any intermediate stop should any instrument, equipment or systems become inoperative...”

Attachment G to the ICAO Annex 6 gives the explanation of the object, as well as the principle of MEL:

“If deviations from the requirements of States in the certification of aircraft were not permitted, an aircraft could not be flown unless all systems and equipment were operable. Experience has proved that some unserviceability can be accepted in the short term when the remaining operative systems and equipment provide for continued safe operations”.

In foreign practice legal policy and norms for establishing Master Minimum Equipment List (MMEL) and Minimum Equipment List (MEL) are set forth in the Aeronautical Requirements, in particular JAR-OPS 1.030 state: “Operator’s Responsibilities:

(a) An operator shall establish, for each aeroplane, a Minimum Equipment List (MEL) approved by the Authority. This shall be based upon, but no less restrictive than, the relevant Master Minimum Equipment List (MMEL) (if this exists) accepted by the Authority.

(b) An operator shall not operate an aeroplane other than in accordance with the MEL unless permitted by the Authority. Any such permission will in no circumstances permit operation outside the constraints of the MMEL.”

However, as the ICAO Convention (Annex 6) states, MMEL should also take into consideration the existing airworthiness standards in order to ensure that the aircraft meets these standards. In this connection the process of approving MMEL is similar to the process of certification: MMEL is the sanctioned deviation from the aircraft Type Certificate.

MMEL Development Process

MMEL development is a process which involves many employees of the company in particular system development specialists, flight safety specialists, etc.

For each MMEL component specialists take into account:

- The influence of this component failure on flight safety;
- Results of the flight tests and/or flight simulator tests;
- Failure influence on the flight crew work load;

- Influence of several malfunctions;
- Influence of the additional critical failure.

Interaction between the systems is being carefully analyzed in order to make sure that multiply failures will not lead to the unsatisfactory flight safety level. Moreover, not only the consequences of the given component failure are being considered in the course of the analysis but also the consequences of the additional critical failure.

When an aircraft is prepared for the departure then if MMEL/MEL is available the acceptable flight safety level is maintained by means of:

- Transferring the function to the other equipment component (reservation); or
- Other equipment component (reserve instrument) giving the required data; or
- Observing the appropriate limitations and/or procedures (flight crew operating procedures and/or maintenance procedures).

MEL development procedure presupposes the analysis of the failure consequences, including critical failures. Aircraft components are included in MEL if the failure consequences are inessential and the required flight safety level is maintained. However, aircraft components may be included in MEL in case when the failure consequences are essential or the required flight safety level is not ensured but the actions of the flight crew or engineering and technical personnel may minimize the failure consequences.

Adopting Decisions about Aircraft Operational Clearance with the Use of MEL

MMEL is the result of the comprehensive study and analysis including the review of a great number of operating conditions and factors with the aim of ensuring safe flight operations and normal aircraft operation.

MMEL sets a time-limit in the course of which the aircraft may be operated with the defective components this limit is determined in order to:

- Maintain the acceptable safety level;
- Prevent poor quality maintenance;
- Prevent multiple failures which may accumulate in the course of time and thus affect flight safety and the efficiency of the aircraft operation.

“Airbus” MMEL sets 4 time intervals necessary to eliminate malfunctions (A, B, C and D):

Time periods of eliminating malfunctions	A	B	C	D
Number of calendar days (excepting the day of detection*)	**	3	10	120

* Not applicable to the ‘A’ type. The time for the elimination of malfunctions is limited by the number of flights or flight hours.

** Category ‘A’ does not set the standard time for the elimination of malfunctions.

Interval ‘C’ corresponds to the period of time adopted by the Authorities till the next repair of the aircraft main/standard system. After the analysis of the failure influence on flight safety it is sometimes necessary to apply the less prolonged ‘B’ interval.

Interval ‘D’ corresponds to the majority of auxiliary systems.

Interval ‘A’ is applied to the components which can’t be referred to the ‘B’, ‘C’ or ‘D’ intervals. Interval ‘A’ may be shorter or longer than specified for the ‘B’, ‘C’ or ‘D’ intervals.

An aircraft can’t be cleared for flight after the time required to eliminate malfunctions, specified in the MEL, has run out. However, there is a possibility to prolong this term in accordance with the special procedure stated in JAR-MMEL/MEL.

Prolongation of the Time Period for the Elimination of Malfunctions

An aircraft shall not be cleared for flight operations after the time required to eliminate malfunctions has run out. However, in accordance with the JAR-MMEL/MEL.081 aircraft operators have the possibility of a single prolongation of the period of time required to eliminate a malfunction. Such prolongation is possible for the ‘B’, ‘C’ or ‘D’ intervals but is unacceptable for interval ‘A’.

JAR-MMEL/MEL.081 describes the procedures of a single prolongation of the time period required to eliminate a malfunction and states the requirements to the aircraft operators:

“Having received the approval of the Authorities, an operator may prolong the ‘B’, ‘C’ or ‘D’ time intervals, required to eliminate a malfunction, for the same period as the MEL specify in case if:

- The description of the duties and responsibility for the regulation of the prolongation is determined by the operator and approved by the Authorities, and
- Only a single prolongation of the corresponding period of time required to eliminate a malfunction is permitted, and
- The Authorities are notified about any prolongation in good time acceptable to them, not

exceeding one month, and

(d) The elimination of the malfunction is executed as soon as possible.”

In special cases aircraft operators may directly negotiate with the Authorities about the second prolongation of the time period required to eliminate the malfunction. Such authorization for the second prolongation is given only by the Authorities and does not involve “Airbus”.

Economic Aspect of the Use of MMEL

MMEL not only ensures safe flight operations but also assists an aircraft operator in using the existing “Airbus” aircraft fleet to the maximum advantage within the framework of the current activity. MMEL contributes to the increase of an operator’s profit.

The first economic aspect is connected with the aircraft operation. MMEL makes it possible to operate an aircraft with one or more unserviceable equipment component when the malfunction is detected in flight or during ground handling. The possibility to dispatch the aircraft for flight removes the necessity of unscheduled maintenance, delays or cancellation of flights.

The second economic aspect of MMEL is the optimization of the “primary support” and, thus, reduction of the storage expenses. “Primary support” is a catalogue containing the enumeration of all replaceable equipment – LRU (line replaceable unit), the number of spare parts and their cost.

This primary support is determined proceeding from the complex mathematical model which takes into account several factors, including:

- The number of aircraft in the fleet;
- Total number of flight hours per year;
- Average cost of a spare part;
- Number of components per one aircraft.

This catalogue enables aircraft operators to order spare parts several months prior to the delivery of the aircraft itself, in order to prevent situations connected with the demurrage of aircraft.

One of the factors, which is taken into account in the model, is directly connected with MMEL. This factor is known under the name “Importance Degree Code” (EC) and it corresponds to the status assigned to the component in MMEL:

- EC=1: Corresponds to the “Not permissible” component;
- EC=2: Corresponds to the “Permissible if” component;
- EC=3: Corresponds to the “Permissible” component.

Such organization enables aircraft operators to plan the return of the aircraft to the home base. Thus, the aircraft may continue the flight in the standard mode in accordance with the MEL requirements.

Therefore, MMEL is the main factor promoting operational reliability and may give aircraft operators the possibility to substantially reduce operating expenses.

As an example of the use of MEL in aircraft maintenance let us cite the experience of “Airbus” aircraft operation. The engineering and maintenance personnel of the line and periodic aircraft maintenance divisions use the “Aircraft Maintenance and Spare system” (AMASIS), “Routine Maintenance Module” to enter information on the accomplished works including those postponed according to MEL. In addition to that, in the course of preparing the aircraft for departure the flight crew is given the printed form from the AMASIS system (“Technical Follow-up” group) on the malfunctions postponed to be eliminated in accordance with MEL.

COMPARISON OF THE WEAR ACTIVATION ENERGY (E^P) “ШХ15” IN FUEL “TC-1” WITH ANALOGOUS VALUE “TC-1*” OF A LONG-TERM STORAGE

In the result of tribokinetic tests of the fuel “TC-1” we have determined the kinetic characteristics and activation energy wear of the third stage of triboreaction $E^P_{TC-1} = 20,314 \text{ kJ/mol}$ that is more than the analogous value of activation energy wear for “TC-1” of the long-term storage $E^P_{TC-1*} = 19,581 \text{ kJ/mol}$ and less than $E^P_{PT} = 21,278 \text{ kJ/mol}$ for fuel “PT”. Receiptal result E^P point at the best antiwear properties of the fuel “TC-1” and “PT” it can not be determined while using of the tribotechnical tests.*

Setup of the problem. The development of modern aviation engineering is impossible without increasing the reliability, durability, productivity, cost-efficiency of machines, mechanisms and their units. These requirements are especially important in designing and manufacturing of aviation engineering items as well as in their operation. Increased reliability, durability and cost-efficiency of these items depends on the surface durability of their individual units. In its turn, the surface durability (wear-firmness) of structural materials of triboconnections cannot be increased and the antiwear properties of fuel and lubricants cannot be improved without conducting unified tests, involving universal, energy, integral and invariant criteria, at least in one of the value ranges of loads, speeds of sliding and temperatures. The criterion that meets all the above mentioned requirements is surface destruction activation energy, i.e. wear activation energy E^P , which is the third stage of triboreaction [1]. This criterion is an energy criterion in fact, integral and universal in application, invariant in the normal mechanical-chemical wear range, i.e. in the range of structural adaptation of the triboconnection materials, which has been proved experimentally [1]. The kinetic characteristics and E^P for the fuel “PT” were also determined. Later the same characteristics were determined for the fuel “TC-1” that had been stored for a long time [2]. The characteristics obtained showed a degradation of antiwear properties of the fuel after the long-term storage. The following hypotheses were put forward with respect to this degradation: 1) this degradation may result from oxidation or from other processes connected with long-term storage; 2) this deterioration condition of the different antiwear properties of fuels “PT” and “TC-1”, in spite of the interchangeability the permission to mix up these fuels in any correlation.

Aim of the work – to put up the true causes of deterioration antiwear properties of the fuel “TC-1*” of long-term storage by means of realization of tribokinetic tests to determine the kinetic characteristics and E^P of the fuel “TC-1”, usually fresh and compare the obtained results, firstly with the value of E^P then with the earlier value of E^P for the fuel “PT” $E^P_{PT} = 21,278 \text{ kJ/mol}$ and the fuel “TC-1*” of long-term storage $E^P_{TC-1*} = 19,581 \text{ kJ/mol}$.

Calculation – experimental part. For the achievement of the aim of the tribokinetic tests, conducted under conditions analogous to the preceding tests to determine the kinetic characteristics and E^P of fuel “TC-1*” of long-term storage, i.e. tribokinetic tests to determine the kinetic characteristics and E^P of fresh fuel “TC-1” (DSTU 320.001249943.011-99), a production of the Kremenchug oil – processing plant conducted on the friction machine “КНИГА-2” [3]. Both hard-phased elements were produced with ball-bearing steel “ШХ15” (ГОСТ 801-78). Tests conducted by axis load $P = 98,1 \text{ H}$, speed of slide $V_{ck} = 1,18 \text{ m/c}$ without excess pressure in the cell, at two temperatures: $T_1 = 333^\circ\text{K}$ and $T_2 = 303^\circ\text{K}$. Then, with the help of instrumental microscope “ММ-7” at 70-divisible increment the diameter of the spot wear of every ball, was measured in two interperpendicular directions and the arithmetic value of diameters of the spots wear d , the mean value d of three of spots wear – d_c and mean value d_c of three or more tests were calculated. According to the method of carrying of tribokinetic tests, we calculate the value of the wear of every ball, which is the geometric form of the ball segment, diameter the base of which is the diameter spot wear. The sum of the volume wear of third balls (summary volume wear of one test)

and we calculated the arithmetic mean value of summary value wear of three or more tests V_c . Results of these tests we bring into table 1.

Table 1

Kinetic characteristics of the surface destruction – third of the stage triboreaction - wear

Temperature of the tests, $T, ^\circ K$	Time of the tests, $t_i, \times 10^3, s$	Mean values of summary volumes of wear of the 3 th tests, $V_c \times 10^{-3}, mm^3$	Speed of wear for intervals of time, $\Delta t \times 10^{-6}, mm^3/s$	Order of wear N^p for interval of time Δt	Constants of speed of wear, $K^p \times 10^{-3}, s^{-1}$	Mean values $K^p \times 10^{-3}, s^{-1}$	Coefficient of deviation of the estimation of $K^p, W, \%$	Graphical value of K^p
303	1,8	0,87934	-	0,84	-	0,47455	4,6	$tg\ 24,5^\circ = 0,4557$
	2,4	1,18034	0,50167		0,48713			
	3,0	1,58446	0,67353		0,48722			
	3,6	2,07816	0,82283		0,44931			
333	1,8	0,91013	-	1,01	-	0,98132	8,3	$tg\ 43,5^\circ = 0,9490$
	2,4	1,71737	1,3454		1,02565			
	3,0	2,9643	2,07821		0,88781			
	3,6	5,61713	4,42168		1,0305			

The next stage of the tribokinetic experiment is to calculate the speed of reaction wear w:

$$w = \frac{\Delta V_c}{\Delta t_c} = \frac{V_{Cti} - V_{Cti-1}}{t_i - t_{i-1}}$$

where V_{Cti} and V_{Cti-1} – mean value of the summary wear of the three balls at moment of time t_i and t_{i-1} respectively.

The results of these calculations of w for every interval of time Δt are brought into table 1. The order of the reaction wear N^p was calculated for the initial Δt_1 and last Δt_3 interval of time using the next formule:

$$N^p = \frac{\lg \frac{w_1}{w_3}}{\lg \frac{V_{C1}}{V_{C3}}}$$

where w_1 and w_3 – speed of wear for interval of time Δt_1 and Δt_3 respectively;

V_{C1} and V_{C2} – mean of the three balls for intervals of time Δt_1 and Δt_3 respectively.

The results of the calculation of the order of reaction of wear N^p are also brought into table 1.

The constants of speed of wear K^p we calculate with help of the final value of V_c in intervals of time Δt , i.e. using the formule:

$$K^p = \frac{\Delta V_c}{\Delta t \cdot V_{Cap.}} = \frac{w}{V_{Cap.}}$$

where V_{Cap} – mean arithmetic value of V_c at beginning and at the end of the interval Δt .

The results of these calculations we also bring into table 1. We also bring the mean arithmetic values of K^p and coefficient of deviation of the estimation of K^p –W, which is calculated according to method of the calculations of measurement errors of the physical quantity [4].

Thus, knowing the value of K^p at both temperatures $T_1=333^\circ K$ and $T_2=303^\circ K$, according to the equation of Arrenius, the value of the activation energy of the surface destruction, i.e. wear calculated:

$$E_{TC-1}^p = \frac{R \cdot T_1 \cdot T_2}{T_1 - T_2} \cdot \ln \frac{K_1^p}{K_2^p} = \frac{1,9144 \cdot T_1 \cdot T_2}{T_1 - T_2} \cdot \lg \frac{K_1^p}{K_2^p} = \frac{1,9144 \cdot 333 \cdot 303}{30} \cdot \lg \frac{0,9813}{0,4746} = 20,314 \frac{kJ}{mol}$$

where R – universal gas constant.

For control of the correction of the of the determination of the kinetic characteristics of wear w, N^p , K^p along with the results of the tribokinetic tests we build the diagrams of the dependence of $\lg V_c$ from time of the tests (t) (diag.1). The linear dependence of $\lg V_c$ from t confirmed the order of the reaction $N^p \sim 1$ and set the value of K^p graphically, which is equal to the tangent of the angle of inclination of the straight line to the axis OX. This value of K^p is also brought into table 1. The results of the tests are brought into table 1 and on the diagram of the dependence of $\lg V_c$ from t.

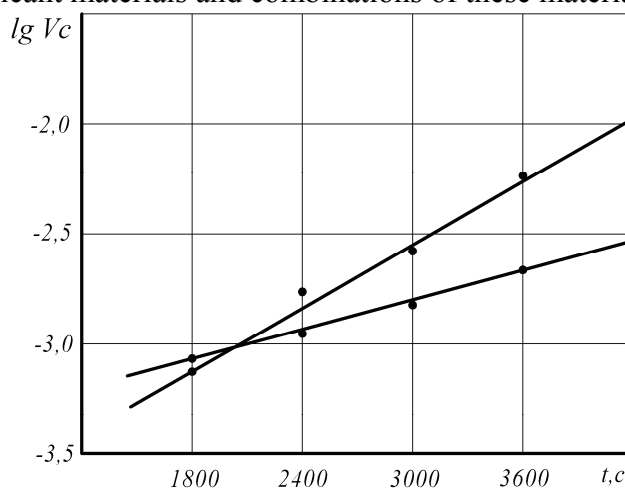
Conclusions

1. Using the obtained values of the kinetic characteristics and $E_{TC-1}^P=20,314$ kJ/mol, place of the causes of the deterioration of antiwear properties of the fuel “TC-1*” of long-term storage was established: it is the consequence of the action of the processes of oxidization and other, which are connected with the length of storage

2. In spite of full interchangeability and permission to mix up the fuels “PT” and “TC-1” in any correlation, antiwear properties, although insignificant, are yet distinguishable – in “PT” a little better ($E_{PT}^P=21,278$ kJ/mol against $E_{TC-1}^P=20,314$ kJ/mol), which was possible owing to the high accuracy of the determination of E^P .

3. Close values of E^P of the tree fuel (“RT”, “TC-1” and “TC-1*” of long-term storage), for which we have determined the kinetic characteristics, confirm the invariance of E^P in diapason of normal mechanical-chemical wear, which correspond to the diapason of the structural-adaptation of the materials of the triboconnections.

4. The established value of $E_{TC-1}^P=20,314$ kJ/mol in the fuel “TC-1” replenished the bank of data of wear-firmness of the steel “ШХ15” and antiwear properties of the fuel “TC-1” and matrixal energy – activation criterion of estimation of construction materials, antiwear properties of combustible – lubricant materials and combinations of these materials



Draw.1. Diagram of the dependence logarithm of mean values of summary volumes of wear of three balls in three tests ($\lg V_c$) from of the tests (t): 1 – at 333°K, 2 – at 303°K.

References

1. Богданович А.И. Кинетические и энергетико-активационные характеристики износостойкости и совместимости материалов трибосопряжений: автореф. дис. канд. техн. наук. – Киев, 1987.-20с.
2. Богданович О.И. Енергія активації протизносних властивостей авіапалива ТС-1 довготривалого зберігання. – Тези доповіді IV Міжнародної науково-технічної конференції НАУ, 23-25 квітня 2002 р. Київ, 2002, с. 43.57–43.59.
3. Аксёнов А.Ф. Трение и изнашивание металлов в углеводородных жидкостях. –М.: Машиностроение, 1977.–147 с.
4. Зайдель А.Н. Ошибки измерений физических величин/ изд. перераб. и доп.–Л.: Наука, 1974.–108 с.
1. Бершадский Л.И., Богданович А.И., Назаренко П.В. Энергетико-активационный матричный критерий совместимости. В кн.: Триботехника – машиностроению: Тез. докладов III Моск.: научно-технической конференции (2-4 сентября 1987г.), М.,1987,с.67-68.

*V.I. Burlakov, PhD, engineering, D.V. Popov, O. I. Yurchenko,
I.A. Slepukhina PhD, ph.math.scien, N.V. Korsunenکو,
National Aviation University, Ukraine*

MANAGEMENT PROCESSES OF TECHNICAL OPERATION OF AVIATION TECHNICS

Approach is examined to forming of the optimum modes of technical maintenance of air ships and development of recommendations on the structural improvement with realization on the basis of the automated systems

The obvious became presently, that to promote efficiency of the use of mathematical methods of research the complex systems with renewal it is possible for the wares of **aviation technics** (AT), if to go it is out of the way increases of amount existent methods and their clarification, and on the way of creation high-quality new approach to the security analysis of the complex systems of AT and its providing in exploitation.

The analysis of the most typical mathematical models of prophylaxis shows that they allow estimating influencing of measures on the management by the state of the system only on separate descriptions and properties of technical devices, at assumptions which not fully reflect the external environments of AT wares.

So, in many cases, descriptions of the faultless systems and elements determine in a function only one periodicity of implementation aircraft maintenance, here plenitude maintenance and control is not taken into account. In other cases of description of faultlessness express depending on plenitude and periodicity only one stage of exploitation, and it means on the very limited part of technical resource of item. In practice in most cases takes place multistage maintenance and every appearance differs by the value of plenitude control and periodicity of leadthrough.

For the complex account of influence on descriptions and objects properties of exploitation, managing influences, development of new methodological approach to the management by the state of wares of AT is required, allowing defining the optimum managers of influence taking into account all operating factors.

The management by a volume, modes and periodicity of implementation works on condition of providing the set level of capacity of AT wares with the purpose of minimization expenses is an optimization task. During optimization of technical service maintenance it is necessary to come from structural and operating properties of AT wares.

The complete volume of maintenance works makes the great number Q , which is broken up on the row of under great number Q_i are maintenance modes (operative, intensive labor, repairs), different in a number of the controlled parameters – Π_i , by character of maintenance works and periodicity of their implementation. Regulations works are executed repeatedly and include:

- continuous control of the state of AT wares in the process of application on the great number of parameters Π_H ;
- leadthrough of works on providing of flight Q_e and control of the technical state on parameters Π_n ;
- periodic control the state of AT on the great numbers of parameters $\Pi_{p1}; \Pi_{p2}; \dots \Pi_{pi}; \dots \Pi_{pk}$ and leadthrough of prophylaxis restorations works after working off the wares of certain works $\Delta t_{p1}; \Delta t_{p2}; \dots \Delta t_{pi}; \dots \Delta t_{pk}$ or duration of exploitation $\Delta \tau_{pi}$ in a volume Q_{pi} . Major repairs of AT are conducted after working off the useful life resource R or (refusals of wares) in a volume Q_{Ri} .

The complex systems of AT in the process of exploitation form the countable set of the states:

$$H = \{H_0 H_1 H_2 \dots H_q\}$$

where H_0 is under great number of the capable of working states,

H_q – down state.

Intermediate the states $H_j (j = 1, q - 1)$ are caused by the refusals of separate elements or their great number, which reduce efficiency work of the system, but does not cause the loss of their capacity.

The complete control for all states H makes the great number $\Pi_N = \{\Pi_1 \Pi_2 \dots \Pi_N\}$, however to carry out global verification not always possibly, and not always expediently, in connection, with what use the system of verifications Π_i on certain parameters $(\Pi_{\Pi}; \Pi_H; \Pi_{Pi})$.

For realization of process control of change properties and descriptions objects of exploitation it is necessary to define the possible managers of influence and to optimize organization of their leadthrough at the set limitations for the receipt of the required values of output vector H^T at minimum operating costs.

It should be noted that in the known models of optimization of plenitude and periodicity of prophylactic measures on the management by the state of complex objects of exploitation development poliparametric method of optimization not is completed until now. At developments of regulations AT maintenance the nomenclature of measures on the management by the state of the complex systems concerns largely expertly and is carried out in the following sequence:

1. Specification of item is learned from the point of its maintenance (setting, external environments, structure of the systems, temporal mode of exploitation, requirements to item, repairable of its elements, maintenance man-hours and other).
2. Item is broken up on component parts and knots are commutable or repaired wholly.
3. The possible refusals and disrepairs are analysed from point of their warnings at technical service.
4. For every knot make a list and types of maintenance works (verification, greasing, regulation, replacement of knot, etc.), necessary instruments, devices, adaptations, options and other, determine
5. Calculations charts choose, exactly and the simplified calculations formulas.
6. Make the working method of data capture.
7. Carry out collection of necessary information for a maintenance calculation on the analogues of wares.
8. Set periodicity of all maintenance works for every element individually.
9. Make the groupment of works on the terms of their leadthrough.
10. Make norms for aircraft maintenance.
11. Develop instructions for maintenance of wares.

Within the framework of the processes control system of technical exploitation of AT on operating enterprises civil aviation collection, account and statistical data processing, rely about discovered on wing and on earth refusals and damaged wares of AT and on the basis of analysis of their reasons, results of exploitation, estimation of actual level of reliability of AT, and also results of diagnostic and control of the technical state of wares, decision of the following basic tasks:

- choice of facilities and optimization of the modes of control and diagnostic of AT taking into account concrete external environments;
- development and realization of organizationally-technical measures on warning of aviation incident and pre-conditions by him through the refusals of AT wares, which arose up as through fault IAC and low quality of AT repair, so it is not enough high qualities of operating properties of wares;
- realization of optimum maintenance philosophy of AT wares.

Task of providing of reliability it is impossible to understand in that understanding that it is needed necessarily to promote reliability of wares. There are certain combinations of descriptions:

properties, maintenance modes and other factors at which reach level set reliability of AT wares, - here charges minimum. In this case providing of requirements on reliability is taken to the task of the optimum distributing of facilities, that is sharply complicated, because it is necessary to know a such global having a special purpose function which would allow to define expedient their distributing between the possible alternatives of increase reliability of objects in exploitation. All of it results in the decision of multicriteria tasks in exploitation.

Multicriteria problems have a characteristic feature, the above all difference of which consists in that no single point of view is, and there is the great number of effective decisions, or decisions optimum on Pareto. On Pareto such alternatives which in transition from one alternative to other the values of one or a few criteria can not become better without worsening of even one criterion will be optimum. Determination of great number on Pareto narrows the initial great number of decisions, that it diminishes vagueness. If some additional information about a task is absent, the subsequent narrowing of great number of Pareto by formal methods is impossible.

If criteria and their values get out taking into account a cooperatively, as a result general interest of group of criteria is put higher than interests of every separate criterion, the choice is optimum on Pareto [2].

Every alternative $\nu^i \in V$ there is the set of parameters

$$\nu_{(i)}^i = V^i(\nu_1^i, \nu_2^i, \dots, \nu_n^i), \quad i = 1, 2, \dots, n \quad (1)$$

that and an alternative can be examined as vector in measurable space of parameters.

The improvement of the system of estimations takes place by the change of parameters V_j^i , and acceptability of these changes is estimated by a criterion. Formal consideration task of choice begins since composition of great number of alternatives is certain. The question of theoretical analysis and complication of such analysis can substantially depend on that, how the successfully entered great number the V objects taken for alternatives.

The multicriteria model of decision-making optimum individual is set as vectorial criterion in a kind, which scalar functions which are certain on V and measure the internals of decision on a certain scale are components. In general case they incompatible. On foundation $K(\nu)$ it is needed to choose the decisions the best in the certain understanding.

A not separate alternative and not pair of alternatives which need to be compared, and all great number of variants, which the "best" variant gets out from, is the argument of algorithm of choice.

Construction of the generalized criterion is based on that the generalized internals of alternatives are estimated by distance between an ideal and examined alternative and than less this distance, the best alternative. How ideal take an alternative which a vector answers

$$\nu(t) = [\nu_1(t_0), \nu_2(t_0), \dots, \nu_m(t_0)] \quad (2)$$

where the maximal values are components for maximized and minimum values for the minimized criteria of optimum, which are achieved on the great number of alternatives V . Distance between two alternatives s and t certainly in ordinary evklyds

$$D_{Sl} = \left[\sum_{j=1}^n (U_j^s - U_j^t)^2 \right]^{\frac{1}{2}} \quad (3)$$

so, that $D_{st} = D_{ts}$ and $D_{ss} = 0$.

In this expression the generalized criterion can be formulated in a kind:

a) most absolute deviation from an ideal alternative for criteria, parts of one dimension:

$$F = W[v_1(t), v_2(t), \dots, v_m(t)] = \max |v_i(t_0) - v_i(t)|, \quad (4)$$

б) most relative deviation from an ideal alternative for criteria, parts of different dimension

$$F = W[v_1(t), v_2(t), \dots, v_m(t)] = \max \left\{ \frac{v_j(t_0) - v_i(t)}{v_i(t_0) - v_i^{\min}(t_0)} + \frac{v_i(t) - v_i(t_0)}{v_i^{\max}(t) - v_i(t_0)} \right\}, \quad (5)$$

For the grant of evenness of influencing of each of criteria on the final value of integral criterion it is necessary to level turn-downs values of criteria by the down-scaling and taking them to the range $[1; 0]$.

Selection of great number of base alternatives, determinate measure for their comparison and setting of the system of advantages between them - are foundation of decision-making the best. The selection of this great number will shorten the subsequent analysis and will decrease the amount of calculations for the processes control of technical exploitation.

References

1. *Дмитрієв С.О., Бурлаков В.І., Салімов Р.М.*, Концептуальні положення збереження льотної придатності повітряних ships of України Сб.науч.тр. «Сучасні авіацій технології» Матеріали IV міжнародної науково-технічної конференції «ABIA-2002», -Т.3. – К.: НАУ,2002.- 157 р.
2. *Ногин В. Д.* Принятие решений в многокритериальной среде: количественный подход.– М.: ФИЗМАТЛИТ, 2002.–144с.
3. *В. І. Бурлаков к.т.н., Д. В. Попов, О. В. Попов*, Прийняття рішень при вирішенні багатокритеріальних задач технічної експлуатації. Сб.наук.пр. «Сучасні авіацій технології» Матеріали VIII міжнародної науково-технічної конференції «ABIA-2007», - Т.2. – К.: НАУ,2002.- С.33.26–33.29.

A CONCEPT OF AN AIRCRAFT ENGINE HEALTH MONITORING PLATFORM

This paper presents a general concept of engine health monitoring platform for commercial aircraft. The paper contains the results of practical situation investigation with the purpose of identifying the problems of the shortcomings of appropriate systems. The state of the research allows defining the list of key positions, which should create the background for the elaboration of mentioned platform.

Introduction

Aircraft engines constitute a complex system, requiring adequate monitoring to ensure flight safety and timely maintenance. Ten years ago Gas Turbine (GT) Diagnostic Systems were ordered in less than 10 % of new units. Today this has changed dramatically; almost all newly ordered gas turbines are equipped with at least a basic Diagnostic System. A main reason is the constantly progressing gas turbine technology. To minimize the risk for vendor and customer, diagnostic benefit starts from the beginning of gas turbine life time with product development and engineering, continues during plant shop test, commissioning, acceptance test and warranty period and closes the loop with maintenance and service .

In the recent years enormous advances were made in the fields of development of computer power, network technology, as well as specific diagnostic tools. This provided the information technology basis (IT) for advanced Monitoring and Diagnostics in an on-line mode, with remotely, centralized performed interrelated data analysis and diagnostics. These were so-called Diagnostic Platforms.

Diagnostic System Platform: Task and Concept

In the early 90's, a number of different hard- and software Systems were necessary to perform the diagnostics tasks. To reduce the complexity of those configurations the development goal was to achieve a common platform for data acquisition and diagnostics. The profit has been taken from the information technology evolution. Through one common platform different analysis and diagnostics tasks can be handled. In addition new diagnostic functions were incorporated in the same manner: one Windows-PC now exceeds the tasks which were then performed by a number of computer devices. So, the Diagnostic System Platform became *one* host for *all* Technologies. The following goals were achieved:

- Depending on the gas turbine-technology requirements, the customer has access to more than twenty different analysis and diagnostic modules
- Market available technologies from different companies in combination with the competence of gas turbine producers should compliment the diagnostic platform.
- Less hardware and software equipment, along with less administration effort provides synergy and cost reduction and prevent computer farms around a gas turbine.
- Combination of different data in one database allows more complex and interrelated data conditioning, analysis and diagnostics.
- There is a common tool used by the technologists for visual evaluation of different kinds of data. This allows easy handling and focus on the technological evaluation and interpretation.

Typical applications of Gas-Turbine On-line Monitoring and Diagnostics System is shown on fig.1.

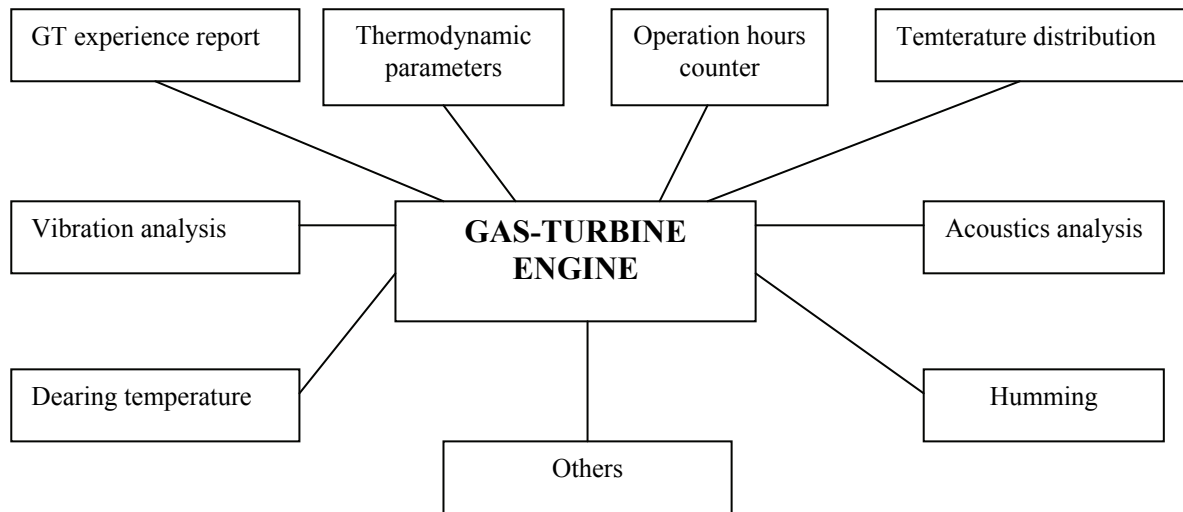


Figure1. Gas turbine monitoring and diagnostics system with typical diagnostics tasks

Typical Diagnostic Platform has modular structure (fig.2). The system contains a basic system frame with the interface to Instrumentation and Control, to networks, to remote access, and the data base and archive infrastructure. The modular Diagnostic System has access to many of the operational installed sensors and obtains between 300 and 1000 signals. Additionally to these signals, a high speed data acquisition for selected signals is included for analog and binary signal analysis. Together with Database, Archive and Remote Access, this is the basic system frame. The valuables in the center of the system are the technology modules which can be selected according to the unit's task specific requirements.

Background information technologies supporting diagnostic platforms

The traditional Engine Health Management (EHM) approach uses fleet statistical data and signal processing techniques to detect and isolate faults. Modern EHM approaches enhance the traditional approach with physics-based models, individual engine performance tracking, predictive algorithms, and decision support capabilities. A modern approach typically measures key operating variables, compares model-estimated values with the measured values, and applies various algorithms and reasoning logic to make health management decisions; therefore, modern EHM capabilities often include model-based diagnostics (or prognostics) and model-based reasoning.

A review of engine monitoring systems for commercial aviation revealed two practical problems facing EHM:

- 1) too many false alarms,
- 2) insufficient sampling and data storage.

On-going research areas in the field of EHM are:

- 1) anomaly detection,
- 2) replacing standard threshold method with feature extraction,
- 3) automated fault diagnosis,
- 4) combination of theory, knowledge, and test information to develop more reliable fault libraries,
- 5) combination of rule-based (e.g., expert system) diagnosis with Artificial Neural Network (ANN or NN) or Fuzzy Logic (FL),
- 6) knowledge discovery.

As EHM has become mainstream, there is a wealth of aircraft engine monitoring data being collected routinely. Extracting useful information from these data, for making better technical and

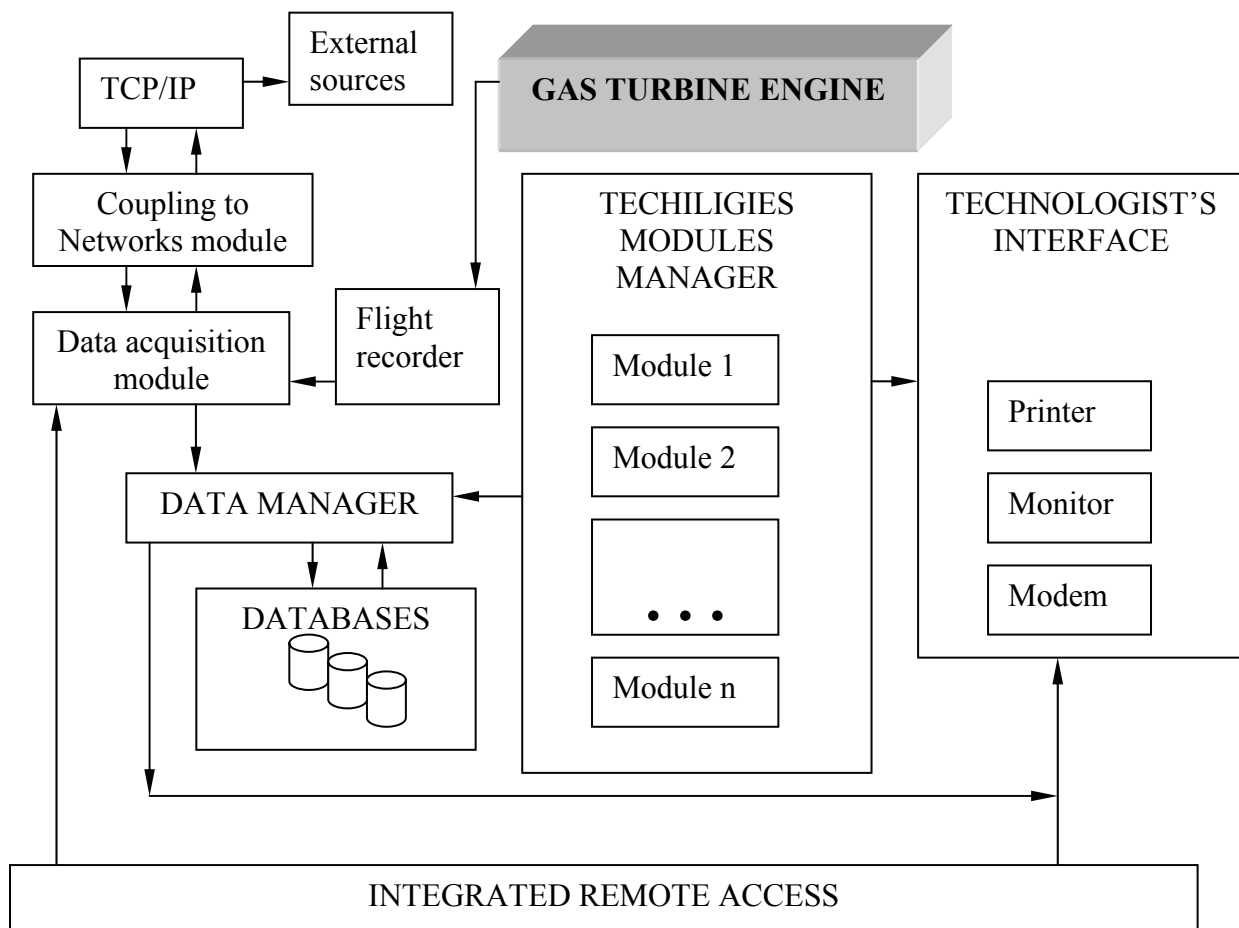


Figure2. Diagnostic Platform for All Technology Modules

strategic decisions, is the next challenge. Knowledge discovery in databases is a data-driven approach that is widely applicable in many fields of research. For example, decision tree learning is one of the most widely used methods for inductive inference, which approximates discrete-valued functions and is capable of learning disjunctive expressions. The output of the algorithm is a decision tree describing the data. The central choice in the algorithm is selecting which attribute to test at each node. One popular algorithm grows the tree top-down, at each node selecting the attribute that best classifies the local training example. Some other potential knowledge discovery techniques propose the use of fuzzy cognitive maps, fuzzy belief nets, and other soft computing techniques for diagnostics and prognostics. The methods make use of whatever data and knowledge is available to achieve reliable diagnosis in cases where failure modes are not thoroughly understood for reliable detection and diagnosis

Fuzzy Logic (FL) approach lends itself for fault detection with incomplete or imprecise information. FL is typically applied to detecting short time-scale degradations.

Genetic Algorithm (GA) has attracted attention as a global search technique that has the potential to “escape” local optima. Seemingly random, GA follows specific rules to reproduce subsequent cases (or strings) to minimize an objective function, and it does not require the calculation of derivatives

Neural network-based diagnosis is another means of complementing rule-based diagnosis. Neural network models can be used instead of traditional models as a means of providing a nonlinear modeling technique. Neural network models can also provide a general tool for classifying test data for comparison to theoretical data from other models. The main advantage of neural networks is their ability to learn the faulty and normal operating signatures from actual test data and help with the reliable classification of faults in engines, without requiring detailed system models. However, a thorough neural-based diagnostic tool requires the collection of extensive training data,

including all possible fault signatures, to develop the model. One possible source of training data is from flight tests.

Hybrid, or cooperating, approach to EHM has the benefit of collecting the strengths of individual approaches; it can also reduce the sensitivity of individual approach for a specific type of data or problem. Examples of hybrid approaches include:

- Genetic Algorithms and classification ,
- Artificial Neural Networks and physics-based model
- Artificial Neural Networks and Genetic Algorithms,
- Genetic Algorithms and gradient search ,
- Artificial Neural Networks and Kalman Filters .

Key principles of developing an aircraft engine health monitoring platform

All considered prerequisites, current approaches to the realization of diagnostic techniques and appropriate information technologies enable to generate the architecture and the list of key principles for hardware and software implementation of an aircraft engine health monitoring platform.

The architecture of an aircraft GT engine health monitoring platform is schematically shown on fig.3.

The key principles for hardware and software implementation of an aircraft engine health monitoring platform are the next.

1. To define the phase (or phases) of an engine life cycle, on which the health monitoring platform will be applied. This will generate the objective of functioning of the health monitoring platform.
2. The objective of functioning of the health monitoring platform enables to select the object (objects) for diagnostics. It may be the whole engine, or its elements.
3. The list of objects for diagnostics makes it possible to define the index of performances.
4. Selected performances define the appropriate diagnostic techniques.
5. Selected performances define also the sources of necessary data, and enable to reveal the information type and structural arrangement of them.
6. The list of information sources gives the opportunity to make the decision about the coupling to Networks.
7. Both diagnostic performances and diagnostic techniques enable to select the appropriate information technologies in order to realize the data acquisition, storing and processing.
8. Selected sources of information demonstrate the quality of data, and reveal the uncertainty administration of them.
9. The objective of diagnostic platform functioning and the diagnostic techniques define the type of diagnostic system essentially: it may be the real time or discrete time system.
10. The information taken from positions 1-9 enables to generate the architecture of the diagnostic platform, and the strategy of its hardware and software embodiment.

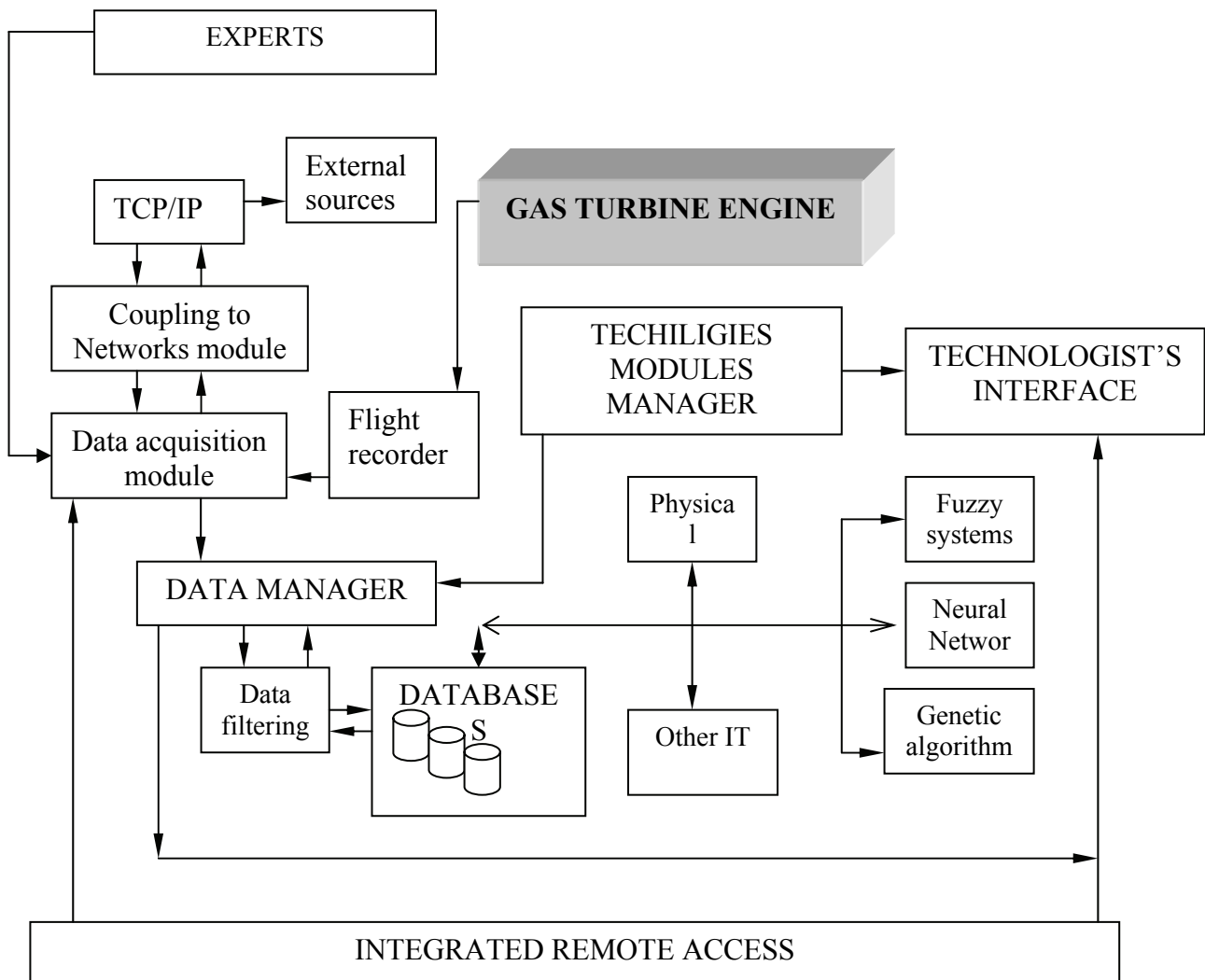


Figure 3. Diagnostic Platform for All Technology Modules

Conclusion

Nowadays the traditional maintenance concept based on periodical inspections after a set number of flight hours or time period of the aircraft usage, is being replaced by a modern, generally accepted, maintenance concept according to the condition. This concept has been applied to a new modular engine design providing fast and simple access to engine parts and significant use of diagnostic equipment for state monitoring. Consequently, the quantity of hardware and software units increase dramatically, and it was difficult to coordinate the efficient functioning of these. This situation revealed the new generation of health monitoring systems – so-called health monitoring platforms. The using of such diagnostic platforms increases the maintenance efficiency, reliability and flight safety.

References

1. Angeli C., Chatzininikolau A. On-Line Fault Detection Techniques for Technical Systems: a Survey./ International Journal of Computer Science&Applications Vol. I,No. 1, pp. 12-30.
2. SAE ARP 1587. Aircraft gas turbine engine monitoring system guide. Aerospace Recommended Practice, April, 1981.
3. Verma R., Ganguli R. Denoising Jet Engine Gas Path Measurements Using Nonlinear Filters.- IFAC Journal: Control Engineering Practice, Vol.5, 1997, pp. 639-652.

*Dokuchayev V. G., Ph. D., Engineer,
Tugarinov A. S., Ph. D., Engineer,
Kazarinov Yu. I., Ph. D., Engineer
(National aviation university, Ukraine)*

INFLUENCE OF THE NEUTRAL ENVIRONMENT ON THERMAL LOADING OF STRUCTURAL MEMBERS OF BRAKE WHEELS AND THEIR DURABILITY

Results of the carried out researches of frictional discs of aircrafts' brake mechanisms, with respect to influence of the neutral environment (of nitrogen) on their wear resistance, are stated in the article. It is shown, that decrease in total wear of brake discs is connected with reduction of their volume temperature and with formation of nitrides in working layers of materials of friction pair under the influence of nitrogen.

Long-term exposure of high temperature on elements of wheels, repeatability of cycles of heating and cooling lead to decrease in fatigue strength of details and aging of rubber materials [1-3]. Thermal exposure promotes accumulation of plastic deformation in materials of discs, that conducts to forming (shape distortion, shrinkage) of those ones and, as a consequence, to change of the brake moment and decrease in a disc resource. All of this affects the operational reliability and durability of a brake wheel as a whole [4-5].

Researches of the brake wheels thermal loading in extreme conditions (landings without activation of engines' thrust reversal, high-lift device extension, braking of wheels at the raised speeds and so on), and also usual practice of airplanes operation, show, that heating of some details and wheel units can exceed admissible norms. It can cause failure of structural components and provoke a precondition to flight incidents.

An overheat of brake wheels appears at performance of excessive number of take-offs and landings, infringement of time modes, and also in the case of wheel forced cooling absence after an interrupted take-off.

More often the overheat of brake wheels occurs on the airplanes serving airlines with short routes and frequent take-offs and landings when total time of flight and parking is found insufficient for dispersion of thermal energy accumulated by a brake, to the value, safe for its separate elements and units.

Development of the means promoting aerodynamic braking at run (flaps, slats, spoilers, brake flaps), application of engines with the increased reverse thrust do not solve the problem.

In connection with increase in landing weights and landing velocities of aircrafts, there is a necessity of further increasing of power intensity of brake wheels by perfection of design, application of various cooling systems, and increase in heat capacity of brakes.

However, the further increase in dimensions of a brake disk pack is practically impossible because of the limited volume of a wheel. The certain limit of power intensity of serially made heat-absorbing materials, such as cast iron CNMH, cermet FMK-11, FMK-845, MKV-50A, is also reached.

Rubber elements of a wheel (tyre cover, chamber, sealing rings of brake cylinders) have certain admissible temperature of heating, excess of which can lead to the loss of efficiency or destruction of both separate elements, and wheels as a whole. The analysis of brake wheel operation and results of flight tests have shown, that the maximum heating of a number of their elements after landing performance in extreme conditions (an interrupted take-off etc.) occurs in 5-7 minutes after braking completion. In these cases after taxiing-in of the airplane on parking place, it is necessary to cool wheels with water, which, getting on brake discs, is evaporated and abruptly reduces their volumetric (average weight) temperature.

Forced air cooling is applied now for reduction of thermal loading and cooling acceleration of a brake and a wheel as a whole by means of a fan, set into rotation by electric motor, located in a wheel axis. The fan, sucking in cold air from the outside, drives it through orifices in wheel cases sidewalls between separate elements of a brake as though "washing" it. Thereby the original screen, protecting a tire from overheats, is created, and at the same time the cooling of discs surface is increased.

One of the solutions to this problem of increasing of durability and efficiency of brake mechanisms is change of operation conditions of frictional materials depending on an environment.

A number of laboratory and bench tests of various frictional materials has revealed the influence of neutral gases on occurrence and development of physical and chemical processes in frictional materials at brake mechanism operation.

As the results of conducted researches have shown, frictional sintered material MKB-50A has lower oxidising persistence (in comparison with other frictional materials, for example, FMK-11), therefore, for localisation of oxidising processes at carrying out of researches, nitrogen was fed in a friction zone of frictional discs which promoted formation of nitrides in working layers of materials of a friction pair that has allowed to raise their wear resistance.

For comparison of brake mechanism operational characteristic in neutral gas (nitrogen) and air medium in real operation conditions, flight researches of specially modified brake wheels KT-140D had been carried out.

The modification consisted in setting of a collector for the gas environment feeding in a chamber of the brake mechanism and obturator on the block of cylinders for partial pressurization of the chamber of the brake mechanism from the environment. The nitrogen feed system has been mounted on the panel and established in the cabin. Gaseous nitrogen went in the brake mechanism of the wheel from a portable cylinder through 2 reducers that reduce the pressure to 1,5 - 2,0 kgs/sm². Feed time of neutral gas in the brake mechanism was regulated by a timer.

Following parametres were registered during the flight researches :

- Landing speed and speed of the beginning of braking of wheels;
- Pressure in the brake mechanism of wheels of the left and right chassis;
- Speed of brake wheels;
- Amount of closures (travels) of shock-absorbers of the main landing gear;
- Temperature conditions of elements of brake mechanisms of wheels;
- Run length of the aircraft after landing and braking distance;
- Feed pressure of nitrogen in a brake cavity of the wheel.

All records of working parametres were carried out with the general synchronisation on time.

Under flight tests the temperature loading of brake wheels elements both at aircraft run modes and at taxiing had been compared. Temperature was measured in a wheel brake (in the tenon of pressure plates and bimetallic discs), in the block of cylinders and in the flange (under a tyre board) of the wheel. After the aircraft taxiing-in on parking the temperature condition gauging of elements of wheels was performed by contact way with application of temperature sensors.

For keeping of the set (established) taxiing speed of the airplane and realization of its turns on a taxiway it is necessary to carry out 2-3 slight brakes, as a result of which wheel elements are heated up. As temperature measurements have shown, at "cold" aircraft taxiing with all working engines after landing to 3000 m, heating of frictional discs had been 90÷95⁰C. During aircraft landing with application of effective wheels braking at run when the temperature of frictional discs reaches high values, it is necessary to take into consideration their additional heating, possible at long-term aircraft taxiing to a parking lot.

Character of the volumetric (average weights) temperatures change of bimetallic discs of two wheels working in different mediums had been determined at the time of individual aircraft landings with various landing weight and beginning speed of braking of wheels (while as a reverse thrust (RTC) is on or off). Graphs (fig. 1 and 2) show that character of increasing and maximum values of volumetric temperature in brake mechanism discs under nitrogen exposure is lower (~ on 60⁰C), than in the brake mechanism working under normal operational conditions (in air

environment). This is explained by better cooling and heat transfer from discs surfaces into environment.

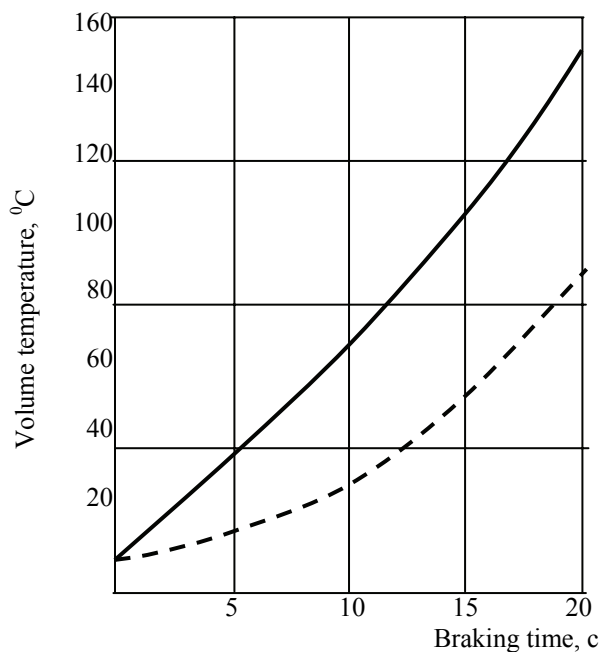


Fig. 1. Character of change of volume temperature of bimetallic wheel disks of KT-140D during plane braking at run ($G_{\text{land.}} = 19,2$ tons, $V_{\text{n.t.}} = 160$ km/h, $P_{\text{Tmid}} = 51$ kgs/sm², landing without RTU inclusion).

----- under brake feeding with neutral (nitrogen) gas;

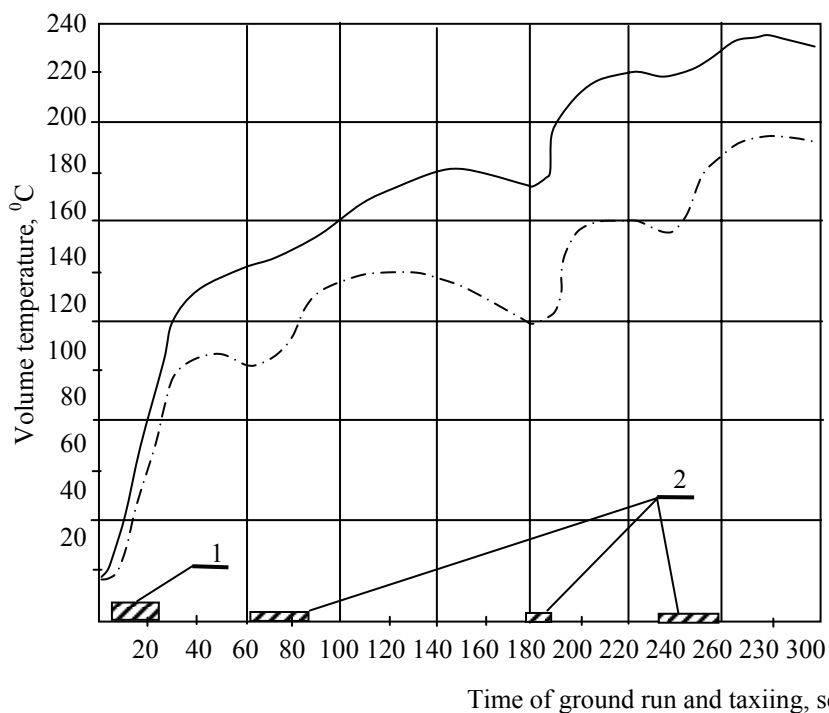


Fig. 2. Character of change of volume temperature of bimetallic wheel disks KT-140D in a transit time and at aircraft taxiing to parking lot $G_{\text{land}} = 13,6$ tons, $V_{\text{n.t.}} = 155$ km/h, $P_{\text{Tmid}} = 45$ kgs/sm²):

----- under brake feeding with neutral (nitrogen) gas;

— . — 1 - a brake way; 2 – braking during taxiing ($V_{\text{tax.}} = 35$ km/h).

Thickness of sectors of bimetallic and metal discs of brake mechanisms of wheels were measured before and after tests for definition of wear of a frictional material. For the purpose of more exact measurement and obtaining of profile wear of sectors (on disc radius) the special device was applied. Four sectors (from each party of the disc) in seven points on its radius were putted to measurement.

The results of measurements of wear for sectors of KT-140D wheels brake discs are illustrated in table 1.

Table 1

KT-140D wheels brake discs sectors wear in air and nitrogen for one take-off and one landing

Environment	Disk type, material			
	Clamping CNMH	Ceramic-metal MKV-50A	Bimetallic CNMH	Supporting CNMH
Air	0,017	0,016 - 0,017	0,014	0,007
Nitrogen	0,008	0,009 - 0,011	0,006	0,006

As it's seen from the table 1, nitrogen application makes essential impact on wear resistance of frictional discs of brake mechanisms. So, at nitrogen giving in a friction zone of the brake discs made of frictional materials MKV-50A and CNMH, their total wear is decreased more, than in 2 times in comparison with the wear of a similar friction pair in air environment, moreover, their frictional characteristics remain practically invariable.

Conclusions:

1. Flight tests of specially modified brake wheels KT-140D have allowed to reveal positive influence of neutral gas (nitrogen) feeding in a friction zone of frictional discs.
2. Under nitrogen feeding the volumetric (average weight) temperature in bimetallic discs is lower (\approx on 60°C), than in the discs working in air medium.
3. Application of nitrogen reduces total wear of frictional materials of discs, more than in 2 times.
4. The reason of increase of wear resistance of frictional discs with feeding in a zone of a friction of nitrogen is formation of nitrides in working layers of a friction pair.

References

1. *Ermilov J.S., Pejko J.N., Germanchuk F.K., Dokuchayev V. G., Malyutin M.V.* Comparison flight tests on research of brake wheels characteristics in the neutral gas (nitrogen) and air medium (in Russian). Collected Papers of State Research Institute of Civil Aviation, №.203, 1981, 163 pp.
2. *Kim S.H., Malyutin M. V., Ermilov J.S., Dokuchayev V. G.* Influence of braking of wheels at taxiing of an airplane on durability of brake discs (in Russian). Collected Papers of State Research Institute of Civil Aviation, №. 214, 1982, 172 pp.
3. *Yermilov Yu.S.* Influence of operational and climatic factors on temperature loading of brake wheels (in Russian). Collected Papers of State Research Institute of Civil Aviation, №. 222, 1983, 168 pp.
4. *Hazanov I.I., Sakach R. V., Pejko Ya.N., Kokonin S.S., Mozalev V.V.* Maintainability of aviation wheels (in Russian). M: Transport, 1974, 224 pp.
5. *Zverev I.I., Kokonin S.S.* Designing of aviation wheels and brake systems (in Russian). M: Mashinostroenie, 1972, 224 pp.

*Kuchaev A.A., Doctor of Science,
(National aviation university, Ukraine)*

ALGORITHM OF BUILDING THREE DIMENSIONAL MAGNETOHYDRODYNAMIC MODEL FOR SUBMERGED NOZZLE-LINER ELECTROMAGNETIC STIRRER SYSTEM OF CONTINUOUS CASTER

Boundary problem for calculation of coupled three-dimensional electromagnetic, hydrodynamic and non-stationary heat transfer processes leaking in a liquid steel flow at an effect on a conductive medium of a travelling magnetic field is formulated. The expressions for a numerical simulation of electromagnetic forces in a submerged nozzle-liner electromagnetic stirrer system on basis of the second-order Fredholm's integral equations are derived.

INTRODUCTION

Reliable and complete computer models of three-dimensional (3D) magnetohydrodynamic (MHD) and heat transfer processes for design and choice of operating mode optimum of continuous casters are required [1, 2].

MHD gates used for confinement of a molten metal in a furnace with the help of the travelling magnetic field in process of long-length rolled products aluminizing have been already found an application for industry [3]. In the paper [4] by physical modelling method was determined that vortex character of electromagnetic forces (EMF) leads to intensive forced convection of the liquid metal in a channel of the MHD gate. It is reflected negatively on operation effectiveness of the MHD gate. In the paper [5] the MHD gate mathematical model is suggested. Here initial 3D electrodynamics problem is reduced by means averaging MHD equations throughout the channel thickness and then is transformed in the 2D problem. The integral and local characteristics of idealised MHD gate are found. Two-pole stator of the travelling magnetic field creates the electromagnetic force. The distribution of total magnetic field amplitude along the stator length, EMF distribution and Joule heat density in the liquid metal have also been discussed. The mathematical model of an electromagnetic pouring submerged nozzle for the steel billet continuous casting is described in the paper [6].

1. PROBLEM DEFINITION

On the liquid metal flowing in the submerged nozzle of continuous caster affects a force of gravity, EMF created by LEMS and a force of flow resistance. Those forces are collinear with moving direction of the liquid metal in the submerged nozzle and influence on molten metal immediately. Like that total force determinative the metal motion it equals to algebraic sum given forces. The force of gravity depends on height of the liquid metal column. The EMF was defined from problem solution of the electromagnetic field in the liquid metal volume filling submerged nozzle. The force of flow resistance is defined on procedure accepted in calculation of a pressure loss in channels of liner induction pumps.

One of the important directions of steel continuous casting advancement is the development of mathematical modelling of 3D MHD processes taking place at control by motion velocity of the liquid steel in the submerged nozzle-liner electromagnetic stirrer (SN-LEMS) system on the basis of coupled fundamental combined equations of electrodynamics, hydrodynamics and heat transfer.

The full mathematical model of MHD processes in the SN-LEMS system includes the following models:

- mathematical model of 3D magnetic field of the LEMS;
- mathematical model of 3D distribution of eddy currents and EMF in the liquid steel induced by LEMS magnetic field;

– mathematical model of 3D distribution of velocities field in the molten steel;
– mathematical model of 3D heat transfer processes in the liquid steel and submerged nozzle lining.
Let us write down the boundary problem of the coupled 3D electromagnetic, hydrodynamic and non-stationary heat transfer processes in the SN-LEMS system for creation of full MHD mathematical model and heat transfer processes leaking at the control by motion velocity of the liquid steel in the submerged nozzle at effect of the travelling magnetic field.

2. ELECTROMAGNETIC FIELD EQUATIONS FOR SUBMERGED NOZZLE-LEMS SYSTEM

The magnetic field equations in a volume V^- of the LEMS ferromagnetic core take the following forms:

$$\nabla \times \mathbf{H}^- = 0, \quad \nabla \cdot \mathbf{B}^- = 0, \quad \mathbf{B} = \mu_0 \mu^- \mathbf{H}^-, \quad (1)$$

where \mathbf{H}^- is magnetic field intensity vector, \mathbf{B}^- is magnetic flux density vector, μ_0 is magnetic permeability of a free space, μ^- is ferromagnetic core magnetic permeability.

The magnetic field in the volume $V^* = V_o + V_m + V^+$ can be described with the help of the following equations:

$$\nabla \times \mathbf{H}^* = \mathbf{J}, \quad \nabla \cdot \mathbf{B}^* = 0, \quad \mathbf{B} = \mu_o \mathbf{H}^*, \quad (2)$$

where V_o is LEMS winding volume, V_m is liquid metal volume, V^+ is space surrounding liquid metal and LEMS, $\mathbf{J}_o, \mathbf{J}_m, \mathbf{J}^+$ are current density in LEMS winding, in the liquid steel and in air.

$$\mathbf{J} = \begin{cases} \mathbf{J}_o - \text{in volume } V_o \\ \mathbf{J}_m - \text{in volume } V_m \\ \mathbf{J}^+ = 0 - \text{in volume } V^+ \end{cases} \quad (3)$$

The second Maxwell's equation and Ohm's law equation in the liquid steel volume V_m needs to be add to given equations:

$$\nabla \times \mathbf{E}_m = -j\omega \mathbf{B}_m, \quad (4)$$

where \mathbf{E}_m is electrical field intensity, $j = \sqrt{-1}$, ω is current angular frequency in LEMS winding.

$$\mathbf{J}_m = \gamma [\mathbf{E}_m + (\mathbf{U}_m \times \mathbf{B}_m)], \quad (5)$$

where γ is electrical conductivity, \mathbf{U}_m is vector of liquid steel velocity that has the appearance in cylindrical system of coordinates:

$$\mathbf{U}_m = u\mathbf{e}_r + v\mathbf{e}_\phi + w\mathbf{e}_z, \quad (6)$$

where v, u, w are the projection of velocity vector on axis x, y, z ; r, ϕ, z are coordinates in cylindrical system; $\mathbf{e}_r, \mathbf{e}_\phi, \mathbf{e}_z$ are unit vectors in cylindrical system of coordinates.

Equations (1)-(5) are solved with boundary conditions:

on the surface S^- of the ferromagnetic core:

$$(\mathbf{n}, \mathbf{B}^+ - \mathbf{B}^-) = 0, \quad [\mathbf{n}, \mathbf{H}^+ + \mathbf{H}^-] = 0, \quad (7)$$

where \mathbf{n} is the normal vector.

On the steel surface S_m :

$$(\mathbf{n}, \mathbf{B}^+ - \mathbf{B}_m) = 0, \quad [\mathbf{n}, \mathbf{H}^+ + \mathbf{H}_m] = 0, \quad (\mathbf{n}, \mathbf{J}_m) = 0. \quad (8)$$

The integral equation method is used for solving of the boundary problem. An initial system of Maxwell's differential equations for the electromagnetic field calculation in the submerged nozzle by using method of potentials are transformed to the second-order Fredholm's integral equations relative to the magnetic charges on the LEMS ferromagnetic core surfaces and the electrical charges on liquid steel surface [7].

Vectors \mathbf{E} and \mathbf{H} are found in the result solving boundary problem (1)-(8) in the steel volume V_m

$$\mathbf{E}^a = \mathbf{e}_r E_r^a + \mathbf{e}_\varphi E_\varphi^a + \mathbf{e}_z E_z^a, \quad (9)$$

$$\mathbf{H}_{ems}^a = \mathbf{e}_r H_{emsr}^a + \mathbf{e}_\varphi H_{ems\varphi}^a + \mathbf{e}_z H_{emsz}^a, \quad (10)$$

$$\mathbf{E}^p = \mathbf{e}_r E_r^p + \mathbf{e}_\varphi E_\varphi^p + \mathbf{e}_z E_z^p, \quad (11)$$

$$\mathbf{H}_{ems}^p = \mathbf{e}_r H_{emsr}^p + \mathbf{e}_\varphi H_{ems\varphi}^p + \mathbf{e}_z H_{emsz}^p, \quad (12)$$

where \mathbf{H}_{ems}^a and \mathbf{H}_{ems}^p are the real and the imaginary components of LEMS magnetic field intensity,

\mathbf{E}^a and \mathbf{E}^p are the real and the imaginary components of the electrical field.

The average value of the EMF volumetric density \mathbf{F} is defined from expressions (13)-(15) according to vectors obtained in expressions (9)–(12) [8]:

$$F_r = \mu_o \gamma \left\{ \left(E_\varphi^a H_{emsz}^a - E_z^a H_{ems\varphi}^a \right) + \left(E_\varphi^p H_{emsz}^p - E_z^p H_{ems\varphi}^p \right) \right\}, \quad (13)$$

$$F_\varphi = \mu_o \gamma \left\{ \left(E_z^a H_{emsr}^a - E_r^a H_{emsz}^a \right) + \left(E_z^p H_{emsr}^p - E_r^p H_{emsz}^p \right) \right\}, \quad (14)$$

$$F_z = \mu_o \gamma \left\{ \left(E_r^a H_{ems\varphi}^a - E_\varphi^a H_{emsr}^a \right) + \left(E_r^p H_{ems\varphi}^p - E_\varphi^p H_{emsr}^p \right) \right\}, \quad (15)$$

where F_φ , F_r , F_z are vector \mathbf{F} components, E_φ^a , E_z^a , E_r^a , $H_{ems\varphi}^a$, H_{emsz}^a , H_{emsr}^a and E_φ^p , E_z^p , E_r^p , $H_{ems\varphi}^p$, H_{emsz}^p , H_{emsr}^p are the real and the imaginary components of the electrical field and the magnetic field intensity accordingly.

3. HYDRODYNAMIC EQUATIONS FOR LIQUID STEEL FLOW

Let us write down equations system describing motion of incompressible viscous liquid that under effect of the travelling magnetic field for definition of the velocity field in conductive medium taking into account obtained EMF distribution.

Equation of motion on coordinate r –

$$u \frac{\partial u}{\partial r} + \frac{v}{r} \frac{\partial u}{\partial \varphi} - \frac{v^2}{r} + w \frac{\partial u}{\partial z} = -\frac{1}{\rho} \frac{\partial P}{\partial r} + \frac{\mu_{eff}}{\rho} \left[\frac{\partial}{\partial r} \left(\frac{1}{r} \frac{\partial ru}{\partial r} \right) + \frac{1}{r^2} \frac{\partial^2 u}{\partial \varphi^2} - \frac{2}{r^2} \frac{\partial v}{\partial \varphi} + \frac{\partial^2 u}{\partial z^2} \right] + \frac{1}{\rho} F_r, \quad (16)$$

equation of motion on coordinate φ –

$$u \frac{\partial v}{\partial r} + \frac{v}{r} \frac{\partial v}{\partial \varphi} + \frac{vu}{r} + w \frac{\partial v}{\partial z} = -\frac{1}{\rho} \frac{1}{r} \frac{\partial P}{\partial \varphi} + \frac{\mu_{eff}}{\rho} \left[\frac{\partial}{\partial r} \left(\frac{1}{r} \frac{\partial rv}{\partial r} \right) + \frac{1}{r^2} \frac{\partial^2 v}{\partial \varphi^2} + \frac{2}{r^2} \frac{\partial u}{\partial \varphi} + \frac{\partial^2 v}{\partial z^2} \right] + \frac{1}{\rho} F_\varphi, \quad (17)$$

equation of motion on coordinate z –

$$u \frac{\partial w}{\partial r} + \frac{v}{r} \frac{\partial w}{\partial \varphi} + w \frac{\partial w}{\partial z} = -\frac{1}{\rho} \frac{\partial P}{\partial z} + \frac{\mu_{eff}}{\rho} \left[\frac{1}{r} \frac{\partial}{\partial r} \left(r \frac{\partial w}{\partial r} \right) + \frac{1}{r^2} \frac{\partial^2 w}{\partial \varphi^2} + \frac{\partial^2 w}{\partial z^2} \right] + \frac{1}{\rho} F_z, \quad (18)$$

continuity equation –

$$\frac{1}{r} \frac{\partial(ru)}{\partial r} + \frac{1}{r} \frac{\partial v}{\partial \varphi} + \frac{\partial w}{\partial z} = 0, \quad (19)$$

where μ_{eff} is effective viscosity, P is pressure, ρ is liquid steel density.

The EMF obtained from expressions (13)-(15) is used in hydrodynamic model. The magnitude and character of the distribution in conductive medium are played determining part in creation of velocity field in the liquid steel. As molten steel flow in the submerged nozzle at effect of the travelling magnetic field is turbulent then effective viscosity μ_{eff} incoming in equations (16)-(18)

represent the sum of two components

$$\mu_{eff} = \mu_l + \mu_t, \quad (20)$$

where μ_l is laminar viscosity, μ_t is turbulent viscosity.

For calculation of the turbulent component is used the popular $(k-\varepsilon)$ model of turbulence [9] including two equations:

balance equation of the turbulent kinetic energy (TKE) –

$$\frac{\partial wk}{\partial z} + \frac{1}{r} \frac{\partial ruk}{\partial r} + \frac{1}{r} \frac{\partial vk}{\partial \varphi} = \frac{1}{\rho} \left[\frac{\partial}{\partial z} \left(\frac{\mu_{eff}}{\sigma_k} \frac{\partial k}{\partial z} \right) + \frac{1}{r} \frac{\partial}{\partial r} \left(r \frac{\mu_{eff}}{\sigma_k} \frac{\partial k}{\partial r} \right) + \frac{1}{r} \frac{\partial}{\partial \varphi} \left(r \frac{\mu_{eff}}{\sigma_k} \frac{\partial k}{\partial \varphi} \right) \right] + \frac{1}{\rho} G - C_D \varepsilon, \quad (21)$$

where

$$\frac{G}{\mu_t} = 2 \left[\left(\frac{\partial w}{\partial z} \right)^2 + \left(\frac{\partial u}{\partial r} \right)^2 + \left(\frac{1}{r} \frac{\partial v}{\partial \varphi} + \frac{u}{r} \right)^2 \right] + \left(\frac{\partial w}{\partial r} + \frac{\partial u}{\partial z} \right)^2 + \left(\frac{\partial v}{\partial z} + \frac{1}{r} \frac{\partial w}{\partial \varphi} \right)^2 + \left(\frac{1}{r} \frac{\partial u}{\partial \varphi} + \frac{\partial v}{\partial r} - \frac{v}{r} \right)^2 \quad (22)$$

balance equation of the dissipation rate TKE –

$$\frac{\partial w\varepsilon}{\partial z} + \frac{1}{r} \frac{\partial ru\varepsilon}{\partial r} + \frac{1}{r} \frac{\partial v\varepsilon}{\partial \varphi} = \frac{1}{\rho} \left[\frac{\partial}{\partial z} \left(\frac{\mu_{eff}}{\sigma_\varepsilon} \frac{\partial \varepsilon}{\partial z} \right) + \frac{1}{r} \frac{\partial}{\partial r} \left(r \frac{\mu_{eff}}{\sigma_\varepsilon} \frac{\partial \varepsilon}{\partial r} \right) + \frac{1}{r} \frac{\partial}{\partial \varphi} \left(r \frac{\mu_{eff}}{\sigma_\varepsilon} \frac{\partial \varepsilon}{\partial \varphi} \right) \right] + C_1 \frac{\varepsilon}{\rho k} G - C_2 \frac{\varepsilon^2}{k}, \quad (23)$$

$$\mu_t = \frac{C_\mu \rho k^2}{\varepsilon}, \quad (24)$$

where C_μ is constant, k is turbulent kinetic energy, ε is turbulent energy dissipation rate.

Those equations are solved with the following boundary condition:

in the liquid metal flow –

$$u = v = 0; \quad w = w(r); \quad \frac{\partial k}{\partial z} = \frac{\partial \varepsilon}{\partial z} = 0, \quad (25)$$

at walls of the submerged nozzle –

$$u = v = w = 0. \quad (26)$$

The hydrodynamic fragment of the full mathematical model in SN-LEMS system is built on integro-differential methods for solving boundary problems (16)-(26).

4. HEAT BALANCE EQUATION

In volume of the liquid steel V_m the temperature distribution θ is described by equation [10]:

$$\frac{\partial \theta}{\partial t} + u \frac{\partial \theta}{\partial r} + v \frac{1}{r} \frac{\partial \theta}{\partial \varphi} + w \frac{\partial \theta}{\partial z} = \frac{1}{c\rho} \left[\frac{1}{r} \frac{\partial}{\partial r} \left(\lambda r \frac{\partial \theta}{\partial r} \right) + \frac{1}{r^2} \frac{\partial}{\partial \varphi} \left(\lambda \frac{\partial \theta}{\partial \varphi} \right) + \frac{\partial}{\partial z} \lambda \frac{\partial \theta}{\partial z} \right], \quad (27)$$

where λ_m is liquid steel thermal conductivity.

The temperature field in walls of the submerged nozzle:

$$\frac{\partial \theta}{\partial t} = \frac{1}{c\rho} \left[\frac{1}{r} \frac{\partial}{\partial r} \left(\lambda r \frac{\partial \theta}{\partial r} \right) + \frac{1}{r^2} \frac{\partial}{\partial \varphi} \left(\lambda \frac{\partial \theta}{\partial \varphi} \right) + \frac{\partial}{\partial z} \lambda \frac{\partial \theta}{\partial z} \right]. \quad (28)$$

At the border of the molten steel and the internal surface of the submerged nozzle S_{mSN} –

$$\theta = \theta_{SN}, \quad -\lambda_m \frac{\partial \theta_m}{\partial n} = -\lambda_{SN} \frac{\partial \theta_{SN}}{\partial n}, \quad (29)$$

where λ_{SN} is the internal surface of submerged nozzle thermal conductivity.

at the border of the external surface of the submerged nozzle and ambient space S_{SN-SE} –

$$\lambda_{SN} \frac{\partial \theta_{SN}}{\partial n} = -\alpha_{HT} (\theta_{SN} - \theta_{SE}), \quad (30)$$

where α_{HT} is heat-transfer coefficient, θ_{SN} is the temperature of the external surface of the submerged nozzle, θ_{SE} is the temperature of the surrounding environment.

For solving (27), (28) equations jointly with boundary conditions (29), (30) the integro-differential method have been used [11].

CONCLUSION

The mathematical model for calculation of EMF, field of velocities and non-stationary of temperature distribution in the liquid steel volume at effect of the travelling magnetic field is presented.

The numerical model of 3D distribution of Lorentz forces in the submerged nozzle on basis of the second-order Fredholm's integral equations is developed. The developed model allows effectively to take into account the powerful diffusion magnetic field, presence of open ferromagnetic cores and complex geometry of the winding of the liner electromagnetic stirrer. It is necessary note the efficient method of solving boundary problem of the electromagnetic field is application of the integral equations. At the same time the initial Maxwell's equations by potential theory methods are transformed to equivalent integral equations relatively of magnetic field source. Therewith magnetic field sources are occupied little space such transformation significantly reduces a calculation area. The number of unknown at numerical solving of problem is reduced significantly and accuracy of the calculation is increased. Like that EMF mathematical modelling in the non-homogeneous conductive medium is simplified.

The hydrodynamic and heat transfer fragments of the full mathematical model for submerged nozzle-liner electromagnetic stirrer system are built on basis of the integro-differential equations.

References

1. *Preissl H., Obermann W., Hubner N., Juza P., Schrack P.* Advances and future aspects in continuous casting automation // *Steel Times*. – 2001, No. 3. – P. 98–100.
2. *Маркс К., Пютц О, Редл З., Хигеман М., Тиман Т., Ввальшайд Л.* Оптимизация процессов производства стали - применение новых способов моделирования нестационарных состояний процесса // *Черные металлы*. – 2001. – № 10. – С. 42–46.
3. *Круминь Ю.К., Биргер Б.Л.* Применение линейных МГД машин для управления потоками расплава алюминия и его сплавов // *Цветные металлы*. – 1989. – № 1. – С. 107–108.
4. *Дементьев С.Б., Сипин К.К.* Исследование циркуляции электропроводной жидкости в мелкой ванне с внезапным расширением под действием бегущего магнитного поля одностороннего индуктора // *Магнитная гидродинамика*. – 1990. – № 2. – С. 136–139.
5. *Валдманис Я., Шишко А., Чо Я.В., Шим Я.Д.* Разработка теоретических основ расчета плоского индукционного МГД затвора. 1 // *Магнитная гидродинамика*. – 1997. – т. 33. – № 1. – С. 81–94.
6. *Pavlicevic M., Codutti A., Kapaj N., Poloni A., Fireteanu V.* Electromagnetic nozzle for continuous casting of steel billets // *Int. Seminar on Heating by Internal Sources, Padua, 12–14 September 2001: Proc.* – Padua, 2001. – P. 395–401.
7. *Кучаев А.А., Петрушенко Е.И., Филиппова Г.А.* Моделирование 3-х мерного распределения синусоидальных вихревых токов и электродинамических усилий в жидкой стали в печь-ковше при индукционном перемешивании // *Методы и средства компьютерного моделирования: Сб. научных трудов*. – К.: Ин-т проблем моделирования в энергетике НАН Украины, 1997. – С. 84–86.
8. *Кучаев А.А.* Алгоритм численного решения трехмерного электромагнитного поля для установки ковш-печь // *Техническая электродинамика*. – 2001. – № 1. – С. 21–25.
9. *Флетчер К.* Вычислительные методы в динамике жидкостей: В 2-х т.: Т.2.: Пер. с англ. - М.: Мир, 1991. - 552 с.
10. *Андерсон Д., Таннехилл Дж., Плетчер Р.* Вычислительная гидромеханика и теплообмен. – М.: Мир, 1990. – т. 2. – 728 с.
11. *Кучаев А.А., Петрушенко Е.И., Филиппова Г.А.* Компьютерная модель трехмерного нестационарного распределения температуры в ковш-печи с электродуговым нагревом и индукционным перемешиванием жидкой стали // *Зб. наукових праць*. – К.: Ін-т проблем моделювання в енергетиці НАН України. – Львів: Світ, 1998. – Вип. № 3. – С. 41–53.

FEATURES OF REALISATION OF A COMPLEX CONTROL-CALCULATED METHOD IN PROCESSES OF DIAGNOSING OF COMPOSITE DYNAMICAL OBJECTS AIRCRAFT TECHNICIANS

Methodological stages of implementation universal complex kontrol-calculated method and feature of its practical realisation in the environment of the automated calculated-information systems for maintenance of an operative profound estimation of a current technical condition of standard difficult objects aircraft technicians are considered.

Introduction. Modern objects aircraft technicians (AT) from aircrafts as a whole to their constructive parts (such as a glider, a power plant, functional systems) concern to difficult dynamical technical objects. After their manufacturing and in regular use to destination there is a necessity of definition current technical conditions (TC) of each separate copy of object of an AT and acceptance on it of the particular operational solution. Thus, to the aviapersonnel which executes operation of a standard AT, it is constantly necessary to search for the answer to two traditional questions: "In what technical condition there is a given object of an AT?" And "what to do further with this object of an AT?". Thus methods and means which are used for obtaining of the answer to the first question are developed within a scientific direction "technical diagnostics", and methods are applied to search of the answer to the second question and means of support of decision-making.

Among a significant amount of existing methods and control devices and diagnosing of objects of an AT which are applied in processes of their maintenance service and lotno-technical maintenance to control of the current TC, the most widespread is the constant parametrical control with data recording from built-in regular systems with the subsequent estimation of presence (or absence) a trend of controllable parametres methods of likelihood statistics. Decision-making is thus provided by use by the aviapersonnel onboard (type MSRP, BASK, BUR, etc.), land (type "Luch", "Analys", "Control", etc.) or land-onboard (EIDS, XMAN, EXPERT, etc.) Monitoring systems and diagnosing (MSD) for standard objects of an AT. Nevertheless, considering that circumstance, that the overwhelming majority of modern difficult air objects of operation (such as aircraft engines and their functional systems) are equipped with insignificant quantity of means of direct measurement of parametres, efficiency existing regular MSD and quality of the analysis of the parametrical information remains on a low level, that leads to untimely detection of faults of constructive knots (elements) of these objects of an AT and impossibility of operative acceptance by the aviapersonnel of corresponding operational solutions. As consequence of it quantity of failures and the preschedule termination of operation of difficult expensive objects of an AT is increased and level of an air safety of aircrafts is reduced.

Therefore and pressing question for air branch the solution **of a scientifically-applied problem** of increase of efficiency of regular monitoring systems of parametres and quality of the analysis of the parametrical information of difficult dynamical objects of an AT for maintenance of operative support of acceptance with the aviapersonnel of operational solutions both in flight, and during the interflight period is especially important at fulfilment of operative maintenance service.

Model of realisation CKC of a method of diagnosing. One of perspective ways of the solution of the indicated problem for processes of current diagnosing of difficult objects of an AT of low level suitable to checking and operative decision-making is working out new complex calculated-information (CI) methods with depth of diagnosing to constructive knot (element) which are realised in the environment of the hybrid dynamical automated systems of diagnosing and decision-making support (ASD DMS). In this connection it is developed conceptual information model of application of the automated estimation of the current TC of difficult object of an AT with use land both

onboard ASD DMS and its methodological model (fig. 1) which is based on application new CI methods of diagnosing of constructive knots (elements) of standard difficult dynamical objects of an AT and information technologies, that realise them in the environment of ASD DMS type "EXPERT-Object AT".

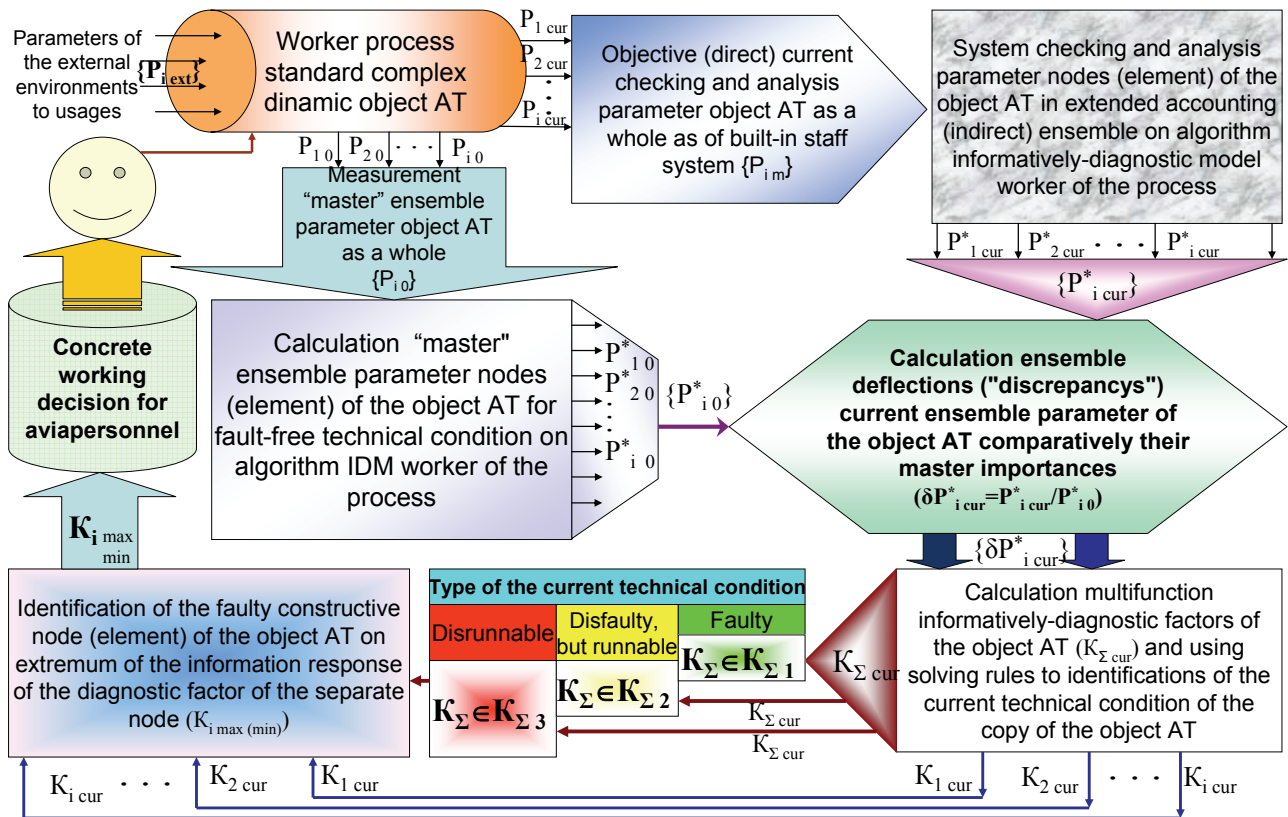


Fig. 1. Methodological model of application of a complex control-calculated method of profound diagnosing of standard difficult objects of an AT

On the basis of the given model of the complex information-analytical approach to processes of diagnosing of standard difficult objects of an AT it is offered to realisation new universal complex control-calculated (CKC) a method of an operative estimation of their current TC which unlike existing likelihood methods parametr-trends diagnosings, provides the consecutive complex determined definition of a kind of the current technical diagnosis of copies of objects of an AT as a whole and at profound levels (to knot/element) with the simultaneous proposal of corresponding technological recommendations to the aviapersonnel from ASD DMS environment knowledge base. It allows to increase (several times) essentially a degree of quality of the analysis of the parametrical information and to reduce duration and labour input of processes of diagnosing of difficult dynamical objects without their constructive adaptations. Realisation CKC of a method is based on the determined system analysis of parametres in the expanded diagnostic space which is provided with application of working algorithms analytical multiparametres informatively-diagnostic models (IDM) their working processes, specialised knowledge bases of aviation specialists, informatively-search methods of identification of the current TC of each copy of diagnosed objects, techniques of forecasting of dynamics of degradation of the TC and automated indicative means of operative informing of the aviapersonnel about results of diagnosing with granting to it of particular technological recommendations for acceptance of operational solutions. Features of realisation of the given method on each of four conditional stages of process of diagnosing of standard difficult object of an AT are (fig. 2): 1 stage – formation of base of current data of a copy typical object of an AT in the form of set $\{P_{i\ m}^*\}$ measured and registered regular MSD current average values of parametres and environment conditions on the established operational mode of the given copy of

object of an AT; reduction of measured parameters to standard atmospheric conditions and a diagnostic mode; set representation $\{P_{i\ m\ br}^*\}$ On an input of

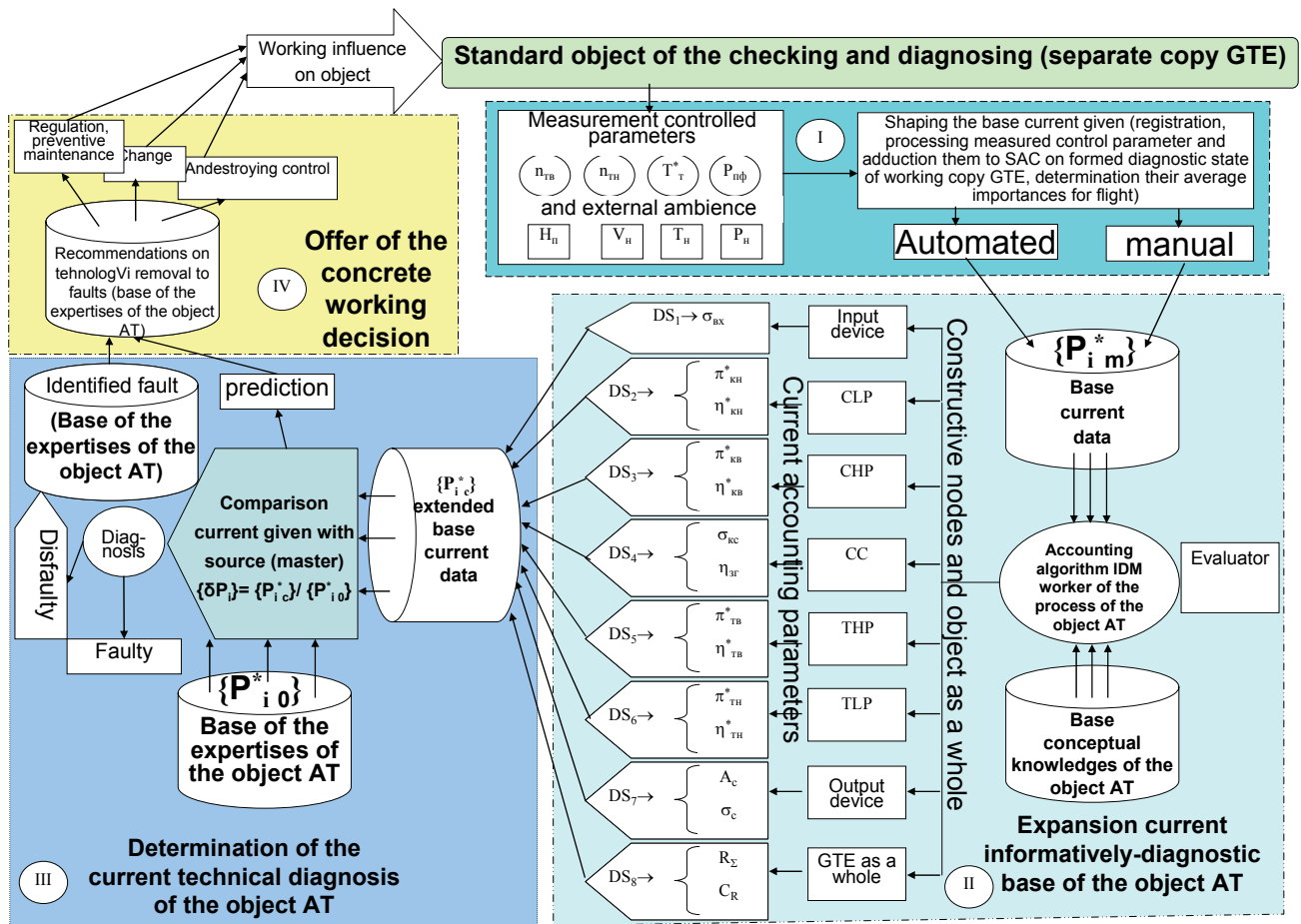
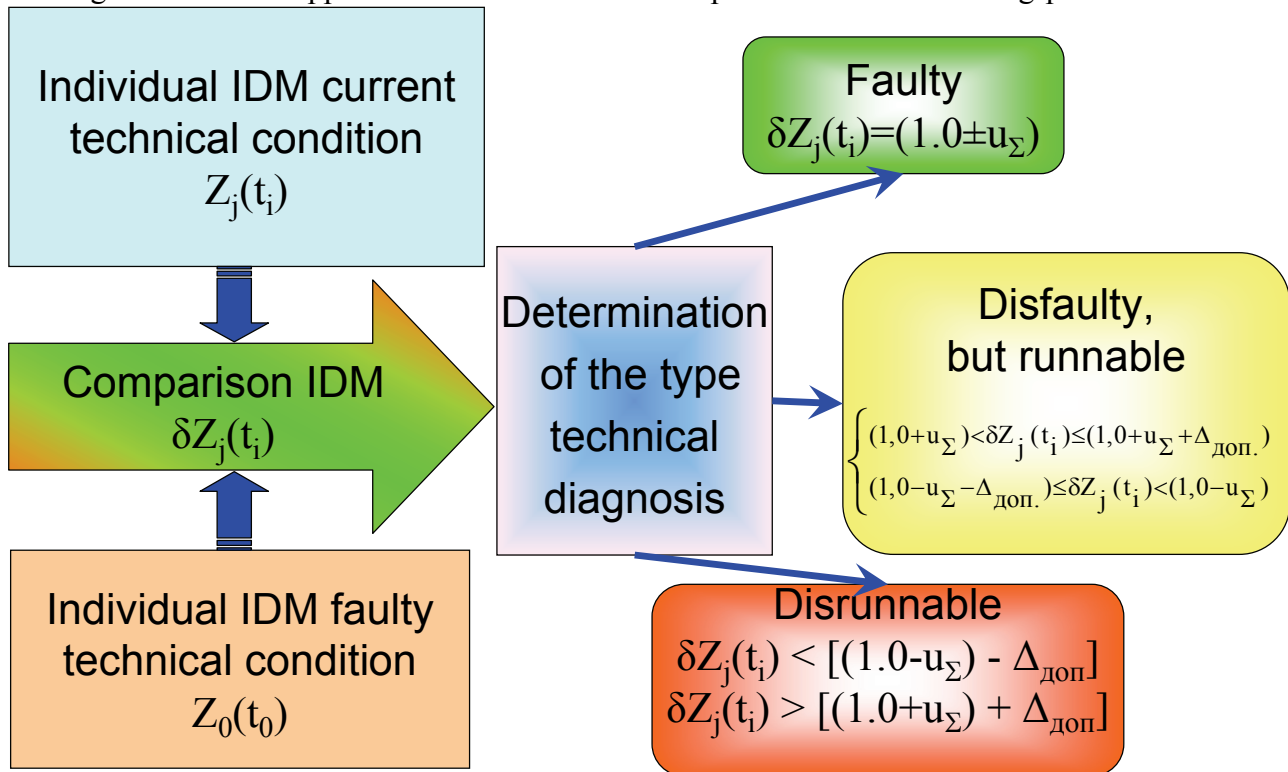


Fig. 2. Model of realisation CKC of a method of diagnosing of difficult dynamic object of an AT (on an aircraft engine example)

knowledge base ASD DMS of type "EXPERT – object AT"; II stage – cardinal expansion of current informatively-diagnostic base copy object of an AT by realisation of special settlement algorithm multyparameters IDM its working process and formation of the expanded current set $\{P_{i\ ac}^*\}$ settlement parameters which characterise the current TC both the given object of an AT as a whole, and its knots (elements); set representation $\{P_{i\ ac}^*\}$ on an input of the unit of comparison of values of parameters in knowledge base ASD DMS; III stage – definition of a kind of the current technical diagnosis of a copy of object of an AT by comparison of current set $\{P_{i\ ac}^*\}$ values of parameters with "reference" set $\{P_{i\ 0}^*\}$ the same parameters of the same copy of object of an AT which are measured and calculated in advance in the beginning of its operation, characterise its serviceable TC and are saved in the archival unit of knowledge base ASD DMS; After definition of set of relative deviations $\{\delta P_i\} = \{P_{i\ ac}^*\} / \{P_{i\ 0}^*\}$, that presence or absence of essential deviations of parameters characterise, and applications of special deciding rules is determined as the general technical diagnosis of the given copy of object of an AT and its estimation at profound levels (to constructive knot/element); representation of results of an estimation of the current diagnosis on an input of the unit of operational solutions of knowledge base ASD DMS; IV stage – definition of the operational solution and technological recommendations to the aviapersonnel by results of an estimation of the current technical diagnosis by granting of a special report of information and a set of technological operations which are in advance developed for each possible version of the technical diagnosis of standard object of an AT and are saved in archive of knowledge base ASD DMS. Thus, essentially higher efficiency CKC of a method in comparison with the existing consists in association of modern information technologies in the form of the generated knowledge base, the special

settlement algorithms, deciding rules and their software which are realised in the environment of ASD DMS type "EXPERT – object AT", with the determined information environment regular MSD a copy of standard object of an AT. Such association of information environments provides efficiency of an estimation of a kind of the current TC, support of acceptance by the aviapersonnel of the solution and the minimum expenditures of labour on technology of diagnosing of difficult objects of an AT at profound levels, and also cardinal increase of levels parametrical informationally objects of an AT and quality of the analysis of their parametres without essential constructive adaptations, and also a practical capability of realisation of their operation on the TC with the control of parametres. One of main differences CKC of a method from existing is application of a method of comparison IDM of working process of object of an AT, which is in serviceable (reference) TC with IDM working process of the same object, which is in the current TC (fig. 3) [1].

Fig. 3. Model of application of a method of comparison IDM of working process of standard



object of an AT

It gives the chance in a complex and more deeply, than now, to supervise and estimate changes of the TC of knots of separate copies of objects of an AT without their constructive adaptations in the conditions of real operation. The analytical structure of model of conditional comparison IDM of the current and reference TC has the following appearance:

$$\delta Z_j(t_i) = Z_j(t_i) / Z_{0j}(t_0) = \delta \phi_j [\delta x_i + \delta y_i + u_\Sigma],$$

where δx_i , δy_i , - accordingly relative deviations of current values of the measured and settlement controllable parametres of object of an AT from their initial values which answer technical requirements, u_Σ - a total error of measurement (calculation) i-s parametres IDM. Proceeding from an essence of the offered model of realisation CKC of a method of the current control and an estimation of the TC of difficult dynamical objects of an AT are offered is functional-analytical (fig. 4) and structurally-information to model ASD DMS of type "EXPERT - object AT" (fig. 5) which explain processes of interaction of the knowledge base and functioning ASD DMS in processes of diagnosing of copies of objects of an AT. Thus applied model ASD DMS of standard object of an AT should satisfy to following analytical models of its technical conditions:

1. Analytical informatively-diagnostic model of working process of object of an AT for the serviceable (reference) TC:

$$Z_0(t_0) = f(\{X_i = Y_{nom}; t_0\}).$$

2. Analytical informatively-diagnostic model of working process of object of an AT for the faulty TC:

$$Z_{Si}^*(t_i) = f(\{X_i \geq Y_{max}; t_i\}) \text{ or } Z_{Si}^*(t_i) = f(\{X_i \leq Y_{min}; t_i\}).$$

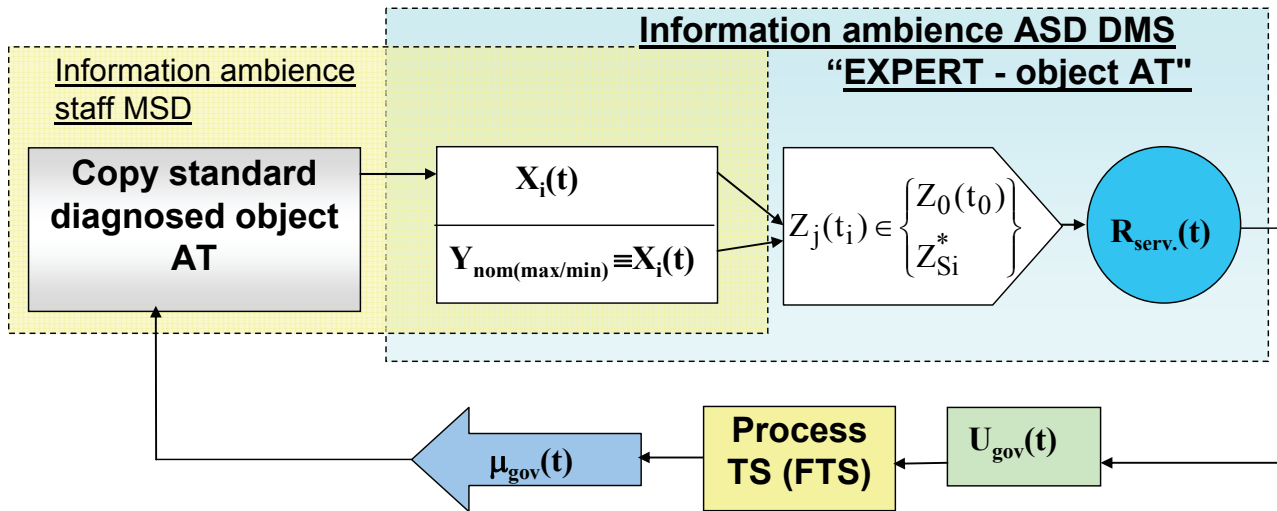


Fig. 4. Functional-analytical model of realisation CKC of a method

Boundary conditions:

- Set of the faulty TC of object of an AT the final:

$$\{S_i\}_{S, \in i = 1, 2, \dots, |S| \dots}$$

- Set of separate operational faults of object of an AT the final:

$$\{O_i\}_{O, \in i = 1, 2, \dots, |O| \dots}$$

- Full compatibility ASD DMS with regular MSD is provided, i.e. conformity of the knowledge base (KB), contained in ASD DMS ($KB|_{ASD DMS} \{Y_{HOM} \text{ takes place}; Y_{max}; Y_{min}\}$), in the environment of base of current data (BCD), generated regular MSD standard object of an AT ($BCD|_{MSD} \{X_i(t_i)\}$):

$$KB|_{ASD DMS} \{Y_{HOM}; Y_{max}; Y_{min}\} \equiv BCD|_{MSD} \{X_i(t_i)\}.$$

- All separate copies of diagnosed objects of an AT belong to a class of objects of diagnosing of continuous action, i.e. values of controllable parameters and diagnostic signs change on time of their operating time continuously:

$$\{X_i = f(t_i)\}.$$

- Solutions-recommendations for the aviapersonnel concerning operation $\{R_{serv.}(t_i)\}$ in operating time ASD DMS depend on value функционала $\{Z_j(t_i)\}$ which estimates a kind of a current technical condition of object of diagnosing (i.e., a kind of its technical diagnosis):

•

$$\{R_{serv.}(t_i)\} = f\{Z_j(t_i)\}.$$

3. Analytical informatively-diagnostic model of working process of object of an AT for the current TC:

$$Z_j(t_i) = f(X_j = Y_i; t_i) \in \{Z_0(t_0) \text{ or } Z_{Si}^*(t_i)\}$$

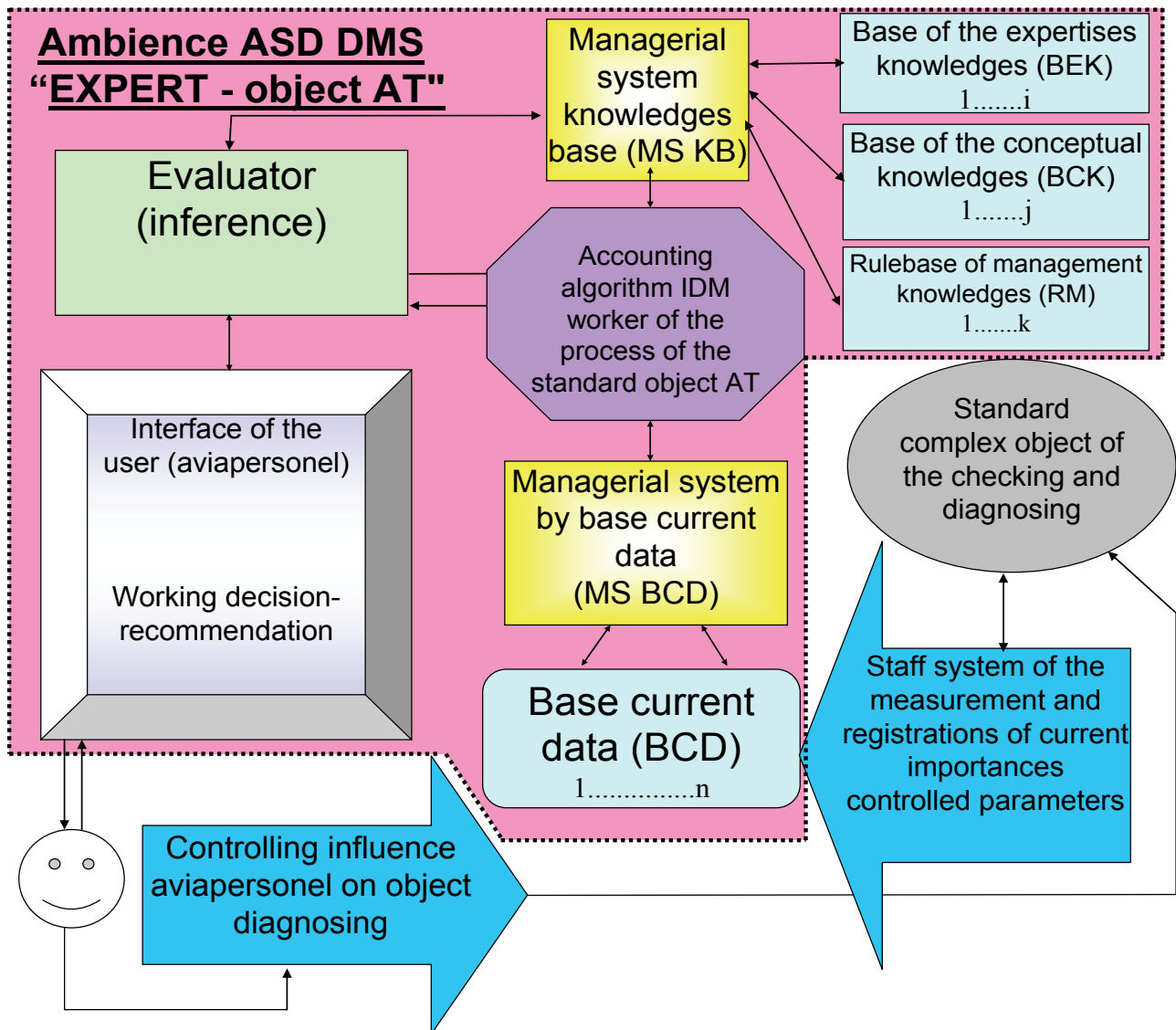


Fig. 5. Structurally-information model ASD DMS of type " EXPERT - object AT"

Conditions of practical use CKC of a method. For operational use of the given method of diagnosing it is necessary to satisfy following conditions:

► necessary:

- definition by the Customer of particular types of objects of an AT which require operative diagnosing and the automated support of decision-making under operating conditions;
- presence of the theoretical and practical bases of construction of the specialised hybrid dynamical automated systems of diagnosing of difficult objects;
- presence of the generated collective of experts-developers (experts, engineers on knowledge and system programmers);
- maintenance of financial support;

► sufficient:

- realisation of applied techniques of synthesis adequate multyparameters informatively-diagnostic models of working processes of standard objects of an AT;
- use of special methods of operative identification of a kind of the current TC of separate copies of objects of diagnosing without their dismounting;

- application of the modern software for modelling of environments of specialised knowledge bases of the automated systems;
- use of the newest tool means of processing and display of different types of information;

Information technologies of realisation CKC of a method in the environment of ASD DMS type "EXPERT - object AT"

For approbation CKC of a method and fulfilment of the indicated sufficient conditions of its realisation on particular difficult object of an AT (a standard aircraft engine) are developed:

1) Applied techniques and settlement algorithms analytical IDM working processes of two-circuit turbine engines [2] in which the full system of the nonlinear equations and criteria of the dynamic similarity is used, describing parametres on an input and an exit of each constructive knot of the flowing part, considering them *совмещенно* activity and control lawes on the established operational modes. It allows essentially (more, than 10 times) to expand informatively-diagnostic base of objects of an AT of low level suitable to checking and gives the chance definitions of change of parametres of knots (elements) depending on versions of possible operational damages. Functionability and adequacy IDM is provided with realisation of a method of linear optimisation of parametres with limitation on specifications, and their acknowledgement implemented by comparison of the received results of analytical modelling with known test experimental data on separate types of the aircraft engines received in EDB their manufacturers, and also with data of the complex experimental researches executed on full-scale gasdynamics a bench of a standard aircraft engine.

2) the algorithm of realisation of a new kind of the informatively-search approach to the operative automated recognition in the form of combined is functional-test (CFT) a method of identification [3] is developed. This method, unlike existing functional or test methods of identification, is based on use of a consecutive combination of special settlement-functional algorithms and deciding test rules for identification of a kind of the current TC as separate copies of difficult objects of an AT which diagnose as a whole, and their constructive knots. The given method is realised in the form of working algorithms and adapted in limits consider above CKC a method of diagnosing of objects of an AT at four conditional stages with application plainly state deciding rules on an example of diagnosing of standard difficult objects of an AT (type of aircraft engines).

3) Is designed and presented generalized algorithm of the decision of the problem of the diagnostics standard complex dynamic object AT before node CKC method in combination with algorithm of the realization CFT method to identifications on example different types engines and automated informatively-diagnostic annunciator [4,5] (fig. 6) with knowledgebase and software variant, which practically realize them in ambience ASD DMS of type "EXPERT - object AT" for support of the taking the working decisions. The Results to test approbation of the offered method demonstrate his capacity to work, validity, efficiency and possibility to realization in real condition of the usages complex object AT in aircraft enterprise. Is it herewith shown that use automated ASD DMS on all stage of the process of the estimation TC power installation before constructive node allows to provide increase a level his operatively in 3,3 times (for power installation Yak -40) and in 2,7 times (for power installation IL-76),but level quality analysis to parametric information in process diagnosing such complex object AT increases in two times. This brings about cardinal qualitative increasing level parametric informatization processes their diagnosing from existing low before high level without significant economic expenseses and allows in significant measure to reduce the factors to duration and labour content of this process.

Conclusions. To advantages considered CKC a method of diagnosing of difficult dynamical objects of an AT with application of environments of the automated systems of support of decision-making it is necessary to attribute:

- universality of application of a method for polytypic objects of an AT;

- efficiency of definition of an estimation of a current technical condition of each separate diagnosed copy of object of an AT without its dismounting from an aircraft under operating

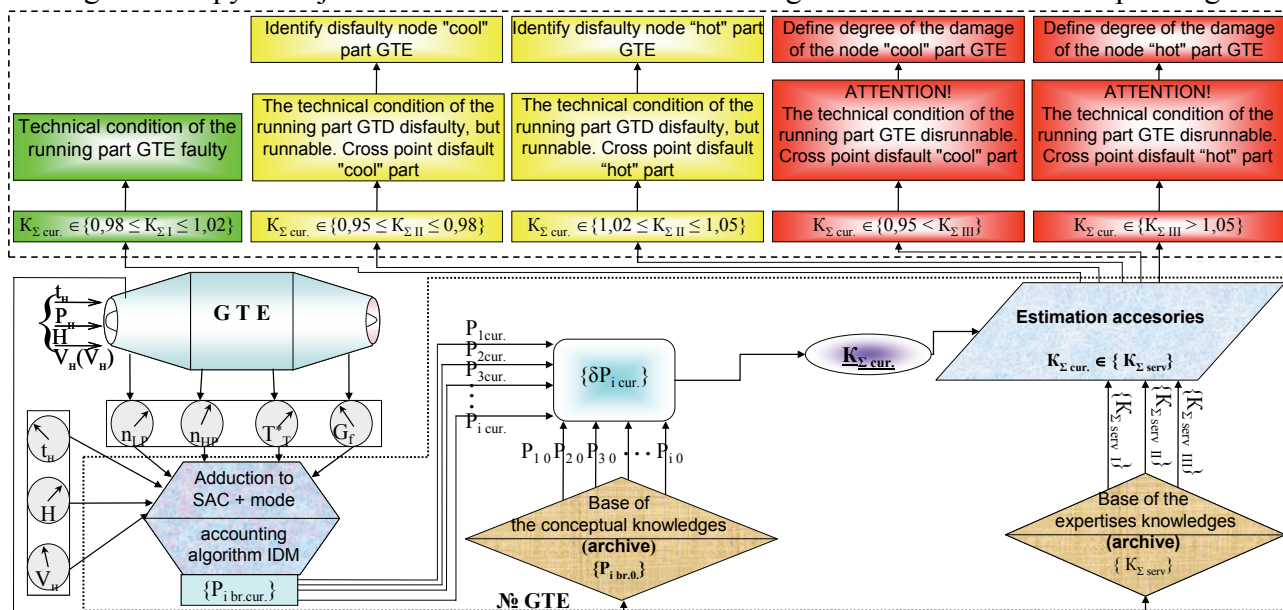


Fig. 6. The Structurally functional scheme of the automated informatively-diagnostic warning indicator for the operative control and an estimation of a technical condition of a flowing part of a turbine engine

conditions with definition of particular technological recommendations to the aviapersonnel for support of acceptance of the operational solution;

- the minimum expenditures of labour on technology of diagnosing of difficult object of an AT in whole and separate constructive knots; - maintenance of diagnosing of standard objects of an AT at profound levels (to constructive knot/element);

- cardinal increase of levels parametrical інформативності, контролепридатності and maintainability without essential constructive adaptations of modern objects of an AT;

- substantial increase of levels of automation and a supply with information of processes of diagnosing of difficult dynamical objects of an AT; - practical provision of realisation of strategy of operation of objects of an AT on a technical condition with the control of parametres.

References

1. Чоха Ю.М., Лихоманенко В.А., Федорчук О.П. Реалізація комплексного контрольно-розрахункового методу діагностування в середовищі експертної системи типового ГТД // Труды Национальной академии обороны Украины. –2005. –Вип. № 58. – С.297-302.

2. Чоха Ю.М. Математична діагностична модель робочого процесу ТРДД з низьким рівнем контролепридатності. // Вестник двигателестроения. –Запоріжжя: ОАО"Мотор Січ"2003. -№ 1. – С.100-103.

3. Чоха Ю.Н. Методика применения функционально-тестового метода идентификации неисправностей ТРДД в среде динамической ЭСД // Вестник двигателестроения. –Запоріжжя: ОАО "Мотор Січ", 2004. – № 2. – С.173-176.

4. Пат. 30615 Україна, МПК G07C 3/14. Сигналізатор автоматизований інформативно – діагностичний для оперативної оцінки технічного діагнозу складних динамічних об'єктів технічної експлуатації / Ю.М. Чоха та ін. - НАУ. - №2007 06233; Заявл. 05.06.2007; Опубл. 11.03.2008, Бюл. №5.

5. Заявка №2007 06234 Україна. Спосіб комбінований функціонально-тестовий оперативної оцінки технічного діагнозу газотурбінного двигуна і його конструктивних вузлів проточної частини / Чоха Ю.М. та ін. – Заявл. 05.06. 2007, позит. ріш. № 7443/1 від 04.06.2008.

ALGORITHM OF DIAGNOSING JET ENGINE AT IN COMBINED DAMAGED UNITS OF A FLOWING PART

One of approaches of the decision of a problem of diagnosing of the aviation turbojet dual-duct engine is considered at combined damage structural units of a flowing part with use methods of recognition of images and neural networks classifications

The diagnostic models of various levels developed at present are applied as to debugging and tests of algorithms of diagnosing as simulators of initial data, and is direct as a part of these algorithms. The given diagnostic models represent functional dependences of parameters of a flowing part FP (pressure, temperatures and consumption of a working body and fuel, rev of rotors etc.) from entrance and mode parameters (temperature and pressure upon an input in the engine, humidity, etc.), and also parameters of characteristics of units. The last allow to correct dependences between characteristics of units, simulating thereby various defects of these units. Algorithms of localization of the defects, based on identification of such models, represent a separate direction in parametrical diagnostics gas turbine engines (GTE) [1].

Now the in-depth studies directed on working out of algorithms of diagnosing which are based on the theory of recognition of images [2, 3] which theoretically allow to spend an estimation of a technical condition (TC) of the engine without attraction of models of high level are spent. According to this approach at first in space of measured parameters or diagnostic signs classes of conditions of object of diagnosing are formed, and then to use of the received classification there is an acceptance of the diagnostic decision on conformity of a current condition of the engine to one of the generated classes at training of system [1-3]. Thus, types and the general number of classes should be chosen and fixed at a grade level – prior to the beginning of direct diagnosing GTE. It is necessary to notice, that at such approach it is necessary to limit the general number of classes, differently reliability of recognition of each class (condition) decreases [1].

The estimations of technical condition GTE developed before system are based on a hypothesis about possible occurrence of malfunction only in any one structural units. However the analysis of operating experience of some engines shows, that acceptance of the given hypothesis is not absolutely correct. The analysis of statistical data about refusals and damages of units and elements dual-duct engine (DDE) promotes an establishment of more accurate interrelations between functional parameters of a working body and characteristics GTE taking into account influence of such damages as: erosion, corrosion or pollution of disks vanes, guide vanes, nozzle vanes (NV), nozzle diaphragm (ND) and turbine bucket, burnout structural elements of the combustion chamber (CC), change of radial backlashes in the compressor, change of area NV of the high (HPT) and low pressure turbine (LPT), adjournment of products of combustion on vanes, breakages vanes, etc. [4].

The physical nature of occurrence of the damages leading to occurrence of refusals is different for various units of the engine. The compressor, as a rule, is subject to the damages, caused by hit of an extraneous subject and abrasive deterioration while damages CC and turbines carry thermofatigue and wear character. At abrasive deterioration of structural units of flowing part (FP) the stock gas dynamic stability decreases; carbonization fuel nozzles leads to such phenomenon as "jet burning" to a flame and, as consequence, to heterogeneity of a field of temperatures before ND with the subsequent melting, burnout vanes of ND and wheels vanes. Carbonization atomizers and change of the area of apertures combustion pipes CC for pass of a secondary stream, leads to incompleteness of combustion of fuel, adjournment of products of combustion on vanes ND, wheels etc. On figure 1 results of the spent analysis directed on revealing of in combined damaged (CD) constructive units of a flowing part of by-pass engine (BPE) D-36 are presented (fig. 1).

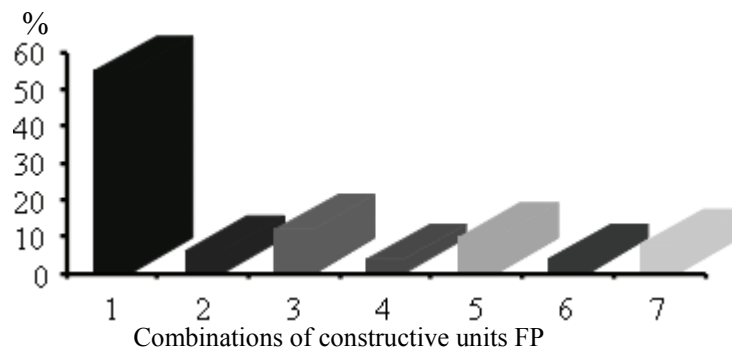


Figure 1 – Distribution CD units GTE Д-36:

- 1 – Compressor,
- 2 – CC,
- 3 – Turbine,
- 4 – Compressor – CC,
- 6 – CC – Turbine,
- 7 – Compressor – CC – Turbine.

Now for localization (recognition) of malfunctions GTE various analytical, mathematical, numerical methods are used: recognition by angular position of a vector of measurements, a method of dividing planes, a method of diagnostic matrixes, a method of statistical classification. However complex use of a mathematical apparatus of the theory of recognition of images for an estimation of technical condition GTE is worked more not enough [5,6]. In practice, especially in systems of operative technical diagnostics, to similar methods and algorithms special demands are made, major of which is the simplicity of realization connected, including, with speed of performance of operations.

Recently, for construction of qualifiers of a technical condition of objects at the decision of diagnostic problems more and more a wide circulation receive self-trained structure on the basis of artificial neural networks. Heightened interest to neural networks to the structures, observed at the decision of problems of forecasting, classification and management, is caused by possibilities of neural networks such operations of processing, comparison and classification of images which are inaccessible to the traditional mathematics, self-organizing and self-training possibilities. Neural networks are a powerful method of imitation of processes and the phenomena, including nonlinear, for reproduction and research of extremely difficult dependences in space of signs and space of conditions (classes) GTE [5,6]. For approbation of process of recognition of classes of conditions GTE with use of classical methods of recognition of images and networks classifications, have been carried out complex research with attraction of data, both bench tests, and modeling experiment [3]. On the basis of the spent researches, the scheme of algorithm of training of system and algorithm of an estimation technical condition GTE on the basis of a logic conclusion of results of diagnosing (fig. 2) have been developed. Distinctive line of the given algorithm, complex use of methods of recognition of images is: the discriminate analysis, a method of minimization of risk, and also networks classifications taking into account compatibility of damage of constructive units of flowing part GTE. By working out of algorithm of the control of technical condition GTE the assumption under operating conditions is accepted, that till the moment of identification of malfunctions or damages of constructive units of a flowing part of the engine the portrait of malfunctions is known. It means, that the system has passed preliminary training and possible conditions of the faulty engine are classified. At formation of initial matrixes it is necessary to approach individually to each type GTE as the quantity of possible conditions depends on design features of object of diagnosing.

Result of an estimation of the TC of object of diagnosing is recognition of malfunction of constructive units FP of the engine, based on three best methods of recognition of images: clusters, discriminate analyses and minimization of risk and neural networks method, by association of their

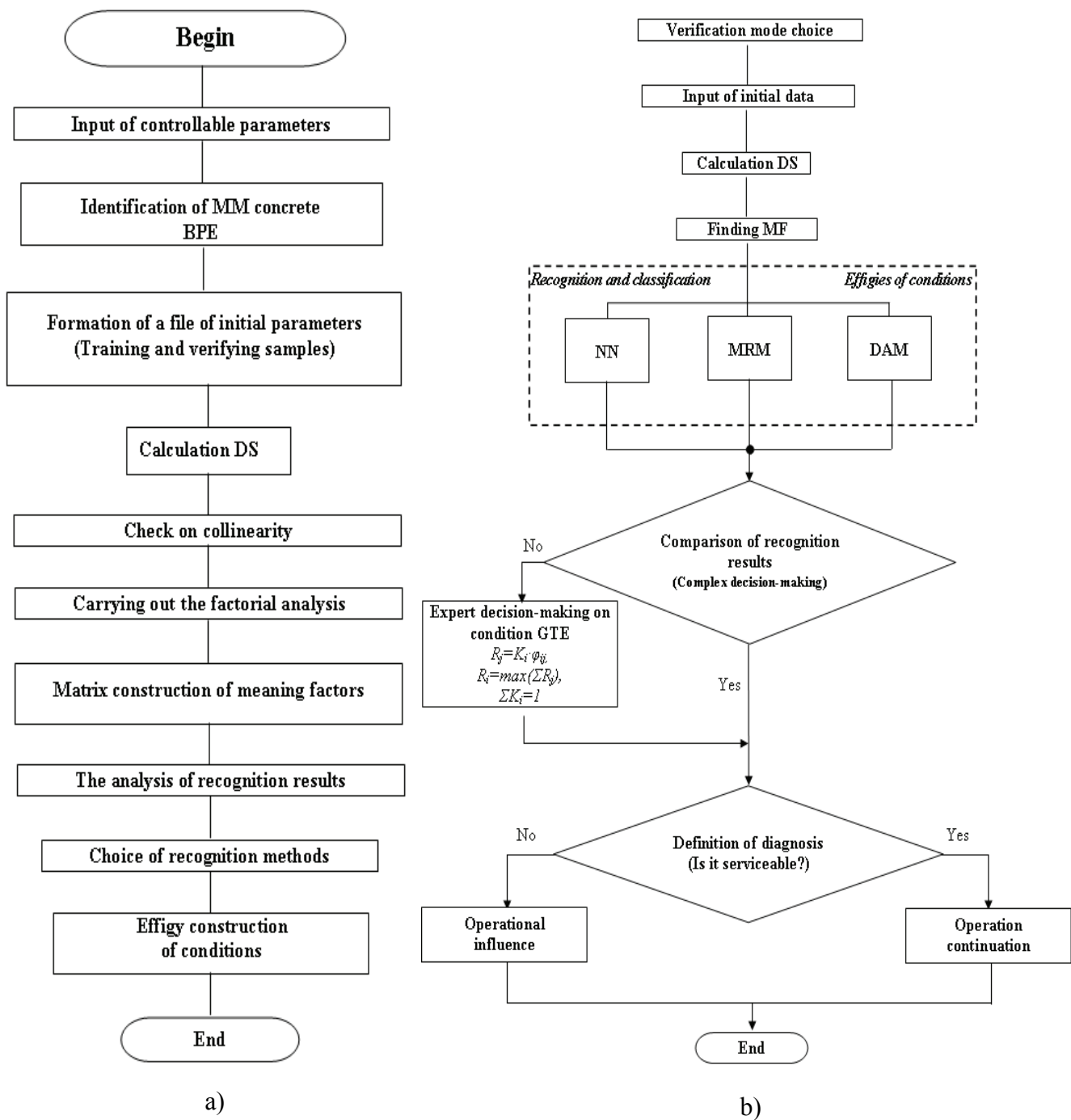


Figure 2 – Procedure of diagnosing BPE at damage of constructive units of a flowing part:
a) - the scheme of algorithm of training of system,
b) - algorithm of an estimation technical condition GTE.

estimations on the basis of procedures of a logic conclusion. Procedure of a logic conclusion is under construction on a condition that the accessory to a certain class GTE proves to be true at its acknowledgement for not less than two different methods. Separately this procedure is carried out on base only methods of recognition of images and separately for all selected methods taking into account a significance value of each method (fig. 3).

As a result of the spent researches, the problem of diagnosing of a flowing part of the aviation dual-shaft engine with depth of localization of malfunction to constructive unit with a logic conclusion on the basis of complex use of such methods of recognition of images as has been solved: minimization of risk, the discriminate analysis and neural networks.

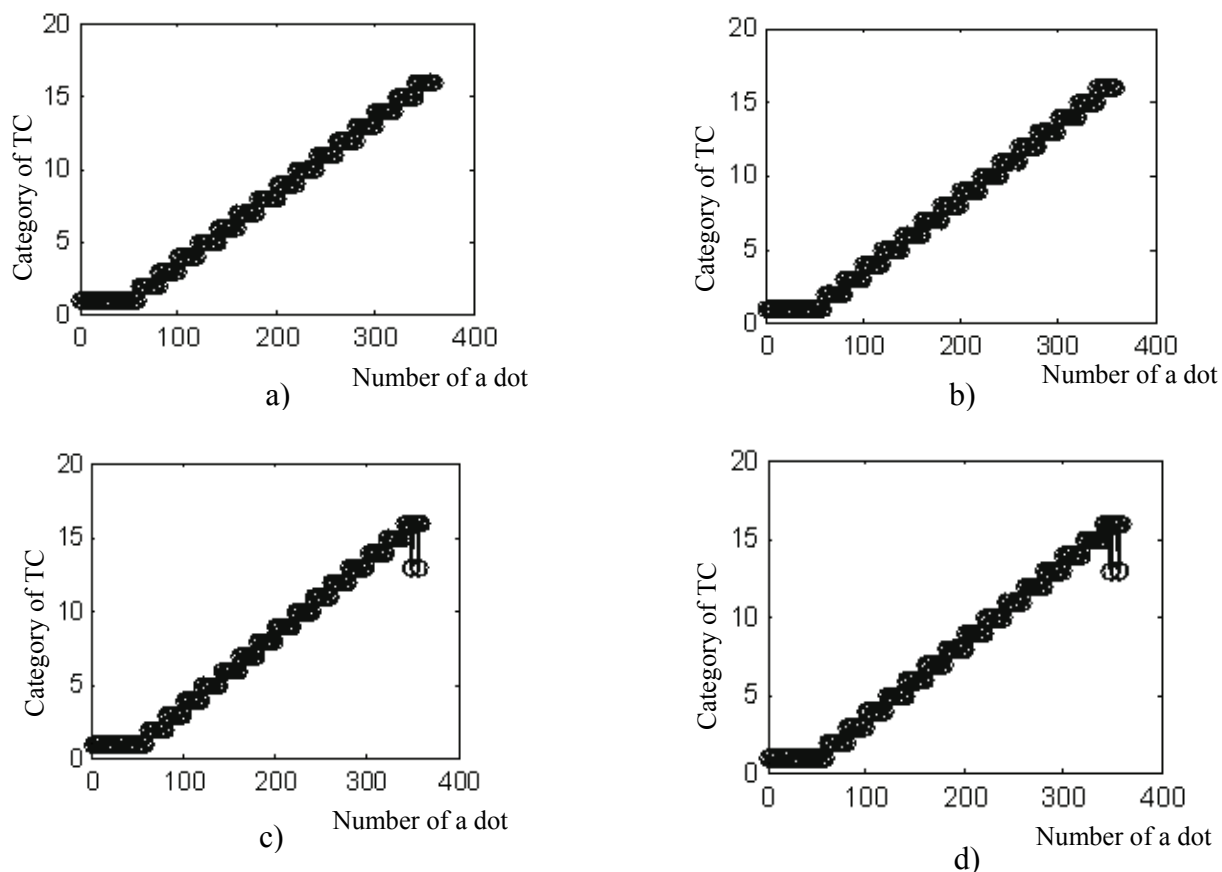


Figure 3 – Results of a complex estimation on the basis of a logic conclusion:
a)– training sample for 2 methods of recognition of images (MRI),
b)– training sample for 3 methods together with NN (MRI+NN),
c)– verifying sample for 2 methods of recognition of images (MRI),
d)– verifying sample for 3 methods together with (MRI+NN).

References

1. Епифанов С.В., Лобода И.И. Идентификация статической и динамической моделей проточной части как средство диагностирования ГТД // Вестник двигателестроения. – 2004. №2. – С. 206-212.
2. Епифанов С.В., Кузнецов Б.И., Богаенко И.М., Грабовский Г.Г. / Синтез систем управления и диагностирования газотурбинных двигателей. – К.: Техника. – 1998. – 312 с.
3. Кучер А.Г, Дмитриев С.А., Попов А.В. Определение технического состояния ТРДД по данным экспериментальных исследований с использованием нейронных сетей и методов распознавания образов // Авиационно – космическая техника и технология. – Х.: – 2007. – № 10/46. – С. 153-164.
4. Попов А.В. Исследование динамических характеристик ТРДД с перемежающимися неисправностями проточной части на установившихся режимах его работы // Авіаційно-космічна техніка і технологія. – Х.: – 2007. – №2/38. – С. 63-67.
5. Концевич А.Г Распознавание неисправностей ГТД искусственной нейронной сетью // Авиационно – космическая техника и технология. – Х.: – 2003. – № 7/42. – С. 113-117.
6. Бурау Н.И. Классификация состояния объекта виброакустической диагностики с использованием нейротехнических структур // Авиационно – космическая техника и технология. – Х.: – 2002. – № 31. – С. 181-185.

V. Ushakov^A Hab.Dr.Sc.Eng., V. Gopeyenko^B Dr.Sc.Eng,
G.Filipsons^A Mag.Sc.Eng., N.Sidenko^A Mag.Sc.Eng.

^{A)} Riga Technical University, Aviation Institute, Latvia

^{B)} Information Systems Management Institute,

Department of Natural Sciences and Computer Technologies, Latvia

NUMERICAL ANALYSIS OF PERIODIC PULSATION INTERACTIONS OF EXTERNAL FLOW ON CYLINDER'S AERODYNAMICS AND HEAT-EXCHANGE.

Annotation: The computer analysis results of the aerodynamic characteristics of the cylinder in the non-stationary gaze flow with periodic low-frequency pulsation with respect to the average velocity at subcritical Reynolds numbers are presented. It is shown that periodic pulsations of the flow velocity significantly effects on the frequency of the vortex separations and the form of the Karman trail behind the cylinder, on the pulsation frequency of the aerodynamic coefficients, heat-exchange coefficient, their average and amplitude values.

INTRODUCTION

In the last years the significant attention is given to the questions of the pulsing flow influence on the bodies' aerodynamics and heat-exchange [1]. It was found that the flow pulsations and the mechanical vibrations of the construction may improve or worsen the aerodynamic properties and the intensity of the bodies' heat-exchange. The financial expenses for the execution of the physical research with pulsing flow and the heat-exchange in the wind tunnel are sufficiently large. Therefore, to solve the problems of the applied aero-hydro- dynamics and heat-exchange the computer modeling technologies or CFD-technologies (CFD – Computational Fluid Dynamic) is found to be more and more implemented. By now the series of universal computer software of different level are developed (FLUENT, STAR-CD, VP2/3, FLOW3D, ANSYS-CFX, CFDesign, CosmosFloWorks etc.), that are based on the numerical solution of the non-stationary Navier-Stocks equation systems, that include the heat-exchange and turbulent transfer processes.

In this work the influence effect of the velocity low-frequency periodic pulsations of the external air flow on the aerodynamic and heat-exchange characteristics of the cylinder at subcritical flow conditions (at Reynolds numbers $300 < Re < 50000$) is numerically researched using SolidWorks/CosmosFloWorks applications. Long-wave velocity pulsations, amplitude of which is lower than the velocity of sound (i.e. acoustic pulsations), but typical body size (diameter of the cylinder D) is smaller than half of the pulsations wave length $D < L/2$ ($L = V_0 T = V_0/f$, L – wave length, V_0 – average velocity of the external flow, T – pulsations period, f – pulsation frequency) are considered. Pulsations velocities are of the sinusoidal and rectangular type ($V(t)$ – flow velocity, t – time):

$$V(t) = V_0(1+A \sin(2\pi ft)) \text{ m/s,}$$

$$V(t) = V_0(0.1+A \cdot \text{sign}(\sin(2\pi ft))) \text{ m/s, } \text{sign}(\varphi) = \begin{cases} 1; \varphi > 0 \\ 0; \varphi = 0 \\ -1; \varphi < 0 \end{cases}$$

The periodicity of the vortex separation that form vortex trail behind the cylinder is defined by the dimensionless frequency (Strouhal number) that expresses the correlation between the vortex separation frequency f_0 , typical body size and typical flow velocity V_0 :

$$Sh = f_0 D / V_0$$

Here f_0 is the frequency of the vortex separation from one side of the cylinder (or the separation frequency of the vortex pair of the cylinder). Another interpretation of the Strouhal number is also possible: it is the relation of the typical body size (diameter of the cylinder) to the flow pulsations wave length. Yet, another alternative of the physical meaning of the Strouhal number for the Karman trail in the stationary flow was proposed in the work [2]: it is the relation of the transverse distance between the chains of the separation vortexes to the longitudinal distance between the vortexes. All three definitions of the Strouhal number are required for the analysis of the pulsation flow influence on the cylinder aerodynamics and heat-exchange.

At subcritical cylinder flow conditions by the stationary flow the dimensionless vortex separation frequency practically does not depend on the Reynolds number $Re = V_0 D / \nu$ (ν is kinematic viscosity coefficient) and is equal to the $Sh \approx 0.21$ (fig.1) [3]. The results of the verifying numerical calculations [4] that were performed in this work by authors is in good agreement with known experimental results.

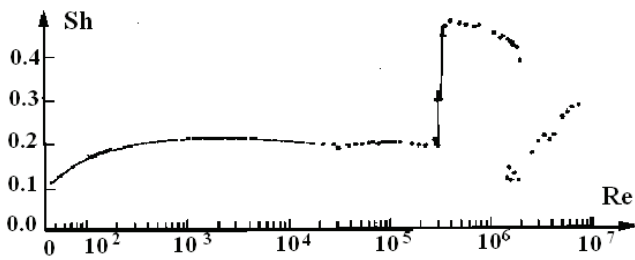


Fig.1 The Strouhal number for a smooth circular cylinder as a function of the Reynolds number

The periodic vortex separation creates the periodic pulsations of the flow in the vicinity of the cylinder (the vortex energy is significantly larger than the energy of the turbulent pulsations), as well as aerodynamic and heat-exchange coefficients. In the stationary flow the pulsation frequency if the Lift force coefficient C_y coincides with the frequency of the vortex separation f_0 , and the pulsation frequency of the head resistance C_x is two times larger than f_0 and pulsation frequency C_y .

The intensity and the frequency of the vortex separation in the pulsating flow depend on time, frequency, the form and amplitude of the pulsating flow. In this case usual Karman vortex trail behind the cylinder deforms in longitudinal and transverse directions and consists of the periodic system of the free vortices with variable step and variable intensity. That is why it is necessary to begin the assessment of the flow pulsation effect possibilities on the cylinder flow parameters from the establishment of the relation between the flow pulsation frequency and the frequency characteristics of the separation vortices.

The objective of the work is to define the conditions and peculiarities of the flow periodic pulsations on the flow character, vortex separation frequency, the form of the Karman vortex trail, aerodynamic and heat-exchange coefficients of the cylinder at subcritical flow conditions.

RESULTS AND DISCUSSION

The calculations results have shown that the flow pulsations effect has the universal character, if the dependence of the researched dimensionless parameters on the dimensionless flow pulsation frequency $Sh = fD/V_0$ (f – flow pulsation frequency) at the same Reynolds numbers is analysed. There exist the Sh frequency ranges where the pulsations significantly affect the non-stationary picture of the velocity field near the cylinder or change the frequency of the vortices separation and the form of the Karman trail as well as pulsation characteristics of the aerodynamic and heat-exchange coefficients.

The dependence character $C_x(t)$ and $C_y(t)$ at the increase of the dimensionless flow frequency in the range of the $0 \leq Sh \leq$ is shown on fig.2 and fig.3. It is obvious that the influence character of the dimensionless flow pulsation frequency on the $C_x(t)$ and $C_y(t)$ coefficients is significantly different. The $C_x(t)$ coefficient pulsations form is close to the form of the velocity pulsations (sine curve in this case) in the whole range of the Sh number variation, but Ac_x pulsation amplitude increases with the Sh number increase. The $C_y(t)$ coefficient pulsations form depends on the frequency of the velocity impulses in the significant extent. At $Sh > 0.14$ the local extremes the intensity and the quantity of which increase with the increase of the Sh number appear. In comparison to the Ac_x the pulsation amplitude of Ac_y changes insignificantly with the increase of the Sh number and in the range of $Sh > 0.5$ remain practically constant.

The intensity of the vortices in the time of the separation may be approximately assessed by the numerical values of the pulsation amplitudes $C_y(t)$ based on the known expression of relations between C_y and the velocity circulation.

This indicates on the necessity to define and assess the influence not only of the first but also of the consequent harmonics of the separation vortices frequencies spectrum. The analysis of the calculation results showed that it is necessary do define no more than two first spectrum harmonics to research the subcritical flow conditions. Therefore the appearance of the local (weak) extremes in the pulsating flow on the $C_y(t)$ curves gives the evidence of the separation vortices formation the separation frequency and intensity of which differs from the main vortices. This indicates on the necessity to define and assess the influence not only of the first but also of the consequent harmonics of the separation vortices frequencies spectrum. The analysis of the calculation results showed that

it is necessary to define no more than two first spectrum harmonics to research the subcritical flow conditions.

Characteristic frequencies of the first and second harmonics of the separation vortices frequencies spectrum may be defined using the dependency plots $C_y(t)$. The main frequency $f_0^{(1)}$ (the frequency of the first harmonic) is defined by the number of the positive (negative) half-periods on the plots $C_y(t)$ at the given time interval in this case. The sub-harmonic frequency (the second harmonic) $f_0^{(2)}$ is defined by the number of the local extremes at the same time interval. The conversion to the corresponding dimensionless frequencies $Sh_0^{(1)}$, $Sh_0^{(2)}$ is performed using the expression for the Strouhal number.

Another method to define the characteristic frequencies is the numerical method that is based on the spectral analysis of the calculation data for $C_y(t)$ using the fast Fourier transformation and the assessment of eigenfrequencies using the Pisarenko method of harmonic expansion [5]. The processing of the calculations results has shown that both methods give the characteristic frequencies that are close to each other. Each of the described methods has its own advantages and disadvantages. The simultaneous usage of these methods allows performing the reciprocal monitoring and to interpret the results more justified.

From the fig.2 and fig.3 it follows that the influence of the second harmonic that changes the signal form practically appears only on the $C_y(t)$ and $Nu(t)$ curves. In the beginning the local extreme on the $C_y(t)$ curve appears on its positive branch at $0 < Sh < 0.14$. Then with the increase of the flow frequency it gradually moves to the negative branch, and at last it appears on both branches. The average Lift force coefficient value for the period is equal to zero $\langle C_y \rangle = 0$ in throughout the frequency range. The $Nu(t)$ curve is affected by the first pulsation harmonic C_x and by both pulsation harmonics C_y . The analysis of the characteristic $Nu(t)$ coefficient's pulsations frequencies will be given later.

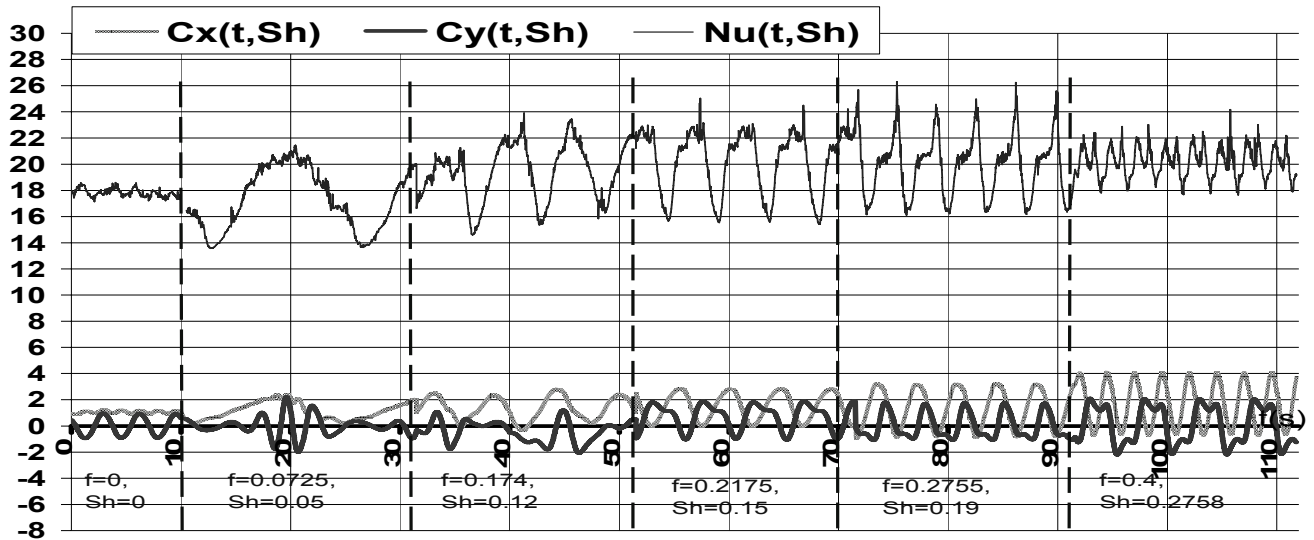


Fig.2 Dependence $C_x(t)$, $C_y(t)$ и $Nu(t)$!! for different pulsation frequencies of the running flow ($0 \leq Sh \leq 0.19$), $Re = 1000$.

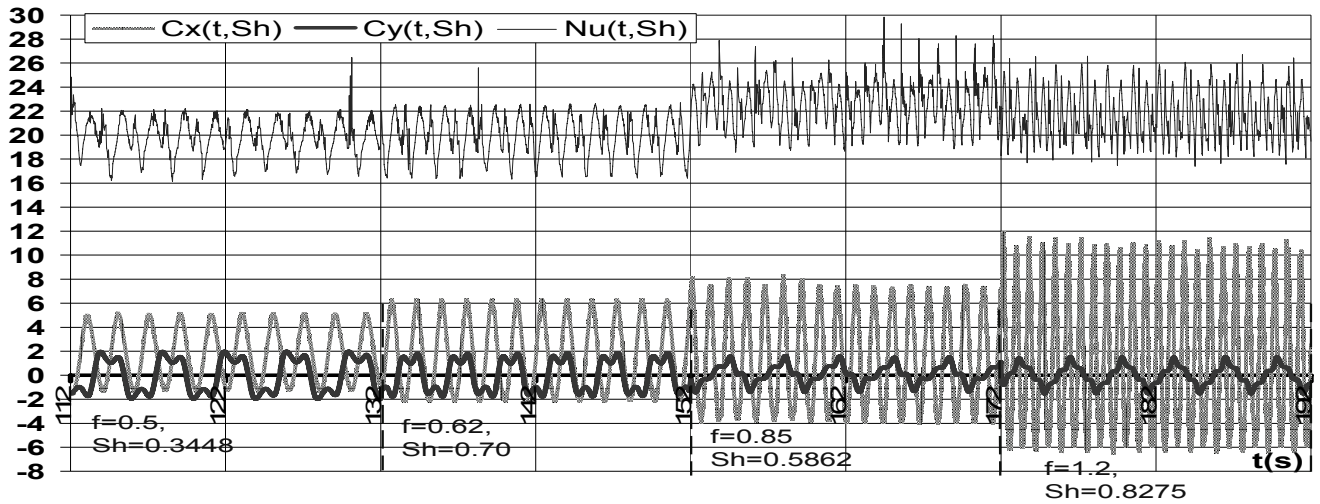


Fig.3 Dependence $C_x(t)$, $C_y(t)$ and $Nu(t)$!! for different pulsation frequencies of the external flow ($0.19 \leq Sh \leq 0.83$), $Re = 1000$.

The dependence on the Sh number averaged for the period of Drag coefficient $\langle C_x \rangle$ value and amplitude values A_{C_x} of the coefficient $C_x(t)$ is shown on fig. 4. The character peculiarity of the flow pulsations effect on the instantaneous values $C_x(t)$ lies in the significant growth of the Drag coefficient pulsation amplitude and the appearance of the negative values $C_x(t)$ at pulsation frequency $Sh > 0.15$ (fig. 2 – 4). The condition $C_x(t) < 0$ implies that the pushing force directed against the flow will periodically affect on the cylinder instead of the resistance force directed along the flow. Sign-alternating amplitude values of the A_{C_x} Drag coefficient values in the area $Sh > 0.5$ increases approximately linearly with the increase of the frequency (e.g. $A_{C_x}(\max) \approx 1.1 + \text{const} \cdot Sh$) and at $Sh \approx 1$ are approximately 10-12 times larger than the corresponding value in the stationary flow (fig.4).

The averaged Drag coefficient $\langle C_x \rangle$ for the period throughout the frequency range $0 < Sh < 1$ is always larger than zero and it changes significantly smaller with the increase of the pulsation frequency than pulsation amplitudes. In the frequency range of $Sh = 0.02 - 0.45$ the flow pulsations cause the increase of $\langle C_x \rangle$ at approximately (40-50)% in comparison with the corresponding value in the stationary flow. In the area of the relatively large Strouhal numbers at $Sh > 0.5$ it is possible to approximately assume that $\langle C_x \rangle$ weakly increases according to the linear law and at $Sh \approx 1$ is 1.25 – 1.5 times larger than the corresponding value in the stationary flow. The Reynolds number at $Sh > 0.5$ as in the case of the stationary flow also practically does not affect the character of the $\langle C_x \rangle$ variation.

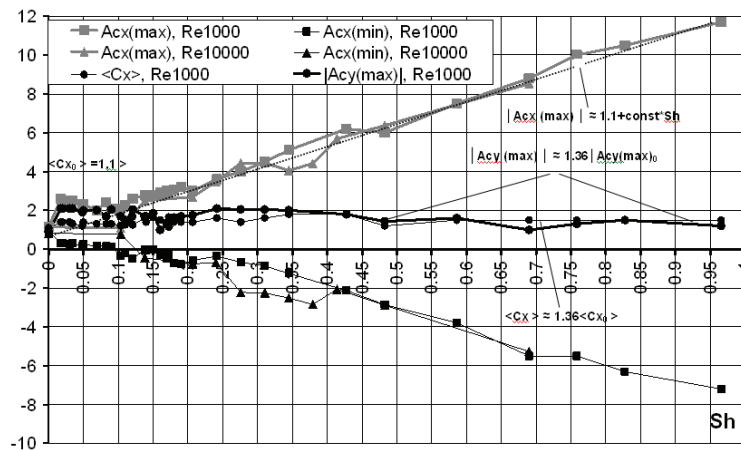


Fig.4 Influence of frequency of the flow Sh on variations of $A_{C_x}(\max)$, $A_{C_x}(\min)$, $\langle C_x \rangle$, $A_{C_y}(\max)$ for $Re=1000$, $Re=10000$, $D=0.1m$.

Lift force coefficient A_{C_y} amplitude values in the zone of the large Strouhal numbers of $Sh > 0.5$ are approximately constant and are 35 – 36% larger than A_{C_y} in the stationary flow in contrast to the A_{C_x} value (fig.4). In the range of $0.02 < Sh < 0.5$ the A_{C_y} value is also approximately constant and is 2 – 2.5 times larger than A_{C_y} in the stationary flow. In the

range of $0 < Sh < 0.02$ and $0.08 < Sh < 0.18$, the A_{C_y} value sharply changes reaching the maximal and minimal values that is the evidence of the considerable nonlinear effect of the flow pulsations on the separation vortexes intensity.

The particularities of the Sh number effect on the characteristic pulsations frequencies of the C_x , C_y coefficients and their amplitude values may be analysed on the basis of the results presented

in fig.5. It was shown earlier that the Sh number variation of the first and second harmonic frequency of the separation vortexes coincides with the frequencies of the corresponding Lift-force coefficient pulsation harmonics $Sh_0^{(1)} = Sh_{Cy}^{(1)}$, $Sh_0^{(2)} = Sh_{Cy}^{(2)}$. The data presented in fig.5 confirms the Sh flow number influence on the mechanism of the vortex separation from the cylinder surface, and $Sh_{Cy}^{(1)} = \varphi_1(Sh)$, $Sh_{Cy}^{(2)} = \varphi_2(Sh)$ curves show the character of this influence. Let's note that in contrast to the Cy the frequency of the first and of the second Cx Drag and Nu Heat-transfer coefficients pulsations harmonics are related with the vortexes separation frequency by other laws that were also defined and analysed on the basis of numerical experiments.

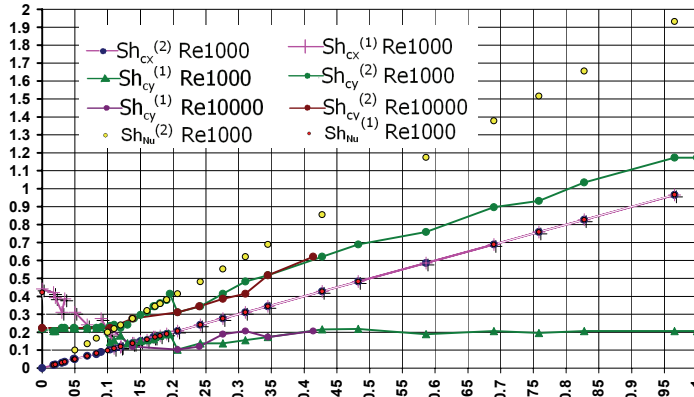


Fig.5 Dependence of dimensionless frequencies of vortex separation $Sh_0^{(1)}$, $Sh_0^{(2)}$ and $Sh_{Cx}^{(1)}$, $Sh_{Cx}^{(2)}$, $Sh_{Nu}^{(1)}$, $Sh_{Nu}^{(2)}$ from flow pulsation frequency Sh for $Re1000$, $Re10000$.

At the low pulsation frequencies of the flow in the range of $0 < Sh < 0.09$ (let's call it „the first zone“) the frequency of the vortex separation is approximately constant and is equal to the frequency of the separation in the stationary flow $Sh_0^{(1)} \approx Sh_{00} \approx 0.21$ (fig.5), i.e. the flow pulsations practically doesn't influence the character

of the flow around the cylinder in the first zone.

In the second zone ($0.08 < Sh \leq 0.42$) the flow pulsation influence becomes considerable. In the range of $0.08 < Sh \leq 0.11$ the vortex separation frequency is partially suppressed by the flow pulsations and decreases until $Sh_0^{(1)} = 0.5 \cdot Sh_{00} = 0.11$. Then with the increase of the Strouhal number from $Sh = 0.11 = 0.5 \cdot Sh_{00}$ until $Sh = 0.21 = Sh_{00}$ the frequency of the first harmonic $Cy^{(1)}$ becomes equal to the flow pulsations frequency $Sh_0^{(1)} = Sh$ and increases until the value of $Sh_0^{(1)} = Sh_{00}$ at $Sh = 0.9Sh_{00} = 0.19$. This is the evidence of the full “capture” condition of the vortex separation frequency by the flow frequency at the given range of the Sh numbers. The frequency of the second harmonic is two times larger then the frequency of the flow $Sh_0^{(2)} = 2 \cdot Sh$ (fig.5) in this case. The further increase of the pulsation frequencies leads to the fast decrease of the vortex separation frequency until the value of $Sh_0^{(1)} = 0.5 \cdot Sh_{00}$ at $Sh = 0.21$ and to its consequent more gradual increase at value of $Sh_0^{(1)} = Sh_{00}$ at $Sh = 2Sh_{00} = 0.42$ again. Let's note that the character of the vortex separation frequency variation in the first zone and in the range of the frequency “capture” of the second zone ($0.08 < Sh \leq 0.21$) qualitatively coincides with the analogical data in the case of the cylinder oscillating across the stationary flow [6]. However, in the range of the flow pulsation frequency variation $0.21 < Sh < 1.0$ the character of the Cx and Cy on the Sh value dependence for the cases of the flow around the stationary cylinder in the pulsating flow and around the oscillating cylinder in the stationary flow significantly differs, especially in the range of the large values of $Sh > 0.42$.

In the third zone ($Sh > 0.42$) the flow pulsation frequencies increase practically does not affects the frequency of the first harmonic $Sh_0^{(1)}$ that is approximately 5% smaller then the vortex separation eigenfrequency Sh_{00} . the value of $Sh_0^{(1)}$ in this zone does not depend on the Reynolds number. In the range of $Sh > 0.42$ the dimensionless frequency of the second harmonic $Sh_0^{(2)}$ that defines the separation frequency of the additional vortexes and the appearance of the local extremes on the $Cy(t)$ curve (see figures for the frequencies $f \geq 0.4\text{Hz}$, $Sh \geq 0.2758$ in fig.2 and fig.3) linearly depends on the flow pulsation frequencies (fig.5) and approximately can be defined using the expression $Sh_0^{(2)} = Sh + C \cdot Sh_{00}$, where $C \approx 0.95 \div 1$.

The frequency characteristics of the Drag coefficient $Cx(t)$ in the range of $Sh \geq 0.5 \cdot Sh_{00}$ is completely defined by the flow pulsations frequency (frequency “capture” conditions) and are described by the relation $Sh_{Cx}^{(1)} = Sh_{Cx}^{(2)} = Sh$ (fig.5). The increase of the flow pulsations frequency in this area leads to the linear increase of the pulsations amplitude Ac_x and to the periodic appearance of the longitudinal force directed against the flow as described earlier (fig.2 – 4). The main part in the creation of the periodic longitudinal force significant by the value in the condition of the capture is played by the vortex separation with the frequency that is equal to the flow pulsations frequency.

The convective heat-exchange of the heated cylinder in the pulsating flow to a considerable degree depends on the condition of its non-stationary flow and therefore on the frequency and the

intensity of the vortexes separation. The intensity of the non-stationary heat-exchange is described by the dimensionless Heat-exchange coefficient (Nusselt number) $Nu = \alpha D / \lambda$, where α [W/(m²*K)] - Heat Transfer coefficient, λ [W/(m*K)] – gas Heat Conduction coefficient. The influence of the flow pulsation frequency on the dependence character $Nu(t)$ may be assessed according to the data in fig.2, fig.3, fig.5. In the stationary flow the pulsation frequency $Nu(t)$ coincides with the Drag coefficient pulsation frequency and is two times larger than the pulsations frequency Cy or vortex separation frequency (fig.2). The appearance of the additional separation vortexes in the pulsating flow causes the formation of the local extremes both on the $Cy(t)$ curves and on the $Nu(t)$ curves (see, e.g. the frequency range $f > 0.2$, $Sh > 0.14$ in fig.2, fig.3). As a result the $Nu(t)$ curves obtain complicated enough configuration that indirectly reflects both the influence of the Cy and Cx pulsations. The influence character of the flow pulsation frequency Sh on the frequencies of the first $Sh_{Nu}^{(1)}$ and of the second $Sh_{Nu}^{(2)}$ Heat-exchange coefficient pulsation spectrum harmonics is shown in fig.5. The frequency of the first harmonic is fully defined by the flow pulsation frequency practically in the whole range of Sh numbers that was researched (excluding the narrow range of $0 < Sh < \dots ?$) and is described by the linear dependence $Sh_{Nu}^{(1)} = Sh$ (fig.5). Therefore only one condition is typical for the frequencies of the first Heat-exchange coefficient pulsations harmonic – the condition of their capture by the flow pulsations. The second harmonic is also proportional to the flow pulsation frequency and is described by the expression $Sh_{Nu}^{(2)} = 2Sh$ (fig.5).

The variation of the separation frequency and of the separation vortexes intensity affects the form of the separation zones and of the heat transfer intensity between the cylinder and the flow in the general case. In the aerodynamic trail behind the cylinder the heat trail with zones (cores) of the increased temperature is formed in case of the heated cylinder cooling or of the decreased temperature at the cylinder heating with hot flow. The calculations showed that the heat trail is similar to the Karman vortex trail moreover the temperature cores zones practically coincide with the zones of the regular vortexes positions [7].

The analysis of the flow pulsation frequency Sh influence on the value of the average Nusselt number $\langle Nu \rangle$ by the period has shown that it is possible to distinguish conventionally three characteristic zones (fig.6). In the first zone $0 < Sh < 0.09$ (the vortex separation frequency is approximately constant) the flow pulsations almost does not affect the separation zone's form and it is possible to consider $\langle Nu \rangle \approx \langle Nu_0 \rangle$, where $\langle Nu_0 \rangle$ – is the average value of the Nusselt number in the stationary flow.

In the second zone ($0.08 < Sh < 0.5$ fig.6) the flow pulsation frequency increase leads to the 30÷40% increase of the relative Nusselt number depending on the heat flow direction (the cooling of the heated cylinder or the heating of the cylinder by the hot flow). In the third zone at Strouhal numbers of $0.5 < Sh < 1.0$ the heat-exchange coefficient stabilizes and the value of the relative Nusselt number is $\langle Nu \rangle / \langle Nu_0 \rangle = 1.3 \div 1.4$.

Hence the presented data gives the evidence of the considerable enough increase of the heat-exchange intensity in the pulsating flow and of the heat-exchange process control in the range of the dimensionless flow pulsation frequencies of $0.08 < Sh < 0.5$.

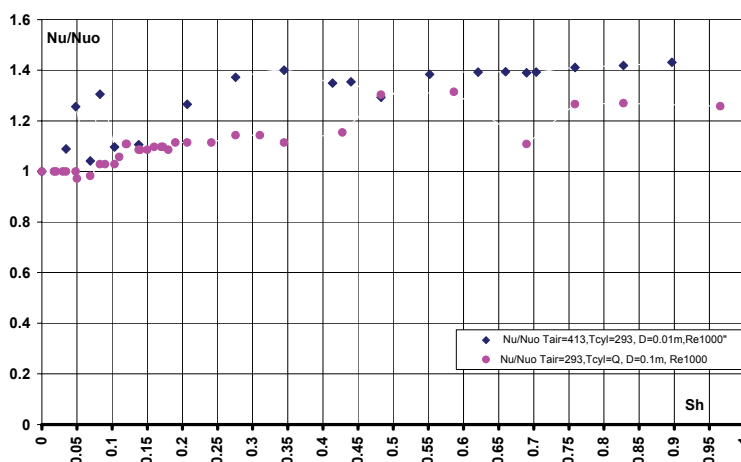


Fig.6. The dependence of the relative Nusselt number $\langle Nu \rangle / \langle Nu_0 \rangle$ on the dimensionless flow pulsation frequencies Sh .

CONCLUSION

1. In the periodic pulsating external flow the intensity of the cylinder Lifting vortex varies periodically and the free separation vortexes are formed. The Karman vortex trail behind the cylinder has been deformed both in longitudinal and in transverse directions and consists of the

system of the free vortexes with the alternating step and intensity. As a result the periodic pulsations of the flow velocity significantly affect the frequency of the vortex separation, the form of the vortex trail, the pulsation frequency of the aerodynamic coefficients C_x , C_y and of the dimensionless Heat-exchange coefficient Nu , their average and amplitude values.

2. For the analysis of the flow pulsation effect on the aerodynamic and heat-exchange of the cylinder it is appropriate to select three characteristic variation ranges of the flow dimensionless Strouhal number Sh .

In the first range of $0 < Sh < 0.09$ the pulsations of the external flow does not affect the vortexes separation frequencies and the heat-exchange intensity.

In the second range of $0.09 < Sh < 2Sh_{00} = 0.42$ the pulsations of the external flow partially suppress the vortexes separation frequency. In this range there are the areas with the condition of the full "capture" of the vortexes separation frequency by the flow frequency. The increase of the average head-resistant coefficient $\langle C_x \rangle$ does not exceed 40÷50%, but the Lifting force Ac_y pulsation amplitude does not exceed 35÷40%. The amplitude values of Ac_x are two times larger than the average values of $\langle C_x \rangle$ (Sh). At pulsation frequency of $Sh > 0.15$ the negative instantaneous values of the Drag coefficient appear periodically.

At the third range of the dimensionless flow frequencies of $Sh \geq 2Sh_{00} = 0.42$ the average Drag coefficient of the cylinder does not vary and is approximately 35% larger than the Drag coefficient in the stationary flow. The pulsation frequency and the amplitude values $C_x(t)$ increase proportionally to Sh (at $Sh \approx 1$ the amplitude values of $C_x(t)$ are 10-12 times larger than the corresponding values in the stationary flow). The pulsation frequency and the amplitude values $C_y(t)$ are constant and are approximately equal to their values in the stationary flow. The average Heat-exchange coefficient also remains constant, but the average Nusselt number is 30÷40% larger than the corresponding value in the stationary flow. The frequencies of the first and of the second heat-exchange coefficient's pulsations harmonics are proportional to the flow pulsations frequency.

3. The received results give the evidence of the necessity to consider the peculiarities of the aerodynamic coefficients variation, as well as the possibility of the significant increase and control of the heat-exchange process of the cylinder that is streamlined by the subcritical external pulsating flow.

REFERENCES.

1. *М. А. Промтов*, Машины и аппараты с импульсными энергетическими воздействиями на обрабатываемые вещества, Москва, Машиностроение, 2004.
2. *Каменков Г.В.*, Теория крыла в закритической области, Избранные труды, т. 1, Москва, 1971, 259 стр.
3. *Williamsons C.H.K.*, Vortex dynamics in cylinder wake, Annual Review of Fluid Mechanics, 1969 (a), 28, 477-539.
4. *V.Ushakov, N.Sidenko, S.Svichkar*, Physical features of drying process of capillary porous materials in a pulsing gas flow. Part 1. Features of aerodynamics. Annals of Warsaw University of Life Sciences. Forestry and Wood Tehnology № 62, 2007.g.
5. *S. Lawrence Marple Jr.* Digital Spectral Amalysis with applications. Prentice-Hall, Inc., Cliffs, New Jersey 07632.
6. *К.К. Федяевский, Л.Х. Блюмина*, Гидроаэродинамика отрывного обтекания тел, Москва, Машиностроение, 1977.
7. *V.Ushakov, V. Gopeenko, N.Sidenko*, Physical features of drying process of capillary porous materials in a pulsing gas flow. Part 2. Features of thermo- and mass transfer. Annals of Warsaw University of Life Sciences. Forestry and Wood Tehnology № 62, 2007.

EXTRUSION-INTRUSION PATTERN AS AN INDICATOR OF ACCUMULATED FATIGUE DAMAGE

The results of the tests show that quantitative estimation of accumulated fatigue damage may effectively be performed by computer-aided optical analysis of the surface state using damage parameter and fractal dimension. Such method can be applied for alclad aluminum alloys which are used for modern aircraft skin manufacturing. New approach allows to indicate more troublesome points of aircraft structures, predict fatigue crack under full scale test of aircraft structures as well as estimate remaining service life.

Introduction

It is well known that the visual inspection of aircraft is the most widely used method employed for ensuring the structural integrity of an aircraft skin and its substructure. For example, a typical heavy inspection carried out on a commercial aircraft after every 12,000 flying hours, is about 90% visual and 10% non-destructive inspection (NDI) [1].

Pressurization and depressurization of the aircraft during each flight cycle causes its body to expand and contract. This expansion and contraction induce stress in the skin that leads to the resulting in the growth of cracks outward the rivets. There are many reliable models which predict crack growth quite accurately as a function of the number of pressurization and depressurization cycles. The goal of visual inspection is to detect cracks that are above a minimum threshold length. This threshold length provides a safety margin that allows a crack to be missed in two or three consecutive inspections before it is big enough to endanger the aircraft structure.

The investigations show that the aircraft visual inspection can be sufficiently improved by the application of computer aided optical tools at initial stage of fatigue.

New method background

The life of a fatigue crack has two stages, initiation and propagation. Dislocations play a major role in the fatigue crack initiation phase. It has been proved by laboratory tests of the alclad aluminum alloys that after a certain number of loading cycles dislocations pile up and form structures called persistent slip bands (PSBs). An example of a PSBs is shown in fig. 1.

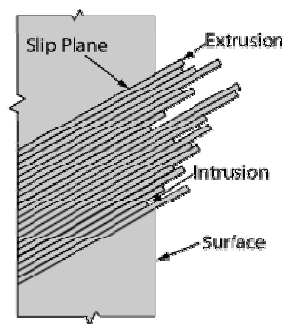


Fig. 1. Persistent slip bands.

PSBs are the areas that rise above (extrusion) or fall below (intrusion) the surface of the component due to material movement along slip planes. This leaves tiny signs on the surface that serve as stress risers where fatigue cracks can be initiated.

Observation of the extrusion and intrusion intensities gives the information about the accumulated fatigue damage. For quantitative assessment of accumulated fatigue damage some parameters of the surface relief have been proposed.

Aluminum alloys D16AT, 2024T3 and 7075T6 have been explored in our previous experiments. These materials are widely used for manufacturing modern aircraft skin in Ukrainian, Russian and Western aircraft industry. As a result of cyclic loading, the deformation relief (extrusion-intrusion pattern) is initiated and developed.

As it was proved before the intensity of the relief as well as the fractal dimensions of clusters depend on the maximum stress level, number of cycles and corresponds to distribution of the stress near the stress concentrator.

Presented results show that the asymmetry of cycle must be taken into account for precise estimation of accumulated fatigue damage.

Experimental procedure

Specimens have been loaded with the wide range of stresses at frequency 25 Hz. The surface was polished with diamond paste. Geometry of specimens with the hole as a stress concentrator is shown in fig. 2.

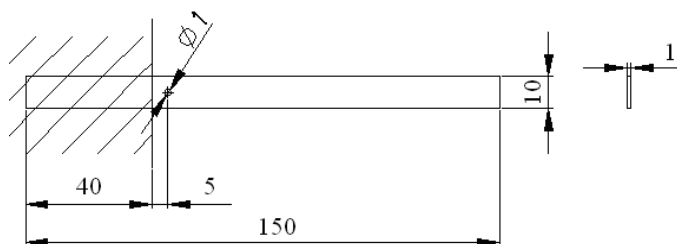


Fig. 2. Specimen for fatigue test.

The procedure for accumulated fatigue damage estimation used in the research includes the applies digital images (fig. 3a) of the deformation relief observed by the light microscope.

Correspondence of the studied structures to the well-known scheme of the extrusion and intrusion formation [2] was proved by the scan microscope investigation of aluminum specimens at the wide range of the loading modes.

In fig. 3b the digital photo of the specimen surface with developed deformation relief obtained by the scan microscope SEM-515 – “Phillips” with the voltage 30 kV is presented.

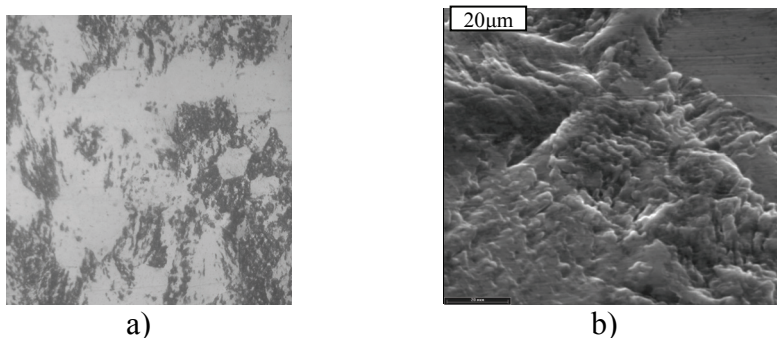


Fig. 3. Aluminum layer surface of alclad aluminum alloy D16AT: a) Light microscope (x 390); b) Scan microscope SEM-515.

In papers [3-6] the processing steps of digital images of alclad aluminum alloys surface that allows quantitative estimation of the surface saturation level with the microplastic deformation signs and correspondent accumulated fatigue damage were shown.

In papers [7] it was shown that the fractal dimensions of deformation relief describe the shape of relief clusters and could be considered as an additional damage parameter that significantly improves the accuracy of the accumulated fatigue damage estimation.

Nowadays there are a lot of methods for the fractal dimensions calculation of the nature objects. One of the more widespread is “a box counting” [8].

The method gives the possibility to calculate fractal dimension of the relief cluster boundaries. Fractal dimension of the cluster boundaries is designated as D_p .

For some fractals the most informative parameter is a fractal dimension of the ratio of perimeter to area. It is known that this ratio characterizes the shape of objects. For the regular geometrical figures this parameter is a constant value and it doesn't depend on the object size.

In paper [9] such kind of dimension describes the shape of clouds and rains.

Correspondent fractal dimension for the clusters of deformation relief is $D_{p/s}$.

For the data processing automatization special software has been developed.

Main stages of calculations are: transformation of digital images of a surface into the monochromic; separation of single clusters of deformation relief; determination of the deformation relief clusters contours; overlapping of the box net on the cluster's contours or on their surfaces; calculation of the box number, overlapping contours of clusters or their surfaces; graphs construction of the relationships $\ln N_p = f(\ln(1/b))$; $\ln N_s = f(\ln(1/b))$ and $\ln N_p = f(\ln(N_s))$, where N_p – number of cells (boxes), overlapping contours of deformation relief clusters; N_s – number of cells overlapping surface of deformation relief clusters; b – the size of the cell.

Typical graph of the relationship $\ln N_p = f(\ln(N_s))$, obtained during the research is presented in fig. 4.

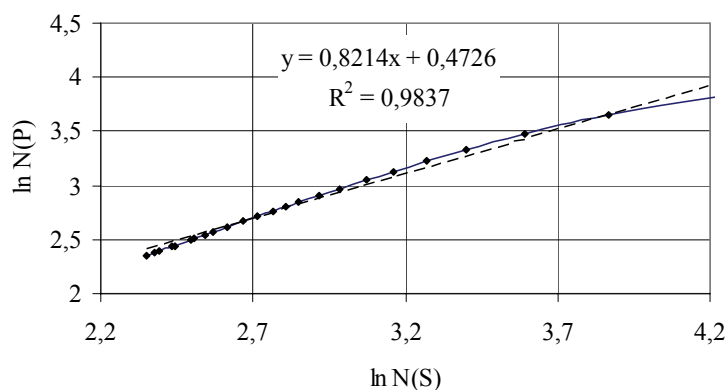


Fig. 4. The relationship between number of cells overlapping clusters contours and number of cells overlapping clusters area.

Fractal dimension $D_{p/s}$ obtained by application of geometrical method was estimated as a doubled absolute tangent value of the slope angle of the middle part of the fractal graph in its linear approximation in log-log coordinates [9].

Fractal dimensions of the deformation relief clusters contours as well as the fractal dimensions determined by the ratio of perimeter to area exceed topological dimension of the line and are within the range of 1 to 2.

Experimental results

The design of specially constructed test machine allows to carry out optical observation of the specimen surface after several initial cycles of loading. Thus, the monitoring of surface state began from the moment of the first evidence of extrusion-intrusion pattern appearance.

Damage parameter D and fractal dimension $D_{p/s}$ have been considered as main diagnostic parameters.

As a typical example of the surface relief evolution one can consider evolution of damage parameter D and fractal dimension $D_{p/s}$ during the process of one specimen loading, tested under the maximum cycle stress 234,5 MPa with zero minimum stress level.

As the practical task of the accumulated fatigue damage monitoring is to forecast the residual life of the aircraft structure components, the ratio of the damage parameter D and fractal dimension $D_{p/s}$ to the remaining number of cycles have been investigated (fig. 5 and 6).

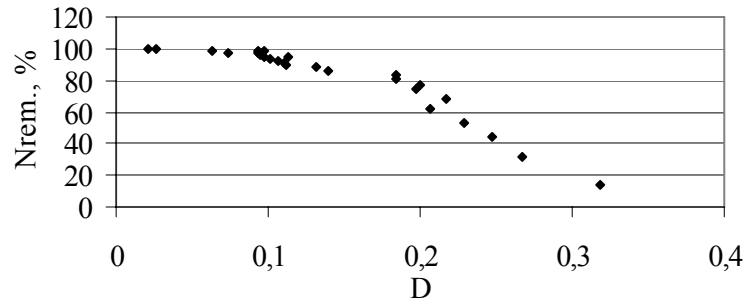


Fig. 5. Relationship between remaining life and damage parameter D.

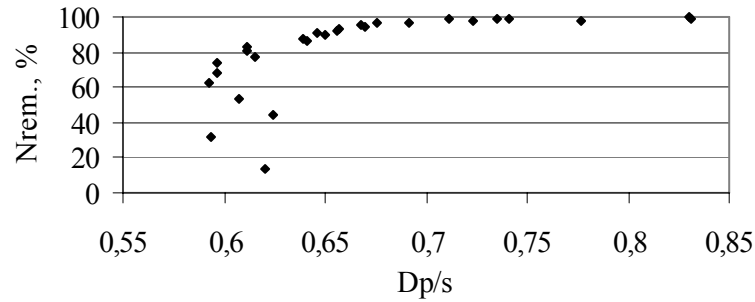


Fig. 6. Relationship between remaining life and fractal dimension $D_{p/s}$.

As it is seen from the graphs above, both parameters correlate with accumulated fatigue damage.

By this relation damage parameter D denotes the intensity of the extrusions and intrusions pattern that forms deformation relief, while changing of the fractal dimension $D_{p/s}$ characterizes the process of the deformation relief clusters coalescence.

In this connection we can apply multiple correlation models for the life forecast process. Thus both parameters of the deformation relief could be taken into account.

Dispersion and regression analysis made by module “ANOVA” of the “Statgraphics Plus” has shown the possibility of the following multiple correlation model application: $N_{res.,\%} = 228,252 - 385,169 D - 69,067 D_{p/s}$, where: D – value of the damage parameter; $D_{p/s}$ – fractal dimension; $N_{res.,\%}$ - residual number of cycles, %.

Correspondent value of the R^2 equals 92,2851 %. Standard error is 6,48.

The analysis performed proves the significance of both considered models parameters: damage parameter D and fractal dimension $D_{p/s}$.

Parts of the aircraft can be subjected to different modes of loading. Hence, it is possible to compare some typical regimes, particularly under symmetrical and nonsymmetrical loading, with stress ratio $R=0$, (fig. 7 and 8).

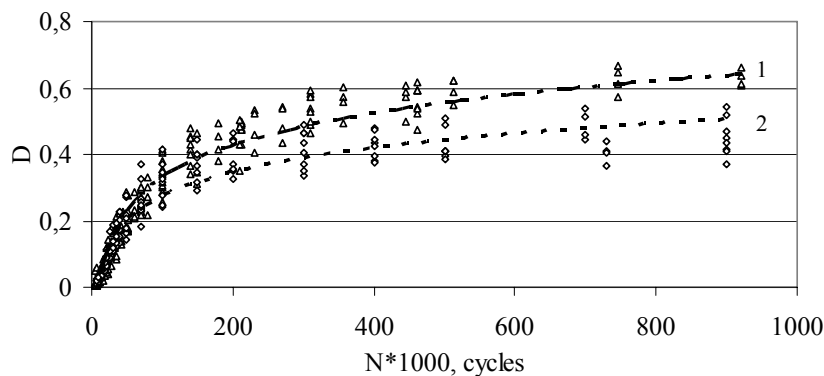


Fig. 7. Evolution of the damage parameter under $\sigma_a=86,58$ MPa at loading with stress ratio $R=0$ (1) and symmetrical cycle (2).

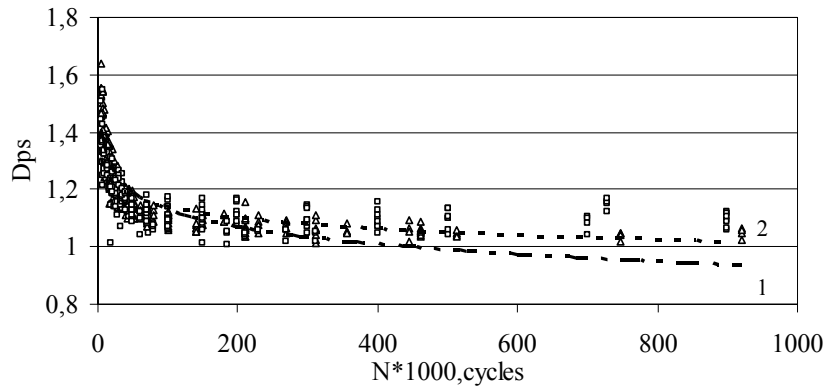


Fig. 8. Evolution of the fractal dimension under $\sigma_a=86,58$ MPa at loading with stress ratio $R=0$ (1) and symmetrical cycle (2).

As it is seen from the presented graphs accumulated damage accelerates with the increase of a maximum stress level despite of the equal amplitude stress σ_a for the tested specimens.

Another important factor of loading is a value of the static component of the fluctuated load under the loading regimes with fixed maximum stress level (fig. 9 and 10). We have carried out tests under the $\sigma_{max}=234,5$ MPa with different values of the static components: $\sigma_1=67,85$ MPa ($R=0,3$), $\sigma_2=117,78$ MPa ($R=0,5$), $\sigma_3=140,4$ MPa ($R=0,6$).

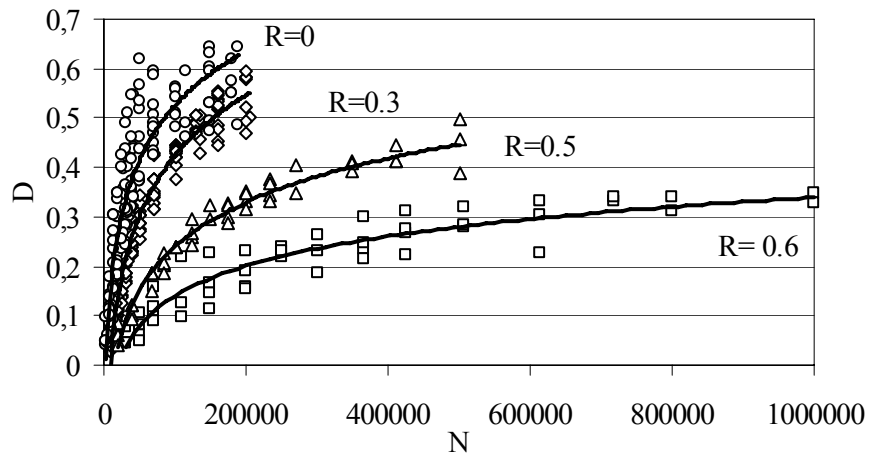


Fig. 9. Evolution of the damage parameter under the various cycle asymmetry coefficients R and fixed maximum stress level.

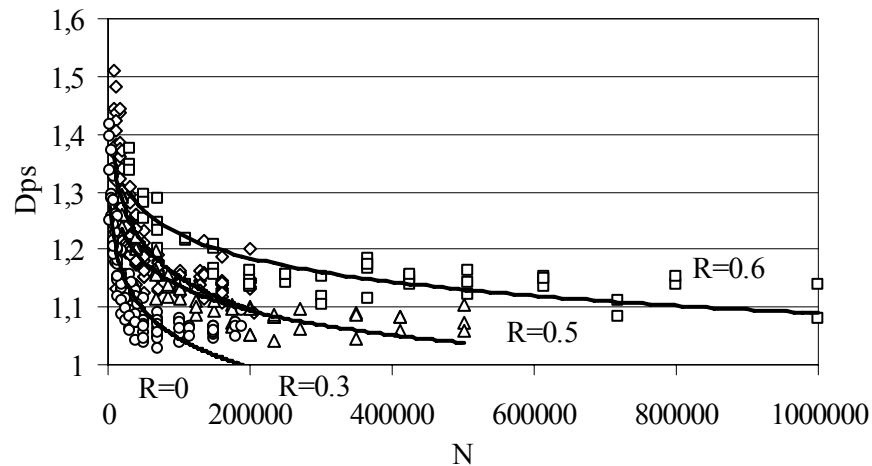


Fig. 10. Evolution of the fractal dimension under the various cycle asymmetry coefficients R and fixed stress level.

The conducted tests show that the decrease of the asymmetry coefficient increases the rate of the fatigue damage accumulation on the initial stage of fatigue.

We can point out, that at all regimes of loading the most appropriate equations for the relationships between damage parameter D and number of cycles is: $D=a\ln(N)+b$.

The relationships between fractal dimension $D_{p/s}$ and number of cycles are: $D_{p/s}=a\ln(N)=b$.

As a result of scheduled researches, the following exemplary procedure for aircraft fatigue analysis might be proposed: 1. Operating range of loads, load distribution along the structure, and material characteristics are determined. 2. Structure parts to be investigated are determined. 3. Laboratory fatigue tests of structure elements (specimens) are carried out to create data bank as to evolution of the element surface state. The test program is scheduled taking into account operating range of loads. As a result of the laboratory tests correlation models for fatigue prediction are developed 4. Monitoring of fatigue process of aviation structures under full-scale test is performed. 5. The analysis of an inspected part of a structure is conducted by estimation of damage parameter D and fractal dimensions. 6. The prediction of the aircraft component residual life is performed by the application of laboratory tested mathematical models.

Conclusions

The presented results indicate the possibility of the accumulated fatigue damage estimation as well as possibility of the remaining life forecast for aircraft structure components, of alclad aluminum alloys made by using the computer aided optical method of the surface deformation relief analysis.

For the structure components remaining life prediction multiple correlation models, including damage parameter D , that characterizes saturation of the surface with the signs of microplastic deformation, and fractal dimension $D_{p/s}$ determined by the ratio of the deformation relief clusters perimeter to their area can be used.

The evolution of the extrusion-intrusion pattern is influenced by the maximum stress level and the asymmetry of cycle.

References

1. C. Seher, "The national aging aircraft nondestructive inspection research and development plan", Proceedings of the International Workshop on Inspection and Evaluation of Aging Aircraft May 21, 1992.
2. Goritskiy V.M., Terentiev V.F. *Structure and fatigue fracture of metals* (Metalurgija, Moscow 1986).
3. Карускевич М.В., Игнатович С.Р., Карскевич О.М., Пантелеев В.М. Диагностика усталости плакированных алюминиевых сплавов // Вестник НТТУ КПИ. Машиностроение. – 2002. – № 43. – С. 53 – 55
4. Карускевич О.М., Игнатович С.Р., Карускевич М.В., Хижняк С.В., Якушенко О.С. Моніторинг утоми конструційних алюмінієвих сплавів // Вісник НАУ. – 2004. – № 1(19). – С. 88 – 91
5. Карускевич О.М., Игнатович С.Р., Карускевич М.В. Эволюция поврежденности сплава Д-16АТ у концентратора на стадии до зарождения усталостной трещины // Авиационно-космическая техника и технология. Журнал Национ. аэрокосм. ун-та им. Н.Е. Жуковского ХАИ. – 2004. – № 4(12). – С. 29 – 32.
6. Карускевич О.М. Влияние уровня напряжений на развитие деформационного рельефа // Вестник двигателестроения. – 2005. – № 2. – С. 79 – 83
7. Karuskevich M.V., Korchyk E.U., Maslak T.P., Zhan Z.H. The fractality of the deformation relief of polycrystal aluminium // Visnik NAU. – 2006. – №2. – P.78-81.
8. Ivanova V.S., Balankin A.S., Bunin I.Zh.: Synergetic and fractals in the material science (Nauka, Moscow 1994).
9. Lovejoy, S. Area-perimeter relation for rain and cloud areas. Science, 216, 185 – 187, 1982.

METAL FATIGUE PROCESS INVESTIGATION BY THE INTERFERENCE NANOPROFILOMETER

The evolution process of deformation relief of D16AT alloy being cyclic loaded was studied. Possibility of material extreme condition prediction in the fatigue process is discussed.

Introduction

The aircraft service life and planning of the periodic check of the technical condition and overhauls is tightly connected with necessity to predict the construction remain resources and fatigue process influence on the construction units.

The main feature of the fatigue process is its locality. As the results of the damage accumulation in any overloaded area of the construction unit, the fatigue cracks are appearing, it leads to the load-carrying ability reduction and unit damage. The second peculiarity of the process is its vicissitude. The fatigue process is the summaries of two different processes: the damage accumulation process following to the fatigue crack and the process of fatigue crack expansion [1]. However the aircraft construction has some parts where the cracks are unacceptable. Therefore it is required to predict the extreme condition based on the information of damage accumulation.

The damage accumulation conception is used for formalization of the gradual machine failure phenomenon, moreover the material damage in the time period is explained as a deviation of its controlled properties [2]. The controllable parameters such as plastic deformation, wearing and corrosion level, crack length are often used as a damage criteria. The current damage condition may be estimated in these cases and the extreme condition or safe life prediction may be determined with high accuracy level.

The units properties deviation doesn't always appear on microscopic level. For example the fatigue damage in the latence period appears on micro – nano scale level.

Fatigue damage in the latence period in many cases is followed by deformation relief formation [3]. A metallographic investigation shows the difference in the processes of the deformation relief formation in the high and low stress amplitudes. The extrusion and intrusion appearance on the surface of the clad aluminum alloy makes possible quantitative estimation of the accumulated fatigue damage with the use of relief formation intensity and relief dimensioning parameters. Such estimation can be evaluated by analysis of surface image obtained while using microscope with high magnification. However optical microscopy gives only qualitative information about surface deformation relief. But this information is not enough for prediction of remaining service life and accumulative fatigue damage. Quantitative relief properties can be obtained by using optical inteferometric profiler "Micron-alpha" [4] which was developed at the department of aircraft structural design of the National Aviation University. Sensitivity of this instrument allows to solve a problem of quantitative estimation of specimen surface geometry (topography) changing under fatigue. [5]

In this work results of surface deformation relief changing of aluminum alloy D16AT, obtained by optical interferometric profiler "Micron-Alpha" under fatigue loading are represented.

Experimental procedure and results

The subject of investigations is polished specimens of duralumin alloy D16AT.

Specimen dimension is 400×80×1,5 mm. The concentrator with diameter 4 mm was made in the center of specimen (fig. 1.a)

Fatigue tests were carried out using servo- hydraulic test machine Bi00-202V with loading frequency $f=11$ Hz. Loading cycle is sinusoidal, from zero.

Specimens were tested on fatigue at cyclic loading. Maximum loading of the cycle is 120 MPa.

Specimen loading was performed with periodicity 10 000 cycles. After each loading specimen surface relief was measured. Investigations were carried out till appearance of well-defined crack with length 0,5 mm.

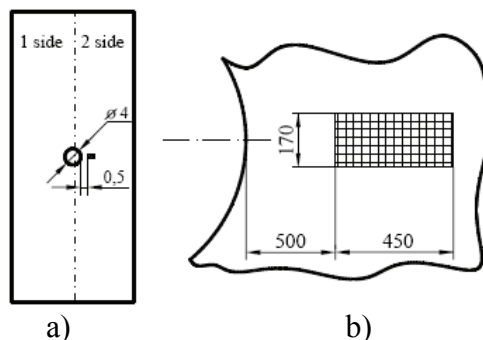


Fig 1. Specimen sketch : a) general specimen sketch (dimensions, mm); b) area of specimen where surface relief was measured (dimensions, μm)

Measured area of specimen was positioned on distance 0,5 mm from edge of concentrator in perpendicular direction to the axis of loading. (fig. 1.b).

Its position was controlled according to the image obtained by instrument. Magnification of instrument is 500 times. Relief features are clearly visible at this magnification.

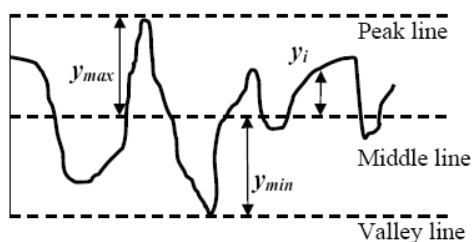


Fig.2. Surface profile and roughness properties

Parameter R_a , arithmetic average of roughness deviation was chosen as index which shows surface relief changing. Surface roughness is a measure of the texture of a surface. It is quantified by the vertical deviations of a real surface from its ideal form [6]. According to [7] value of arithmetic average of roughness deviation we find from the formula

$$R_a = \frac{1}{l} \int_0^l |y(x)| dx. \quad (1)$$

To determine relief changing due to nonfailure operating time measurements were performed by two methods. Measurements were made along 20 lines. In the first case lines were oriented in cross direction to the axis of loading (fig.3.a), in the second case they were oriented in longitudinal direction.

Values for lines along which roughness is determined from dimensions of measured area which is equal to 450x170 (table):

Table

Determination of lines parameters

	cross direction	longitudinal direction
Length of lines, μm	400	160
Step between lines, μm	8	20
Number of lines	20	

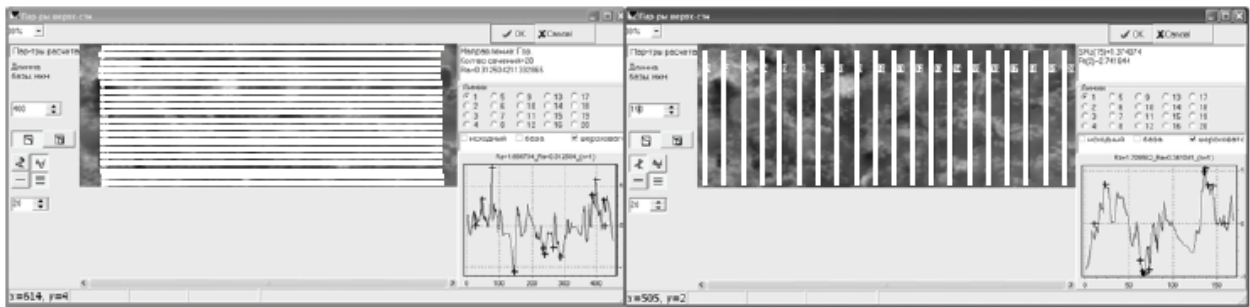


Fig. 3. Methods of relief determination roughness

Value Ra was determined for each line. For further analysis of surface deformation relief changing we used meaning value \overline{Ra} along 20 lines.

$$\overline{Ra} = \frac{\sum_{i=1}^{20} Ra_i}{20}. \quad (2)$$

Data analysis shows (fig. 5) that difference between \overline{Ra} obtained by two methods is very small and it is possible to assume that values of roughness parameters for first and second cases are equal. However to determine stress influence of concentrator on specimen surface the first method of roughness measuring was chosen in longitudinal direction to the axis of loading.

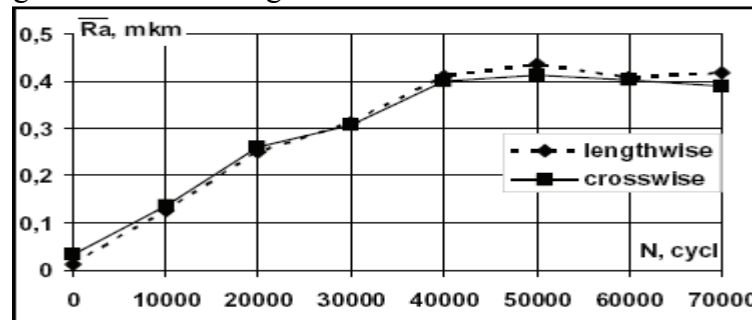


Fig.5. Influence of lines directions on Ra value

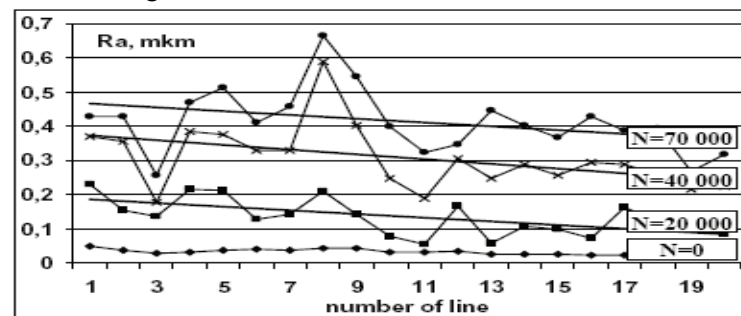


Fig.6. Changing of Ra due to operating time depends on distance from stress concentrator

As an example let's consider results obtained on specimen after experiment. Dynamics of surface relief changing due to operating time are showed on fig. 6 and fig. 7.

Fig. 6 shows that surface topography of the specimen changes in dependence on distance from concentrator, inclination of mean line Ra indicates it. In this connection it is necessary to choose location of measured area very thoroughly.

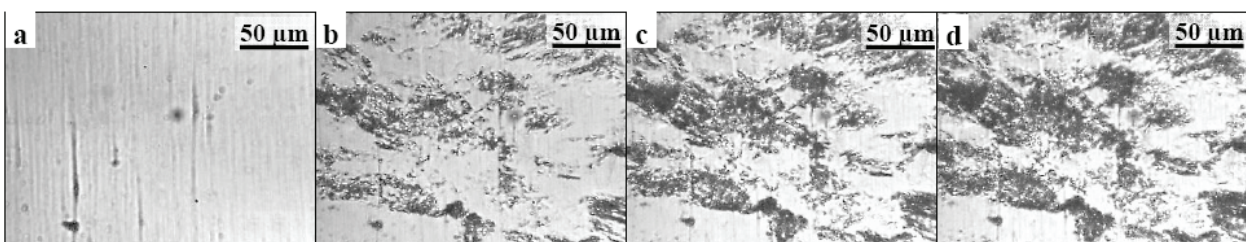


Fig. 7. specimen surface relief changing due to operating time

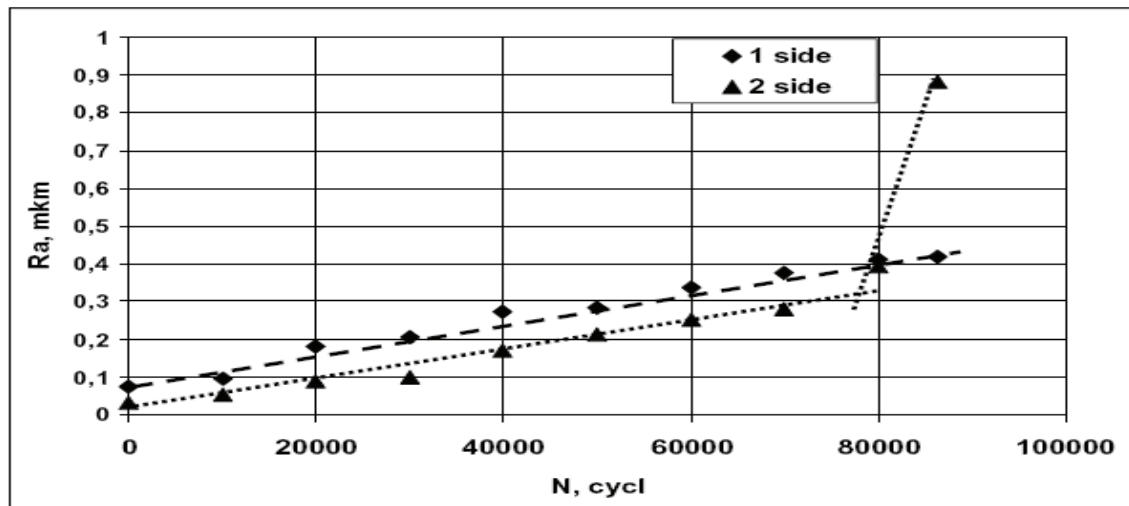


Fig. 8. Graph of dependence of \overline{Ra} changing due to operating time

At operating time $N=86\ 300$ testing was stopped because specimen was brought up to extreme condition (crack propagates up to 0,5 mm on side №2)

For Side №1 it's clear that changing of \overline{Ra} is directly proportional to operating time and is given by straight line. For side №2 the similar tendency is observed till the moment of crack formation. Fig 8 shows inflection of curve in the area $N=80\ 000$ which is caused by crack formation. However in particular case changing of \overline{Ra} due to operating time has a view represented in fig. 5.

Conclusions

The received results show, that the values describing a roughness of a material surface changing with an operating time and can be used to forecast time of a specimen limiting state achievement . The jump of the roughness parameter changing is connected with local cyclic plastic deformations in top of the crack. It allows to detect crack occurrence.

References

1. Vorobiev A.Z., Olkin B.I., Stebenev V.N. Fatigue resistance of structure elements (Mashinostroenie, Moscow 1990).
2. Pronikov A.S. Machines reliability (Mashinostroenie, Moscow 1978).
3. Gorickiy V.M., Terentiev V.F. Metals structure and fatigue failure (Metallurgiya, Moscow 1980).
4. Ignatovich S.R., Karuskevich O.M., Zakiev I.M., Zakiev V.I., Fatigue damage diagnostic by the contactless registration method of the object relief in nanometer range // Material of 13 international conference "Modern methods and means of nondestructive control and technical diagnostic" (Yalta, 3.11.2005), - P. 80 – 82
5. Ignatovich S.R., Zakiev I.M., Zakiev V.I., Detail surface condition control by the contactless profilometer / Aerospace technique and technology – № 8 – Kharkov: KHAI, 2006.. – P. 20 – 22
6. Samohvalov Ya.A., Livitskiy M.Ya., Grigorash V.D. Reference book of technician-constructor (Tehnika, Kiev 1978).
7. GOST 2789-73 — Surface roughness. Parameters and characteristics.

V. Astanin, prof.
M. Borodachov, prof.
S. Bogdan, assoc. prof.
(National Aviation University, Ukraine)

THE STRESS-STRAIN STATE OF AVIATION THIN-SLAB STRUCTURE ELEMENTS OF UNDER IMPACT LOAD

The problem concerning transversal impact of a body in form of a mass point or a finite body of different form to the sheet-formed structures was considered. For solution the finite element method (FEM) was used. The influences of velocity value, the impact body mass, the effect of presence strengthened ribs and damages in web of plate on the structure stress-strain state were studied. In addition different plate boundaries fixing was considered.

1. Statement of problem. *The problem concerning transversal impact of a body in form of a mass point and a finite body of different form to the sheet-formed structures of following type: a plate, a plate strengthened by ribs, a plate with damages was considered. The stress-strain state of above mentioned structures by elastic approach is defined under different level of impact impulse and plate boundaries fixing applying finite element method (FEM).*

As such model the stress-strain state of a plate, rigid fixed along perimeter, under impact was studying. For that plate it is impossible to obtain exact analytical solution, especially if the problem is complicated by presence of the ribs, damages, strips etc. Therefore, for calculation the approximate analytical and numerical methods were applied. The represented calculation approach is based on a combination of numerical methods and basic principles of impact theory under expansion by oscillation modes.

The problem of load impact to plate in point with coordinates $x = a/2$, $y = b/2$ is considered (Fig. 1). Let analyzed the plate with rigid fix along edges. At $t \leq 0$ the plate is under stressless and strainless state, but at moment of time $t = 0$ the plate is impacted by a load, which have a mass M and velocity v_0 . The velocity vector v_0 is directed at right angle to the center surface of plate plane. In other words

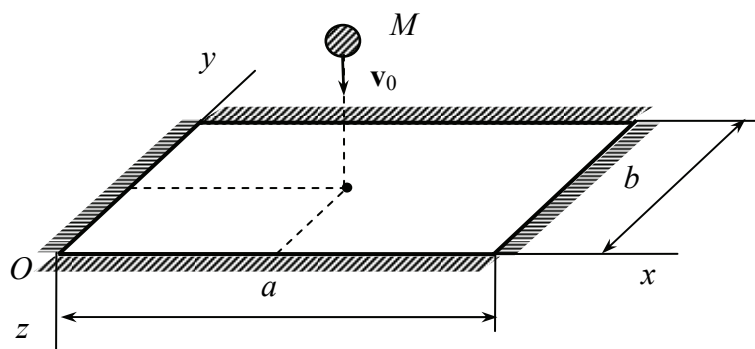


Fig. 1 Problem design diagram

2. The basic statement of studying. *The differential equation of induced transversal oscillations of a plate is presented in following view*

$$D \left(\frac{\partial^4 w}{\partial x^4} + 2 \frac{\partial^4 w}{\partial x^2 \partial y^2} + \frac{\partial^4 w}{\partial y^4} \right) + m \frac{\partial^2 w}{\partial t^2} = q(x, y, t), \quad (1)$$

where $D = \frac{Eh^3}{12(1-\nu^2)}$,

D – cylindrical rigidity of plate, h – plate thickness, E – modulus of elasticity (Young's modulus), ν – Poisson's ratio, w – vertical deflection, m – plate unit area mass ($m = \gamma h/g$), γ – relative density of plate material, g – gravitational acceleration.

Initial condition of the problem

$$w = 0 \text{ and } \frac{\partial w}{\partial t} = 0 \text{ at } t = 0. \quad (2)$$

Due to plate rigid fixing along its perimeter the boundary conditions will be in following view

$$\begin{aligned} w = 0 \text{ and } \frac{\partial w}{\partial x} = 0 \text{ at } x = 0 \text{ and } x = a, \\ w = 0 \text{ and } \frac{\partial w}{\partial y} = 0 \text{ at } y = 0 \text{ and } y = b. \end{aligned} \quad (3)$$

It is practically impossible to obtain strong analytical solution for the equation (1), which would be met the initial conditions (2) and boundary condition (3). Therefore, it is expedient for put problem solving to apply the approximate analytical and numerical methods.

For solution of denoted problem concerning load impact to the plate we used a numerical method, which is based on the finite element method (FEM) in form of displacement.

The theorem of mass point momentum alteration at impact is represented in following view

$$M(\mathbf{v}_1 - \mathbf{v}_0) = \sum \mathbf{S}_j, \quad (4)$$

i.e. mass point momentum alteration during impact is equaled to sum of impact momentums (\mathbf{S}_j) acting to the mass point. There \mathbf{v}_0 , \mathbf{v}_1 – accordingly velocity of the impacted load at the beginning and the end of impact. The formula (4) could be written by axis z projection in following view

$$M(1+k)v_{0z} = \sum S_{jz}, \quad (5)$$

where k – restoring coefficient under impact.

Impact momentum

$$\mathbf{S}_{\text{imp}} = \int_0^\tau \mathbf{F}_{\text{imp}} dt = \mathbf{F}_{\text{imp}}^{\text{av}} \cdot \tau, \quad (6)$$

where \mathbf{F}_{imp} – impact force, τ – time of momentum duration.

Usually it is accepted that

$$\tau = 2,5T_1 = 2,5 \frac{2\pi}{\omega_1}, \quad (7)$$

where ω_1 – first circular frequency of plate natural oscillation.

Based on formulae (6) and (7) was obtained

$$F_{\text{imp}(z)}^{\text{av}} = \frac{M(1+k)v_{0z}}{\tau}. \quad (8)$$

It is assumed in formula (8) that only one impact occurs (without repetition). The impacting force, which should be applied to plate during time τ , is defined by formula (8).

The references [1 – 3] are dedicated to impact load theory. The up-to-date results concerning impact calculations are presented in references [4 – 9].

3. The plates under impact of mass point. The developed procedure is illustrated by a calculation example of steel plate, design diagram of which shown in Fig. 2. The analysis of stress-strain state of the structure member, caused by impact load of different level intensity at a constant impact momentum view, was fulfilled applying FEM.

The plate dimensions are: side $a = 1$ m and thickness $h = 1,25$ cm. It is made of low-carbon steel with following properties: $E = 2,1 \times 10^5$ MPa; $\nu = 0,28$; $\gamma = 77$ kN/m³. The plate is rigid fixed along its perimeter and modelled by uniform finite-elements mesh. The impact of load occurred at point K with coordinates $x = y = a/2 = 0,5$ m. The plate circular frequencies of natural oscillations $\omega_1 = 692,772$ s⁻¹, $\omega_2 = \omega_3 = 1408,08$ s⁻¹ were taken into account. The time $\tau = 0,023$ s of impact momentum duration at first circular frequency of plate natural oscillation was considered.

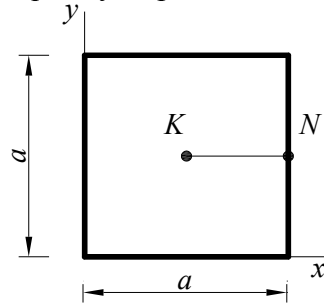


Fig. 2 Design diagram of plate

For the studying plate at load mass $M = 3$ kg and initial impact velocity $v_{0z} = 20$ m/s it is given the fields of deflection intensities distribution w for plate central surface (Fig.3) and the fields for main σ_1 , σ_3 and equivalent σ_{eq} stresses for the plate based layer were researched.

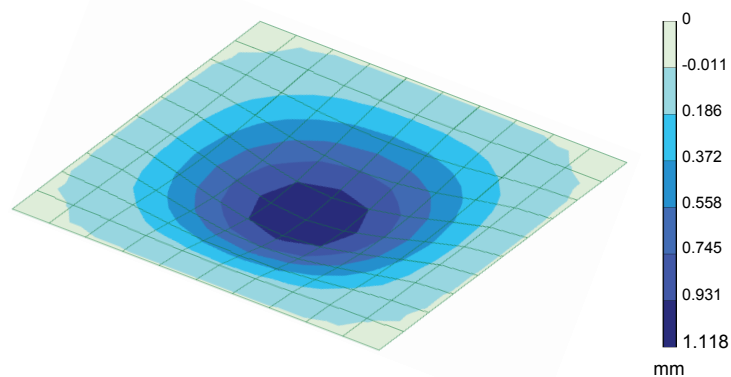


Fig. 3 Fields of deflection intensities distribution w for plate central surface

The analysis of the plate stress-strain state under dynamic impact load with different impact momentum intensity is presented in view of plotting some functional relations of the equivalent stresses level σ_{eq} and deflections w around a zone of extreme values at point K caused by load mass magnitudes that impacted into plate (Fig. 4).

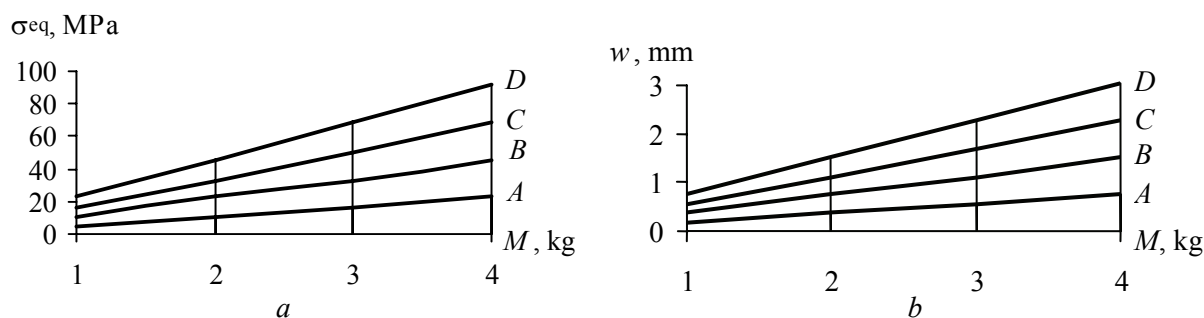


Рис. 4 Relations at variation of impact initial velocity v_{0z} at point K

$A - 10$ m/s, $B - 20$ m/s, $C - 30$ m/s, $D - 40$ m/s:

$a -$ equivalent stresses $\sigma_{eq} = f(M)$; $b -$ deflections $w = f(M)$

While studying influence of impulse view form on structure member stress-strain state it was taken into account the linear (Fig. 5 a, b, c) and curvilinear relations (Fig. 5 d, e) for impulse loading $F = f(t)$.

The diagrams of intensity of the deflections w and equivalent stresses σ_{eq} in plate cross-section KN for different impulse view form are presented in Fig. 6 under load mass $M = 3$ kg and impact initial velocity $v_{0z} = 20$ m/s, accordingly. The comparison of calculation results is given in Table 1.

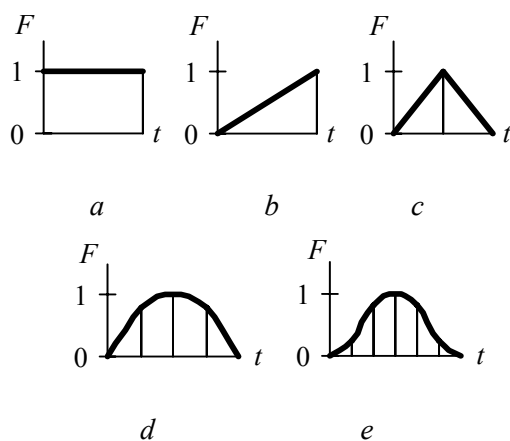


Рис. 5 Impulse form of view

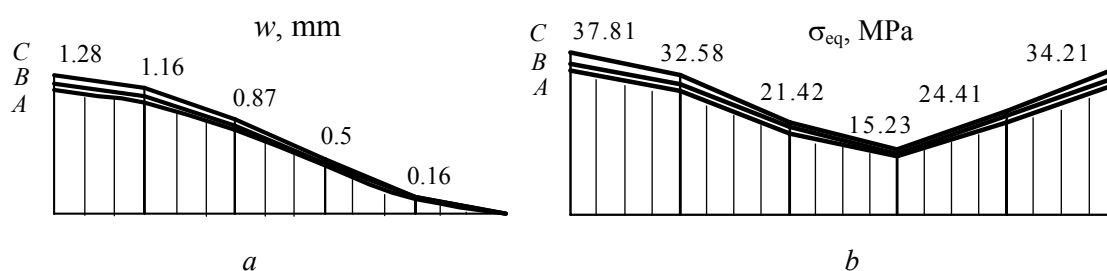


Fig. 6 Deflection w (a) and equivalent stress σ_{eq} (b) intensity distribution diagrams in cross-section KN depending on view of impulse: $A -$ Fig. 5, d ; $B -$ Fig. 5, b ; $C -$ Fig. 5, c

View form of impulse

Relations	Fig. 5, <i>a</i>	Fig. 5, <i>d</i>	Fig. 5, <i>b</i>	Fig. 5, <i>c</i>
w_{\max} , mm	1,12	1,14	1,20	1,28
$\sigma_{\text{eq}(\max)}$, MPa	33,02	33,56	35,40	37,81

4. The plates under impact of a massive body. It was also considered a plate under impacting of a body in the finite dimensions. The impact square is 40×40 cm. A magnitude of impulse load intensity and mass of impacting body were distributed on impact interface area accordingly.

The analysis of structure member stress-strain state was performed at constant view form of impact momentum intensity. The value of maximum deflection at point *K* was decreased to $w_{\max} = 0,831$ mm. The deflection distribution diagram onto plate surface is given in Fig.7. The maximum equivalent stress in our case occurred at *N* (see. Fig. 2) and equals to $\sigma_{\text{eq}(\max)} = 23,25$ MPa that proves a distribution of maximum stress intensity towards external plate contour.

The distribution field of the plate equivalent stresses σ_{eq} is given in Fig. 8.

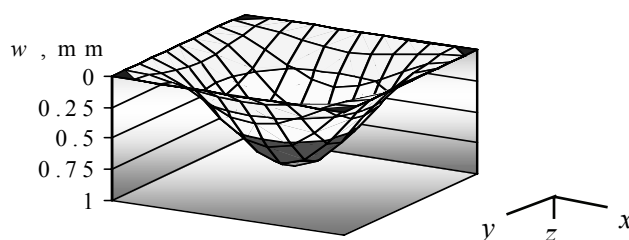
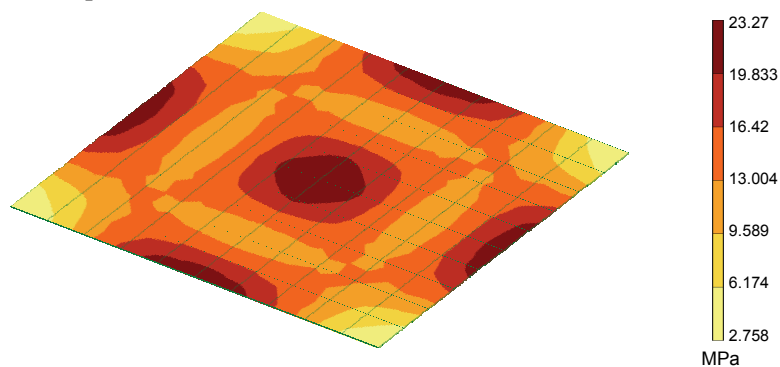


Fig. 7 The diagram of plate's deflections

Fig. 8 The stress field σ_{eq} of the plate caused by impact body of finite dimensions

5. The damages of plate caused by impact loadings. For the maintenance practice of sheet structure members the issues related to appearance of damages on structure surface due to material corrosion and others causes. The damages of such types often occur during operation of the aircrafts, ground-based machinery and military equipment.

This problem takes on special significance in cases when dynamic loadings occurs, for instance at impacting the damage sheet structures by bodies with significant intensity of impact momentum due to a great body mass or impact velocity.

The analysis of plate stress-strain state with damage area of 40×40 cm at its centre and thickness of $h = 0,5$ cm under constant view form of impact momentum intensity is illustrated by fields of its deflections and equivalent stresses (Fig. 9).

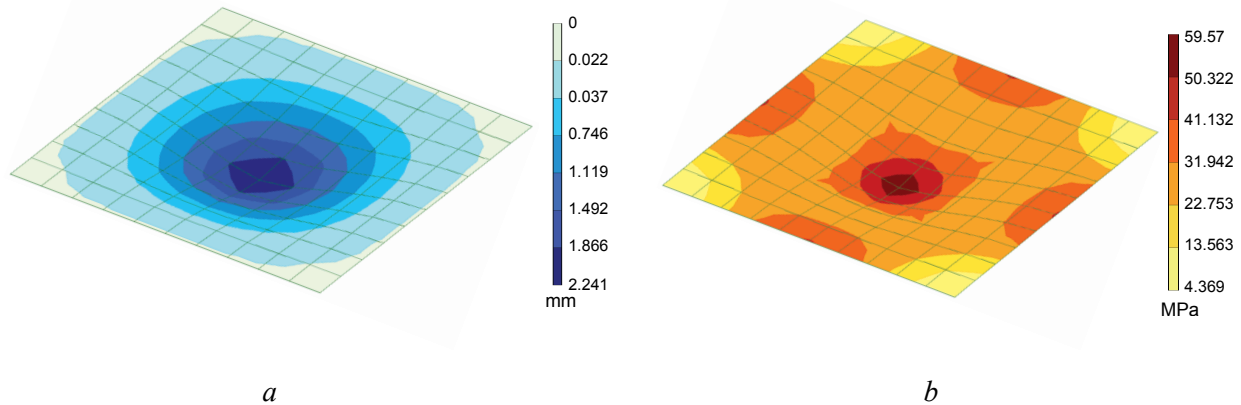


Fig. 9 The field of deflection w (a) and equivalent stress σ_{eq} (b) intensity distributions for damage plate

6. The plates with strengthening ribs under impact loadings. The effect of presence strengthening ribs in various cross-sections and its locations in area extend of plate was investigated. The stress-strain state variations due to failure one or several ribs were considered as well. The presence of damages in plate web also was analyzed.

It was considered a plate with stringers during action of mass point impact at the centre of plate under following conditions: $a = 1$ m, $b = 1,6$ m, $c = 0,4$ m, $d = 0,8$ m; two stringers in cross-section dimensions $50 \times 50 \times 3$ mm (Fig. 10). The analysis of structural member stress-strain state under constant view form of impact momentum intensity was performed. The value of maximum deflection at point K comes to $w_{max} = 2,244$ mm. The field of deflection intensity distribution onto plate surface is presented in Fig. 11. The field of equivalent stresses σ_{eq} intensity distribution of the plate based layer is presented in Fig. 12.

During analysis of damages in plate web the defects in the plate centre of dimensions 40×40 cm and deep of 2,5 mm and 5 mm were considered.

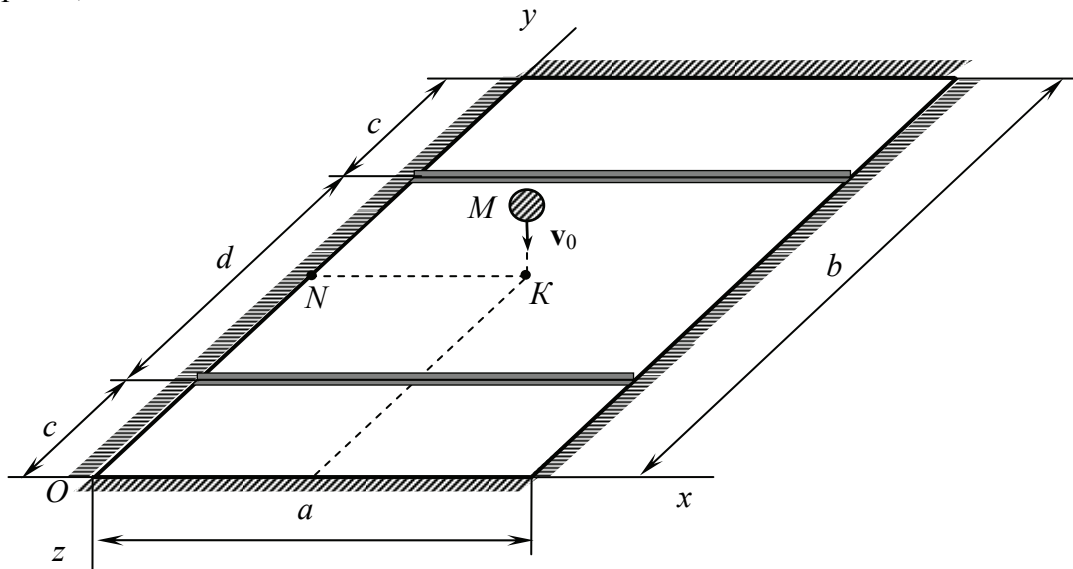


Fig. 10 The structure diagram of plate with stringers

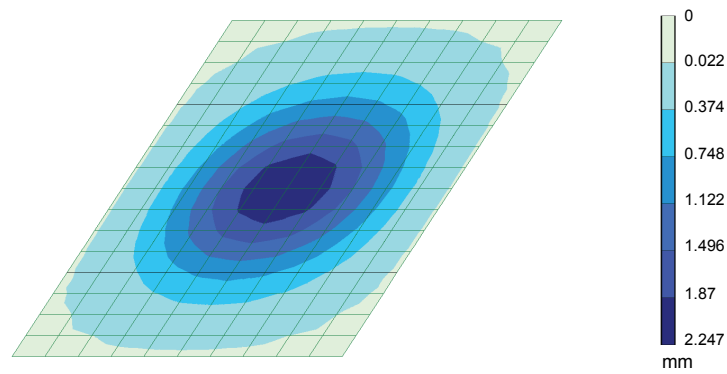


Fig. 11 The deflection field of plate with stringers

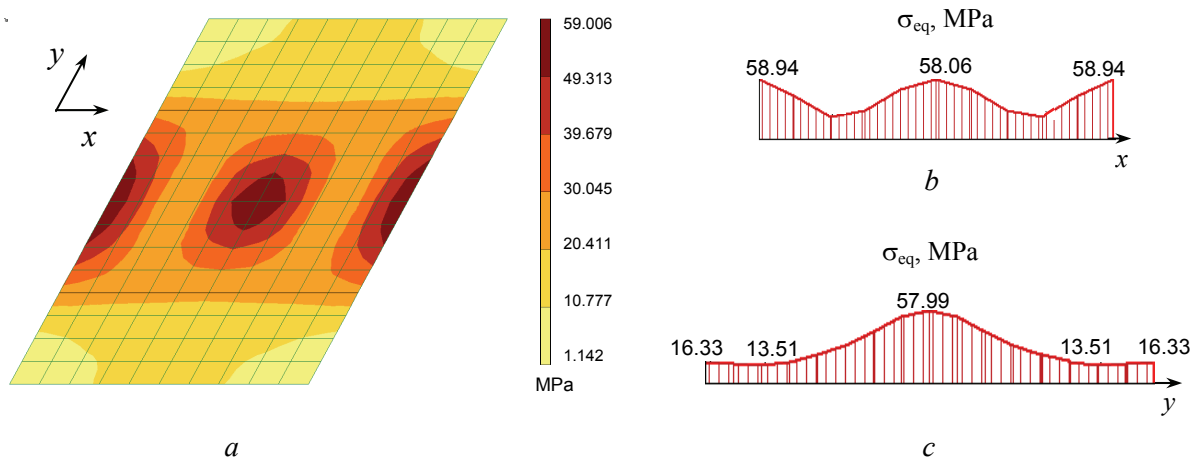


Fig. 12 Distribution of equivalent stresses σ_{eq} : *a* – in plate with stringers; *b* – in central cross-section along axis *x*; *c* – in central cross-section along axis *y*

The extreme values of deflections of the plate central surface w_{max} and equivalent stresses $\sigma_{eq(max)}$ of plate based layer depend on damage deep are given in Table 2. Corresponding diagrams of the plate equivalent stresses σ_{eq} in central cross section along axis *x* are shown in Fig. 13.

Table 2

Deep of damage, mm			
Relations	0	2,5	5
w_{max} , mm	2,244	2,962	4,18
$\sigma_{eq(max)}$, MPa	58,94	73,797	101,829

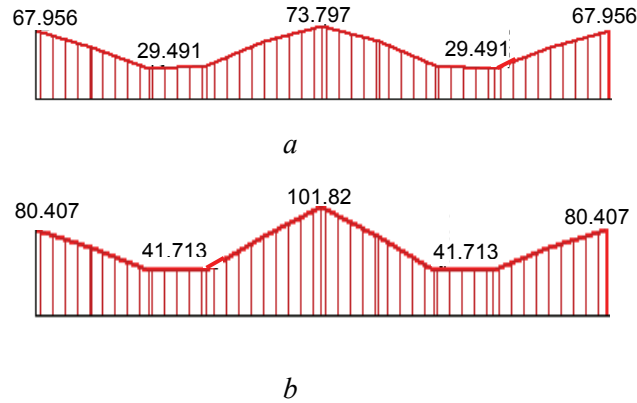


Fig. 13 Diagrams of equivalent stresses σ_{eq} (MPa) of plate with stringers in central cross-section along axis x at damage depths: $a - 2,5$ mm; $b - 5$ mm

7. The views of plate fixing. The influences of different plate boundaries fixing (Fig. 14) on their stress-strain conditions were studied. During analysis the diagonal matrix of masses under permanent view of impact momentum intensity were considered. The duration of impact momentum τ were taken into account under first circular frequency of plate natural oscillation ω_1 .

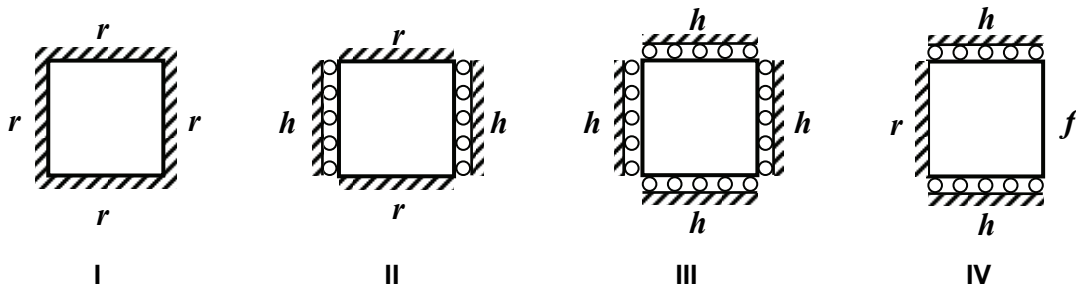


Fig. 14 The views of plate fixing along its edges:
 r is rigid fix; h is hinged fix; f is free end; I, II, III, IV are plate types

The stress-strain state was performed for the square plates of side dimensions 1 m and thickness $h = 1,25$ cm made of low-carbon steel with mentioned about mechanical properties. The plates are subjected to transversal impact of a point mass $M = 5$ kg into the centre under $v_0 = 50$ m/s. The values of maximum equivalent stresses $\sigma_{\text{эKB max}}$ and deflections w_{max} for different plate types and their cross-sections are shown in Figures 15 and 16 respectively.

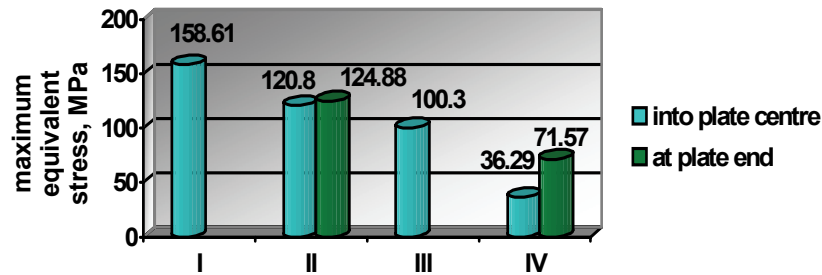


Fig. 15 The values of $\sigma_{\text{эKB max}}$ for different plate types: I – into plate centre;
 II – into plate centre and fixing; III – into plate centre; IV – into plate centre and free end

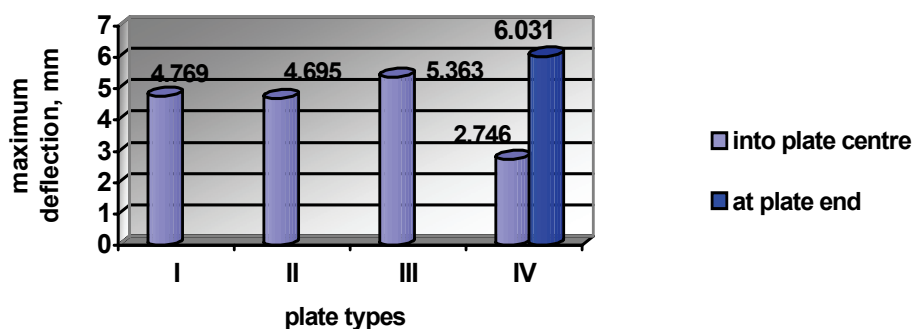


Fig. 16 The values of w_{\max} for different plate types: I, II, III, – into plate centre; IV – into plate centre and free end

8. Conclusions. Based on results of numerical analysis performed applying presented approach one may formulate the following statements:

1. It is suggested an effective procedure, which enables sufficiently solving the problems concerning impact action of load, that is based on FEM and impact theory, for plate formed structure analysis.
2. The influence of impact momentum view form was studied (four cases were analyzed). Here discovered that the most dangerous is impact momentum view form presented in Fig. 5,c).
3. Performed calculations demonstrated that considering dimensions of the impacting body leads to decreasing of the values of dynamic deflections and equivalent stresses.
4. The influence of plate corrosion damages was studying as well. The analysis of stress-strain state shown that under decreasing of plate thickness at damage area up to 40 % the maximum deflection value increased to 100,5 % and equivalent stress increased to 80,2 %.
5. The effect of strengthening ribs on stress-strain state of structure member was studied.
6. The influence of corrosion damages on plate with stringers was analyzed.
7. The effect of different plate boundaries fixing was studied.

The obtained results may be applied for analysis of the sheet structure members' stress-strain state under action of impact loading.

References

1. Гольдсмит В. Удар.: М., Стройиздат, 1965. – 448 с.
2. Харрис С.М., Криз Ч.И. Справочник по ударным нагрузкам.: Л., Судостроение, 1980 – 359 с.
3. Тимошенко С.П., Янг Д.Х., Уивер У. Колебания в инженерном деле.: М., Машиностроение, 1985. – 472 с.
4. Акимов А.А. Пространственное моделирование соударения компактного элемента с преградой методом сглаженных частиц./ 9 Всерос. съезд по теор. и прикл. механике. Аннотации докладов. Т. 3.: Нижн. Новгород, Изд-во НАГУ, 2006. – с. 11.
5. Радченко П.А. Численный анализ высокоскоростного взаимодействия анизотропных тел./ Физика и химия наноматериалов. Сб. матер. межд. школы-конф.: Томск, Изд-во ТГУ, 2005. – с. 442-445.
6. Sburlati Roberta An exact solution for the impact law in thick elastic plates. / Int. J. Solids and Struct, 2004.41, № 9 – 10. – p. 2539-2550.
7. Gao Zhen, Gu Yong-ning, Hu Zhi-giang. Impact strength analysis of ship hull. Shanghai Jiao Tong University, China. Chanbo lixue. / J. Ship Mech., 2005.9, № 2. – p. 77-82.
8. Онищенко А.В. Повреждаемость пластин при действии ударных нагрузок. / Матер. 4-ой межд. научн. конф.: Донецк, Юго-Восток Лтд, 2006. – с. 283-285.
9. Орлов А.С., Шатров А.К. Расчетно-экспериментальная оценка нагружения космических аппаратов при высоко-интенсивных импульсных воздействиях. / Вестник Сиб. гос. аэрокосм. ун-та, 2005, № 6. – с. 153-155.

V. V. Astanin, prof.
G.O. Olefir, mas.
(National Aviation University, Ukraine)

MATERIAL IMPACT STRENGTH RESEARCHES IN THE CONTEXT OF CIVIL AVIATION SAFETY

Test run of three layered composite material specimens with load-bearing metal frames and spacer mediums of several types is carried out using developed and manufactured experimental impact strength research installation "GANCHEN". It includes piercer accelerator, ballistic pendulum and residual deformation measurement device. Composite structures showing better impact energy absorption characteristics and consequently protection properties in the view of safety provision are determined.

1. Introduction

At the high level of technical equipment evolution the increasing attention is given to reliability of and construction usage safety maintenance while their development and operation. Besides more and more considerable requirements are exposed to specialized designs intended for protection. The problem of construction and material stability at impact loadings arises in many areas, starting with creation of protective designs and ending with constructing transport. Impact loading is a kind of dynamic loading, namely a pulse action at occurrence of a non-stationary strained deformed state in a volume of the loaded body that is quickly changing in time because of distribution of resilient-plastic and impact wave fronts and is transformed into a quasistatic or harmoniously changing state with the strain intensity reduction in time after the end of the transients [1]. This question is actual in aircraft because of the necessity of support of properties of technical and operational modern aviation equipment after collision with extraneous subjects and receptions of residual external deformations of construction members because of operation of aviation technical equipment in boundary modes or gradually accumulated residual deformations and also on account of transition to its on-condition maintenance. Bottom parts of fuselages, motor-gondolas, chassis gondolas and of aerodynamic aircraft surfaces intensively interact with thrown out from under the wheels or entrapped with the air-gas streams of aviation engines while taking off and landing stones, extraneous objects, sand, dust etc. This problem is important for helicopters that are used at small heights and with unprepared take-off platforms, for high-speed on-ground vehicles, such as automobiles and locomotives, for estimation of deformations of automobile bodies after road accidents. Construction ability for a troubleproof work in a wide range of operation conditions and its survivability degree directly influence upon the safety level as good as its protective qualities in the situations of intentional wrongful acts execution contra people, cargo, techniques using means, which action is aimed at construction destruction under the action of impact loading.

2. Problem Statement

Temporary situation in the sphere of civil aviation safety demands elaboration of new complicated composite impact proof materials and corresponding science intensive experimental installations for researches of their impact strength. Theoretical description and consequently practical usage of properties of solids and liquids at high pressures which exist in powerful impact waves, represent a very difficult problem rather wide of its final solution at present. Therefore experimental research methods of condensed substance in a compressed state take on special significance [2-4].

Thus the safety problem solution in aviation the same way as in other fields of human activities determine urgency of study of construction property and behavior under the action of external forces, which result in elastic or residual deformations depending on material structure and nature, and also the problem of comparison of deformation characteristics of different design

variants. All this is possible to be executed by means of development of a specialized research complex uniting opportunities of such impact interaction initiation and following definition and analyzing of reaction of material patterns to it, their characteristics.

3. Theoretical Experiment Grounds

Elastic pressure constituent in shock waves with pressure of about hundreds of thousands atmospheres and below predominate if it occurs in condensed substances in contrast to gaseous matters. All the intrinsic energy obtained by the substance in the wave is spent for repulsion forces overcoming at the body compression and is concentrated in the form of potential, elastic energy. The pressure range of about several tens and hundreds of thousands atmospheres has a great importance for practice. These are typical pressures mounted at explosive detonation, at water blasts, at impact of detonation products with metal obstacles etc. Mechanically solid equilibrium position at zero temperature and pressure is characterized with mutual compensation of interatomic attractive and repulsion forces and also with elastic potential energy minimum, which may be taken as its zero reference datum $\varepsilon_x = 0$. Scrutinizing shock waves of not too significant amplitude it is possible to ignore electronic pressure and energy constituents and to consider Gruneisen coefficient Γ to be constant and equal to its value Γ_0 at normal conditions. At the same time it is assumed that the wave is not too weak, so that it is possible to ignore also the initial unperturbed substance energy ε_0 . In fact it corresponds to admitting the start temperature to be equal to zero and to making no difference between the normal volume V_0 and the starting volume V_{0k} at temperature absolute zero. Such wave slightly differs from the acoustic one. It extends with speed close to acoustic speed, compresses the substance only to several or tens of percents and gives it velocity behind the wave front which is several times less than the wave eigen transmission speed. The atmospheric pressure is negligibly small in comparison to the pressure, which takes place at even very small body volume changes. So there is no difference if it is in vacuum conditions ($p_x = 0$) or in the atmosphere ($p_x = 1 \text{ atm}$).

The pressure p and specific inner energy ε of a solid substance may be considered in their two parts. The first ones, which are their elastic constituents p_x and ε_x , are bound only with interaction forces, which act between body atoms and completely do not depend on the temperature. The other ones which are thermal constituents are associated with the body heating, i.e. with its temperature. Elastic constituents p_x , ε_x depend only upon the substance density ρ and are equal to the full pressure and specific inner energy at the temperature absolute zero. So they are named below as cold pressure and energy for short. At the temperature absolute zero atoms perform null oscillations associated with the energy of $h \cdot \nu / 2$ per one normal frequency variation ν . This energy may be included into potential energy $\varepsilon_x(V)$ so that ε_x is observed starting from the zero oscillation level in the body equilibrium state at $p_x = 0$. The elastic pressure is connected with the potential energy with the relationship $p_x = -d\varepsilon_x/dV$. It has a natural mechanical meaning of equality of the energy increment to the compression work. This correlation may be considered as isotherm or adiabatic cold compression equation. Potential energy and elastic pressure dependences on solid specific volume are schematically shown in the fig. 1,a.

Mass, impulse and energy flow conservation law for the shock wave front have completely general meaning without regard to aggregative state of the substance in which the wave propagates. Shock wave transmission speed in the unperturbed substance is designated as D and mass speed surge in the wave front is designated as u and is equal to the substance speed after the front in the laboratory coordinate system if the substance initially rests. Omitting index for values after the wave front the mass and impulse conservation laws are written as $V_0/V = D/(D-u)$ and $p = D \cdot u/V_0$. Excluding the speed u in these equations the pressure gets calculation formula

$p = D^2 \cdot (1 - V/V_0)/V_0$. In capacity of third energetic correlation percussive adiabat equation is taken at $p_0 = 0$: $\varepsilon - \varepsilon_0 = 0,5 \cdot p \cdot (V_0 - V)$ [5].

The full energy obtained by one mass unit of a substance in the result of impact compression $p(V_0 - V)$, is distributed equally between the kinetic $u^2/2$ and inner $\varepsilon - \varepsilon_0$ energy. It holds for the coordinate system in which unperturbed substance rests. In turn the inner energy variation consists of elastic and thermal energy changing. If to consider a shock wave distributing in the body at zero temperature $T_0 = 0$, the variables have the next values: $\varepsilon_0 = 0$, $V_0 = V_{ok}$. The continuous substance p, V - diagram for impact compression of (fig. 1, b) contains cold compression adiabat curve p_x and percussive adiabat p_H . The last one is naturally above the cold compression curve because the full pressure after the wave front combines both elastic and thermal pressures.

The obtained by the substance elastic energy ε_x is numerically equal to the horizontally hatched curvilinear triangle OBC area: $\varepsilon_x = \int_V^{V_{ok}} p_x dV$. The full inner energy ε according to the impact adiabat equation is equal to the triangle OAC area. The difference of these areas, which is vertically hatched, performs the thermal energy of the substance which was subjected to impact compression. As it may be seen from the fig. 1, b, the area OAC is necessarily greater than the area OBC, if only the cold compression curve is bulged relative to the volume axis ($d^2 p_x / dV^2 > 0$), that is usually true. So the substance is always heated in the shock waves and its entropy increases. It is completely general statement arising for solids from the elastic substance properties.

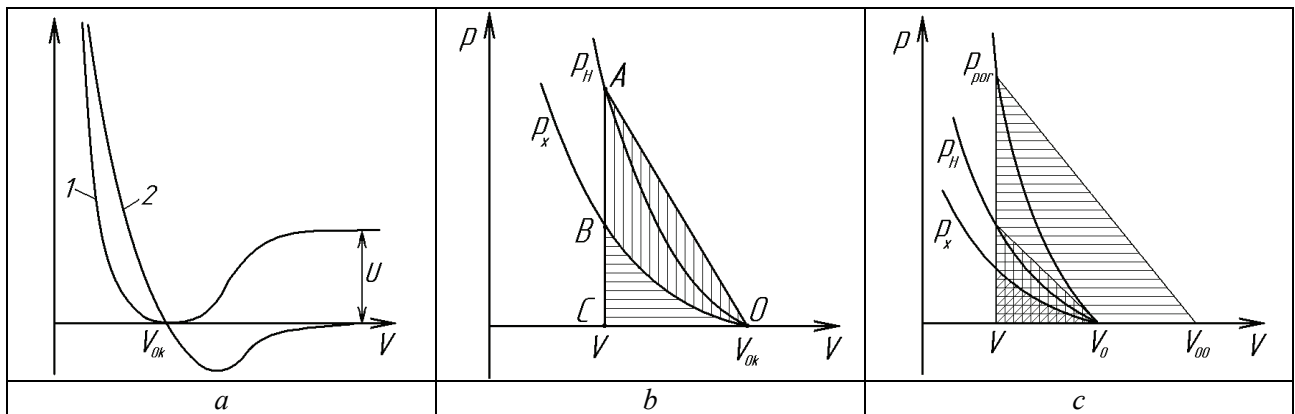


Fig. 1. Graphic chart of dependences of solid parameters on volume: a – curves of potential energy ε_x (1) and elastic pressure p_x (2); b – p, V - diagram for impact compression of continuous substance; c – p, V - diagram for impact compression of porous substance; p_x – cold compression curve, p_H – continuous substance percussive adiabat, p_{por} – porous substance percussive adiabat

There are significant differences in impact loading action for porous substances comparing to the continuous ones. The porous bodies may have very different nature and structure and may be powders, bodies with inner interstices, fibrous bodies. All of them are characterized with presence of more or less coarse particles and continuous substance zones with normal density of $\rho_0 = 1/V_0$ and hollow zone thanks to which the average specific volume V_{00} is greater then the normal one V_0 and the average density ρ_{00} is less then the normal one ρ_0 . At impact porous body compression to high pressures the usual continuous substance adiabat may be considered being coincident with the cold compression curve. The effects connected with strength and initial temperature $T_0 \approx 300^\circ \text{C}$ distinction from zero are neglected.

If the substance is continuous and homogeneous behind the shock wave front in the final state, the percussive adiabat is given by the fig. 1, c in accordance with the conservation laws for the shock

wave front and the substance constitutive equation. The corresponding to the normal volume V_0 and zero pressure $p = 0$ point is laying in the percussive adiabat. The obtained by the substance in the shock wave inner energy $\varepsilon = 1/2 \cdot p(V_0 - V)$ is equal to the horizontally hatched triangle area. Its elastic part is equal to the curvilinear triangle area, which is limited with the curve $p_x(V)$ and thickly hatched in the fig. 1. The more is the initial volume V_0 , i.e. the higher is the initial substance porosity, the more is the difference between the areas, which corresponds to the thermal part of the energy at porous substance compression to the same final volume. Here the elastic energy at a given volume does not change and the full one is increasing. So the more is porosity, the more steeply is the percussive adiabat. Specifically percussive adiabat points are situated higher for porous body then for continuous body. For porous substance compression to the same volume as the analogous continuous substance much higher pressures are necessary. They are the higher the higher is the substance porosity degree. The situation does not change qualitatively if to consider the initial temperature and entropy to be not equal to zero [6].

Therefore it is possible to suppose that porous substance usage as medium layers for three dimensional composite materials will promote to increase of impact energy absorption by the construction, which is made of it, because of initiating of its dissipation in the form of thermal intrinsic composite substance energy. To check this supposition it is necessary to carry out a series of comparative experiments of specimens with the same supporting layers but with inner layers of different porosity and subsequently of different density and nevertheless made of identical material so they provide equal mass of the produced constructions.

4. Research Equipment Elaboration

The extreme short impact loading duration demands usage and elaboration of special measurement methods, which allow definition of physical parameters in the conditions of high speed process, demand creation of corresponding devices. Specially for carrying out of experiments on research of impact durability of monolayer materials or materials of complex composite structure and constructions of them, computerized research complex is developed and produced. It serves for carrying out experiments on impact interaction of specimens with an accelerated to a certain velocity piercer. The complex includes "GANCHEN"-type thermal gas ballistic gun for piercer accelerating, piercer velocimeter, ballistic pendulum for measurement of integral energy datum of piercer-specimen interaction, and "ODD" device for measurement of residual deformation of the specimen. The principle of thermodynamic gas expansion processing at chemical reaction of burning with energy eduction is used for the piercer racing. The experiment progress control, gauging equipment sensor signal processing and obtained information data storage are accomplished at researches. The elaborated system and research techniques permitted carrying out a series of comparative check tests of specimens of different metal-composite constructions.

Impact strength researches are strictly regulated with numerous state and international standards. Among them are European standards CEN, Germany police administration's standard DIN 52290. They were considered at development of the research equipment. The used method essence is as follows. The researched samples are punched with a piercer as obstacles. Energy characteristics of the impact process are defined with the ballistic pendulum on which the investigated samples are fixed. It receives an impact pulse while punching which causes the pendulum deviation of size S from the equilibrium position that may be used for calculation of the power absorbed by the sample during its deformations and fracture according to the energy balance equation [2, 5]:

$$E = \frac{m}{2} \left[2V_0^2 \cdot \frac{S}{S_1} - V_0^2 \left(\frac{S}{S_1} \right)^2 \right] = \frac{mV_0^2}{2} \left[2 \frac{S}{S_1} \left(1 - \frac{S}{2S_1} \right) \right],$$

where m – piercer weight, V_0 – collision speed, S_1 – pendulum position, $S_1 < S$.

The laboratory installation "GANCHEN", which principal scheme is given in the fig. 2, is a computerized equipment complex, which consists of the thermal gas ballistic accelerator – the flouncing device 3 for the piercer 5 racing, the piercer velocity measuring set 4, the ballistic pendulum 6 for researched material specimen 10 fastening and data acquisition and analysis system 1. The flouncing device 3 also includes the power supply unit 2, working gas supply system 7, diaphragm unit 8 and acceleration tube 9. Data acquisition and analysis system 1 serves for the experiment process controlling, processing of measuring equipment sensor signals and the received information saving. The ballistic pendulum 6 is used for estimation of the impact interaction energy characteristics. The installation also includes residual deformation damage definition system 11.

The action principle of the developed thermal gas dynamic flouncing device in the structure of the research ballistic installation is as follows. At guidance of the system 4 and with help of the working gas supply system 7 the flouncing device chamber is filled with working gas at a certain pressure. The ignition system due to work of the power supply unit 2 creates the electric spark discharge on a specially developed lengthened electrode located directly in the chamber. It initiates the chemical reaction of burning accompanied with a temperature and pressure increase that results in destruction of the diaphragm and accelerating of the piercer in the tube 9.

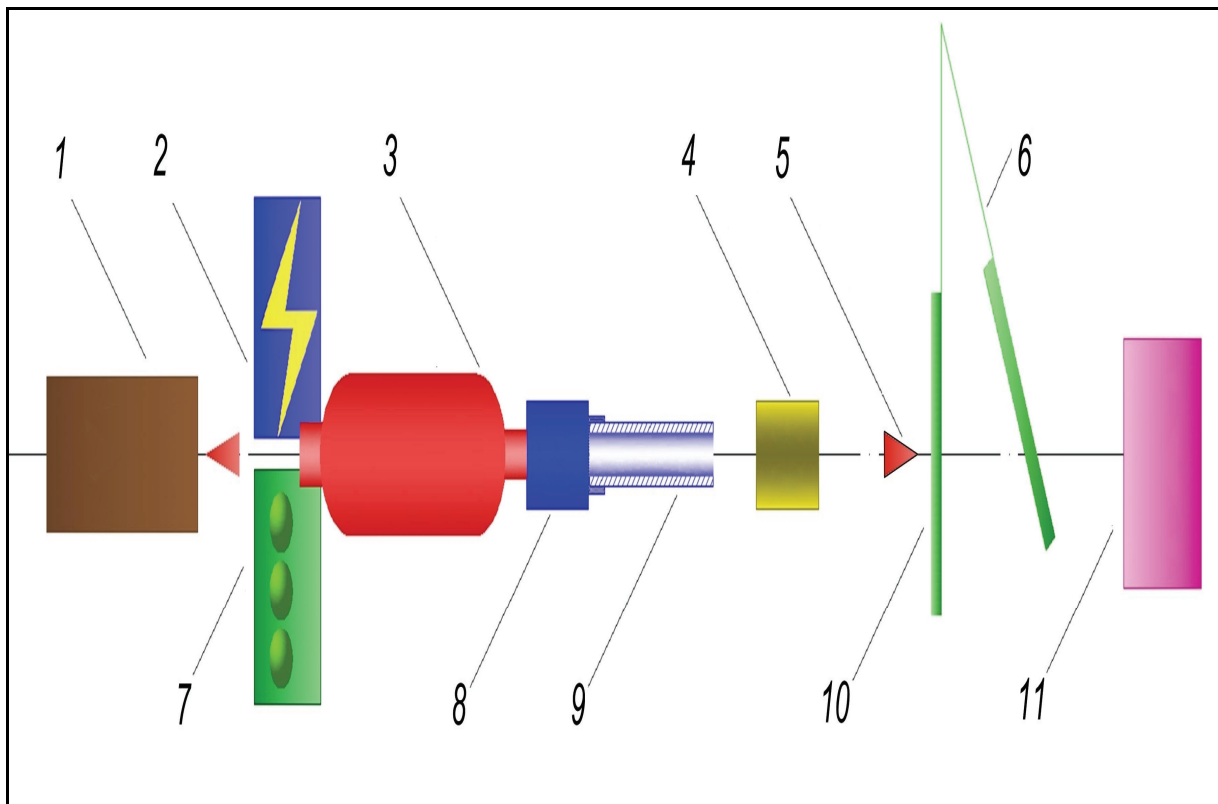


Fig. 2. Thermal gas ballistic laboratory installation "GANCHEN" principal scheme: 1 – data acquisition and analysis system; 2 – power supply unit; 3 – flouncing device; 4 – piercer velocity measuring set; 5 – piercer; 6 – ballistic pendulum; 7 – working gas supply system; 8 – diaphragm unit; 9 – acceleration tube; 10 – researched material specimen; 11 – residual deformation damage definition system

A butane-air mixture is used as the working gas in the constructed installation. The electric ignition unit provides a voltage of 25-30 kV for the spark creation. Power supply is effected from a network (220 V). The power supply unit 2 transforms the alternating current to direct current with voltage of 27 V for work of the hydraulic automatics of the unit 7, the electric ignition unit and particularly for the controlling unit 1. A special working chamber internal surface form is designed for receiving a cumulative effect and thus considerable increase of the installation effectiveness is

obtained. Several safety levels are incorporated in the working gas supply system design, which are duplication of the gas access overlapping cranes, the fulfilled gas release system for the case of unforeseen pressure increase and others. The unit 1 provides control remotability and consequently safety of work with the installation. The installation advantages are compactness, simplicity of work and control remotability, modular structure that makes possible not only replacement of the deteriorated units, but also experimentation with usage of different types of igniters, diaphragms, acceleration tubes, power supply units of different capacity. The experiment is carried out according to the following procedure. The piercer is accelerated to a fixed velocity and the level of the remainder deformation or destruction after the impact is determined for each material of the list of the researched ones. The piercer velocity is measured with a device communicated with the data acquisition and analysis system and transmitting the data on its values for usage in the further calculations.

For an operative complex qualitative and quantitative estimation of macro and micromechanical damages of material surfaces with calculation of both the damage geometry and complex integrated parameters of deformation destruction a special device was created and patented – optical deformation detector ODD [7, 8]. Its modification ODD-L was used at the experiment execution. Its operation principle consists in projection of an obtained with a laser radiator grid image on the studied surface and the following surface image receipt with the help of a photosensitive matrix. Specially designed program software allows definition of coordinates of surface points and calculation of residual deformation cavity parameters by means of analysis of the initially projected grid image curvatures. Precision of definition of the surface coordinates depends on the created laser beam quality, the matrix sensitivity, computer algorithm of the data processing etc. In the realized device the received precision is 0.01 mm.

5. Experiment Operation and Analysis of Research Results

The developed installation and research techniques allowed carrying out a series of tests of composite material specimens. Three layered composites with load-bearing metal frames and spacer mediums of several types were studied. Three test runs were executed, in each of them a quantity of specimens enabling building a statistical distribution of obtained results was analyzed. Specimens of two types were researched. For the sake of convenience the specimen layers were numbered in the following way. Metal layer facing towards the piercer is marked as the first one. The layer, after which the shock wave exit out of the specimen takes place, is numbered as third. Accordingly the medium layer is considered as the second one. In the first test run the medium composite layer was made of polyvinylchloride, in the second test series it was cellular polystyrene and in the third one it was a metal grating structure. In the specimens of the both types the second layer was made of the same material, but it had porous structure in the first case and continuous structure in the second case. Specimens of one test series have the same weight and chemistry. In the third test run grating usage allowed obtaining porous metal layer. In the corresponding specimens of the second type metal plates of the same mass were utilized.

With the help of the elaborated thermo gas ballistic accelerator the piercer was raced to the speeds of accordingly 200 ± 0.4 , 350 ± 1.2 , and 450 ± 2 m/s for every test series. Piercer velocity support was realized by proportioning the actuating medium amount in the flouncing device working chamber. The velocity selection is explained with provision of the not throughout specimen punching condition. So that in the result of interaction the material gets only residual deformation of the third layer in the form of a cavity. Specimens with work area of 100 x 100 mm were fixed on the ballistic pendulum. So the energy transferred to the specimen from the piercer but not absorbed by the material layers was defined. By definition of the track passed by the reflected from the specimen piercer in the opposite to its initial motion direction it was found out that amount of its residual kinetic energy after interaction with the specimen was too small in comparison to the initial one.

Appearance of the material specimens with the medium layer of cellular polystyrene after punching with the piercer is given in the fig. 3.

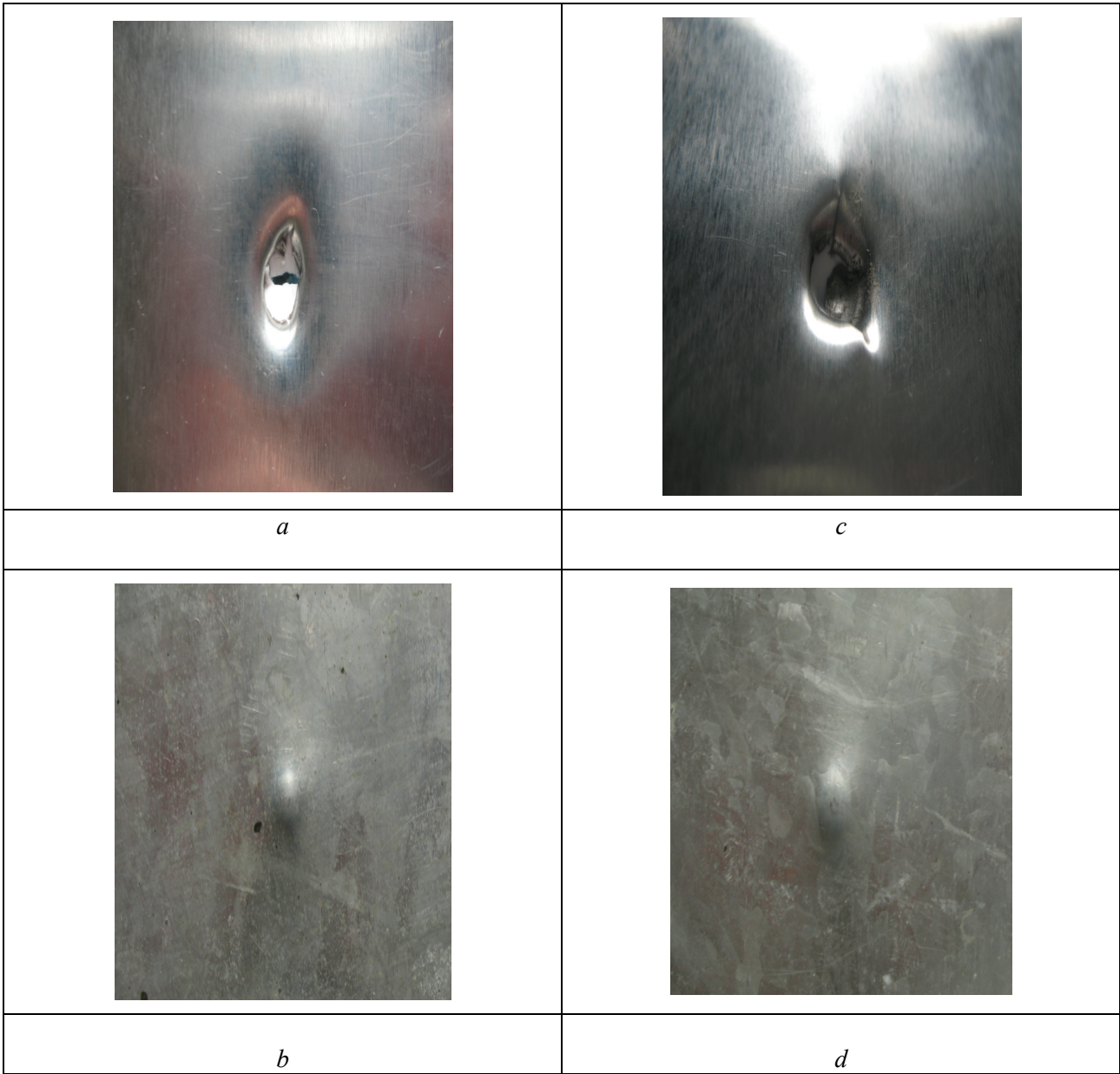


Fig. 3. Material specimen appearance after interaction with the piercer in test with a specimen of the first type (porous) from the front (a) and from behind (b) and in test with a specimen of the second type (continuous) from the front (c) and from behind (d)

In the fig. 4 three-dimensional cavity models are shown with color and numerical representation of their parameters. The models were obtained as a result of residual deformation measurement for both types of specimens of each test run. As it is seen from the given models, there is a clearly defined dependence of residual deformation value upon the medium specimen layer porosity in each experiment series.

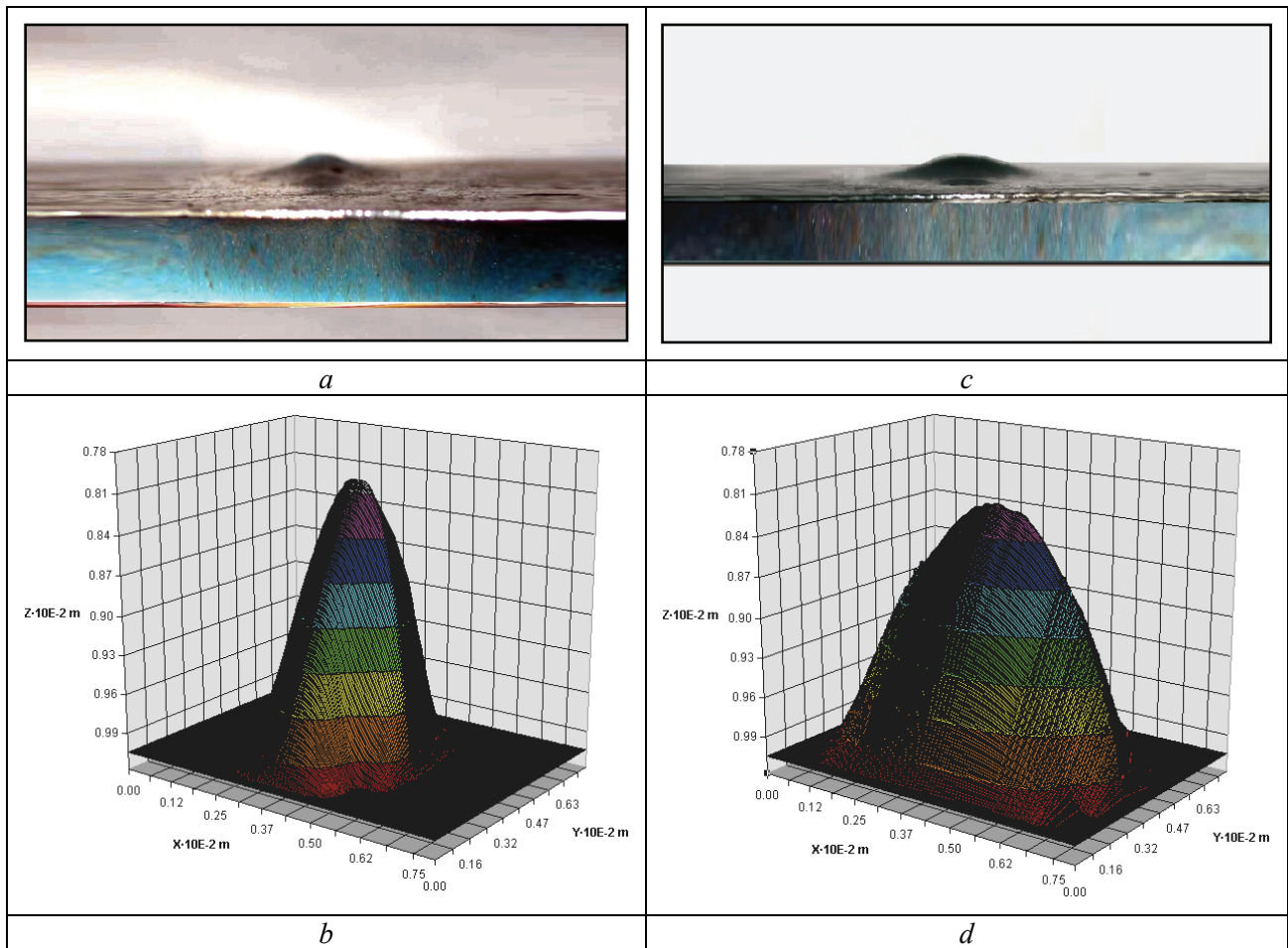


Fig. 4. Cavity appearance (a) and deformation model (b) in test with a specimen of the first type (porous); cavity appearance (c) and deformation model (d) in test with a specimen of the second type (continuous)

Moreover in each case the higher porosity is accompanied with less strongly pronounced residual deformations of the third specimen layer. Percentage ratio of the working area residual deformation degree at interaction realization in all the three cases is given in the table 1. The observed according to its volume deformation is differing from about 1.2 to almost 2 times. Therefore differs the damage of potentially protected by the composite constructions.

Table 1.

Specimen residual deformations in the three test runs

Test run	Average specimen deformation, $\cdot 10^{-6} m^3$		Residual deformation value ratio, %
	with porous spacer mediums	with continuous spacer mediums	
1	0.025	0.03	0.83
2	0.018	0.034	0.53
3	0.020	0.027	0.74

As it implicates from the considered above theoretical analysis of the impact interaction processes, which was given in the third section, the elastic constituent of the energy obtained by the specimen as a result of impact should not essentially differ for specimens of one test series. Pendulum suspension deflection values received for each separate experiment verify that such supposition was righteous in practice to 4.5 %. This deviation may be explained by the initial piercer velocity fluctuations, specimen fixation rigidity distinctions in each separate test and by other variations in experiment holding conditions. Taking into account the clear tendency of the general regularities evincing, the deviation is small for influencing on their revelation. In that case the given in the table 1 values testify to different levels of resulting shock wave energy acting onto the third material layer. Its decrease for composites with porous materials is explained with its transition into the form of potential and intrinsic energy of the second layers.

Thus carrying out of comparative impact interaction tests of three layered material specimens with load-bearing metal frames and spacer mediums of porous and continuous structure showed that utilization of porous substances for medium layers contributes to increased impact energy absorption by construction made of it.

6. Conclusion

For properties of constructions and behaviour estimation under the action of high-speed impact loadings and comparison of corresponding characteristics of materials and different constructions' execution variants at the stage of their material development or engineering of the compete design, specially for carrying out of experiments on research of shock durability of monolayer materials or materials of complex composite structure and constructions of them, laboratory research ballistic installation "GANCHEN" is developed and produced. The developed system and research methods enabled carrying out a series of comparative researches of material specimens with computer processing of gaging equipment sensor signals and obtained information saving. Impact interaction parameters of materials with load-bearing metal frames and spacer mediums of porous and continuous structure were learned. The experiments were considered according to the shock wave transmission theory.

While carrying out of the tests it was shown that usage of porous substances as spacer layers of three layered composite materials facilitates to increased impact energy absorption by construction made of it. So such materials have heightened protective qualities at the same mass of produced of them construction. It is perspective in spheres of surface protection of transport vehicles, such as aircrafts, helicopters, automobiles, trains, cutters and yachts, for light armoring system elaboration. Such materials may be utilized in constructions of divide walls and partitions, pilot and passenger chairs, doors and floor panels and also for shockproof constructions used in water, wheeled transport, in another fields.

Obtained results gave an opportunity to state the next aims and research directions for development of impact-resistant composite materials applicable in aviation, ground transport and protective constructions.

References

1. Прочность материалов и конструкций / Редкол.: В.Т.Трощенко и др. – К.: Академперіодика, 2005. – С. 574-703.
2. Астанін В.В. Деформирование и разрушения преград при пробивании цилиндрическим ударником. В кн.: Динамическая прочность и трещиностойкость конструкционных материалов. – Киев, 1986, с. 23-27.
3. Степанов Г.В. Прочность при импульсных нагрузках // Механическое поведение материалов при различных видах нагружения.— Киев: Логос, 2000, с. 421-536.
4. Зубов В.И., Степанов Г.В., Широков А.В. Деформирование и разрушение образцов из высокопрочных металлов при высокоскоростном нагружении //Артиллер. и стрелк. вооружение. -2004.- В. 2. - С. 17-22.
5. Астанін В.В., Галиев Ш.У. Численно-экспериментальные исследования упругопластического взаимодействия ударника с преградой. – Проблемы прочности, 1987, № 11, с. 97-100.
6. Зельдович Я.Б., Райзер Ю.П. Физика ударных волн и высокотемпературных гидродинамических явлений. – М.: Наука, 1966.
7. Сканування механічних пошкоджень поверхні конструктивних елементів / Астанін В.В., Олефір Г.О. // Вісник НАУ. – К.: НАУ. – 2006. – №1. – С. 95-99.
8. Патент UA 31774. Пристрій для автоматизованого визначення координат тривимірної криволінійної поверхні об'єкта. Національний авіаційний університет. Астанін В.В., Олефір Г.О. – Опубл. в Б.В. №8, 2008.

V.V. Astanin, Dr Sc. Prof.
P. Vynogradskyy, PhD
(National Aviation University, Ukraine)

MULTIPURPOSE DATA ACQUISITION SYSTEM FOR INVESTIGATION OF MECHANICAL PROPERTIES OF MATERIALS

Multipurpose mobile data acquisition system (DAS) of Laboratory of strength of materials, Mechanics chair of NAU is intended for strength testing of materials and aviation/industrial structures as well as for automation of educational laboratory works. DAS permits to control testing machines and experimental rigs and perform measurements of up to 32 analog signals of appropriate transducers.

Introduction

With the development of microelectronics and computer hardware a great progress has been achieved in development and implementation of sophisticated test rigs for experimental investigation of different physical phenomena. In the field of strength of materials a number of firms begin to produce computer-controlled testing machines with appropriate software permitting to conduct the set of standardized tests with controllable regimes of loadings. Such machines however are very high-priced and often are intended for routine everyday testing. Ukrainian plants and scientific/educational institution like that in other post-soviet countries for almost two decades were unable update their park of testing machines. Still now the regular cost of order of \$100 000 is too high for many Ukrainian entities equipped with aged machines. This is even more true for educational institutions, which need from one hand a number of machines for educational purposes and from other hand a flexible multipurpose test rigs to perform scientific investigations. In Laboratory of Strength of Materials of Mechanics chair of National Aviation University of Ukraine the approach of creation of multipurpose expandable data acquisition and control system has been chosen to satisfy the demands of up-to-date testing. This permitted step-by-step improving of testing capabilities with gradual automation of different scientific and educational testing rigs and no high lump sum payment.

Nomenclature

DAS	data acquisition system;
GUI	graphic user interface;
I/O	input/output;
K_A	strain gage amplifier gain coefficient;
ksps	kilosamples per second – number of signals measured per second;
LVDT	linear variable differential transformer;
P	load;
ΔL	absolute deformation;
ε	relative deformation;
σ	stress;

1. Data Acquisition and Control System Concept and Composition

Modern data acquisition systems are usually include regular or specialized computer with one or more extension boards for data acquisition and control. It could be a multifunctional data acquisition board with opportunities to measure and generate analog and digital signals or a set of specialized boards capable to perform specific task, for instance only measurement of analog signals or generation of analog output signals. These boards could be installed in the expansion slots of

computer's motherboard (ISA, PCI) or connected to computer via different ports – USB, COM, SCSI, etc.

Several aspects should be taken into account to make a decision concerning DAS architecture. At the beginning of the work a set of tests to automate and park of existing machines and test rigs have been analyzed and list of parameters to be measured and controlled have been created. According to scientific and educational load on the laboratory it was found appropriate to create one multifunctional system rather than a number of separate systems with individual DAS in each. The hardware from different vendors was investigated on the cost-beneficial basis accounting to both hardware cost and the complexity of software development and implementation for a specific task. The issues of accuracy and measurement errors as well as opportunities of dynamic measurements and possible sampling rates were taken into account.

The concept of multiple functionality requires that DAS should be mobile and be easily connected to any test rig in the laboratory. That is why all the equipment must be mounted in the single and transportable unit. This forced to use internal expansion board(s) installed inside the computer and the latter is to be mounted in the same rack with all necessary signal conditioners, power sources, wiring and computer peripheral devices such as monitor, keyboard with mouse. The composition of hardware in this unit is defined by scope of tasks to be performed by DAS. The analysis have shown that almost all measurements performed in the laboratory include not more than two parameters such as load (or pressure) and displacement and a number of signals of strain gages, which often exceed 16 – the number, typical for multifunctional data acquisition boards.

The final requirements to DAS were formulated as follows:

- Number of analog measuring channels – up to 32;
- Signal types – high-level pressure transducer signals, deformation sensor signals, strain gage bridge signals, etc.;
- Opportunity to acquire discrete signals of test rig state;
- Opportunity to generate discrete and continuous (analog) control signals.
- Connection to external instrumentation using serial communication ports (RS-232, USB) and to LAN.

The main requirements to computer were:

- Easy software coding using “rapid prototyping” approach;
- Graphical representation of measured parameters in the course of experiment;
- Opportunity of remote observation and control of the experiment.

These requirements have led to the following hardware composition. DAS is mounted in wheel-based Schroff's “Proline” industrial cabinet (figure 1), where all the other instrumentation is mounted:

1. Industrial on-line uninterruptible power supply to prevent equipment damage from power supply failure;
2. Stabilized DC power source 24 V, 3 A to power transducers and signal conditioners;
3. Industrial computer with expansion boards, monitor; keyboard with mouse. Expansion boards are from Advantech company and include:

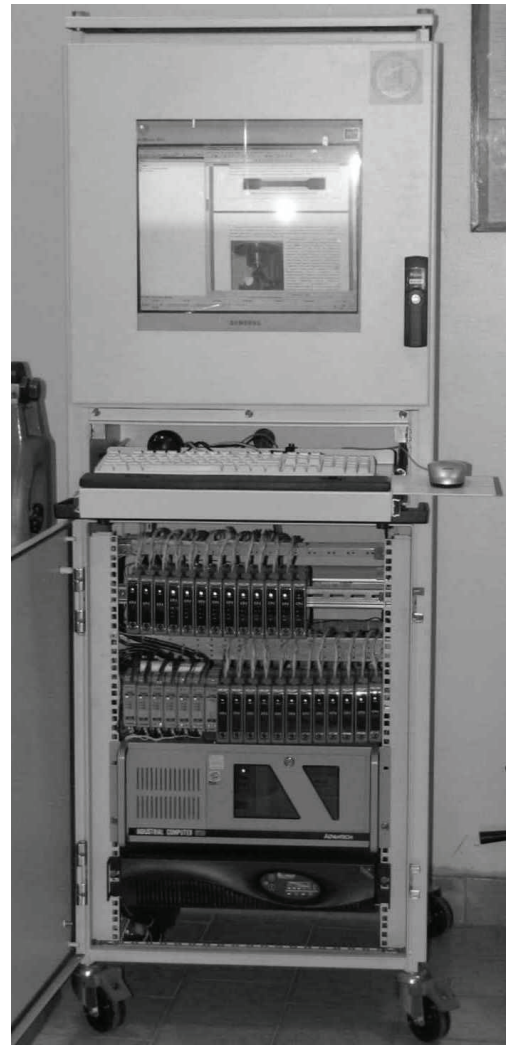


Fig. 1 DAS Front View

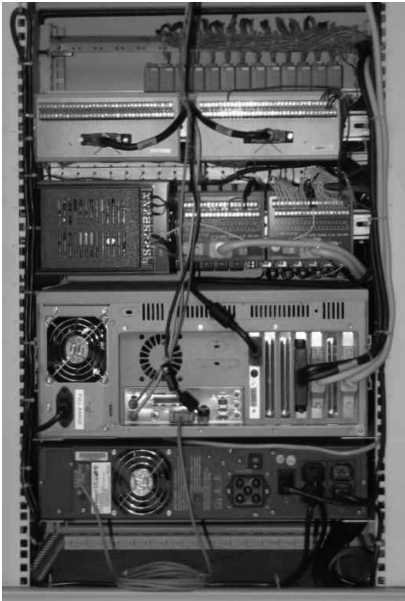


Fig. 2 DAS Rear View



Fig. 3 DAS Output Connectors

- a) PCI-1713 32-channel analog input board with 12-bit analog-to-digital converter and up to 100 kbps sampling rate;
 - b) PCI-1720 4-channel 12-bit analog output board;
 - c) PCI-1753 12-byte digital I/O board;
 - d) All boards have galvanic insulation up to 2500 V to prevent system damage in harmful industrial electromagnetic surrounding.
4. 30 strain gage amplifiers;
 5. Web-cam for remote observation;
 6. Appropriate internal wiring with screw terminals and connection cables to connect respective signal sources and external controlled devices to expansion boards (figure 2);
 7. Three output multipin connectors and power supply connector are located in a special holder on the left-down part of the cabinet (figure 3) and intended to reach easy connection to outer devices.

DAS composition and mobility provide its multiple functionality together with output connectors. One of them is universal 45-pin connector containing six 4-wire strain gage channels, 2 analog input channels, 2 analog output channels, 3 digital input and 2 digital output channels, 24 V DC pin and common (GND) pin, 2 pins for RS-485 connection and 8 pins for LAN connection. Two other are identical 50-pin connectors containing twelve 4-wire strain gage channels each. This permits

connection of any test rig in laboratory for both measurement and control.

All software has been created using MATLAB package and appropriate toolboxes. Individual programs may include Simulink blocks with real-time windows target blockset. This permits to avoid low-level programming of data acquisition procedures and gives access to easy-implementing real-time graphics together with extensive and sophisticated data processing tools. MATLAB approach to data acquisition tasks utilizes both “Switch-and-measure” and “Easy prototyping” concepts. For simple single-mission tasks it is possible to compose very easy software program with minimal coding and graphic representation of measurement results. For routine tasks it is relatively easy to create software program with necessary graphic user interface, which permits software and hardware tuning and which could contain soft real time blocks for test rig control. As compared to LabView software package widely used for solving measurement tasks, it could be mentioned that it is intended mainly for specialists in data acquisition and requires understanding of functioning of data acquisition hardware. Matlab's data acquisition concept on the contrary is oriented to specialists in particular branch of knowledge (engineers and scientists), say specialists in strength-of-materials, who's business is strength testing, not data acquisition.

2. DAS Application Examples

2.1 Tension test of standard specimen

Standard 8 mm in diameter specimen was tested using ZDMU-30 test machine. It was controlled manually because automation of hydraulic drive of this machine requires servo drive with loop-back, which could not be easily built. Measurement of tensile force was performed using Danfoss pressure transducer installed in the pressure line of power cylinder of the machine. The correlation between measured pressure and applied force was obtained via preliminary calibration using standard (reference) dynamometer. Absolute deformation of the specimen was measured using precalibrated strain gage deformation sensor connected to one of strain gage amplifiers. In the

course of the experiment instantaneous values of load and absolute deformation were displayed on the monitor. After specimen rupture the data were recalculated and two plots were displayed on the monitor in “ $P-\Delta l$ ” and “ $\sigma-\varepsilon$ ” coordinates as shown in figure 4. Specific values were calculated including maximal load, maximal deformation, stress and relative deformation. All obtained data together with plots were saved to hard disc in MATLAB format. Another required values, such as limit of proportionality, limit of elasticity, modulus of elasticity, etc. could be calculated programmatically provided that more precise deformation sensor is installed on the specimen.

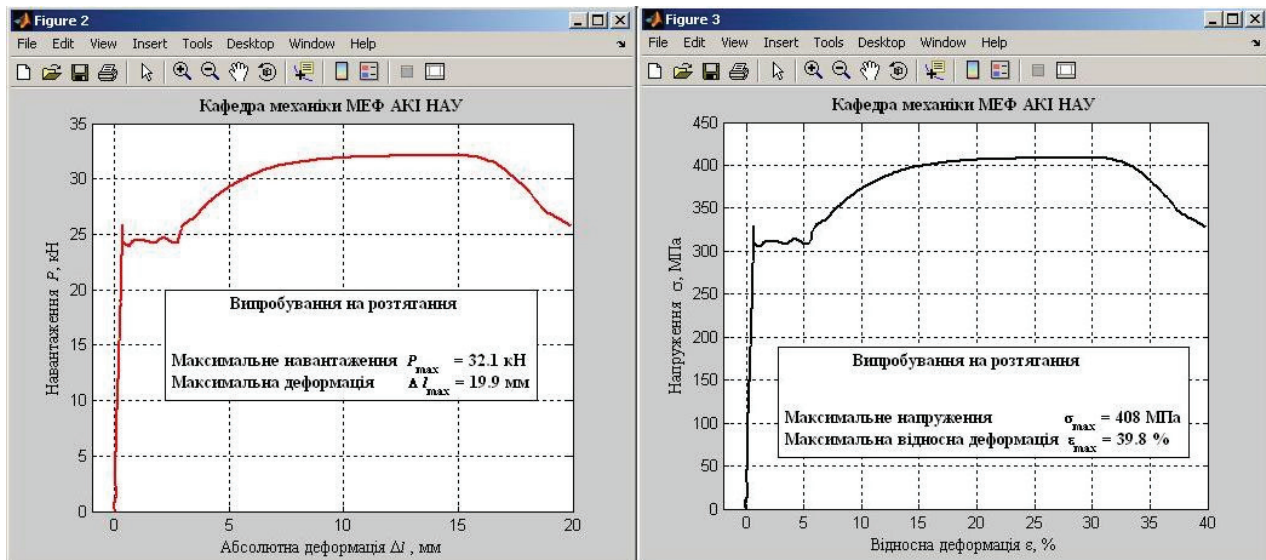


Fig. 4 Resultant Plots in “ $P-\Delta l$ ” and “ $\sigma-\varepsilon$ ” Coordinates

2.2. Aviation panel testing

This is an example of multipoint strain measurements using DAS. Aviation panel specimen with typical operational damage was tested [1]. The main task of this investigation was experimental verification of computational model for mode of deformation determination of aviation structures with stress concentrators. Investigated specimens were made of aluminum alloy sheet and had different modeled defects. Totally 26 strain gages were glued to each of them in and round the modeled damage. Tests were performed on P-5 test machine (Fig. 5) and loads were applied manually. This set of tests was performed at the beginning of DAS creation that is why only measurements of strain gage were performed by DAS. The values of load were input in the software program from keyboard.

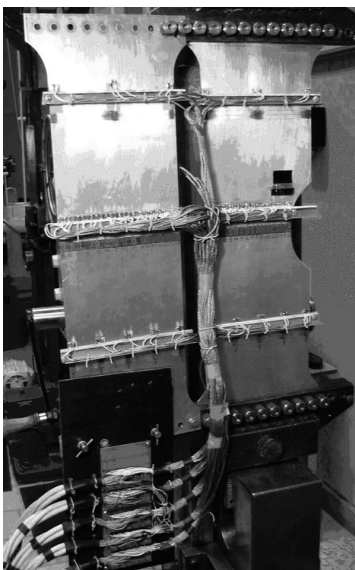


Fig. 5 Aviation panel specimen

To obtain precise data, all strain gage amplifiers were calibrated to set the same gain coefficient equal to $K_A = 500$. To reduce random errors caused by both electrical noise and inaccuracy of load setting, each load value was repeated three times and at each point multiple measurement were performed during 2 s at sampling rate of 2 ksp/s. Mean values were calculated programmatically within in each sample and then mean value of three sets was calculated. Measurements were performed at each level of loads and permitted to obtain strain distribution over specimen width as shown in Fig. 6.

2.3 Pipeline section testing with internal pressure

A scientific investigation of residual capability of pipeline section with modeled corrosive damage to withstand internal pressure

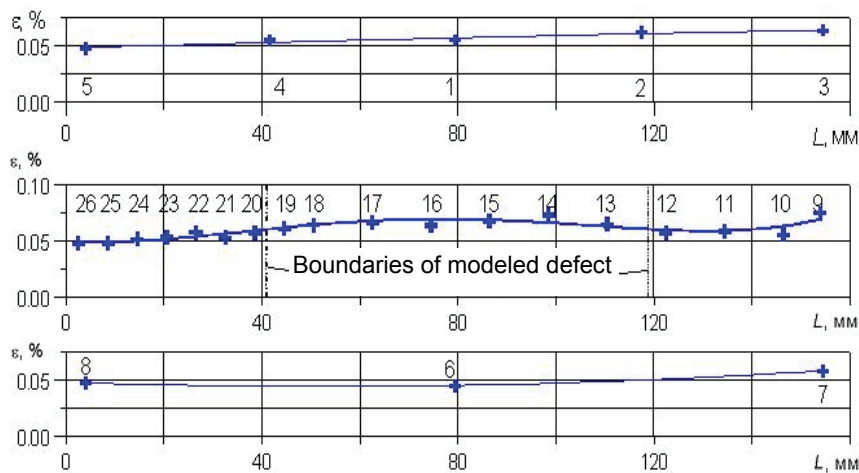


Fig. 6 Strain distribution across aviation pane specimen

data concerning mode of deformation of the specimen in the neighborhood of modeled damage, 12 strain gage sensors were glued to the specimen according to the scheme shown in figure 7. During testing pressure value was set up manually using built-in pressure regulator and pressure measurement was made using similar to the tension tests Danfoss pressure transducer. Similarly, calibration of the transducer was performed using machine's manometer as a reference standard gage.

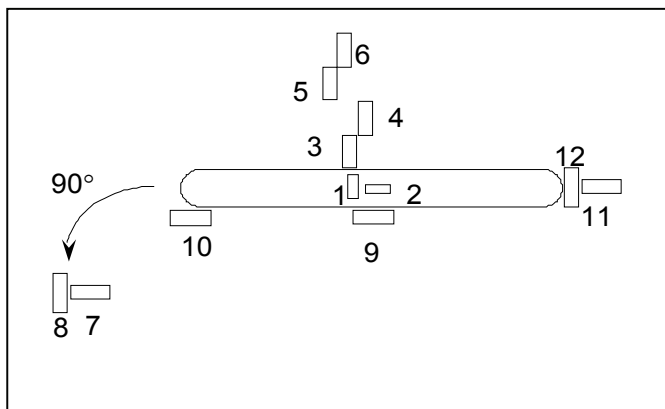


Fig. 7 Strain Gages Layout on the Pipeline

relatively slow, here 0.1 s samples were obtained continuously at sampling rate of 2 kps. Mean values of each sample were considered the result of measurement at certain pressure.

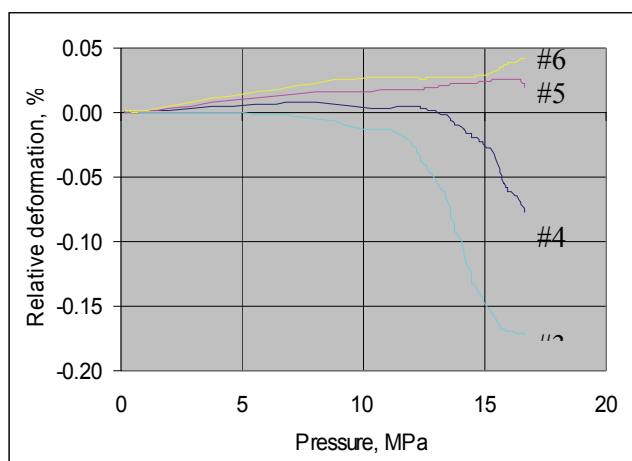


Fig. 8 Relative Deformations vs. Internal Pressure

was conducted at ZDMU-30 test machine. Modeled corrosive damage was 100 mm long milled-out cavity, which decreases pipe wall thickness from 5.0 to 1.5 mm. End faces of pipeline section were corked with thick flanges welded to it, and the pipeline was filled with water. In the upper flange two threaded openings were performed, one of which was used to supply pressure and another one – to drain residual air. The later had a stopcock.

To obtain comprehensive

The procedure of testing was the following. Oil from test machine was pumped into the pipeline section and 13 parameters were continuously measured during the experiment. They were internal pressure and 12 strain gage signals referencing to relative deformations in specific points of the pipeline. Two of them namely longitudinal and circumferential relative deformations in undamaged portion of pipeline, measured by strain gages #7 and #8 respectively were plotted on the monitor versus internal pressure in the course of experiment. To reduce electric noise and accounting for that pressure changed

In the test non-trivial results were obtained [2]. It was found that at pressures exceeding 4 MPa plastic deformation began in the place of weakness and circumferential deformations very quickly exceeded 1.0 % and reached measuring rage of strain gage sensor. Longitudinal deformation was much less and at pressure level of 10 kPa it did not exceed 0.025%. Circumferential deformations in the vicinity of place of weakness (fig. 8) changed from tensile to compressive, which was measured by strain gages #3 and #4. Deformations under strain gages #5 and #6

remained tensile but still much less than that in undamaged region. Rupture pressure was 16 MPa, which is much less than for undamaged pipe. The data concerning deformation distribution were later proved by numerical modeling and by similar investigation performed by Belorussian researchers [3].

2.4 Impact loading of simple beam - educational laboratory work

For educational purposes DAS is used to demonstrate and perform measurements and control in different laboratory works including strain gage calibration, stress concentration, loading of cylinder vessel with internal pressure and other. Among them there are two works with dynamic

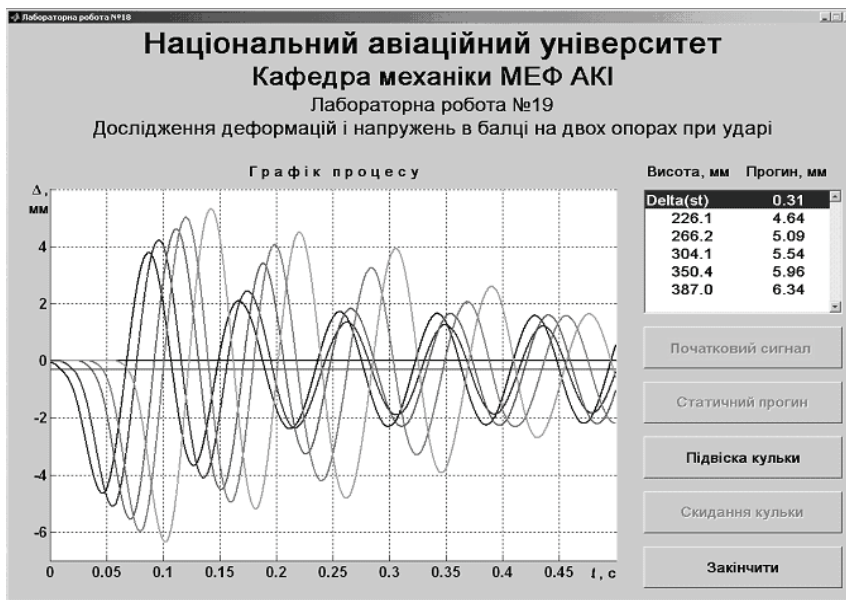


Fig. 9 Graphic User Interface of Laboratory Work #19

processes measurements [4], for which DAS permits to obtain much more reliable data than analog recording equipment. Laboratory work "Investigation of stresses and deformations of simple beam under impact loading" demonstrates dynamic deflection of the beam under the action of falling weight and stipulates comparison of dynamic factors obtained from experimental data with those calculated from theoretical considerations. Graphic user interface (GUI) of laboratory work is shown in figure 9.

Test rig includes simple beam with weight trap attached to it in the middle of beam span. Solenoid for weight holdup and drop is installed above the trap with the opportunity of vertical movement along guide path. Lateral deflection of the beam is measured by strain gage bridge glued to it. Height of drop is measured by linear variable differential transformer (LVDT) with appropriate signal conditioning circuit. Switching ON and OFF of the solenoid is realized from DAS via digital output signal generated by digital input/ output board.

After initial signals measurement of unloaded beam the weight is placed into the trap and static deflection is measured. Then by pressing hold-on button ("Підвіска кульки") on GUI the signal is generated (logical "1" is set) to switch the solenoid on. The weight, which is steel ball is put under the solenoid and holds there with magnetic force. After drop button ("Скидання кульки") is pressed the measurement of height of drop (LVDT output signal) is performed, solenoid is switched off (respective digital output signal changes to "0") and measurement of beam deflection output signal is started with 10 kps. Measurements are performed during 0.6 sec and obtained instantaneous values of output voltage are recalculated into deflection values using preliminary obtained calibration function, digitally filtered to remove noise and graphically output to the monitor. Maximal deflection of the beam is found and its value together with height-of-drop value are placed into the respective window of GUI in digital form. Theoretical and experimental values are calculated in hidden mode and could be printed for a lecturer to control students' results. All data are logged to disk into a separate file.

2.5 Vibration and resonance study - educational laboratory work

Laboratory work "Investigation of elastic oscillations of mechanical systems" is aimed to experimentally verify the correctness of theoretical values of amplitudes of forced oscillations of a



Fig. 10 Graphic User Interface of Laboratory Work #20

time of the beginning of each individual measurement. This permits calculation of both amplitude and frequency of oscillations. Speed of rotation of electric motor is regulated from DAS via analog signal, generated by analog output board, which voltage is set programmatically from the GUI. The change of oscillation amplitude can be viewed in digital oscilloscope screen. GUI of laboratory work is shown in figure 10.

Pressing of start button (“Пуск”) (see fig 10) switches electric motor ON and required speed of rotation (and frequency of excitation force respectively) is set up by slider position. Oscillation amplitude varies according to excitation frequency. After transient process is finished, operator performs measurements by pressing respective button on the GUI (free or forced oscillation button). Measurements during 1.2 sec are performed and instantaneous values of strain gage output signals are used to calculate beam deflection values according to its calibration function. Obtained data are plotted to upper window. Oscillation period is calculated as mean value of times between eight sequential maximal and minimal values of deflection amplitudes. The mode of oscillation is defined using Fourier transformation and magnitude-frequency plot is output to lower plot window. A pair of “amplitude-frequency” data is output to digital data window. A set of measurements with different excitation frequencies permits to obtain the dependency of amplitude of forced oscillations versus frequency of excitation and gives students the understanding of resonance phenomenon, its danger to mechanical structures and means for its overcoming.

3. Problems and Prospects

The main problem of implementation of computer-controlled testing using hydraulic-driven test machines is the difficulties of creation of servo actuators instead of manually controlled ones. Today several firms in the world propose computer-controlled pump stations with servo valves but their prices are too high and only slightly less than testing entire machine. From the other hand a lot of test machines have good enough pumps capable to produce rated pressures and flows and need only appropriate control units. This is particularly true for educational and scientific institutions where operation time of machines are relatively small despite their physical age. For these machines suitable computer-controlled servo valve block seems to be the best choice to obtain up-to-date testing capabilities for minimal cost and with minimal labor expenditures, but only few vendors of such equipment are available in the world.

Another problem associated with previous one is the implementation of standardized procedures of testing, which also requires computer-controlled regimes of load application and could not be implemented without closed-loop control. This requires installation of appropriate sensors and development of corresponding real-time software to control testing machines. For

instance, for tension and compression tests it is planned to equip electrically driven P-5 testing machine with load cell and displacement transducer for load and deformation measurements. Control of loading speed and/or strain rate according to requirements of regulations is planned to perform by electric motor regulation using frequency converter. These are the main tasks to be solved in future to expand testing capabilities of DAS presented.

One more task at which the works are in progress, is utilization of image processing for determination of metal macrohardness using digital images of the dents obtained according to Brinell, Vickers, and Rockwell hardness tests. Images of footprints of respective intruders are obtained using digital camera or web-cam and microscope, if necessary. Software for sophisticated image processing is included in Matlab's image processing toolbox.

In educational sphere it planned to rise up the level of automation of several laboratory works and to expand their nomenclature.

Conclusion

Multipurpose mobile DAS of Laboratory of strength of materials, Mechanics chair of NAU proved its applicability and efficiency in solving tasks of strength testing of standard specimens and aviation/industrial structure. It showed easy and quick adaptation and tuning for particular testing task and capability to provided high volumes of measurement information with improved accuracy. The opportunity of graphic representation of measured parameters in the course of experiment permits a higher-level control of testing procedure even if it is performed manually. Quick and easy documentation of testing results and opportunity to perform sophisticated processing of obtained data directly after test completion is another advantage of the DAS presented.

Application of DAS in educational sphere improves the level of specialists.

Further works are needed to expand testing capabilities of DAS including new sensors installation and software development.

References

1. *V.V. Astanin, N.M., O.A. Shevchenko, P.M. Vynogradskyy.* Determination of Deformation Mode and Limiting State of Structural Elements Using Data Acquisition System. VII International Scientific Conference «AVIA-2006». Kiev, Ukraine, September 2006. (In Ukrainian).
2. *V.V. Astanin, N.M. Borodachev, S.Ju. Bogdan, V.A. Koltsov, N.I. Savchenko, and P.M. Vynogradskyy.* Strength of Pipelines with Corrosive Damages.//Strength and Reliability of Transit Pipelines. “TP-2008”, International Conference, Kiev, Ukraine. 5-7 June, 2008. pp.9-10 (in Russian).
3. *A.A. Kostyuchenko, A.M. Bordovskiy, A.N. Kozik, V.V. Vorobyov, and L.A. Sosnovskiy.* Experimental Study of Destruction of Pipes of Oil Pipelines with Corrosion Defects on the Internal Surface. //Strength and Reliability of Transit Pipelines. “TP-2008”, International Conference, Kiev, Ukraine. 5-7 June, 2008. pp.55-56 (in Russian).
4. *V.V. Astanin, P.M. Vynogradskyy.* Application of Data Acquisition System to Laboratory Works in Engineering Mechanics. //Science and Methodological Commission of Ministry of Education and Science in Engineering Mechanics. Mariupol, Ukraine. 5-8 September 2006. Pp. 21-29 (in Ukrainian).

NON-DESTRUCTIVE INSPECTION OF AIRCRAFT COMPOSITE PLATES BY USING IMMERSION ULTRASONIC METHOD

In this study, for aircraft structural composites immersion ultrasonic test method is optimised by changing test prob scan range and test piece immersion time. Laminated fiber composites and honeycomb composites are analysed by using pulse-echo and through transmission test techniques. Obtained results are discussed in the conclusion and advantages of the method are also listed.

1. INTRODUCTION

Advanced composite materials are different from homogeneous metal alloys. Laminated structures and continuous fibers are used in them. Generally, there are long fibers such as graphite, carbon, boron and Kevlar 49 in matrix phase such as epoxy. Aircraft structural composites have many advantages such as high strength to weight ratio, stiffness, environmental degradation resistance [1]. They have good resistance during long service time for both civil and military application. But, wide range of defects such as ply delamination damage, impact damage, moisture absorption damage can be occur during curing processes and service life time [2].

Damages should be detected as possible as in early stage. Discontinuities can be detected by non-destructive inspection (NDI) both in design full scale tests to assess maintenance planing schedule and in maintenance facilities during components service life [3]. Two important fact about component condition appear by using NDI techniques. This methods show that component doesn't contain discontinuities. Second is NDI obtain the guarantee that if the component's discontinuities reach critical dimension. In modern aircraft maintenance planing especially for damage tolerance analysis NDI methods are vital [4].

Inhomogeneity and low density of composites cause many problems for application conventional NDI methods such as radiography, eddy current and ultrasonic. On the other hand, ultrasonic immersion method is capable to detect small discontinuities in the aircraft composites [5].

2. THE PRINCIPLE OF IMMERSION ULTRASONIC METHOD

As a principle of this method, test piece and prob are immersed in the test tank. Tank generally contains water as liquid couplant. During the contact test to protect couplant thickness homogeneity is difficult. This change affects sensitivity of results. But in immersion method water column between test piece surface and prob is constant. Automatic scanning is used and prob is commanded by manipulators.

The interface reflects high percentage of the ultrasonic energy because of highly differences between acoustic impedance of water and test piece. For example, the percentage of the transmitted ultrasonic energy through the interface water/carbon-epoxy is 72% [6].

3. DIFFERENT MEASUREMENT TECHNIQUES

Two different measurement techniques can be used in ultrasonic immersion control. These are pulse-echo and through transmission techniques. In pulse-echo technique, one prob is used as transmitter and receiver. As one prob using is practical, this technique is generally preferred. Because damage echo can be shown in A-scan display, pulse-echo is more successful for laminated composites testing as shown in Figure 1.a. C-scan display is also possible. The most important inconvenience of pulse-echo is front and back surface of test piece should be parallel.

Damage detection capacity of this technique is listed for different damage type in Table 1. For example, to assess delamination of glass-epoxy laminates up to 16 mm thick, pulse-echo is capable [1].

The other technique is through transmission. In this technique, two prob are used. One prob is transmitter. This prob doesn't have receiving function. The other prob is only receiver, this prob doesn't study as transmitter. For sandwich composites this technique is more successful than pulse-

echo as shown in Figure 1.b. Especially for thick laminated composites testing, this technique have advantage. The other advantage of this thecnique is two prob can be placed in angle position as shown in Figure 1.c and 1.d. [7].

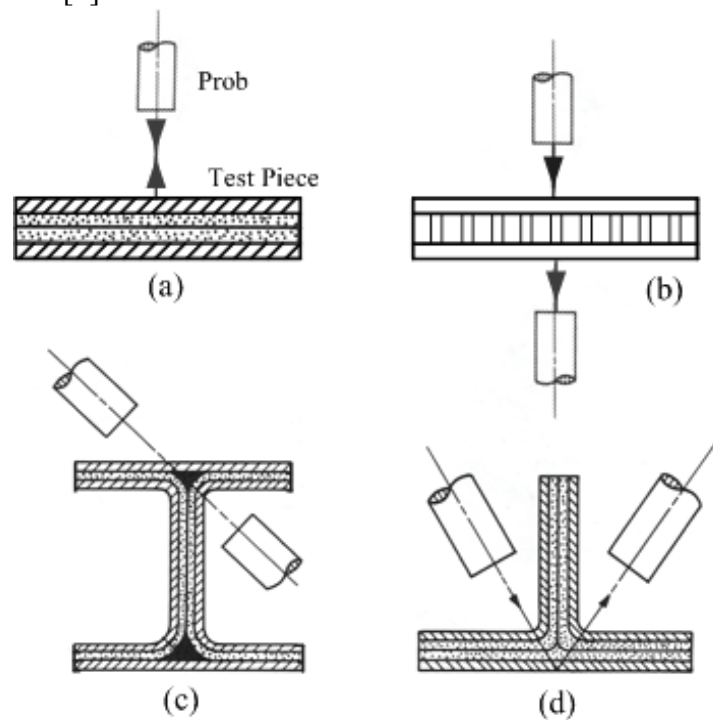


Figure 1 Different immersion techniques

- a. Pulse-Echo for laminated structure
- b. Through transmission for honeycomb structure
- c. Through transmission for "I" section
- d. Through transmission for "T" section

Through transmission technique have high sensitivity for small defects in test piece. For example, 1.6 mm dimension defect can be detected in boron-epoxy composite. Damage detection capacity of this technique is listed for different damage type in Table 1 [8].

Table 1 Damage detection capacity of test techniques

Test Technique Damage Type	Pulse-Echo	Through Transmission
Delamination	●	●
Crack		
Void	●	●
Thick Bond		●
Core Damage	●	●
Density Variation		
Inclusion	●	●

● Effective Technique

4. THE OPTIMISATION OF IMMERSION TEST SYSTEM

For this optimisation study, carbon-epoxy (T300-914) test pieces are used. Each piece is 28 plies and 3.5 mm total thicness. Each of them has impact damage created by 20 joule impact energy. Immersion test system contains one immersion tank with manipulator moving x,y,z axes and Usip 12 Krautkramer unit and computer system. C-scan display can be used. For this study pulse-echo measurement technique and diminution of background echo is regarded. Reflector plate and focusing immersion prob are used [9].

4.1. Assessment of Prob Scanning Range

Scanning range affects the test time and damage shape picture on C-scan display. Prob scanning range can be choice depends on test system capacity. For small defect analysis scanning range should be small enough. In this study, testing ranges are between 0.2 mm and 1mm by changing in each step 0.1mm. C-scan examples are given in Figure 2. As shown in Figure 2, for damage shape picture quality, about 0.2 mm value is obtained as optimum scanning range.

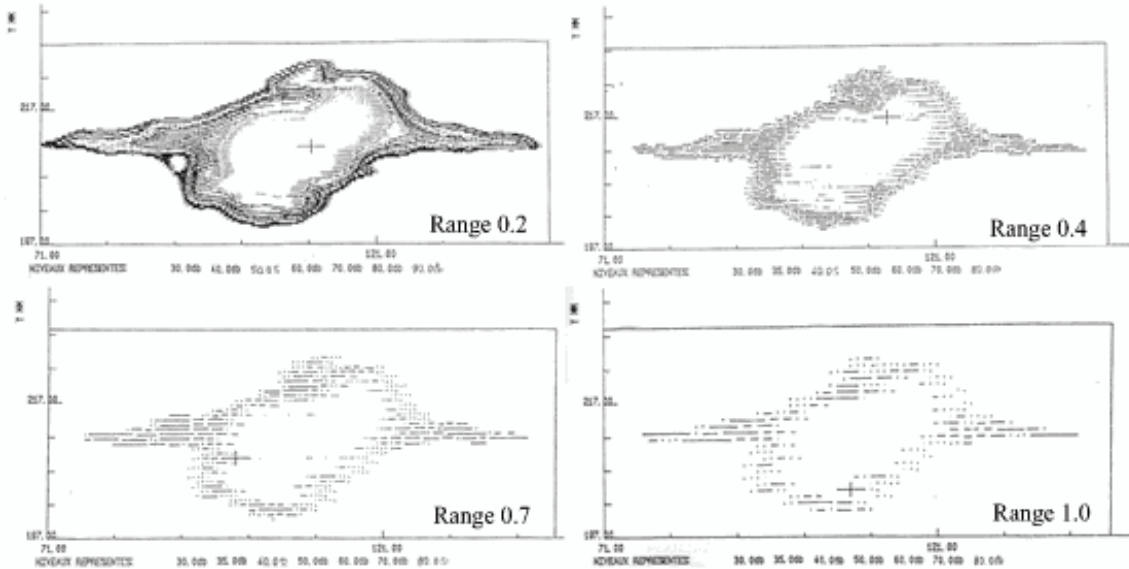


Figure 2 Different scanning range examples

4.2. Assessment of Immersion Time

Test piece's surface dimensions affect the scanning time for C-scan display analysis. Composite materials absorb the water. This cause debonding and delamination problem. For composite testing immersion time should be short enough. In this study for impact delamination damaged composite laminates, after 3 days immersion time water absorption problem was detected. As given in Figure 3, after 3, 8 and 10 immersion days analysis results show that C-scan damage picture change. Immersion time should be restricted by only scanning time. After the test, test piece should be taken off the tank and immediately dry.

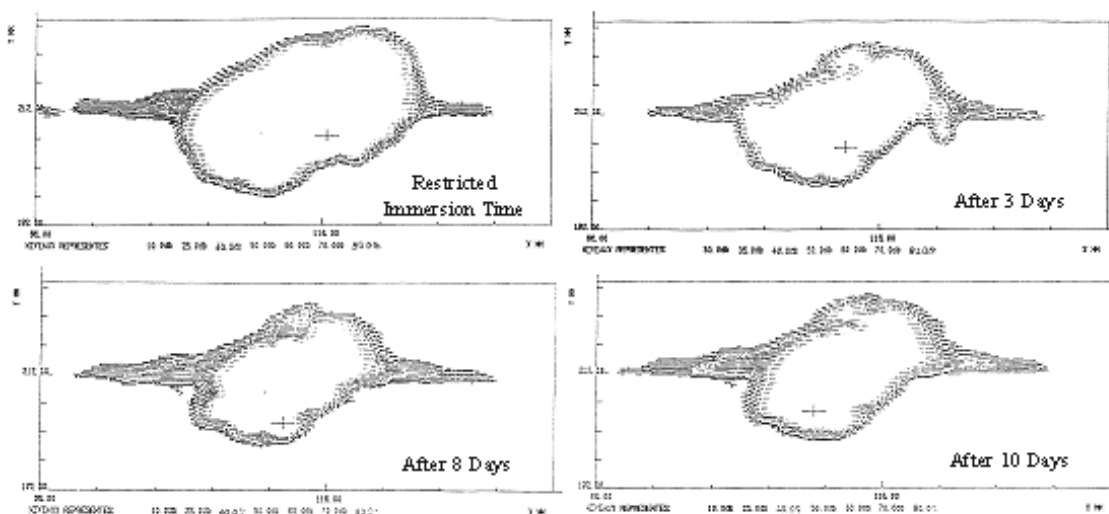


Figure 3 Different immersion time test results

5. CONCLUSION

Immersion ultrasonic method is more successful than contact ultrasonic test method, especially to test thin composite plates. This method can be used to analyse damage tolerance design requirements at laboratory level. In this test method, nearfield perturbation problem of ultrasonic beam can be eliminated in the water column. The other advantages of this method can be listed as below.

Test prob angle can be changed easily.

As automatic scanning is possible, test speed is high.

For small defects high sensitivity.

Test piece surface condition such as surface roughness and shape don't affect the test results.

For thin composite plates testing, high sensitivity focusing prob using is possible, as focal distance stays in water column.

Test piece dimension should be small enough to immerse into the tank and immersion time should be short enough. In this case, advanced water squirting probs may be used instade of immersion into the tank. Only longitudinal waves should be used in immersion method, as other transversal and Lamb waves don't transmit in the water. Because high percentage of the ultrasonic energy reflects from the test piece surface, high test frequencies should be used.

References

1. *Schwartz, M.M.*, Composite Materials Handbook, McGraw-Hill Inc., 1984.
2. *Armatlı Kayrak M.*, Non-Destructive Inspection Methods for Aircraft Maintenance, Anadolu University, Eskisehir/Turkey, 2001.
3. *Assler H., Telgkamp J.*, Design of Aircraft Structures Under Special Consideration of NDT, <http://www.ndt.net/article/wcndt2004/pdf/aerospace/817-assier.pdf>.
4. *Cowie W. D.*, Fracture Control Philosophy, Non-Destructive Evaluation and Quality Control, Metals Handbook, Volume 17, ASM International, 1989.
5. *Cohen Y.B., Mal A.K.*, Ultrasonic Inspection, Non-Destructive Evaluation and Quality Control, Metals Handbook, Volume 17, ASM International, 1989.
6. *Matthews F.L.*, Composite Materials Engineering and Science, Chapman and Hall Inc., 1994.
7. *Stone D.E.W.*, Non-Destructive Inspection of Composite Materials for Aircraft Structural Applications, AGARD CP-234, pp 14-1/14-18, Technical Editing and Reproduction Ltd., London, March 1978.
8. *Kaitatzidis M.*, Inspection of Carbon Parts After Fabrication and During Service, AGARD CP-234, pp 16-1/16-16, Technical Editing and Reproduction Ltd., London, March 1978.
9. *Armatlı Kayrak M.*, Contribution a L'Optimisation D'une Procedure De Control Non Destructif Par Ultrasons en Immersion, ENSICA, MA Thesis, Toulouse/France, 1990.

INDIRECT THRUST MEASUREMENT DURING THE GROUND TESTS OF THE TURBOROP ENGINES

The new method of propeller thrust measurement is proposed. Also it's compared two different means of blade pitch measurement with their advantages and disadvantages

INTRODUCTION

At the end of 20-th century a lot of regional turbojet like ERJ-145, CRJ100 CRJ200 etc. were set in operation in Western Europe and North America. In this case the most of aviation experts were unison in opinions that time of turboprops is finished [1, 2]. But some years ago, after new European noise admission rules implementation and particularly after the beginning of the petroleum crisis, the biggest regional carriers came back to discussion about the possibility of using of turboprop aircrafts. From this point in 2006 the new life of turboprops was started.

In witness of this fact, in 2007 ATR, which is affiliated company with the biggest European aircraft consortium EADS, announced the record level of orders for their ATR 42-500 and ATR 72-500 aircrafts in all history of ATR [3]. More than that, Bombardier – the other biggest manufacturer of regional aircrafts is also optimistic in their forecasts about the future of turboprops [4]. Bombardier analytics suppose that in next twenty years regional carriers will increase their turboprop fleets and in 2026 the part of turboprop in global regional fleet will be assigned up to 36 percent.

The increasing of amount of turboprops in next ten years had remade the problems of turboprop exploitation again. That's why the solving of the most of this problems but on from the new point of view with new test equipment, with modern algorithms of problem searching etc are very important task which will allow to increase the level of flight safety and economical efficiency.

The problems of turboprops operation

During the manufacturing and operation all aircrafts assumed some specific attributes. The typical attribute of the turboprops is the aerodynamic quality degradation in consequence of asymmetric thrust of the left and right engines [4, 5]. In such case the crews are trying to compensate this asymmetric with rudder, ailerons or flaps using but the result of this compensation could be dramatic [6]. The other side of asymmetric thrust is increasing of the fuel consumption which could reach up in some cases to 6 percent. That's why the periodic control of thrust of turboprop is very important procedure which will allows keeping a high level of flight safety.

In addition, precise determination of turboprop thrust is of much interesting as it allows, in principle, to verify the specified engine performance and propeller characteristics as well as to quantify the lift and drag characteristics of the aircraft.

The exist thrust measurement methods

In the case of turboprop, the thrust of the propulsion unit can be obtained from measurements of the variables related to the propeller thrust and the jet thrust of the engine. Several techniques to obtain propeller thrust and jet thrust already exists. In general, they require the measurement of several engine and propeller variables and also airdata like temperature, airspeed, humidity etc.

The most simple method of thrust measurement is the using a force balance method [7, 8] which is widely used during designing or testing of a power plants in a couple with the measurement of total pressure behind the propeller [9, 10]. Both of these methods are terminated only for designing and special manufacturer testing because they require a special equipments and conditions which couldn't be provided during all period of engine operation.

In other case the thrust of turboprop could be obtained through the power measurement [11, 12, 13], but this method is also limited and not allows to measure the trust level of power plant on the ground which is very important for plane crash preventing especially during the take-off.

So, at present some thrust measurement method were created but all of them are not answered for in full requirements which were raised by air carriers. Therefore it's necessary to continue technical investigations which could solve the problems of turboprop operation without using special equipment in all periods of turboprop exploitation.

Method of thrust measurement during the ground tests

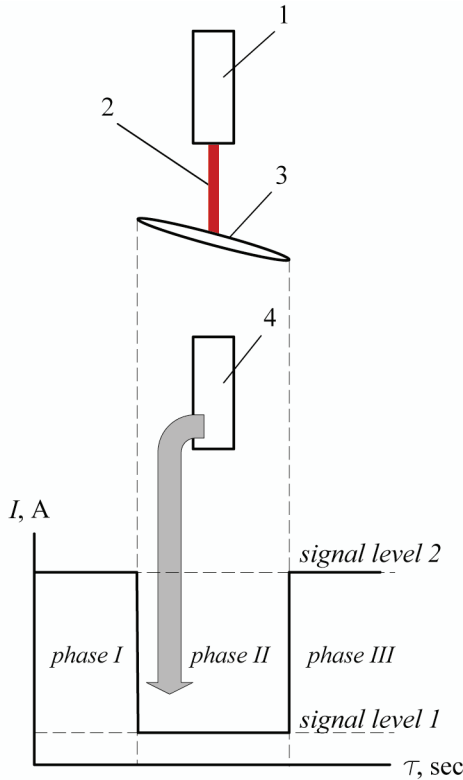


Figure 1. The schema of light beam crossing by blade

- 1 - the light source,
- 2 - the light beam,
- 3 - the propeller blade,
- 4 - the light detector.

to obtain the blade pitch (fig. 2)

The radial angle $\gamma_{\text{рад}}$ of blade projection could be obtained from equation

$$\gamma_{\text{рад}} = \frac{\pi n_{\text{TB}}}{30} \Delta t. \quad (1)$$

The same angle could be obtained (but in degree mode) with formula

$$\gamma = 2 \arcsin \left[0,5 \frac{b_x}{R} \cos(\varphi_0 + \varphi) \right]. \quad (2)$$

where b_x – blade chord length on radius R_x ;

φ_0 – blade geometric twist on radius R_x ;

φ – blade pitch.

In consideration of (2) the radial angle $\gamma_{\text{рад}}$ could be written with formula

$$\gamma_{\text{рад}} = 2 \arcsin \left[0,5 \frac{b_x}{R} \cos(\varphi_0 + \varphi) \right] \frac{\pi}{180}. \quad (3)$$

The result of substitution (3) in (1) is

$$3n_{\text{TB}} \Delta t = \arcsin \left[0,5 \frac{b_x}{R} \cos(\varphi_0 + \varphi) \right].$$

The proposed method is based on the “shadow” time duration measurement which is detected by the special optical device (fig. 1) during the propeller blade rotation. In more detail, if the blade is crossing the light beam then an optical “shadow” is created and fixed by photo detector (fig. 1, phase II).

And if the lights beam is following to the optical detector without obstruction then detector registered a signal and transforms it to electrical signal (fig. 1, phase I and phase III). This signal is more power in compares with the “shadow” signal so it allows calculating the “shadow” duration $\Delta t = t_2 - t_1$. This conception of the blade pitch measurement is very simple and it's not required any kind of airframe construction modification.

The length of “shadow” projection could be obtained with known rotation speed n_{TB} :

$$V = \frac{\pi n_{\text{TB}}}{30} r_{\text{неп.гб}} \Rightarrow l_{\text{np}} = V \Delta t,$$

where V – linear propeller rotation speed;

$r_{\text{неп.гб}}$ – selected propeller radius;

l_{np} s – the “shadow” length.

It's obvious; the “shadow” length will change if propeller blades move from one angle to other.

The propeller characteristics like chord length b , and profile curvature \bar{c} are, as usual, well known parameters of each type of propeller so it's not difficult

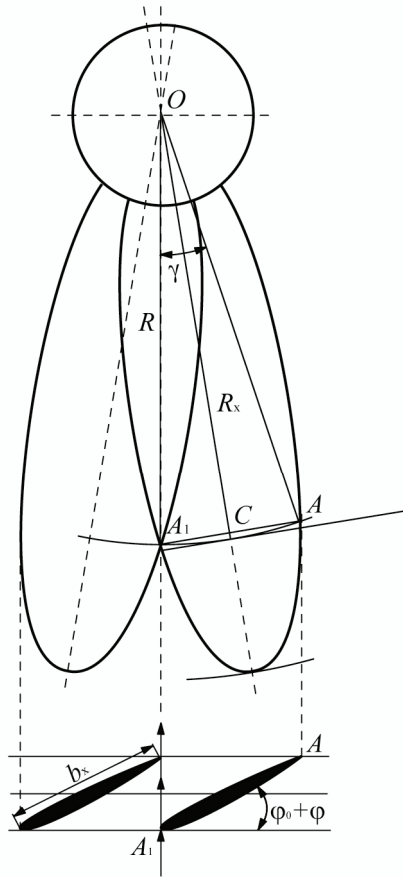


Figure 2. The propeller blade angle position during the frontal optic measurements

mathematical modeling of a gas turbine engine. At the end both propeller thrust and jet thrust should be added one to one which will represent the full thrust of turboprop.

The blade pitch measurement tests

The first attempt of propeller blade pitch measurement was done with the 2 blade propeller model via portable PC-integrated oscilloscope Handyprobe 2.

This measurement strategy allowed indicating the different blade pitch with 1 degree step (fig. 3). But a high parasitic noise and insufficient precise form of signal (fig. 4) are jamming the final result.

The second strategy is based on using of Schmitt trigger which allows obtaining nearly ideal meander. The tests result in this case could be obtained in graphical mode and also in table mode (table 1).

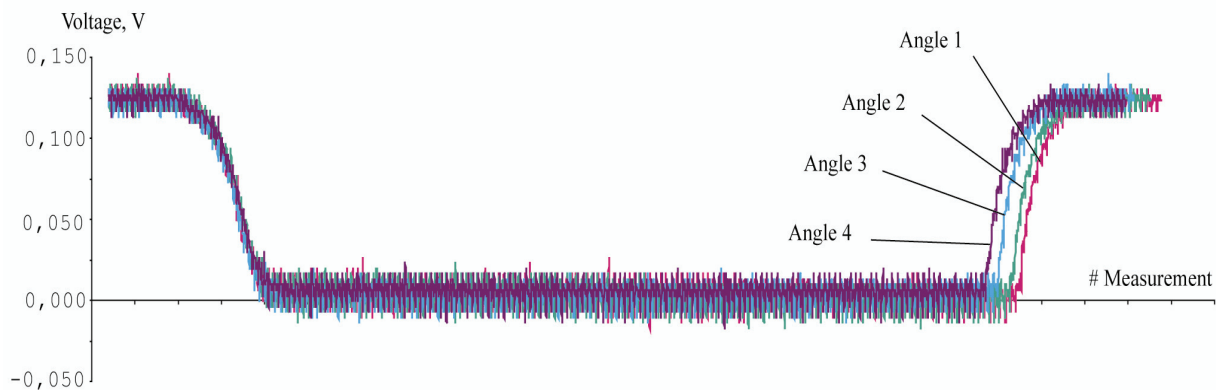


Figure 3. The “shadow” for different blade pitch

The relation between radiuses R_x and R is estimated by the following equation

$$R_x = \sqrt{R^2 - [0,5b_x \cos(\varphi_0 + \varphi)]^2}.$$

So far as the chord length b_x and blade geometric twist φ_0 are not constant and changed along the blade the blade pitch calculation procedure should be amendment with next equations

$$\bar{b}_x = f(\bar{R}_x); \varphi_0 = f(\bar{R}_x),$$

where $\bar{b}_x = b_x / D$;

$$\bar{R}_x = R_x / 0,5D;$$

D – propeller diameter.

With known propeller blade pitch φ , propeller manufacturer characteristics and atmosphere conditions, it becomes possible to calculate the thrust coefficient α and power coefficient β which allow obtaining the thrust and power produced by propeller.

The propeller thrust could be obtained with following equation

$$P = \alpha \rho n^2 D^4,$$

where ρ – air density.

The propeller power could be calculated with formula

$$N = \beta \rho n^3 D^5$$

The jet thrust of turboprop as usual could be obtained from

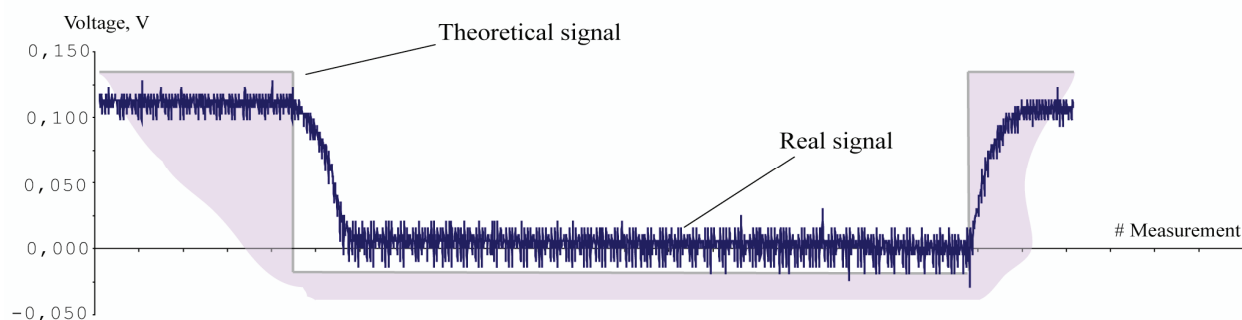


Figure 4. The signal distortion

Table 1.

The “shadow” and light detection duration

#	“Shadow” duration	Light detection duration
1	657	2207
2	655	2234
3	635	2197
4	655	2207
5	661	2225
6	641	2226
7	660	2194
8	655	2208
9	654	2231
10	632	2196
11	656	2211

Conclusion

The model based experimental testing of proposed method indicated that the using simplicity and adequate accuracy are the good indicators before the in full ground tests with turboprop aircraft.

However the proposed method has a limitation which consists in the possibility to measure the thrust only during the ground tests. This fact restricts the range of implementation of proposed method but the simple mathematical apparatus, the lack of any construction modification and using readiness for all types of aircrafts with variable-pitch propeller are unchallenged advantages of this method which could serve for it widely using.

References

1. Hess H. Fairchild Dornier 328JET thrusts into new class // Flug Revue. - 1998. - № 4. - p. 30 – 31.
2. Стопу У. мл. Эксклюзивные соглашения перекаривают планы двигателестроителей // Авиатранспортное обозрение. – 2001. – № 8 (35).
3. ATR registers Record Year of Orders with 113 new Aircraft // ATR Press Release. – Paris, 23rd January 2008.
4. Bombardier Aerospace – Commercial aircraft market forecast 2007-2026 // Bombardier Press Release. – Belfast, 1st May 2007.
5. Ударцев Е.П. Динамика пространственного сбалансированного движения самолета: Уч. пособие – Киев: КИИГА, 1989. – 115 с.
6. Propeller Governor Assembly: AD/PT6A: Civil Aviation Safety Authority of Commonwealth of Australia 04.2002. – Canberra, 2002. – 1 p.
7. Bass R.M., Munniksm B., van Hegst J. Aerodynamic and structural aspects of propeller and drive for 1/5 scale model wind tunnel programme. AGARD CP-136, 1985.
8. Munniksm B. Test technique for establishing propeller performance and propeller/airframe interference. NLR Memorandum AV-88-014 U. – National Aerospace Laboratory, The Netherlands, 1988.
9. Broek J.J. The use of total-head rise across the propeller of the De Havilland Canada DHC-2 Beaver as a similarity parameter to simulate power-on flight in the wind tunnel // Report VTH-190. – Delft: Delft University of Technology, 1976.
10. Vries O. Preliminary tests with a yaw meter rake in the slipstream of an operative propeller // NLR Memorandum AI-87-010 L. – National Aerospace Laboratory, the Netherlands, 1987.
11. Александров В.Л. Воздушные винты. - Москва: Государственное издательство оборонной промышленности, 1951. – 448 с.
12. Мхитарян А.М. Аэродинамика. – Москва: Машиностроение, 1976. – 446 с.
13. Домотенко Н.Т., Кравец А.С., Никитин Г.А. и др. Авиационные силовые установки. – Москва: Транспорт, 1976. – 321 с.

P.S. Abdullayev,
A.S. Yakushenko,
A. J. Mirzoyev,

(National Aviation Academy, Azerbaijan)

THE COMPLEX APPROACH TO THE DECISION FORMING OF AVIATION GAS TURBINE ENGINE TECHNICAL CONDITION

The offered method of aviation gas turbine engine monitoring based on the complex system, allowing to perform multiply – stage identification the engine actual condition. The separate stage of complex system for realization of offering method was considered.

The investigation of the Aviation Gas Turbine engine (AGE) technical condition automatized system's creating shows the insufficiency valid of application system based only on the one of the monitoring method. As know no one methods are not universal and absolutely reliable. Naturally, the like diagnostic systems, build only on the one classifier could not satisfy the requirements presenting to the engine diagnostic entirely as in the online as in the offline regime.

Under this condition the complex method applying is stipulated by using the Soft Computing new technology and Mathematical Statistics in the AGE monitoring process. Applying such method is requested the steady and effective investigation of modern information technology resources [1].

The creating AGE complex monitoring system allowing to perform the multiply-stage online and offline engine condition identification by flight recorder and manual parameters registered parameters, shows on the Figure 1.

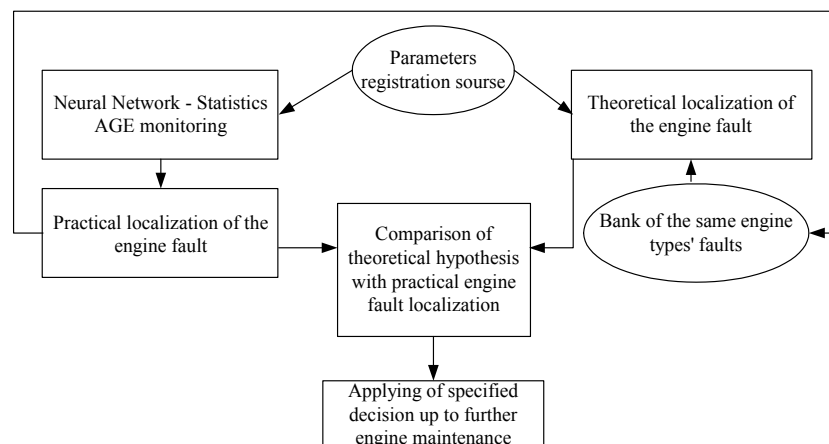


Fig. 1 Common scheme of AGE complex diagnostic

The first stage of suggested AGT complex monitoring system is allowed to determine only the tendency of engine inclination to the fault condition by the Neural Network and Statistic methods without engine fault localization [2].

The statistics determination of the engine fault is based on the forming of the flexible diapason registered parameters and comparing their values with upper and lower calculated possible boundaries by formulas:

$$P_n^U = \bar{P}_n + K_{l,n} \sqrt{S_n^2} ; P_n^L = \bar{P}_n - K_{l,n} \sqrt{S_n^2} ,$$

where \bar{P}_n and S_n - the average values and standard deviation of engine parameters, $K_{l,n}$ - tolerance coefficient, depending on the measuring number n , applying amount's layer and confidence probability. The context of the Neural Network is the engine fault determination on the basis of the upper and lower threshold forming of output diagnostic parameters the suited to the beginning of AGE condition fault. The output diagnostic parameter in the engine neural network model is

making more exact, borrowing of main distribution parameter's characteristics efficient which forming of engine condition fault threshold by below formula:

$$U_{II}^U = P_n + \gamma_u, \gamma_u = P_b * \alpha_1;$$

$$U_{II}^L = P_n + \gamma_L, \gamma_L = P_b * \alpha_2,$$

where P_n - the last measured value of output diagnostic parameter, P_b - base (baseline) value of output diagnostic parameter, determined as centre line average for three subsequent measured, $\alpha_1 = 0.5 \div 0.6$ and $\alpha_2 = 0.2 \div 0.3$ - the experiment coefficients were found out by investigation of real faults of engine PS90A-76SW, D30KU – 154 and RB-211-534E.

The recommendation requirement for the further engine maintenance is handed by the Logical Decision Block (LDB) by comparing the Neural Networks and Statistics analysis result of actual engine condition.

The fault localization up to engine module based on the practical and theoretical result is the second stage of the offering AGE complex monitoring system. The practical result of the engine fault localization is based on the table which was formed by correlation and regression analysis of real AGE faults. It will be enough to find out the output diagnostic parameter of neural networks engine's model and recognize the activity rate of parameters the effectiveness which characterized the engine actual condition [3].

The forming of theoretical engine fault localization is carried out by engine actual condition identification steady simulation parameters values characterized the real engine fault trained by static neural network. The real source of main calculated point's volume for static neural network training is bank of parameters values faults which archived during engine maintenance [4].

The final stage of suggested engine identification method is applied the specified actual condition of the engine by comparing the theoretical hypothesis with the practical engine fault localization. The comparison of hypothesis is based on the correct combination of practical and theoretical engine fault localization results by the LDB. At the same time the logical model has the following structure:

- the identification results are coincidence;
- the identification result are different

In case the actual engine condition is defined by the second presenting option therefore as a basis decision is applied the result of practical localization, but the engine fault module is become the theoretical localization result take into special consideration and without ground deep analysis the engine don't admit up to the further maintenance.

The creating automatized AGE monitoring system is being passed the successful experiment realization on the engines PS-90A-76SW, D30KU-154 and RB-211-534E.

Reference

1. *M.G. Shaxtaxtinskiy, P.S. Abdullayev, A.C. Mirzoyev, A.S. Yakushenko, V.N. Oxmakevich: "Application Of Soft Computing Methods In Complex Condition Monitoring System For Aviation Gas Turbine Engines", Матеріали 8 МНТК "АВИА - 2007". Т.2 – К.: НАУ, 2007, с. 31.14-31.17*
2. *А.Д. Мирзоев «Комплексная система диагностирования авиационных газотурбинных двигателей» // Авиационно-космическая техника и технология, ХАИ, 2007, № 6 (42), с. 47-59.*
3. *P.S. Abdullayev, A.M. Pashayev, R.A. Sadiqov, A.J. Mirzoyev Fuzzy Condition Monitoring System for Aviation Gas Turbine Engines // Proceeding of IMECE2007: ASME International Mechanical Engineering Congress and Exposition, November 11-15, 2007, Seattle, Washington, Paper IMECE2007-43902, 14p*
4. *П.Ш. Абдуллаев, А.Д. Мирзоев "Диагностирование авиационных газотурбинных двигателей с использованием нейронных сетей"// Elmi Məcmuələri, 2006 cild 8, №3 с. 3-7.*

*Yury I. Belykh (technical director of air company "Aeroflot", Russia)
Vladimir A. Naida (associate professor of department «Technical Exploitation of Aircrafts and
Aviation Engines», Russia)
Anton S. Pozolotin (6 year student of Mechanical Faculty, Russia)*

TECHNOLOGICAL ASPECTS OF DEVELOPMENT OF ELECTRONIC TRAINER FOR ACQUISITION OF SKILLS AND ABILITIES ON A START AND TESTING OF AVIATION ENGINE

The substantive provisions of aviation electronic trainer development technology are presented for engineer-technical personnel. The features of a sound row creation of electronic trainer and his synchronization are shown with the system of reflection of information.

Complication of modern air courts and aviation equipment attained such level at which an omission in procedures of technical service and repairing can appear pre-condition to dangerous flying incident or to the conclusion from the line-up of expensive equipment. On these reasons very rigorisms are produced to professional preparation of specialists on technical maintenance of air courts which are impossible to satisfy the following to traditional programs and methods of the primary teaching and practice only on the real air courts.

For development of complex of skills of operative management processes of technical exploitation aviation operating trainers are used.

Last years the theory of exploitation of the difficult technical systems got considerable development, especially in area of aviation.

Basis of simulation model of trainer is a functional model of aviation engine. The functional model of aviation engine consists of interactive graphic flight compartment which cooperates with program-mathematic model of the functional systems of engine. The model is realized in the technological pointing and other technical documents on a start and assay of engine.

The display imitators of device boards of flight compartment, and also imitators of management organs, enter in the complement of trainer: switches, levers, and buttons. On the structural and colour registration imitators largely correspond real organs of management.

Dynamic processes of start and assay of engine, switching and moving of organs of engine management, and also text of prompts is accompanied by sound effects and voice of the announcer.

Switching of position graphic toggle switches, protective hubcaps, lids and handles of management is carried out after admission of cursor on the image of organ of management and successive pressure of the left key of a "mouse".

Switching of graphic position button switches is carried out after admission of cursor on the image of organ of management and successive pressure of the left key of a "mouse".

Moving of graphic organs of management having more than two positions (rotary switches, levers of management engines, steering wheel and other) must be carried out after admission of cursor in the set position and pressures of the left key of a "mouse".

A graphic flight compartment provides a call on the screen of monitor of necessary organs of management and control to provide the implementation of cabin procedures on a start and assay of engine.

A graphic flight compartment consists of two fields: working (left part of the screen) and official (right part of the screen). The areas of device boards, related to the current step of start and assay of engine, are represented in working part. In official part of the screen the side system of signaling and alphanumeric field is represented for prompts.

The scenario of start of engine is executed in accordance with the algorithm of start and reflects maintenance of every step of process of start, parameters of work of engine and their value controlled on this step. The actions of a student are described in the process of management of the engine start. For example, the scenario of start of auxiliary power-plant includes the followings steps:

- To push the button «main pumping»;

- To switch «emergency brake»;
- To switch the screen «auxiliary power-plant»;
- To commute toggle switch «launching - cold rolling»;
- To commute toggle switch of stop and choice of the mode of operations of auxiliary power-plant;
- To press button «launching».

Development of the electronic trainer reflection system.

The system of the electronic trainer reflection system consists of a set of graphic images, presenting the workplace of a flight engineer of airplane IL-96. The followings panels of device board and desktop of a flight engineer were used:

- Panel of the air conditioning system
- Panel of auxiliary power-plant
- Panel of the fuel system
- Panel of engine control devices
- Launch of engine pad on earth
- Launch of engine pad in mid air
- Control engines stand.

The panels images of flight engineer workplace are got by digital photography in a flight of airplane IL-96 compartment. The got pictures were used as a model for subsequent creation of electronic version in the environment of graphics editors of Corel Draw, Adobe Photoshop, Adobe Flash and Microsoft Powerpoint.

Sound row creation of of electronic trainer and his synchronization with animation.

Sound accompaniment of process of start of engine consists of noises of started auxiliary power-plant, engine and voice of announcer. Two methods of creation of sound accompaniment were used: record of noises at the start of engine in the conditions of the air field by a dictaphone and editing of sound file from the program «Microsoft Flight Simulator». The last shift gave more high-quality sound accompaniment, as the sound is synthesized, and does not cause problems with filtration of extraneous noises, as a dictaphone record. To creat necessary effects of permanent maintenance frequency of rotation, and also sound effect of increasing frequency of rotation in the process of output on the mode, a cyclic segment was selected long in 1 second. Then by the dynamic change of frequency and amplitude of this segment the effect of growth of turns was attained in the program Adobe Audition Professional. In the process of importation a sound was used in the format of Mp3. For the improvement of sounding quality, by facilities of the program Adobe Audition Pro, superfluous noises and echo, arising up at the increase of amplitude were remote.

Facilities of ActionScript were used so far as events of animation must coincide with the events of sound, programmatic synchronization. Start, stop, volume of reproducing of every sound, and also amount of cycles of his sounding, are set with the valid for one occasion commands of ActionScript. It allows to avoid a mess with importation of sounds and complications with synchronization. All sounds here are in the internal library of executable file.

Trainer software is functionally linked base of educational materials, teaching and supervisory programs. It provides individual preparation of a trainee taking into account his primary level of preparation.

Development framework:

Application software of the trainer is developed with the use of Macromedia Flash 8 software framework and programming language ActionScript 2.0 and takes into account the standard requirements of airline “Aeroflot”.

Macromedia Flash 8 software product is the last version (in the moment of beginning of development) of one of the most widespread in the world and the widely applied applications, allowing to execute author works and animation. Reliability, productivity and variety of Flash possibilities, rises with every update version. In respect of traditional animation and graphic program possibilities, support of developers in that became more complete than never. This support

is not only limited by animation, as Flash 8 package evolved in an effective multimedia tool, able to integrate a wide set of languages and multimedia formats.

An object-oriented programming language ActionScript 2.0 is used in Flash 8, which passed the considerable way of development from the primary programming a method «drag&drop» in the version of Flash 4 to reliable and standardized object-oriented language nowadays.

Technology of Flash-document development includes a few stages. Being in development framework, a designer creates a so called author file (document). During this process visual elements, colour chart of project, are developed, and appearances which find embodiment through the vectorial editor of the program are also created. On this stage, if there is a necessity, the import of graphic arts (vectorial or raster) is carried out from external editors, its optimization and integration in a detail design.

Then the animator joins in business. He «animates» characters through an assembling line (or simply decorative elements). The structure of document is formed. The import of video files or sequences, created in external applications is carried out if necessary.

The document is supplied with a phonogram (by sound accompaniment). For this purpose it is necessary to import a sound file (created beforehand in one of the programs specially intended for this purpose).

Then the programmer forms a program framework document and fills the project with interactive maintenance. The range of script language application can be very various depending on tasks. The necessity of the intensive use of programming is conditioned the presence of large number of interactive elements and also non-linearity of implementation of document.

The document has a phonogram (sound accompaniment). For this purpose it is necessary to import a sound file (created beforehand in one of the programs specially intended for this purpose).

We will show development technology of electronic trainer in a general view on the example of the step “Choice of operation mode of auxiliary power-plant”.

As the step «mode of operations of auxiliary power-plant» is intermediate, all necessary elements to continue the work are already drawn, layers are distributed. We open the panel of Actions of scale of Timeline and write a code «stop();» to stop reproducing in while expecting managing influence. We choose the button « 3 pozic 2» and on a panel “Actions” we write the code of passing to the next shot. Thus it is necessary to stop the before started sounds. For this purpose on a panel “Actions” we write a code «sound_7.stop();». We move the losing head of scale of Timeline on the next shot, write a code «stop();». We make a substitution « 3 pozic 2» on «gaz». Button is also commutable «5» on «5_Active». Pressing Ctrl+F12 compile and test the prepared file. **Trainee action control** is carried out due to ActionScript code program. 2 types of errors are counted up separately: errors of choice of necessary devices and management organs, and errors of violation of algorithm of start. A warning signal sounds and an error is set off when incorrect key being pressed. After implementation of exercise there is a general amount of errors, and also a type of perfect errors specification is represented in the field of text-tips, and can be both looked over and unsealed on a printer. Time of implementation of exercise is there represented.

The use of electronic trainer in an educational process allows substantially to reduce bringing in engineer-technical personal of the educational air field in teaching students technology of start and assay of engine PS-90A on the airplane IL-96. In addition, it is possible to replace training of students and test start of engine on an airplane by acquisition of skills on a start and assay of engine on the trainer.

The trainer is intended for working off the correct sequence of executions of a trainee at a start and assay of engines PS-90A on the airplane IL-96.

Work of the trainer is based on the simplified mathematic model of engine work. Control of actions of the trainee is carried out on the basis of actions of a member of the crew in obedience to Guidance on flying exploitation.

The trainer can be used for individual preparation in the educational process of aviation technical schools and training centers of Civil Aviation. The trainer has tree operating modes:

- Self-control (training);
- Control (certification);
- Demonstration.

OPTIMIZATION OF PARAMETERS OF TURBOFAN AFT-FAN ENGINE

Peculiarity of turbofan engine with aft-fan calculation is considered in the paper. It is described adjustment parameters of gas generator and aft-fan of turbofan engine based on optimal gas flow free energy balance between primary and second flows providing the optimal ratio of velocity at the exit plane of the core exhaust nozzle and velocity at the exit plane of the fan exhaust nozzle.

Introduction

Principal ways of turbofan engine development direct at efficiency increasing, rise of specific thrust and as result of it mass reducing.

These problems are solved by choosing optimal engine parameters and air-gas channel configuration. The choice has to meet engine operational requirements and aircraft requirements.

Purpose of the article is investigation of resources for turbofan engine parameters improvement at the expense of aft-fan geometry optimization.

Turbofan engine aft-fan consists of two elements: internal part (core) and external part. Internal part of aft-fan operates in turbine mode. External part operates in propeller mode. Gas flow coming from low pressure gas generator turbine is the working fluid for turbine of the turbofan engine aft-fan. Power developed by aft-fan turbine is transferred virtually without loss into turbofan engine secondary flow and increases energy of air passing through secondary flow.

Adjustment parameters of gas generator and aft-fan of turbofan engine

Thermodynamic calculation of turbofan engine with aft-fan consists of base thermodynamic calculation of gas generator and aft-fan optimal parameter calculation. To obtain optimal parameters of turbofan engine having separate exhaust nozzles it is necessary to partition useful cycle work to primary and secondary flow so as the optimal ratio of velocity at the exit plane of the core exhaust nozzle c_1 and velocity at the exit plane of the fan exhaust nozzle c_{II} is realized. Bypass parameters optimization is carried out for concrete design flight conditions of aircraft taking into consideration different variants of engine design arrangement.

Aft-fan rotor blades have an elaborate design. The fan blades are performed as extension of the turbine blades. The root end of airfoil operates in turbine mode and has corresponding airfoil profile. Tip end of airfoil operates in compressor mode and has compressor blade parameters.

The turbine part of blade row characterizes by extension ratio $\pi_{T,BII}^*$ and extension work required for compression air passing through turbofan engine secondary flow. The external part of aft-fan characterizes by pressure ratio π_{BIII}^* and compression work.

Optimal gas flow free energy balance (optimal parameters value of internal and external parts of aft-fan) that sets conditions for minimum specific fuel consumption for given flight conditions exists.

Given data for calculation aft-fan optimal parameters are results of engine gas generator thermodynamic calculation and operating conditions.

Value of cycle work L_i and parameters of gas flow after gas generator turbine are determined from gas generator thermodynamic analysis findings. Gas generator cycle work is calculated with the assumption that efficiency of compression process (η_c) is equal to compressor efficiency (η_k^*) and efficiency of expansion process (η_{ex}) is equal to gas generator turbine efficiency (η_T^*)

$$\eta_c \approx \eta_k^*; \eta_{ex} \approx \eta_T^*.$$

This assumption is sufficiently correct for preliminary optimization calculation.

Design flight conditions are characterized by design altitude, flight speed V_p and estimated value of air temperature and pressure at the engine and aft-fan inlets (T_H^*, p_H^*).

In design mode efficiency of aft-fan is set on the basis of statistical data for propellers and fans. The aft-fan efficiency is taken $\eta_{BII} = 0,8 \dots 0,85$ in Mach number range $M_H = 0,5 \dots 0,7$.

Optimization conditions

Turboprop engines and turboshaft engines can conventionally be considered as turbofan engines with high bypass ratio (greater than 10). For these engines condition of cycle work optimal distribution between propeller and direct thrust can be written as

$$\left(\frac{c_c}{V_p} \right)_{\text{opt}} = \frac{1}{\eta_B}.$$

Applying this principle to aft-fan parameters calculation the mean value of gas velocity at the exit plane of the core exhaust nozzle

$$c_{cII\text{opt}} = \frac{V_p}{\eta_B}.$$

Optimal free energy balance between aft-fan primary and secondary flow provides at this velocity. It characterizes the minimal specific fuel consumption.

According to thrust creation the turbofan engine with aft-fan is the turbofan engine with separate exhausts. In ideal case for turbofan with separate exhausts condition of optimal distribution of core cycle work W_i is equality of gas velocity at the exit of primary c_{cI} and secondary flow c_{cII}

$$c_{cI} = c_{cII}.$$

According to considered requirement velocity at the exit of primary and secondary flow for design flight speed V_p and optimal parameters of turbofan engine with aft-fan are

$$c_{cI} = c_{cII} = \frac{V_p}{\eta_{BII}}.$$

Determination aft-fan parameters

1. Useful gas generator cycle work which considered as free energy is determined as

$$L_i = \frac{k}{k-1} RT_H \frac{e-1}{\eta_c} \left(\frac{\bar{m} \Delta \eta_c \eta_{ex}}{e} - 1 \right),$$

where $e = \pi_{\kappa\Sigma}^{*k-1}$; $\Delta = \frac{T_\Gamma^*}{T_H}$; $\eta_c \approx \eta_\kappa^*$; $\eta_{ex} \approx \eta_\tau^*$; $\bar{m} = 1,04$.

2. External work transferred by aft-fan turbine to secondary flow can be evaluated using the equation

$$L_e = L_i - \frac{c_{cII}^2 - V_p^2}{2}, \quad (1)$$

taking into account that $c_{cI} = c_{cII} = \frac{V_p}{\eta_{BII}}$, we get optimal value of external work at given flight speed and fan efficiency

$$L_e = L_i - \frac{V_p^2}{2} \left(\frac{1 - \eta_{BII}^2}{\eta_{BII}^2} \right).$$

3. External work transforms to the change in kinetic energy of air flow passing through secondary flow. Taking into account bypass ratio m we have

$$\frac{\eta_{BII,p}}{m} L_e = \frac{c_{cII}^2 - V_p^2}{2}.$$

Subject to the optimal ratio flight velocity and velocity at the exit of primary and secondary flow of aft-fan

$$L_e = \frac{m \left(V^2 \frac{1}{\eta_{BII}^2} - V^2 \right)}{2\eta_{BII}} = V^2 \frac{m}{2} \left(\frac{1 - \eta_{BII}^2}{\eta_{BII}^3} \right). \quad (2)$$

4. From equations in items 2 and 3 we get

$$V^2 \frac{m}{2} \left(\frac{1 - \eta_{BII}^2}{\eta_{BII}^3} \right) = L_i - \frac{V^2}{2} \left(\frac{1 - \eta_{BII}^2}{\eta_{BII}^2} \right),$$

from this we get optimal bypass ratio for given flight conditions and fan efficiency:

$$m_{opt} = \frac{L_i - \frac{V^2}{2} \left(\frac{1 - \eta_{BII}^2}{\eta_{BII}^2} \right)}{\frac{V^2}{2} \left(\frac{1 - \eta_{BII}^2}{\eta_{BII}^3} \right)}.$$

5. Estimated value of fan pressure ratio $\pi_{BII \text{ II opt}}^*$ is calculated according to got optimal bypass ratio:

$$\pi_{BII \text{ opt}}^* = \left(\frac{L_e \frac{\eta_{BII}}{m_{opt}}}{\frac{k}{k-1} RT_b^*} + 1 \right)^{\frac{k}{k-1}},$$

where $L_e \frac{\eta_{BII}}{m_{opt}}$ determined from equation (2).

Value $\pi_{BII \text{ II opt}}^*$ alloys determine flow parameters at the secondary flow nozzle exit. Further aft-fan calculation is determined by conditions of engine design as a whole.

After the definition of the optimal meaning of the by-bass ratio and pressure ratio in the fan, it's necessary to coordinate the parameters of the turbine and of the aft-fan. For solution this problem, it's impossible to use the complex parameter, which is propose in work [1].

$$\Pi = \frac{u_k^2 \bar{G}_k m_g}{\sigma MFP(M_g)} \quad (3)$$

where u_k rotor velocity,

\bar{G}_k = mass flow rate coefficient for fan,

$m_g = 0.0396$,

σ = tensile stress,

$MFP(M_g)$ = mass flow parameters for turbine.

The impossible of using the complex parameter can be explained, that the equation (3) has been received when stretch stress in the turbine blades become clear from equation (4) and depend on the exit turbine square in near the rotation of the rotor constant. In the turbine blades the tensile

$$\sigma = 2\rho \frac{\pi}{3600} N^2 A_t \Phi \quad (4)$$

where ρ = density of the turbine blade alloy,

N = rotor revolution per minute,

A_t = exit turbine area,

Φ = shape coefficient for turbine blade.

Depend not only from parameters, that is used in (4), but from centrifugal forces of the compressor blades too. The centrifugal forces of the compressor blades are perceive by turbine blades.

The influence of compressor blades shape and the turbine blade form for the tensile stress could be considering by the coefficient Φ which is present in equation (4). After substitution of the turbine exit area for gas flow rate and for middle gas parameters the equation (3) could be written in following form

$$\Pi = \frac{m \sin \alpha \sigma_b \pi_k^* \sqrt{T_H^*}}{\Phi_0 K_G f \pi_T^* \sqrt{T_T^*}} 2,32 \cdot 10^{-4} \quad (5)$$

where α = the outlet angle of the gas flow from the turbine nozzle set,

$K_G = 0,93 \div 0,95$ experimental coefficient,

f - fuel / air ratio,

π_k^* - the compressor pressure ratio,

T_H^* - the total temperature at the engine inlet,

π_T^* - the turbine pressure ratio,

T_T^* - the total temperature after turbine.

σ_b - total pressure loss coefficient for main burner,

Φ_0 - empirical coefficient. Its determination is difficult and that is why the simplified formula can be used instead formula (5):

$$\frac{u_k^* \bar{G}_k}{u_T^2 \bar{G}_T} = 0,98 \frac{m}{K_G f} \sigma_b \frac{\pi_{B\pi}^*}{\pi_T^*} \sqrt{\frac{T_H^*}{T_T^*}}, \quad (6)$$

where $\pi_{B\pi}^*$ –fan pressure ratio.

Rotor speed ratio is replaced by tip diameters ratio $\left(\frac{u_k}{u_T} = \frac{D_k}{D_T} \right)$. Tip diameters ratio expresses from hub/tip ratio of fan:

$$\bar{d}_k = \frac{D_k}{D_T} (1 + \Delta),$$

where Δ – length of fan blade root. Mass flow rate coefficient for aft-fan turbine \bar{G}_T is determined from equation (7) using calculated optimal bypass ratio and optimal fan pressure ratio $\pi_{B\pi, \text{opt}}^*$ for given \bar{d}_k and \bar{G}_k .

$$\frac{\overline{G}_K}{\overline{G}_T} = 0,98 \frac{m}{K_G f (1 + \Delta)^2} \sigma_b \frac{\pi_{Bл.опт}^*}{\pi_T^*} \sqrt{\frac{T_H^*}{T_T^*}} \quad (7)$$

Then turbine and fan diameters are calculated from continuity equation and tensile stress in turbine blades is checked.

If aft-fan is assembled with production gas generator having specified air flow rate on the design mode then secondary flow air flow rate G_{II} , engine thrust R_Σ and specific fuel consumption C_R are determined as

$$\begin{aligned} G_{BII} &= m G_{BI}; \\ R_\Sigma &= G_{BI} (1 + m) R_G; \\ C_R &= \frac{3600 g_{II} c_{II} (T_\Gamma^* - T_K^*)}{\eta_\Gamma H_u \cdot R_G (1 + m)}, \end{aligned}$$

where g_{II} - relative fuel consumption, H_u - specific fuel caloricity, c_{II} - fuel specific heat, T_Γ^* - total temperature before turbine, η_Γ - burner efficiency.

If engine thrust is given on the design mode R_Σ then air flow rate through the primary and secondary flows and specific fuel consumption are determined in accordance with the same equations.

Conclusions

The method described in article can be used for calculation geometric parameters of aft-fan at optimal bypass ratio and optimal fan pressure ratio.

References

1. Холщевников К.В. Согласование параметров компрессора и турбины в авиационных газотурбинных двигателях. – М.: Машиностроение, 1965.- 200 с.
2. Холщевников К.В. Теория и расчет авиационных лопаточных машин. – М.: Машиностроение, 1970.- 603 с.
3. Терещенко Ю.М., Волянская Л.Г., Кулик Н.С., Панин В.В. та ін. Теория авиационных газотурбинных двигателей. – Киев: Книжное издательство НАУ, 2005. – 500 с.

CRISIS OF VISCOUS FLOW IN AIRFOIL CASCADE

Flow of viscous compressible gas is considered in the airfoil cascade with big negative angles of attack. Influence of wall boundary layer upon the flow stall modes is estimated in the article.

Introduction

Aerodynamic research of the axial-flow compressor stages begins with calculation of the air flow in elementary stages, are designed as airfoil cascades.

Characteristics of the axial-flow compressor stages and modes' of operation typical restrictions, are determined by using cascade aerodynamic characteristics.

The modes of operation main restrictions are of such types: restrictions for gasdynamic stability, are caused by flow separation under big positive angles of attack, and compressor stage stall modes for the air consumption.

Separation flows are widely spread in nature and practice, description of them plays important role in engineering calculations. Separation appears in the result of viscous-nonviscous interaction between flow layers, that is why viscous processes, as well as nonviscous should be exactly modeled to foresee flow separation. Processes interact nonlinear, this fact have to take into account.

It is well known, that position of a separation point depends on boundary layer condition in front of interaction zone.

Turbulent boundary layer is more stable for separation than laminar, because viscous displacing tension, that has counteracted to pressure gradient is higher. Therefore, during separation flows research it is necessary to consider and to model at quite exactly level condition of boundary layer.

Researches and publications analysis

A number of researches on characterization of the airfoil cascades were made [1, 2, 3]. Functional dependences have received, on the basis of researches' results analysis, and used to forecast an appearance of the flow stall modes for air consumption.

On the Fig. 1 [2] airfoil cascade characteristic in the ideal gas flow was represented. It allows to evaluate an appearance of the flow stall modes depend upon the relation of the throat crosscut flow area to the normal crosscut flow area at the entry into cascade. (F_T/F_1).

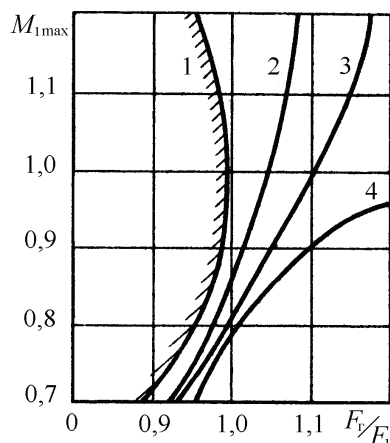


Fig. 1. Dependence of the M_{\max} values from the relation of F_D/F_1 :

- 1 – theoretical attitude(experiment);**
- 2 – supersonic cascade(experiment);**
- 3 – transonic cascade(experiment);**
- 4 – subsonic cascade(experiment).**

The wall boundary layer is formed on a plates surface under real gas flow. Throat crosscut flow area of the blade channel becomes lower, this influences on flow mode and appearance of the stall mode[2, 3].

Target setting

Influence of flow compressibility and viscosity is taking into account to foresee need of quite exact definition of the separation zones' arrangement and intention, also to correct pitch angle and the cascade density, which is calculated for nonviscous flow under different M numbers.

The goal of this research was to define real flow viscosity influence level on stall modes. Target setting like this allows to analyze exactly viscosity influence on stall modes of the airfoil cascade without taking features of aerodynamic plates form into account(plates "bodily").

Geometrical parameters of the airfoil cascade (cascade density $\frac{t}{b}$; plates pitch angle γ), are corresponded to similar parameters for aerodynamic plates cascade. Choking modes overall performance. Air flow under this modes can be divided into confusor (up to throat) and diffuser(after throat) sections.(Fig. 2). If the air flow in the blade channel's throat area corresponds to condition $w_T = a_{cr}$, there will be stall mode with maximum possible air consumption.

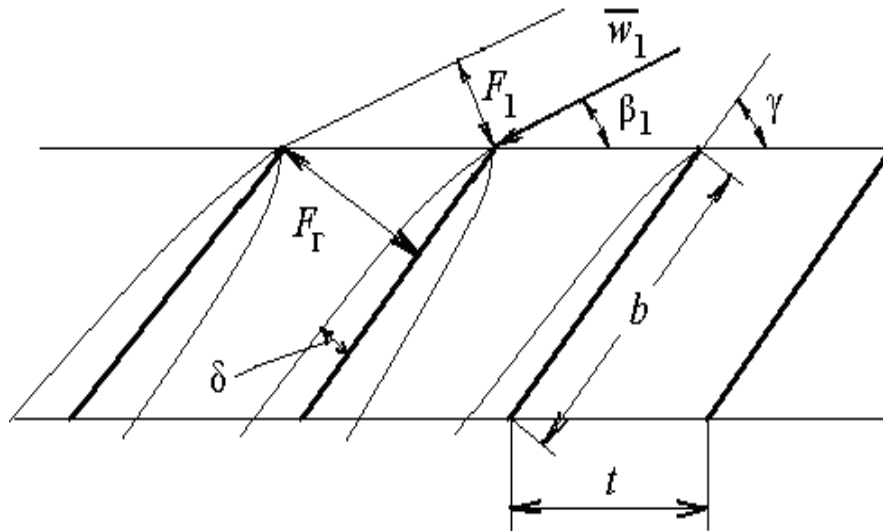


Fig. 2. The airfoil cascade flow scheme

On the Fig. 2 flow parameters are designated: w_1 — is the velocity vector on cascade input; γ — is the plate pitch angle; β_1 —is the angle of attack; b —is the plate chord; t —is the grid spacing; F_1 —is the normal crosscut flow area at the entry into cascade; F_D —is the blade channel throat flow area; δ —is the boundary layer thickness on the profile surface.

Analysis of viscous compressible gas flow in the airfoil cascade

Let's examine gas flow in the cascade of the thin plates(Fig. 1) for two cases: nonviscous compressible gas flow and viscous compressible gas flow.

To the first case consumption equation for sections F_1 and F_T is written down in the form of:

$$mF_1 \frac{P_1^*}{\sqrt{T_1^*}} q(\lambda_1) = mF_D \frac{P_D^*}{\sqrt{T_D^*}} q(\lambda_D),$$

where m — air consumption coefficient, considers features of actuating fluid's physical

property, equal: $m = \left(\frac{2}{k+1} \right)^{\frac{k+1}{2[k-1]}} \sqrt{\frac{k}{R}}$;

R – is the gas constant; F_1 – is the normal crosscut flow area at the entry into cascade; F_D – is the blade channel throat flow area; P_1^*, T_1^* – is the impact pressure and temperature in F_1 crosscut; P_r^*, T_r^* – is the impact pressure and temperature in F_D crosscut; $q(\lambda_1)$, $q(\lambda_r)$ – relative current density in characteristic crosscut.

From equality $P_1^* = P_r^*$ and $T_1^* = T_r^*$ we get:

$$\frac{q(\lambda_r)}{q(\lambda_1)} = \frac{F_1}{F_r} = \frac{t \cdot \sin \beta_1}{t \cdot \sin \gamma}; \quad \frac{q(\lambda_r)}{q(\lambda_1)} = \frac{\sin \beta_1}{\sin \gamma}; \quad q(\lambda_1) = q(\lambda_r) \frac{\sin \gamma}{\sin \beta_1}.$$

Value of the consumption function in F_1 crosscut, corresponds to the flow stall mode in throat F_T is written down in the form of: $q(\lambda_1) = \frac{\sin \gamma}{\sin \beta_1}$.

Quantity $M_{\max} = \frac{w_1}{a}$, corresponds to the appearance of stall flow in the blade channel throat, is written down in the form of:

$$M_{\max} = \left(\frac{\frac{k+1}{2}}{1 + \frac{k-1}{2} M_{\max}^2} \right)^{\frac{k+1}{2(k-1)}} = \frac{\sin \gamma}{\sin \beta_1}.$$

To the second case equation of continuity with taking boundary layer into account, is written down in the form of:

$$m F_1 \frac{P_1^*}{\sqrt{T_1^*}} q(\lambda_1) = m (F_r - \delta^*) \frac{P_r^*}{\sqrt{T_r^*}} q(\lambda_r),$$

where δ^* – boundary layer displacement thickness in F_1 cross section.

From equality $P_1^* = P_r^*$ and $T_1^* = T_r^*$ we get:

$$\frac{F_1}{(F_r - \delta^*)} = \frac{q(\lambda_r)}{q(\lambda_1)}; \quad \frac{t \cdot \sin \beta_1}{(t \cdot \sin \gamma - \delta^*)} = \frac{q(\lambda_r)}{q(\lambda_1)}; \quad \frac{\sin \beta_1}{\left(\sin \gamma - \frac{\delta^*}{t} \right)} = \frac{q(\lambda_r)}{q(\lambda_1)}.$$

To the stall mode under: $q(\lambda_r) = 1$ Derivable:

$$q(\lambda_1) = \frac{\left(\sin \gamma - \frac{\delta^*}{t} \right)}{\sin \beta_1}. \quad (1)$$

where $\frac{\delta^*}{t}$ is the relative boundary layer displacement thickness on the profile surface in the throat area; t – the grid spacing ($t = b \cdot \left(\frac{t}{b} \right)$); b – the profile chord; $\frac{t}{b}$ is the cascade density.

For the viscous gas flow the cascade stall mode is defined by algebraical expression:

$$M_{\max} = \left(\frac{\frac{k+1}{2}}{1 + \frac{k-1}{2} M_{\max}^2} \right)^{\frac{k+1}{2(k-1)}} = \frac{\sin \gamma - \frac{\delta^*}{t}}{\sin \beta_1} . \quad (2)$$

To evaluate the influence of the boundary layer parameters on the stall modes, we use the determination method of turbulent boundary layer's integral characteristics in the blade channel throat. Calculation formula:

$$\delta_r = kx_r \cdot \frac{1}{\sqrt[5]{Re_r}} .$$

Where: x_r is the coordinate of the throat channel (from the profile nose); k is the coefficient characterizing geometric parameters of the cascade and is defined by data of experimental researches (for cascade of the thin plates with grating density of $\frac{b}{t} < 1.5$ and the coefficient of $k \approx$

0.37); $Re_r = \frac{w \cdot x_r}{\nu}$ is the Reynolds criterion for the point with coordinate of x_r . For compressor cascades, transfer point of the laminar boundary layer to the turbulent boundary layer is located near blade entrance edge. Thus making boundary layer calculation as for the turbulent one can be executed for the whole length of blade chord.

The displacement thickness for crosscut in the blade channel throat can be defined by formula:

$$\delta_r^* = \delta_r \cdot \frac{1}{n+1}, \text{ where the coefficient } n = 1.43 \dots 2.5.$$

For the cascades with grating solidity $\frac{b}{t} = 0.8 \dots 1.5$ chord $b = 80 \dots 120$ mm, angle of pitch $\gamma = 38 \dots 45^\circ$, flow parameters correspond to the numbers of $Re = 3 \dots 5 \cdot 10^5$, impulse losses thickness $\delta = 0.3 \dots 0.4$ mm. Based on the fact, that boundary layer integral characteristics are interrelated by formula:

$$\frac{\delta^*}{\delta^{**}} = \frac{2+n}{n} , \quad (3)$$

The displacement thickness of the boundary layer in the cross section of the blade channel throat is:

$$\delta^* = \delta^{**} \cdot \frac{2+n}{n} = 0.76 \dots 0.92 \text{ mm}.$$

We receive the M_{\max} values by formula (2) taking into consideration displacement thickness of the boundary layer by formula (3) and can evaluate gas viscosity influence on stall of axial-flow compressor stages. Fig. 2 shows the M_{\max} values, are calculated for nonviscous gas flow in the airfoil cascade by following dependence:

$$M_{\max} = f\left(\frac{F_r}{F_1}\right).$$

Fig. 3 shows calculation dependences of M_{\max} values for the flow without taking boundary layer into consideration, and M_{\max}^* values with taking boundary layer into consideration

Analysis of these dependences proves that throat channel stall under significant reduction of speed values at the cascade entrance takes place, as a result of the viscous real flow influence. In the airfoil cascade, discrepancy of M_{\max} and M_{\max}^* values is from 5 to 15%. Comparison of stall modes

characteristics for airfoil cascade (Fig. 3) and experimental data for aerodynamic profiles gratings (Fig. 1) proves that the offered method of calculation is correct enough.

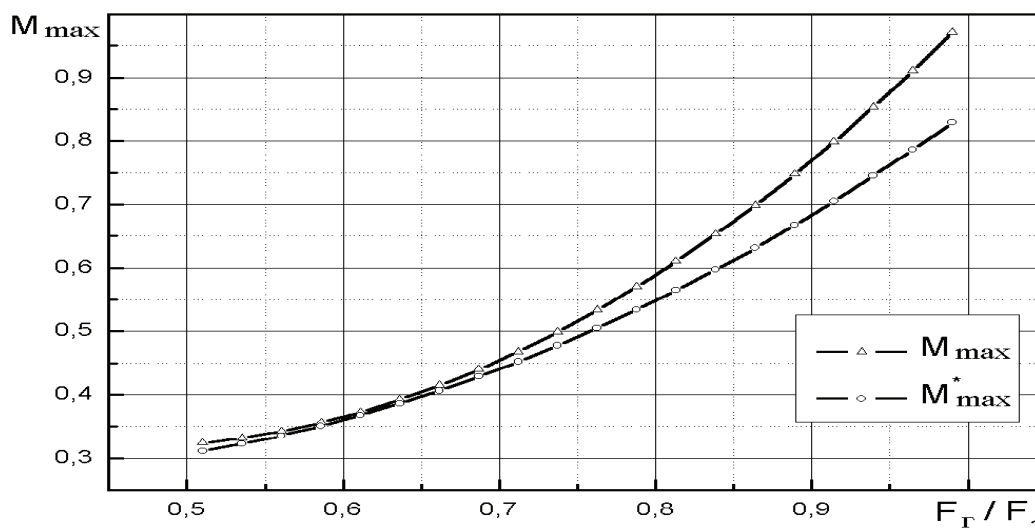


Fig. 3. Dependence of the M_{\max} values from the relation of F_T / F_1

The M^*_{\max} values had defined with the help of the formulas (1) and (2) under quality signs contemporized with the experimental research results, that are shown on Fig. 1 (curves 2-4). Continuation of researches in this direction should be oriented to determine the calculation dependences to evaluate flow viscosity influence on subsonic and supersonic airfoil cascades characteristics.

Conclusions

1. Offered method allows to evaluate the estimation of the flow viscosity influence on cascade aerodynamic characteristics during streamline of them with the big negative angles of attack . Comparison of stall modes characteristics for the airfoil cascade (Fig. 3) and experimental data for aerodynamic profiles (Fig. 1) proves that offered method of calculation is correct enough.

2. Taking flow viscosity into account leads to lowering the M_{\max} calculation value, corresponds to the compressor cascade stall mode for the air consumption. For the airfoil cascade the M_{\max} and M^*_{\max} values discrepancy is from 5 to 15%.

3. The aim of the further research is to obtain results and to analyze the influence of peculiarities of the aerodynamic form of cascade blades profiles on the grating blocking modes in the viscid gas flow.

Reference

4. Терещенко Ю.М., Мітрахович М.М. Авіаційні газотурбінні двигуни.–К.: КВІЦ, 2001.– 312 с.
5. Терещенко Ю.М. Аэродинамика компрессорных решеток. – М.: Машиностроение, 1979. – 120с.
6. Терещенко Ю.М. Аэродинамическое совершенствование лопаточных аппаратов компрессоров.–М.: Машиностроение, 1987.-168 с.

OPTIMISATION OF PROCESSES OF AIRLINE LOGISTICS

Methods of optimisation of logistics support system of maintenance processes by repair parts on the basis of the reliability analysis and resource state of airline aircrafts park are observed.

Introduction

To aviation technique (AT) provision by repair parts major attention is constantly paid. It results from the fact that to create absolutely reliable object is impossible and for its maintenance repair parts (SP) are always necessary. They are necessary for elimination of random failures and substitution of the wearing out parts. It demands coordination of logistics processes and process of aircrafts maintenance as a whole with logistics support of airline activity, in particular, with the its maintenance service (MS).

1. Supply optimisation and forming of necessity in material resources

In operation practice for estimation and maintaining of reserves and spar parts various models of spar parts optimization are used. Most often in these purposes stochastic model are used. They are based on data about AT failures and faults for the previous period and also data about resources residuals and aircraft run on predictable period. There are two the most justified and accommodated for operating time accounting system models .

Model 1 is grounded on use of law of small numbers by comparison of observable number of failures n_ϕ with regulating upper bound (RUB), representing admissible level of reliability. The observable number of failures in certain times has character random from null to RUB. Value of RUB is determined with use of law of small numbers. RUB determines with the accepted probability $P_{\text{зад}}$ high limit of failures n = received which will not be exceeded with the given probability $P_{\text{зад}}$ in the presence of only stochastic reasons [7]:

$$P_{\text{зад}} = \sum_{n=0}^{n=BTP} \frac{(\omega_{cT}Ta)^n}{n!} e^{-\omega_{cT}Ta}$$

Where T – run of airplanes park; a – number of similar airplane types; ω_{cT} –planned failure rate; $P_{\text{зад}}$ – probability of failures number, which does not exceed regulating upper bound.

On fig. 1. it possible to see monograms of quantity of articles not exceeding regulating upper bound with the given probability $P_{\text{зад}} = 0,975$ for various predictable failure rates and $\omega_{cT} = \{0,4; 0,65; 0,8; 1,2; 1,6\} \times 10^{-3}$, $a = 1$

Model 2 is grounded on estimation of quantity of the spare parts required for maintenance of article on set interval $[0, t_k]$, at major enough interval of maintenance in comparison with mean time between failures [4].

$$m(t) = \frac{t}{T} + u_\alpha \frac{\sigma\sqrt{t}}{T^{3/2}},$$

where $m(t)$ – quantity of spare parts, $U_{1-\alpha}$ –quantile of normal distribution for probability, equal to $(1-\alpha)$, T –mean time between failures, σ^2 – time variance between failures, t – total operating time.

On fig. 2. monograms of quantity of spare parts depending on probability are resulted at $p=1-\alpha$, mathematical expectation and mean standard deviation of time between failures equal $T = 500$, $\sigma = 200$.

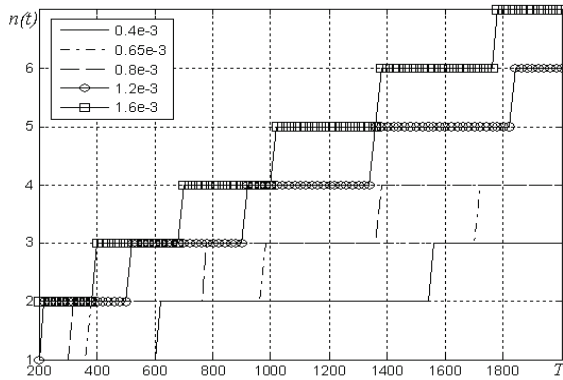


Fig. 1. Quantity of articles not exceeding regulating upper bound with probability $P_{\text{зад}} = 0,975$ for various parameter values of failures flow (model 1).

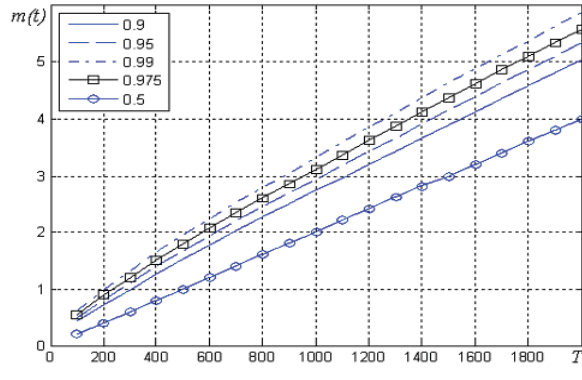


Fig. 2. Relation of required number of articles instead of failed articles providing given probability (model 2).

2. Airline park supply by spar parts by maximum of probability of non-failure operation criterion on the basis of rational selection of reserve elements at limited financing

The common statement of problem on spare parts provision can be formulated thus: let the average of failures m_{cp} and cost of recovery c_i of each i -th part which works in system throughout time t_i is known ($t_i \leq t$). Considering that quantity of spar parts should be not less then quantities of failures, definition of quantity of spare parts of one type is reduced to m_p determination from the equation [5]

$$P(m_p) = e^{-\Lambda t} \sum_{i=0}^{m_p} \frac{(\Lambda t)^i}{i!} = e^{-m_{cp}} \sum_{i=0}^{m_p} \frac{(m_{cp})^i}{i!}.$$

The number of spare parts can be discovered also by approximate formula

$$m_p = \Lambda t + U_r \sqrt{t \Lambda}.$$

It is necessary to determine the quantitative structure of spare parts for the greatest possible probability of non-failure $1-\alpha$ of engineering system throughout time t . Quantity of spare parts is determined taking into account limitation

$$\sum_{i=1}^k c_i m_i \leq C,$$

where m_i – number of spare parts of i th type, c_i – cost of one part of i th type, C – total sum for spare parts purchase.

Thus maximisation of probability of non-failure in case of the normal law:

$$\sum_{j=1}^k \left[\frac{t}{T_j} + U_{1-\alpha} \sqrt{\frac{\sigma_j^2 t}{T_j^3}} \right] c_j \leq C,$$

where T_j – mean time to failure of j th part, σ_j^2 – time to failure variance, t – total operating time, $[\cdot]$ – integer part of number.

In the equation it is required to discover such maximum value of quantile of distribution ($U_{1-\alpha}$) at which the inequality is fulfilled. It is necessary to note, that the minimum financing of spare parts should be not less then the costs of average of parts failed at the indicated period t , i.e.

$$C > \sum_{j=1}^k \left[\frac{t}{T_j} \right] c_j.$$

On fig. 3, optimum quantity of spare parts of each type, their greatest possible probabilities of non-failure and total costs of complete sets of the same type repair parts for normal ($P_{hj} > 0,889$) and exponential ($P_{pj} > 0,905$) distributions (the Poisson flow of failures) are shown. $P_{hj} > 0,889$ $P_{pj} > 0,905$ at initially set quantity of failures and cost of parts for base period and the limiting financing $C=190000$ y.e.

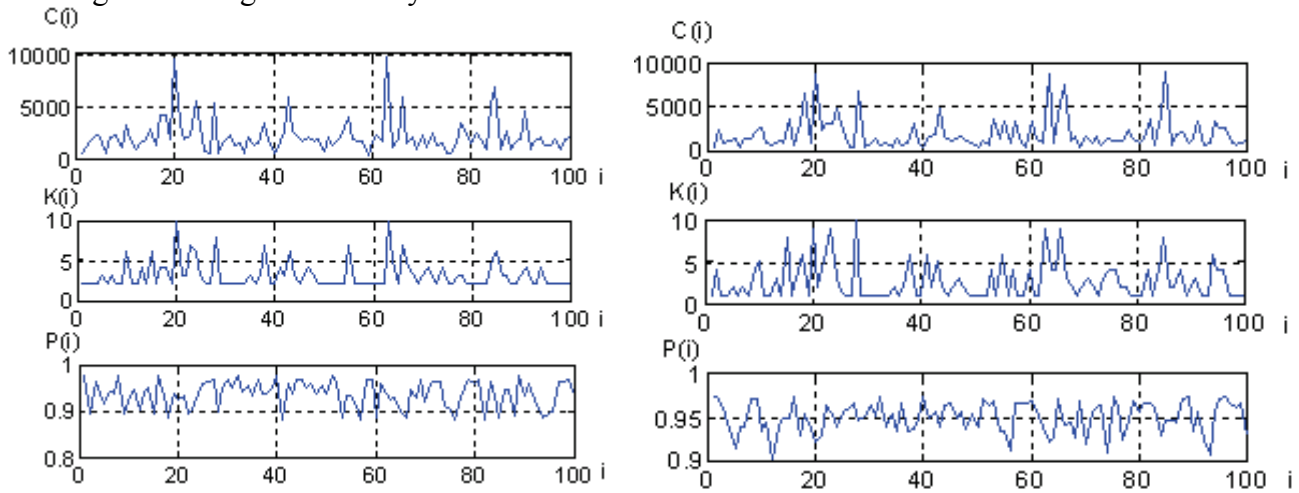


Fig. 3 Maximization of probability of non-failure operation on the basis of rational selection of reserve elements at the limited financing: a - normal distribution; b - Poisson flow of failures.

3. Optimisation of supply process to provide given probability of non-failure of the complex engineering system

For complex systems at RUB calculation methods of structural, logical circuits and functional method are used. These methods can be used in problems of optimisation of spare parts logistics system. In this case at failure of system consisting of n part parts, each part is substituted by another one with the same performances of reliability. The formula of calculation of probability of non-failure for the scheme with m -multiple unloaded reserve looks like [2]

$$P_i = \exp(-\lambda_i t) \sum_{j=0}^m \frac{\lambda_i^j t^j}{j!}$$

Thus, probability of part non-failure is increased at each adding of the reserve element and consequently systems RUB increases too. The problem consists in discovering sequence of substitutions of parts which, by each selection of part, maximises probability of system non-failure.

For security of non-failure operation of fuel system number of logical (fig. 4) [9]. should be executed.

On the scheme through A_i the events consisting in non-failure operation are marked out,: aircraft part of fuel system (event A_1); automatics of fuel rate control (event A_2); pilot using manual selection of fuel delivery pumps (event A_3); fuel flow-meter (event A_4); parts of manual selection of delivery pumps (event A_5); automatic control unit of centre-drilling (event A_6); system of fuel supply of left engine (event A_7); system of fuel supply of right engine (event A_8).

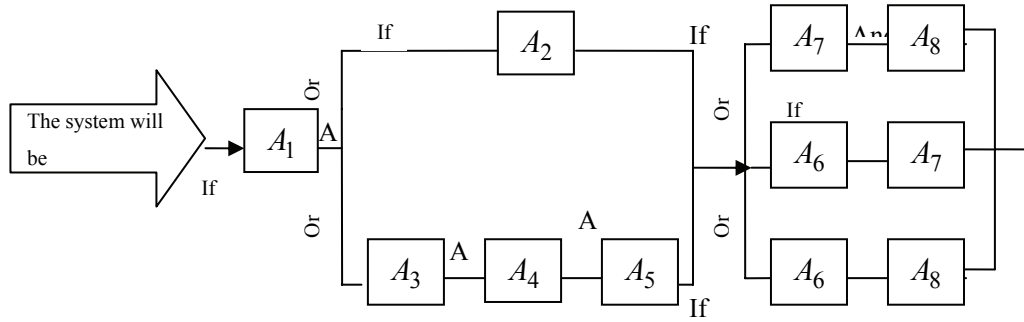


Fig. 4. The Logical circuit of non-failure operation of fuel system.

Probability of non-failure of fuel system of airplane, P_{cucm} according to the scheme, it is possible to be calculated by method of logical circuits by formula

$$P_{cucm} = P_1(P_2 + P_3 \cdot P_4 \cdot P_5 - P_2 \cdot P_3 \cdot P_4 \cdot P_5)(P_7 \cdot P_8 + P_6 \cdot P_7 + P_6 \cdot P_8 - 2P_6 \cdot P_7 \cdot P_8)$$

Where – $P_1, P_2, P_3, \dots, P_8$ probabilities of implementation of i th events (failures).

On the basis of statistical data of failure rate of fuel system parts are resulted in tab. 1.

Table 1.

The statistical given rates of failure of parts of fuel system

Events	Symbol	Value of intensity $\lambda = \frac{1}{m}$
A_1	λ_1	$2,5 \cdot 10^{-4}$
A_2	λ_2	$10 \cdot 10^{-5}$
A_3	λ_3	0
A_4	λ_4	$8 \cdot 10^{-5}$
A_5	λ_5	$10 \cdot 10^{-5}$
A_6	λ_6	$10 \cdot 10^{-5}$
A_7	λ_7	$5 \cdot 10^{-5}$
A_8	λ_8	$1 \cdot 10^{-5}$

If time in flight is equal to four hours ($t = 4$), that, receiving distribution of mean time between failures at all parts of fuel system under the exponential law, $P_i = e^{-\lambda_i t}$ we gain $P_{cucm} = 0.99820130$. For small t , accepting $P_i \approx 1 - \lambda_i t$ it is possible to gain approximate value for probability $P_{cucm} = 0.99820072$, which coincides with exact within the sixth signs.

If to accept for prediction interval $t = 5000$ h. and for RUB - $P_{cucm}^{np} = 0,975$ on the basis of the statistical given values of failure rate of fuel system parts (tab. 1) number of the added parts as RUB maximum modification are placed as follows

$$n(t) = [7, 1, 1, 2, 1, 7, 2, 1].$$

Thus, systems RUB accepted values

$$P_{cucm} = [0,2014, 0,4532, 0,6105, 0,7539, 0,8348, 0,9040, 0,9470, 0,9757].$$

At total number of spar parts equal, $k_s = 8$ quantity of the added on type parts is equal

$k(i) = [4, 2, 0, 0, 0, 0, 2, 0]$ (fig. 5 a).

If in calculations of fuel system RUB the consecutive scheme, in sense of reliability, by the order of RUB maximum modification is used (fig. 5 b)

$n(t) = [1, 2, 5, 6, 4, 1, 7, 1, 2, 5, 6, 4, 8, 1, 7, 2, 5, 6, 1]$.

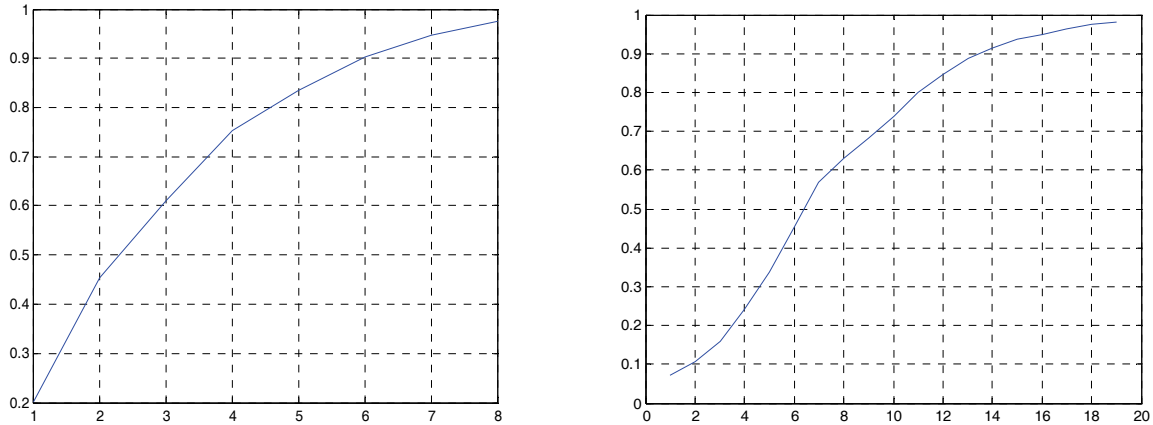


Fig. 5. RUB modification of fuel system: a - at schematic connection; b – at consecutive connection

4. Optimisation of spare parts supply of recovered AT articles

The important problem of AT maintenance is calculation of recovered spar parts reserve where for the purpose of minimisation of idle time of airplane failed aggregate is immediately replaced by spar part and it is guided to repair. The repaired aggregate supplements with itself the spar parts reserve. Insufficiency of the spar parts reserve increases airplane idle times, and redundant spar parts reserve fixes money resources and demands expenses on storage of articles. The similar scheme is widely applied at AT maintenance of large airlines, which has major number of the homogeneous aggregates. The classical approach to the solution of this problem of storekeeping is application of methods of queueing theory, in particular, for model with failures $M/M/1/S$. Required articles is observed as the channel holding, each request calls the ordering for fulfilment (repair), duration (delay) is interpreted as maintenance time.

The problem solution is the optimum volume of the spar parts reserve which is set by the formula [6]:

$$s^* = \left\lfloor \frac{\ln(d(1-\rho)/h)}{\ln(1/\rho)} \right\rfloor,$$

Where h – the price of article storage; d – the price of idle time of airplane for the same unit time (the penalty price); $\rho = \lambda/\mu$ – load factor of system recovery, λ – failure rate; μ – intensity of recovery.

On fig. 6 plots of ratio of logs from right member of the formula for load factors from 0,05 to 0,975 and the norm of the penalty ($\frac{d}{h} 10^2 \dots 10^6$) are resulted. The rounding off of nonintegral numbers should be yielded for obtaining of optimum reserve in the smaller side.

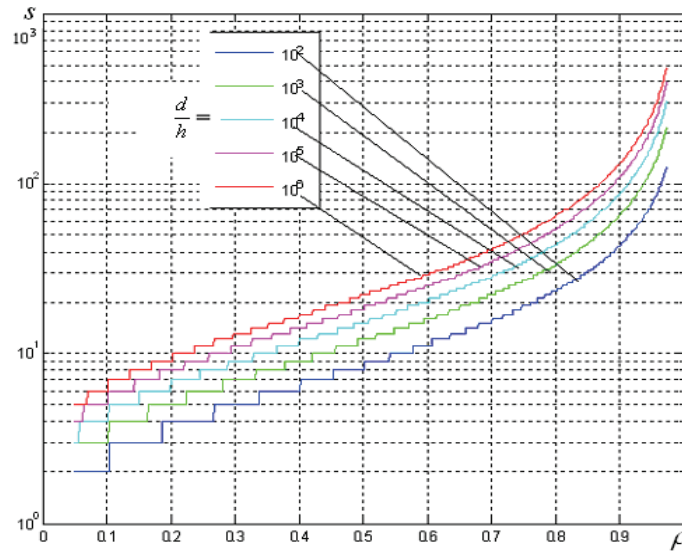


Fig. 6. Relation of optimum reserve to the penalty $\frac{d}{h}$ and load factor norm $\rho = \lambda/\mu$

5. Forming of optimum size of the ordering of spar articles

In the course of delivery of spar parts there is problem of optimisation of size of the ordering and frequency of deliveries in the form of separate complete sets for consumptions minimisation of offtheir delivery and storage, which can be expressed as follows[8]:

$$\Gamma = AS/Q + SC + ZQ/2 \rightarrow \min,$$

where C – the price of unity of ordered article; Z – charges on reserve unity storage; Q – ordering size; S – necessity in material for certain period; A – cost of delivery of one complete set of the ordering.

Calculation of optimum size of ordering Q^* is executed by formula [1]:

$$Q^* = \sqrt{\frac{2AS}{Z}}$$

Point of the repeated ordering:

$$P = LS/N$$

where N – number of the working days in period; L – period of obtaining of the ordering

Interval of time between orderings:

$$T = N \cdot Q^* / S$$

As display practical calculations expenditure for orderings are approximately equal to storage charges.

If products are delivered from one manufacturer or geographical zone (city) it is possible to present functional in kind:

$$D + \sum_{i=1}^n A_i \frac{S_i}{Q_i} + \sum_{i=1}^n S_i C_i + \frac{1}{2} \sum_{i=1}^n Z_i Q_i \rightarrow \min,$$

where A_i – cost of registration of the ordering on i -й kind of products D – cost of delivery of one complete set of the ordering.

6. Optimisation of aircraft engines supply of airline park

The most adequate methods of long-term prediction of processes of maintenance and reproduction of aircraft engines park are simulation models, which are grounded on simulation of engine service life (fig. 7) [3].

In the simulation model service life is executed in four stages: initial distributions of objects in all states (maintenance, repair, storage), advancing of system time and accumulation of

modifications in all parts of system; analysis of modifications in each part; decision making on each part of system according to the selected strategy of maintenance[10].

For implementation of this strategy all service life states plane and engine are dissected on n internal states, which match to i -th value of operating time, from initial to limiting, equal to the assigned service life of engine.

The mathematical presentation of all processes is executed on the basis of discrete Markovian circuit looks like Kolmogorov-Chepmen differential equations. For process of maintenance the set of equations looks like

$$\begin{cases} \frac{d}{dt} P_{2,1}(t) = -\lambda'_1(1)P_{2,1}(t) - \lambda_2(1)P_{2,1}(t) + \lambda_1(t)P_1(t) \\ \frac{d}{dt} P_{2,i}(t) = -\lambda'_1(i)P_{2,i}(t) - \lambda_2(i)P_{2,i}(t) + \lambda_1(i-1)P_{2,i-1}(t), \quad i = \overline{2, n} \end{cases}$$

where $\lambda_1(i)$ and $\lambda_2(i)$ – intensity of exit / entry (-/+) from maintenance state (Θ_2) accordingly on resource and on failure; $P_{2,i}(t)$ - probability of determination in i -th state of maintenance Θ_2 with operating time H_i

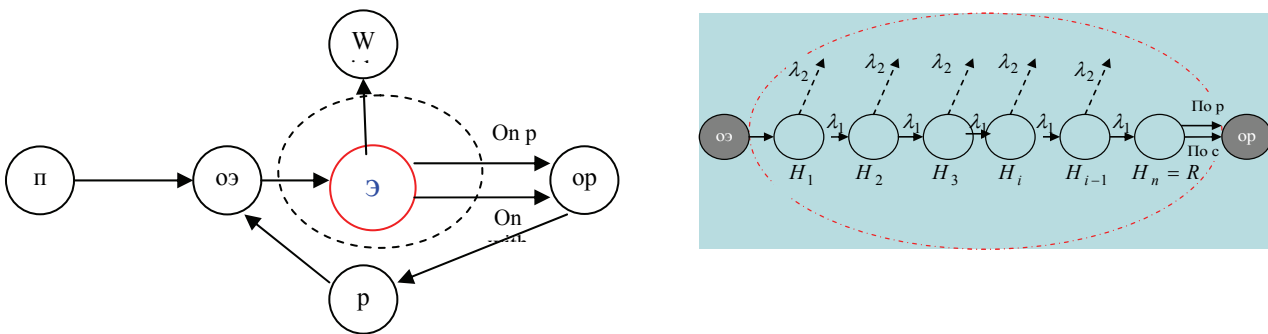


Fig. 7. Structure of processes: a - maintenance and repair (life cycle) of engine; b - fragment of maintenance process (Π – manufacture; OΘ – maintenance expectation; Θ – maintenance; P – repair; OP – repair expectation; C – discarding;

H_i - State with operating time H_i ; λ_1, λ_2 – intensity of passage on resource and failure.

Information about initial resource state of airplanes park , engines and their operating time on the prediction beginning, and also rates of run modification of park, considering seasonal oscillations for last two years are gained within the limits of AT system reliability. One of versions of such calculation is presented on fig. 8 and rice 9.

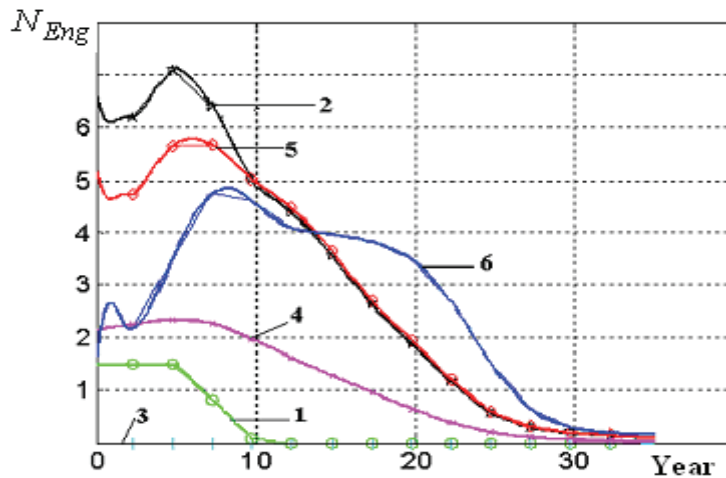


Fig. 8. Quarterly performances of engine cycle:

1 - manufactured in quarter, 2 – used in quarter, 3 – repair waiting, 4 – removed for repair before the term, 5 – under repair for quarter, 6 – discarded for quarter

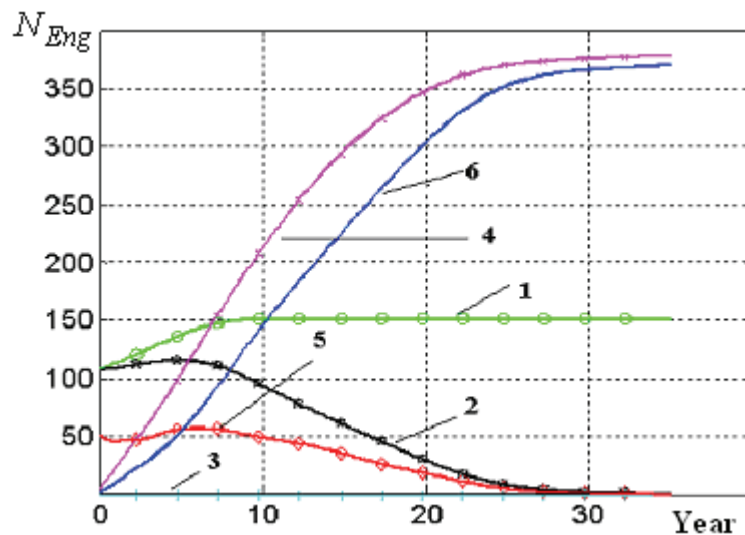


Fig. 9. Integrated performances of engine cycle:
 1 - manufactured in quarter, 2 – used in quarter, 3 – repair waiting, 4 – removed for repair before the term, 5 – under repair for quarter, 6 – discarded for quarter

References

1. Kazshncke A.M. Aloysius: Manual for students. – 12-th edition. – Moscow:(Dashkov and K) , 2006. – 432 p.
2. Komarov. A. A. Aircrafts reliability Manual for students. Комаров А.А. – К.: КМУКА, 1997. – 416 p.
3. Olexiy Kucher., Mustafa A.S. Mustafa. Air-engine demand planning and forecasting of airline's air fleet // Visnyk NAU. – 2007. – № 3-4.–p.77–84.
4. Engineering systems reliability: Manual/ Bereverzev E. Albarto A. Danuev Y. – Dnipropetrovs'k: Boroku, 2002. – 396 p.
5. Ostrenkovskiy B.A. Theory of reliability – Moscow, 2003. – 463 p.
6. Rechekov Y. E. Queues theory and reserves management. – SPB.: Peter, 2001. – 384 p.
7. Smernov N. N. In conditions maintenance and repair of aviation technique.– Moscow: Transport, 1987. – 272 p.
8. Cohen M.A., Kleindorfer P.R. at al. Multi-item service constrained (s, S) Policies for spare parts logistics systems // Naval Research Logistics. – 1992. – no. 4. – p. 521 – 529.
9. Douglas S. Carmody Airplane Maintenance and Repair: A Manual for Owners, Builders, Technicians, and Pilots, Paperback. – 1998, McGraw – Hill. – 346 p.
10. Michael J. Kroes, William A. Watkins (contributor), Frank Delp (Contributor) Aircraft Maintenance & Repair (Aviation Technology), Paperback. 6th edition, 1993, Glencoe McGraw – Hill. – 648 p.

*M.S.Kulyk (Ph D Engineering, Professor), A.A.Tamargazin (Ph D Engineering, Professor),
I.I.Linik (Ph D Engineering) (National aviation university, Ukraine)*

AIR TRANSPORT INTEGRATION PROCESS MANAGEMENT

The modern problems of aircarriers integration are considered. Basic scientific and practical recommendations on the choice of forms and methods of air transport integration processes development in Ukraine and estimation of their efficiency are defined.

Low-income popular majority of the country on the one hand, and high level of running expenses on the other hand, do not allow even to the large domestic carriers to use their sizable financial resources for updating the aging airline fleet and modernization of infrastructure objects. A situation is aggravated by the modern market of aviation services, characterized by destructive competition which continues to exhaust resource potential of airlines. Competition is stepped up by the foreign carriers. There is the passengers outflow to the foreign airlines which widely use the integration as a method of raising of their competitiveness. These factors require industry consolidation, collaboration and cooperation development.

The international market of passenger transportations in fact turns out to be shared between global alliances of the world largest airlines. Consolidation of airlines in the form of aviation alliances or other economic unions is one of methods for raising the efficiency of transportations under the severe competition conditions. And world air transport itself, strictly speaking, is found hard up: the regular global airlines for 5 years in succession suffer losses, there is the large surplus of unused carrying capabilities, regularity of flights, their safety etc., is violated.

Unlike world practice, integration processes development in civil aviation of Ukraine still takes place in very small scales, or «convolves» on the earliest implementation phases.

The analysis of global market development of air traffic showed that a period from 1996 to 2007 was characterized on the whole by growth of air traffic with the average annual growth rates of passengers transportations by 4%, freight by 6 %; 20 global airlines out of 811, carrying passengers on international and domestic regular air-routes, transport more than 50% all passengers of regular routes. In the structure of regular passenger transportations of global airlines the share of the transportations volume, carried out on the international routes, was 60%. The dynamics of volume indices of air traffic in different regions of world differed from average level. The highest growth rates are shown by the carriers of Near East and African airlines.

In spite of steady growth rates of air traffic volume, global air carriers experience deep crisis (i.e. airlines work with negative profitableness). The main reasons of this, besides the growth of political instability in the world mentioned, are the price increase of air fuel, increase of cost of airplanes, ground service, taxes, collections and payments set by governments and airports, and also the personnel costs.

In the global fleet of airplanes the share of transportations performed by aircraft with the specific fuel consumption over 30 g/pass. km, does not exceed 5%, while in Ukraine such airplanes make 80%. The modernization of aircraft fleet is carried out with extremely low rates.

The tendency of sharp decreasing of domestic internal transportations while increasing the international sector influenced the development of the airport system of the country.

The volume of state support of airports for modernization of material and technical base has made about 20-30% from the general volume of investments lately, and participation of regional budgets in an investment process makes less than 10%.

The research showed that, with the development of air traffic sector, the necessity for the high-quality ground infrastructure increases. Nowadays there is an urgent necessity for creation of international transport hubs. By the experts estimate, the construction of one hub gives, by the most pessimistic estimation, annual increase of no less than 1,5 mln. pass., and the regional hubs available – up to 7 million

The process of competition strengthening of the Ukrainian airlines with foreign aircarriers is underlined. Mainly it is related to the passengers outflow to the western airlines. Booking of business-class on the routes of domestic aircarriers, as a rule, does not exceed 40%. Industry consolidation both for saving of leadership at the internal market, as well as for joining international market is required. The analysis of airlines collaboration and cooperation development showed that integration processes in global air transport have taken place by stages, in a definite sequence, within the framework of general tendencies.

The first stage was characterized by confluence of airlines of one country, because the international law did not allow the receipt of commercial rights to those companies in which more than 25 % foreign participation was present. First to appear on international lines were alliances not supposing to exchange ownership. Next stage of integration development is related to the process of liberalization of air transport regulation. Appearance of countries with the minimum regulation and control of rights for access to the market, its capacities and pricing, promoted the strengthening of integration processes and appearance of large coordinating centers.

Nowadays, the main tendency at the international market is deepening of cooperation of airlines in different regions of the world, including sharing codes, implementation of transportations and participation in the programs of encouragement for the passengers who fly regularly. There is still the process of market liberalization. Greater part of mergence and acquisitions is carried out within the same country. More of possibilities for the mergence of transactions on confluence with foreign airlines and their acquisition appeared, mainly owing to the fact that many states adopted a new policy or changed effecting rules with regard to foreign investments and control of national carriers for the purpose of rising of efficiency and search for new investments for the airlines development. As the analysis showed, the airlines interested in gaining the access to the internal market of the competitors come forward for abolition of limitations most actively.

Presently in the world there are about ten global alliances which develop actively. At the start of 2008 about 80 % world aviation market has been controlled by global aviation alliances.

Marketing alliances having temporary character and allowing to the airlines to keep legal and financial independence became the preferable form of union in Ukraine. The attempts of voluntary union in other forms are undertaken by the Ukrainian airlines, but duration of their existence so far does not allow to draw conclusions how successful they are.

Absence of clear determination of integration in entrepreneurial activity in the Ukrainian legislation, as well as difficult and contradictory character of integration processes showed up in existence of different approaches to determination of this notion. It is possible to select two aspects of the considered phenomenon, which can be classified by their development in time: aspect of dynamics, characterizing process as an action and the action itself of creating integrated structures; aspect of statics, characterizing the result of this process, that is functioning of newly- formed structures.

As the analysis showed, according to the theory of the systems the integration is considered as the state of the system separate components intercommunication and the process which stipulates such state. Consequently, integrity of the system is expressed by the high-quality specific property which is created in the process of continuous cooperation of elements and is absent in the simple sum of properties of separate elements. The latter allows asserting that when the system integrative properties are available, the effect of synergy appears, and the main purpose of airline integration is the achievement of synergetic effects, which in market economy appear, first of all, in achieving of competing advantages due to the integrity of the object.

There is also an approach which determines integration as the interconnection with the market of corporate control. By the integration the process of acquisition/union of rights for the control over a company is meant. In this case integration processes will be realized by means of corporate mergence.

The analysis of different definitions of integration allows asserting that they should not be considered as alternatives, for all of them reflect the main source of effect – synergy, which provides the receipt of competitive advantages. So principle of competition will be realized with

larger effect in the integration systems.

Taking into account the world three basic systems of corporate management (English-American, European and Japanese), in international practice three basic models of integration are selected: Anglo-Saxon, Continental and Japanese, distinctions in which to a great deal are determined by the features of corporate management in that or another country. Such features are: instruments of economical-legal infrastructure within the framework of which shareholders can realize the right of ownership, and also character of distributing of joint-stock ownership in a country. Thus absence or relatively rare use of certain mechanisms is connected, for example, with the market intercept of corporate control, and can be compensated by the other one, such as, owning the large share holding, domestic control, belonging to the created group.

Classification by the organizing and legal registration (corporation, business concern, holding, conglomerate, strategic alliances and etc) and by the direction of integration is the most widespread (horizontal, vertical, conglomerate and etc).

The analysis of world experience allows to determine seven basic reasons of integration: receipt of synergetic effect; upgrading of quality management; tax motifs; possibility of the surplus resources use ; the personal motifs of managers; difference in the market price of company and cost of its substitution; difference between liquidating and current market value. Practically there is no situation in which an enterprise during integration would aspire the achievement of a certain single purpose. As a rule, the question is about the system of purposes, that, in its turn, presents a serious problem at planning of integration of companies. It is related to the decision of such questions, as: estimation of the integration object cost, mechanism of realization of transaction on integration, adjusting of postintegration co-operation of subdivisions and others. So there is no universal formula by which it is possible to estimate or realize an integration process, but there is a mechanism of the given process control.

As a methodological tool at the integration process control on the air transport the conception of project management can be recommended as the most complete, responding to the requirements of complexity in the development of air transport. The given conception is based on the «project» notion, which comes forward as the object of management, possessing specific features effluent from the essential features of every concrete project.

Determination of purpose is the starting point of the project management methodology – the desired state of the guided object, which must contain the basic idea of the project and determine the project and activity on its realization on the whole. Further in the project management the purpose is decomposed into the realized and guided elements of activity, logically and organizationally bound in complexes and packages of works.

At the level of Ministry of transport the mission of passenger transportations by the air transport, primary purposes and strategies of industry in investing, financial and other spheres must be defined. The project management allows considering the market of air transportations as a system of large scale, uniting commercial (profitable transportations) and socio-economic (regional and local transportations) subsystems. This is especially important for the choice of mechanism of government control of economic processes in the commercial and social sectors of transport market. The purpose of project must be open up in the detailed plan of actions, which reflects different aspects of project and can be expressed depending on its content in different documents. It allows removing the lack of coordination on the levels of management by an air transport, resulting in the decline of efficiency and quality of transport service.

Methodical approach to the economic substantiation of choice of the air transport integration variant can be developed on the basis of application of the unclear set (TUS) theory and method of analysis of hierarchies (MAH). TUS is used for research of economic problems of activity of enterprises in the conditions of vagueness. At planning of integration practically it is impossible to build mathematically strict (adequate) formal model of the incorporated company (alliance) due to the fact that a number of parameters of the enterprises integration process, considerably affecting the results of the task decision, turns out to be indefinite. Complex hierarchic structure of integration purposes suggests using the special methods of optimum decisions acceptance theory,

including MAH.

Two-stage procedure of integration processes simulation is suggested.

On the first stage the model of unclear set estimation of the integration alternatives efficiency with the use of linguistic variable is made, i.e., the variable, the meanings of which are not numbers, but words or sentences of natural or formal languages. From feasible solutions 2-3 variants of integration are selected, which are characterized by the largest potential of synergetic effects according to the results of the multicriteria estimation. These variants are considered as «perspective» from the point of realization of purposes and development of airline, and are the «approximate» ones. Perspective variants further come forward as elements of great number of effective decisions on integration and pass to a next stage of simulation.

On the second stage additional, specifying information for the simulation with the use of the MAH is involved. The use of new information increases the level of requirements to the considered variants and solves the problem of high-quality variety of alternatives. From the great number of effective variants the optimum decision on integration development of airlines with taking into account horizontal and vertical connections in the hierarchy of economic criteria and indices is selected. Additional information must comply with the requirements of the content, for it should give the answers to the following questions: does this additional information contradict to the current one, and, if not, does it carry anything new? For this purpose on the second stage of simulation the analysis of the already involved information with taking into account the estimations received from the compared variants is conducted, that purposefully allows to complement information about the preferences.

Thus, the conducted researches allow concluding and suggesting the following:

- activity and plans of the Ukrainian carriers as for the integration by their purposes, tasks and methods on the whole correspond to the world tendencies and approaches. However development of integration processes on the air transport of Ukraine so far is not realized to a due measure. Mainly it is connected with insufficiently studied efficiency of integration and mechanism of choice of the best variants of integration decisions;

- marketing alliances became the most widespread form of union in Ukraine. Main trunk air carriers tend to be united with regional companies, however the latter reluctantly go to voluntary unions: integration often takes place in the form of mergence by the main airlines of flat-broke regional ones. For the industry the appearance of alliance agreements between air carriers and railway operators is also a common thing, which means transition to interbranch integration.

- efficiency of integration depends on the quality of management and organization of this process on every stage. As a methodological device at the integration process control in the air transport it is offered to use conception of project management, as the most completely compliant with the requirements of complexity in the development of air transport. Within the framework of this conception the air transport must be considered as a large system with various functions and complete set of criteria of the system;

- the important element of the successful integration of companies is establishing of inter-corporate cooperation which is reasonably to be carried out in the following directions: integration of corporate strategies; integration of the management system; integration of product line, which is carried out on the basis of optimum principle within the framework of a new corporate structure; integration of the system of orders distributing (works, services); integration of corporate cultures;

- in a particular branch developments in solving of the problems related to organization of integration processes and estimation of their efficiency, the retrospective analysis is accentuated as a rule, because of the lack of the required initial information. As the research showed, for the choice of effective integration decisions the perspective approach realized within the framework of technology of project management using the unclear set theory, with the acceptance of optimum decisions, including the method of analysis of hierarchies is the most significant and important.

CRACKED BLADE PRESENCE INFLUENCE ON BLADED DISK DYNAMIC RESPONSE

Process simulation of the cracked blade identification is presented. Crack induced nonlinear problem formulation is performed by harmonic balance method. Main efforts are directed on development of bladed disk model containing cracked blade, which takes into account external excitation phase lag, system mistuning and able to simulate cracked blade localization phenomenon.

Introduction

Cracked blade identification procedure is very important task and it is under investigation of many researchers [12-14]. The problem can be divided in the following tasks: (I) understanding of the crack nature appearance and its subsequent propagation; (II) precision of the crack most probable location depending on particular external conditions; (III) defining crack probable critical sizes that allows or forbids consequent operation of the damaged assembly; (IV) development of the appropriate cracked blade model within the frameworks of the bladed disk dynamic model; (V) application of the blade amplitude measurement methods with goal of cracked blade identification.

The aim of the presented study is to offer the model of the cracked blade behaviour which contains as much as possible information to describe its identification process in the most realistic way.

The bladed disk model was created containing cracked blade. The cracked blade simulation involved introducing of the relative DOF between coinciding nodes of the crack location region. Due to absence of cyclic symmetry caused by crack presence it was necessary to implement a reduction procedure of the bladed disk model to reduce computational expenses, which are high at full solution, moreover, in the case of nonlinear solution methods requiring iteration procedures. The reduction approach was applied using crack location as interface between two blade model parts. They were considered as sub-structures for subsequent fixed-interface method application.

The questions of crack nonlinear behaviour under periodically varying load were considered and the solution on the base of harmonic balance method application was proposed. Application of the nonlinear solution procedure depends on centrifugal forces forming initial gap. Such gap can result in always open crack case and thus in useless of crack nonlinearity simulation.

The excitation model of the bladed disk is able to take into account external force phase lag caused by difference between number of rotor and stator blades. Then mistuning model basing on different blades structural properties deviation was added. It can directly affect cracked blade detectability. Cracked blade dynamic behaviour localization plays here important role. As cracked blade dynamic localization we will understand blade localized frequency response. At certain level of mistuning it seems to be impossible to identify cracked blade presence, even in the case of its localization.

1. Bladed disk model with cracked blade

Generally bladed disk dynamic problems present by themselves the objects for cyclic analysis techniques application due to their behaviour symmetry in circumferential direction. The presence of mistuning, alias spread of structural properties from one blade to other, or in cyclic representation between the sectors, disrupts the symmetry. And even in this case, from the work [10], we can see the ability to continue with cyclic analysis of the mistuned bladed disks. In our study we will deal not only with mistuning caused by manufacturing inequalities. The crack presence in the blade will induce its nonlinear behaviour that will lead to impossibility to utilize cyclic analysis and will require full assembled disk model to simulate its influence on disk dynamic response.

In order to create full bladed disk model containing one or some cracked blades the disk sector with cracked blade finite-elements model was initially developed using ANSYS. Then its structural matrices were transferred to MATLAB to continue sequential assembling process.

As it was mentioned earlier, as the initial, the sector with cracked blade was taken. And to obtain the disk model with one or some cracked blade it is enough to merge DOF in the cracks areas of the blades accepted as uncracked. In order to facilitate this procedure the relative crack DOF was introduced. These relative DOF present by themselves displacements between nodes, which comes into contact at crack breathing. Thanks to such approach it is necessary to delete these DOF from system matrices in order to pass to the uncracked state. Also introducing of the relative displacements will decrease in 2 times number of nonlinear DOF retained for cracked blade nonlinear behaviour simulation.

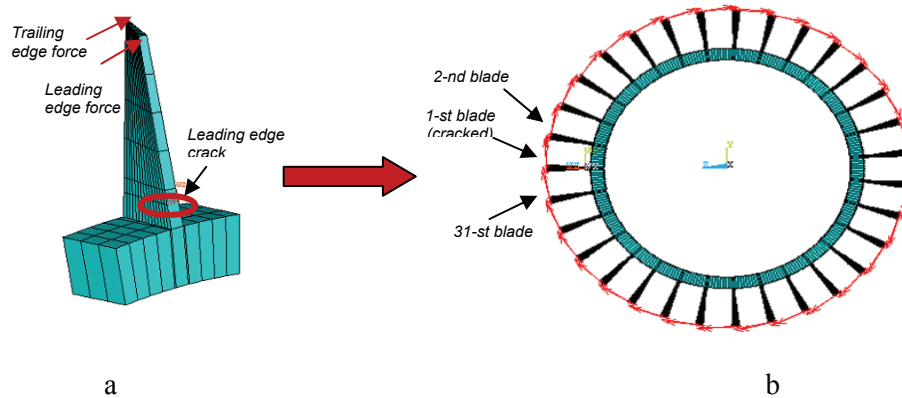


Figure 1 Bladed disk finite-elements model:
a - sector with cracked blade, b – assembled disk with applied external forces

2. System reduction methods application

When doing an analysis of vibration performances of a structure with required high accuracy we meet the problem of enormous DOF number taking part in the solution procedure. The exclusive solution is to reduce system size by implementing one of the existent reduction methods based on system sub-structuring like fixed interface sub-structuring method of Craig-Bampton [6] and free interface sub-structuring method of Mac Neal [7].

In the case of the disk model with cracked blade the sub-structuring approach can be understood on individual cracked blade. Crack location forms interface between two blade parts (fig. 2). It should be noted that in this case we do not have classical sub-structuring, because these parts are not fully independent. Some DOF are remained shared between upper and lower blade sub-structures. They are relative displacement between contact nodes.

In our case, it is possible to apply two approaches of the sub-structured system reduction:

- Reduction of the full assembled system (fig. 2 a). This approach was used for the analysis as the most favourable at the present moderate number of full system DOF.

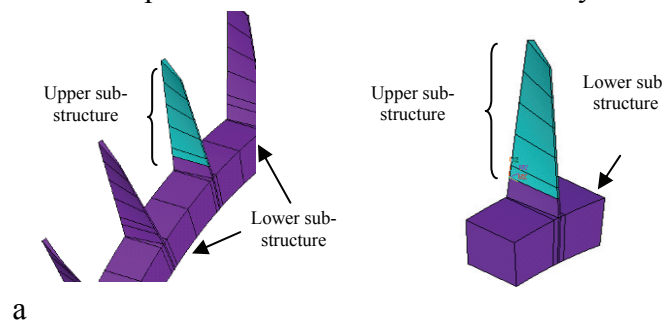


Figure 2 System sub-structuring: a – using full assembled system; b - using disk sector
– Reduction on the base of the disk sector (with cracked blade, fig. 2 b). In this case the cracked blade sector is reduced and then full system assembling is performed.

After having established two approaches for system reduction the fixed-interface method was chosen to be applied.

As interface or master DOF the relative displacement between contact pairs were accepted. Additionally, a certain number of modes describing uncracked bladed disk behaviour were retained. Also DOF of external force application were added to this set. The initial full model of the assembled bladed disk contained 28284 DOF and it was reduced to the model of 136 DOF plus certain number of additional modes. Comparing system eigensolutions it is enough to retain 50 modes additionally to be able to properly approximate dynamic behaviour of the full model within the range of the 1-st blade flexural modes.

3. Frequency response of the bladed disk

3.1 Linear crack case

The linear presentation of the cracked blade consists in simulation of the crack presence supposing the crack to be always open. Generally, crack influence on dynamic response is simulated by stiffness reduction when solving eigenvalues problem. The crack models used in these analyses are divided into two categories:

- open crack models – linear statement;
- opening and closing or breathing crack models – nonlinear statement [1-2, 8].

Most researchers use always open crack models in their studies and have claimed that the change in natural frequencies might be a parameter for crack presence detection.

Let the bladed disk be described by the equations of motion

$$\mathbf{M}\ddot{\mathbf{u}} + \mathbf{C}_\xi \dot{\mathbf{u}} + \mathbf{K}\mathbf{u} = \mathbf{F}e^{i\omega t}, \quad (1.1)$$

where \mathbf{M} , \mathbf{C}_ξ , and \mathbf{K} are the symmetric mass, damping, and stiffness matrices of the disk model, \mathbf{F} – amplitudes vector of external excitation force. Damping matrix was calculated on the base of structural damping ratio ξ and stiffness matrix $\mathbf{C}_\xi = \xi\mathbf{K}$.

Then, in the linear case we assume that system response is steady-state and has the form $X(t) = xe^{i\omega t}$ that yields to the set of algebraic equations

$$\mathbf{H}\mathbf{x} = \mathbf{F}, \quad (1.2)$$

where $\mathbf{H} = \mathbf{K} - \omega^2\mathbf{M} + i\omega\mathbf{C}_\xi$ is the impedance matrix at the excitation frequency ω .

Application of external excitation forces is shown on fig. 2. Forces are applied in points of blade tip: at leading and trailing edges. The system frequency response solution we will perform within the range that covers blades 1-st flexural modes. On graphs of fig. 3 solutions of the full system assembled in chapter 1 and the reduced system elaborated in chapter 2 are presented.

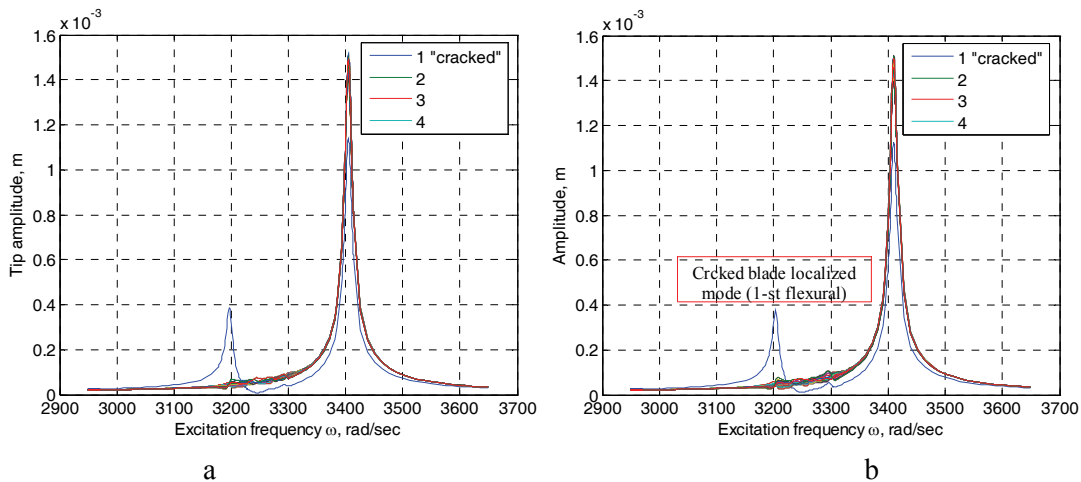


Figure 3 Full (a) and reduced (b) bladed disk models frequency responses

At the absence of the excitation force phase lag (all externally applied to blades forces have same phase) we observe two system response peaks: principal peak of all blades and additional peak which corresponds to frequency localized response of the cracked blade.

A localization phenomenon is very important diagnostic sign that gives us the most information about crack presence in the blade. Simulations concerning cracked blade localization cases will be interrogated in the chapters 3.3-3.4 in combination with the presence of mistuning and excitation force phase lag.

3.2 Nonlinear crack case

However, the assumption that crack is always open in vibration is not realistic because compressive loads may close the crack. The main results obtained through simulations or experimental studies were that the observed decrease in the natural frequencies is not sufficient to be described by a model of open crack [12-14]. So, the real changes in resonances can be calculated only on the base of nonlinear cracked blade dynamic model. Two approaches of crack breathing process simulation might be used:

- periodical varying stiffness introduction [8];
- contact simulation between crack sides in the moment of crack closing [2].

In most cases analytical solutions of such dynamical systems are practically impossible to obtain. Thus researchers and engineers turn to numerical techniques. Firstly, systems are discretized as a set of nonlinear ordinary differential equations with high dimension. Then traditional direct time integration solution techniques are then applied. However, this process is extremely time-consuming. Therefore, it seems to be necessary to examine more efficient techniques to reduce the computational costs. One such technique is harmonic balance (HB) method [4-5]. Earlier a simple mathematical model able to simulate such nonlinearity was created [2]. In such way it was possible to prove correctness of the method formulation by comparing its results with direct integration. Now this approach can be projected on more complex cracked blade model.

In nonlinear case system motion equation (1.1) is expressed by:

$$\mathbf{M}\ddot{\mathbf{u}} + \mathbf{C}_\xi \dot{\mathbf{u}} + \mathbf{K}\mathbf{u} + \mathbf{F}_{nl}(\mathbf{u}) = \mathbf{F}(t), \quad (1.3)$$

where \mathbf{F}_{nl} – nonlinear force vector.

Then we are searching for the $u(t)$ in the form of the truncated trigonometric series of $k=1, \dots, N$ harmonics:

$$u(t) = a_0 + \sum_{k=1}^N a_k \cos k\omega t + \sum_{k=1}^N b_k \sin k\omega t, \quad (1.4)$$

where a_0, a_k, b_k – Fourier series coefficients, ω – excitation frequency.

If we put equation (1.4) to (1.3) the last would be changed to:

$$\mathbf{A}\tilde{\mathbf{u}} + \mathbf{b}(\tilde{\mathbf{u}}) = \mathbf{C}, \quad (1.5)$$

where \mathbf{A} is diagonally symmetric in block matrix:

$$\mathbf{A} = \begin{bmatrix} \mathbf{L}_0 & 0 & \dots & 0 \\ 0 & \mathbf{L}_1 & \dots & 0 \\ \dots & \dots & \dots & \dots \\ 0 & 0 & \dots & \mathbf{L}_N \end{bmatrix}_{N_{dof}(2k+1) \times N_{dof}(2k+1)}; \quad \mathbf{L}_0 = \mathbf{K}; \quad \mathbf{L}_k = \begin{bmatrix} \mathbf{K} - (k\omega)^2 \mathbf{M} & k\omega \mathbf{C}_\xi \\ -k\omega \mathbf{C}_\xi & \mathbf{K} - (k\omega)^2 \mathbf{M} \end{bmatrix}. \quad (1.6)$$

where \mathbf{b} – nonlinear member, \mathbf{C} – external excitation force vector and $\tilde{\mathbf{u}}$ – vector of Fourier series coefficients.

Nonlinear solution requires taking into account system nonlinearity, in our case - nonlinear contact force between two nodes. The governing equation (1.5) of HB method represents by itself the system of nonlinear equations to that some linear transformation could be applied in the for a Newton-type iterative solver of nonlinear algebraic equations system implementation.

The nonlinear force representation is one of the most important tasks in any nonlinear analysis, as well as for the harmonic balance method. In our case we have some nonlinear degrees of freedom (relative vertical displacements between contact nodes). For the contact force determination the Lagrange multipliers or penalty methods could be utilized [1]. The easiest way is to use the penalty method to approximate this force by the following expression:

$$F_{nl} = k_{nl} \cdot \left(\frac{u_{nl} + |u_{nl}|}{2} \right), \quad (1.7)$$

where k_{nl} – penalty stiffness and u_{nl} – nonlinear dof displacement. Penalty stiffness value should be chosen to provide minimum penetration in the contact zone.

It should be mentioned the disadvantage of such nonlinear force approximation when it crosses the zero. So then $u_{nl}=0$, $\partial F_{nl} / \partial u_{nl} \rightarrow \infty$. In order to pass up such problem the smoothing function should be applied. In the work [3] tangent function was used for smoothing. We applied it with some modification and have gotten the next expression:

$$F_{nl} = \frac{1}{\pi} k_{nl} (\arctan(su_{nl}) - \frac{\pi}{2}) u_{nl}, \quad (1.8)$$

where s – coefficient, the sufficiently high level of that is required to accurately represent force-displacement relationship smoothing.

The nonlinear solution and as the linear one in the time domain are reconstructed by inverse Fourier transformation and shown for: relative vertical displacement between two coinciding contact nodes – “crack point” (fig. 4 a) and excitation force application node horizontal displacement – “tip point” (fig. 4 b).

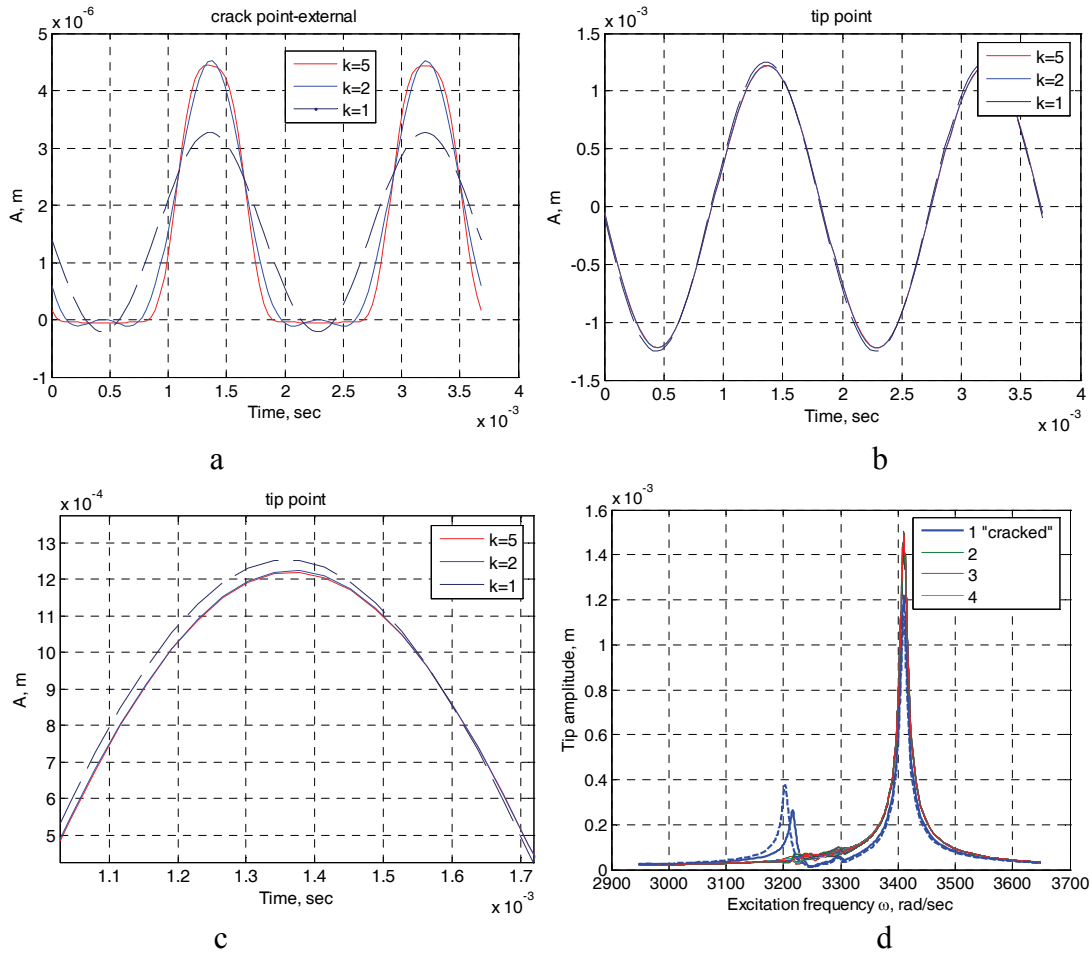


Figure 4 Nonlinear solution by HB method for different harmonics numbers: a – “crack point”, b – “tip point”, c – “tip point” (zoom), d – frequency response function at “tip point” (dashed line - linear solution of the cracked blade)

Fig. 4 presents the simulations accomplished for different numbers of retained harmonics (1.4). Their number is critical for solutions computation times. The set value of penalty stiffness is enough to avoid penetration and nonlinear force approximation (1.8) allows us to precisely simulate system nonlinearity.

For all following simulation the nonlinear model with 2 harmonics was used as it accurately enough describes system nonlinear behaviour. Also we can see that system response stays almost sinusoidal and this fact will be utilized for more simple formulation of tip-timing method governing equation.

3.3 Excitation frequency phase lag influence on the bladed disk dynamic response

For external excitation force vector construction for all force application DOF of the assembly (fig. 1) it is necessary to take into account force phase lag. It is caused by inequality between blades numbers of the rotor wheel and preceding stator stage. An engine order excitation is assumed, which is harmonic in time and differs only in phase from blade to blade. The excitation force on j -th blade can be expressed as:

$$\mathbf{F}_j = \mathbf{F} \mathbf{a}_j e^{i\psi} e^{i\omega t}, \quad \psi = 2\pi \frac{n_s}{n_r} (j-1), \quad (1.9)$$

where \mathbf{F}_j - excitation force vector of j -th sector, ψ - phase, ω - excitation frequency, n_s - stator blades number, n_r - rotor blades number.

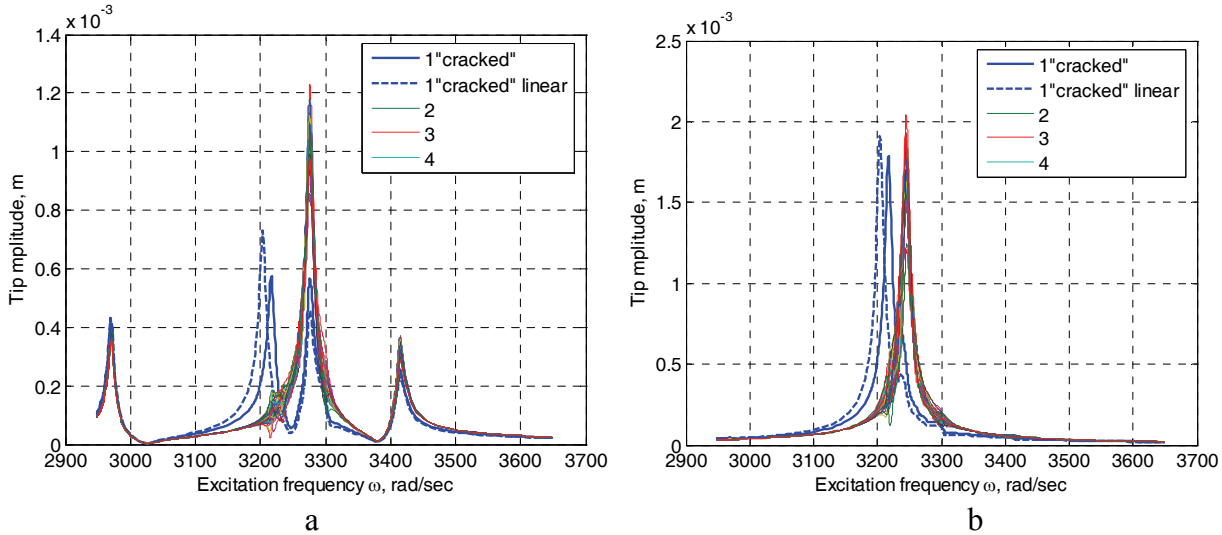


Figure 5 Excitation force phase lag influence on bladed disk forced response:
a - $n_s=28$; b - $n_s=23$

On fig. 5 simulations of reduced bladed disk model forced response are presented at different number of stator blades that induce different phase lag values of excitation force. We can observe that with increase of phase lag the amplitude peak is going to increase. Also we can see from these results that crack imposed nonlinearity shifts cracked blade localized peak closer to the main system response. This fact is very critical in the view of further mistuning consideration because it hides cracked blade frequency localization among other mistuned blades.

3.4 Mistuning effect on frequency response of the bladed disk

After having established the influence of the excitation force phase lag we pass to the examination of the mistuning effect. It will be simulated the possibility to localize cracked blade dynamic response at the certain mistuning level. The prediction of the mistuning effects on the bladed disk response is a mainly challenging problem as indicated by the many authors [9-10].

In our case we considered that main effect of mistuning on bladed disk forced response would be represented by blades stiffness mistuning and as far as we are working with the range of the blade

1-st flexural mode only, the mistuning model can be represented by perturbation of the individual blade partition of the bladed disk stiffness matrix [9]:

$$\mathbf{K}_{jbm} = (1 + m_j) \mathbf{K}_{bj}, \quad (1.10)$$

where m_j – mistuning coefficient relatively to the 1-st blade and randomly generated by normal law with mean $\mu = 0$ and standard deviation σ .

Having obtained the fundamental mistuning model, a major concern becomes the prediction of the ability to detect cracked blade on the base of the bladed disk forced response. The easiest case, at the presence of certain level of mistuning, is if we have a case of cracked blade frequency localization. As it was mentioned before it will result in appearance of the additional resonance peak caused by crack presence in a blade. In linear statement crack presence can be equated to the blade mistuning. Therefore at a certain mistuning level we can obtain uncracked blades frequency localization. This will results in cracked blade detection problems.

Generally, the maximum forced vibration response of a subcomponent (blade) of a mistuned structure is larger than that of a perfectly tuned structure. Thus mechanical energy stored in a subcomponent of a mistuned structure is different from those stored in other subcomponents. This is called the vibration localization of a mistuned structure. Localization occurs because waves propagating away from the energy source are rejected by the boundary between the slightly different subsystems constituting the nearly periodic structure. The resulting energy accumulation may lead to much higher amplitudes locally than would be predicted if perfect periodicity has been supposed, this possibly can have disastrous effects, for example in turbomachinery [11].

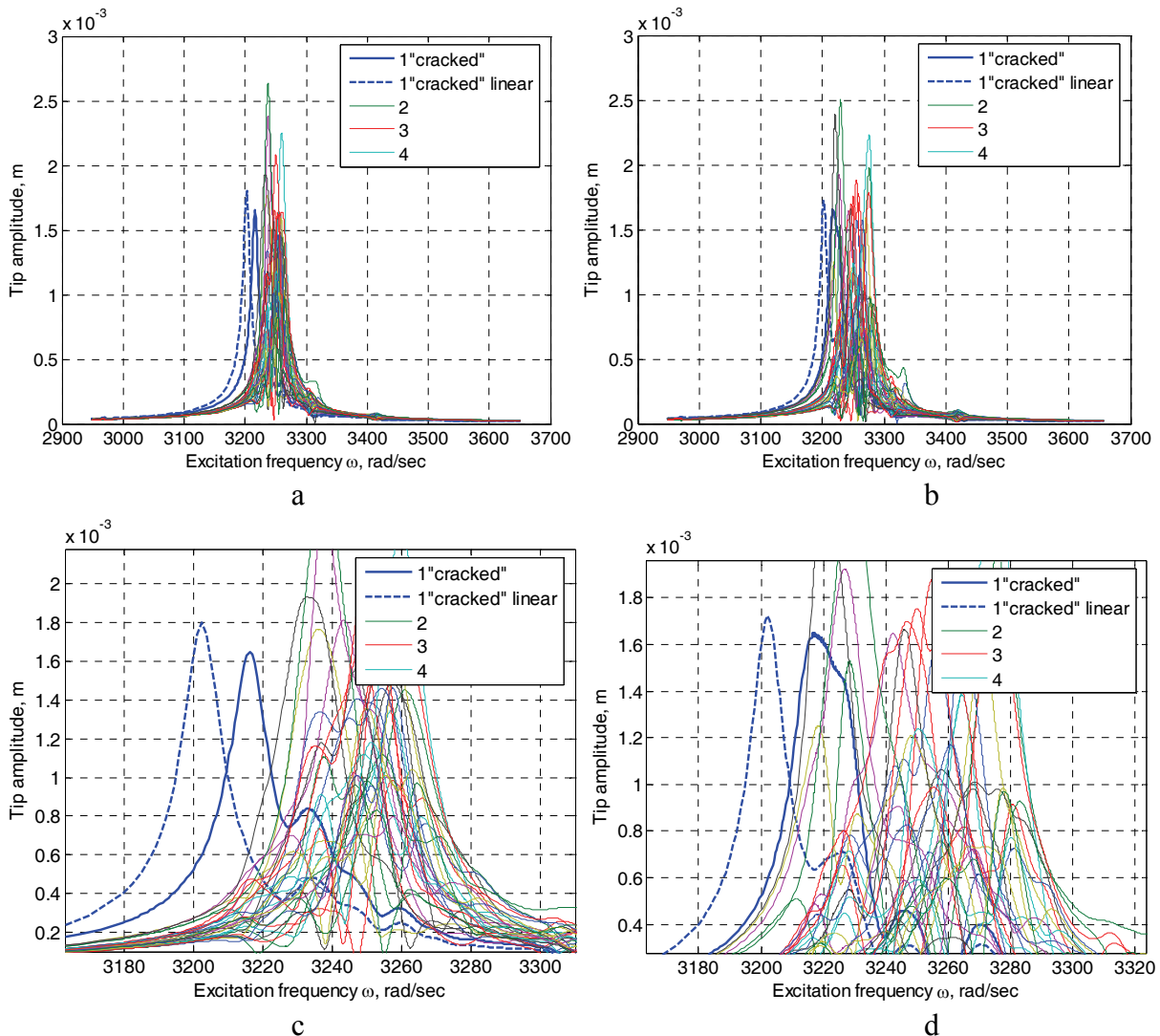


Figure 6 Excitation force mistuning influence on bladed disk forced response ($n_s=23$):
a - $\sigma=0.01$; b - $\sigma=0.02$; c - $\sigma=0.01$ (zoom); d - $\sigma=0.02$ (zoom)

From the results of different mistuning level simulations (fig. 5-6), we can observe stated earlier, that taking into account of cracked blade nonlinear behaviour leads to difficulties of crack identification. Sometimes it becomes impossible to distinguish cracked blade localized dynamic behaviour. The linear model at mistuning level of 2% allows us to recognize cracked blade, whereas taking into account the nonlinearity makes this process unrealizable.

Conclusions

The presented above study was devoted to describe cracked blade detection process that can be performed during operation or maintenance of the aviation gas-turbine engine. It consists of bladed disk model with cracked blade development. Much attention was made of cracked induced nonlinearity simulation by crack inside contact approach. The influence of combined excitation force phase lag and bladed disk structural mistuning was studied. Certain level of the mistuning was decided to be critical for ability to detect presence of the cracked blade. Also it is necessary to point out that taking into account cracked blade nonlinear behaviour decreases such abilities due to the shift of cracked blade natural frequencies closer to the uncracked one.

References

1. *J.-P. Laine, V. Kharyton* **Cracked structure response on external harmonic excitation** // Aerospace technics and technology. - 2006. - Vol. 61. - pp. 1057-1074.
2. *O. Kucher, V. Kharyton, J.-P. Laine, F. Thouverez* **Harmonic balance method implementation for crack breathing process simulation** // Aerospace technique and technology. – 2007. – vol. 8(44). – P. 150-156
3. *Chengwu Duan, Rajendra Singh* **Dynamic analysis of preload nonlinearity in a mechanical oscillator** // Journal of Sound and Vibration. – 2007. – Vol. 301. – pp. 963-978.
4. *G. von Groll, D. Ewins* **The harmonic balance method with arc-length continuation in rotor/stator contact problems** // Journal of Sound and Vibration. – 2001. – Vol. 241(2). – pp. 221-233.
5. *L. Liu, J.P. Thomas, E.H. Dowell, P. Attar, K.C. Hall* **A comparison of classical and high dimensional harmonic balance approaches for a Duffing oscillator** // Journal of Computational Physics. – 2006. – Vol. 215. – pp. 298-320.
6. *R. Craig, M. Bampton* **Coupling of substructures for dynamic analysis** // AIAA Journal. – 1968. – Vol. 6(7). – pp. 1313-1319.
7. *R. Mac Neal* **A hybrid method of component mode synthesis** // Computers & Structures. – 1971. – Vol. 1. – pp. 581-601.
8. *S. Cheng, X.Wu, W. Wallace, A. Swamidas* **Vibrational response of a beam with a breathing crack** // Journal of Sound and Vibration. – 1999. – Vol. 225. – pp. 201-208.
9. *J. Rivas-Guerra, M. P. Mignolet* **Local/Global effects of mistuning on the forced response of bladed disks** // ASME Journal of Engineering for Gas Turbines and Power. – 2004. – Vol. 126. – pp. 131-141.
10. *Bladh R., Castanier, M. P., Pierre* **Component-Mode-Based Reduced Order Modeling Techniques for Mistuned Bladed Disks - Part I: Theoretical models** // ASME Journal of Engineering for Gas Turbines and Power. – 2001. – Vol. 123(1). – pp. 100-108.
11. *G. Ottarsson* **A transfer matrix approach to free vibration localization in mistuned blade assemblies** // Journal of Sound and Vibration. – 1996. – Vol. 197(5). – pp. 589-615.
12. *R. Ruotolo, C. Surace, P. Crespo, D. Storer* **Harmonic analysis of the vibrations of a cantilevered beam with a closing crack** // Computers and Structures. – 1996. – Vol. 61. – pp. 1057-1074.
13. *E. Douka, L. Hadjileontiadis* **Time-frequency analysis of the free vibration response of a beam with a breathing crack** // NDT&E International. – 2005. – Vol. 38. – pp. 3-10.
14. *M. Kisa, J. Bradson* **The effect of closure of cracks on the dynamic of cracked cantilever beams** // Journal of Sound and Vibration. – 2000. – Vol. 238(1). – pp. 1-18.

EXERGoeCONOMIC ASSESSMENT OF AIRCRAFT TURBOFAN ENGINES

Exergy analysis has been widely used in the design, simulation and performance evaluation of thermal systems. Besides providing savings on fuel consumption, exergoeconomic analysis is quite useful for environmental protection issues. However, utilization of this tool over the aircraft turbofan engine is a relatively new research area.

An exergoeconomic analysis of an aircraft turbofan engine is performed in this study. Exergy and exergoeconomic analysis methods based on both first and second laws of thermodynamic along with economic parameters are used for understanding how close the system to the ideal operation conditions, where the imperfection points or components could be and how further recoveries and improvements could be possible from the technical, economical and environmental points of view.

A new parameter, the so-called specific thrust cost (STC), which has been recently developed by the authors, is used in this paper. This parameter may be considered to be more useful than specific fuel consumption (SFC) for comparing the aircraft propulsion systems. Based on the analysis performed, the STC values are found to be 139.01 \$/kNh and 306.44 \$/kNh for the cold and hot thrusts, respectively. On the other hand, the effects of various parameters, such as system life time, annual operation hour and interest ratio, on the STC are also investigated and discussed.

1. INTRODUCTION

Currently, one of the most two problems that suffered by the world community are the risk of depletion of the energy resources and their environmental and ecological impacts. Some offer the alternative energy and sustainability, while the others insist on the nuclear energy. Beyond these options on the other hand, the perception of efficient utilization of the present energy resources reveals as a simple and required step before switching the energy format to the new ones.

A number of studies on alternative energy resources have been conducted in many countries. (i.e., hydrogen in Canada, ethanol in Brazil and wind in Denmark, Spain and Germany). Utilization of many alternative energy technologies, such as solar, biomass, has significantly increased [1]. Among them for instance, one of the promising technology, called solar chimney, was experimentally studied in Spain in 1982. This plant gave a power output of 50 kW with a collector diameter of 240 m and a chimney height of 195 m [2]. Furthermore, since 2001, in Australia, a study on a solar chimney with a height of 1 km has been implemented. This chimney is considered to give a power of 200 MW and also to abate 900,000 tones of greenhouse emissions [3].

Exergy analysis is one of the most practical method that makes engineers measure the system performance quite accurately. Using the both first and second laws of thermodynamics, it deals with the heat and work independently. Using exergy analysis method, it is searched the answer of the how systems could work better. This could be done by determining the work potential based on the thermodynamics laws, at the inlet and outlet of the single units, and the figuring out the difference between these two points. Catching a similar non ideal condition by exergy analysis provides making an exergoeconomic analysis and getting results more sense (i.e. cost). Cost at every system components makes enable to know if the improvement work on the system and system design is really profitable, e.g. one unit could have a high efficiency, but the high capital investment could eliminate the benefits having with the efficiency. Similarly even a component has a relatively low efficiency, it could be worse if trying to increase the efficiency in the meaning of capital investments. For further studies one could refer the Refs. [4-6].

2. MODEL

The model used in this study is a turbofan engine with a high by-pass ratio of 5.4:1. The overall pressure ratio and the specific fuel consumption (SFC) values are 28.4 and 0.357, respectively. It consists of one stage fan, 3 stages low pressure (LP) compressor, 14 stages high pressure (HP) compressors, an annular type combustion chamber and 2 and 4 stages HP and LP turbines. It is used with especially middle and long range aircrafts (i.e., B747, B767, A300, A310, A330, MD-11 and DC-10). The thrust range of this engine is changed between 214-334 kN at a maximum take off. Since this is a turbofan engine, there are two exhaust parts named as fan and core engine. The thrust obtained by the fan exhaust depends on the fan unit and there is no any burning of fuel or air, while the thrust obtained by the core engine exhaust is due to the discharging of the combusted gas from this part. Because of the air or gas mass flow exiting the exhausts are not the same, the thrust of these parts is also not the same. As a rule of thumb, 75%-80% of the total thrust is produced in fan exhaust and the rest of thrust comes from the core engine exhaust.

3. ANALYSIS

In this two-step analysis program, the main objective is acquiring the cost rate of thrust which is produced by the fan and core engine exhausts, independently. Since the cruise phase is the longest period of a flight and consumes the most fuel, for this analysis, the cruise phase was chosen under the proper operation conditions. An exergy analysis was carried out first. The data required for the exergoeconomic analysis were then collected. Finally, using these data, capital investment and the expenditures of operation and maintenance, an exergoeconomic analysis was conducted. The operational cost was included in the maintenance cost value.

The detailed calculation and method about either exergy or exergoeconomic analyses could be found in thermodynamics textbooks, while some papers could be obtained from Refs. [7-12]. Therefore only the basic equations were included in this study.

3.1. Exergy analysis

Here, two exergy components are considered in exergy analyses, namely physical and chemical exergies as [8]

$$\overline{ex}_{ph} = \overline{h} - \overline{h}_0 - T_0 (\overline{s} - \overline{s}_0) \quad (1)$$

$$\overline{ex}_{ch} = \sum_k x_k \overline{ex}_k^{ch} + \overline{R} T_0 \sum_k x_k \ln x_k \quad (2)$$

where h , s and T in Eq.(1) denote the enthalpy, entropy and temperature, while x and \overline{ex}^{ch} in Eq.(2) are the mole fraction and the standard chemical exergy value for the corresponded air components, respectively. When the gas flow is assumed to be ideal, Eq. (1) can be expressed as

$$\overline{ex}_{ph} = \overline{c}_p T_0 \left(\frac{T}{T_0} - 1 - \ln \frac{T}{T_0} \right) + \overline{R} T_0 \ln \frac{P}{P_0} \quad (3)$$

where \overline{c}_p and \overline{R} denote specific the heat at constant pressure and the universal gas constant, while T and P are the temperature and pressure of the system, respectively. However, for physical exergy, acting as Eq.(3) could give inaccurate results in such cases particularly after combustion or a similar chemical reactions [13].

The other two most known exergy items are called potential and kinetic exergy. Since there are no elevation differences, the potential exergy is neglected. On the other hand, at the exhaust parts, due

to the high speed discharge there are serious amount of kinetic exergies at those parts. The kinetic exergy is given as,

$$ex_{ke} = \frac{V^2}{2000} \quad (4)$$

where V denotes the velocity and the number of 2000 is used to convert $(m/s)^2$ to (kJ/kg) .

In this analysis, the environment temperature and pressure are taken as 246.9 K and 0.363 bar, respectively. These values are the environment temperature and pressure values at the flown altitude of 10060 m (33000 ft). The air mole fractions at this altitude are assumed to be the same those in the sea level and taken from Ref. [8] as 77.48% for N_2 , 20.59% for O_2 , 0.03% for CO_2 and 1.9% for H_2O , respectively.

3.2. Exergoeconomic Analysis

The second and last step of the analysis is the exergoeconomic analysis, which is used to take into consideration of the cost concept. Without an exergoeconomic analysis, the results are sense only for the thermodynamics studies, but not for the case of practical applications of the result obtained from those studies.

Three basic important equations used in exergoeconomic analyses are given by [8]

$$CRF = \frac{i(i+1)^n}{(i+1)^n - 1} \quad (5)$$

$$CA_{i,k} = \frac{PEC_k (\$) \times CRF (y^{-1})}{5110 (h y^{-1})} \quad (6)$$

In Eq.(5), CRF denotes a parameter called capital recovery factor, which is used to levelized the purchased equipment cost (PEC) of a separate unit as well as the entire system. Among the other symbols, i , n and CA are the interest ratio, system life time and the levelized capital cost, respectively. The other equation is obtained from

$$\sum_i \dot{C}_{i,k} + \dot{C}_{Q,k} + \dot{Z}_k^T = \sum_e \dot{C}_{e,k} + \dot{C}_{W,k} \quad (7)$$

where \dot{C} and \dot{Z} denote the cost rates (exergetic costs) and the non-exergetic levelized cost values with the units of $\$h^{-1}$, while the subscripts of i , e , W and Q define the inlet, exit, work and heat transfer, respectively. Eq.(7) should be run for all of the system components, such as fan, compressors, combustion chamber, turbines and exhaust parts. The \dot{Z} term is usually composed of capital investments (CI) and operation and maintenance (OM) costs and is given by

$$\dot{Z}^T = \dot{Z}^{CI} + \dot{Z}^{OM} \quad (8)$$

4. RESULTS AND DISCUSSION

In order to define a merit for the thrust cost, a new parameter, the specific thrust cost (STC), is developed in this paper for the first time to the best of the authors' knowledge. The STC, similar to the specific fuel consumption, is used to obtain the kN based cost of the thrust. It is also called the most sense parameter of the exergoeconomic analysis conducted in this paper.

In this paper, the parameters, which are tried to be searched for the effects on the cost rates and specific thrust costs (STC), are listed as fuel cost, interest ratio, system life time, maintenance coefficient and annual operation hours. Using the Eqs.(1-8), the calculated STC values are obtained

as 139.01 $\$/\text{kNh}$ for cold thrust and 306.44 $\$/\text{kNh}$ for hot thrust, respectively. In the following paragraphs, the effects of some variables on the STC are studied.

In Fig. 1, the STC variation of cold and hot thrusts due to the fuel price is shown. As seen in this figure, both thrusts increase with the fuel price as expected. In this analysis, the fuel (kerosene) price is taken as 1.8719 $\text{kg}/\text{\$}$ and this case is marked as the circles. Also, increasing the fuel price only 0.5 $\text{\$/kg}$ (from 1.5 to 2 $\text{\$/kg}$) can result in 35.8 $\text{\$/kNh}$ and 79.6 $\text{\$/kNh}$ ascends of cold and hot thrusts, respectively. Therefore the fuel prices have quite dominant effects on the STC.

The variation of the STC due to the annual fuel price increase is illustrated in Figure 2. In the present analysis, the annual fuel price increase is estimated as 6%. This estimation is made by considering kerosene fuel prices of the last three years in Turkey. However, it is not possible to determine a fixed annual fuel price increase. Therefore, assuming some different annual fuel price increase, one could have case results about the STC. According to the diagram, it is clearly seen that the hot thrust is affected much more than cold thrust because the cold thrust produced by the fan, which is operated by the low pressure turbine, while for producing the hot thrust it is required much more energy to operate high pressure turbine. Also not all the energy provided by the low pressure turbine is given to both the fan and the low pressure compressor.

In Figure 3, the interest ratio effect is shown. Although it is assumed that the constant interest ratio among all of the system life time of 15 years in this analysis is hardly possible, in conclusions of the descend and ascent, nearly constant interest ratios might be expected. Between the values of 5% and 15%, the interest ratio is responsible of an increase about 160.1 $\text{\$/h}$ at the levelized total capital investment and the operation & maintenance expenditures. In this paper, the purchased equipment

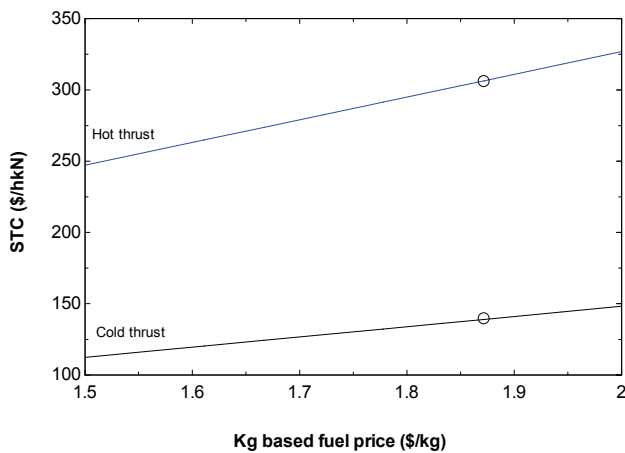


Figure 1. Fuel prices effects on the STC. Cold and hot thrusts denote the thrust obtained from fan exhaust and core engine exhaust, respectively. The circles show the value of fuel price ($=1.8719 \text{ kg}/\text{\$}$) which used in the present analysis.

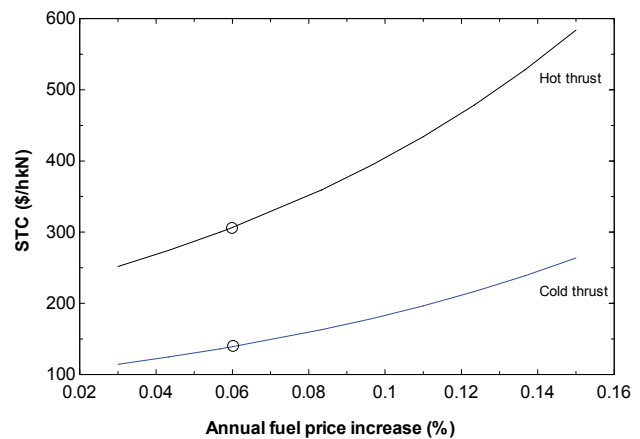


Figure 2. Variation of the STC due to the annual fuel price increase. Cold and hot thrusts denote the thrust obtained from fan exhaust and core engine exhaust, respectively. The circles show the value of annual fuel price increase ($=6\%$) which used in the present analysis.

cost (PEC) of the entire engine is assumed to be 10 M\$. This value can be levelized as 281.7 $\text{\$/h}$ for an interest ratio of 10%. It can also be noted that, decreasing the interest ratio from 10% to 5% and increasing the interest ratio from 10% to 15% are resulted as descend at 75.3 $\text{\$/h}$ and as ascent at 84.8 $\text{\$/h}$, respectively.

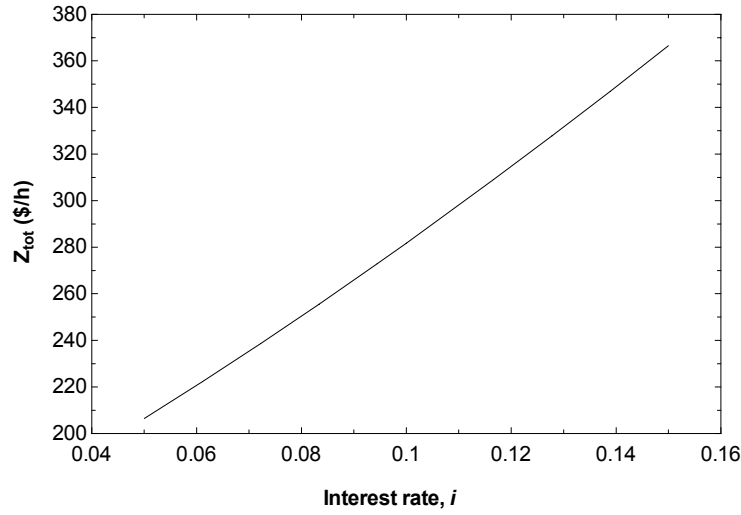


Figure 3. Variation of the levelized capital investment and operation and maintenance costs (Z_{tot}) due to the interest ratios. In this paper, the interest ratio is assumed as %10 (i.e., 0.1) and constant among the system life time.

In Figure 4, the Z values belonging to the major components of the engine are given. Since there are 3 PEC groups which can be listed as; (1) Fan, LPC and HPT as the PEC at 1 M\$, (2) HPC and LPT as the PEC at 3 M\$ and (3) CC as the PEC at 300,000\$. As seen in the figure, components having high PEC values are affected more than those having relatively low PECs. For instance, increasing the interest ratio from %10 to %15 is resulted in 25.4 \$/h for HPC, 8.48 \$/h for fan and 2.54 \$/h for combustion chamber.

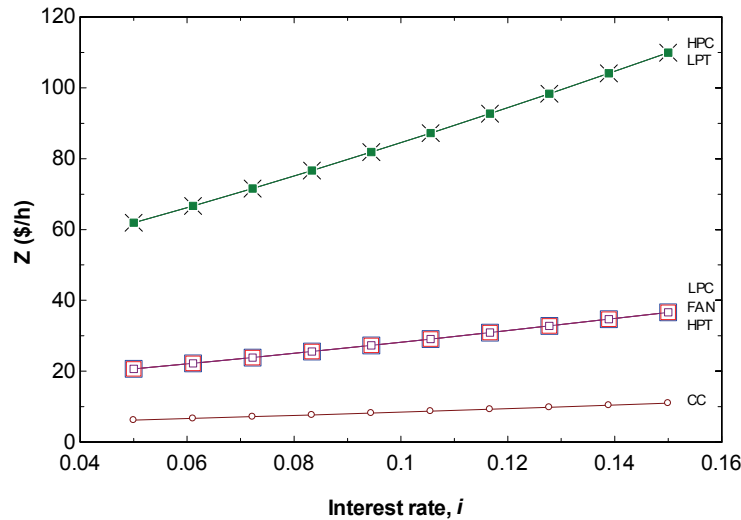


Figure 4. Variation of the levelized capital investment and operation and maintenance costs (Z_{tot}) of all major component of the engine due to the interest ratios. In this paper, the interest ratio is assumed as %10 (i.e., 0.1) and constant among the system life time. HPC and LPT denote High Pressure Compressor and Low Pressure Turbine, while LPC and HPT are Low Pressure Compressor and High Pressure Turbine, respectively. CC is Combustion Chamber.

Regarding to the system life time effects, it is interest to get a relation as an inverse proportion at the first glance, but it is an expected result because that increasing the system life time will increase the operation & maintenance expenditure. Meantime, this cost ascent should not consider alone, because there will be a revenue ascent as well. Considering the net profit, on the other hand, despite having a relatively low values than the first years revenues, it is still possible to speak about a serious amount of profit. This case is shown in Figure 5.

In Figure 6, the similar results are obtained as explained in Figure 5. For the values varying between 2930 h/year (8 h/day) and 6570 h/year (18 h/year), the variation of STC for both hot and

cold thrusts are found to be 205.00 \$/h and 90.68 \$/h, respectively. For the current analysis, the operating hour p.a. of the engine is assumed as 5110 h (14 h/day). Therefore, increasing the operating hour from 5110 to 6570 h/year (14 h/day to 18 h/day) is resulted as 37.01 \$/h with an increase of %26.68 for cold thrust and 83.36 \$/h with an increase of %27.20 for hot thrust.

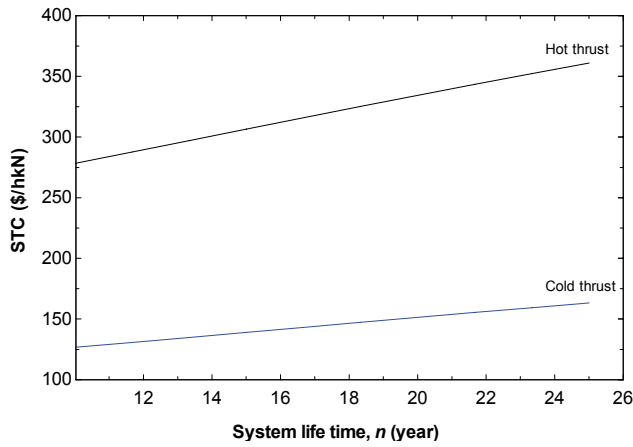


Figure 5. Variation of the STC due to the system life time. Cold and hot thrusts denote the thrust obtained from fan exhaust and core engine exhaust, respectively. In this analysis, $n=15$ years.

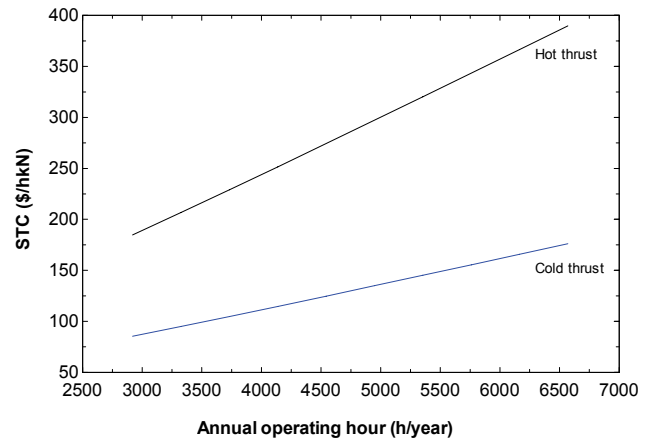


Figure 6. Variation of the STC due to the annual operating hours of the system. Cold and hot thrusts denote the thrust obtained from fan exhaust and core engine exhaust, respectively. In this analysis, annual operating hours is taken as 5110 hours which equals 14 h operating per day.

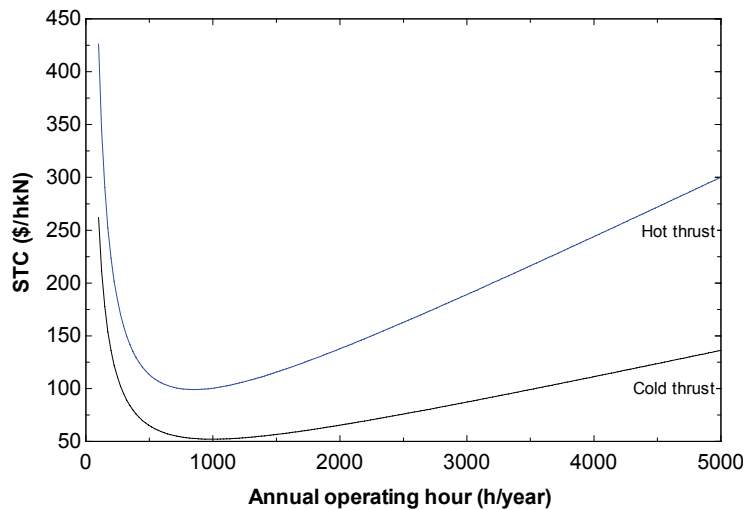


Figure 7. The variation of the STC due to the annual operating hours. The annual operating hours limits vary between 100 h (0.3 h/day) and 5000 h (13.7 h/day). Cold and hot thrusts denote the thrust obtained from fan exhaust and core engine exhaust, respectively.

After examining the annual operating hours effects over the STC for the values between 2920-6570 hours (8-18 hours/day), the variation of STC for the smaller values of operating hours should be considered. Performing a parametric study, it is found that there is a decent until a value of 1000 h/year (2.7 h/day) for the cold thrust and 850 h/year (2.3 h/day) for hot thrust, then after those values there is an ascent as seen in Figure 7. From this result, it might be concluded that there must be a further research on figuring out the close relation between the STC and the revenue obtained by the aircraft operator. Since there have no any data about the revenue in this paper, it is not possible to estimate which annual operating hour is the most profitable at the manner of STC.

5. CONCLUSIONS

In this study, an exergoeconomic analysis is performed for an aircraft turbofan engine. Exergy and exergoeconomic analysis methods are used to measure the real performance of thermal systems dealing with both first and second laws of thermodynamics. Exergoeconomic analysis is established after an exergy analysis.

The examining parameters in this study include annual operating hours, system life time, fuel price and interest rates. The main conclusions, which may be drawn from the results of the present study, may be listed below:

- a) kg based fuel price and the annual fuel price ascents have drastic effects over the STC
- b) increasing the interest rates increase the levelized total (and component by component) capital investment and operation & maintenance expenditure
- c) there is an inverse proportion between the system life time and STC since increasing the system life time increase the cost because of the higher operation % maintenance cost due to the aging.
- d) furthermore, considering some parameters such as annual operating hours which studied in Figure 7, it is revealed that for obtaining the actual profit, the cost values found by the exergoeconomic analysis might be taken into consideration with the revenue which came from the ticket selling. But in this case, one should consider the other cost not only deal with the engine, but also deal with the other items such as aircraft, airport, real estates and so on.

The authors plan to perform such a study by widen the range of the exergoeconomics.

Nomenclature

i	Interest ratio
\dot{Z}	Levelized capital and OM costs
CA	Levelized capital cost
n	Life time
\bar{h}	Molar specific enthalpy (kJkmol^{-1})
\bar{s}	Molar specific entropy ($\text{kJkmol}^{-1}\text{K}^{-1}$)
x	Mole fraction
\bar{ex}^{ch}	Standard molar specific chemical exergy (kJkmol^{-1})
T	Temperature (K)
R	Universal gas constant ($8.314 \text{ kJkmol}^{-1}\text{K}^{-1}$)

Subscripts

0	Ambient
CH	Chemical
k	Component indices
e	Exit
Q	Heat
i	Inlet
KE	Kinetic
l	Levelized
PH	Physical
T	Thrust
W	Work

Superscript

CI	Capital investment
OM	Operation and maintenance

REFERENCES

1. Cengel Y.A., *Green thermodynamics*, *International Journal of Energy Research*, 31 (12) (2007) 1088-1104.
2. Onyango F.N., Ochieng R. M. *The potential of solar chimney for application in rural areas of developing countries*, *Fuel* 85 (2006) 2561–2566
3. Enviromission, <http://www.enviromission.com.au>: Access date: May 2008-05-26
4. Hepbasli A., *A key review on exergetic analysis and assessment of renewable energy resources for a sustainable future*, *Renewable and Sustainable Energy Reviews*, Volume 12, Issue 3, April 2008, Pages 593-661.
5. Granovskii, M., Dincer I., Rosen M.A., *Exergetic life cycle assessment of hydrogen production from renewables*, *Journal of Power Sources*, Volume 167, Issue 2, 15 May 2007, Pages 461-471.
6. Dincer I., Rosen M.A., *Exergy analysis of renewable energy systems*, *EXERGY*, 2007, Pages 163-228.
7. Szargut, J.M., Morris, D.R. and Steward, F.R., *Exergy Analysis of Thermal, Chemical and Metallurgical Processes*. John Benjamins Publishing, 1988.
8. Bejan, A., Tsatsaronis, G. and Moran M., *Thermal Design and Optimization*, Wiley, USA, 1996.
9. Tsatsaronis G., Czesla F., *Thermoeconomics*, *Encyclopedia of Physical Science and Technology*, Third Edition, Volume 16, Academic Press, 2002, pp. 659-680.
10. Xiang, J.Y., Cali, M. and Santarelli, M., *Calculation for physical and chemical exergy of flows in systems elaborating mixed-phase flows and a case study in an IRSOFC plant*. *International Journal of Energy Research*, 28 (2) (2004) 101-115.
11. Turgut E.T., Karakoc T.H., Hepbasli A., *Exergetic analysis of an aircraft turbofan engine*, *International Journal of Energy Research*, 31 (14) (2007) 1383-1397.
12. Balli O., Aras H., Hepbasli A., *Exergoeconomic analysis of a combined heat and power (CHP) system*, *International Journal of Energy Research*, 32 (4) (2008) 273-289.
13. Karakoc, T.H, Turgut. E. T., Hepbasli A., *"A Study on Exergy Analysis of a Hydrogen Fuelled Turbofan Engine"*, 3rd International Green Energy Conference, Sweden, 2007.

*V.I. Dvoruk, M.V. Kindrachuk, Doctor of Science, professor
(National Aviation University), Ukraine*

METALLOPHYSICS OF WEARING FRICTION SLIDING IN THE PRESENCE OF ABRASIVE MATERIAL

New direction of researches of wearing down ability of the ground surfaces is offered on principle of display by the metal of electronic relaxation. The calculation-analytical model of surface wearing down capabilities is developed and estimation of influencing of factors incoming in it is conducted

Introduction. During deterioration of friction surfaces of initially free abrasive particles, which are in the conjugation space [1], it is observed charging effect fixation of the abrasive material on one of the friction surfaces. In that conjugations of friction sliding, where movable surface is made of more tough metal than fixed one, usually charge last. Due to this effect, the deterioration ability of movable surface appreciably reduces. Never the less, deterioration of fixed friction surface under heavy load is very considerable [2]. The deterioration mechanism of charging surface is not completely elucidated.

Theoretical concept and its analysis. The result of study of this problem [3; 4] showed that structure because of charging fixed surface gets composite. Abrasive deterioration of such "composite" represents fatigue disruption under low-cycle loading. Frictional low-cycle fatigue takes place at the fixation points of the abrasive particles on the friction surface and the destruction has a viscous character. This process occurs because of abrasive particles enforced vibration which charges into metal under action of changeable forces or forced by movable surface. Due to vibration of particles in the places of their fixation deformations will appear and tensions which are in accord with them. Scheme of powered action of friction movable surface on the abrasive particle which is fixed on fixed surfaces depicted in fig. 1.

According to [5] it can be assumed take that speed of deterioration of fixed surface is

$$V_i = h/\tau = h\omega/N \quad (1)$$

where h_A – penetration of abrasive particle on the fixed surface; τ – material durability at the place of abrasive particle fixation with penetration h ; ω – enforced vibration frequency; N – quantity of cycles till material destruction at the place of abrasive particle fixation with penetration h_A .

Charging layer can be regarded as the enforced vibrations source from which in the depth of fixed surface amplitude vibrations will be spread.

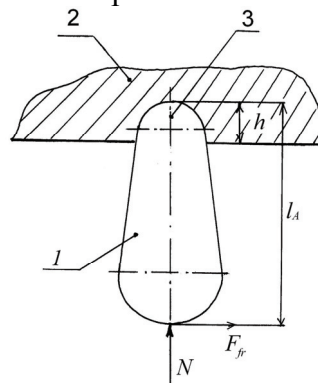


Fig. 1. Scheme of power action of mobile surface of friction on abrasive particle, that:

1 – abrasive particle; 2 – immobile surface of friction; 3 – center of oscillation of the particle

Due to such vibrations in the fixed surface metal acoustic waves spread which with at distant from the surface disappear. As charging layer is the source of acoustic vibrations are

spread lower layer then for flat external surface it's possible to take acoustic wave as flat (fig. 2) wave with finite value of shift

$$A = Am \sin \omega \left(t - \frac{x}{a} \right) \quad (2)$$

where A – source shift from equilibrium position; Am – vibrations amplitude; t – time interval; x – wave front coordinate; $a = \sqrt{\frac{E}{\rho_{II}}}$ speed of sound (phase velocity); E – metal resilience module of the fixed friction surface; ρ_{II} – metal particle of the fixed friction surface.

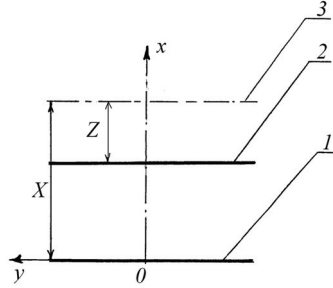


Fig. 2. Scheme of spreading flat wave in immobile surface of friction:
1 – source of oscillation; 2 – immobile surface of friction; 3 – front of wave

Due to enforced constant frequency, intensity of sound depends on amplitude vibration am only. It is possible to find Am formula on the basis of solution of the expression of energy consumption process in the body with unbounded external surface, which moves in the deterioration process.

After the solution of this equation the following formula for amplitude vibrations, a has been obtained

$$Am = Am_0 e^{\chi \rho (-V_i b^{-2} z)} \quad (3)$$

where Am_0 – amplitude of enforced vibrations on the fixed friction surface; $b^2 = \frac{\lambda}{c\rho}$ – temperature conductivity of metal; λ – heat conductivity of metal; c – heat capacity; z – depth on which enforced vibrations are spread inside the metal; V_i – metal deterioration rate.

If in the equation (3) instead of deterioration rate V_i its expression is put from (1) we will get a well known from vibration theory formula for finding amplitude of fading vibrations.

$$Am = Am_0 \left(-\frac{\pi \varepsilon}{a} \omega z \right) \quad (4)$$

where ε – acoustic loss factor [6]; $\frac{\pi \varepsilon}{a}$ – metal physical constant of an immovable surface. From equalizations (3) and (4) for suppression velocity V_i will have

$$V_i = \frac{\pi \omega b^2}{a} \varepsilon. \quad (5)$$

Acoustic loss factor is recommended to determine from the following correlation

$$\varepsilon = \frac{8\pi}{3} \frac{\omega(1+l)}{E} \eta. \quad (6)$$

where $l = Ta = \frac{2\pi}{\omega} a$ – wave length; T – vibration period; η – metal viscosity of immovable surface.

In general, viscosity of immovable surface η is determined through its connection with inner metal friction. But the approach exists [6], that the notion of inner friction includes energy losses of different types which have no direct relation to the notion of viscosity. It is reflected negatively on the exactness of viscosity estimation.

The analysis of new relations with high-level characteristics is necessary for increasing exactness. Besides, if to take into account the interaction, fact of friction tensions with electronic system of metal, the approach from the position of electronic relaxation is to be considered perspective [7].

According to this approach, sound fading is a result of a sound wave interaction, that is spread with electronic gas of metal.

The gas, that electrons create in metal, is highly degenerated (i.e. has quantum character of interaction between electrons) and is a subject of Fermi-Dirak statistics. [8] Quantum state of electron is described by wave vector K , directed toward the side of spreading electronic wave in metal. One of the most important characteristics of the metal electronic system is the Fermi surface – the surface of constant energy at a K – sphere, which answers Fermi's energy. In the metal conductivity only conductivity electrons which are on the Fermi's surface take part. According to [7] electrons may be regarded as effective viscous environment, viscosity of which

$$\eta = \frac{N_e m_e l_e \bar{V}}{3} \quad (7)$$

where $N_e = \frac{N_A \rho_{II}}{\mu}$ – quantity of electrons in a volume unit; N_A – Avocado's number; ρ_{II} – metal viscosity; μ – metal molecular weight; m_e – electron mass; l_e – average length of electron free run; \bar{V} – average velocity of electrons conductivity.

Because of this viscosity, sound wave transfers a pulse and energy to the electronic gas and as a result of this fades.

Taking into account, that near the Fermi's surface $\bar{V} = V_F$ equitation can be written as follows

$$\eta = \frac{N_e m_e l_e V_F}{3} = \frac{N_e m_e V_F^2 \tau}{3} \quad (8)$$

where $\tau = \frac{m_e}{N_e e^2 \rho}$ – relaxation time; e – electron charge; ρ – specific electric resistance of metal;

$V_F = \sqrt{\frac{2E_F}{m_e}}$ – velocity of electrons near the Fermi's surface; $E_F = \frac{\hbar^2}{2m_e} (3\pi N_e)^{2/3}$ – Fermi's energy

$\hbar = \frac{h}{2\pi}$ – Plank's constant; h – Plank's constant.

After the introducing all these correlations in to the formula (8) and correspondent transformations.

We obtain

$$\eta = \frac{\hbar \left(3\pi \frac{N_A \rho_{II}}{\mu} \right)}{3e^2 \rho}. \quad (9)$$

If we take into account (9) formula (60) looks like

$$\varepsilon = \frac{2\hbar^2 (\omega + 2\pi a) \left(3\pi \frac{N_A \rho_{II}}{\mu} \right)^{2/3}}{9\pi^2 e^2 \rho E}. \quad (10)$$

And now, returning to the formula (5), after the substitution (10) we definitely have

$$V_i = \frac{2}{9} \left(\frac{h}{e} \right)^2 b^2 \frac{\omega(\omega + 2\pi a)}{\rho E a} \left(3\pi \frac{N_A \rho_{II}}{\mu} \right)^{2/3} \quad (11)$$

Using known correlations of quantum mechanics, i.e. de – Broil's formula

$$\lambda_e = \frac{h}{m_e V_F} \Rightarrow h = \lambda_e m_e V_F \quad (12)$$

where λ_e – de – Broil's wave length, and also formula of gyro magnetic ratio of electron spin moments

$$g_s = e/m_e \quad (13)$$

equalization (11) can be rewritten form which is in a more comfortable for subsequent analyses form.

$$V_i = (\lambda_e V_F)^2 \left(\frac{N_e^{2/3} \gamma}{g_s^2} \right) \left(\frac{\lambda}{C} \right) \left(\frac{1}{\rho_{II} E} \right) \left(\frac{1+l}{a} \right) (\omega) \quad (14)$$

Single out in the equation six groups of factors, which characterize:

1) Quantum characteristics of electrons

$$K = (\lambda_e V_F)^2; \quad (15)$$

2) Electronic system

$$E_e = \frac{N_e^{2/3} \gamma}{g_s} \quad (16)$$

where $\gamma = \frac{1}{\rho}$ – conductivity of metal

3) Thermal characteristics

$$T = \frac{\lambda}{C} \quad (17)$$

4) Mechanical characteristics

$$M = \frac{1}{\rho_{II} E} \quad (18)$$

5) Acoustic characteristics

$$3 = \frac{1+l}{a} \quad (19)$$

6). The soiree of oscillations

$$D = \omega \quad (20)$$

After substitution (15-20), the equation may be written in the following form.

$$V_i = K E_e T M 3 D \quad (21)$$

Results from (21), show that increase of all six groups of factors favours the increase of wearing ability. The most influence is exerted by parameters λ_1, V_F, g_s – so as they are pouts of equation (13) with index of power. 2. The smallest influence has parameter N_1 which has index of power $2/3$. The rest of parameters have the index of power 1, so their influence should be considered as essential.

Conclusion. The equation (13) revels the nature of wearing ability, defines ways of regulation by this tribological characteristics, and also it is an instrument for calculation of wearing ability. So as it is evident the amplitude A_m is not a part of this equation, the for application in tribotechnical

calculations it is necessary to know temperature of fiction (defined experimentally or by calculation way), as well as temperature dependences on all parameters.

References

1. *Икрамов У.А.* Расчетные методы оценки абразивного износа. – М.: Машиностроение, 1987. – 288с.
2. *Дворук В.И.* Научные основы повышения абразивной износостойкости деталей машин. – К.: КМУГА, 1997. – 101с.
3. *Дворук В.І.* Особливості утомного руйнування трибосистем ковзання при абразивному зношуванні // Вісник НАУ. – 2002. – №3. – С.56-58.
4. *Дворук В.І., Кіндрачук М.В.* Механізм утворення частинок зносу при терті ковзання металів у присутності абразиву // Проблеми трибології. – 2004. – №1. –С.130-137.
5. *Ханин М.В.* Механическое изнашивание материалов. – М. Изд. стандартов, 1984. – 152с.
6. *Красильников В.А., Крылов В.В.,* Введение в физическую акустику. – М.: Наука, 1984. – 400с.
7. *Новик А., Берри Д.* Релаксационные явления в кристаллах. – М.: Атомиздат, 1975. – 472с.
8. *Епифанов Г.И.* Физика твердого тела. – М.: Высшая школа, 1977. – 288с.

*A.A. Kornienko, Ph.D. engineer, assistant professor, L.A. Lopata, Ph.d. engineer, senior researcher (National Aviation University), Ukraine
M.V. Luchka, Ph.d. engineer, senior researcher (Frantsevykh Institute for Problems of Materials Science of NAS of Ukraine), Ukraine*

TRIBOENGINEERING OF COMPOSITE ELECTROLYTIC GRADIENT COATINGS

In the work research of dependence of wear resistance single and multi-layer composite electrolytic coating from structure and composition of a matrix-filled type is carried out. Influence of a gradient of properties of multi-layer coating on their wear resistance is considered

Introduction. An effective solution to the problem of increasing the wear resistance of parts made from construction materials is the formation on them of wear-resistant gradient layers with a heterogeneous structure of a matrix-filled or a skeleton types.

This solution has been successfully realized thanks to using composite electrolytic coatings (CEC), composed of a ductile metallic matrix and wear-resistant powdered filler. In this case, gradient coatings are composite matrix-filled coatings whose regular character is broken in the gradient direction, with the shape, quantity, and dimension of inclusions changing in accordance with a definite law [1, 2].

The present work aims at obtaining data on the wear resistance of matrix-filled single- and multilayered gradient deposits containing SiC inclusions in the Ni matrix and at clarifying the effect of the gradient in the coating depth direction on their wear resistance.

Experimental procedure.

Composite electrolytic coatings were produced through silting of strengthening SiC powders of various dispersivities with electrolytic nickel. The coatings were deposited on prismatic 10x10x5 mm samples. Deposits containing coarse particles (fractions 100/80, 50/40, and 28/20 μm) were deposited onto the horizontal cathode under impulse stirring of the electrolyte at a current density of 5-10 A/dm². The coatings containing more disperse particles (fraction 5/3 μm , SiC_N nanoparticles 50 nm) were obtained on the vertical cathode under continuous stirring of the electrolyte at a current density of 4-5 A/dm².

Tests were performed on a M-22M unit under conditions of dry friction. Prismatic 10x10x5 mm samples were studied at a friction speed of 0.5 m/s and a load of 20, 40, and 60 N. Steel HRC 45 was as a counterbody, a shaft-plane as a scheme of coupling, the friction path was equal to 1 km. Wear was evaluated from the data on mass loss and the linear wear of the friction couple.

Results and discussion.

The coatings obtained were examined using a chemical analysis and wear tests.

The contents of inclusions in the Ni matrix were (mass %): SiC_N=2, SiC₅=4, SiC₂₈=12, SiC₅₀=20, and SiC₁₀₀=24. It was established that the larger particles, the better they are inserted into a coating. By the data [3], the optimal inclusion content in a coating, from the viewpoint of increase in wear resistance, is 20-30%.

We have developed multilayered gradient coatings the wear resistance of which was higher than that of single-layer coatings for both the direct – fig., *a* (base from Steel 20, layers with inclusions of particles sizing (from base to surface) from 100/80 μm to nanometers) and reverse – fig., *b* (base, fine particles, coarse particles) gradients. The structure of the multilayered coating with a gradient in the depth direction is shown in Fig.

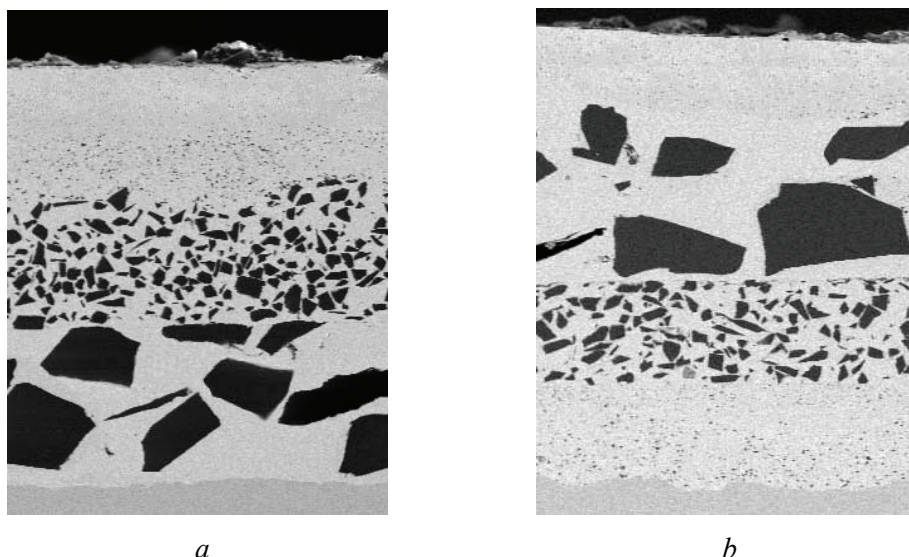


Fig. Microstructure of multilayered gradient CEC containing SiC inclusions in Ni matrix, Augmentation $\times 130$: *a* – direct gradient; *b* – reverse gradient

The results of friction and wear tests are listed in Table.

As seen, the coatings obtained by filling of nickel matrix with silicon carbide powder (fractions from 50/40 to 28/20 μm) have the highest wear resistance among single-layered CECs, which is far higher than that of mild Steel 20; the friction coefficient being lower by a factor of 1/3. These data are in good agreement with those obtained before [1].

Table

The data of friction and wear tests of CECs with various fillers

Coating type	Load, N	Friction coefficient	Weight wear of sample, mg/km	Weight wear of counterbody, mg/km	Linear wear of friction couple $\mu\text{m}/\text{km}$
1	2	3	4	5	6
Steel 20	20	1,3	75,7	34,6	62
	40	0,91	83,8	24,5	72
	60	0,75	61,5	26,4	56
Ni+SiC _N	20	1,3	32,4	5,0	47
	40	0,8	33,9	5,4	48
	60	0,7	36,6	6,8	50
Ni+SiC ₅	20	1,3	27,7	1,8	42
	40	0,63	34,2	2,5	48
	60	0,69	38,7	8,9	53
Ni+SiC ₂₈	20	1,1	1,7	5,7	11
	40	0,9	3,4	10,2	22
	60	0,73	9,0	37,4	40
Ni+SiC ₅₀	20	0,75	1,2	4,5	10
	40	0,62	3,2	9,4	22
	60	0,8	7,7	10,6	25

1	2	3	4	5	6
Ni+SiC ₁₀₀	20	1,1	69,7	37	49
	40	0,82	93,2	42,5	105
	60	0,66	121,7	54,1	118
Direct gradient	20	1,15	4,0	7,1	40
	40	0,82	10,8	8,7	59
	60	0,75	6,5	17,0	38
Reverse gradient	20	1,3	3,8	13,5	48
	40	0,91	9,3	20,5	65
	60	0,75	6,2	30,0	52

Coatings containing smaller and larger particles are characterized by significantly greater wear. For example, under the selected scheme of friction, CECs containing 24 mass % filler with a particle size of 100 μm sharply decreases the capacity for work over the entire load range (20-60 N). However, in the presence of a multilayered CEC with a gradient of quantity and location of inclusions in the layers, the wear resistance increases.

Estimating the total wear (linear and by weight loss), we see that the basic regularities are similar for both small (20 N) and maximal (60 N) loads and the optimal SiC dispersivity is in nickel CEC (50/40 and 28/20). Despite the fact that the content of nanostructured (50 nm) SiC filler is below 2 mass %, the wear resistance of these CECs is not lower than that of Ni-SiC (5/3 μm , 4 mass %) CECs.

Of the greatest interest is the fact that the wear resistance of CECs with both direct and reverse gradients, containing in the upper layer inclusions with dispersivities of 5/3 and 100/80, respectively, is far higher in comparison with that of deposits with no gradient sublayer. It is explained by the fact that such gradient layers have higher dissipative properties than single-layered coatings and more effectively disseminate stresses in nickel matrix that is confirmed by the analytical calculations.

Conclusion.

Single-layered composite electrolytic coatings on the basis of nickel have been produced with optimal filler dispersivity from the viewpoint of high wear resistance under selected friction conditions.

The work needs further elaboration. Nevertheless, the conclusion about the positive effect of a gradient sublayer on the wear resistance of coatings can be drawn. The use of such gradient coatings makes it possible to significantly increase the wear resistance of deposits containing fine inclusions (including nanoparticles), which do not have a required wear resistance when used in single-layered coatings.

References

1. Лучка М.В., Кіндрачук М.В., Мельник П.И. Износостойкие диффузионно легированные композиционные покрытия. – К.: Техника, 1993. – 143с.
2. Покрыття градієнтного типу поверхні триботекстату ковзанням / Лучка М.В. – Київ, 1998. – 53с. (Препр. / НАН України. Інститут проблем матеріалознавства ім. І.М. Францевича: 98-5).
3. Кіндрачук М.В., Куницький Ю.А., Дудка О.І. Структурутворення та формування триботехнічних властивостей евтектичних покриттів. – К.: Вища шк., 1997. – 120 с.

E.A. Kulkhavyi, Ph.D. engineer, senior researcher, A.S. Kryzanovskiy, Ph.D. engineer, assistant professor (National Aviation University), Ukraine

TRIBOLOGICAL PROBLEMS OF AIRCRAFT SAFETY

Results of this work show that for failure probability reducing it is necessary to enhance tribostructure stability, i.e. to reduce their entropy. Prospects are connected with reducing of friction factor of technical tribosystems in two-three orders and approaching of this factor to the level of biological systems

Safety of an airplane as a technical object is mainly determined by its strength and tribological properties. Strength features characterize the ability of the structure to resist its destruction under permissible operational conditions. Tribological properties mean the ability of aircraft movable joints to maintain the required operational ability during given service life.

In order to ensure required safety relative to strength criteria special systems have been developed which include prior information, static and endurance calculation methods, experimental check of all engineering solutions under laboratory and working conditions beginning from initial design stages to the aircraft phasing out of operation.

The main criterion of strength is the destruction probability that can be expressed by load condition characteristics during operation and strength properties of the structure as

$$Q = \int p(X)F(X)dX, \quad (1)$$

where $p(X)$ is the density of distribution of external loads during operation; $F(x)$ is the distribution function of the structure strength.

Tribological aspects are not considered during the first stage of the process of design. In other words, at the initial stage of design prior information is used. After that on the basis of actual and operational testing the full-scale maximum load and service life are determined.

In this case required safety level is based by the application of traditional materials and constructions as well as homogeneity of tribology objects with respect to small number of failure signs. Trouble-shooting and elimination of failure reasons takes up to 80 % of all of expenditures for aircraft and aero-engines maintenance. In this case failure of tribocouplings is the main source of aircraft accidents which occur owing to technical reasons.

Complicated, multifactor, non-equilibrium contact process are the reason of the fact that the designed methods for tribocouplings have not been elaborated. In order to obtain the estimation of the processes (1) it is necessary to have multi-dimensional characteristics of materials in tribocontacts as well as operational conditions in the range of all factors influencing operation. Due to the fact that external and internal conditions of tribological objects are indefinite it is very difficult to determine all characteristics with the accuracy necessary for calculation and design. The present paper describes methods of calculation and design based on specific properties of tribosystems and triboprocesses.

Two contacting solid bodies and a lubricant (grease, oil, gaseous or combination of these) the elements of a tribosystem. In the process of relative displacement under load, the interaction of substances of tribosystem elements takes place. These substances under the action of fluctuating potential power and temperature fields rather quickly achieve final physical-chemical and aggregate condition.

During the evolution stage of running-in, the tribosystem spontaneously transfer from the state preset by technological processes to the state determined by the process itself. At this stage in the place of a contact tribological structures are being formed and later on, in these structures at stationary mode the triboprocesses are realized. Tribostructures are formed from products of interaction of all tribosystem elements that are in the final physical-chemical and aggregate state. For example, iron oxides properties are invariable up to temperature 1000° K. Oxides, sulfides,

phosphates, cokes, metallorganic salts and complexes in the form of molecules, clusters, superdispersed particles are tribostructure elements and provide their resistance to external actions.

In tribostructure forming mechanism randomness has the main effect. In the fluctuate potential field of the tribological contact probability peaks arise in a random way. During evolutionary process the weakest peaks of potential probability correspond to abrupt peaks of concentration of transferred substance. Final molecules, clusters, superdispersed particles form structures in the form of separate portions, meshes, cells, wedge-shaped and wavy systems that can be observed at the end of the process on the elements and samples friction surfaces and can be analysed in the metastable state. During tribostructure formation entropy decrease is iteratively compensated by entropy increase during heat removal from the tribosystem. These conditions are favourable for self-organization and formation of dissipative structures.

Having been formed tribostructures operate according to nonlinear laws of synergetics in the stationary mode. Their overgrowth is limited by entropy and their low level is restrained by free energy.

Using linear approximation of Boltzman's transfer equation we can present triboprocesses as function of time in the following form

$$dy(t)/dt = -(y_0 - \langle y \rangle)/T \quad (2)$$

$$y(t) = (y_0 - \langle y \rangle)\exp(-t/T) + \langle y \rangle \quad (3)$$

$$Y(t) = (y_0 - \langle y \rangle)T[1 - \exp(-t/T)] + \langle y \rangle t \quad (4)$$

where y_0 and $\langle y \rangle$ are initial and stationary values of the process; T is running-in time of relaxation; $Y(t)$ is integral process.

In tribological contact friction, wear and failure processes are realized. Energy, substance and failure flows correspond to these processes. Mentioned above equations are correct for all of three flows. If we deal with friction process $Y(t)$ corresponds to friction energy $E_{fr}(t)$ and $y(t)$ is friction power $N(t) = dE_{fr}(t)/dt$; for wear process $Y(t)$ corresponds to wear $I(t)$ and $y(t)$ is wear rate $i_t = dI/dt$; for failure process $Y(t)$ is failure probability $\Pi(t)$ and $y(t)$ corresponds to failure rate $\pi(t) = d\Pi(t)/dt$.

Functions presentations (3) and (4) correspond to classical curves that describe wear rate and failure rate depending upon time. Exponents of right parts characterize running-in evolutionary process, running-in duration determines relaxation time T and running-in effect on integral process is characterized by function $Y_0 = (y_0 - \langle y \rangle)T[1 - \exp(-t/T)]$. At this stage free energy tends to minimum, aggregation of transferred particles occurs, substance internal flows form the tribostructure and increase its volume, failure flows and substance flows from the system are reduced till they achieve stationary level. In this case tribostructure substance is in its finite state, temperature and entropy are constant, and tribostructure entropy is proportional to its volume. When the entropy effect becomes predominant tribostructure collapses. Tending to uniform distribution leads to partial destruction of the tribostructure and removing some amount of its substance from the system in the form of wear debris. In this case, the volume and the entropy of the tribostructure decrease and tend of free energy to minimum becomes predominant. Consolidation of transferred particles occurs and tribostructure recovery is observed. The cycle is repeated.

Stationary state level is determined not by all produced entropy but only by its small part that is connected with tribostructure substance. It is proportional to the volume and may either be increased or reduced. During friction process the total entropy always increases. Competition of free energy G and entropy ST_v generates steady periodical processes under non-equilibrium conditions. Models of Lotki – Volter, brusselator models and others correspond to these processes in $G-ST_v$ coordinates.

In any tribosystem in the positive quarter of velocity range $V_m/sec(X_1)$ and loads $P\Pi a(X_2)$, where \vec{X} is the predetermined coordinates, there exists an area C in every point of which there is a stationary state where friction, wear and failure process have constant in time and dispersion features (Fig.1). This area is limited by states in which failure probability is increased from zero to one.

In friction units of aircraft systems velocities and loads are changed depending upon modes of typical flight and random fluctuations. Triboprocess level is also changed together with these states. In order to choose an optimum tribosystem for the specific friction unit it is necessary to have the method to estimate friction, wear and failure under variable operational conditions.

Let us consider basic physical phenomena and mechanism of this calculation.

In every point of C area stationary state is an attractor. At the stage of running-in all processes tend to this state. When the system moves along area C all three processes follow to the path of motion. In this case motion is considered as changing of states in time. In other words it is motion in the area of states where the process corresponds to new state in every following point.

In the solid body mechanical signals are spread with sound speed. Tribostructures activated by friction have high relaxation ability. That is why triboprocesses follow to states without inertia up to high rate of change of loads and accelerations. Attraction of stationary states and high relaxation properties of triboprocesses allow to use superposition principle and linear summation in combining characteristics of tribosystem $y(X)$ and medium $p(X)$ in the form of

$$Y(t) = \int_0^t dt \int_{\vec{D}} y(X)p(X) dX \quad (5)$$

Inner integrals determine average values of processes and their dispersions for all states in \vec{X} coordinates during time dt , $Y(t)$ and $\sigma^2(t)$ are correspondingly integral value of the process and its dispersion during time from 0 to t . Outer integral is used for non-stationary operational conditions when contact area is increased together with wear and this fact leads to change of states probability $p(X)$. If operational characteristic $p(x)$ is not changed the inner integral is multiplied by the time of process realization t .

Let us consider the structure of states area \vec{X} on the basis of operational conditions of the aero engine friction unit. These conditions are changed during aircraft typical flight from the ground idling condition when velocities and loads are minimal to take-off mode with maximum velocities and loads. For any part of the engine we may determine rectangle $D(\vec{X})$ in \vec{X} coordinates within which all its operational states are located. This rectangle has to be in limitations of stationary states area $C(\vec{X})$ because outside this limitations failure probability tends to one.

After dividing this rectangle by lines which are parallel to axes and are located at equal distance we obtain a set of elementary rectangles. Identical velocity and load interval correspond to every of this elementary rectangle. During typical flight time T any time t_{jk} corresponds to every elementary part. Besides, we shall assume that value $p_{j,k} = t_{j,k}/T$ is the probability of a given state with respect to time. If we preset corresponding probability to every elementary part of $D(\vec{X})$ we obtain operational characteristics of the friction unit $p_t(\vec{X})$. This characteristic is a single mapping of the time line on \vec{X} . In this case every portion of these lines has exact place on $D(\vec{X})$. Inverse mapping $p(\vec{X})$ on t is ambiguous. It shows the probability with which the given state may appear at any point of the time line. In this case one elementary part $D(\vec{X})$ may have several mappings on t .

Expression (5) is generalization of integral (1) for multi-dimensional spaces and non-stationary processes with respect to medium state $p(X)$. In this case medium is functional area of velocities and loads X .

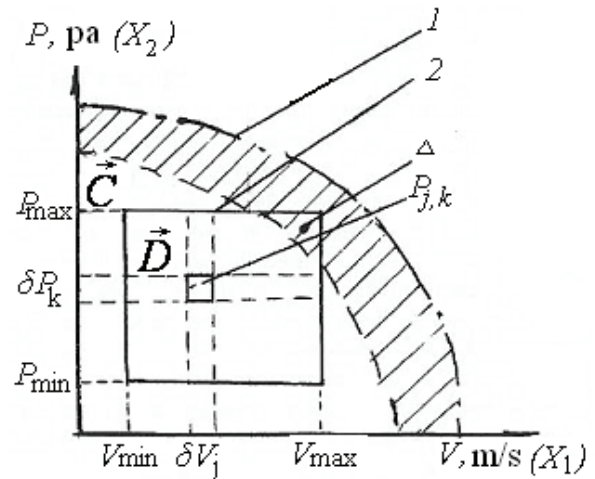


Fig 1. Preset area \vec{X} tribosystem conditions: 1 is boundary of area C; 2 is boundary of area of friction unit D operational states; 3 is state probability; 4 is critical operational part.

In order to find energy losses for friction, wear or failure probability per time t it is necessary to calculate integral (5) for every process. For performing this calculation we should know operational characteristic of the friction unit $p(X)$ that is one for all of three processes as well as tribosystem characteristics for every stationary process on C such as friction factor $\mu(X)$, wear rate $i(X)$ and failure rate $\pi(X)$.

Operational characteristic of the friction unit can be obtained as a result of calculations and by means of analysis of synchronous measurements of velocities and loads during operation.

At every point of area C average values with respect to time and dispersions of processes are constant. Besides, dispersions are homogeneous on C . That is why we can use average values functions and common dispersion for every process on C as tribosystem characteristics.

Owing to stability of tribostructure properties the friction factor is usually changed lightly in the area of stationary states C . That is why it is possible to use average value and dispersion of the friction factor as characteristics of tribosystem stationary process of friction. For determination of these characteristics we have made several experiments at different points of area C .

Function $i(\bar{X})$ that describes parameters of wear stationary process in all points of area C on X can be obtained in laboratory environment by means of making quite complicated and long-term experiments and analysis of their results.

Application of methods of multi-variant statistic and mathematical models of regression analysis allows to reduce essentially material and time expenditures for the experiment and to represent characteristics in the analytical form that is handy for use and storage.

Stationary processes of the wear are homogeneous in area \bar{C} with respect to dispersions. Consequently, for its estimation it is enough to make several parallel experiments at one point, for example at the centre of area \bar{C} .

If wear is a result of partial and reversible destruction of the tribostructure the failure process occurs under partial non-reversible tribostructure destruction and after that it progresses till the final fracture. Failure process leads to serviceability loss of the frictional unit due to excessively high friction forces and comes to either seizure for example, in a cylinder and the piston group of the aircraft piston engines, in frictional units of the landing gear and other or to fire due to failure of support bearing of the gas turbine engine rotor and so on. Failure due to excessively high level of wear leads to high dynamic loads and to blades destruction of structural elements. In particular owing to wear of strip flanges blades of the gas turbine engine rotor are destructed. Such failures can be the reason of emergency and catastrophic situations. But because of the fact that for aircraft the probability of such situations can not be higher than 10^{-7} or one during 1100 years of service life we can come to the conclusion that the failure probability of the most responsible units approaches to zero.

The large part of the stationary state area C corresponds to these conditions. The increase of the failure probability in the marginal area is connected with stationary imbalance between energy and entropy in the tribostructure. When the entropy is excessive with respect to stationary states high mobility of tribostructure elements reduce their load-carrying ability. Direct contact of solid surfaces and cohesive separation of relatively large particles occur.

When the entropy is quite small we observe tribostructure breakdown that occurs due to low mobility of elements, direct contact of solid bodies and cohesive separation of particles. These particles form stress concentrations at the contact. They cause separation of new particles. The process is developed according to self-catalyzed mechanism and brings to non-reversible tribostructure destruction. Thus, instability of stationary states and development of failure processes are connected with appearance of self-catalyzed reactions at the contact.

As a rule, failure processes arise at the intersection of critical and operational areas Δ (Fig.1) If for a friction unit the state probability during operation is $p(\Delta)$ and the probability of appearance of the tribosystem failure process E is $\pi(E/\Delta)$ we can find the average failure frequency $p(E)$ along operational area as $p(E) = p(\Delta) \pi(E/\Delta)$. After multiplying this expression by t we obtain the analogue of the integral (5) for failure probability during time t where $p(\Delta)$ is friction unit operational characteristic and $\pi(E/\Delta)$ is tribosystem failure process characteristic.

Obtained relation represents existing knowledge about failure processes. Frequency of failure is uniformly distributed in time. In other words it has maximum information entropy. This information allows to localize failure process and to improve quality of forecasts in the presence of corresponding characteristics as well as to reduce the failure probability in case when characteristic features are not present. The reduction of indeterminacy as a result of diagnostics may be assumed as quantity of obtained information i.e. information is inversely proportional to indeterminacy

Information relative to failure E contained in characteristic F probability E changing from its prior value $p(E)$ to its posteriori value $p(E/F)$. In the information theory information amount contained in event F with respect to event E is determined as

$$I(E, F) = \log \{p(E/F) / P(E)\} \quad (6)$$

In this expression the base of the logarithm determines a unit of measurements of the information. When the logarithm base is 2 the information unit relative to E is obtained if $p(E)$ is doubled; when the logarithm base is 10 the information unit corresponds to increase of $p(E)$ in ten times.

When diagnostics is performed according to two characteristics simultaneously the property of additivity of the information amount is carried out in the following way

$$I(E; F_1 F_2) = I(E; F_1) + I(E; F_2/F_1) \quad (7)$$

Failure appearance is always connected with tribostructure non-reversible destruction. That is why it is accompanied with identical phenomena for different tribosystems which are used as diagnostic characteristics. Among them there are changes in acoustic and vibration spectra, change of friction surfaces state, friction force fluctuation, presence of solid bodies' particles in the wear debris. Tribosystem homogeneity relative to failure characteristics permits to use very wide information basis for expert objectives and to obtain reliable estimation of prior probabilities even for very seldom events. Conclusion.

Information obtained during aircraft service life, modern means of technical diagnostics and operational inspection system allow to determine development of failure processes at an early stage. On the other hand the posteriori information and Bayesian calculation with required accuracy permit to localize a failure when the first signs appear and to reduce failure probability when they are absent to the level determined by requirements of airworthiness standards.

This level, according to which aircraft accidents rate is not greater than 10^{-7} per flight hour is not changed during fifty years. It means that classical methods of aircraft safety improvement exhaust themselves.

Results of this work show that for failure probability reducing it is necessary to enhance tribostructural stability, i.e. to reduce their entropy. Classical method consists of increasing energy flow rate from the system. Modern cooling systems attain their perfection many years ago. That is why reserves are minimal in this direction.

Prospects are connected with reduction of friction factor of technical tribosystems in two-three orders and approaching of this factor to the level of biological systems. Principal solution of this problem is connected with activation of repulsive phase states of interatomic ties in technical systems tribostructures.

In technical systems multiple reducing of friction forces simultaneously allows to solve different problems of wear, failure and ecology besides saving energy expenditure.

References

1. Селихов А.Ф., Чижев В.М. Вероятностные методы в расчетах прочности самолета. – М: Машиностроение, 1987. – 240 с.
2. Зельдович Я.Б. Перемещаемость в случайных средах. – УФН. Т.152 – Вып.1, 1987 – С. 33-41
3. Пригожин И.А. От существующего к возникающему. – М: Наука, Физматгиз, 1985 – 328 с.
4. Кульгавый Э.А. Триботехнические характеристики и их применение. – Проблемы трибологии. – 2003 – №3 – С. 51-61
5. Нормы летной годности гражданских самолетов СССР. – МАП, МГА, 1974 – 344 с.

*G.V. Tsybanov (Institute of strength problems in the name of G.S. Pisarenko of NAN Ukraine)
V.E. Marchuk, V.V. Zhiginas (National aviation university, Ukraine)*

FRETTING-RESISTANCE OF AIRCRAFT TRIBOLOGICAL ASSEMBLY DETAILS IN THE CONDITIONS OF ALTERNATING LOADS

The technical state of units and details of aircraft undercarriage, made from high-strength construction steel 30XГCA, was analysed. The experimental researches of 30XГCA steel in the conditions of fatigue and fretting-fatigue were conducted.

Today aerotechnics are a difficult technical complex, which includes plenty of details and units, forming a part of equipment, engines, frame and control system. The analysis of the technical state of aircraft basic units and details in the last few years testifies that they fall out by reason of various surface damages, related to violation of geometrical size and worsening of surface layer quality which assisted by high operating loads. So in 100% aircraft defects are exposed in the construction of fuselage, 47% - in a construction of wing and undercarriage and to 60% - in gas turbine engine, which are concerned with the damage of compressor-blades, turbines and other details [1].

Among the mentioned power elements the least operating reliability, from the point of strength, have the details and units of aircraft undercarriage, which work under hard operating conditions and high level of variables loads, operating at take-off, landing and taxiing. Such details are power constructions, joint-screw-bolt connections, axes, suspension brackets, bushes and other. To maintain the high reliability and strength of undercarriage the most of its power construction details and units are made from high-strength construction steels (fig. 1), the most widespread of them is 30XГCA and 30XГCHA [2-4].

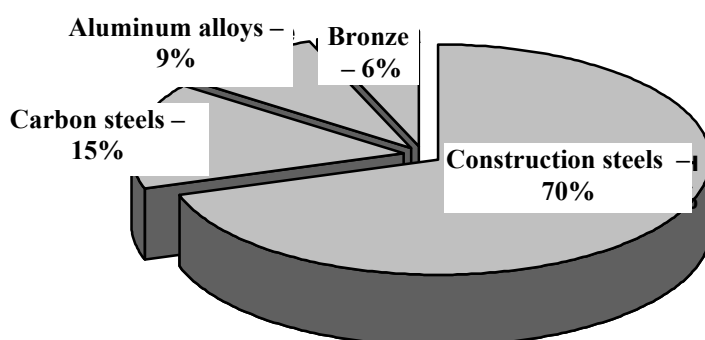


Fig. 1. Allocation of materials by the elements of the aircraft undercarriage construction

The construction steels have substantial dispersions of characteristics and fatigue resistance, and also high sensitiveness to the stress concentrators. An analysis of statistical data of the undercarriage power construction failures in exploitation showed, that more than 60% of the

undercarriage construction elements are liable to fatigue damages, thus 26% from them behave to the failures of joint-screw-bolt junctions. A nature of detail surface damages testifies of the joint influence of the alternating loads and fretting-corrosion.

A high wear in movable joints can result in the loss of kinematical precision of undercarriage gear power construction that, in same queue, can create the redistribution of loads and, on occasion, impacts in joints. Therefore, today, a research in area of tribology and mechanics of contact damage is an urgent task. They predetermine the considerable part of operating failures. If a wear conduces to the severe financial losses, then a fatigue damage can result in sudden destruction of responsible units and details. So, in the general issue of aircraft and air-engines details wear the fate of fretting-corrosion makes from 35 to 50%, and the amount of fretting-fatigue damages makes, approximately, 40% from general fretting ones [5, 6].

Thus, an analysis of aircraft undercarriage elements damage testifies about the necessity of further deep study of power elements, made from construction steel 30XГCA (30XГCHA), fretting and fretting-fatigue, and methods of its durability increase in the operating conditions.

Method of researches. The samples for research of fatigue resistance characteristic were made from high-quality alloy steel 30XГCA (module of elasticity $E = 194$ GPa), which is widely used in an aviation engineering. The samples were exposed to heat treatment in the following mode: hardening to 910°C and cooling in oil, after that tempering at temperatures of 500°C during 1 hour. The material of counter-samples is steel 30XГCA.

An experimental determination of fatigue and fretting-fatigue resistance characteristic was conducted on VLZ plant (on the base of electrodynamics vibrostand; certification No UA6.001.H.313) in the mode of resonance vibrations at normal laboratory conditions. The flat cantilever corset type samples were put to the test under conditions of symmetric cross-bending (fig. 2). For the criterion of sample destruction was taken a drop of self-frequency vibrations on 1%, by comparison to an initial resonance value which conformed to an origin in the «dangerous» section of surface semi-elliptic macro-crack sample with a depth to 0,1 mm. A frequency of sample resonance vibrations in the process of fatigue tests made of 130 Hz, on a fretting-fatigue ~ 75 Hz.

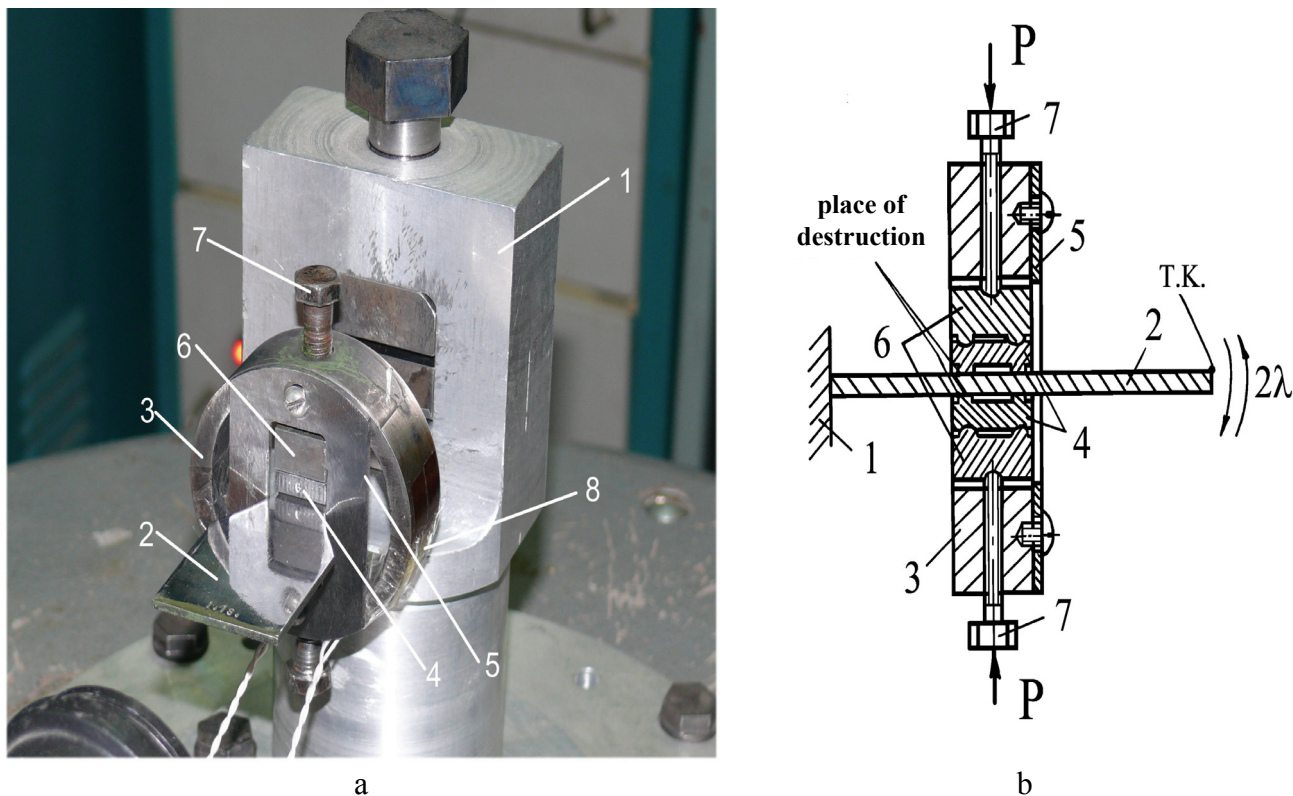


Fig. 2. A sample with a dynamometric ring for the fretting-fatigue tests: a - a general view, b - a schematic image (a transverse section): 1 - a clamp, 2 - a sample, 3 - a dynamometric ring, 4 - a counter-body, 5 - a plate-holder, 6 - a bush, 7 - the bolts, 8 - the tenso-resistors 4Г1-10-400

Before the beginning of tests a dynamic calibration of sample was conducted without and with fixed on it dynamometric ring with counter-bodies and static calibration of ring by the tenso-resistors of KΦ-4 type with a base of 3 mm and 4Г1-10-400 with a base of 10 mm. The dynamic calibration was conducted by a method, developed in the Central institute of aviation motor-building (CIAM, Moscow) and recommended for dynamic calibration on the enterprises of aviation industry [7].

Results of researches and their analysis. After the research method described higher were got the curves of 30XГCA steel fatigue on corset samples (curve 1 on a fig. 3) and on the same samples at presence of pressed to them fretting-brackets (curve 2 on a fig. 3). Effort of pressing of brackets to the sample was chosen starting from realization of the most damaged level of contact stress. Given on a fig. 3 results testifies, that the presence of fretting reduces the border of 30XГCA steel fatigue from 718 MPa to 375 MPa. Thus the angle of slope of the fatigue curve is also increased to abscissa.

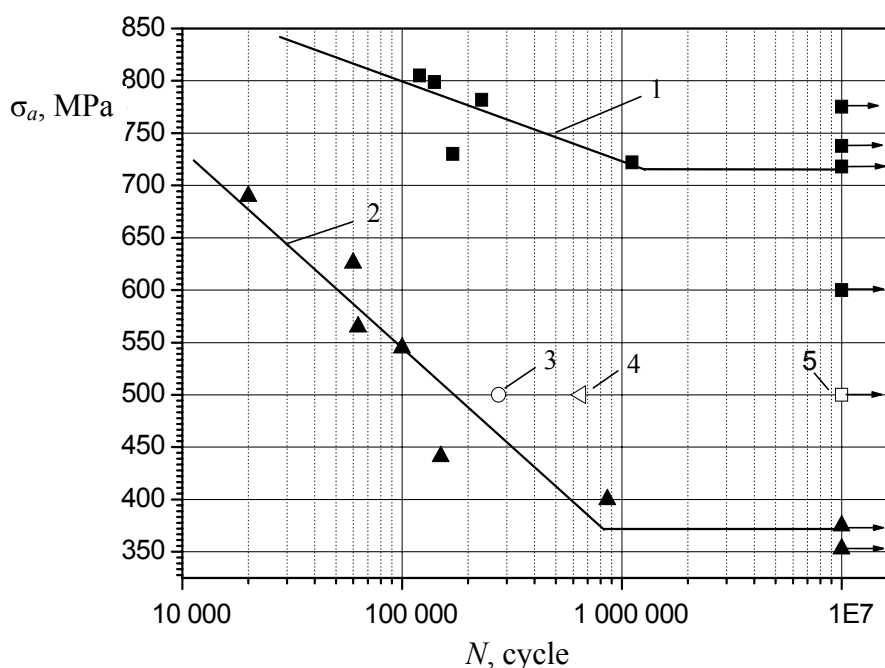


Fig. 3. The results of 30XГCA steel researches on a fatigue and fretting-fatigue: 1 - a curve of the smooth samples fretting; 2 - a curve of those samples fatigue in the conditions of fretting in contact with that steel at contact pressure of 140 MPa; 3, 4, 5 - a fretting-fatigue of samples at contact pressure of 56, 70 and 14 MPa accordingly.

In a table are resulted the numeral values of the statistical processing data results on a fatigue and fretting-fatigue of investigated steel as a line of regression

$$\lg N = A - B \sigma_a,$$

where N is an amount of destruction load cycles of the sample; σ_a is an amplitude of the applied stress in a section, in which destruction was happened.

Table

Data of the statistical treatment of fatigue and fretting-fatigue curves

Type of research	Free member, A	Coefficient of regression, B	Coefficient of correlation, R	Standard deviation, S
Fatigue	16,233	0,014	-0,7150	31,4942
Fretting-fatigue	7,9104	0,00535	-0,9307	44,372

Note: Results are got during minimization of the deviation squares sum on \lg .

It should be noted that, not looking on the near values of standard deviations for both of the curves, dispersion of results more meaningfully for the case of «clean» fatigue, because samples which did not destroyed on the base of tests of $N = 10^7$ cycles at the level of stress amplitudes higher than the border of endurance were not taken into account during treatment of results.

Because a level of contact stress in tests on a fretting-fatigue was selected coming from literary sources, and at such level of brackets pressing a slippage in a contact can be insignificant and the adhesion zone of a sample with a counter-body prevails, that decreases the damage from fretting, it was executed a few experiments at less values of contact stress and amplitude of cyclic stress $\sigma_a = 500$ MPa. On a fig. 3 these points marked with numbers 3, 4, 5 ($S_{K\Phi}$ is equals to 158, 192 and 77 MPa, accordingly). They show that durability at these contact stress exceeds those which are determined at this σ_a level on the fretting-fatigue curve. Thus, the level of contact stress chosen for researches is most damaged from investigated. Starting from that in the conditions of fretting-fatigue there is a level of brackets pressing, after exceeding of which influence of this parameter remains almost at the same level [8], it is possible to consider that this level is achieved. In addition, a re-calculation to actual stress in a contact testifies that they changed in the different investigations at the building of the samples fretting-fatigue curve in the range of $S_{K\Phi} = 276...290$ MPa.

Conclusions.

1. The short review of the aircraft undercarriage power elements load conditions and the reason of destruction statistics testifies that the 30XГСА (30XГЧА) steel, which is utilized in these constructions, fatigue and fretting-fatigue further researches are necessary, taking into account possible application of the newest technologies of resistance characteristics increase to the mentioned factors of the steel surface layer.

2. The method of cantilever samples fretting-fatigue researches in contact with П-like fretting-brackets at their loading in the resonance mode on an electro-dynamic vibro-stand, which can be applied for verification of the different methods of materials surface modification influence to resistance a fatigue at presence of fretting-contact, was developed and tested.

3. The decrease of 30XГСА steel endurance limit in $\sim 1,9$ times at presence of fretting was experimentally determined. It's showed also, that realized in the experiments for building of the fretting-fatigue curve contact stress are the most damaged from investigated choices, and dispersion of the experiment results at «clean» fatigue is higher, than at fretting-fatigue.

References

1. Шапкин В. Проблемы поддержания летной годности воздушных судов //Авиапанорама.- Сентябрь-октябрь.- 2003. - С. 24-26.
2. Бойцов Б.В. Надежность шасси самолета. М.: Машиностроение, 1976. - 216 с.
3. Марчук В. Є., Колесник В. І, Кравець В. В. Проблеми надійності шасі літальних апаратів // Труды академп. - К.: НАОУ, 2005, №62, с. 240-244.
4. Купрін А.П., Марчук В.С, Лабунець В.Ф., Жигінас В.В. Підвищення надійності шасі літальних апаратів нанесенням дискретних структур на поверхні зношених деталей //Проблеми тертя та зношування: Науково-технічний збірник - К.: НАУ, 2006. - Вип. 46. - С. 149-159.
5. Ковалевский В.В. Малоамплитудный фреттинг-износ и фреттинг-усталость металлов и сплавов: Автореф. дис... д-ра техн. наук: 05.02.04 / ВНИИЖТ. - М., 1985. - 36 с.
6. Шевеля.В.В., Калда Г.С. Фреттинг-усталость металлов. - Хмельницкий: Поділля, 1998.-299 с.
7. Трощенко В.Т. Грязнов Б.А., Малашенко И.С. та ін.Циклическая прочность рабочих лопаток ГТД из никелевых сплавов // Пробл.прочности. - 2007.- № 2. - С. 5-14.
8. Tanaka K., Muton Y., Sakoda S.. and Leadbeater G. Fretting fatigue in 0,55C spring steel and 0,45C carbon steel //Fatigue Fract.End.Mater.Struct. – 1985. – Vol.8,No 2. – P.129-142.

MONITORING OF FRICTION NODE TRIBOLOGICAL PARAMETERS IN CONDITIONS OF MASS REMOVING

The process of friction surface monitoring in the dynamic mode is presented. The processes of reparation are considered in the electrical conduction environments of polyethylene glycol for creation of positive gradient on the surfaces of friction. The results of recovered layer formation by the dynamic materials are shown, appointed the influence of magnetic lines direction on the conditions of material removing.

Introduction

A difficult structure and technical decisions of various system details of hydraulic actuators, which are used in the newest transport vehicles, are need service and repair with time. The main reason of their failure, in the process of work, is a wear of surfaces of touch. Creation of friction surfaces with the beforehand set properties and with subsequent unhandled service.

Purpose of research. To create a complex for testing on wearing capacity of materials in the directed magnetic field. To work off technology of friction surfaces renewal, due to unhandled technologies, by triboelectrochemical method.

General problem and its connection with science tasks. Quality of details and knots of transport vehicles can be substantially arisen, if apply new technologies of details and constructions restoration, which are based on the achievements of physics and material engineering.

The basic method of wear intensity decline, at a friction, there is the using of lubricating materials, however, there is a number of the working modes and their efficiency isn't enough.

Researches showed that copper tape in a pair steel-bronze appears as a result of anodal dissolution of bronze. Thus alloying elements of Pb, Zn, Sn, Al, Fe go to lubricating material and surface of friction enriched by them.

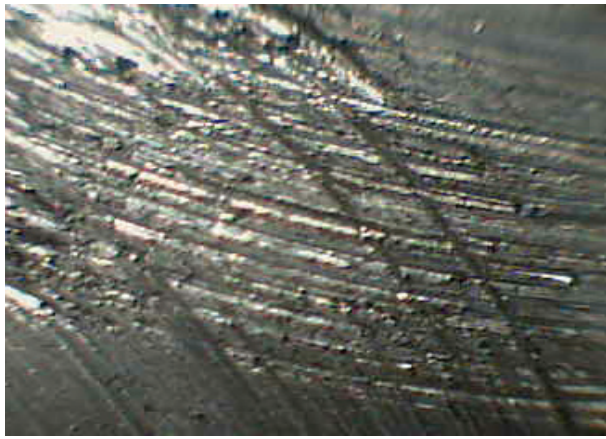
Thus the capacity of mechanism is explained the different ways to the condition of friction. Co-operation of surfaces can be mechanical or molecular. Mechanical cooperation is expressed in mutual penetration and hooking of inequalities of surfaces in an aggregate with their collision, in the case of sliding of rough surfaces

1. World experience in tribological sphere

Use of materials and pair, which co-operate in the process of friction, has a considerable spectrum, to both properties: chemical and mechanical.

The corps of fuel and oil pumps of the different setting are made from aluminium alloys, in particular Al9. Wear of an aluminium corps under the gearing of oil pump to renew by galvanic method is impossible. The details of plunger pair are made from steel of 25X5MA.

All friction knots of machines are in the tense state, for their capacity power and material losses are used. Due to the friction surfaces power state change, between them, the third intermediate body appears with the operating parameters, to which energy or work of friction is spending, done from the taking efforts in a mechanism. A total power stream is outlaid on flowing of tribological changes in the area of friction, which divided into a mechanical constituent and electrochemical changes, with formation of the third body. Deformation of superficial layer actively takes friction energy for microstructure alteration of new structures formation, so called third body.



a)



b)

Fig.1 a) aluminium alloy friction surface after the interaction with an alloy on the basis of iron;
б) alloys friction surface on the basis of iron.

Basic principles of tribosystem work power providing are [1] expressed and the triboelectrochemical method of their power states control is offered. In eighty percents the failures in machines are happen as a result of failure of details in the knots of friction. Charges on maintenance of aircraft to 7th one time exceed it's cost, the same situation and in an engineer.

Basic determination of friction, it is the phenomenon only of destructive character and processes appear in an area of surfaces collisions are the slump of material. But, it is possible to create such conditios of work in the friction knot, by which a wear was not. It is set that in opened tribosystems, which constantly get negative entropy and matter from an external environment, there can be non-equilibrium states with the high degree of organization. Such systems are name without wear. Without wear effect is experimentally certain more than half century ago, however, and presently there is not a single idea in relation to the mechanism of it's origin, in particular, mechanism of mass transfer in without wear mode. The phenomenon of spontaneous formation of copper tape, by the thickness of 1...2 mkm, was observed on steel or bronze, the coefficient of friction decreased approximately on an order. A process is not endless, since a surface was enriched by copper, dissolutions halted and set mode of selective transference.

I. Kragel'skiy and D. Garkunov [2] specified that character of friction, which is conditioned by the exchange of friction knot with an external environment, energy and matter, also by the collective conduct of coppers ions , which is farmed thin copper tape which protects the friction surfaces from a wear. A friction can not destroy tape, it creates it. There is the phenomenon of selective transference - transference of copper on steel and its reverse transference, which is accompanied by diminishing of friction force and as the results the considerable decline of friction pair wear. With the development of selective transference, the limits of unworn were wider. Gradually were passed to creation of lubricating composition materials, which in a complex with basis of lubricating material, can cause the mode of excitation and self-regulation of process - to activate oxide-renewal reactions at the beginning of work of friction knot, to provide their fading in the set mode and to assist in the selection of necessary materials for creation of the modified structure of surface.

Main factors, which determine the principle possibility of settling two and more metals and relative composition of alloy, are:

- sizes of equal potentials of each metal in material, which removes the material, this electrolyte, cathode polarization of each metal;
- relative concentration of ions of each metals, which must be covered on a surface, especially in cathode space;
- overstrain of hydrogen on a set alloy;

- the mode of electrolysis is a temperature, size of current, removing, presence in the span the colloids or other perfunctory-active materials.

Using of perfunctory-active environments one of the electrons transference ways in liquids, which positively influence on frictions and wear conditions. Electrode potential of material is not always comfortable at the account of it's transference conditions, both, material and superficial material.

Perfunctory-active materials (PAM) are chemical compounds, which reduce superficial interference of water. PAM used for the production of cleaning detergents, as effective corrosive depressor for metals in water environments, also shown that they prevent the process of stainless steel pitting. Their properties of corrosive depressing, related to their ability to fix in a metal, detaining, thus, superficial reactions and to form not reliable connection with the steel through the amino acid part of molecule. There is a negligible quantity of works on the PAM using on the basis of polyethylene glycol in the pair of friction. Polyethylene glycols – polyethylene oxide (polyethylene) the polymers of ethylene oxide (E) have a general formula $[-OCH_2CH_2-]_n$. Viscous liquid by molecular mass to 400, the unlimited dissolves in water, but falls out in sediment from water solutions higher 100°C, and also at engagement of inorganic salts. The hydroxyl groups of glycols react independent of each other or simultaneously, that is why the proper mixtures of products appear sometimes.

Soft metals (molybdenum, tin, copper, silver and other) can be brought in the area of friction or in the molecular micronized type, or at ionic level as a result of chemical reactions of liquid oil components with the source of soft metal.

2. Experimental part

2.1. Probed materials

The most responsible parts of plunger pairs are the piston, which are made from iron-bearing materials and tempered on a martensite. For a specimen we chose steel 45, treated on offered structure, load changed from 5 to 10 MPa.. For providing of positive friction gradient, the work materials is lead, which is used as an auxiliary electrode fig.3. Glass served as a rider, as very thin, hard material, and chemically neutral. Possibility to conduct monitoring of friction surface transformation appears only on pinhole material.

2.2. Research method

The method of wear calculations (its general chart) consists in consistently done the following operations:

- determine loading, operating in the friction knot;
- determine deformation of friction knot, at the action of this loading, area, form of contact spot and size of operating contact tensions (for their determination the method of eventual volume elements and proper program providing are used);
- on each of contact area laying out elements determine the actual area of contact of A_r and actual pressure of R_r , that change depending on the mode of friction knots operations. For example, for aviation products: start, mode of taxiing, flight, set of height, cruiser mode, landing, braking, and others like that.

Ability of material to form protective tapes on surface in the process of oxidization from the action of environment in different technical conditions under the action of friction and in stationary conditions, considerably differ. In stationary conditions, by potential electrolysis, it is possible to define enough exactly time of surface passivation. Considerably heavier to get a passivating surface during a friction. Permanent derangement of protective tapes, which appear, does not enable a surface stabilized in any solution. Chemical influence of environment with the surface of material, that appeared again, and speed of actual contact moving, considerably influence on the aggregate of parameters, which characterize the vital functions of oxide tapes on the friction surface. By the tribological complex [3] developed in a laboratory, for determination of tribological characteristics of friction knot, we conducted monitoring of surface topography change, estimated the quantitative

parameters of the created oxide tapes and their geometrical sizes. The friction knot is the transparent glass plate from photographic glass, which is able to skip light through itself without breaking and distortion of surface, which is observed. Opposite a specimen, through glass, the lens of microscope is mounted. Through the system of microscope lenses light focuses in the photo camera "PC Camera" with the standart software, for treatment and fixing on the screen of computer, with possibility of record on electronic transmitters, states and qualities of friction surface. This system gives a possibility to control the friction conditions of metallic specimen surfaces on «absolutely» hard rider, which is neutral electric glass. For determination of tribological parameters of metallic specimen, if it is necessary, it is possible to use the metallic surface of the rider. But in this case surface monitoring, without the handle of friction knot, is impossible to do Due to the finger-plane friction chart, where a finger is a specimen with the diameter of 3mm in 94 times longer, than it's diameter ($S=2\pi r = 2 \times 3,14 \times 45 = 282,6\text{mm}$) to the next touch with the same point, which is ground on a surface. Due to the moving mechanisms of carriage with a specimen on the plane of glass, it is possible to change the diameter of friction path, that enables to take pictures a specimen on the clean area of glass, in the area of lens action.

A camera is mounted under a microscope so that the ray of light lighted up eyeshot of the «working field of specimen through glass», and images were shown on the computer screen.

Knowledge of wear periodicity sizes will allow to extend our pictures of physical processes of contact interaction and will enable more grounded to speak about the questions of wear diagnostics. In this work the method of adhesive wear periodicity estimation is offered with the use of acoustic analysis of signals, registered during friction [4]. The dimension of current characterizes power of oxide tapes formation on the surface of metal. Taking off tension from the friction surface, which researches are conducted with, it is necessary to insulate the non-working surface of specimen from a hit liquid on it, usually for this purpose dope or shrink isolation are used. Thus, measuring a current between a specimen and any calibration electrode, better such, which has large corrosive firmness, being an electro-explorer with positive potential (gold, platinum, rules) which will pass on the reserved electric circle: working specimen - working liquid – reference specimen - ammeter - working specimen, will get a current, proportional to the amount of electrons, which go out from the surface of s specimen or directed on it's surface.

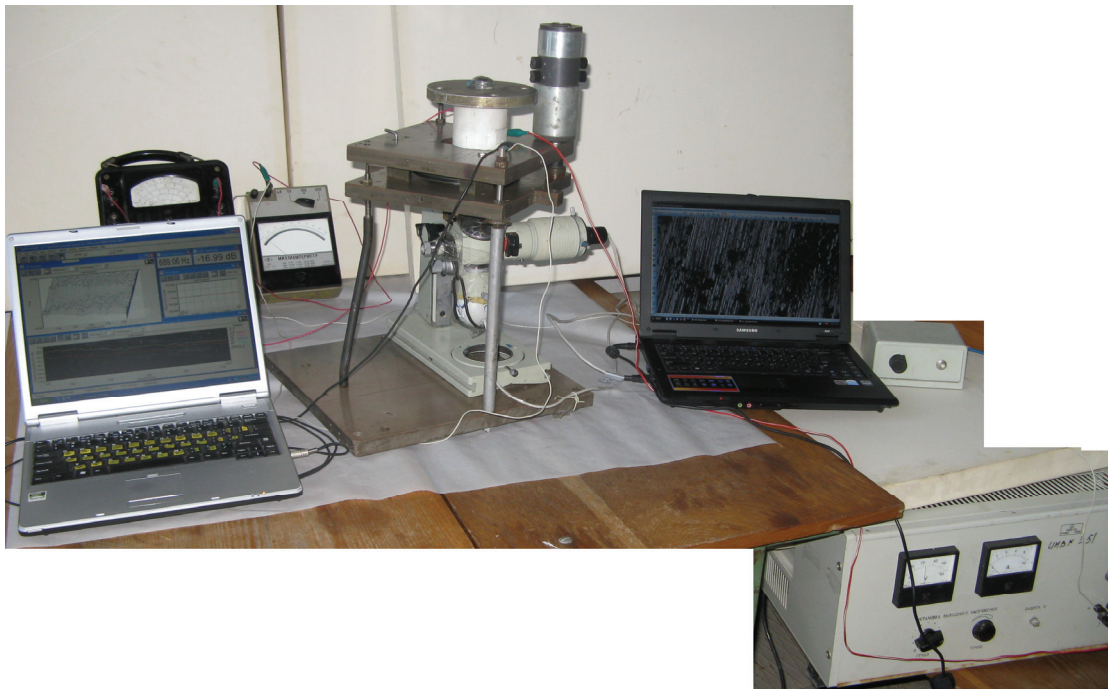


Fig.2. General view of tribological complex

Taking into account that the process of friction always radiates frequency signals, tribological complex is equipped by acoustic belongings, for the removal of frequency description in the friction process of metallic specimen on glass, or other surfaces. Tribological complex is provided with an acoustic piezoceramical sensor and standard software of SPECTRA-LAB_434 for a computer. The program works in connection with the sound card of computer.

For accuracy of measuring and diminishing of extraneous sounds influence from working mechanisms, all details of tribological complex are made from non-metal materials. Bearings are made from a fluoroplastic 4, their working frequency hesitates in the range of low values from 700 to 950 Hz, a carriage with the fixed specimen has working frequency about 800 Hz. Engine, taken away outside the tribological complex, and a tourk moment is passed by rubber passes. Velocity of the relative moving of specimen changes fluently from a 0,05 m/sec to 2 m/sec. The friction moment is measured by two mechanisms: the first - the change of current is registered on an engine, depending on loading; the second - by a тензометрической beam, mounted in a carriage, in which an acoustic sensor and spring of loading are mounted.

The moment of oxide tape increasing is accompanied by additional force of sound, which looks as raising of general frequency curve on all length of voice signal. In the moment of blowing off the oxide tape from the surface of metal on middle and high frequencies, from 20 to 20000 Hz, there is a splash of frequency constituent as peaks.

Moving of metal in the atomic state is accompanied de alteration of structure, which is formed in the direction of the maximal strengthening and orientation in relation to direction of moving.

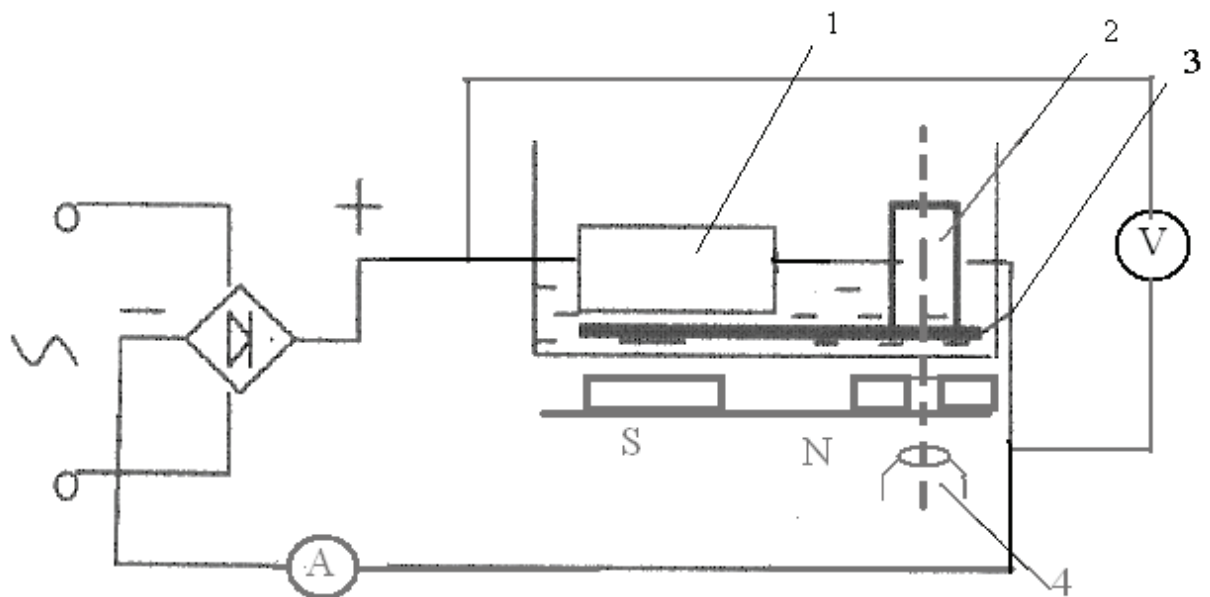


Fig. 3 Electric chart of specimen connection:
1 –auxiliary electrode; 2 - specimen; 3 – glass; 4 - microscope

The surface of specimen was ground on abrasive skin–micron. Then wiped by spirit and weighed on the analytical scales AIB-200M with accuracy 10^{-4} grammes. On the tribological complex [5] during 2 minutes rub a specimen to appearance of contact spot, external view of which was observed on the screen of monitor with work on wear approximately 0,0005 gramme. Then the voltage connected due to electric chart (fig.3) in the mode of permanent voltage 30V, at which an initial current was 10,5 mA. By switching it is possible to change direction of current.

3. Results of experiment

Was put a task to conduct friction surface monitoring in the dynamic mode.

The lead transfer on the metal surface was carried out by the tribochemical method in the environment of 25% polyethylene glycol-400, water-diluted. Loading was 0,2 kg of normal one,

velocity of relative rotation - 0,1 m/sec on a moment of contact spot appearance in field of view. During an experiment in the area of photographing, a specimen was taken off and weighed. If addition of weight was detected, a specimen was abandoned for research on the PEM microscope. A next specimen was exposed the same researches, but time of work was increased on 20%. Finding the contact spot resulted to the subsequent gravity measuring.

Thus, doing 5 measurements, detected the considerable causing of leaden coverage on the specimen surface, to 70% of area is covered by lead fig.4., soft tribological material.

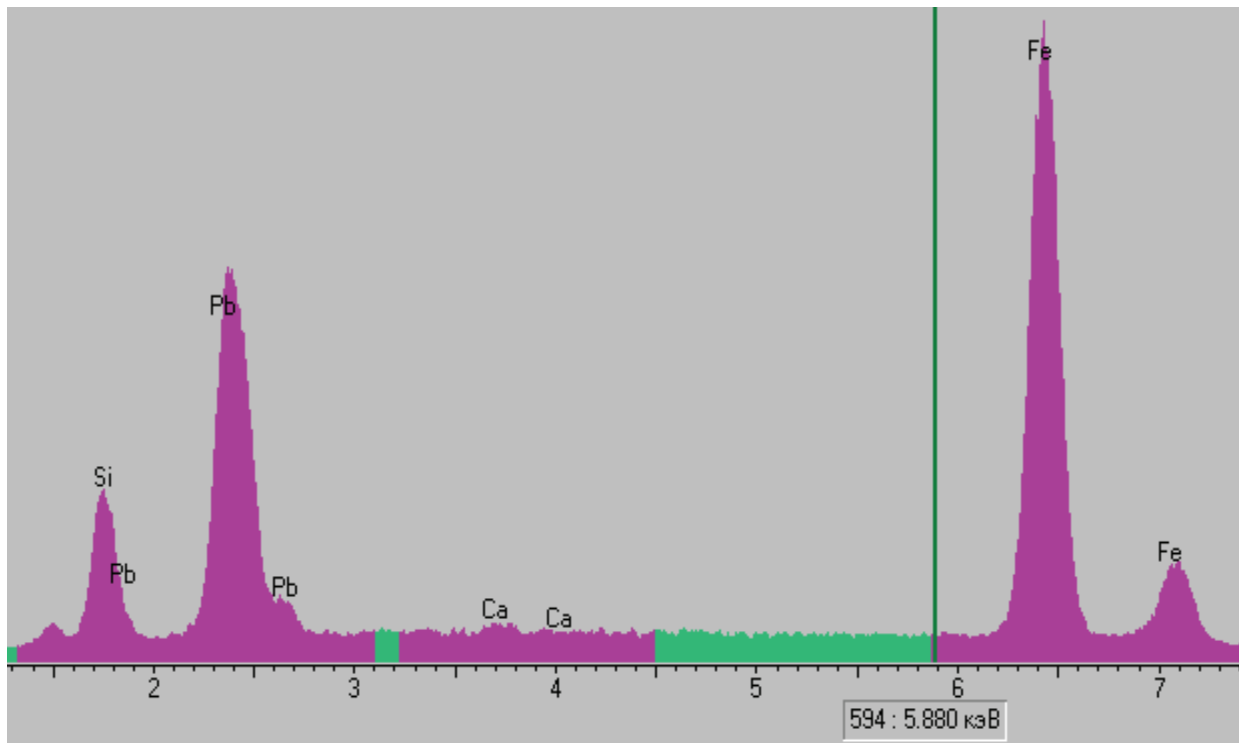


Fig. 4. Chemical composition of steel 45 friction surface after triboelectrochemical treatment in an environment of 25% solution PEG-400. (Fe~29%, Si~4%, Pb~65%)

4. Discussion of experiment results

There is an endless amount of various dopants on the basis of soft metals (molybdenum, tin, lead, copper, silver and other) which can be brought in the area of friction in the molecular micronized kind, or at ionic level, as a result of chemical reactions of oil components, with the sources of soft metal. Realization of the first method is related with two problems:

- 1) creation of the proof suspension of soft metals thin particles;
- 2) ratio between the possible concentration of such metals, in circulatory butter and concentration sufficient for providing of plating effect even on the oil complete resource, very limited at time of work. In addition, the thin dividing layer of soft metals is not guarded the friction surface from the burrages in extreme cases, that is at stopping of oil circulation. The second method is related to realization of electrol removing, control of which carries while especially casual character and explores very seldom. Dopants, which activate forces of oil tripping with the friction surface can be very effective on unwearing and, especially, to unburrage characteristics.

But they have the substantial disadvantages:

- 1) the action of such dopants proceeds until they are in oil in a sufficient concentration;
- 2) such dopants, as a rule, not only are not anti-friction, but even able to increase resistance of friction;
- 3) usually high concentrations of such dopants can influence on oil reology.

Material which is activated is isotropic body for which it is always possible simply to define the border of durability and module of resiliency, which are the generalized descriptions of physical mechanical properties of material. And friction forces work will be always proportional to destruction work $A_{fr} = k_0 Ad$.

Resistance of material, at the bias, depends on dimensionless description h/R - relations of depth h , introduction of single inequality, designed by spherical segment, to it's radius R .

Depending on character of superficial layer deformation distinguish an external friction at resilient one, plastic contacts and at microcutting. In certain conditions, dependence on loading and mechanical properties of each friction pair, an external friction passes to internal, for which absence of velocity jump is characterized in removing from one body to other. Loading at which an external friction is violated, for this friction pair, is named the weir of external friction.

So in water solutions the nonpolar hydrocarbon radicals of PAM molecules form the micelle kernel, and polar groups are turned to water. PAM split in water solutions, and they are subdivided into anionic (hydrocarbon radical in composition of anion), cationic (with organic cation) and ampholytic (amphoteric). Formation of micelles in colloid PAM solutions is the most thermodynamics-advantageous process in comparison of the processes of true solution formation or division of phases. Formation of micelles in colloid PAM solutions, as adsorption of PAM molecules, in external layer flows involuntarily.

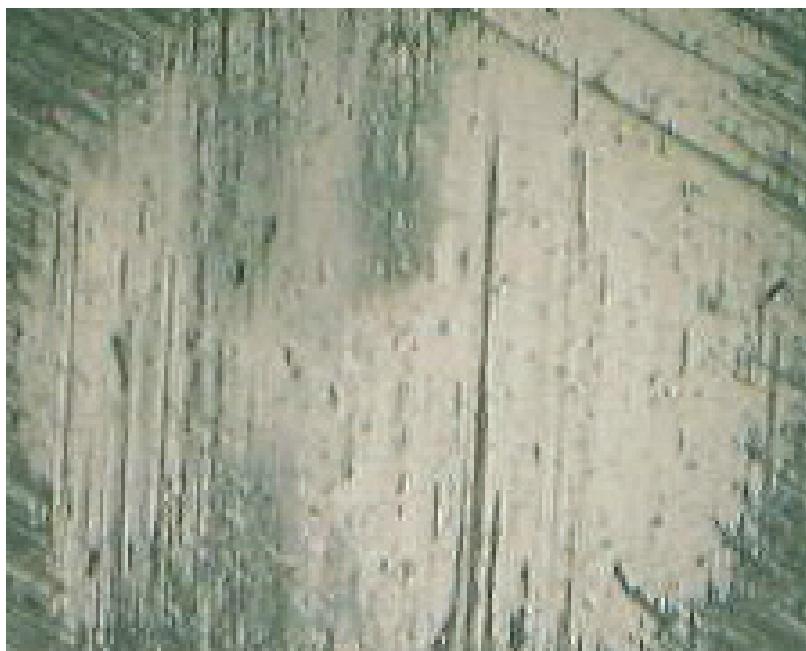


Fig.5. Renewal surface of steel 45 by lead

The conditions of liquid friction are accompanied by smoothing of surface, due to deformation of surface topography apexes. The subsequent smoothing of surface in perfunctory-active liquids passes at piling of elements from a liquid. For the increase of aggressiveness of auxiliary electrode ions settling the directed electric current was used. At deformation of surface most power instability is concentrated in the places of actual contact. There where instability is, there always will be a change toward diminishing of superficial energy, which can pass at interference of metal ions in the produced surface with formation of protective tapes.

A lead is diamagnetic material, influence of the magnetic field on it's transformations is minimum, if specimen is located between the poles. But on poles, at the change of direction of the magnetic field, moving of lead from N poles to the S pole is increased.

Technology of renew process passes under the action of friction. On surfaces which are ground many process are issue at the same time : stream of heat; streams of material; physical and chemical processes of interaction of bodies with an environment; deformation; structural, phase transformations and other Some of these processes are caused directly by friction, streams of heat

from the area of friction, streams of matter from one area of friction to other one, and the main is deformation. On fig.5 the renewal surface of steel 45 with an auxiliary electrode from lead, at the using of polyethylene glycol and magnetic constituent. These processes are caused, as a rule, by the gradients of intensive sizes, which arose up as a result of friction: temperatures of chemical potential, tensions. Thus, the general making of entropy in the system, conditioned by friction, will be equal the sum of entropy proper streams in the environment of polyethylene glycol. By the directed action of electric current there is transference of matter from an auxiliary electrode to the PEsteel 45 surface. On fig.6 lead, the nonmagnetic material, is presented.

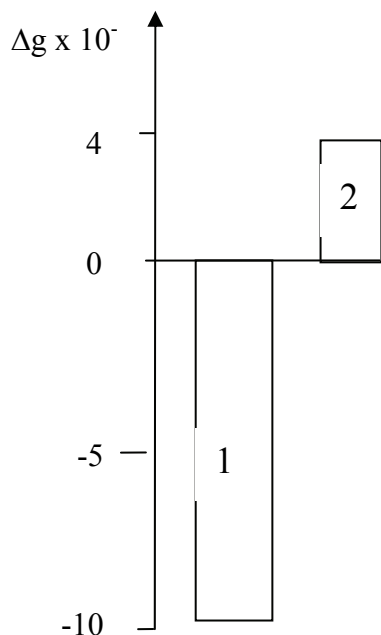


Fig.6.1 – Wear of steel 45 in 25% solution of PEG; 2 - Changing of specimen mass from steel 45 in conditions of reparation by Pb, when voltage 30V, linear velocity $V=0,1$ m/sek., load 0,2kg normal load

Conclusions

Presented higher scientifically - methodical and practical results of scientific work allowed to do the following conclusions: 1. At the friction of carbon steel 45, hard-tempered on a martensite, in a pair with glass, is shown, that it is possible to use glass as rider for the monitoring of tribological processes.

2. The triboelectrochemical parameters of friction surface renewing are set for displacement of positive potential of friction.

3. These researches are shown the principle new method of renewal of machines details friction pairs by the triboelectrochemical methods. Attitude of the power state of friction surface is shown to the mechanism of causing of metallic material on the workings surfaces of detail, in the conditions of unhandled renewal. The results of researches can be applied for the exhaust friction surfaces of oil pumps and plunger pairs.

References

1. В.Э. Бурлакова **Триботехника эффекта безизносности**: [моногр.] / В. Э. Бурлакова; ДГТУ. - Ростов н/Д, 2005. - 211 с.: ил. – ISBN 5-7890-0323-0 : 65-00.
2. Д.Н. Гаркунов **Триботехника** (знос и безизносность): Ученик. – 4-е узд., перераб. И доп. – М.: «Издательство МСХА», 2001. 616с., ил.280.
3. **Проблеми тертя та зношування**: Науково-технічний збірник. – К.: НАУ, 2006. – Вип.45.- 204с., Свирид М.М., Паращанов В.Г., Онищенко А.В., - Комплекс для дослідження трибологічних параметрів вузла тертя
4. **Проблеми тертя та зношування**: Науково-технічний збірник. – К.: НАУ, 2007. – Вип.48.- 230с., Свирид М.М., Паращанов В.Г., Прыймак Л.Б., Шевченко А.Л., - Мониторинг трибологических характеристик в полиэтиленгликоле.
5. А.И. Кравець **Репаративная регенирация трибосистем**. Т.: Издательство Бережанського агротехнического института 2003. – 284с.

FATIGUE CRACK GROWTH IN AIRCRAFT STRUCTURAL ELEMENTS AT REAL OPERATION CONDITIONS

Abstract. *The analytical and experimental researches concerning predicting of fatigue crack growth in the operating conditions are presented. Theory of fatigue crack growth indication is developed. There is planned and executed a flight experiment using the crack growth indicator (CGI) located on two aircraft An-24 and An-26. Results of crack growth in CGI at operational load allowed evaluating the parameters of generalized Paris-Erdogan law and statistical properties of crack increment per flight.*

1. Introduction

At the same time the precise predicting of the fatigue crack growing is difficult problem, because there are many effects causing large range of the rate of fatigue crack growth.

$$\frac{dl}{dN} = C(\Delta K)^m \quad (1)$$

where ΔK is the range of the stress intensity factor, C and m are material coefficients. Usually m lies between 2 and 7. This relationship that is known as Paris-Erdogan' law [1] can be used to predict the remaining lifetime of a structural component, if the stress amplitude remains approximately constant. There are known others, more complex models used a stress intensity factor as main motive factor of fatigue crack growing. First of all if the stress amplitude varies, then the growth rate may depart markedly from the simple power law. The single overloads can reduce the crack growth rate drastically. There are a number of models for description of overload effect. First physical models [3-5] explain this effect on the basis of residual and active stresses interaction in plastic zone of the crack front. Recent results for modeling of crack growing at the load with variable amplitude are some versions of these models. The more perspective approaches of the crack growing at variable amplitude load are methods for predicting flight-by-flight crack growth [6-13]. These methods use the load spectra for one flight as a unit of generalized periodic load. As a result all effects of overloading are accumulated in a fatigue crack increment for one flight and generalized Paris-Erdogan law (or similar formulas) can be used for predicting of crack propagation. Obviously better accuracy of predicting can be achieved. But in all cases it is necessary to reduce real flight loads to some idealized spectra for its using in fatigue tests or analysis. It is common disadvantage of all these approaches. Furthermore for example, small changes in the concentration of corrosive agents in the environment can also produce very different results in comparison with predicted ones.

In this paper the results of analytical and experimental researches concerning predicting of fatigue crack growth in the operating conditions are presented. The problem of fatigue crack growth at the stresses of variable amplitude was analyzed and an approach of description of this process is performed. Theory of fatigue crack growth indication is developed. There is planned and executed a flight experiment using CGI located on two aircraft An-24 and An-26.

2. A fatigue crack predicting at the complex spectrum of load.

The remarkable properties of asymptotic representation of elastic stress in front of a some mode crack provides the description of distribution of stresses as functions of coordinates by means of unique parameter – the stress intensity factor. Therefore the condition of similarity of stress in two points of front of a crack is carried out automatically, if the ratio of corresponding of the stress intensity factors on time does not vary. Thus, for cracks of the first mode, for example, the condition of full similarity of the stress state is transformed to a simple view

$$k_s = \frac{K_I^{(1)}}{K_I^{(0)}} \quad (2)$$

Thus if the set function $\bar{P}(t)$ of structure of loading process is stationary in sense of its parameters identity at all possible intervals of loading, the uniform characteristic of fatigue failure for the given loading spectrum (cyclic loading, stationary random process, periodic program loading) can be presented in the form of generalized Paris-Erdogan law

$$\frac{dl}{d\tau} = C_s (k_s \bar{K})^{m_s} = C_s^* \bar{K}^{m_s} \quad (3)$$

where C_s and m_s parameters cracking resistance of a material at the set function of loading structure obtained at some base loading intensity σ_0 .

$\bar{K} = \frac{K_I^{(0)}}{\sigma_0}$ it is relative stress intensity factor independent of a level of external load. It defines character of effect of length of a crack to stresses intensity near front of a crack. The factor k_s considers influence of intensity of the given loading in comparison with basic process. In the formula (3) τ is the parameter of an operating time which can be estimated in flight hours, number of flights, number of cycles of program periodic load or other units.

Thus, using the formula (2) it is possible to predict growth of the crack in a structural element, if conditions of all concomitant factors are satisfied and external loading has similar structure with basic process, but different intensity. Below it is shown the results of generalization of data about fatigue crack growth of at test of samples of a material 7075-T651 by thickness 12.7mm and width 152.4 mm[15]. The loading program spectrum was similar with an operational spectrum of the airplane. The maximal stress in a spectrum was 169, 211.8 and 254 MPa. If to accept the basic parameter of loading intensity $\sigma_0=169\text{MPa}$, then $k_s=1.0, 1.253, 1.503$ accordingly. For each level of loading intensity the direct processing of results of tests “the length of a crack – number of blocks of loading” has allowed to define value of the constant C_s^* , and under the formula $C_s^* = C_s \cdot k_s^{m_s}$ to define these constants for the second and third level of loading, using value C_s^* of the first level. It was accepted average value of a parameter $m_s=3.2$. Results of processing are presented in table 1.

Table 1. Theoretical parameters of the fatigue crack growth with experiment

Maximum Stress, MPa		169.00	211.8	254
k_s		1.0	1.253	1.503
$C_s^* \cdot 10^4$	experiment	1.907	4.2814	7.6655
	theory	1.907	3.928	7.025
Error, %		0	-8.25	-8.35

Other example: Fatigue test of samples from a titanic alloy Ti-6Al-4V with thickness 6.35mm and width 152.4mm was executed at the program loading [16]. Each block of program contained 17 levels and cyclic load and modeled aircraft load in operation during one flight. At conservation of internal structure of the loading block the test has been lead at four values of a stresses 386.6, 421.8, 456.9 and 492.1 MPa. Average value of a parameter $m_s=3.6$ was accepted. Results of calculations are presented in table 2.

Table 2. Theoretical parameters of the fatigue crack growth with experiment

Maximum Stress, MPa		386.6	421.8	456.9	492.1
k_s		1	1.091	1.182	1.273
$C_s^* \cdot 10^4$					7.665
	2.592	3.802	4.768	5.955	5
	2.592	3.548	4.730	6.179	7.025
Error, %		0	-6.703	-0.797	3.77

Thus, if the program block of loading is used as unit of an operating time predicting, a fatigue crack average growth rate estimated by the law (3) satisfied to data of test with accuracy (6-8) %. It allows to assume, as at use of the information on growth of a fatigue crack under action of real operational loadings it is possible to obtain enough reliable value of generalized law (3) constants and to use them for predicting remaining lifetime of structural elements.

3. Indication of fatigue crack growth.

At the same time the simulation of a flight loading spectrum in laboratory test does not guarantee exact definition of characteristics of cracking resistance in real operation (change of duration of flight, flight weight, weather and climatic conditions, rare random overloads, an environment), because it is difficult to consider all factors of operation in the program of fatigue tests with the ordered, limited number of loading levels. Therefore for increase of reliability of predicting and efficiency of aircraft operation it would be desirable to obtain the experimental data on growth of fatigue cracks directly during operation. Such attempts are known. In Refs.[17,18] results of data processing about growth of cracks in operation in a covering of a wing of the C-130 aircraft are stated. For crack reconstruction the crack growth rate was measured between two sequential inspections. Paris' law exponent was accepted 3, but constants were defined by numbers of cycles and length of cracks for each one.

However, the cracks in primary structural elements are not admissible at regular flights of civil aircraft. If the crack is found out, the structural element either should be repaired or replaced. So long observation of a growing crack that necessary for reliable definition of cracking resistance constants is not possible at operation.

Therefore an idea of inclusion in dynamically loaded structure some device for indication and measurement of a crack is the logical conclusion of this situation. There are many solution of different aspects of this problem (for example, US Patents No.3,979,949; 5,319,982; 6,983,660; 5,614,680; 5,816,530; 6,443,018; Japan Patent 46359-78; SU 1504548-1989; 938093-1982 and others),[15,22]. All type of these devices must be subjected the same load but its destruction must not influence to the fatigue lifetime of a structure. These are common properties.

Common disadvantage of all these solutions is low reliability of fatigue damage predicting connected with that of other significant difference of initiation and development of fatigue damage in comparison with original structure. Here the version of device [23] is used for definition of characteristics of crack resistance in real operation of aircraft. This device is free from mentioned

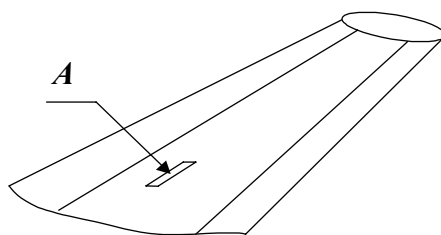


Figure 1. The scheme of CGI mounted at the wing panel of

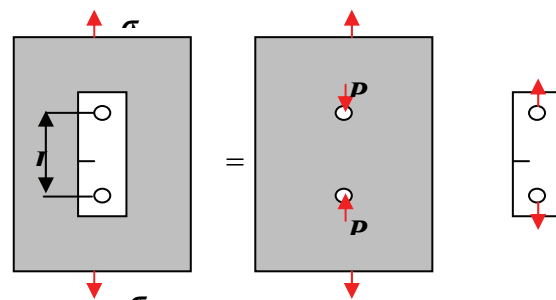


Figure 2. Crack Growth Indicator Mounted

disadvantage because it is created in complete accordance with general theory stated above. The general theory allows to solve a problem of obtaining of material constants at the set function of loading structure. It is obvious the device must have a sensitive element containing a fatigue crack. Such device is named by the crack growth indicator (CGI). Constants of material for some structural element can be correctly obtained at following conditions:

- 1) All concomitant conditions (the mark of a sensitive element material, technology of its mechanical and thermal processing, thickness, etc.) should be same, as at an investigated structural element.
- 2) CGI should be fixed on a structural element so that to have the same history of loading, defined by function $\bar{P}(t)$ of structure of loading process.

In this case growth of a crack in CGI will be caused by action real operational load and influence of all concomitant factors (temperature, humidity, a chemical compound of environment, etc.).

Figure1 shows principal scheme of CGI mounted at the wing panel of aircraft (Unit A). The scheme of structural element and CGI interaction is presented in Figure 2.

Disregarding nonlinear effect, it is possible to accept the operational stress $\sigma(t)$ and the force $P(t)$ acting on the CGI are proportional. Therefore, the stress intensity factor $K(t)$ on a crack front in CGI is proportional to $\sigma(t)$. It means both structural element and CGI have the same function $\bar{P}(t)$ of structure of loading.

The stress intensity factor \bar{K} is some function of a crack length. For this function determination the energetic method of mechanics can be used. First of all interaction force P (Figure 2) can be defined by the formula

$$P = \frac{\sigma L}{E_0(\lambda_0 + \Delta\lambda_i)} \quad (4)$$

where λ_0 is structural element, indicator without crack and fastening device common elastic compliance; $\Delta\lambda_i$ is elastic compliance increment , caused by the growing of a crack, L is base of CGI., E_0 is elasticity module of structural element material.

The elastic compliance λ_0 can be calculated theoretically or obtained experimentally. Elastic compliance increment $\Delta\lambda_i$ can be determined in accordance the theorem of displacements reciprocity [19]. Effect of a crack can be expressed by displacement increment Δ_i in direction of appropriate generalized force Q_i

$$\Delta_i = \Delta\lambda_i Q_i \quad (5)$$

As a result elastic compliance increment is defined by known formula of the linear fracture mechanics

$$\Delta\lambda_i = \frac{2}{Q_i} \int_s \left[\int_s \frac{(1-\nu^2)}{E} (K_I^2 + K_{II}^2) + \frac{1+\nu}{E} K_{III}^2 \right] dS \quad (6)$$

where E and E_0 are elasticity modules of CGI and structural element materials, δ is sensitive element thickness.

The function $\varphi(l)$ determines the stress intensity factor for crack in sensitive element at action of concentrated forces P , it is $K = P\varphi(l)$.

4. Flight experiment and processing of its results

In this case the sensitive element of CGI is around compact specimen of aluminium alloy D16T with 5 mm thickness and a basic size $D = 54$ mm. Others geometric relations and basic function $K = P\phi(l)$ can find out in [25] for such configuration of isolated sensitive element. Using this function and formula (10) it is possible to define the function “Relative stress intensity factor - Crack length”. The analytical approach for determination of elastic compliance λ_0 was created for a thin-walled structural element and two-points fastening of CGI. For experimental determination of initial elastic compliance λ_0 the special device was designed and made. It allows also direct experimental obtaining of function “Relative stress intensity factor - Crack length”. Desirable degree of amplifying can be obtained by the increasing of CGI installation base L (distance between the CGI fastening points to structural component).

Figure 4 presents CGI typical main characteristics “Relative stress intensity factor - Crack length” for two L . They were made for special flight experiment described below. It is seen, for fixed base of CGI installation L the stress intensity factor variation is small in wide interval of crack length. Therefore a fatigue crack growth rate in this interval of crack length also will be relatively small. Otherwise if the base L will be increased, then both the stress intensity factor and a growth rate of a crack increases.

There was planned and executed a flight experiment using two aircraft An-24 and An-26 in operation. CGI was used for the evaluation of parameters of law (6) for bottom panel of central part

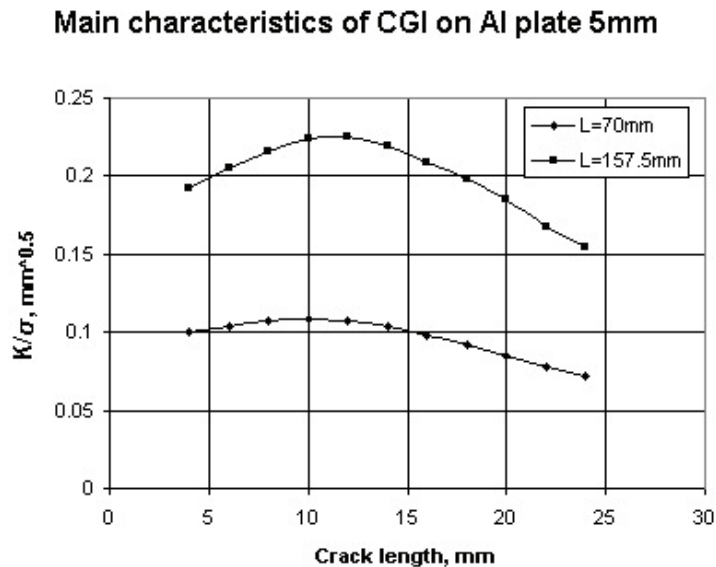


Figure 3. CGI main characteristics

of a wing. This part is located between fuselage and a compartment of engine. CGI was attached to the back longeron (here there are maximum nominal stresses in section of a wing). It was attached by bolts using the holes of the joint of bottom technological panel and the longeron.

Previous analysis of CGI influence to structural elements of wing was executed. Before installation to the aircraft the preliminary initiation of a fatigue crack was executed in laboratory by relatively low level of cyclic loading which could not cause the effect of crack braking.

The range of operating time of CGI sensitive element was from 5 to 300 flights. After taking down the sensitive element was prepared for fractography analysis of a crack surface. It is known the quantitative fractography was successfully used for coupons to generate crack growth curves under flight spectrum loading [10-12,26,27]. Fractography research was carried out by the electronic microscope. During the flight experiment the parameters of aircraft loading in each flight were strictly fixed: take-off weight, payload and fuel, flight range and duration. So the opportunity to estimate effect of these parameters to the crack growth rate was achieved. Typical view of a crack surface of CGI after 294 flight is presented in the picture (Figure 5). The bands caused by the flights

could be distinguished on the fracture surface and an accurate reconstitution of the crack growth curve could be made. The crack increments occurring in the flights were measured (it is possible to see the marks for identifying each flight).

The attempt of an evaluation of the statistical characteristics of a crack growth was undertaken. Below the results of statistical analysis of CGI in 231 flights experiment, are presented. The crack growth was fixed precisely in 202 flights.

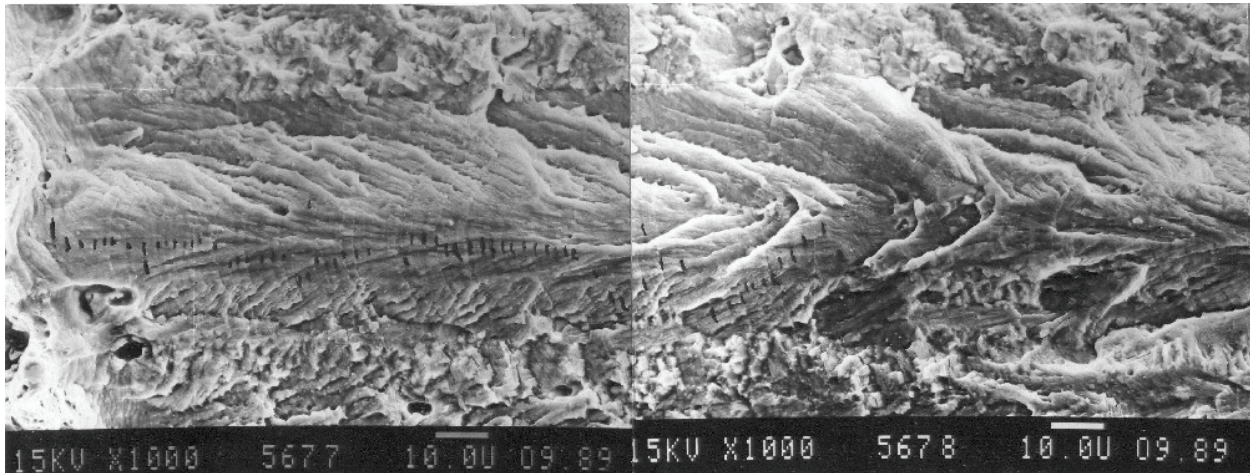


Figure 5. View of a crack surface in CGI after 294 flight

The measurement of width bands was executed with use of a special technique with maximum error no more than 10%. The estimated average increment is equal $2.72 \cdot 10^{-3}$ mm/ flight, and standard deviation $1.44 \cdot 10^{-3}$ mm/ flight. The constant of generalized Paris-Erdogan law $C_s^* = 0.0102$ and $m = 2.5$, if relative stress intensity factor is measured in \sqrt{m} and a crack growth rate in mm/flight. The statistical hypothesis about lognormal distribution low of a crack increment was carried out with positive result. Figure 6 presents the lognormal distribution function (continues line) and points of empirical cumulative distribution.

5. Conclusions

The fatigue damage having significant influence on remaining strength and remaining lifetime is very difficultly predicted, especially at a stage of initiation of a fatigue crack. Therefore, if the high accuracy of a prediction of remaining lifetime of some structural element is needed, then conditions of testing must correspond as much as possible with conditions of real operation. The proposed approach of this problem solution assumes such theoretical analysis and experiment at which the stress state in critical points of samples and its variation for time would be same as in an investigated structural component. This is main condition of reliable predicting of fatigue damages initiation and its development. The second condition assumes identity of concomitant factors which are not the direct cause of fatigue degradation, but can significantly accelerate it. If these conditions are exactly satisfied, then it provides practically reproduction in experiment of the investigating phenomenon. In this case the experimental mechanical properties of a material will be exact and can provide a reliable prediction of remaining lifetime of a structural component. It is obvious also, that the area of use of these characteristics is limited, especially, for initiation of a crack. However, at the careful analysis this area can be widespread to separate classes of critical places of a structure. It is shown the fatigue crack growth allows obtaining more common solution in comparison with the initiation of a crack. The variant of effective solution offered above assumes evaluation of the fatigue crack resistance properties of material in conditions of real operational load at action of all concomitant factors influencing intensity of fatigue damage development. The approach assumes use of special device, fatigue crack growth indicator, for which all necessary conditions for determination of fatigue crack growth are satisfied practically precisely. On the other hand, the

combination of CGI with fractography of a fatigue crack surface allows decreasing necessary tests, terms of their carrying out and increasing accuracy and reliability of results.

Acknowledgments This research was induced by the authors' participation in 6FP research project AISHA (Aircraft Integrated Structural Health Assessment). The authors are grateful to European Commission for financial support and all partners for scientific and technological collaboration. Especially the authors are grateful to the Kiev Mechanical Plant (Antonov Design Bureau) for collaboration in the flight experiment organization and high quality of fractographic investigation.

References

1. Paris P.C., Erdogan F. A critical analysis of crack propagation laws.- Trans. ASME, Ser.D, J. Basic Eng., Vol.85, No 4, 1963, pp.528-534.
2. N.E. Dowling, Mechanical behavior of materials, engineering methods for deformation, fracture and fatigue, Prentice Hall, New Jersey (1993).
3. O. Wheeler, Spectrum loading and crack growth, J. Basic Eng., **94** (1972), pp. 181–186.
4. Willenborg J, Engle R, Wood R. Crack growth retardation model using an effective stress concept. Air Force Flight Dynamics Laboratory Report, Technical Report AFFDL-TM-71-1-FBR.
5. J. Bannentine, Fundamentals of metal fatigue, John Wiley, New York (1980).
6. R.A. Pell, P.J. Mazeika and L. Molent. The comparison of complex load sequences tested at several stress levels by fractographic examination. Engineering Failure Analysis, Volume 12, Issue 4, August 2005, Pages 586-603
7. L. Molent, R. Jones, S. Barter and S. Pitt, Recent developments in crack growth assessment, International Journal of Fatigue, Volume 28, Issue 12, 2006, pp. 1759–1768.
8. Levy M., Kuo A.S., Grube K.P. A Practical Method for Predicting Flight-by- Flight Crack Growth in Fighter Type Aircraft for Damage Tolerance Assessment. – ICAS-80, 19.2, pp.666-675.
9. Broek D., Smith S. The Prediction of Fatigue Crack Growth Under Flight-by- Flight Loading. _Engineering Fracture Mechanics, 1979, Vol.11, No.1, Pages 123-141.
10. W. Zhuang, S. Barter and L. Molent. Flight-by-flight fatigue crack growth life assessment. International Journal of Fatigue, Volume 29, Issues 9-11, September-November 2007, Pages 1647-1657
11. R.A. Pell, P.J. Mazeika and L. Molent. The comparison of complex load sequences tested at several stress levels by fractographic examination. Engineering Failure Analysis, Volume 12, Issue 4, August 2005, Pages 586-603
12. O. Pártl and J. Schijve. Reconstitution of crack growth from fractographic observations after flight simulation loading. International Journal of Fatigue, Volume 12, Issue 3, May 1990, Pages 175-183
13. J. Schijve, M. Skorupa, A. Skorupa, T. Machniewicz and P. Gruszczynski. Fatigue crack growth in the aluminium alloy D16 under constant and variable amplitude loading. International Journal of Fatigue, Volume 26, Issue 1, January 2004, Pages 1-15
14. Pavelko V. STRESS STAT IN THE RIVET JOINTS: THE APPLIED THEORY OF THE FATIGUE FRACTURE. ICAS 2006-4.3.1, 25th Congress of the International council of the Aeronautical Sciences, Hamburg, Germany, 3-8 September, 2006
15. J.P. Gallagher, H.D.Stalnacer. Developing Normalized Crack Growth Curves for Tracking Damage in Aircraft.-Journal of Aircraft, 1978, Volume 15,No 2, Pages 114-120.
16. Broek D., Smith S. The Prediction of Fatigue Crack Growth Under Flight-by- Flight Loading. _Engineering Fracture Mechanics, 1979, Vol.11, No.1, Pages 123-141.
17. W.S.Johnson, R.A.Heller and J.N.Yang. Flight Inspection Data and Crack Initiation Times.- Proceeding 1977 Annual Reliability and Maintainability Symposium , 1977, pp.148-154.
18. R.A.Heller and G.H.Stevens. Bayesian Estimation of Crack Initiation Times from Service Data// J. of Aircraft, 1978, Volume 15, No 11, pp.794-798.

19. Pavelko I., Pavelko V. The valuation of stiffness of rods with cracks. Warszawa : Informator inst. tech. wojsk lot., 1997. - Pp.105 - 110.
20. Gallagher J.P. et all. Tracking Potential Crack Growth Damage in US Air Force Aircraft.- Journal of Aircraft, 1978, Volume 15, No 7, Pages 435-442.
21. Pfeiffer F. Bestimmung des Schädigungsverlaufs bei Dauerschwingbeanspruchung mittels Ermüdungsindikatoren.-IfL-Mitteilungen, 1978, Vol.17,Nr 6,s.220-223.
22. Gallagher J.P. et all. Tracking Potential Crack Growth Damage in US Air Force Aircraft.- Journal of Aircraft, 1978, Volume 15, No 7, Pages 435-442.
23. SU Patent 1290412. Kondratiev A., Pavelko V. Method of Definition of Structure Fatigue Lifetime. – 1985.
24. Pavelko I., Pavelko V. The valuation of stiffness of rods with cracks. Warszawa : Informator inst. tech. wojsk lot., 1997. - Pp.105 - 110.
25. J.C. Newman Jr., Stress Intensity Factor and Crack-Opening Displacements for Round Compact Specimens.- Int.Journal of Fracture, Volume 17, No 6, December, 1981, Pages 567-578.
26. Joonpyo Hong and Joseph Gurland. Direct observation of surface crack initiation and crack growth in the scanning electron microscope. Metallography, Volume 14, Issue 3, September 1981, Pages 225-236
27. J. Siegl, J. Schijve and U. H. Padmadinata. Fractographic observations and predictions on fatigue crack growth in an aluminium alloy under miniTWIST flight-simulation loading. International Journal of Fatigue, Volume 13, Issue 2, March 1991, Pages 139-147

I.Pavelko, V.Pavelko, S.Kuznetsov, E.Ozolins, I.Ozolins
(Aviation Institute of Riga Technical University, Latvia)

FATIGUE CRACK INDICATION BY LAMB WAVE NON-DESTRUCTIVE TESTING

Abstract. Investigation of ultrasonic Lamb wave interaction with a fatigue crack has been executed on flat samples of 1mm thickness aluminum alloy 2024-T3. Quite definitely it is possible to conclude, that the given technology of NDT over use of ultrasonic waves is quite capable to provide high stability and necessary accuracy at the continuous integrated SHM of thin-walled aluminum components of aircraft. It is shown also the accuracy of damage predicting is one of the most significant parameter of SHM efficiency

1. Introduction

This article is result of the authors' participation in European project AIHA. This project aims at realizing a breakthrough in aircraft health monitoring technology by exploring the capabilities of ultrasonic Lamb waves as the basic sensing principle and by providing an integrated and multidisciplinary research path.

The safe use of complex engineering structures such as aircrafts can only be guaranteed when efficient means of damage assessment are in place. Whereas aircraft design is nowadays based on a damage tolerance approach and time based inspection cycles, it is envisaged that the large cost associated with this approach can be drastically reduced by switching to a condition based maintenance schedule. This does require continuous health monitoring capabilities using integrated sensing technology and autonomous damage assessment. Structural Health Monitoring (SHM) is becoming important for preventing catastrophic failures and also for the uninterrupted operation. Reducing the costs associated with inspection and maintenance will have a large impact on airline profitability and competitiveness. But the most important feature of SHM is reliable detection of all possible kinds of damage in structural elements of aircraft. For metallic components the fatigue is one of the most dangerous damage mechanisms in aircraft structures. Multi-site fatigue damage,

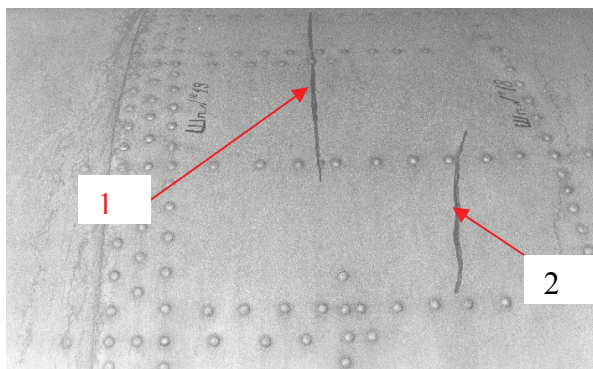


Figure 1. The fatigue cracks in a skin are initialized by the stress concentration 1) near the most loaded fastening point in rivet-joint 2) on small hole in skin

hidden cracks and corrosion, which, especially when combined, can lead to threatening damage states. Figure 1 shows two typical modes of fatigue crack in the skin of tail beam of helicopter MI-8 (at full scale fatigue test).

Elastic waves and their propagation have been used for many years to analyze impact response problems, mechanical properties of various materials and structural damage. Various types of methods based on sound and ultrasound are applied for nondestructive testing (NDT). Modern NDT ultrasound equipment and technology allows hope that SHM problems can be successfully solved. In articles [1,2] it is present an example of calculation and experiment of implementation health monitoring of aircraft

fuselage structures using ultrasonic waves: RMS of calculated and measured signal have good correlation as "healthy", as damaged structures. For health monitoring of aging aircraft structures, two main detection strategies are considered: the E/M impedance method for near field damage detection, and wave propagation methods for far-field damage detection [3]. Two damage identification techniques are integrated in this paper, including impedance methods and Lamb wave propagations. Examples of successful using PZT materials in the areas of active and local sensing

are Lamb wave propagations [5,6] and the impedance-based structural health monitoring methods [7].

But very important side of SHM is the reliable prediction of remaining strength and remaining life time. Two variants of models “signal - remaining lifetime” are essentially probable:

1) Direct model “signal - remaining lifetime (remaining strength)”. It may be established by results of direct tests of samples or structural elements in conditions completely conterminous with operating conditions of a structural element. In this case the model will represent statistical connection between parameters of a signal and remaining lifetime.

2) Indirect model “signal - damage - remaining lifetime (remaining strength)”.

It is obvious the first variant is preferable from the point of view of accuracy and reliability. In some situations such model may be constructed. However a variety of materials, structural forms of elements, variants of mechanical loading, aggressive influence of environment does not allow to hope for reception in such immediate prospects of universal linking suitable for any probable conditions of operation.

Therefore in all other cases the second variant is really feasible: “signal - damage - remaining lifetime (remaining strength)”. Analysis of damage phenomena, including its parameters and degradation conditions allows forming main functions those are basis of modeling “signal - remaining lifetime”. For all damage phenomena there is some common scheme of remaining lifetime determination: after damage initialization its parameter grows. At some moment it is detected by the system of inspection. It is initial value of parameter. During damage development the remaining strength is decreasing. Durability of damage development to some parameter when the remaining strength has decreased to minimal level is remaining lifetime. A fatigue phenomenon is possible practically for all structural materials of aircrafts. Mainly a parameter of fatigue damage is length and /or depth seen fatigue crack. Paris’ law or similar regularities allows establishing of tight correlation between crack sizes and structural element remaining lifetime. So, in this case the basic point of remaining lifetime predicting is the correlation “signal – crack size” establishing and its features defining.

The establishment of reliable correlations between parameters of damage and a sensor response during automatic NDI is one of the most important conditions of successful creation of the SHM system of aircraft. It is first aim of present paper. Second, and it is main aim, is estimation of efficiency different approaches of the fatigue crack prediction at use of scalar parameters of a signal-response.

2. Experimental Investigation

2.1. Material, Samples, Equipment

Investigation of ultrasonic Lamb wave interaction with a fatigue crack has been executed on flat samples from an aluminum alloy 2024-T3 by thickness 1mm. The sketch of a base configuration with the sizes 80x300mm is presented in Figure 2. For initiation of a fatigue crack in a middle part of the sample the concentrator of stress was carried out. In experiment described here the sample with the central circular hole with diameter 4mm was used. The sample was tested by the servo-hydraulic test machine Instron with frequency of variable loading 10 Hz, the maximal stress in a cycle

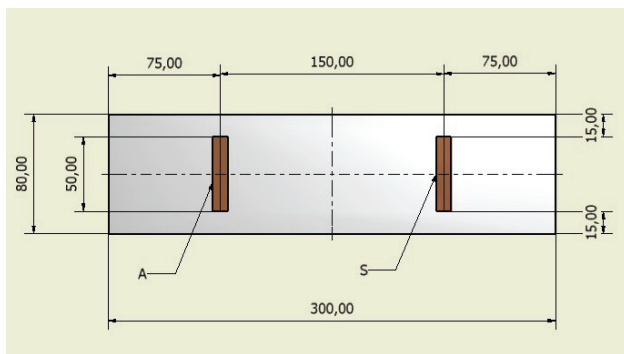


Figure 2. Sketch of a sample with sensors in basic experiment

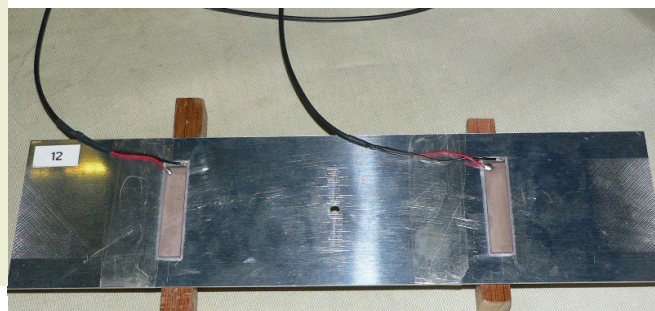


Figure 3. Experimental sample: Al 2024-T3, 1x80x300mm, 4mm central hole

150MPa and factor of a cycle 0.333.

At the first stage of tests the initial crack at edges of a hole with a size up to 1 mm was initiated. Before the beginning of the second stage of tests installation of PZT transducers was made in conformity with the scheme Figure 2. As transducers the Piezoceramic PIC 151, 0.5x10x50mm (PI Piezoceramic) was used. PZT transducers were pasted directly to a surface of the sample by means of one of types Hysol paste. The preliminary tests executed in laboratory KUL (Catholic University Leuven) have shown that at a considered configuration and a level of loading PZT keep strength and working capacity. The picture of a sample prepared for tests is shown in Figure 3.

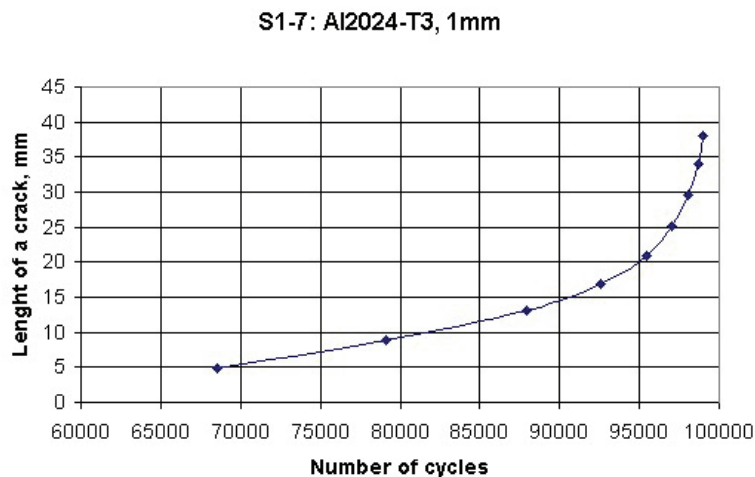


Figure 4. Curve of a fatigue crack propagation

At the second stage of tests the fatigue crack was growing from the central hole in the sample during cyclic loading. The size of a crack on a surface of the sample was fixed by means of a microscope with tenfold increase. The crack developed practically symmetrically concerning the center of the hole. The crack growth history it is shown in Figure 4. Growth of a crack is well described by Paris' law with an exponent $=3.78$ and a constant $=1.69 \cdot 10^{-8}$, if growth rate to measure in mm/cycle, and stress intensity factor in $\text{MPa} \cdot \text{m}^{0.5}$.

Loading was being interrupted and the non-destructive testing of a sample by means of the built in monitoring system described above was being made when after each end of a crack had growth approximately in 2mm.

Electronics LWDS45 of firm Cedrat Technology with software of KUL was used for excitation of ultrasonic impulses.

A impulse 5-cycle sine burst signal at 250 kHz used to excite the actuators at their resonance frequencies. Time extent of an impulse was 20 μs , and the amplitude did not exceed 1.5 V (Figure 4a). The Lamb waves excited by the actuators propagated along the plate and were received by the sensor. The response was amplified and transferred to a digital oscilloscope PXI-5105 (National Instrument).

The typical response is presented on Figure 4b. The signal has complex structure, but it is possible to notice, it represents some set of the impulses these are the transformations of an excitation impulse during its propagation from actuator up to a sensor as a result of interaction with borders of the sample, a hole and a crack. Thus intensity of an impulse, frequency and, as a result, the form of

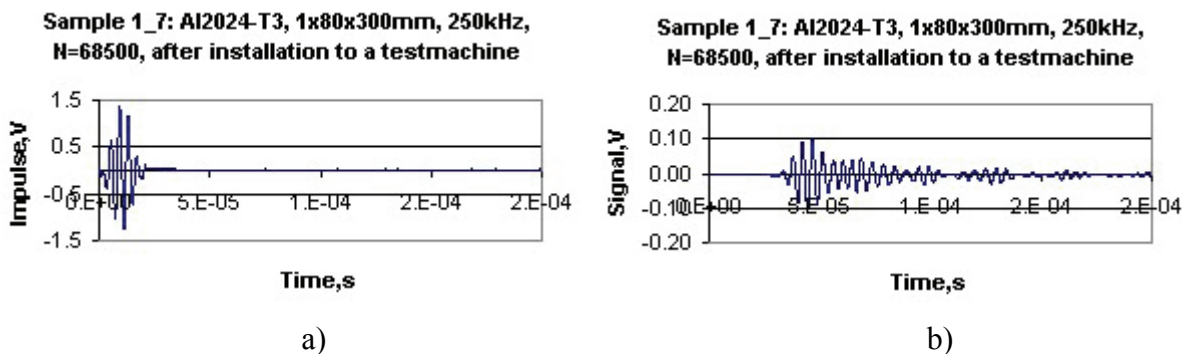


Figure 4. Form of an impulse of excitation (a) and Sensor response (b) in Al sample with the 4mm central hole and initial crack

the direct and reflected impulses can vary. During fatigue experiment the essential change of conditions of signal propagation is connected with the growing of a crack. Therefore, the analyses

of features of the response and detection the most essential of them which are caused by propagation of a crack is the key problem of processing of ultrasonic NDT results.

2.2. Signal Processing and Features Extraction

There are a number of simple time domain measures in structural damage detection [7]. These include response maximum and minimum and peak-to-peak of a response (a difference between the maximum and minimum), arrival time - absolute time when the signal first crosses the threshold level and others simple parameters of a response. The Root Mean Square (RMS), statistical moments are more complex parameters of signal.

Three parameters of response were choused for their efficiency comparison:

- Peak of amplitude - maximum amplitude of the signal (half of a peak-to-peak of a response);
- Maximum of the $RMS(t)$ on time interval $[0, t]$, $t < T$, where T is duration of a record;
- Global maximum of the smoothed function $S(t)$ on time interval $[t - \Delta t, t + \Delta t]$, $\Delta t < t < T - \Delta t$, where $2\Delta t$ is trimmed interval of a record.

First parameter can be easy defined using of a response record (Figure 4).

Second parameter, maximum of the $RMS(t)$ on time interval $[0, t]$, can be defined by the following way. First of all the $RMS(t)$ on time interval $[0, t]$ must be calculated by the formula

$$RMS(t) = \sqrt{\frac{\sum_{i=1}^{n(t)} (s_i - \bar{s})^2}{n(t)}} \quad (1)$$

where $n(t)$ is number of samples in a response record, s_i is the value i of digital record, \bar{s} is mean of process.

Then

$$RMS_{max} = \max_{t \in [0, T]} [RMS(t)] \quad (2)$$

An example of $RMS(t)$ as the time function is shown in Figure 5. Usually this function has one peak and in all cases first peak is maximal.

Third parameter, global maximum of the smoothed function $S(t)$ on time interval $2\Delta t$ is defined by similar way.

$$S(t) = \sqrt{\frac{\sum_{i=n-\Delta n}^{n+\Delta n} (s_i - \bar{s})^2}{2\Delta n}}, \quad (3)$$

where Δn is number of samples in time interval Δt .

An example of this function $S(t)$ is shown in Figure 6. In contrast to the previous case this function usually has several peaks and maximal peak is not ever first. The largest peak is named global.

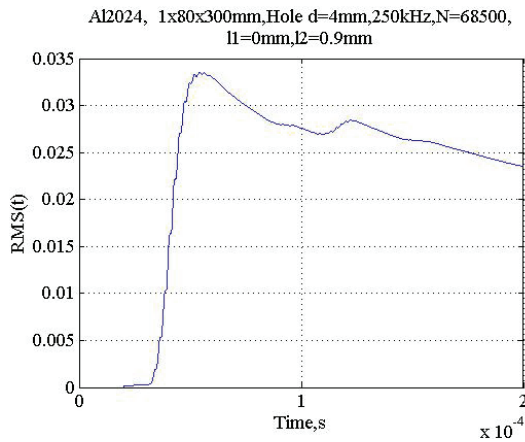


Figure 5. The $RMS(t)$ as a function of the time

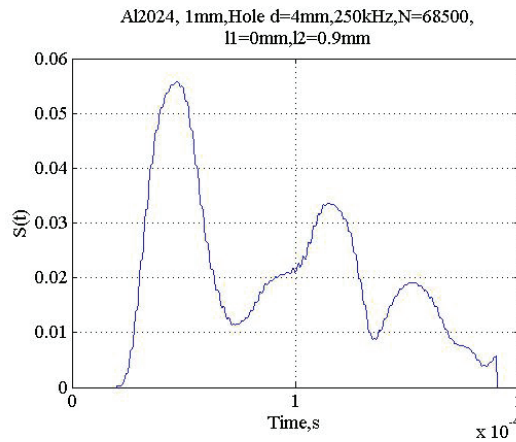


Figure 6. The $S(t)$ as a function of the time

After processing experimental data the correlation functions “parameter of signal – length of the crack” were obtained (Figures 7, 8, 9) for each of three kind’s parameters.

S1-7: Al2024T-3, 1mm, 250kHz

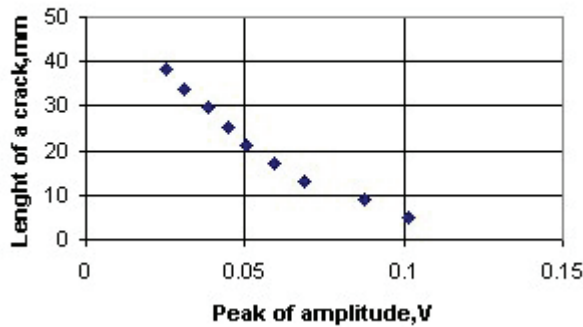


Figure 7. Correlation function for the first parameter of response

It is visible, that the obtained correlation functions have similar shape. Parameters of a signal noticeably decrease, if length of a crack increases. It can be explained by the shading effect of a crack. Because the crack is placed down on a way of direct distribution of an elastic wave from actuator to a sensor, there is its partial reflection from a surface of a crack. The degree of reflection increases with increase in the size of a crack that causes both change of the form, and the signal intensity received by a sensor. Because all of three parameters characterize signal intensity its reduction during growth of the crack is natural.

S1-7: Al2024T-3, 1mm, 250kHz

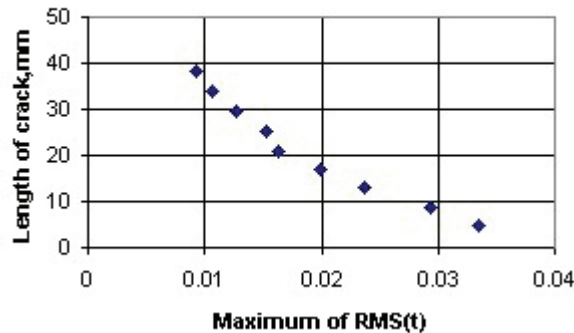


Figure 8. Correlation function for the second parameter of response

S1-7: Al2024T-3, 1mm, 250kHz

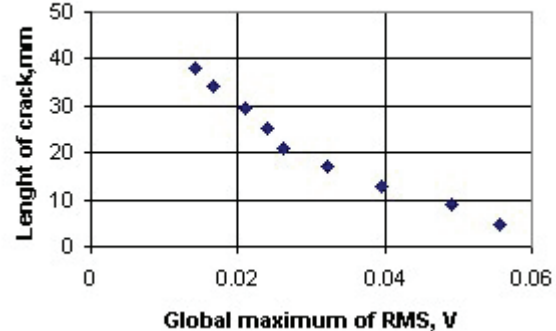


Figure 9. Correlation function for the third parameter of response

2.3. Comparison of Efficiency of Different Parameters of a Response

One of the main tasks of present paper is the comparison of efficiency of the use of different scalar parameters of a signal-response at the predicting of the size of a fatigue crack. Natural criterion is the mistake of predicting of length of a crack as a result of natural dispersion of measured values of parameter. So the variance and the standard deviation may be used as the measure of natural dispersion. The variance is the second central statistical moment. The variance describes the variability of a signal from the mean. The standard deviation from the mean is used widely in statistics to indicate the degree of dispersion.

It is supposed the X is a simple scalar parameter of a response. It is random and has some distribution law $F_X(x)$. Let the length of a crack is the parameter of a signal function $y = f(x)$. It is obvious, that in this case the predicted length of crack Y is also a random with the law of distribution $F_Y(y)$. If the function $y = f(x)$ is relatively smooth, then

$$(y - y_0) \approx \left. \frac{\partial f}{\partial x} \right|_{x=x_0} (x - x_0) \quad (4)$$

If for some fixed x_0 is the mean of random X , then variance $D(Y)$ of random Y and its standard deviation $\sigma(Y)$ can be expressed under formulas

$$D(Y, y_0) = \left(\left. \frac{\partial f}{\partial x} \right|_{x=x_0} \right)^2 D(X, x_0), \quad \sigma(Y, y_0) = \left. \frac{\partial f}{\partial x} \right|_{x=x_0} \sigma(X, x_0), \quad (5)$$

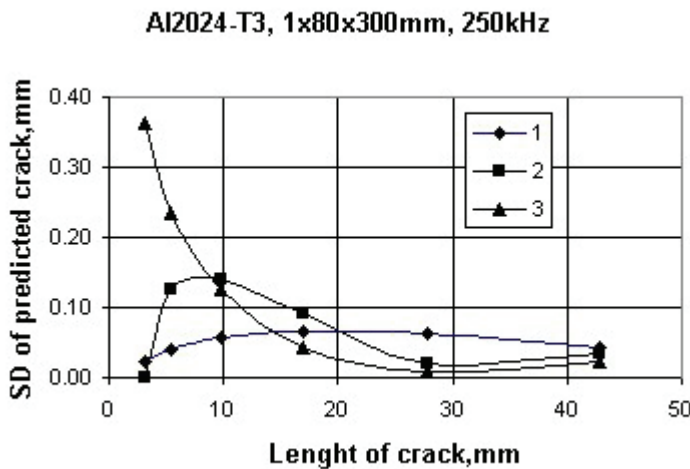


Figure 10. Standard deviation of the crack length, predicted at the use of three parameters of a response: 1- peak of amplitude, 2- maximum of the $RMS(t)$, 3 - global maximum of the $S(t)$.

length of a crack and preferred for small crack.

2) Integral criterions 2 and 3 are preferred for large crack.

3) The criterion 3 for small cracks can give sufficient difference predicted length of a crack.

It is necessary to notice, that the received estimations are based on the limited experimental data. The increasing the volume of statistical data can undergo the certain changes. However, quite definitely it is possible to conclude, that the given technology of NDT over use of ultrasonic waves is quite capable to provide high stability and necessary accuracy at the continuous integrated SHM of thin-walled aluminum components of aircraft. Result of this research shows that multi-parametric criterion can be used.

If there is experimental data of the random X for different means x_0 , then the variance $D(Y)$ of random Y and its standard deviation $\sigma(Y)$ can be estimated. Statistical data obtained in experiment is sufficient for such estimation. Final results of statistical analysis are presented in Figure 10.

3. Conclusions

It can see any of three parameters of response has relatively small dispersion. Thus the length of a crack predicting with their use, especially for more than 10mm crack, is acceptable for SHM. Comparison of this parameters shows:

- 1) Peak of amplitude is stable criterion in large interval of the

It is shown also the accuracy of damage predicting is one of the most significant parameter of SHM efficiency.

Acknowledgement

This research was induced by the authors' participation in 6FP research project AISHA (Aircraft Integrated Structural Health Assessment). AISHA has brought together major European aircraft manufactures, research and academic institutions in order to provide effective integrated system of continues detection of damages in the aircraft structure.

The authors are grateful to European Commission for financial support and all partners for scientific and technological collaboration.

References:

1. Victor Giurgiutiu, Andrei Zagrai and Jing Jing Bao. Piezoelectric Wafer Embedded Active Sensors for Aging Aircraft Structural Health Monitoring// SHM, Copyright _ 2002 Sage Publications, Vol. 1(1): 0041–61.
2. Z. Q. Zhou, W. K. Chiu, M. K. Bannister. Health monitoring of aircraft fuselage structures using ultrasonic waves // Proceeding of 25th international congress of the aeronautical sciences, Hamburg, September of 3-8th 2007.
3. Jeannette R. Wait, Gyuhae Park* and Charles R. Farrar. Integrated structural health assessment using piezoelectric active sensors// Shock and Vibration, 12 (2005), 389–405.
4. S.S. Kessler, S.M. Spearing and C. Soutis, Damage Detection in Composite Materials using Lamb Wave Methods, Smart Materials and Structures **11** (2002), 269–278.
5. J.B. Ihn and F.K. Chang, Detection and monitoring of hidden fatigue crack growth using a built-in piezoelectric sensor/actuator network: II. Validation using riveted joints and repair patches, Smart Materials and Structures **13** (2004), 621–630.
6. G. Park, H. Sohn, C.R. Farrar and D.J. Inman, Overview of Piezoelectric Impedance-based Health Monitoring and Path Forward, *The Shock and Vibration Digest* **35** (2003), 451–463.
7. Health Monitoring of Aerospace Structures — Smart Sensor Technologies and Signal Processing. Edited by W.J. Staszewski, C. Boiler and G.R. Tomlinson © 2004 John Wiley & Sons, Ltd ISBN: 0-470-84340-3
8. Staszewski, W.J., Read, I. and Foote, P. Damage detection in composite materials using optic fibers - recent advances in signal processing// Proceedings of the SPIE's 7th International Symposium Smart Structures and Materials, Conference on Smart Structures and Integrated Systems, Newport Beach, California, 5-9 March, 2000.
9. Worden, K. a. Structural fault detection using a novelty measure, Journal of Sound and Vibration, \ 1997, 201, pp. 85-101.
10. Worden, K. 1997. Damage detection using a novelty measure, Proceedings of the 75th International Mot Analysis Conference, Orlando, pp. 631—637.

*D.M. Krasnoshapka, PhD (National Aviation University)
A. Skalyga, post-graduate student (National Aviation University)*

FEATURES OF CALCULATION OF THE ESTABLISHED MODES OF THE CASCADE ASYNCHRONOUS MACHINE

The technical decision of construction of the generator of own needs gas turbine engine (GTE) in the form of the cascade machine used also as a starter for starting GTE is offered. Features of calculation of starter mode of the cascade machine are considered

Gas-pumping plants (GPP) with gas turbine engine compound 63% from total amount of GPP of Ukraine. The majority of them become out of date and requires replacement by modern, more reliable and economic plants. In this connection, searching of new constructional solutions, including turbine engine starting systems is actual.

Now initial run-up of a rotor of a turbine engine is carried out with a compressor part of the GTE at the expense of pumping of gas which one is burnt further in a flare [1]. Such system makes essential ecological impact on an environment. At the same time, as a part of each GPP there is a generator of own needs. Hence, searching of such construction of the generator which one is capable to execute functions of a starter of gas turbine engine is expedient.

Cascade machine can be such starter-generator. Because of its noncontact construction the electrical starting system based on asynchronous cascade answers the basic demand of explosion safety GPP.

The cascade machine consists of two asynchronous machines placed in one body and linked mechanically and electrically (fig. 1). The rotors of both machines are on one shaft, and their three-phase rotor windings are switched on one on another. Thus the rotor winding of the first machine 2 is connected to a rotor winding of the second machine 3 with an inverse phase interchange. Windings of stator of asynchronous machines (1 and 4) are made in the form of separate three-phase windings. Ration quantity of pair poles defines synchronous velocity of cascade.

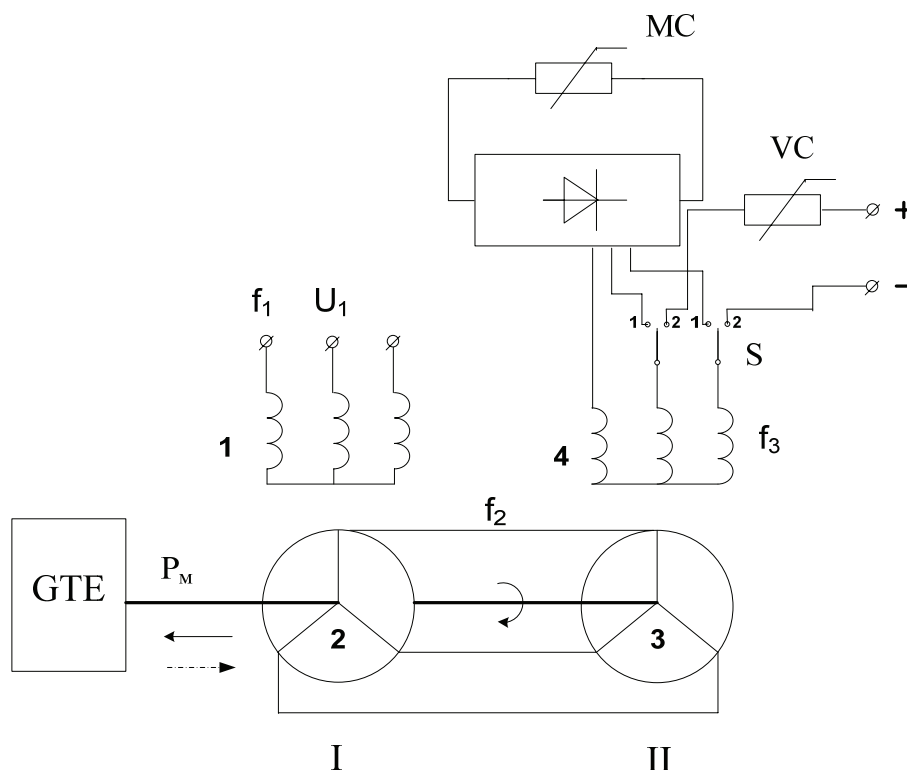


Fig. 1 The scheme of set of starter-generator cascade

The cascade machine in such modification can be used as:

- a noncontact asynchronous motor with a resistance starting;
- a noncontact synchronous generator of higher frequency.

In a mode of a noncontact asynchronous motor the cascade machine ensures turbine engine launch, i.e. is a starter. Thus the winding of the stator of the first machine is switched-on on the three-phase network and stator winding of the second machine - on a moment controller (MC) - a switch position (S) is 1-1. After starting-up of turbine engine the cascade machine works in a mode of the noncontact synchronous generator. Thus second machine infused by a direct current from the stator and it is implicit-pole synchronous generator. A switch position is 2-2 (fig. 1).

Let's observe in more details operating mode of a starter of cascade.

In noncontact modification the cascade asynchronous machine has one synchronous velocity [2] defined by a network frequency (f_1) and the total number of pair poles of the first and second machines ($p_1 + p_2$) by formula (1)

$$n_c = \frac{60 \cdot f_1}{p_1 + p_2}. \quad (1)$$

Sliding of first machine s_1 defines by known expression. Sliding of asynchronous cascade s_2 (2) is sliding a rotor of the second machine concerning a field of the rotor.

$$s_2 = \frac{n_{n2} - n}{n_{n2}} = \frac{(n_{n1} - n) - n \cdot \frac{p_2}{p_1}}{n_{n1} - n}, \quad (2)$$

where n_{n1} - velocity of a field of the first machine concerning the stator, and n_{n2} - velocity of a field of the second machine concerning a rotor (3), f_2 - frequency of currents of rotor windings of cascade machine [2].

$$n_{n1} = \frac{60 \cdot f_1}{p_1}, \quad n_{n2} = \frac{60 \cdot f_2}{p_2}. \quad (3)$$

The real rotating speed of a working shaft of an asynchronous cascade (n) taking into account sliding (s_2) [2] is defined by the formula (4)

$$n = \frac{60 \cdot f_1}{p_2 + p_1 \cdot (1 - s_2)}. \quad (4)$$

The physical equivalent circuit of asynchronous cascade for one phase is present on fig. 2. Observing the processes proceeding in the cascade asynchronous machine, it is necessary to mark out three head loops merged by a transformer coupling by means of flows of interinduction Φ_{m1} and Φ_{m2} . It is the stator of the first machine (1), a rotor head loop (2) and the stator of the second machine (3). Accordingly, the equations of voltage in the complex form [3] for these head loops look like (5):

$$\begin{aligned} \dot{U}_1 &= \dot{I}_1 \cdot \dot{Z}_1, \\ \dot{E}_{21} - \dot{I}_2 \cdot (\dot{Z}'_{21} + \dot{Z}'_{22}) &= \dot{E}_{22} \\ \dot{E}_3 &= \dot{I}_3 \cdot (\dot{Z}_3 + \dot{Z}'_{306}), \end{aligned} \quad (5)$$

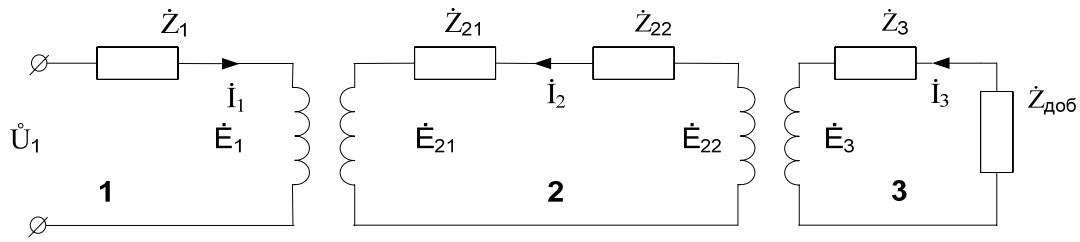
where U_1 - a mains voltage;

$\dot{Z}_1, \dot{Z}_{21}, \dot{Z}_{22}, \dot{Z}_3$ - complex resistances of head loops of a stage MC (fig. 1);

\dot{Z}_{006} - complex resistances MC;

$\dot{I}_1, \dot{I}_2, \dot{I}_3$ - complexes of currents of the applicable head loops of a cascade;

$\dot{E}_{21}, \dot{E}_{22}, \dot{E}_3$ - an EMF of windings of head loops of a cascade.



Fi

g. 2 Physical equivalent circuit of a cascade

For account of steady runs of the cascade asynchronous machine the equivalent circuit of substitution gained by consecutive reduction in two stages of arguments of a stage to a network is used. The first stage - reduction of stator winding of the second machine to a rotor head loop. Second - reduction of a rotor head loop of a stage to the stator of the first machine. Used reduction coefficients of an EMF, currents and resistances are defined by known relationships.

For account of modes of operation it is expedient to use an exact gamma-type equivalent circuit of an asynchronous stage (fig. 3). Thus, account becomes simpler thanks to that under this circuit design with sliding alteration currents of the principal circuit vary only a little, and the current of a circuit of magnetization remains invariable at invariable meaning of a mains voltage.

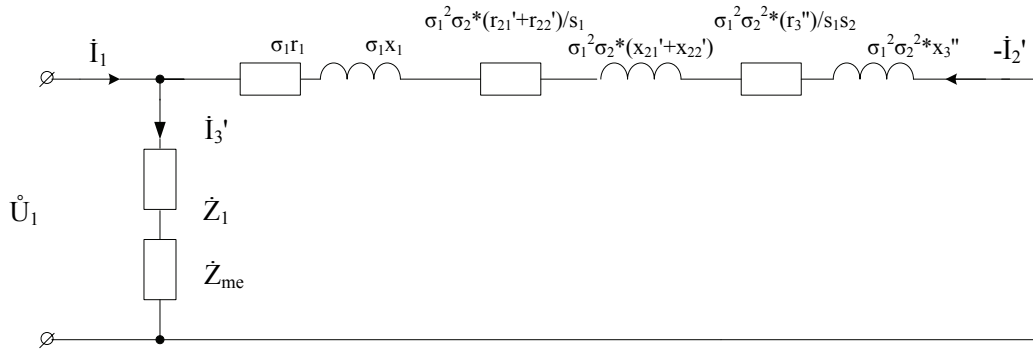


Fig. 3 Exact gamma-type equivalent circuit

σ_1, σ_2 - complex dissipation coefficients of the stator first and a rotor second asynchronous machines (6)

$$\sigma_1 = 1 + \frac{\dot{Z}_1}{Z_{m1}}, \quad \sigma_2 = 1 + \frac{\dot{Z}_{22}}{Z_{m2}}. \quad (6)$$

Z_{me} - equivalent resistance of magnetizing head loops of a cascade

$$Z_{me} = \frac{x_{m1} \cdot (x_{m2}' + x_{21}' + x_{22}')}{x_{m1} + (x_{m2}' + x_{21}' + x_{22}')}, \quad (7)$$

where x_{m1} - inductive resistance of a magnetizing branch of the first machine;

$x_{m2}', x_{21}', x_{22}'$ - resulted inductive resistance of a magnetizing branch of the second machine, resistance of dissipation of rotor windings of the first and second machines accordingly.

Currents of branches of the exact gamma-type circuit design are defined by expressions (8):

$$-i_2' = \frac{U_1}{\dot{Z}_1' + \dot{Z}_2' + \dot{Z}_3'}, \quad i_3 = \frac{U_1}{\dot{Z}_1 + Z_{me}}, \quad i_1 = i_3 - i_2', \quad (8)$$

and the moments of asynchronous machines of a cascade (9)

$$M_{1asm} = \frac{3 \cdot I_2^{2'} \cdot R_2}{\Omega_1}, \quad M_{2asm} = \frac{3 \cdot I_2^{2'} \cdot R_3}{\Omega_2}, \quad (9)$$

$$R_2 = \sigma_1^2 \cdot \sigma_2 \cdot \frac{(r_{12}' + r_{21}')}{s_1},$$

$$R_3 = \sigma_1^2 \cdot \sigma_2^2 \cdot \frac{r_3''}{s_1 \cdot s_2},$$

where Ω_1, Ω_2 - frequency of a field of the first and second asynchronous machines in a cascade.
The total electromagnetic moment of a cascade (10):

$$M_{em} = M_{1em} + M_{2em} \quad (10)$$

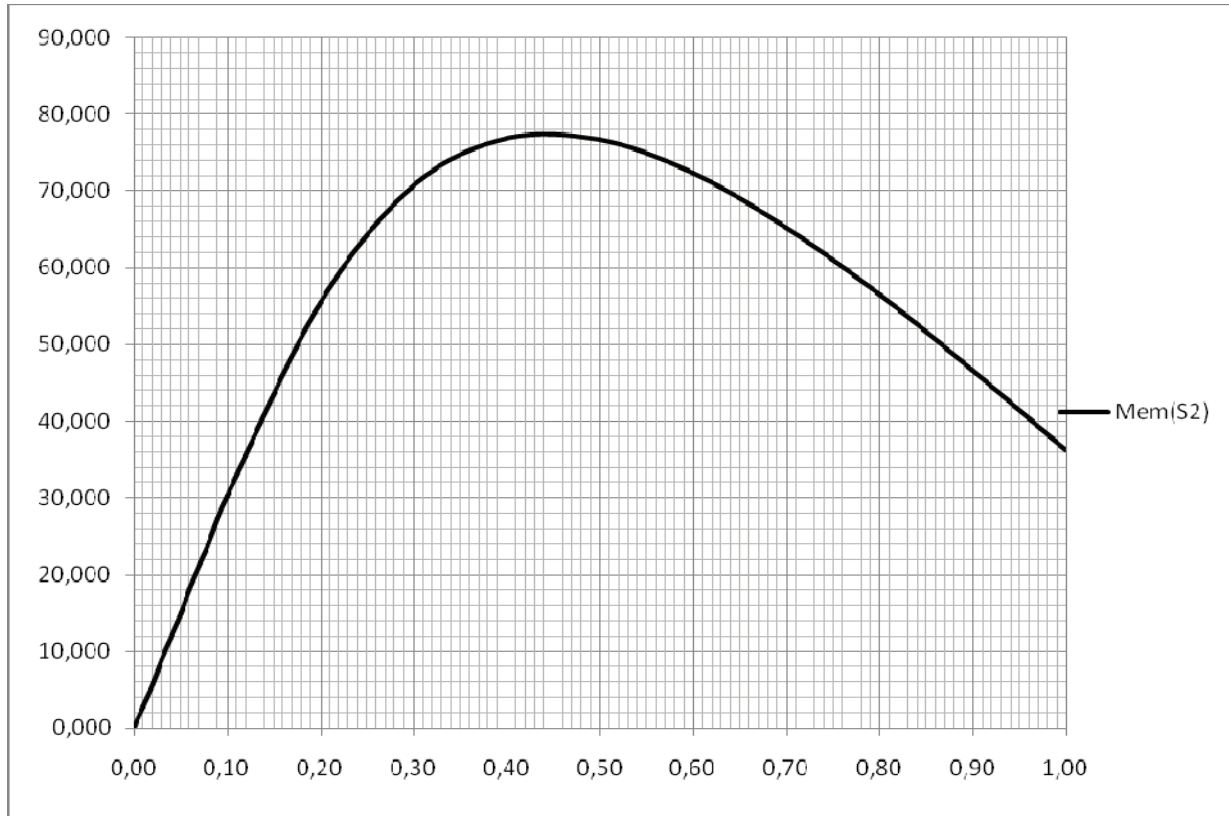


Fig. 4 Moment characteristic of an asynchronous cascade

On fig. 4 the characteristic gained computational by on an equivalent circuit of asynchronous cascade in case of the six-pole machine, fed from a network and the bipolar machine is introduced. Through stator winding operating of a cascade is realized. The full rated power of a cascade 90 kVA.

The technical decision of construction of the generator of own needs gas turbine engine allows to create a noncontact generator without gyrating rectifiers and to use it in the capacity of a starter for turbine engine starting. The resistance starting of the cascade asynchronous machines allows to realize run-up of a rotor of a turbine engine with the constant dynamic moment on its shaft.

References

1. B.M. Kats, E.S. Zharov, V.K. Vinokurov. Starting systems aviation gas turbine engines. – M.: «Mashinostroenie», 1976.
2. Works of the third all-Union conference on contactless electric machines. Volume 2. «Zinatne», Riga 1966.
3. M.P. Kostenko, L.M. Piotrovski Electric machines. In 2 p. P.2 - Machines of an alternating current. The textbook for students high techn. Studies. Institutions. The edition 3, nepepa6. – L.: «Energia», 1973.

*Krasnoshapka D. M., PhD, professor of National Aviation University, Ukraine
Mazur T., post-graduate student of National Aviation University, Ukraine*

AUTOMATIC CONTROL OF PROCESS OF DESIGN OF THE ASYNCHRONOUS MUFF WITH MASSIVE FERROMAGNETIC CARTRIDGE CASE ON THE SECONDARY ROTOR

The design procedure of optimum parameters asynchronous муфты with a massive ferromagnetic sleeve on a conducted rotor is offered

Statement of a problem Interest to creation of optimum electric machines has arisen for a long time. For a substantiation of optimum parities classical methods of search of a maximum and a minimum of functions of many variables were used. However these methods not always are suitable for the decision of complex and special problems of optimum designing electrical machines. With reference to asynchronous motors with a massive ferromagnetic cartridge case on a rotor the problem of definition of the optimum geometrical sizes of a cartridge case is actual. This problem is connected by the value of nonlinear frequency dependent parameters that a ferromagnetic massive brings in rotor's circuit of the asynchronous machine.

The analysis of the last researches and publications Development of methods of optimum settlement designing electrical machines were engaged in M.P.Kostenko, G.N.Petrov, I.M. Postnikov, I.P.Kopylov, D.A.Avetisyan.

The formulation of the purposes of article Purpose of this article is development of a technique of the automated designing asynchronous muff (AM) with special design secondary squirrel-cage rotor. The feature such type of rotor consists in essentially nonlinear dependence its parameters from frequency and size of rotor's currents.

The basic aspects of a problem Application of methods of optimum settlement designing the characteristics of asynchronous machines allows to solve problems of search of such combination of the linear sizes of the machine and to choose of electro-magnetic loadings at which the criterion of quality (criterion function) has the best value from all possible and at which demands made the machine proceeding from conditions of operation with high efficiency is satisfied. With reference to asynchronous engines with a massive ferromagnetic cartridge on a rotor the problem of definition of the optimum geometric sizes of a cartridge is actual. The geometrical sizes of a massive cartridge case will be optimum if the demands of simultaneous maintenance of an extremum of criterion function (criterion of an optimum) will be satisfied. Hence, for calculation of the optimum geometrical sizes of a ferromagnetic cartridge case it is necessary:

1. To make mathematical model of object of optimization, in our case model asynchronous muff with a special design of secondary rotor;
2. To define criterion of an optimum;
3. To define operational requirements in the form of necessary restrictions;
4. To describe constants and variable initial data, an index point of search;
5. To develop the algorithm and the program of calculation on the personal computer, which connects parameters of optimization with criterion of an optimality and restrictions.

Let's consider more in detail each of these components. At transformation of conceptual model on mathematical language set of used variables and qualitative dependences are translated in quantitative: criteria of an optimality - in criterion functions; restrictions are translated in the equations or inequalities; communications between variables in functional parities.

We shall use mathematical model AM with frequency dependent parameters in secondary rotor's circuit, namely functional dependences between the geometrical sizes of a massive cartridge case, sizes of equivalent parameters, which is brought in secondary rotor's circuit and electromechanical characteristics of AM.

According to the basic settlement parities [2] communication between equivalent parameters of a ferromagnetic cartridge case, which is brought in secondary rotor's circuit and frequency of a rotor of the asynchronous machine and the geometrical sizes of a cartridge case is established. $M = \frac{m_1 p_{am} (r'_2 + r'_e)}{2p f_{rel} s_{am}} |I'_2|^2$; (1)

$$I'_2 = \frac{U_q}{\left[r_1 + c_1 \frac{r'_2 + r'_e}{s_{am}} \right]^2 + \left[x_1 + c_1 \left(x'_2 + \frac{x'_e}{s_{am}} \right) \right]^2}; \quad (2)$$

$$n = \frac{th \alpha h + tg^2 \alpha h \cdot th \alpha h}{1 + tg^2 \alpha h \cdot th^2 \alpha h} + \frac{th^2 \alpha h \cdot tg \alpha h - tg \alpha h}{1 + tg^2 \alpha h \cdot th^2 \alpha h}; \quad (3)$$

$$m = \frac{th \alpha h + tg^2 \alpha h \cdot th \alpha h}{1 + tg^2 \alpha h \cdot th^2 \alpha h} - \frac{th^2 \alpha h \cdot tg \alpha h + tg \alpha h}{1 + tg^2 \alpha h \cdot th^2 \alpha h}; \quad (4)$$

$$\alpha = \sqrt{\frac{\mu \omega \gamma}{2}}; \quad (5)$$

$$H_s = \sqrt{2} \frac{2 \cdot m_1 (k_{\omega 1} w_1)^2}{\pi d} I'_2; \quad (6)$$

Relative magnetic permeability μ_s we could find by means of the basic curve of magnetization for a material of cartridge case. For definition of equivalent parameters of a ferromagnetic cartridge case made from carbonaceous steel, it is expedient to use the approximated expression of a curve of magnetization [3].

$$\mu_s = \frac{c}{H_s + a} + \frac{c_1}{H_s + a_1} + \mu_0; \quad (7)$$

c, c_1, a, a_1 - factors of approximation of a curve of magnetization;
 μ_0 - magnetic constant.

$$\mu = \mu_0 \mu_s; \quad r'_e = 4n \sqrt{\frac{\mu \omega}{2\gamma}} \frac{m_1 (k_{\omega 1} w_1)^2}{\pi d} l; \quad (8)$$

$$x'_e = 4m \sqrt{\frac{\mu \omega}{2\gamma}} \frac{m_1 (k_{\omega 1} w_1)^2}{\pi d} l; \quad (9)$$

In formulas auxiliary quantities are designated:

m_1 - number of phases AM;

r_1, x_1 - active and inductive resistance of a phase of a winding of leading (primary) rotor of AM in view of removal of a contour of a magnetizing current;

r'_2, x'_2 - active and inductive resistance of a phase of the squirrel-cage secondary rotor of AM, led a winding of a leading rotor in view of removal of a contour of a magnetizing current;

f_{rel} - frequency of rotation of a field concerning leading rotor AM;

s_{am} - sliding of AM equal to the attitude of frequencies of secondary and leading rotors AM.

$$s_{am} = \frac{f_2}{f_1} = s \left(\frac{p_{am}}{p_{cm}} \pm 1 \right),$$

s - sliding of electrodynamic reduction unit (ERU);

$\frac{p_{am}}{p_{sm}}$ - attitude of numbers of pairs poles of the synchronous machine and AM ERU;

$k_{\omega 1}$ - factor of winding of a leading rotor;

w_1 - number of coils of leading rotor AM ;

d - diameter of a secondary rotor ;

l, h - length and thickness of a ferromagnetic cartridge case.

Proceeding from equivalent circuit of ERU (fig.1), let's assume that parameters of secondary rotor of AM are led to a leading rotor and for leading rotor we can say that $U_1 = const$, and $f_1 = const$. Such approach allows us to use AM as system with the concentrated parameters.

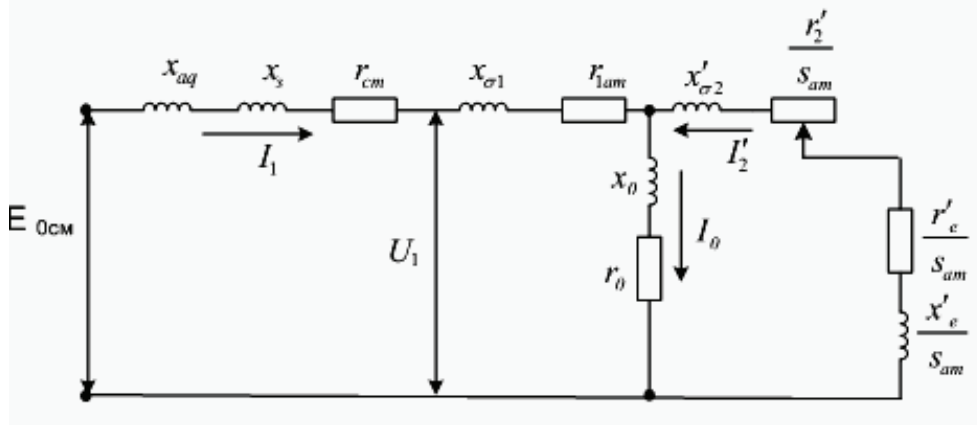


Fig.1 The equivalent circuit of SM and AM cascade in view of equivalent parameters of a massive ferromagnetic cartridge case, which is brought in secondary rotor's circuit of AM.

Thus in secondary rotor's circuit of AM besides constant parameters appear nonlinear frequency depended parameters. Therefore calculation of modes of AM by traditional ways (a method of the theory of circuits, etc) is impossible. Sizes of these equivalent parameters depend on the geometrical sizes of a ferromagnetic cartridge case (radial thickness and axial length). In turn, the geometrical sizes of a ferromagnetic cartridge case essentially influence a kind of the mechanical characteristic. Let's find such geometrical sizes of a cartridge case at which the kind of the mechanical characteristic of AM will be close to excavator characteristic. For this some conditions should be carried out: the rigidity of an initial site of the mechanical characteristic and size of the starting moment would be enough. Thus it is the most expedient to enter restrictions on a kind of the mechanical characteristic of AM, namely to make necessary demands to its rigidity.

The criterion of definition of the optimum geometrical sizes of a massive cartridge case can be formulated as follows: to find a maximum of the starting moment:

$$M_n(l, h) \rightarrow \max ;$$

at performance of conditions of necessary rigidity of the mechanical characteristic in the field of small slidings:

$$M_1(l, h, s_1) \geq M_1$$

$$M_2(l, h, s_2) \geq M_2 .$$

$$l, h > 0$$

This problem concerns to problems of nonlinear programming. Its complexity is defined by that restrictions are set in the form of inequalities.

A task is solved by means of the search methods of optimization based on search of values of parameters of optimization on a grid with constant step and consecutive approach an optimum variant [1]. The algorithm of the program decision represented on fig.2 provides a variation of parameters of a cartridge case: lengths l and thickness h .

First we choose an index point of search: such values when the length and thickness of cartridge case have the minimal values. Further we vary length of a cartridge case at a minimum of its thickness. During calculations some length of a cartridge case at which the moment reaches the

maximal size is defined. After that thickness of a cartridge case increases up to new value. Then the cycle of calculations of search of the maximal size of the starting moment repeats. Thus the new length of a cartridge case will be less, than calculated earlier. The given algorithm works until the increase in thickness of a cartridge case leads to reduction axial lengths of cartridge case simultaneously with performance of restrictions on a kind of the mechanical characteristic. The found geometrical sizes of a massive cartridge case will be optimum.

As follows from (1) between varied parameters M_{st} (the starting moment) and l (axial lengths of cartridge case) on the previous and subsequent steps there is a mutual communication: at reduction of axial length of a cartridge case in comparison with the previous step there is an increase of the starting moment.

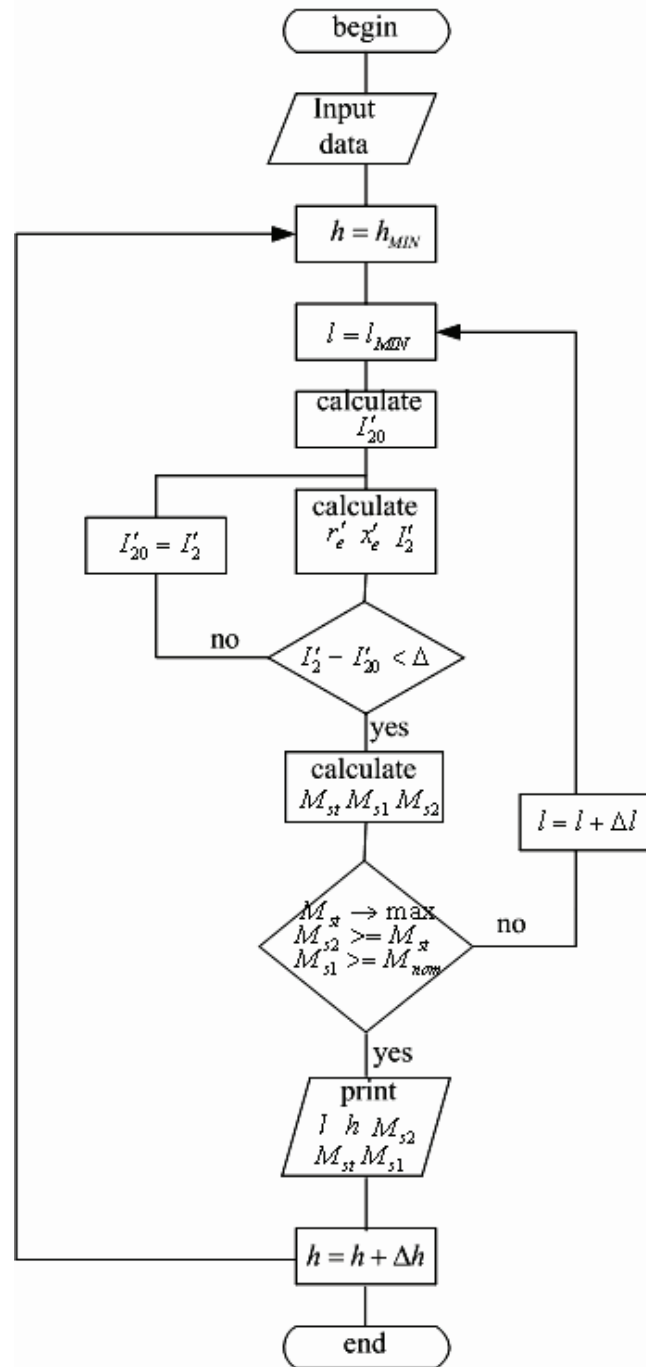


Fig.2. Algorithm of the program of search of the optimum sizes of a massive cartridge.

Calculation of equivalent parameters of cartridge case also is carried out by an iterative method. On a first step of calculation absence equivalent resistance is supposed. That gives the overestimated value of secondary rotor's current I'_2 . According to this value of a current make calculations of

equivalent parameters under formulas (1) – (9) and the next iteration rotor's current is defined. Process proceeds until the difference between values rotor's current on adjacent steps does not become less than some set size delta.

To make calculations we suppose, that known sizes are: numbers of pairs poles of synchronous and asynchronous machines, quantity of coils and factor of winding of a leading rotor, parameters of equivalent circuit AM, factors of approximation of a curve of magnetization of a material of a ferromagnetic cartridge case.

Thus, on each step (stage) most favourable of possible decisions get out.

It is necessary to note, that purposeful approach an optimum variant on each step of increase in thickness of a cartridge case is accompanied by approach of a kind of the mechanical characteristic to set kind. Results of work of the program are shown on the schedule (fig.3)

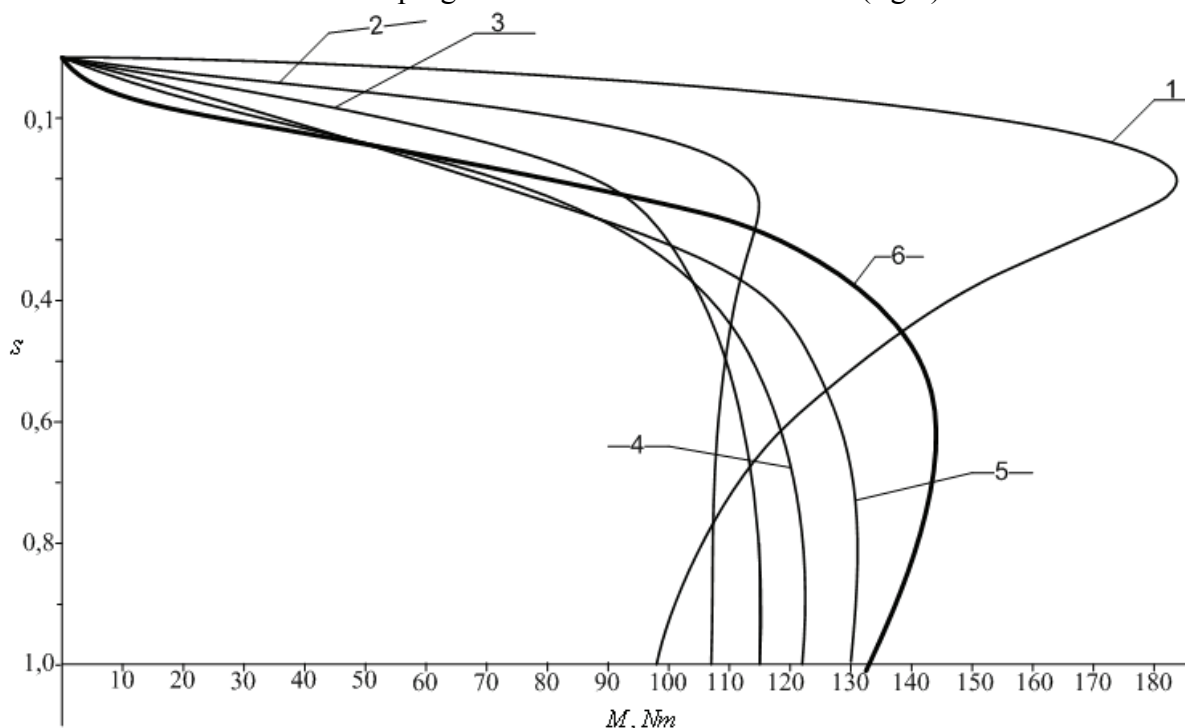


Fig.3. A series of mechanical characteristics of AM at constant frequency of rotation of a leading rotor, for different values of length and thickness of a ferromagnetic cartridge case: 1 - $h = 7mm$, $l = 5.4cm$; 2 - $h = 8mm$, $l = 9.4cm$; 3 - $h = 9mm$, $l = 10.4cm$; 4 - $h = 10mm$, $l = 11cm$; 5 - $h = 12mm$, $l = 11cm$; 6 - $h = 16mm$, $l = 11cm$.

As we can see from the schedule (fig.3) the most suitable variant is the mechanical characteristic № 2 with the optimum sizes of a ferromagnetic cartridge case $h = 8mm$, $l = 9.4cm$, its kind comes nearer to excavator kind.

Conclusions The offered technique of definition optimum geometrical sizes of a massive cartridge case allow designing AM with frequency depended resistance in a circuit of the secondary rotor, which have the improved starting properties and the set rigidity of the mechanical characteristic in the field of small slidings.

References

1. Аветисян Д.А., Соколов В.С., Хан В.Х. Оптимальное проектирование электрических машин на ЭВМ. – М.: Энергия, 1976. – 208с.
2. Красношанка Д.М., Устименко Н.И. Расчет эквивалентно вносимых параметров асинхронного короткозамкнутого двигателя с индукционными сопротивлениями в цепи ротора //Техническая электродинамика. – 1985. - №2 – С. 72 - 78.
3. Панасенков М.А. Электромагнитные расчеты устройств с нелинейными распределенными параметрами. – М.: Энергия, 1971. – 216с.

DEVELOPMENT OF ALGORITHM OF GENERATION OF ADVISORY INFORMATION FOR CREW UNDER EVOLUTION OF ABNORMAL CONDITION IN FLIGHT

The algorithm of generation of advisory information for crew under evolution of abnormal condition in flight is proposed.

Introduction. The world aircraft service experience shows that the main task of modern air transportation development is ensuring of flight safety and flight high efficiency.

Problem statement. The analysis of flight safety according to International Civil Aviation Organization (ICAO) [1, 2] shows that the main causes of accidents (of about 70 %) are crew errors. In this case the overwhelming majority is related to untimely and incorrect operation of crew. First of all it is connected by that the evolution of abnormal situation has rapid nature and crew not always have time required to counteract or stabilize development of condition occurred. In this connection for problem solving it is essential to search the ways to reduce the time required for crew to counteract development of abnormal condition or to prevent transition of a hazardous situation into catastrophic. This time will depend on nature of development of condition occurred, airplane aerodynamic characteristics, dynamic and psychophysiological characteristics of crew in particular abnormal condition, as well as from environment condition (6). This is why the concept of system "airplane-crew-environment" in abnormal condition during flight [7] has been introduced and justified for the further researches of possible ways of reduction of time required for crew. The concept definition takes into account the airplane aerodynamic properties, dynamic and psychophysiological characteristics of crew, environment condition, as well as nature of abnormal condition development.

Solution of problem. One possibility of reduction of time required for pilot to counteract or stabilize the development of standard abnormal condition can become implementation of information system output advices for crew. The analysis of the information obtaining by crew in case of abnormal condition has shown that available indication system includes aural and light signals which can be of warning or notifying type. The publication proposes the algorithm of generation of advisory information in the form of prescriptive prompting messages. These messages essentially will be advices for actions, prompting to crew what of possible alternatives they should use in the given occurred flight condition. To solve this problem the publication suggests to apply the mathematical tool using the controller based on fuzzy logic [3-5]

With that end in view the block diagram of manual control mode for the longitudinal channel including the fuzzy controller has been developed (fig. 1). The fuzzy controller algorithm can be presented as follows. The current value of derivative of pitch angle $\dot{\theta}_\tau$ is compared to its preset value $\dot{\theta}_s$, and the following error ε_θ passes to the fuzzification unit for transformation of its current value to its linguistic analogue. The fuzzy variable ε^* passes to the main component of fuzzy controller - the knowledge base. It is supposed to form the knowledge base of fuzzy controller on the basis of the algorithm: "If..., then..., else - aggravation of abnormal condition". Each control rule represents a fragment of knowledge and looks like "condition - action". This rule is presented in the knowledge base as follows:

- if ε will be ε^* then u will be u^* , else - aggravation of abnormal condition;
- if ε will be ε^{**} then u will be u^{**} , else - aggravation of abnormal condition;
- if ε will be ε^{***} then u will be u^{***} , else - aggravation of abnormal condition.

where $\dot{\varepsilon}$, \dot{u} – derivative of the following error, pitch control, while ε^* , ε^{**} , ε^{***} , u^* , u^{**} , u^{***} , – their linguistic estimations.

The defuzzification unit transforms the linguistic values u^* , u^{**} , u^{***} to their crisp numerical value u_{1g}^* , u_{2g}^{**} , u_{3g}^{***} . The found crisp value of control action will pass to multifunction display (MFD) in the form of advisory information for crew.

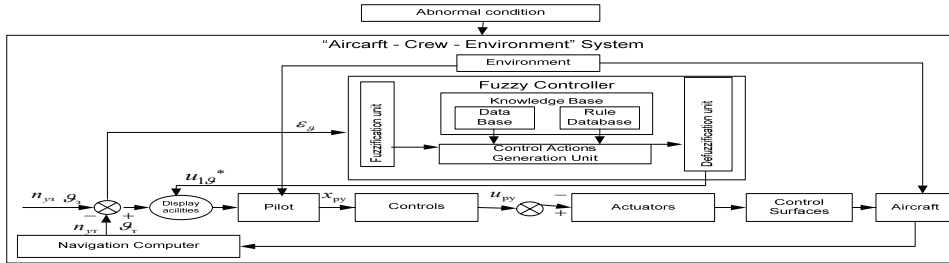


Fig. 1. Block diagram of manual control mode for the longitudinal channel including fuzzy controller .

where: $\dot{\mathcal{G}}_3$ - a predetermined value of derivative of pitch angle; $\dot{\mathcal{G}}_\phi$ – an actual value of derivative of pitch angle; n_3 - a predetermined value of acceleration; n_ϕ - an actual value of acceleration; x_{py} - a control action produced by crew.

However, the linguistic control rules by themselves cannot be realized on modern computers. To formalize its, it is offered to define the referred above cause-and-effect relations in natural language with application of the fuzzy set theory and linguistic variables with account for positive previous experience of actions of crews in the similar conditions received by results of cognitive simulation.

For this purpose we shall present the "Aircraft-Crew - Environment" system under abnormal condition as object having n inputs and one output [3]:

$$p = f(m_1, m_2, \dots, m_n), \quad (1)$$

where p - an output variable; m_1, m_2, \dots, m_n - an input variables.

The variables m_1, m_2, \dots, m_n and p are quantitative, therefore the limits of their variation are assumed as known:

$$M_i = [m_{i \min}, m_{i \max}], i = \overline{1, n};$$

$$P = [p_{\min}, p_{\max}],$$

where $m_{i \min}$ ($m_{i \max}$) p_{\min} (p_{\max}) - minimal (maximal) value of input and output variable.

The problem lies in the fact that for a vector $M^* = [m_1^*, m_2^*, \dots, m_n^*]$ of the fixed values of input variables $m_i^* \in M_i, i = \overline{1, n}$ of the specified "Aircraft-Crew-Environment" system under abnormal condition in flight it is necessary to determine required control action $p^* \in P$, i.e. crisp value of the controlled variable feed as advices on MFD. To estimate linguistic variables m_i , $i = \overline{1, n}$ and p the fuzzy sets will be considered: $S_i = [s_i^1, s_i^2, \dots, s_i^{l_i}]$ - fuzzy set of a variable m_i , $i = \overline{1, n}$; $V = [v_1, v_2, \dots, v_r]$ - fuzzy set of a variable p . These fuzzy sets s_i^q and v_j will be determined by ratio [1]:

$$s_i^q = \int_{m_{i\min}}^{m_{i\max}} \mu^{s_i^q}(m_i) / m_i ; \quad (2)$$

$$v_j = \int_{p_{\min}}^{p_{\max}} \mu^{v_j}(p) / p , \quad (3)$$

where $s_i^q(m_i)$ - function of an input variable membership $m_i \in [m_{i\min}, m_{i\max}]$ to the set $s_i^q \in S_i, q = \overline{1, l_i}, i = \overline{1, n}$; $\mu^{v_j}(y)$ - function of an output variable membership $p \in [p_{\min}, p_{\max}]$ to the solution $v_j \in V, j = \overline{1, r}$.

On the basis of expressions (2), (3) the ratio (1) defining relation between input parameters, describing the occurred abnormal condition m_i and necessary to prevent development of this abnormal condition by control action p , is formalized in the form of system of fuzzy logic expressions which are based on the knowledge matrix . Its fragment is shown in Table 1. The available expert data presented in the form of the knowledge matrix define relation between a set of input data describing the current state of "Airplane - Crew - Environment" system under abnormal condition $m_1 - m_n$ and corresponding sets of system conditions requiring control actions $v_j, j = \overline{1, r}$ as logic expressions of type "If (there is a condition), then (the certain control action is required to prevent its development), else - aggravated development of abnormal condition" (ref. Table 1).

Table 1

Knowledge matrix

No. of input value combination	Input variables				Output variable
	m_1	m_2	$\dots m_i \dots$	m_n	p
11	s_1^{11}	s_2^{11}	s_i^{11}	s_n^{11}	v_1
12	s_1^{12}	s_2^{12}	s_i^{12}	s_n^{12}	
...	
$1 k_1$	$s_1^{1k_1}$	$s_2^{1k_1}$	$s_i^{1k_1}$	$s_n^{1k_1}$	

It is supposed to solve the problem of filling the knowledge base of advices by use the knowledge base created on experience of previous successful actions of crews in similar conditions on the basis of cognitive simulation which is based on the subjective opinions of experts and analysts concerning to the condition occurred and possible recovery actions.

The principle of knowledge base generation with use of cognitive simulation, we shall consider by the example of standard abnormal condition. For the purpose the pitch angle following errors are accepted as input linguistic variables (fig. 1) ε_g and by its derivative $\dot{\varepsilon}_g$, and as an output linguistic variable the value of control action $\Delta \delta_{PB}$ (elevators) which in the form of advice will pass to MFD is accepted. The values of linguistic variables are offered to be defined according to stated below qualitative scale which is formulated in terms of the theory of fuzzy sets: NL - negative large; NM - negative middle; NS - negative small; N0 - negative close to zero; C0 - close to zero; P0 - positive close to zero; PS - positive small; PM - positive middle; PL - positive large;

It is supposed to generate the control actions in the knowledge base connecting linguistic values of input and output variables on the basis of the algorithm: «if, then, else - aggravation of abnormal condition».

To define a grade of linguistic values membership to the specified fuzzy sets, the team of experts has been offered to estimate ranges of values of input variables ε_g , $\dot{\varepsilon}_g$ and output variable Δ for the chosen standard condition δ_{pb} , then in regular intervals to locate between the maximal negative and positive values of these variables.

10 respondents - pilots and test-pilots having high and approximately equal level of authority took part in anonymous individual polling.

Then the experts has been offered to define a range of values of linguistic variables: ε_g pitch angle following errors and its derivative $\dot{\varepsilon}_g$, as well control actions $\Delta \delta_{pb}$ according to stated above qualitative scale which is formulated in terms of the theory of fuzzy sets. The results of testing for each linguistic variable are shown in Table 2.

Table 2

Knowledge base

No.	Error value ε_g	Error value $\dot{\varepsilon}_g$	Control action value $\Delta \delta_{pb}$
1	NL	NL or NM	PL
2	NL or NM	NS	PM
3	NS	PS or P0	PM
4	N0	PL or PM	PM
5	N0	NL or NM	NM
6	P0 or C0	N0	N0
7	P0	NL or NM	PM
8	P0	PL or PM	NM
9	PS	PS or N0	NM
10	PL or PM	NS	NM
11	PL	NL or NM	NL
12	N0	PS	PS
13	N0	NS	NS
14	P0	PS	PS
15	P0	PS	NS

In this case the fuzzy sets NL, NM, NS, N0 for $\{\varepsilon_g\}$ for a linguistic variable $\Delta \delta_{pb}$ correspond to control wheel position "Push", and fuzzy sets PL, PM, PS, P0 correspond to control wheel position "Pull".

The principle of advisory information generation on the basis of the developed knowledge base (ref. Table 2) can be explained as follows: "If the value of pitch angle following error $\varepsilon_g = 6$ corresponds to fuzzy set PS (positive small) with grade of membership 0,8" and "Value of rate of change of pitch angle following error $\dot{\varepsilon}_g = 3$ corresponds to fuzzy set PS (positive small) with grade of membership 0,6, then "NM (negatively middle) control action is required that corresponds to control wheel position "Push", else "Aggravation of abnormal condition". It is offered to display as advisory information: variation of the constitutive parameter, required control action. Since $\Delta \theta = \Delta \alpha + \Delta \beta$, and variation of flight path inclination angle, describing long-period longitudinal motion of an airplane occurs essentially slowly than variation of an angle of attack we shall made

assumption, that $\Delta\theta \approx \Delta\alpha$. On the basis of this assumption it is offered to output on MFD not pitch angle following error, but variation of an angle of attack (fig. 2).

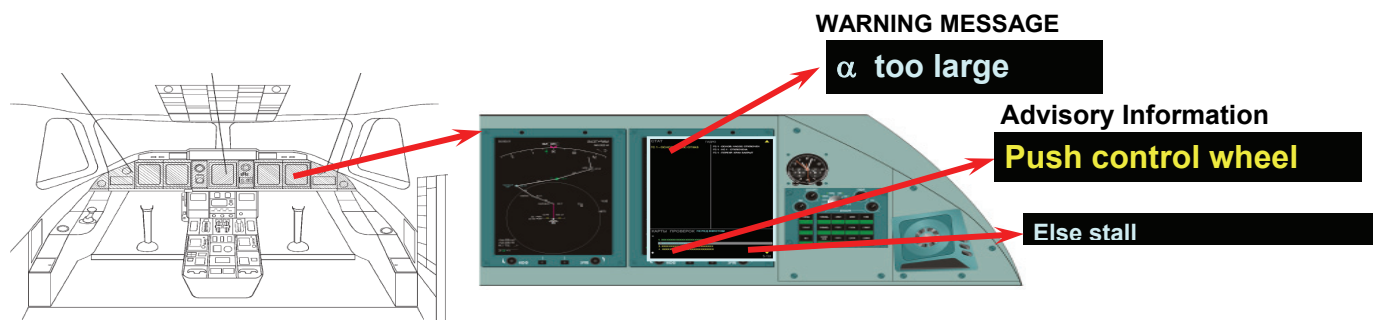


Fig. 2. Example of display frame of advisory information for crew on MFD.

Conclusions. Thus, the proposed algorithm of advisory information generation based on positive previous experience of experts - pilots allows formalizing the flight data in view of current development of abnormal condition in the form of fuzzy logic propositions connecting fuzzy variables and output control action displaying in the form of advice on MFD.

References

1. Полтавец В.А. Обобщение материалов расследования авиационных происшествий самолетов гражданской авиации, анализ и классификация ошибок их экипажей. - Отчет № 119-00-III. НИИАО, 2000.
2. Ноздрин В.И. Программа ИКАО дальнейшего исследования человеческого фактора и его влияния на уровень безопасности полетов.- М.: ВИНТИ, Проблемы безопасности полетов.- 2003.- №3- С. 8-26.
3. Прикладные нечеткие системы: Пер с япон./ К. Асаи, Д. Ватада, С. Иваи и др.; под редакцией Т. Тэрано, К. Асаи, М. Сугэно.- М.: Мир, 1993.-368 с.
4. Силов В.Б. Принятие стратегических решений в нечеткой обстановке. -М.: ИНПРО-РЕС, С.1995.С-148 .
5. Тачинина Е.М., Шевчук Д.О., Акмалдинов Е.Ф. Оценка возможности применения нечеткого регулятора для восстановления живучести воздушного судна и его управляемости // Матеріали 11-ї міжнар. конф. з автоматичного управління «Автоматика – 2004». – К.: НАУ. – 2004. – Т.4 – С.27.
6. Тачинина Е.Н. Казак В.Н. Оценка возможности сокращения времени требуемого экипажу для предотвращения особой ситуации в полете путем применения нечеткого регулятора. // Міжнар. наук. конф. «ISDMIT'2007». – Херсон: Видавн. Херсон. морськ. ін-ту.- 2007.-Т.ІІ.-С.64-68.
7. Тачиніна О.М. Казак В.М. Математическая модель системы «самолет-пилот-среда» в условиях развития особой ситуации в полете.// Проблеми інформатизації та управління: Зб. наук праць: Випуск 3 (18). К.: НАУ, 2006.-165 с.

*V. Vorobyev, P.h.D. (National Aviation University, Ukraine)
V. Zakharchenko, P.h.D. (National Aviation University, Ukraine)
S. Enchev, P.h.D. (National Aviation University, Ukraine)
V. Tikhonov, P.h.D. (National Aviation University, Ukraine)*

PROBABILISTIC DYNAMIC MODEL OF ESTIMATION OF FAIL-SAFE FEATURE BOOTHING ERGATIC INTERFACE

Booth integrated interface of the system is a «crew–aircraft–environment» is a key complex in the tasks of realization of strength security of flights of air ships. Amount of the aviation incidents accomplished through fault of «human factor», achieves 80 % from an incurrence. International organization of civil aviation of ICAO offered to the entire countries to create the control system by safety of flight on new principles of organization and quality.

Introduction. Modern to aircraft with the functional computer-controlled systems, crew with all system of preparation to activity, influences of environment and system of their warning require the estimations of quality and depth of joint co-operation in questions perfection of the system of the crews, system of priorities and values of providing of safety of flights training, to development on principle new side equipment.

Such approach is grounded by the analysis of aviation incidents (AI): on the stake of *human factor* is from 65 to 85 % all AI, from which to 80 % behave to erroneous actions of crews in difficult situations. Cost of error of crew constantly grows from permanent growth of primary cost of modern airplane increase of capacity of passenger salons and growth of cost of the crews training. Catastrophe of aircraft with the large number of passengers is perceived as state and national calamity. Exactly a high accident rate at passenger transportations disturbs ICAO, offering to the entire countries to create the control system by safety of flight on new principles of organization and quality.

There are the following contradictions in development of the functional systems of aircraft:

1. The faulttolerance of FS rises from one side, the resource of engines is multiplied, sides and ground methods and backer-ups strength security of flights are perfected, and with other - in sky above Europe, Japan, America becomes «all closer». Air space is intensively loaded besides by small aviation.

2. Conception of crew will be realized on the economic considering in composition two persons. The «truncated» crew has the limited possibilities and less chances to go out well from an extreme situation.

3. Introduction of the computer-controlled systems of warning about the collision with the obstacles promoted strength security of flights substantially, however computer-integrated these systems not are in a single informatively-managing complex. The systems not are reliable, subject to electromagnetic influences. The single multifunction complex of computer-integrated information is needed for *the increase of reliability of activity of crew on wing*.

Problem statement. Region A (fig. 1) is examined as probabilistic space of influence of environment only on a pilot (limited flight visibility, inadequate commands of controller, unsatisfactory luminosity, runway other). These factors do not render influence on the capacity of the functional systems and glider [1].

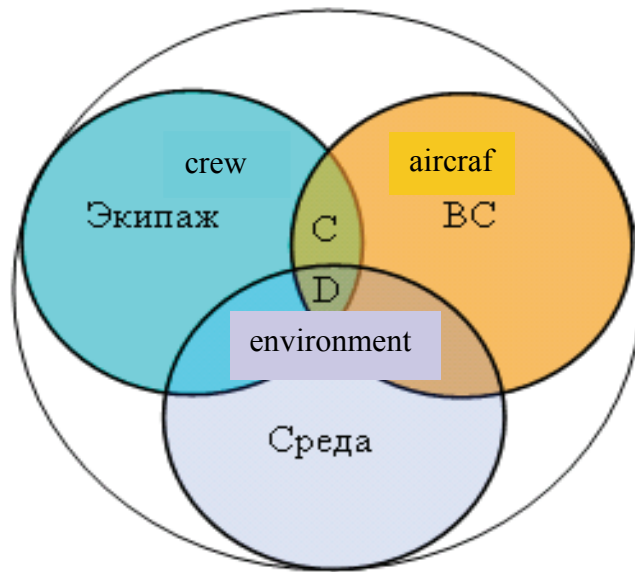


Fig. 1. Cooperation of causal factors on wing

Region B determines influences of environment only on an air ship and indirectly on a crew (temperature, humidity, pressure of air, turbulence). Thus always there is probability of hit in a dangerous environment „displacement” wind, „dust” storm, strong icing meeting with birds and other

Region C corresponds to the cases, when the errors of crew, caused by different reasons, are laid on on structural and ergonomic imperfections of concrete type of aircraft.

Region of D is examined as the incorporated influences of refusals of the functional systems and glider, errors of crew and simultaneous influences of environment on a crew and aircraft. Points of D form space of the most difficult, but rare flights situations, when saltatory probability of aviation incident increases.

Important that here each the component of the aviation transporting system and environment does not exceed possible limits and does not create the threat of safety of flights. Can account for combination of complicative factors by the display of system effect of synergetics character, resulting in the result of negative character – heavy aviation incident [2,3].

Basic assumptions: random events in the system «crew– aircraft – environment» independent and combinations of co-operation of the system take place „on to the chainlets”: A (crew – environment), B (environment - aircraft), C (crew - aircraft) and D (crew – aircraft – environment), where A,B,C,D, are regions of cooperation of elements, and crew, aircraft, environment, are elements of triad accordingly crew, aircraft and environment [4,5].

Solution of problem. Probabilistic dynamic model of estimation of the fail-safe feature system of «crew – aircraft –environment»

We will enter denotations:

$Q_{\text{э}}$ is conditional probability of errors of crew, negative factors caused by an aggregate;

Q_c is conditional probability of negative influences of environment;

Q_{BC} is conditional probability of refusals of the functional systems and glider of aircraft on wing;

Q_D is conditional probability of joint influence of erroneous actions of crew, negative influence of environment and refusals FS and glider (systems «crew–aircraft–environment»).

Conditional probability of origin of event of erroneous actions of crew and negative influences of environment.

$$Q_{A(\text{э}+BC)} = Q_{\text{э}}Q_c - Q_{\text{э}}Q_cQ_{BC} = Q_{\text{э}}Q_cP_{BC} \quad (1)$$

Conditional probability of joint event of negative influence of environment and refusals of FS and glider.

$$Q_{B(C+BC)} = Q_C Q_{BC} P_{\mathcal{C}} \quad (2)$$

Conditional probability of origin of joint event of erroneous actions of crew and refusal of FS and/or glider.

$$Q_{C(\mathcal{C}+BC)} = Q_{\mathcal{C}} Q_{BC} P_C \quad (3)$$

Difficult flight situation compound situation (CS) at joint influences in elements (C-F-E) and possibly heavy aviation incidents (emergencies, catastrophes). Conditional probability of origin of situations: CS, crash situation (CrS) or catastrophe situation (CatS) at combination of all refusals „small” (C-F-E)

$$Q_{\mathcal{A}} = Q_{\mathcal{C}} Q_{BC} Q_C.$$

Passing to probabilities of origin of events of A,B,C, \mathcal{A} , we use expression $Q_i = 1 - P_i$:

$$\begin{aligned} \text{A} \quad & 1 - P_A = (1 - P_{\mathcal{C}})(1 - P_C)P_{BC}; \\ & 1 - P_A = P_{BC} - P_{\mathcal{C}}P_{BC} - P_C P_{BC} + P_{\mathcal{C}}P_C P_{BC}; \\ & P_A = 1 - P_{BC} + P_{\mathcal{C}}P_{BC} + P_C P_{BC} - P_{\mathcal{C}}P_C P_{BC}. \\ \text{B} \quad & 1 - P_B = P_{\mathcal{C}} - P_{OC}P_{\mathcal{C}} - P_{BC}P_{\mathcal{C}} + P_C P_{BC}P_{\mathcal{C}}; \\ & P_B = 1 - P_{\mathcal{C}} + P_{OC}P_{\mathcal{C}} + P_{BC}P_{\mathcal{C}} - P_C P_{BC}P_{\mathcal{C}}. \\ \text{C} \quad & 1 - P_{\mathcal{U}} = (1 - P_{\mathcal{C}})(1 - P_{BC})P_C; \\ & 1 - P_{\mathcal{U}} = P_C - P_{\mathcal{C}}P_C - P_{BC}P_C + P_{\mathcal{C}}P_{BC}P_C; \\ & P_{\mathcal{U}} = 1 - P_C + P_{\mathcal{C}}P_C + P_{BC}P_C - P_{\mathcal{C}}P_{BC}P_C. \\ \text{D} \quad & 1 - P_{\mathcal{A}} = (1 - P_{\mathcal{C}})(1 - P_{BC})(1 - P_C); \\ & 1 - P_{\mathcal{A}} = (1 - P_{\mathcal{C}} - P_{BC} + P_{BC}P_{\mathcal{C}})(1 - P_C); \\ & P_{\mathcal{A}} = P_{\mathcal{C}} + P_{BC} - P_{BC}P_{\mathcal{C}} + \\ & + P_C - P_{\mathcal{C}}P_C - P_{BC}P_C + P_C P_{BC}P_{\mathcal{C}}. \end{aligned} \quad (4)$$

Conditional probability of total effect $Q_A, Q_B, Q_C, Q_{\mathcal{A}}$:

$$\begin{aligned} Q_{\Sigma} &= Q_A + Q_B + Q_C + Q_{\mathcal{A}} = \\ &= 4 - P_A - P_B - P_C - P_{\mathcal{A}}. \end{aligned}$$

Probability of happy end of flight at the job processing:

$$P_{\text{оnn}} = 1 - P_{\mathcal{C}} - P_{BC} - P_C + P_A + P_B + P_{\mathcal{U}} + 3P_{\mathcal{A}}, \quad (5)$$

where P_A is probability of that event And {erroneous actions of crew and negative influence of environment will not happen at the flight job processing}; P_B it is probability of that event In { joint event of negative influence of environment and refusals of FS and/or glider} at the flight job processing will not happen; P_C it is probability of that event with { joint event of errors of crew and refusals of FS and/or glider} at the flight job processing will not happen.

Passing in expression (5) to the probabilistic form of function of time for areas, it is possible to get analytical expression of probability of happy end of flight in the form of time of exploitation. It allows at the known statistical estimation of events A, B, C and to carry out D statistical design of complex index of fail-safe feature aircraft:

$$\begin{aligned} P_{\text{оnn}}(\Delta t_n) &= 1 - P_{\mathcal{C}}(\Delta t_n) - P_{BC}(\Delta t_n) - P_C(\Delta t_n) + \\ &+ P_A(\Delta t_n) + P_B(\Delta t_n) + P_{\mathcal{U}}(\Delta t_n) + 3P_{\mathcal{A}}(\Delta t_n), \end{aligned} \quad (6)$$

$$\text{where } t_n = \sum_{i=1}^n \Delta t_i.$$

Conclusions

1. A probabilistic model (6) is universal for the estimation of fail-safe feature aircraft and can be resulted to the known form for the complex index of fail-safe feature (1) at the independent events of the system «crew is aircraft is environment», when regions A,B,C, and D degenerates in the empty sets.

2. The analysis of statistical information on the stages of flight $(\Delta t_i) \quad t_n = \sum_{i=1}^n \Delta t_i$ allows to draw structural conclusion about the increase of the fail-safe feature system «crew is aircraft is environment» and to expose the tense dynamic areas of stages of flight of aircraft, the coefficient of risk of activity of crew can serve as the numeral index of these modes and capacity of aircraft

3. Automation and cooperation of elements of the system is a «crew is air ship is environment» of cab interface of aircraft are those key bases of increase of strength security of flights and efficiency of the air system, when the variety of processes can be conditioned by the examined probabilistic dynamic model of fail-safe feature and quantitative results of researches.

References

1. *Теймуразов Р. А., Полтавец В. А.* Анализ безопасности полетов самолетов с газотурбинными двигателями за 50 - летний период (1957...2006 г.г.) эксплуатации в гражданской авиации СССР и государствах - участниках соглашения о гражданской авиации и об использовании воздушного пространства (пассажирские перевозки)/Воздушный транспорт. – М.: Воздушный транспорт, 2007 – №48-51.
2. *Шишкин В. Г.* Безопасность полетов и бортовые информационные системы. Иваново: МИК,2005. – 240 с.
3. Руководство по предотвращению авиационных происшествий. М. : ИКАО, 1984. – 18с.
4. *Воробьев В.М., Киселев А.Д., Захарченко В.А., Ваику О.Ж., Воробьев А.В.* Системная эффективность функционирования авионики/Кибернетика и вычислительная техника. 2000. – Вып. 126, С. 48-76.
5. *Воробьев В. М., Киселев А.Д., Захарченко В. А., Семида В. С., Енчев С. В.* Современные проблемы и тенденции автоматизации и взаимодействия кабинного интерфейса комплекса «экипаж – воздушное судно – среда» / Кибернетика и вычислительная техника. – 2008. – 26

BASE COMPLEX OF RADIO ELECTRONIC EQUIPMENT OF AN-148 AIRPLANE

The base complex of radio electronic equipment of AN-148 airplane is reviewed in this article, as well as its descriptions and possibilities, in regard to the task of regional passenger and cargo airplanes modernization.

Introduction to An-148 airplane avionics creation. The excellent example of Russia and Ukraine mutual cooperation in the high-tech sphere and particularly in aircraft building is creation in the required rate and in the possible earliest date of competitive regional airplane AN-148 that has passed its certification tests in 2007. The integrator of An-148 airborne electronic complex (avionics) is OJSC «Aviapribor - Holding» that is included in Russian Air Instrument-Making Alliance. The participation of the leading Russian avionics developer and producer in AN-148 program allowed ANTK of O.K. Antonov to reach considerable success in short terms and with maximal economic efficiency. At designing appearance of AN-148 airplane avionics three variants of avionics complex design were reviewed: design on the equipment base of CIS production; mixed variant and complex with the use of integral crates of the computer systems and complex control of flight navigation and radio engineering systems [1, 2, 3].

Task formation for design and research processes. The task of avionics choice has required taking into account many factors in order to optimize the aircraft quality with minimum expenses and risks, main of which are the following:

- technical avionics descriptions should correspond to the modern level and perspective requirements of ICAO (AP-25, JAR-25);
- equipment systems are to be certificated;
- cost of equipment set is to be at minimal level;
- expenses on the new systems creation, modernization as it applies to the AN-148 airplane conditions, and integration are to be minimized, including expenses on system integration.

An-148 airborne electronic complex or avionics is integrated ensemble of associated computer systems, indication facilities and management, sensors, aggregates and information exchange channels, providing at high-automated level realization of effective co-operation within the system «crew – aircraft – environment» in order to fulfill the requirements to the airplane.

Functions of avionics complex. Implementation of pilotage, navigation, communication and controlled supervision tasks is determined by ICAO, CNS/ATM conceptions:

- automated planning of flight task;
- automation of air navigation and pilotage;
- navigation with following RNP and RNAV requirements ;
- automatic and directive landing according to IIIA category of ICAO;
- granting the crew integral information about the flight and environment parameters, the technical condition of the avionics systems and aggregates, standard airplane equipment (SAE) and power installation;
- co-operation with flight control and air traffic facilities, and other aircrafts;
- avionics automated control and technical maintenance by airplane controls and diagnostics;
- possibility of modern technical service strategies («by the state») use.

For AN-148 airplane *system integrator* of standard avionics complex is ANTK of O.K. Antonov with assistance of OJSC «Aviapribor - Holding» - the developer of the following systems:

- computer system of air navigation with the block of databases (BCC-100);
- complex system of electronic indication and signaling (КСЭИС-148);
- systems of automatic flight control (СAY-148);

- electronic remote control system (ЭДСУ-148).

These systems are basic integrate elements of any airplane. As a technical humanization on AN-148 airplane the following systems of Ukrainian development are installed:

- standard airplane equipment control system (СУ ОКО-148);
- system of the early warning and approaching earth (СПИПЗ-2000);
- informative complex of high-speed parameters (ИКБСП-148);
- integrated (VOR/ILS/MPK) radio engineering system (КУРС-93).

The standard systems of avionics include the following systems:

- collision avoidance system - TCAS-200 (USA);
- laser attitude-and-heading reference system - LCR-93 (Germany);
- satellite navigational - CHC-2 (Russia);
- reserve devices (Russia);
- radio navigation equipment - РСБН-85 and DME-85 (Russia);
- radio communication equipment (USA).

Structure of AN-148 airplane avionics has opened flexible architecture that allows potential Customer to form equipment composition without the airplane revision. Aircraft equipment corresponds to all modern requirements and recommendations of ICAO and EUROCONTROL, and due to the flexibility of architecture provides the requirements of the nearest and distant prospects.

The computer system of air navigation (BCC-100) allows to decide the tasks of automatic aircraft control in four-dimensional space (4D), to execute the automatic maneuvering on the standard charts of arrival (STAR), departure (SID), approach landing (APPROACH) and maneuvering in the area of expectation (HOLD), to carry out the calculations of departure and landing descriptions, including engineless.

The newest system of complex indication and signaling (КСЭИС-148) on the base of five multifunction liquid-crystal indicators (6x8 inches) substantially improves ergonomics of flight compartment. The decline of two persons crew load is carried out with the use of complex management control for the computer systems of air navigation CDU-6200, radio communicational and radio engineering equipment RTU-4200.

Digital service and command communication in ACARS system (on CPDLC channel) together with air traffic management service and in the prospect of CNS/ATM conception implementation is carried out by data transfer equipment CMU-4000.

Realization of «paperless documentation in cockpit» principle foresees the possibility of 3 class electronic informational tablet (EFB) installation, when a technical document (flight operating manual, operating manual, etc.) is replaced with delivery of air navigation, official and certificate information to the crew.

Safety of flights is improved by setting the MNRLS system of the early warning of earth approaching with the function of «wind shift» identification on board of the aircraft.

The standard airplane equipment control system (СУ ОКО-148) allows to automotive information collection and treatment, fulfill administration, control functioning of the airplane systems, while simplifying the device boards arrangement and reducing crew loading during the flight.

The modern high-efficiency protection from atmospheric electricity is introduced on the airplane based on high-power installations tests (lightning protection). The terms of avionics electromagnetic compatibility are provided on the stage of drafting the designer documentation (requirements to avionics equipment technical tasks, recommendations, concordance of designer documentation).

On the airplane the three-level avionics control system is realized with the integral interpretation of information regarding the technical condition of the systems for flight and technical crews [4,5]. Denial localization in the systems is foreseen on the basis of the embedded systems of control (BCK).

New conception on control and exploitation of aircrafts of AN-148 type is developed on the basis of ARINC 624 and ARINC 604 guiding documents and recommendations. It is grounded on unified requirements to the embedded systems of control for functional systems based on board system of technical service (BCTO) as means of integration and cooperation in regard to results of control with centralized access to information.

BCTO and BCK efficiency are provided due to automation of automatic denial identification, its localization and messages transmission to the crew or to the remote terminal. BCTO of the airplane allows to fulfill the following functions [3]:

- to use means of technical service that are economically effective and convenient for use;
- to simplify procedures of technical service and minimize requirements to staff recruiting;
- to lower considerably exploitation expenses (in regard to continuity and labour involvement of technical service).

Conclusions

1. Avionics complex of AN-148 airplane conforms to the requirements of CNS/ATM conception and to the structure of Europe air space (ECAC) and North America air space as navigation strategy of ECAC for the period 2000...2015 year on all stages of the flight:

- *Running approach - take-off* (beginning of introduction 2000...2005, general introduction 2005...2010, without the use ILS 2010...2015).

- *Route*: automatic air navigation with provision of RNP-5 on all stages of the route, RNP-1 - in areas in the mode of RNAV (2005...2010), RNP-1, RNAV «free flight» (2005...2010).

- *Approach and landing*. Standard approaching scheme (STAR). RNP-1. Landing according to III A category of ICAO (2005...2010), co-operation with services of air traffic management and crew.

- *Ground running (after landing)*. Taxiing on the air field with aiming on lateral and longitudinal planes during the run and taxiing (ILS/GNSS - 2005...2010; GNSS/ILS -2010...2015).

- *Echelon on the height* providing shortened minimum levels on height. Crew provision with information about the environment, weather conditions, obstacles (2000. ..2015, taking into account the introduction of RNP, RNAV).

- *4D RNAV four-dimensional zonal navigation* (beginning of introduction in the period 2005...2010 , general introduction in the period 2010...2015).

2. Accurate characteristics of avionics complex:

- according to the co-ordinates of location: from CHC - 10...20 m; in КОИ mode: БКВ, CHC, CBC - 10... 100 m; БКВ, CBC, VOR/DME - 5 km; БКВ, CBC DME/DME - 0,7 km; БКВ, CBC, PCBH - 1 km; БКВ, CBC - 6% of the route:

- according to the way speed: from CHC - 0,15 m/s; in КОИ mode: БКВ, CBC, VOR/DME - 2m/s; БКВ, CHC, CBC - 0,15... 0,5 m/s;

- according to a veritable course: from БКВ - 20'+6'X1(hour); in КОИ mode: БКВ, CHC - 10'.

3. Tasks that are decided by avionics complex:

- flights according to the rules of flight on devices and rules of visual flight;
- aviating according to the methods of BRNAV and PRNAV, with RNP-1 and RNP-5 exactness level;
- maneuvering in the airport area according to SID and STAR charts;
- use of world air-navigation information base;
- III category landing;
- vertical echeloning after 300 m (RWSM);
- early warning of earth approaching (TAWS);
- warning of airplanes collision in mid air (TCAS);
- documenting of crew members negotiations;
- radio communication in MB and ДКМВ range, communication inside the aircraft;
- indication for the crew on LSD indicators (flight and navigation information, information about synoptic formations, including «wind shift», chart of flight routes; exit scheme from the air field area, charts of landing approaching, charts of airports and others).

4. Informational complex equipment co-operation is fulfilled taking into account ARINC429; ARINC 708A; ARINC 604; PTM 1495-75 (3); ГОСТ 18977-79; sound and video signals.

References

1. *Семейство* региональных пассажирских самолетов Ан-148. Краткое описание типовой конструкции (этап макетной комиссии). – К.: АНТК «Антонов», 2005. – 84 с.
2. *Краткое* описание бортового радиоэлектронного и электротехнического оборудования самолетов Ан-148 №01-01, №01-02. – К.: АНТК «Антонов», 2003. – 68 с.
3. *Мир* авионики. Журнал Российского авиаприборостроительного альянса. – Санкт Петербург. - №2. – 2005. – 98 с.
4. Воробьев В.М., Киселев А.Д., Захарченко В.А., Семида В.С. и др. Современные проблемы и тенденции автоматизации и взаимодействия кабинного интерфейса комплекса «экипаж – воздушное судно – среда». Часть 1 // Кибернетика и вычисл. техника. – 2007. – Вып. 153. – С. 71-87.
5. Воробьев В.М., Киселев А.Д., Захарченко В.А., Семида В.С. и др. Современные проблемы и тенденции автоматизации и взаимодействия кабинного интерфейса комплекса «экипаж – воздушное судно – среда». Часть 2 // Кибернетика и вычисл. техника. – 2007. – Вып. 154. – С. 66-81.

*Lysenko A. PhD (National Aviation University, Ukraine)
Kirchu P.I., (National Technical University "KPI", Ukraine)*

COMPUTER CERTIFICATION OF THE ROBUST CONTROL ALGORITHM

Possibility of application of classic method of synthesis of the automatic control system by the methods of logarithmic peak descriptions is described in this work, for creation of robust law of management unmanned flying object. The method of choice of type of regulator and calculation of his parameters is shown, at the change of parameters of the unmanned flying object and action of external revolting influences causing saltatory change of parameters of the automatic control system.

Introduction

One of the modern approaches to the synthesis of an automatic control system is the approach based on the ideas of robustness: the robustness of stability and the robustness of quality – under conditions of indeterminacy. Today, Papers [1], [2] have developed the method of the synthesis of a robust system for the objects being under the action of parametric disturbances belonging to the type of tim-smooth spline-approximated parametric actions. However, for a certain class of control objects, e.g., DPLA of a single action, an impulse external action is characteristic, causing a jumping in the parameters of a control system. The methods, making possible to synthesize a robust control for such objects adequately to a physical nature of disturbance, have not been developed yet practically. Therefore, the subject of this article is actual both from a practical and a theoretical point of view.

Problem statement

The approach to the synthesis of an automatic control system, based on the idea of a robust control, first of all, takes into consideration the fact that the real physical systems and external conditions, under which these systems operate, cannot be simulated in an absolutely accurate manner. The synthesis of a robust control system requires solving two problems: to determine the regulator structure and to adjust its parameters. This article has preserved the structure of the automatic control system prototype and made a channel-to-channel calculation of the PID regulator. The parameters of the regulator are chosen so that the system reaction may meet certain criteria of quality, in particular, the set damping time of transient processes, an acceptable overcontrol, the set reserve of the amplitude and phase stability. [3]

Contents

A two-channel structure has been taken as the basis of a control system, enabling the control of a single-action unmanned flying object (UFO), in two mutually-perpendicular planes of the coordinate system, linked with a selected object. [4] The structure of the mathematic model of a control system is shown in fig. 1. [5]

Explain physical sense of work of this structure. The linear co-ordinates selected by the device accepying laser ray serve as a managing signal, characterizing his deviation from the center of the laser informative ray formed by the special system of aiming.

Let us proceed to the synthesis and computer simulation of a robust control system, having restricted ourselves to the calculation of a relevant coefficient of proportionality for the PID regulators of both channels, as well as the parameters of the rejecter. These coefficients have been chosen by the decibel-log frequency response method and specified in the course of an imitation simulation of the guidance process.

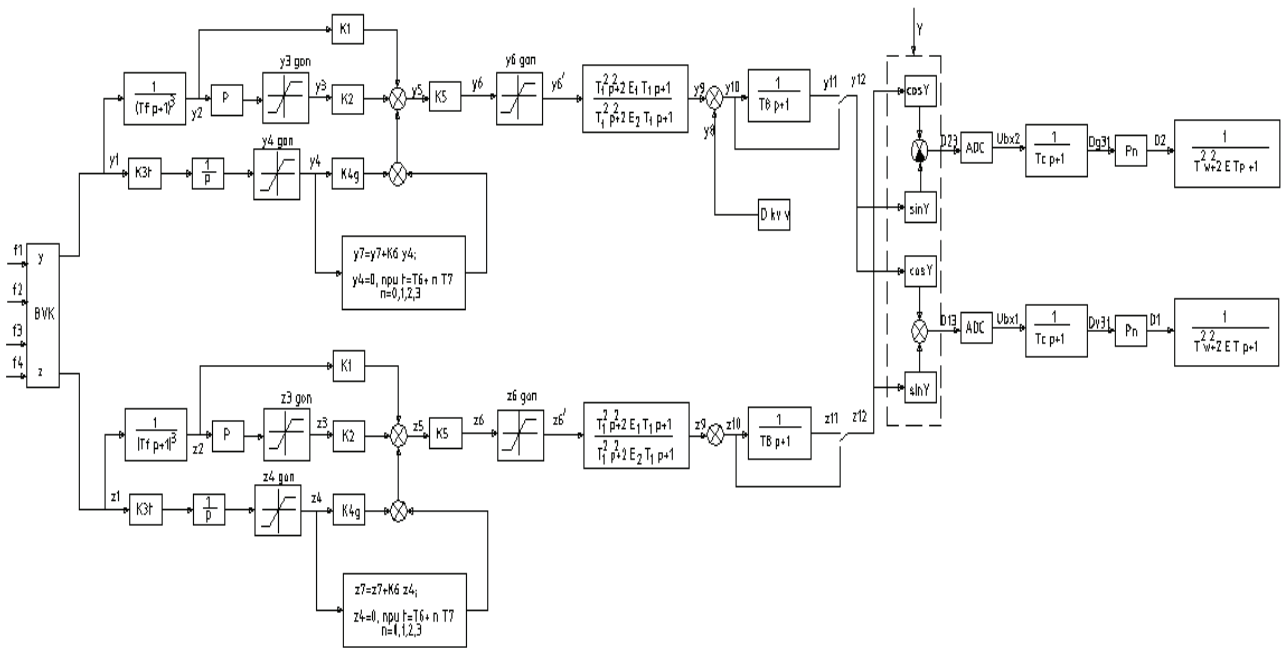


Fig. 1. Structure of the mathematic model of a control system

The amplitude-frequency response and the time change in the natural frequency of the UFO itself have been used in the choice of the parameters of the rejecter. As the structure of the automatic control system prototype is rather complex to be analyzed due to non-linear elements, composing it, the existing system has been suggested to be reduced to a certain shape.(1)

$$W = \frac{1}{p(T \cdot p^2 + 2\xi \cdot T \cdot p + 1)}, \quad (1)$$

Curves drawn on a fig. 2 shows the amplitude-frequency and phase response of the control object for characteristic points of the trajectory ($t = 0 - 16$ s), as well as the wished amplitude-frequency response of the entire system, comparing which the kind of regulator and its parameters are being chosen. The reduction behavior of the existing system, brought to a simplified shape, has enabled to facilitate the calculation of the coefficient of proportionality for the PID regulators and the parameters of the rejecter. The calculated parameters were set into the mathematical model of the automatic control system prototype and checked in the course of the imitation simulation of the initial system.

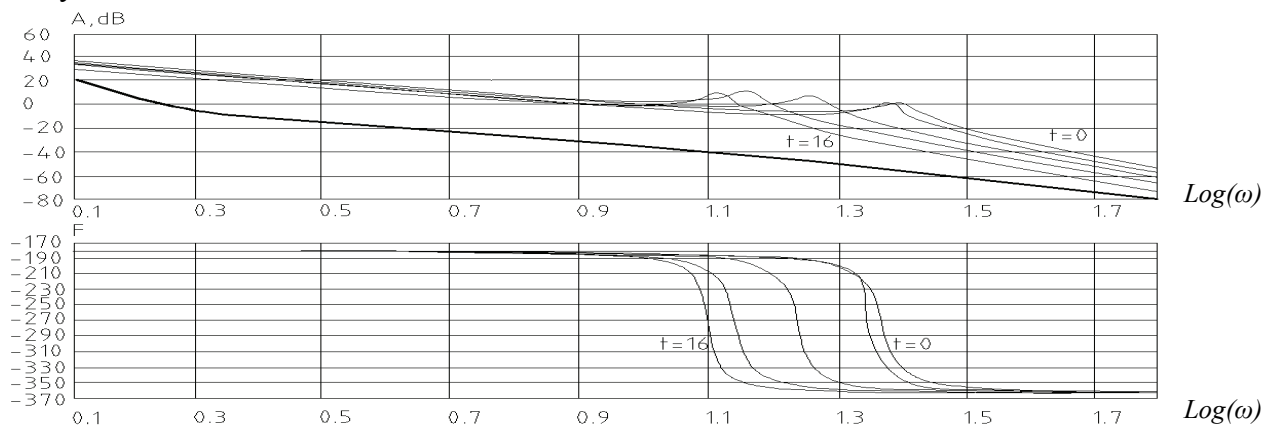


Fig. 2. Flock of the amplitude-frequency response of the control object and the wished decibel-log frequency response of the reduced automatic control system

As the boost of the UFO amplitude-frequency response does not exceed 20 dB at the natural frequency, parameters $\xi_1 = 0.05$, $\xi_2 = 0.5$.

The transfer coefficients of a control path have been chosen such that the maximum reserve of phase stability and an acceptable reserve of amplitude stability might be provided.

Curves drawn on a fig. 3 shows the flock of amplitude-frequency and phase response of the open-loop initial control system for the characteristic points of the trajectory ($t = 0 - 16$ s) with the chosen parameters of the control system.

These characteristics indicate that the reserve of an amplitude stability changes in the range from minus 5 to minus 10 dB, and the reserve of a phase stability from minus 30 to minus 45°. These reserves are sufficient to provide the stability of a closed loop system if the parameters of the control object change.

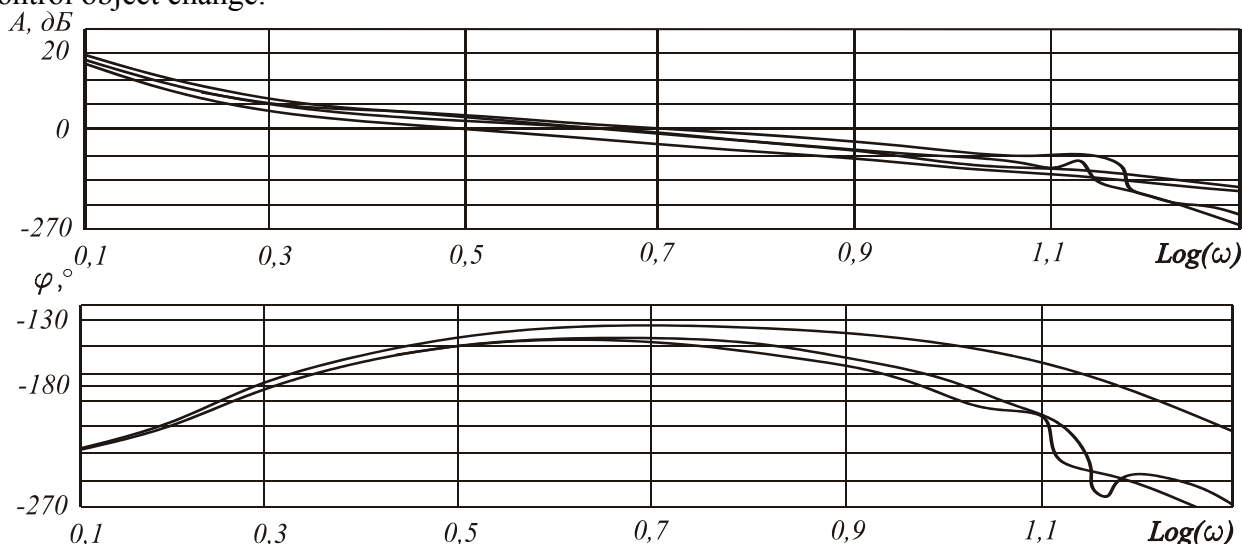


Fig. 3. Flock of the amplitude-frequency responses of the open loop system

Curves drawn on a fig. 4, 6 shows the response of the control system to a stepwise output signal along coordinate $Y_{\text{set}} = 1$ m with the maximum, mean and minimum speed of the UFO.

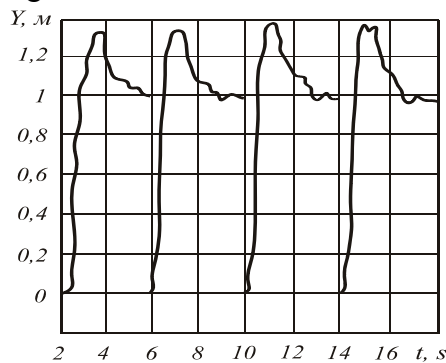


Fig. 4. The response of the automatic control system to the single stepwise signal at the different stages of the flight of the control object

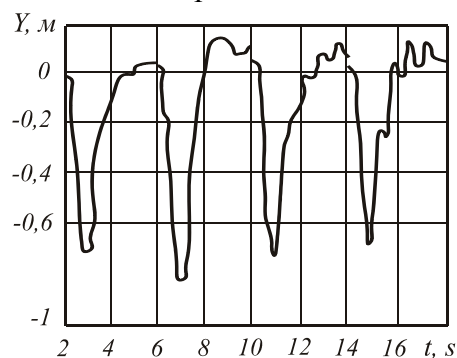


Fig. 5. The response of the automatic control system to the action of the wind disturbance at the different stages of the flight of the control object

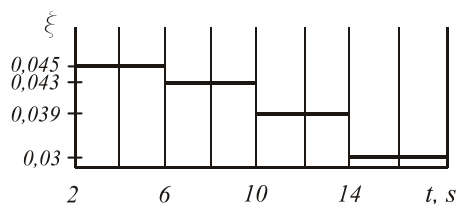


Fig. 6. The corresponding change in the damping coefficient (ξ) at the different stages of the flight of the control object

The quality of the transient process is satisfactory, the overcontrol is not more than 30%, the static error is absent since the control system, having an astaticism of the first order, processes constant control and disturbing effects without errors. Curves drawn on a fig. 4, 6 shows that the characteristics of transient processes do not change practically at all stages of the flight with the change in damping coefficient ξ of the control object.

The response of the control system to the disturbing effect has been estimated as its functioning under the action of a wind disturbance with a constant speed of 30 m/s, reduced to the equivalent rudder angle $\delta_v = 5^\circ$. Curves drawn on a fig. 5, 6 shows the graphs of repulsing disturbances at the different stages of the flight with the changed damping coefficient.

The control system repulses constant wind disturbances with a static error; the overshoot due to the deviation from the center of the ray does not exceed 0.7 m. The calculated coefficient of PID regulators and the parameters of the rejecter remained constant in the process of the imitation simulation, as the rest of parameters of the initial automatic control system changed in time.

Under such conditions, the parameters, characterizing the quality of the initial automatic control system with the synthesized stationary coefficients of the rejecter, remained unchanged, which is evidence of the robustness of the synthesized control law.

Conclusions

A conclusion may be drawn on the basis of an amplitude-frequency and phase response analysis and the simulation of the response of the control system to type actions that the control system with the chosen parameters is stable in a longitudinal motion and possesses sufficient dynamical properties. Curves drawn on a fig. 6 also show the change of damping coefficient ξ of the control object at the different stages of the trajectory. Curves drawn on a fig. 3, fig. 4 and fig. 5, fig. 6 prove that the change in the parameters of the control object does not influence practically the quality indices of the automatic control system and they remain in an acceptable range, which shows that the use of the decibel-log frequency response method to synthesize an automatic control system has enabled a robust control law to be achieved, which was itself the purpose of this article.

Reference

1. Ричард К. Дорф, Роберт Х. Бишоп Современные системы управления. – М.: Лаборатория базовых знаний, 2004. – 831 с.
2. Лебедев А. А., Карабанов В. А. Динамика систем управления беспилотными летательными аппаратами. – М.: Машиностроение, 1965. – 463 с.
3. Доброленский Ю. П., Иванова В. И., Поспелов Г. С. Автоматика управляемых снарядов. – М.: Оборонгиз, 1963. – 447 с.
4. Крикунов Л. З., Усольцев И. Ф. Инфракрасные устройства самонаведения управляемых снарядов. – М.: Советское радио, 1963. – 364 с.
5. Кочерышкина Т. А., Ветрова М. Б. Комплекс управления ракетным вооружение модернизированных танков Т-55М, Т-62М. – М.: Военная академия бронетанковых войск имени маршала Советского союза Малиновского Р. Я., Кафедра электроники и автоматики, 1984. – 59 с.
6. Лебедев А. А. Динамика беспилотных летательных аппаратов. – М.: Машиностроение. 1973.–212с.
7. Лебедев Р. К. Стабилизация летательного аппарата бесплатформенной инерциальной системой. – М.: Машиностроение. 1973.–315с.
8. Лазарев Л. П. инфракрасные световые приборы самонаведения и наведения летательных аппаратов. – М.: Машиностроение. 1973.–290с.

METHOD OF EVALUATION OF RELIABILITY AND VITALITY OF DIFFICULT ELECTROENERGY SYSTEMS OF AIR-PORTS

High strength and regularity of flights security is provided on all stages of litakovodinnya. That is why aspiration to attain the higher level of reliability of functioning of constituent of this process - technological equipment of surface facilities of the air fields providing of flights, fully appropriate. The equipment of surface facilities of providing of flights is especially sensible to quality of electric energy and interruptions of elektropostachannya.

The increase of reliability of his power supply allows substantially to decrease probability of critical situations on the stage "Flight-landing" of air ship (PS), that refusals with direct influence on life and health of people.

For planning, making and exploitation of the difficult electroenergy systems which provide the power supply of this equipment, as criteria of making optimum scheme-technical and organizational decisions use the quantitative indexes of vitality.

Raising of problem

Nateper reliability and vitality of elektropostachannya of responsible electro-receivers (EP) of the first category of the special group is provided due to the set amount of independent sources of power supply without taking into account them nadiynisnikh descriptions which from data of statistics differ in ten and hundreds one times.

The problem of providing of quantitative reliability and vitality of elektropostachannya of responsible EP of air-ports indexes yet and until now is not decided, and its actuality in connection with growth of intensity of flights in the whole world and, accordingly, requirements to their safety and regularity grows incessantly.

Consequently, development of method of evaluation of level of vitality of elektropostachannya of the system of svitlosignal'noy of the air field (SSA) brings in a ponderable stake in the decision of this problem.

Analysis of the last researches

For creation of method of evaluation of level of vitality of the difficult electroenergy systems which the systems of power supply of responsible EP are, were analysed the most widespread are known quantitative estimations in relation to their possible use. Yes, level of vitality of the system L_{ifi} , for which unloading is executed after frequency, that disconnecting of nevidpovidal'nikh EP is used, determine such correlation [1]:

$$L_{ifi} = (\Delta E_m - \sum_{i=1}^m \Delta E_i P_i) / \sum_{i=1}^m \Delta E_i P_i$$

where ΔE_m it is a border of nedovipusku of electric power after which vitality is at maximum level; ΔE_i - there are nedovidpusk electric power subject to the condition I-go indignation for a case, when protiavariyni automatic devices execute unloading after frequency with the purpose of saving of basic

functions of the system; P_i is probability of appearance of I-go indignation; m is an amount of indignations.

But for of air-ports such estimation can not be acceptable through their very low power comparatively with a grid and presence of plenty of responsible EP which can not be disconnected,

and also through impossibility of influencing such method on the brief interruptions of elektropostachannya.

For the evaluation of vitality also use the methods of system informative analysis [1], which operate probabilities of unachieving aims through violation of functioning of object, management knot on condition of a priori incomplete information.

$$\overline{O}_{L_{ef}} = \left| -Z_d(1-\gamma_1\overline{O}_1)\dots(1-\gamma_k\overline{O}_k)(1-\sum_{i=k+1}^n Si\overline{O}_i) \right|$$

Where $Z_d = f(a, z_{ef})$ is a coefficient of organization of management which depends on the estimation of vitality and knot of management and efficiency of work of management knot ;

γ_1, γ_k are coefficients of the reverse and cross influencing between determining aims;

$\overline{O}_1, \overline{O}_k$ - it is disorganization of determining aims; $\overline{O}_{k+1}, \overline{O}_n$ - it is disorganization of

complementary aims; S – is a coefficient of relative importance of complementary aims.

The index of having a special purpose disorganization and naslidkovi copulas between aims use for recognition of emergency situation and decision-making for its liquidation in some electroenergy systems and again due to disconnecting of irresponsible EP.

The quantitative indexes of level of vitality, which do not use probabilistic descriptions are known also, for example [3]:

$$L_j(E) = \min_{l_i \in E} \Phi_j(l_i)$$

Where $L_j(E)$ is an index of vitality of the system for the plural of possible external indignations of $E = \{l_1..l_i\}$;

Φ_j it is an index of quality of functioning of j-go variant of the system during indignation of l_i .

That in the conditions of vagueness for the evaluation of vitality after this index examine the worst case of functioning of the difficult system, here optimization of the designed system is erected to finding of such variant of the system, for which has a maximal value.

In the conditions of air-ports, where registered interruptions of elektropostachannya of centralized vvodiv, most acceptable is such estimation of vitality, as a parameter of stream of refusals of functioning with cascade development of indignation and mass violation of power supply of EP [4].

Raising of task

A purpose of researches is development of method of evaluation of vitality of the difficult electroenergy systems, separation of levers of influence on the got estimations and developments of recommendations in relation to the increase of vitality of elektropostachannya of EP of the first category of the special group.

Evaluation of vitality of the difficult electroenergy system

For the evaluation of reliability of functioning of the system of elektropostachannya of SSA will take advantage of certain in the article [4] criterion of its refusal.

Vector of the states of the system X is the casual function of time $\bar{H}_m(t)$ which takes on a value from the counted plural $X = \{X_m^{\alpha_m}\}$. Will consider the refusals of first multipleness of q_1 from by a successive possible refusal each to the k -go element, then a number of the states of the system is $\tau = k + 1$, and also refusals of second multipleness of q_2 by a successive possible refusal for two elements (at what one of these two lementiv could say no before with unfound out the so-called refusal, such as a refusal defence of breakers of circuits, erroneous spratsyuvannya built on automatic vvodu of reserve (AVR)), then $m = C_k^2 + 1$. At scenario approach the states of the system of m_s appear only and by the certain criterion of refusals, thus $m_s \ll m$.

At determination of criterion of refusal of the systems of reserving of industrial network (SRPM) which has two tires of the assured power supply on an output (SHGZH). ШГЖ1 and ШГЖ2 is used limitation of leading documents for the use of SSA. It is set that at the calculation of reliability of elektropostachannya of SSA the criterion of refusal of elektropostachannya is a refusal of one of SHGZH or two from three independent sources of power supply. This index was compared with violation of regularity of flights of PS.

For the calculation of reliability of elektropostachannya of SSA the power chart of SRPM is analysed and the followings scenarios of m_s are taken away with the refusals of q_1 for the certain criterion of refusal:

1. A short circuit is on the output of ПABP1 or ПABP2. Then will be the disconnected defence one of TSDZH and ADZH;

2. A short circuit is on SHGZH1 or ШГЖ2. Then at normal robotzakhistu and intersectional PAVR will be znestrumlenoy one of SHGZH.

Other scenarios with the refusals of q_2 are not examined on a background the considerable sizes of q_1 .

For all SRPM there is a parameter of stream of refusals at the calculation of reliability Ω will be determined through

$$\omega_{ШГЖ} : \Omega = 4 \cdot \omega_{ШГЖ}$$

Pursuant to operating normative documents there are limitations of the use of SSA on condition of presence of refusals of power supply, or refusals of her constituents, If to generalize different combinations of refusals of all functional groups of SSA and take them to the refusal of power supply, for the evaluation of vitality it is expedient to take no the criterion of refusal at once two SHGZH [4].

The evaluation of vitality of the difficult electroenergy systems upon typical settlements of reliability with average indexes which do not take into account technology of work of air-port, gives considerable errors. That is why there is a necessity in the account of the real division of duration of refusals and rare events, that refusals of AVR protective vehicles with the parameter of stream of refusals, greater than $10^{-3} - 1$, if duration of their existence is considerable enough.

On condition of the use of existent periodicity of verifications of capacity of SRPM of the system of svitlosignal'noy after the first and second categories of IKA0, that one time for a week, a refusal defence or erroneous switching of AVR without the proper signaling can exist at least week, that in the case of appearance of other refusals in the system of elektropostachannya can result in violation of elektropostachannya of responsible EP.

The refusals of power supply EP of the first category of the special group of air-port considerably differentiate on duration as a result of change of configuration of SRPM and introduction to work of different reserve electrical equipment, that is why they can be grouped in three groups:

1) brief interruptions of elektropostachannya of Tk by duration to 3 s, that take place on condition of considerable decline of tension of network, which short circuits lead to, robot niz'kovol'tnikh AVR of fast-actings with small self-controls of time;

2) middle interruptions of elektropostachannya of Tc by duration of 15 s, that take place as a result of refusal of niz'kovol'tnikh AVR and works of AVR of high-voltages, built on automatic repeated include a grid, by introduction to work of autonomous elektroagregativ of diesels;

3) of long durations interruptions of elektropostachannya duration of over 15 s, that take place on condition of refusal of SRPM with the aggregates of diesels, but duration them limited sometimes in 5 khv, as on existent technology after such term of znestrumlennya of surface facilities of providing of flights an air-port will be closed.

Will consider methodical approach to creation probabilistic - the determined model [1] for the evaluation of vitality of elektropostachannya of SSA on the example of typical SRPM [1], that answer all requirements and recommendations of IKAO.

In the case when vid two independent centralized sources of feed (vvodiv) of 1II and 2II through two power transformers of step-downs tension is given to the proper normal working entrance of the first and second built on AVR - A1 and A2. The entrances of emergencies (in the normal state turned off) of these devices are connected to autonomous diesel elektroagregata of R, and outputs through sectional AVR ELEMENT to two sections of IIIГЖ-III1i III2 are connected.

For the calculation of vitality of elektropostachannya of SSA it is necessary more detailed to consider a robot SRPM with the refusals of second multipleness of q2 [1]. Will describe situations which can result in the complete refusal of power supply of SSA.

Situation 1. The refusal of both sections of tires arises up in tom case, when after the refusal of one of the centralized sources with the parameter of stream of refusals to the start of diesel elektroagregata will say no other source accordingly

$$\omega_{2k}(\omega_{1k})$$

In this case brief refusals are possible only with the parameter of stream of refusals Ω or middling the protracted refusals Ω_{1c} elektropostachannya of SSA is in connection with tim, that the start

of diesel elektroagregata lasts 15 s.

Taking into account, that in last case of refusal take place only at the certain sequence of events: at first a refusal is middle or of long duration first or second centralized vvodu with the parameter of stream of refusals

$$\omega_{1C.D} = \omega_{1C} + \omega_{1D} \text{ or } \omega_{2C.D}$$

and then brief - with the parameter of stream of refusals

$$\omega_{1k}(\omega_{2k})$$

will get such expression:

$$\Omega_{1k} = \omega_{1k} \omega_{2k} T_k + \frac{\omega_{1CD} \omega_{2k} + \omega_{2CD} \omega_{1k}}{2} T_c = 3.2 \cdot 10^{-7} (0.2 \omega_{1k} \omega_{2k} + \omega_{1CD} \omega_{2k} + \omega_{2CD} \omega_{1k})$$

(1)

Coefficients in expression (1) certainly for the parameters of streams of refusals.

The parameter of stream of refusals of middle duration can be calculated after similar approach:

$$\Omega_{1C} = \omega_{1CC} \omega_{2CC} T_C = 6.3 \cdot 10^{-7}$$

Situation 2. Refusals two SHGZH of all trivalostey can take place, when during the of long duration refusal of one of centralized vvodiv dissuades any other, and diesel elektroagregat was not started, that said no in the mode expectation with probability of QDAO

If there is only one source of power supply of SSA in work, the leader of flights closes an air-port after adopting PS, which are on a circle. Let this time make $TD = 300$ s.

Then by analogy, it is possible to write down such expressions for the noted sequence of events:

$$\Omega_{2K} = \frac{\omega_{1D} \omega_{2K} + \omega_{2D} \omega_{1K}}{2} T_D Q_{DAO} = 4.8 \cdot 10^{-6} (\omega_{1D} \omega_{2K} + \omega_{2D} \omega_{1K}) Q_{DAO}$$

$$\Omega_{2C} = 4.8 \cdot 10^{-6} (\omega_{1D} \omega_{2C} + \omega_{2D} \omega_{1C}) Q_{DAO}$$

$$\Omega_{2D} = 9.6 \cdot 10^{-6} \omega_{1D} \omega_{2D} Q_{DAO}$$

$$Q_{DAO} = 0.5 \omega_{DAO} T_{n.DA}$$

ω_{DAO} - parameter of stream of refusals of diesel elektroagregata in the mode of expectation "reserve", and TPDA is time between verifications of his capacity.

Situation 3. The protracted shutdown of one of centralized vvodiv is characterized a forced downtime or prophylactic repair of Ko and possibility of refusal in the robot of diesel elektroagregata ratio. It follows to notice that in an air-port repairs of elektroagregativ of diesels and AVR during the difficult terms of weathers appointed will not be usually, and repairs in the centralized network execute regardless of requirements of air-port.

Before the shutdown of one of centralized vvodiv during the planned repair in a grid it is needed preliminary to start diesel elektroagregat and load it higher than minimum possible power. If diesel elektroagregat will say no in the working state with the parameter of stream of refusals ω_{DAP} an air-port on the set technology [4] will be closed after adopting airplanes which are on a circle. Coming from such development of events and their sequence, it is possible to write down such expressions

$$\begin{aligned} \Omega_{3K} &= \frac{(K_{B1} + K_{P1}) \omega_{2K} + (K_{B2} + K_{P2}) \omega_{1K}}{2} \omega_{DAP} T_D = \\ &= 4.8 \cdot 10^{-6} \omega_{DAP} [(K_{B1} + K_{P1}) \omega_{2K} + (K_{B2} + K_{P2}) \omega_{1K}] \\ \Omega_{3C} &= 4.8 \cdot 10^{-6} \omega_{DAP} [(K_{B1} + K_{P1}) \omega_{2C} + (K_{B2} + K_{P2}) \omega_{1C}] \end{aligned}$$

$$\Omega_{3Д} = 4.8 \cdot 10^{-6} \omega_{ДАП} [(K_{B1} + K_{P1})\omega_{2Д} + (K_{B2} + K_{P2})\omega_{1Д}]$$

Situation 4. Related to the possible short circuit on SHGZH with the parameter of stream of refusals $\omega_{ШГЖ}$ and by the refusal of identical protective switches with probability of refusal of one of them Q3.

In the case of origin of short circuit on SHGZH, defence which will disconnect her vid centralized vvodu and zablokue a sectional circuit breaker must work normally. If will say no defence of one of breakers of circuits of vvodiv, next defence, more near to centralized vvodu, will work, and a sectional switch will not be zablokovaniy. If there is not a power supply on any SHGZH, a sectional switch will be included on a short circuit, and at the possible refusal of this defence the second section of SHGZH can be turned off. Coming from the considered possible events, it is possible to write down:

$$\Omega_{4Д} = 2Q_3^2 \omega_{ШГЖ} = 2\left(\frac{\omega_3 T_{ПЗ}}{2}\right)^2 \omega_{ШГЖ} = 0.5 \omega_3^2 T_{ПЗ}^2 \omega_{ШГЖ}$$

ω_3 parameter of stream of refusals defence of breakers of circuits; $T_{ПЗ}$ is time between verifications of their capacity.

It follows to pay attention to te, that a similar situation can arise up in the system of elektropostachannya of air-port and in the case of short circuit on the tires of high-voltages with the parameter of stream of refusals $\omega_{БШ}$ if there is high-voltage AVR. It can result in the origin of refusal of middle duration while diesel elektroagregat will not be started:

$$\Omega_{4C} = 0.5 \omega_3^2 T_{ПЗ}^2 \omega_{БШ}$$

Situation 5. At the short circuit of SHGZH

$$(\omega_{ШГЖ1} = \omega_{ШГЖ2} = \omega_{ШГЖ})$$

turned off defence. Thus diesel elektroagregat is not started automatically, because on the entrance of block of control of tension diesel agregata tension remains normal.

After it the leader of flights informs the crews of PS about closing of air-port. For this time can say no the centralized source of power supply which feeds the second SHGZH.

At presence of ARV on high tension such event is improbable. In the total to the start of diesel elektroagregata there will be a brief refusal both SHGZH, or middle duration.

Respecting, that time on informing of crews Those are not exceeded by 20 s, the parameters of streams of refusals make like the first scenario:

$$\Omega_{5K} = \frac{\omega_{ШГЖ2}\omega_{1K} + \omega_{ШГЖ1}\omega_{2K}}{2} T_i = 3,2 \cdot 10^{-7} \omega_{ШГЖ} (\omega_{1K} + \omega_{2K})$$

$$\Omega_{5C} = 3,2 \cdot 10^{-7} \omega_{ШГЖ} (\omega_{1CD} + \omega_{2CD})$$

Situation 6. AVR is related to erroneous work. Working in the case of refusals of sensible elements at presence of tension with probability of QпABP.

Unlike the first to five reliability of chains of the second commutation is examined in this situation. Parameter of stream of refusals of such events ω_{nABP}

If signaling of such mode is (that is in many air-ports) not, he can last a few hours, or even a few days (let time between verifications make TPAVR). Then in the case of refusal of the centralized source of power supply on both SHGZH will not be tension, while diesel elektroagregat will not be started with probability of Q_{ДАО}.

Like will define the parameters of stream of refusals for a sixth situation:

$$\Omega_{6K} = T_{nABP} (2\omega_{nABP} \frac{\omega_{2K}}{2} + \omega_{nABP} \frac{\omega_{1K}}{2}) = T_{nABP} \omega_{nABP} (\omega_{2K} + 0.5\omega_{1K})$$

$$\Omega_{6C} = T_{nABP} \omega_{nABP} (\omega_{1CD} + 0.5\omega_{2CD})$$

$$\Omega_{6D} = T_{nABP} \omega_{nABP} Q_{d.a.c.} (\omega_{2D} + 0.5\omega_{1D})$$

Similar refusals can arise up and in the case of erroneous work of ARV on high tension, But they can be not taken into account, because time of existence of such mode will be insignificant as signaling of the state of AVR of high-voltages is obligatory, and a duty personnel quickly will interfere in a situation.

The additional stream of refusals can arise up in the case of coincidence of repair of diesel elektroagregata with the difficult terms of weathers or with the features of the system of elektropostachannya of air-port, that is why probability

of him for concrete terms it is needed to calculate and take into account.

For a typical chart with two elektroagregatami of diesels on charts one diesel elektroagregat is replaced two, and for other situations the parameters of diesel elektroagregata (it is needed to understand as generalized) are divided into two.

After the calculation of all constituents of parameter of stream of refusals it is necessary to make them and analyse. The parameter of stream of the together taken refusals of middle and large duration must not exceed 10-3, and brief - (2...5) 10-2 [4]. If they exceed these values, it is needed to develop the plan of influencing on them by the use of more reliable (modern) perfection of methods of exploitation, or loosening the holds on exploitation due to multiplying frequency and volume of works.

From all possible methods it is needed to choose most effective which with the least charges will be able to give a maximal effect.

Conclusions

1. For the evaluation of quantitative indexes of vitality of the difficult electroenergy system a method is developed with the use of statistical information which are registered in every air-port. The normative value of quantitative estimation of index of vitality needs in the special research and clarification only.

2. It follows to consider te, that she allows in wide scopes to regulate the parameters of quantitative estimation of vitality technical and organizational facilities advantages of the developed method.

References

1. Neret V.I., Sushenko O.A. «Method of evaluation of vitality of the difficult electroenergy systems» // Announcer NAU – 2004. - №2. – s. 121-125.

Samkov O.V., National aviation university, Ukraine
 Lytvynenko V.I., PhD, Lomavatsky I.E. J.Zaharchenko
 Kherson national technical university, Ukraine

OPTIMIZATION METHODOLOGY OF FINANCING PROJECTS ON THE BASIS OF IMMUNE ALGORITHM CLONAL SELECTION

The questions of methodology optimization of discounting projects are in-process examined on the basis of immune algorithm of clone selection

Problem decision. In the given job the approach to a choice of projects on the basis of the theory of fuzzy sets [3...5] is considered, at use of fuzzy index of the importance of the project (FIIP). For definition of the best distribution of the finance between projects, on the basis of FIIP, it is offered to use clone algorithm (CA)

Let - $P = \{P_1, P_2, \dots, P_n\}$ the set of the offered projects, which cost represents (b_1, b_2, \dots, b_n) ; $FIIP_i = (c_i^l, c_i, c_i^r)$ - an fuzzy index of the importance of the project ($P_i, i = 1, 2, \dots, n$), presented by fuzzy number with triangular function of an accessory, where - c a point of the greatest possible degree of an accessory, and $c^l - c^r$ the left and right borders of a range to which the estimated size can get; - b the general budget planned on performance of projects; - k quantity of experts which take part in a choice of projects; - m quantity of criteria of a choice.

Let's give to everyone the project a variable which x_i accepts value 1 or 0 depending on that, the project or not (1 – if the project is accepted, 0 – otherwise) is approved.

Thus, the problem consists in a choice of such projects which maximizes the general payment behind fuzzy criteria, and also satisfy to a condition of budgetary restriction:

$$\sum_{i=1}^n FIIP_i * x_i \rightarrow \max, \text{ with } \sum_{i=1}^n b_i * x_i \leq b \quad (1)$$

Let's characterizes each project fuzzy criteria of the choice presented in the form of linguistic variables "quality" (S) and "importance" (W). A scale of a linguistic variable "quality" we will divide into 7 classes: $S = \{EG, VG, G, M, P, VP, EP\}$ where EG - the best, VG - very beautiful, G - beautiful, M - average, P - below an average, VP - bad, EP - very bad. At a ten-mark scale fuzzy numbers with triangular function of an accessory will become: $EG = (9.5; 10; 10)$ $VG = (7; 8.5; 10)$ $G = (5.5; 7; 8.5)$ $M = (3.5; 5; 6.5)$ $P = (1.5; 3; 4.5)$

$VP = (0; 1.5; 3)$ $EP = (0; 0; 0.5)$ A scale of a linguistic variable "importance" we will divide into 5 classes: $W = \{VI, I, F, UI, VUI\}$ where - VI very important, I - important, F - average importance, UI - not important, VUI - very low importance. Value of this variable also we will present in the form of fuzzy numbers with triangular function of an accessory at ten mark scale: $VI = (8; 10; 10)$ $I = (5; 7; 9)$ $F = (3; 5; 7)$ $UI = (1; 3; 5)$ $VUI = (0; 0; 2)$ At necessity, the form of functions of an accessory of such fuzzy numbers can be defined behind the formula:

$$f_{\tilde{c}}(x) = \begin{cases} (x - c_l) / (c - c_l) & c_l \leq x < c, & c_l \neq c \\ (x - c_r) / (c - c_r) & c \leq x \leq c_r, & c_r \neq c \\ 0, & \text{else} \end{cases} \quad (2)$$

Let's assume that already there are fuzzy estimations from the person making the decision (PMD) quality and importance of projects. For association of these estimations we will use averaging. Let: $S_{ijt} = (s_{ijt}^l, s_{ijt}, s_{ijt}^r) \in S, i = 1, 2, \dots, n, j = 1, 2, \dots, m; - t = 1, 2, \dots, k$ there is the linguistic

rating appropriated(given) OPR of the project D_i by P_i criterion C_j . Also we will put, that; $W_{ijt} = (w_{jt}^l, w_{jt}, w_{jt}^r)$ $j = 1, 2, \dots, m - t = 1, 2, \dots, k$ there is the linguistic weight factor given PMD by D_i criterion C_j . We will enter variables:

$$\bar{S}_{ij} = \frac{1}{k} \otimes (S_{ij1} \oplus S_{ij2} \oplus \dots \oplus S_{ijk}), \quad \bar{W}_j = \frac{1}{k} \otimes (W_{j1} \oplus W_{j2} \oplus \dots \oplus W_{jk}), \quad (3)$$

where symbols and \otimes the designated \oplus operations of fuzzy multiplication and addition, accordingly. At the selected designations the variable represents \bar{S}_{ij} an average fuzzy rating of the project by P_i subjective criterion, C_j and is \bar{W}_j an average value of fuzzy weight factor of importance of subjective criterion C_j . Variables and also \bar{S}_{ij} \bar{W}_j are fuzzy numbers with triangular function of an accessory of a following kind:

$$\begin{aligned} \bar{S}_{ij} &= (\bar{s}_{ij}^l, \bar{s}_{ij}, \bar{s}_{ij}^r), \quad \bar{W}_j = (\bar{w}_j^l, \bar{w}_j, \bar{w}_j^r), \\ \bar{s}_{ij}^l &= \frac{1}{k} \sum_{t=1}^k s_{ijt}^l, \quad \bar{s}_{ij} = \frac{1}{k} \sum_{t=1}^k s_{ijt}, \quad \bar{s}_{ij}^r = \frac{1}{k} \sum_{t=1}^k s_{ijt}^r, \\ \bar{w}_j^l &= \frac{1}{k} \sum_{t=1}^k w_{jt}^l, \quad \bar{w}_j = \frac{1}{k} \sum_{t=1}^k w_{jt}, \quad \bar{w}_j^r = \frac{1}{k} \sum_{t=1}^k w_{jt}^r \end{aligned} \quad (4)$$

Generally weight factors of criteria should be normalize:

$$\bar{W}_{jN} = \bar{W}_j \otimes \left(\sum_{k=1}^m \bar{W}_k \right) \approx \left(\frac{\bar{w}_j^l}{\sum_{k=1}^m \bar{w}_k^l}, \frac{\bar{w}_j}{\sum_{k=1}^m \bar{w}_k}, \frac{\bar{w}_j^r}{\sum_{k=1}^m \bar{w}_k^r} \right) = (\bar{w}_{jN}^l, \bar{w}_{jN}, \bar{w}_{jN}^r) \quad (5)$$

$$FIIP_i = \frac{1}{m} \otimes \left[(\bar{W}_1 \otimes \bar{S}_{i1}) \oplus (\bar{W}_2 \otimes \bar{S}_{i2}) \oplus \dots \oplus (\bar{W}_m \otimes \bar{S}_{im}) \right] \quad (6)$$

According to an expansion principle will not be $FIIP_i$ fuzzy number with triangular function of an accessory. However for simplicity in practice approximately $FIIP_i$ consider as fuzzy number with triangular function of an accessory as:

$$FIIP_i \approx (c_i^l, c_i, c_i^r) = \left(\frac{1}{m} \sum_{j=1}^m \bar{w}_j^l \bar{s}_{ij}^l, \frac{1}{m} \sum_{j=1}^m \bar{w}_j \bar{s}_{ij}, \frac{1}{m} \sum_{j=1}^m \bar{w}_j^r \bar{s}_{ij}^r \right) \quad (7)$$

At the decision of a problem of a choice of the project we will use procedure of ranging of fuzzy numbers. Let \tilde{A} the fuzzy number, and its generalized expected value with an optimism index is defined μ as where $E_\mu(\tilde{A}) = \mu E_R(\tilde{A}) + (1 - \mu) E_L(\tilde{A})$ and $E_R(\tilde{A})$ is $E_L(\tilde{A})$ right and left expectations of value of number, \tilde{A} accordingly, $\mu \in [0, 1]$ and also $E_R(\tilde{A})$ are defined $E_L(\tilde{A})$ as:

$$E_R(\tilde{A}) = \int_{\alpha}^{\beta} x f_{\tilde{A}}^R(x) dx, \quad E_L(\tilde{A}) = \int_{\gamma}^{\delta} x f_{\tilde{A}}^L(x) dx \quad (8)$$

The parameters of characterizes $\mu \in [0, 1]$ degree of optimism OPR. For fuzzy number and $\tilde{A} = (c^l, c, c^r)$ optimism level it is easy $\mu \in [0, 1]$ to define, that $E_L(\tilde{A}) = 0.5(c^l + c)$ $E_R(\tilde{A}) = 0.5(c + c^r)$ At some level of optimism fuzzy numbers μ can be ordered by comparison of their generalized expected values at concrete sizes μ . For two fuzzy numbers and \tilde{A} and \tilde{B} ratio $E_\mu(\tilde{A}) < E_\mu(\tilde{B})$ $E_\mu(\tilde{A}) > E_\mu(\tilde{B})$ mean $E_\mu(\tilde{A}) = E_\mu(\tilde{B})$ that, $\tilde{A} < \tilde{B}$ and $\tilde{A} > \tilde{B}$ accordingly $\tilde{A} = \tilde{B}$.

For application clone algorithm it is necessary to define: a way of representation of decisions of a problem in the form of individuals, population of individuals, criterion function (affinity

function) and procedure of a reproduction which are switched on by operators of selection, replacement and hyper mutations of decisions.

Formally clone selection can present algorithm (1– 9):

$$CLONALG = (P^l, G^k, l, k, m_{Ab}, \delta, f, I, \tau, AG, AB, S, M, n, d), \quad (9)$$

where – P^l search space (space of forms); G^k , – space representation; l – length of a vector of attributes (dimension of space of search); k – length of a receptor of an antibody; – m_{Ab} the size of population of antibodies; δ - expression function; f – affinity function; I – function of initialization of initial population of antibodies; τ - a condition of end of job of algorithm; AG – a subset of antigens; AB – population of antibodies; S – the operator of selection; C – the operator of cloning; M – the operator of a mutation; n – quantity of the best antibodies which are selected for cloning; d – quantity of the worst antibodies which are subject to replacement with the new.

Clone the algorithm belongs to the class of evolutionary algorithms, however its advantage before such algorithms as, for example, the genetic algorithm, consists that hyper mutations are beautiful for research of local areas of search, while editing (i.e. removal of antibodies with low affinity) allows to avoid hit of decisions (antibodies) in local optimum. Thus, editing and a hyper mutation play complementary roles in the course of maturing affinity. In addition to a somatic hyper mutation and editing of receptors the part of the individuals generated by a casual rank which arrive in the general fund for safety of a variety of population increases.

The decision of the considered problem is the list of the projects accepted to financing. We will give to everyone the project a variable which x_i accepts value 1 or 0 depending on that, the project or not (1 – if the project is accepted, 0 – otherwise) is approved. Then it is possible to present each decision of a problem in the form and $(x_i, i = 1, 2, \dots, n)$ – a binary variable of a vector, $\bar{X} = (x_1, x_2, \dots, x_n)$ where n - the general number of projects. Thus, each individual of population will be made from the bats n which values will correspond to values of a vector $x_i \bar{X}$. Each individual of population has some estimation, which size similar with fitness of the individual. Value of such estimation is defined by criterion function $f(\bar{X})$. Traditionally CA define as maximizing algorithm. Then, as criterion function we will use ranging value of the total FIIP :

$$f(\bar{X}) = E_{\mu} \sum_{i=1}^n FIIP_i \quad (10)$$

In our research it was used three operators of selection: tournament, elite and selection by a roulette method. For definition of the most effective configuration CA there was a used test problem in which it was necessary to select from 52 projects such which would maximize criterion function at the set value judgment and satisfied restriction on the budget in size from 10000 standard units. Comparative experiments with genetic algorithm [6, 7] have been made.

The made experiments have shown, that the best results are reached at the size of elite in 16 individuals and the size of population in 32 and 128 individuals. On the basis of the developed algorithm of distribution of the finance between alternative projects the developed corresponding technique. It allows to receive rational variants of projects for concrete conditions of balance and restrictions. On the basis of aggregation the fuzzy index of the importance for each project which specifies is received, its realization can be how much useful.

The comparative characteristic of results of iterations

		Quantity of iterations of genetic algorithm		
		50	100	150
Selection method	Tournament	974.5025	1024.797	1028.562
	Elite	1023.135	1119.340	1108.092
	Roulette	1031.777	971.9800	1089.685
		Quantity of iterations clone algorithm		
		50	100	150
Selection method	Tournament	1000.6075	1036.853	1060.667
	Elite	1128.275	2119.125	2999.523
	Roulette	1181.243	1000.7850	2099.125

Conclusions. As a result of researches the solved optimizing problem to a choice of projects for financing and distribution of resources between the selected projects which are characterized by fuzzy criteria of a choice. It is offered to use optimizing procedure on the basis of the device fuzzy bulevogo programming and clone algorithm. The received results specify in higher efficiency clone algorithm at the decision of problems of the given class.

As a result of research methodology optimization of processes is developed on the basis of immune algorithm of clone selection and an optimization task is decided to the choice of projects for financing and allocation of resources between select projects which are characterized by the unclear criteria of choice.

References

1. Самков О.В., Климчук В.П. Особенности разработки и реализации авиационных целевых комплексных программ в Украине//Вестник НАУ. – К.:НАУ,2004.– №4(22).-С.55-60.
2. Самков О.В., Литвиненко В.И. Методологічний підхід щодо вирішення завдань розподілу ресурсів в умовах невизначеності// Зб. наук. праць ДНДІ авіації. – К.: ДНДІА. – Вип..2 (9), 2006. – С.220 – 225.
3. Вороновский Г.К. Генетические алгоритмы, искусственные нейронные сети и проблемы виртуальной реальности– Х.: ОСНОВА,1997.– 112с.
4. Кордзадзе Т.З., Бидюк П.И., Литвиненко В.И. Эволюционная оптимизация распределения финансов между альтернативными проектами на основе нечеткой логики//Искусственный интеллект.– 2002.– №3.– С. 574– 580.
5. Орловский С.А. Проблемы принятия решений при нечеткой исходной информации – М.: Наука. Главная редакция физико-математической литературы, 1981. – 208 с.
6. Litvinenko V., Bidyuk P., Baklan I., Kordzadze T. The evolution approach to optimal funding distribution between alternative projects //Международная конференция по прикладной математике.– К.: КПИ, 2002.– С.80-81.
7. Бидюк П.И., Литвиненко В.И., Гринавцев О.В. и др. Объектно-ориентированный подход к программной реализации задачи выбора проектов для финансирования при помощи генетического алгоритма//Вестник ХГТУ.– Х.: ХГТУ, 2003. №2(18).– С.110-116.

RESOURCE – CONSTRAINED PROJECT SCHEDULING TASK AND THEIR APPLICATION FOR CONFLICT SCENARIOS MODELING

To support the decision making in modern conflict it is important to know different ways of conflict's progress. General scheme of conflict scenario generation needs a generator that could form ramified process and aimed function that plays important role in rules of optimal decision variants selection

Introduction. To support the decision making in modern conflict it is important to know different ways of conflict's progress.

Problem statement. General scheme of conflict scenario generation needs a generator that could form ramified process and aimed function that plays important role in rules of optimal decision variants selection [1].

Under the term scenario we mean certain consequence of events $Sc_i = \Psi\{\theta_{1i}, \theta_{2i}, \dots, \theta_{ki}, \dots, \theta_{mi}\}$, where Ψ - is a relation of order. Event θ_{ki} is listed as set $\langle \{i_A\} \in I_A, \{j_B\} \in J_B, k \in L \rangle$, where $\{i_A\}, \{j_B\}$ - is a number of A and B sides' objects that takes part in the event, k - a unit, an object of one side's infrastructure of the conflict that is the target of the event, I_A, I_B - is a number of A and B sides' objects that takes part in the conflict, L - is the number of units that are the basis of the conflict's space.

Solution of problem. The aim of the conflict's scenario generation is a multi - criterial task [2]. One of the mostly used ways of solving it is a way of transforming it into mono – criterial task. This can be achieved by selecting the dominating criteria and applying restrictions to other. Let us choose the duration of the conflict as dominant criteria. Suppose each side of the conflict tries to imply the blitzkrieg strategy and save their resources during the conflict. The side that has minimal duration scenario, and according to it, loses recourses to the critical rate. Mathematic arrangement of this task is formed like that: on the conflict's scenario number $\{Sc\}$ a suitable scenario $Sc^{opt}(T; x_1, x_2, \dots, x_l) \in \{Sc\}$, should be found that corresponds the conditions:

$$Sc^{opt}(T; x_1, x_2, \dots, x_l): \quad T = \min_{j \in M_{Sc}} \sum_{k=1}^{G_j} \max_{i \in \theta_k} (t_{ik}^j + \Delta t_k^j) \equiv \min_{j \in M_{Sc}} T^j \quad (1)$$

Under limits:

$$\sum_{k=1}^{n+1} \max_{i \in \theta_k} (t_{ik}^j + \Delta t_k^j) = \sum_{k=1}^n \max_{i \in \theta_k} (t_{ik}^j + \Delta t_k^j) + \max_{i \in \theta_{n+1}} (t_{i(n+1)}^j + \Delta t_{(n+1)}^j) \quad (2)$$

$$\forall \theta_k \cap \theta_{k+1} \neq \emptyset: \quad t_{\theta_k}^j + t_{\theta_{k+1}}^j \neq t_{\theta_{k+1}}^j + t_{\theta_k}^j \quad (3)$$

$$G_j: (\forall i \in \overline{1, l}: x_i \leq x_i^k) \wedge (G_j + 1): (\exists i \in \overline{1, l}: x_i > x_i^k) \quad (4)$$

where M_{Sc} - is a conflict's scenario number; T^j - duration of j - conflict's scenario; G_j - number of events in j -scenario; t_{ik}^j - time for attraction of the i - object to the k - event in j - conflict's scenario; Δt_k^j - time for implementation of k - event in j - conflict's scenario; $t_{\theta_k}^j$ - duration of θ_k - event in j - conflict's scenario; $x_i, i = \overline{1, l}$ - conflict's model parameters. Limitations (2)-(4) play the role of the conditions the leads to the end of the conflict.

Tasks (1)-(4) are regarded to the calendar – planning class of tasks with limited recourses (RCPSp task). They are NP – complicated, because packing in the containers task is their part too [3]. Let us list the features of the task (1)-(4):

- Not all events can be applied to the certain conflict's scenario project. At the same time, some events can be applied to the same project more then once;

- Used in the scenario resources are added and the leftovers don't disappear when the event is over;
- The consumption of the resources is not even and depends on the event structure;
- Implementation time is not fixed and depends on the conflict's scenario structure and number of the event on the scenario structure;
- The search of the solutions is made on the set of the two – dimensional matrix of changeable length;
- The results of the conflict's scenario implementation depend from the events order in it.

The methods, targeted at finding precise solution, can not be applied to finding *NP*-complicated solutions. That is why the search of “acceptable solutions” is guided with the help of iterative heuristic methods. Among the last, methods of search with limitations and evolution methods of analysis, genetic algorithms are widely spread. But to apply them directly is impossible because of the mentioned above features of the tasks (1).

To avoid this problems, the method of matrix – genetic modeling – the method that operates two – dimensional matrix code of changeable length was developed . The lines of the given code are arranged set of events that characterize chosen scenario of the conflict, and the columns contains information about the participation of the conflict's side objects in the chosen events.

The method was tested on the results of the conflict between USA (Confederates) and Iraq in 2003. According to different limitations on the variants of the conflict conducting, 3 optimal due to the criteria scenarios were created. Scenario 1 suggests simultaneous attack on Bagdad from the North and South, its coverage and encirclement. The wide use of aviation and missiles carriers is suggested. The given above scenario was not implemented because of the poor support of the northern group of confederates. To include this fact, new filter was added to the model (limitation) that excluded attack from the north. After calculation Scenario 2 was found. This scenario suggested the confederate attack from the north on Bagdad and from the east on Basra. At last the Scenario 3 was found – the scenario of confederate air attack.

Comparison analyzes, gained with the help of the matrix – genetic method of the conflict's scenario modeling of 2003, is listed in the Table 1.

Table 1

Comparison analyzes of the conflict's scenario

Conflict Parameters	Scenario 1	Scenario 2	Scenario 3
Conflict duration, days	25	16	15
Conflict duration, considering parallel actions, days	12	13	15
Complexity of Iraq's infrastructure	0.43	0.44	1
Complexity of Confederates' infrastructure	1.53	1.46	1
Defense potential of Iraq	0.48	0.34	0.44
Defense potential of Confederates	1	1	1
Reserve of Iraq's PMM	0.49	0.39	0.62
Reserve of Confederates' PMM	0.89	0.96	0.89
Ammunition reserve of Iraq	0.53	0.37	0.65
Ammunition reserve of Confederates	0.85	0.94	0.93
Loss of Iraq	43591	21678	28182
Loss of Confederates	814	1082	55
Results of scenario implementation	Seizure of Iraq's territory, encirclement of Bagdad	Seizure of the south and Bagdad	Defeat of the defense potential of Iraq

All parameters of the conflict's scenario, except loss, are given in the Table 1. in percentage, loss – men.

The comparison of the received data with the real conflict of 2003 shows good correlation Table 2.

Table 2

The comparison of the received data

Conflict Parameters	Scenario 1	Scenario 2	Real actions
Conflict duration, days	25	16	25
Loss of Iraq	43591	21678	36800
Loss of Confederates	814	1082	760

From fig. 1. it follows that the comparison of the second scenario to the real events that happened in 2003.

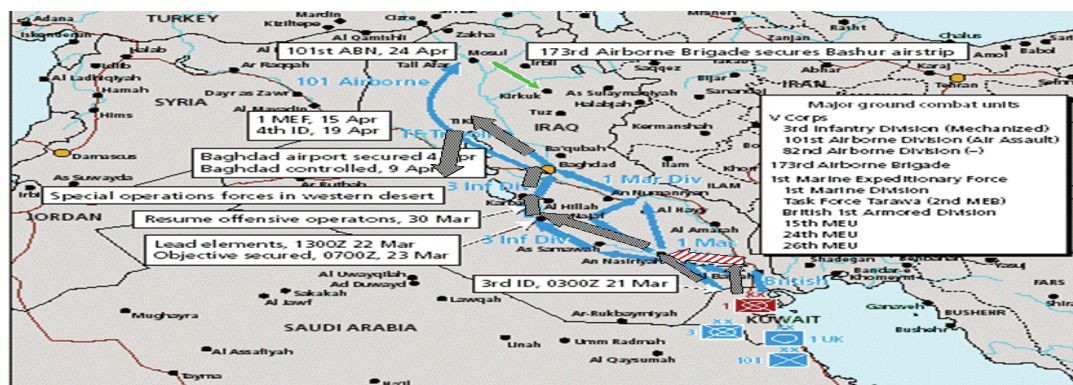


Fig. 1. Mapping of the second variant of the conflict 2003 on the map of Iraq. (scenario 2).

Bold arrows - result of the generated scenario, thin arrows – real actions.

Conclusions. Received results can help to make assumption about availability of this method of generating long – term scenarios of conflicts, and can be applied to the operation planning. Also it can be useful in creating study objects game simulators.

References

8. Слободяник В.А., Чумаченко С.Н. Подходы к генерации сценариев для поддержки принятия решений в конфликтных ситуациях //36. Системи підтримки прийняття рішень. Теорія і практика. – Київ: ІПММС НАНУ, 2005.- С.72-75.
9. Дружинин В.В., Конторов Д.С. Основы военной системотехники. - М. 1983. - 416с.
10. Гэри М. Вычислительные машины и труднорешаемые задачи / М. Гэри, Д.Джонсон. Пер. с англ. А.Фридман – М.: Мир, 1982. - 416 с.

INFORMATIONAL PROVIDING OF TECHNICAL OPERATION “ON CONDITION”

The structure of the integral information computer system for processing of parameters, which are characterizing the technical condition of control object, is offered, that allows to close the control loop of a technical condition of the object by negative feedback, what is enabling to pass from technical operation of object “on resource” to its technical operation “on condition”

Method of technical operation “on resource” with strategy of technical maintenance “on time” is traditional [1] and during operation of control objects with different technical purposes including aviation turbo engines, power-plants of compressors stations on main gas-pipelines, gas-turbines plants for ships is used until now. As is generally known [1], such method of aviation equipment operation results in nonoperation 0,3-0,9 of its actual resource. From other side, economic situation that is presently, forces to prolong the terms of operating whole row of objects (for example, majority of gas-pumping aggregates (GPA), which is on the balance of main gas-pipelines Management «Priкарпаттрансгаз», were entered into operation more than 30 years ago and, presently, the primary task is an extension of operation terms of these aggregates). It should be noted, that, already, after working off by GPA over 15-20 years its technical and economical indexes get worse substantially (the volumes of harmful extras in an atmosphere are increasing, reliability of its nodes diminishes considerably, expenses of maintenance and repairs grow). By a basic normative act, which is used for regulating maintenance organization of GPA with a turbine drive, is the «Temporal position of the preventive repairs system for gas-turbine plants with centrifugal superchargers», in accordance with which, the terms of repairs realization are foreseen. Without taking into account of actual condition of aggregate, its structural features, time from start of operation, identical terms for repairs realizations of all types of gas-turbines plants have been recommended there [2]. At a substantially outspent resource, such strategy of maintenance necessarily includes unplanned works for the plant restoration, because of refusals in separate nodes of GPA, volumes and terms of which are casual and have sufficiently large dispersion.

Characteristic feature of maintenance “on time” strategy is that the control loop of technical condition is unclosed (the statistical feedback that characterized by large delay and dispersion, cannot be examined as a feedback). For object under maintenance, a closing of the technical condition control loop by negative feedback on period between major repairs possibly, exceptionally, at a result of continuous and deep control of parameters that characterize its technical condition. Such control allows exposing disrepairs on the stage of their origin and predicting their further development. At declining from a norm of parameters that characterize a technical condition of control object, a feedback will provide immediately correction of this condition. Because presently, during operation of many control objects the using of maintenance “on condition” strategy is not assumed, and, consequently, the built-in checking systems of determining parameters are absent in them, and determining parameters are have been not assigned by the developer, the task of organization a maintenance “on time” with prognostication of the pre-refuse condition, and also technical maintenance “on condition” must have been decided on the base of regular control-measuring system (CMS). Taking into account this circumstance, integral information-computer system (IICS) of control the technical condition of object, that offered, is represented on fig.1.

The CMS of control object is a primary information generator about the current values of functional parameters. Measurable parameters at the diagnostic value, as a rule, are divided on groups. For example, among parameters measurable the CMS SAT-05 of GPA type GPP 10-01, the most diagnostic value is possessed by next parameters: temperature of working body after a turbine, pressures of air before and after a compressor (at such combination the control of the temperature value before a turbine is provided more reliable, if to compare with its direct measuring),

frequencies of rotation (high accuracy and stability of measuring), temperature of butter in a greasing system, a vibration of billow, temperature of working body on the exit of combustion chamber, a pressure of working body on the turbine exit, temperature in the cavity of turbines wheels, temperature of air on the exit of compressor, expense of fuel [3].

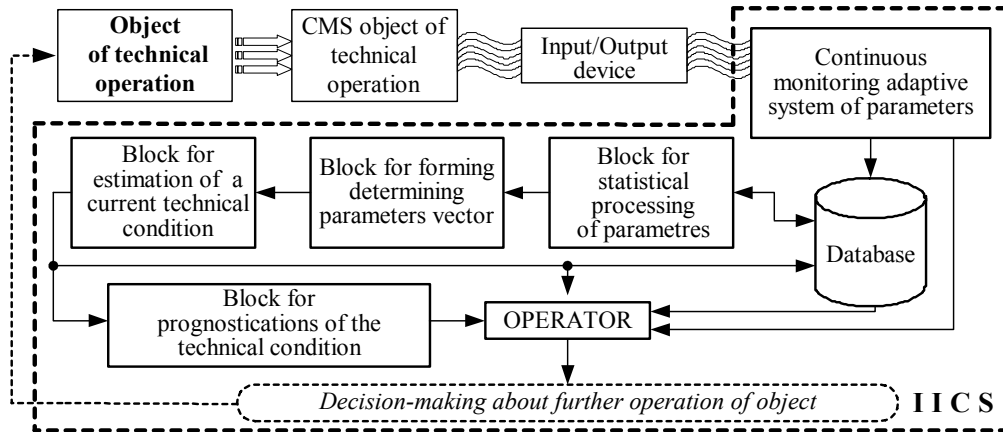


Fig. 1. Structurally functional scheme of IICS processing the parameters characterizing technical condition of object

Because, by the developer, in this example, determining parameters that characterize the technical condition of object, are not assigned; a primary task is a task of forming the vector of determining parameters. In articles [4], [5] the method for choosing of determining parameters that characterize the technical condition of turbo engine, is offered; it is based on a circumstance that at functioning of control object in regular modes, small deviations of functional parameters from their basic values take place. Therefore, as parameters that characterize technical condition of object under operation is offered to examine parameters of its linear dynamic model, in the complement of which functional parameters with most diagnostic value are entered. In this case, continuous monitoring system of parameters that characterize the technical condition of operation object is intended for realization continuous control of parameters of linear dynamic model, determination of moments their correction and new basic values calculation of linear dynamic model parameters that true to changed technical condition of object. Thus, a model and an object “gets older” together. Structure scheme of continuous monitoring system for parameters that characterize a technical condition of maintenance object, is represented on a fig. 2.

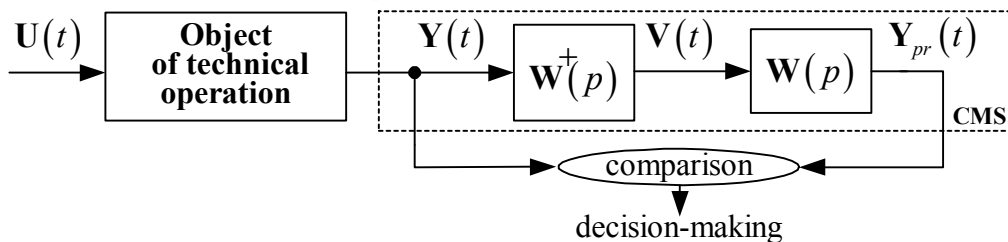


Fig.2. Structure scheme of continuous monitoring system for parameters that characterize technical conduction of object in transient behavior

In structure scheme on fig.2: $W(p)$ – transfer functions matrix of linear dynamic model for control object, $W^+(p) = (W^T(p)W(p))^{-1}W^T(p)$ – pseudo inverse matrix for $W(p)$.

Structure scheme for determination parameters of transfer functions, that format i -th line of object matrix under control, represented on fig.3.

Using the method of main component, between parameters of the dynamic model of control object exude statistically independent (or poorly dependent). Procedure of forming the vector of determining parameters is carried out in the proper block. In addition, in this block the purpose of defining the proactive admittances for determining parameters is carried out. A database is a single general system informative resource which is intended for arrangement storage of all information types at all stages of processing. A database can be divided into two basic blocks: block of

preliminary information, where primitive accumulation is conducted on for every measurable parameter and block of statistical information, where results of statistical processing at different stages are kept. The block of parameters statistical processing is intended for statistical processing thread of information about current values of parameters that characterize a technical condition of object and information from a database. The block of prognostication is intended for estimation of probability that forecast value of determining parameters vector will be in the field of admittance.

Fig.3. Structure scheme that allows parameters determination of transfer functions, formatting i -th line of matrix object under control

1. The structure of the integral information-computer system processing the parameters that characterize the technical condition of maintenance object, is offered, which allows carrying out monitoring and prognostication of these parameters, and is basis of informative support for decision-making at technical maintenance of object.
2. The description of object technical condition by parameters of its linear dynamic model is grounded for the wide class of objects, if their systems of control function on the mode of stabilizing, i.e. on the mode of the small rejections of functional parameters from their basic values.
3. The distinctive feature of approach that offered is: for technical maintenance of object it is possible to use both of maintenance strategy (combined strategy of maintenance “on time” with prognostication of the pre-refusal condition and strategy of maintenance “on condition”), without bringing of the difficult built-in and external checking systems, in conditions of regular functioning and statistical null data about a large number of same objects types, that takes place, for example, for GPA with a turbine drive.

1. Техническая експлуатація авіаційного обладнання / Под ред. В. Г. Вороб'єва – М.: Транспорт, 1990.–296с.
2. Довідник працівника газотранспортного підприємства / За ред. А. А. Рудника. – К.: Росток, 2001. – 1090с.
3. *Зарицкий С.П.* Диагностика ГПА с газотурбинным приводом. – М.: «Недра», 1987.– 199с.
4. *Асланян А. Е., Бельська О. А.* Локалізація несправностей в лінійних динамічних системах ОВТ / Збірник наукових праць ЦНДІ ОВТ. – К.:ЦНДІ ОВТ, 2007. – Вип. 18. – С.3-8.
5. *Асланян А.Э., Бельская А.А.* Забезпечення практичної безвідмовності функціонування газотурбінного двигуна при його експлуатації за технічним станом / Збірник наукових праць ДНДІ авіації. – К.:ДНДІ авіації, 2008. – Вип.19. – С.3-11

ASPECTS THE APPLICATION GAS SUPPRESSION ASSEMBLIES AT THE COMPRESSOR STATION

Process and block scheme of centralized automatic gas fire suppression system MIZHU is described. Strengths and weaknesses of the present system are analyzed.

Nowadays the Unified gas-supply system is one of the most important branches of national economy and dependable service of the international main gas pipelines provides economic stability for a lot of states. It gives the country of gas transit a chance to have a good reputation as a responsible transit country that results in construction of new main gas pipelines and receiving great financial investments into its economy in the future.

A modern compressor stations is the complex engineering structure providing primary of preparation and transportation of natural gas. It is an integral and constituent part of the main gas pipeline providing continuous gas transfer using gas-compressor unit and power equipment placed at the compressor plant. In particular, compressor plant parameters predict the performance of main gas pipeline, and in its turn it has a great effect on stable gas supply to consumers. Reliability level of compressor plant functioning over a period of several decades is still top-flight. Nevertheless, compressor plant is classified as fire and explosion dangerous facility. Fire hazard at the compressor plant and the lineal part of main gas pipe-line depends above all on physical/chemical properties of natural gas which can explode, inflame and result in technogenic accidents associated with fire spread under aberration from safe professional behavior. Gas transfer facilities have fire hazard grade which depends upon their technological process characteristics, such as:

- large fire gases volume in the linear and process parts of pipe line;
- high value of operating pressure figures;
- great many of fuel (steam-turbine oil) needed for gas-compressor unit work.

Statistics and operating experience shows the main ignition causes at the compressor plants as follows :

- oil flaming in the compressor section due to oil pipeline breakoff and his hits on hot surfaces of the gas-compressor unit;
- gas piping arrangement breakage in the compressor section ;
- foreign bodies in the supercharger cavern;
- ingress of inflammable substances through the leakages in shut-off and control valves;
- breakdown in process and fire prevention rules by operating personnel or field personnel (human factor).

In accordance with live regulatory documents the compressor plants fire protection is provided with sprinkler stations. They are obligatory for gas-compressor unit protection. As fire development at the oil and gas transportation facilities is defined by sudden flame spreading and explosion hazard, sprinkler stations should meet some rigid requirements. Thus, sprinkler stations are always chosen under the following requirements:

- operational benefit of fire fighting;
- performance reliability;
- fast response;
- commonality;
- ease of maintenance;
- should cost.

As seen, priority selection of the automatic fire-extinguishing system means technologic effectiveness of heat source suppression. Meanwhile, a wide range of different substances is used as

fire extinguishing agents: water, generated mechanical foam, powder, inactive gases, gas-aerosols as well as their combinations. In the preceding article we analyzed the present fire extinguishing agents and came to a conclusion that the only acceptable and adequate technologic effectiveness of fire suppression at the compressor plants is gas fire extinguishing agent, particularly, carbon dioxide CO_2 . Choice of gas fire suppression technology is also reasonable in view of equipment status of technical production capacities providing reduction in expenditure with relation to repair work and preventive measures carrying out as well as low cost of liquefied carbon dioxide.

Gas-compressor units are placed in the hangar-type installation of container-type, in the base machine halls. The most effective fire suppression systems are specified for each kind of units. For the purpose of unification the following classification of compressor plants fire protection is developed:

- up to 1 000 m^3 (balloons) CS should be protected by gas-fired assemblies based on high pressure modules;
- effectually using gas fire suppression at the compressor plants of volume exceeding 1 000 m^3 is achieved by gas-fired assemblies of low pressure based on isothermal modules (MIZHU).

The process flow of this unit is presented on the Figure.1.

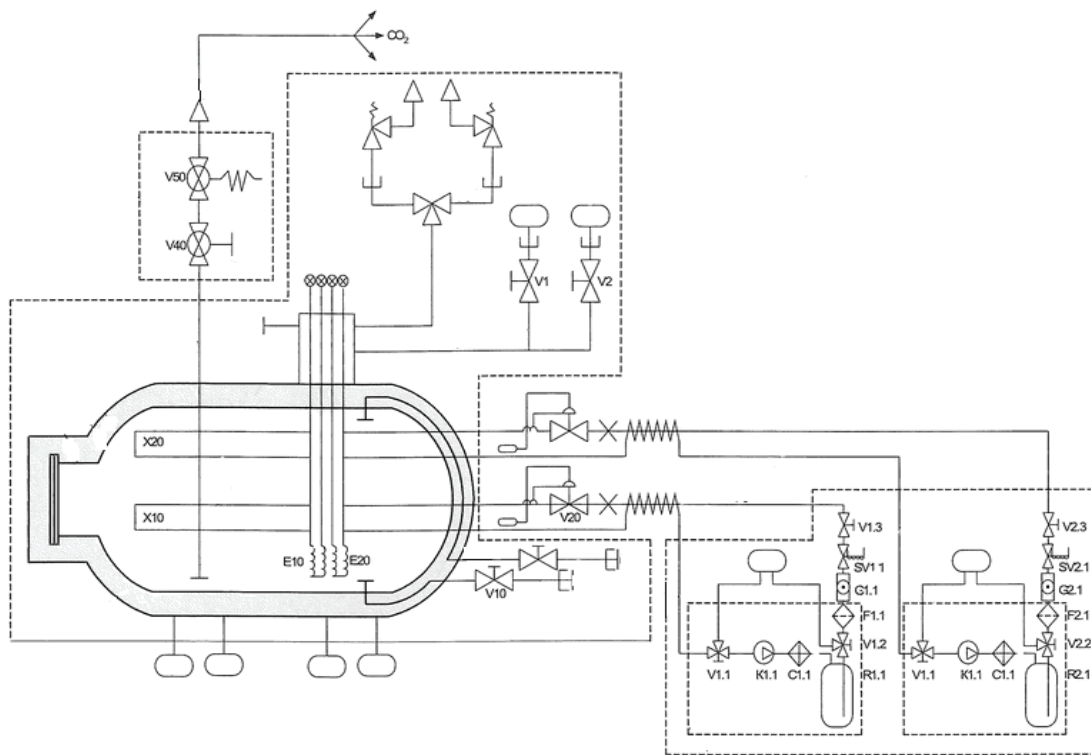


Fig.1.The process flow of automatic gas suppression system MIZHU.

It consists of such basic elements: steel tank; isothermal cover; nipple for fire extinguishing agent release; gas suppression system pipe line; locking-and-release device; globe valves; nipple for electric heating unit installation; electric heating units; protection valves; electric-contact manometers; chilling units; piping arrangement ; evaporators; filling nipple; nipple for pressure balancing while filling; strain gage .

As is clear from this figure 1, automatic gas suppression system MIZHU includes the isothermal module c metal container 1 and urethane foam or foam enclosure 2 of low conducting property for storing liquid carbon dioxide in the volume of 3 - 25 m^3 .

Isothermal module can be used for stocking main and reserve CO_2 at the environmental temperature from -40 to $+50^\circ\text{C}$. Supply time for 50% of fire extinguishing agent– shall not be above 50 seconds. Inertance of locking-and-release device response shall not be above 2 seconds. It

is the fast-acting and effective system of pozharotusheniya to date, which works for a few seconds and possesses ability on 100 % to snuff out flame. It is here possible to take two important factors. The system well cools the area of burning and hinders proceeding in a fire. Moreover after fire suppression or unauthorized startup gas fire extinguishing agent CO₂ in practice does not have unfavorable effect upon protected equipment. To perform effectively fire-extinguishing system is equipped with fire early detection system with execution unit providing fire-extinguishing system automatic switching-on. As combustion process in the places of gas transfer industry is accompanied by high rate of flame spreading and fast temperature rise, the execution unit system shall be provided by integrated equipment including detectors combining with other fire-safety systems such as control of gas contamination, ventilation, and emergency shutdown of gas-compressor units and emergency announcement of operating personnel. Therefore the up-to-date automatic fire protection and gas contamination control system of the compressor plant represents the multilevel and multifunction complex which is capable of processing fire protection total cycle:

- fire detection using sophisticated sensors;
- fire-alarm signal to the automated monitoring system, automatic fire protection system, duty operator and operation personnel by means of sound-and-light indicators;
- automatic fire protection system startup for giving the fire extinguishing agent into the seat of fire ;
- fire isolation and suppression;
- Detection of unacceptable gas level in the protected volume and signal to the operation personnel.

Moreover, using intelligent automation the automatic fire protection system is connected with other significant systems – ventilation and conditioning, alarm system and people evacuation control in fire condition. Operation algorithm of those systems allows fully excluding uncontrolled fire development at the compressor plant.

Block scheme of the recent complex of the centralized automatic gas fire suppression system (CAGFSS) is presented. As is clear from this figure, four gas-compressor units placed in the shelter should be protected by centralized automatic gas fire suppression MIZHU, placed in the detached housing. The base of automatic control of gas fire suppression is program controller, placed in the operator's room of the compressor section, which receives information from automatically controlled fire detection system – program controller of the gas-compressor unit and gives a command impulse to the control cabinet MIZHU to startup one of suppression direction from MIZHU container. Simultaneously with start pulse, information on fire from program controller comes to the rack cabinet of the providing information device and to the operator's automated work place.

First testing MIZHU automatic fire suppression system for fire protection of the compressor plants were conducted more than three years ago at the «Gasprom». According to the project the gas-compressor unit of the Urengoi— Pomary – Uzhgorod gas pipe line placed in the individual shelter with separate division walls should be protected with centralized automatic fire suppression system of low pressure. That system included:

- fire sensor set 12-X27121-000 under the engine casing and at maintenance area in the motor space and supercharger;
- sensors I7698E;
- program controller PC 4510-01 for fire suppression system control;
- isothermal module of gas fire suppression with liquid carbon dioxide MIZHU -16/2.2 including distribution device.

This system is mounted on CS «Pochinki», where to execute of order of vice-chairman rule «Gasprom» A.G. Ananenkova interdepartmental tests which went well were conducted in September, 2003. On results these tests a decision to project the system of the lokal'no-ob'emnogo extinguishing by MIZHU for defence of aggregates, set in general machine halls was accepted. First such system will be tested on CS «Cheboksarskaya» in May, 2005.

Creation of conception of protecting from the fires of objects of « Gasprom» and conducting of single technical policy in this area is an important positive tendency which characterizes passing to more high level of providing of fire safety of industry. The offered conception answers the requirements of operating presently normative documents in area of fire safety, which allow a customer to choose the most effective, worked in practice plug and plays of pozharotusheniya and fire warning taking into account the features of functioning of industrial objects, fully, pozharovzryvobezopasnosti, amount and technological parameters of circulating on a production reagents. Creation of conception of protecting from the fires of objects and conducting of single technical policy in this area is an important positive tendency which characterizes passing to more high level of providing of fire safety of industry. The offered conception answers the requirements of operating presently normative documents in area of fire safety, which allow a customer to choose the most effective, worked in practice plug and plays of pozharotusheniya and fire warning taking into account the features of functioning of industrial objects, fully, pozharovzryvobezopasnosti, amount and technological parameters of circulating on a production reagents.

Therefore, we can conclude that in case of fire reduction of the supply time of the fire extinguishing agent at gas transfer facilities is a key problem for providing fire and explosion safety of energy industries facilities. This problem is considered to be the main objective of our next studies.

STATISTICAL METHODS OF CONTROL OF TECHNICAL STATE OF EQUIPMENT OF CHANNEL OF ELECTRIC POWER SYSTEM

Diagnostics of channel of electric power system to the plug-in unit on the first stage and to the element on the second stage

Providing of invariance of initial values of U and f in the static modes in relation to the basic disturbances allows select the signal dependent on the state of system components, and also on exactness of static error compensation.

According to expressions

$$u_{v\Sigma} = u_{v.st} \quad \text{and} \quad u_{f\Sigma} = u_f + u_{fst}$$

the presence of performance degradation in the blocks of generation channel (GC) will result in increase of absolute value of signals

$$|u_{v\Sigma}| = u_{vn} \quad \text{and} \quad |u_{f\Sigma}| = u_{fn}$$

If fix the value u_{vn} and u_{fn} and then to compare them to the signal of u_{vn}^* and u_{fn}^* , the value of which is conditioned by inaccuracy of compensation of the static U (or f) error, then it is possible with the definite accuracy to judge about the technical state of channel equipment by signals

$$|u_{vn}| - u_{vn}^* \quad \text{and} \quad |u_{fn}| - u_{fn}^*$$

At presence of permanent fault symptom in GC, that is when $|u_{vn}| \geq u_{vn}^*$ or $|u_{fn}| \geq u_{fn}^*$ it is necessary, that the digital test and control system (DTCS) determines the location of fault up to the structurally plug-in unit.

As at the use of DTCS structure of the automatic control system (ACS) of voltage and frequency is two-sectional (fig.1), then at presence of fault symptom $|u_{vn}| \geq u_{vn}^*$ either $|u_{fn}| \geq u_{fn}^*$ the DTCS task consists in the location of fault spot in one of 2-th blocks, that is whether there is a fault in the synchronous contact-less generator, SCG, or in the voltage regulator, VR, (constant speed drive, CSD, or frequency corrector, FK).

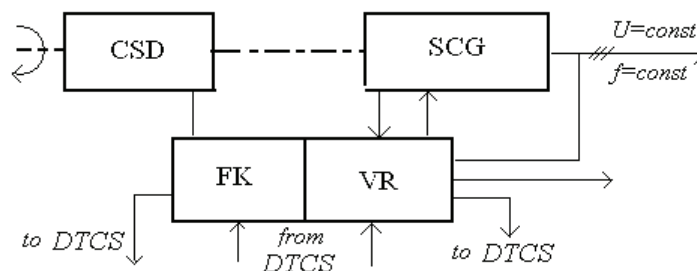


Fig.1. Block diagram of GC

The voltage control system at the two-sectional construction is possible to be presented so (fig.2). The put task is solved by measuring of intermediate output value I_{ex} (current of excitation of exciter) and comparison of it with the computation value proper to the load current I and its $\cos\varphi$. As measuring is conducted at $U = const$ and $f = const$ (even at presence of performance degradation), the calculation is conducted by the algorithm proper to the approximated control characteristic of generator

$$I_{ee}^*(iT) = I_{ee0}^* + K_{ee}^* I(iT),$$

where I_{ee0}^* - exciter excitation current at $I = 0$;

K_{ee}^* - coefficient of the approximated characteristic, dependent on the load and $\cos\varphi$.

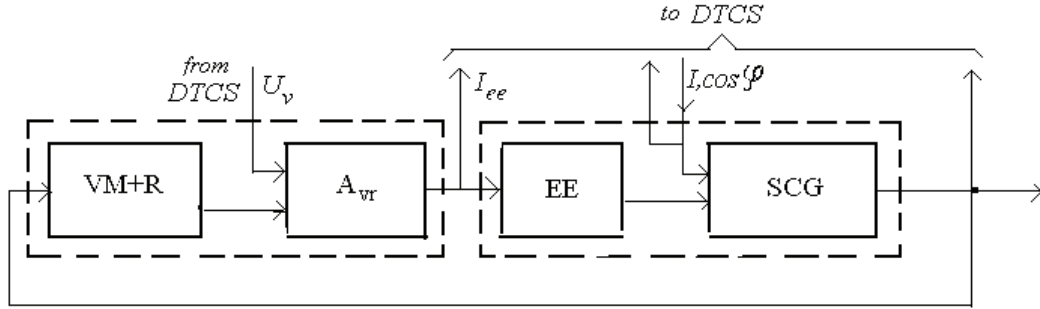
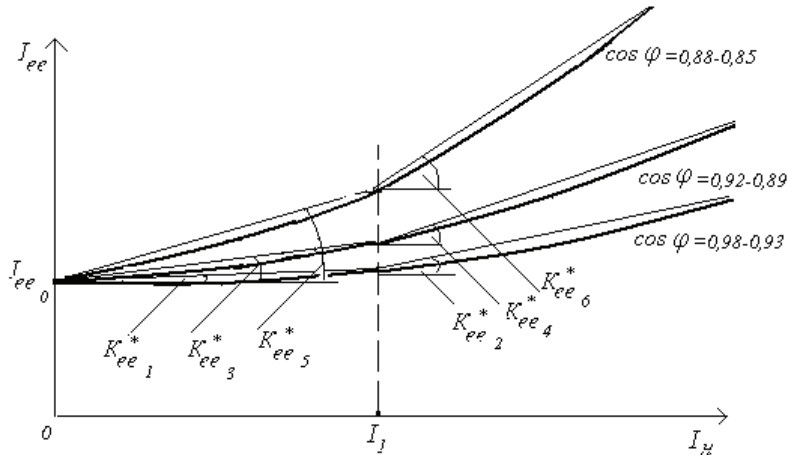


Fig.2. Block diagram of voltage ACS, where VM+R – voltage meter with rectifier, A_{vr} – amplifier of voltage regulator, EE – excitation of exciter

Expediently from point of minimum volume of main memory, family of the control characteristics $I_{ee} = f(I, \cos\varphi)$ is presented as three generalized approximated characteristics (fig.3), each of which appears by two linear areas.



Ris.3. Control characteristics of synchronous generator

For the existing load of the modern electric power systems (EPS) values of $\cos\varphi$ lie in the range 0,85 - 0,96.

K_{ee1}^* at $0 < I < I_1$, $\cos\varphi = 0.98-0.93$

K_{ee3}^* at $0 < I < I_1$, $\cos\varphi = 0.92-0.89$

K_{ee5}^* at $0 < I < I_1$, $\cos\varphi = 0.88-0.85$

K_{ee2}^* at $I > I_1$, $\cos\varphi = 0.98-0.93$

K_{ee4}^* at $I > I_1$, $\cos\varphi = 0.92-0.89$

K_{ee6}^* at $I > I_1$, $\cos\varphi = 0.88-0.85$

If it will appear as a result of control, that $|I_{ee} - I_{ee}^*| \geq I_0^*$, that is a measured value of current of exciter I_{ee} will be more or less of computation value I_{ee}^* on the I_0^* value, caused by the error of measuring and calculations, then an element with the performance degradation is in generator (exciter). If, $|I_{ee} - I_{ee}^*| \approx I_0^*$ and $u_{vn} > u_{vn}^*$ this will mean, that an element with the performance degradation is in regulator.

Thus, for the location of spot fault in the control voltage system up to the structurally plug-in unit it is necessary to measure a current of excitation of exciter I_{ee} and register the signal value of

voltage correction, and also have data in the main memory of DTCS which characterize control characteristics of “exciter-generator”.

The frequency correction system and even active power distribution at the two-sectional construction is possible to be presented in kind (fig.4).

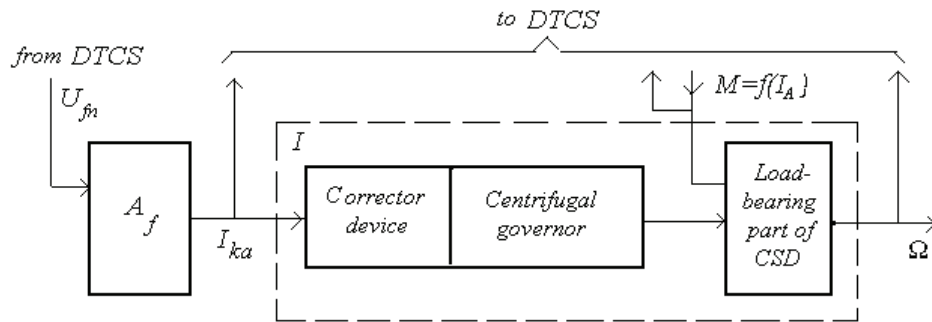


Fig.4. Frequency control system of synchronous generator, where A_f - amplifier of frequency corrector

Controlling a signal value u_{fm} , correction current I_{ka} (intermediate co-ordinate) and frequency departure Δf , it is possible to define a fault block caused by the presence of performance degradation of channel unit.

If it will appear, as a result of control, that $|I_{ka} - I_{ka}^*| > I_{ka0}^*$, that is, the measured I_{ka} value more or less of computation value $I_{ka}^* = f(I_A, \Omega_A)$ by the I_{ka0}^* value, caused by the methodical error and errors of measuring and calculations, then a unit with the performance degradation is placed in the block I (in CSD, correction device) (look fig.4).

On fig.5 principle relation of $I_{ka}^* = f(I_A, \Omega_A)$ is shown for three typical modes of operations of aircraft engine: ground idling condition, cruising mode and take-off regime.

If $|I_{ka} - I_{ka}^*| \approx I_{ka0}^*$, and $u_{fA} > u_{fm}^*$, this will mean, that an element with the performance degradation is in amplifier (A_f).

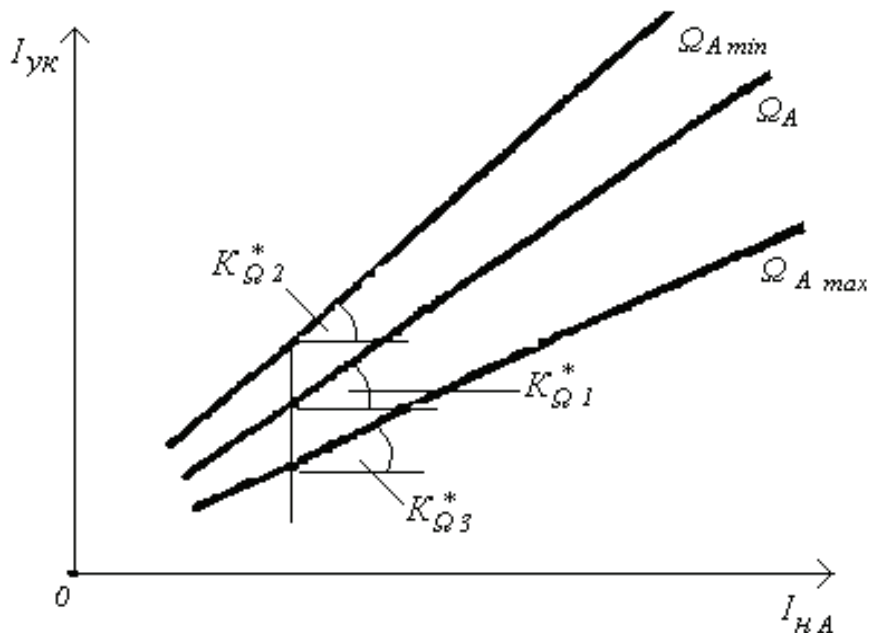


Fig. 5. Control characteristics of frequency corrector

Condition information about one of blocks of the EPS channel, selected by the previous diagnostics, it is possible to get in kind, for example, not sinusoidal functions. The analysis of these functions is possible to be automatically executed with the help of either electronic frequency analyzer or electronic correlation analyzer, or by methods of pattern identification. In the given

work the comparative analysis of these methods is executed and is offered block diagram of diagnostic and prediction complex.

By parallel frequency analyzer it is possible to get composition of harmonics at the non-stationary processes, but the output about the character of fault can give only autocorrelation function:

$$\Phi_{11}(\tau) = \frac{1}{T} \int_0^T u_1(t) u_1(t - \tau) dt$$

or cross-correlation function:

$$\Phi_{12}(\tau) = \frac{1}{T} \int_0^T u_1(t - \tau) u_2(t) dt$$

Naturally, that the data bank is needed in this case. The cross-correlation function allows to explore also influencing of repair measures and facilitates achievement of the desired reaction of device.

The block diagram of parallel frequency analyzer is represented on fig. 6, where: A – input amplifier; F – filters; D – detectors; MD – memory devices; MP – multiplexer; OD – output device; CU – control unit.

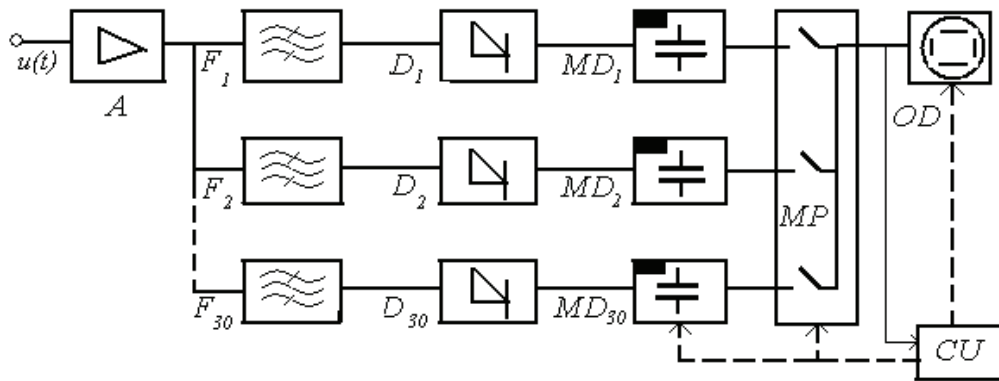


Fig. 6. Block diagram of parallel frequency analyzer

The block diagram of the electronic correlator for the automatic cross-correlation analysis of the measured voltages u_1 and u_2 is represented on fig. 7, where DB – delay block; M – multiplier; I – integrator; CU – control unit; OD – output device.

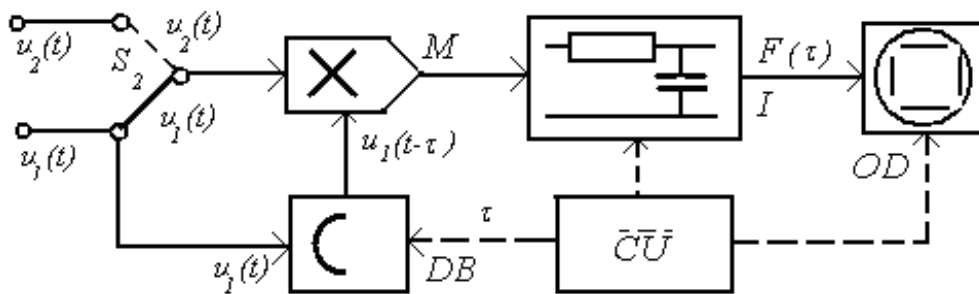


Fig. 7. Electronic correlator

For acceleration of analysis they use a scheme of parallel action in which the quantity of channels equals to a quantity of the simultaneously calculated points of correlation functions. Every channel has DB, which detains a signal according to the given point of correlation function. The simplified scheme of the multiplexed correlator is represented on fig.8.

For the automatic recognition of appearance of not sinusoidal function four characters are used – r, r, b, t , each of which corresponds to a definite area of curve (fig. 9)

The character of r corresponds to the P wave, r corresponds to RS – transition, b corresponds to the flat part which divides S and T extremes, t corresponds to the wave T . If take the P wave as beginning of counting out, then in such denotations the normal function is described by the sequences of characters: $prbtb$, $prbtbb$, $prbtbbb$ and etc

The syntactic descriptions of such kind are possible to be got with the use of G grammar:
 $G = \{Vt, Vn, P, S\}$,

where $Vt = \{p, r, t, b\}$, $Vn = \{S, A, B, C, D, E, H\}$, and the set of P rules of substitutions is such:

$$\begin{array}{lll} S \rightarrow pA & A \rightarrow rB & B \rightarrow bc \\ C \rightarrow tD & D \rightarrow b & D \rightarrow bE \\ E \rightarrow b & E \rightarrow bH & E \rightarrow pA \\ H \rightarrow b & H \rightarrow bS & H \rightarrow pA \end{array}$$

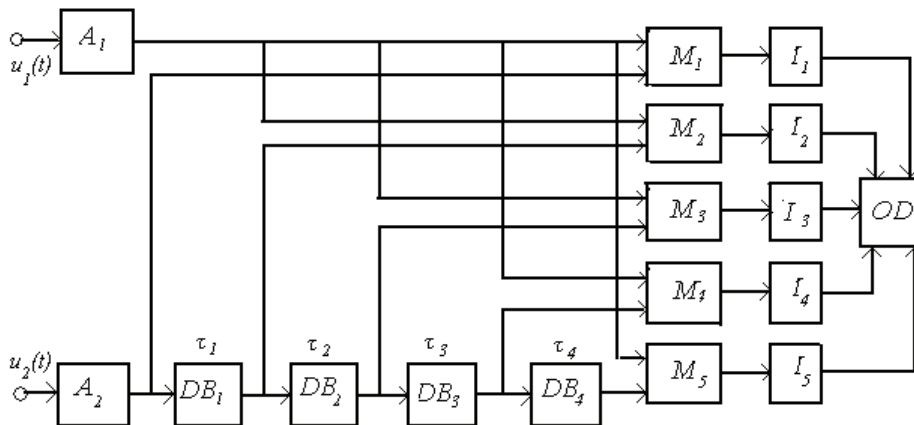


Fig. 8. Multiplexed correlator

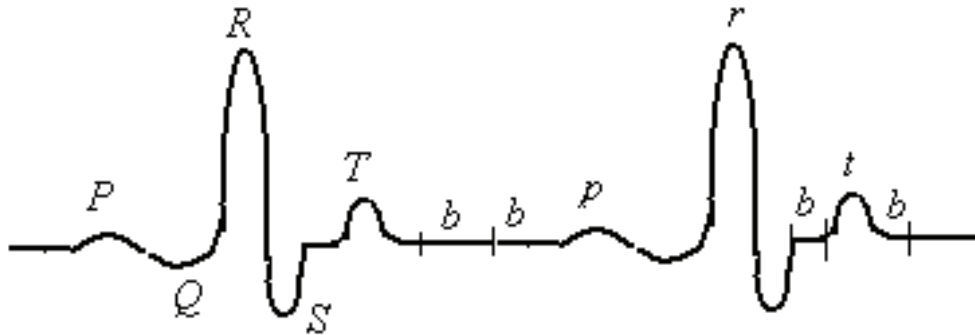


Fig. 9. Arbitrary not sinusoidal function

This grammar gives a language to which in accordance it is possible to put the finite automation, the chart of which is represented on the fig. 10.

In order to expose an anomalous function and distinguish it from normal, use the output «0», if the explored function corresponds to a «normal» standard, and output «1» in the opposite case. On the fig. 10 this output is connected with the lines of transitions.

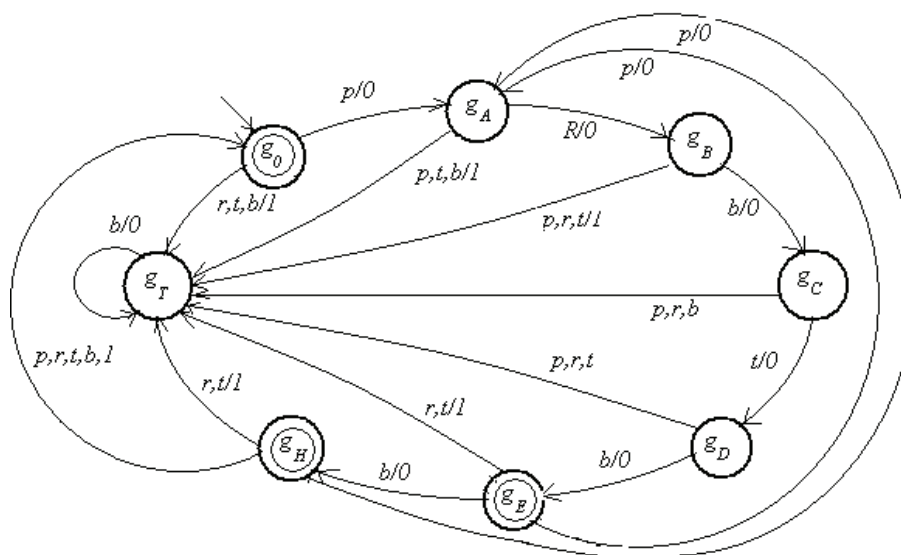


Fig. 10. Finite automation

Conclusions

Thus, it is possible to identify a EPS channel by the statistical methods within the plug-in unit and by the not sinusoidal functions within the element of block. The analysis of these functions is possible to be automatically executed with the help of either electronic frequency analyzer or electronic correlation analyzer, or by the methods of pattern identification.

MODERNIZATION METHODOLOGY OF UKRAINIAN CIVIL AVIATION PARK

In the article researching the scientific aspects of modernization of Ukrainian civil aviation park and forming methodology of modernization.

Introduction

Modernization of transport parks, especially aviation, is one of basic directions of technical policy for greater part of the world powers in modern terms. It allows improving quantitative and high-quality descriptions of transport vehicles, extending their possibilities at charges almost on the order of more small, than purchase of new technique [1]. Receipt of maximal effect from modernization of park of aviation technique (AT) of civil aviation of Ukraine possibly on the basis of decision of two linked complexes of tasks: synthesis of variants of modernization of standards of AT and management projects. For their decision it is needed to develop the proper methodology, which at ground of the having a special purpose complex programs of update AT park will give possibility to develop the scientific aspects of modernization, conduct optimization of variants of modernization of standards of AT taking into account necessary resources.

Problem decision

By the question of development of methodological bases of modernization of aviation technique (AT) and management projects devoted far of works [1...7]. In our time methodological approaches in relation to the ground of variants of modernization for the park of air force [1] and some methodical developments are developed for the park of civil aviation [2]. However, conducting of the program of modernization of aviation park of civil aviation in Ukraine is labored in a number of specific features, related to: by insufficiency of resources (above all things, financial) which are offered on modernization; by the vagueness of their receipt; by complication providing of compatibility of oversea element base with domestic, by the necessity of continuation of the appointed resource indexes of objects of AT, by absence of developers and producers after AT in Ukraine and other. In this connection question of account of terms of insufficiency of the resource providing for programs modernization of aviation park and vagueness of his receipt are important, need operative decision and creation of the methodical providing which must enter as component part in methodology of modernization.

A purpose of this article is forming of methodology of modernization park AT on the basis of development of new methodical constituents and tying up of existing. Such methodology must decide problem tasks on modernization of Aviation Park in modern terms by the complex decision of tasks of synthesis of variants of modernization and optimization of allocation of resources taking into account their possible insufficiency and vagueness of receipt.

Modernization of Aviation Park has two opposite tendencies: from one side of necessary to develop such variants of modernization of air courts and aviation complexes (AC) on their basis, which will satisfy a world level on a long period; from other side - resource possibilities of Customer of modernization are limited and need permanent minimization.

These contradictions generate a scientific problem in relation to creation of methodology of modernization of aviation park, which will give possibility of ground necessary variants of modernization of AC and to form implementation of the program of modernization of AT phases on the basis of optimization of allocation of resources taking into account their possible insufficiency and vagueness of receipt.

With the purpose of decision of the put problem of researches it is suggested to examine modernization from positions of approach of the systems at the level of park AT and as an object of

researches to select AC, which except for an aircraft, includes facilities of surface service, field-technical providing, and management.

Mathematical formalization of problem of researches is conducted for the set aggregate of finite sets with their descriptions: tasks, the decisions of which must provide AC after modernization, types of AC, which are subject modernization, production capacities of aviation enterprises which modernization will be conducted on, possible variants of modernization, after the types of AC, volumes of financing and terms of receipt of finances.

In connection with the presence of vagueness the stochastic raising of scientific task of researches, which consists in finding for certain the type of AC of such optimum variant of modernization, is considered, that provides maximum mathematical waiting of objective function of choice of variants of modernization for indefinite factors taking into account limitations.

The decision of this problem taking into account vagueness presents substantial complication, and the known methods of its decision (expert, adaptive and compromise decision) on the basis of methods of the stochastic programming are developed not enough. For its decision offered approach on principle of decomposition of problem on the row of separate tasks and research of the most unfavorable cases on the basis of pessimistic, optimistic and middle estimations [7].

Principle of general decision of task of synthesis of AC, which is modernized, and task of allocation of resources, is offered also during conducting of modernization. Thus in the conditions of decision-making on realized program of modernization taking into account the selected volumes of financing, set amount of AC, that modernized, the task of realized has priority above the task of synthesis and can bring in corrective in its decision.

Unlike the known approaches to the decision of task of synthesis of variants modernizations of AC, which are based only on the basis of criterion of economic efficiency, application of triad of criteria is offered, where next to the known measure of cost the offered coefficient of potential efficiency (CPE) of AC, and also criterion of safety of flights (SF) of airplane, that has priority above a cost [3].

The basic stages of decision of scientific problem of modernization of aviation park of civil aviation is development of methodology of modernization AC on the basis of general decision of task of synthesis of variants of modernization of AC and optimizations of plans of conducting of modernization. Basic methodical approaches from the based choice of variants of modernization of AP on the basis of triad of criteria of CPE, SF and in are based on methodical decomposition and include [1]: optimization on one criterion, by which accepted decision on the early stages of modernization; optimization to on to many to the criteria at determination of area of effective decisions, built in factor space, and following grounds of optimum variants of modernization of AC; methods of theory of making a decision at the comparative estimation of variants of modernization after the aggregate of indexes which include high-quality indexes.

With the purpose of forming of variants of modernization of AC utilized structurally is functional approach on the basis of theory of the graphs, which allowed to link composition of equipment of AC, which is modernized, with the nomenclature of his decided tasks.

For the comparative estimation of variants of modernization on the basis of to the selected triad of criteria the developed methodical approaches of their determination. Thus for the comparative estimation of variants of modernization the necessity of application in place of indexes of economic efficiency of indexes of technical perfection of AC is grounded, for example, index of increase of CPE AC.

On the basis of methods of theory of volumetric the developed method of increase of CPE AC is as a result of his technical improvement, which takes into account the relative increases of aggregate of compared his descriptions. A method is given by possibility to take into account more large the amount of flying and technical descriptions that is instrumental in objectivity of choice of variants of modernization and their ground [4].

Index of safety of flights, that is on the second place in the triad of criterion, is probability of happy completion of flight of the modernized AC - determined by logic - probabilistic method on the basis of the developed count of the state of AC by adding up of probabilities of his eventual

states. Method of determination of actual strength of flights securities developed to that end for the different variants of modernization of AC.

Determination of cost of modernization of AC is based on the account of all of component charges. The developed methodical approaches after determination of the selected triad of criteria allowed for previous suggestions on modernization of AC to conduct their reduction and form the great number of possible variants of modernization, that is satisfied the set limitations. On the basis of offered approach from the grounded choice of variants of modernization of AC the developed method of synthesis of their variants taking into account sufficientness of financing and other resources.

For the terms of the insufficient financing of modernization AC park the developed method of synthesis of variants of modernization of AC at the stage-by-stage financing with the use of index of specific cost of increase of CPE [3]. Its application is given by possibility to bind the directive and actual levels of increase of CPE to the charges on modernization, grounded priority row on the basis of index of specific cost and in the total to form the proper variants of modernization of AC. At the estimation of realized of conducting of the program of modernization AC the put and decided task of maximization of increase of CPE for the park of civil aviation as a result of his modernization taking into account insufficiency and vagueness of financing. The model of conducting of modernization is developed AC and method parka optimum distributing resources AC Park during conducting of modernization.

Such method includes the row of the stages: determination of necessary resource AC Park on modernization; comparison of necessary and present resources; verification of terms of modernization on maximal, middle and minimum variants. The optimum mixed plan of modernization is determined in the total, which provides the maximal increase of potential efficiency park at providing of the set correlation after the types of AC. The task of maximization of percent of fulfilling the plan of modernization park AC is taken to the canon type of maximal task. For reduction of volume of the analyzed variants there is the offered procedure of "improvement of supporting plan"[3].

In the conditions of the insufficient financing there are some possibilities in relation to cutting of costs AC on conducting of modernization, which are based on the choice of variants of modernization with rational (not optimum) parameters, and also on differential approach to modernization AC after a model. Such approach from one side can considerably shorten necessary charges on the entire program.

Results of researches on the basis of the developed methodological vehicle show that the insufficient providing resources bring implementation over of the program of modernization to derangement. For the removal of it in the conditions of the insufficient providing resources it is needed to bring in corrective to the program, which require the change of variants modernization AC and AC on the whole, reductions amounts of AC, which are modernized, possibilities («depths» of modernization), increase of terms of conducting of modernization and other In modern terms at Ukraine actual is a task of conducting of modernization in the conditions of vagueness of providing resources. For its decision the offered methodological approach in relation to the ground of optimum variants of modernization of AC and allocations of resources in the conditions of vagueness on the basis of the combined use of algorithms of the artificial immune systems [5].

The conceptual raising of tasks of allocation of resources looks like in the conditions of vagueness. For a park AC that consists of units and types, it is necessary to define the plan of modernization where is a plan of modernization of separate unit of AT. It is thus necessary to find the optimum variants of modernization of park AT which will provide the maximal increase of CPE at minimum finance charges for the least time in the conditions of vagueness of receipt of resources for realization of the program of modernization.

Thus, AC and its constituents parka on the basis of development of methodology of modernization: scientific methods, methods, mathematical models, criteria the decided scientific issue of the day of ground of variants of modernization parka AC of civil aviation of Ukraine taking

into account the limited providing resources by the complex decision of tasks of synthesis of variants of modernization and optimization of allocation of resources.

Developed scientifically is a methodological vehicle of ground of variants of modernization AC parka taking into account the limited and indefinite providing resources allows to define the increase of level of technical perfection of AC as a result of modernization, to estimate execution of limits on resources and possibilities in relation to providing of necessary strength of flights security and as a result to ground the variants of modernization of AC taking into account the real possibilities of their realization in Ukraine. He includes: method of estimation of influencing of indexes of technical perfection of AC on efficiency of his application; method of estimation of increase of CPE AC after modernization on the basis of change of the most meaningful descriptions of AC and his functional systems; method of determination of actual strength of flights securities for the different variants of modernization of AC; method of synthesis of variants of modernization of AC, that is based on distributing after importance to the triad of criteria of potential efficiency, safety of flights and price method of synthesis of variants of modernization of AC at stage-by-stage providing resources; method of allocation of resources during conducting of modernization AC of civil aviation parka in the conditions of the insufficient financing; methodological approach in relation to the ground of optimum variants of modernization of AC and allocations of resources in the conditions of vagueness on the basis of the combined use of algorithms of the artificial immune systems and other.

Methodology of modernization park AC is the scientific background of subsequent development of theory of modernization and can be used at planning of development of aviation park of civil aviation on the basis of his modernization, update, and also at accompaniment of the Government programs of development of transport parks, ground of requirements in financing and terms of conducting of such programs, forming of requirement specifications on modernization of AC after types, to the estimation of technical suggestions of modern industry and oversea firms relatively update of aviation technique and other.

Conclusions

Thus, the formed methodology of modernization AC, which allows conducting the grounds of variants of modernization of Aviation Park taking into account the limited providing resources by the complex decision of tasks of synthesis of variants of modernization and optimization of allocation of resources in the conditions of their possible insufficiency and vagueness of receipt.

References

1. *Самков О. В., Коваленко А. В.* Методологія обґрунтування варіантів модернізації парку бойових авіаційних комплексів// Зб. Наук. праць.- К.: Науковий центр ВПС ЗС України. - Вип.6.,2003.-С. 15-20.
2. *Самков О. В., Климчук В.П.* Особливості розробки та реалізації авіаційних цільових комплексних програм в Україні//Вісник НАУ- К.: НАУ, 2004.-№4(22).-С.55-60.
3. *Финадорин Г.А., Харченко А.В., Самков А.В.* Методологические аспекты формирования программы развития военной авиации// Труды научного центра ВВС. - К.: НЦ ВВС- Вых.1, 1997.-С.77-87.
4. *Самков О. В., Казак В.М.* Методичний підхід щодо обґрунтування оптимальних варіантів модернізації складних технічних систем//Системні технології. - Дніпропетровськ: - Вип.6 (47), 2006.-С.212-220.
5. *Самков О. В., Литвиненко В.И.* Методологічний підхід щодо вирішення завдань розподілу ресурсів в умовах невизначеності// Зб. наук, праць ДНДІ авіації. - К.: ДНДІА.-Вип.21-(9), 2006. - С. 220 - 225.
6. *Науково-методологічне забезпечення управління складними проектами/За ред. М.М.Мітраховича.-К.: Техніка, 2002.-369с.*
7. *Зайченко Ю.П.* Исследование операций.- К.: Вища шк., 1988.-552с.

INITIAL ANALYSIS OF THE ORNITHOLOGY SITUATION CONCERNING AIRFIELD IN THE ASPECT OF BIRD STRIKE TO AIRCRAFT

The main goal of the project is to work out methods of airships protection in scope of safety threat from breeding, non-breeding and migrating birds. As the research area, Deblin airfield has been chosen. Authors of the project foresee that researches carried out will bring an algorithm that will expand existing airfield prevention system as far as the potential collision threat is concerned and will have positive influence on flight safety.

1. AVIATION ACCIDENTS COUSED BY BIRDS COLLISIONS

As international statistics show, in the years 1959-1999 in the world's military aviation 286 disasters took place as a result of bird collisions. It is worth to mention that 63 of them were fatal. About 60 of them took place in Germany, 47 in Great Britain and 46 in the USA. The great number of these crashes was on fighters and striking-fighters (not less than 179), 40 on multiengine aircraft and 34 trainee aircraft. It turns out, that despite the fact that the number of flights has decreased lately, the number of collisions has increased. Taking into consideration disasters from 1990 the number of casualties equals 68.

As statistics show, most of the collisions occur on low altitude (not more than 50 m.), during take-off and landing and in vicinities of airfields on the altitude of 300 m. Every year in the US military aviation about 1500 collisions are registered. As a result 15 aircraft have been destroyed and 3 pilots lost their lives.

The US Air Force for years 1985-1996 presents following data:

General number of bird strike accidents amounts to 30907:

- In airfield vicinities – 14887 (48%) of overall number;
- During low altitude flights – 6018 (20%);
- Fatal victims – 33;
- Destroyed airships – 14;
- Material loss – 457 mln USD;
- Average number of collisions per year – 2600;
- Yearly average loss – 38 mln USD.[2]

One of the most tragic disasters in US Air Force history caused by bird strike was an accident of E-3A aircraft which crashed immediately after take-off from the Emendorf airfield (Alaska) in 1995. The aircraft was completely destroyed and 24 aircrew members lost their lives. The disaster was caused by the flock of Canadian Geese. Similar disaster took place in 1996 in Netherlands with the were 34 fatal victims, as a result of strike of C-130 tanker aircraft with the flock of 600 sparrows and seeders [6].

A few disasters caused by the same reason took place in Poland as well. On the 3rd August 1965 cadet of the Polish Air Force Academy, Andrzej Antkiewicz flying training jet TS-11 "Iskra" stroke the flock of pigeons on the altitude of 100 m. It caused engine disorder. During forced landing at the altitude of 12m he grappled two energy lines with a wing and a rudder. As a result, he went down, hit the ground and was killed. The aircraft was totally destroyed.

On the 9th April 1972 during reconnaissance flight aircraft called Lim-2 on the altitude of 400m hit a hawk. The front side of the cockpit was destroyed and the pilot was seriously injured. The other accident occurred on Navy Mi-14 helicopter. Mi-14 hit the flock of pigeons. Engines were destroyed and the altitude was too small to land in autorotation regime. Three crew members were killed in this crash.

On the 17th May 1984 while Su-20 performed zone flight at the altitude of 300m and with the speed of approximately 700-750 km/h bird collision occurred. As a result, the front hardened glass windshield was destroyed. Broken glass and bird fragments got into cockpit injuring pilot's face [3].

On the 14th July 1999 jet TS-11 “Iskra” stroke a stork. The right front fuselage and engine compartment were damaged (Photo.1). The rudder was also blocked.

Except accidents described below there were 4 more damages which took place a result of bird collisions, including Su-22 aircraft, Mig-21 aircraft engine, and a fuselage of TS-11 aircraft. Moreover 37 incidents were recorded without serious consequences. The value of a single collision is estimated to approximately 80 thousands PLN.



Photo. 1. The aircraft called TS-11 “Iskra” after a bird strike

In 2004 in spite of prophylaxis deployed the number of collisions recorded has increased. It does not mean that the real number of collisions drastically increased. It depicts the fact that the reporting system is more efficient in comparison to the previous timeframe and more incidents not causing aircraft damages were reported.

The number of bird collisions varies and is different on different airfields. It depends on:

- geographical location of the airfield;
- natural environment;
- manners and methods of precaution measures deployed;
- flights' intensiveness;

Summarizing, the flight altitude has also a big impact on the statistics of bird collisions. Analyses that were carried out show that taking into account flight altitude criterion the most common altitude at which accidents occur is between 200-300m. It is obvious that at the higher altitude, the number of birds decreases, so probability of collisions is much smaller. The number of accidents is closely related to the stage of flight as well. As statistics show operations such as take-off, departure, approach and landing are the most dangerous, while operations as taxiing or ground run are the safest. It is said that operations as taxiing or ground run are very short and are accompanied by the huge noise. At the same time on many airfields a lot of precaution measures are deployed. On the other phases of the flight, where deterrence is not working probability of bird collisions is much higher.

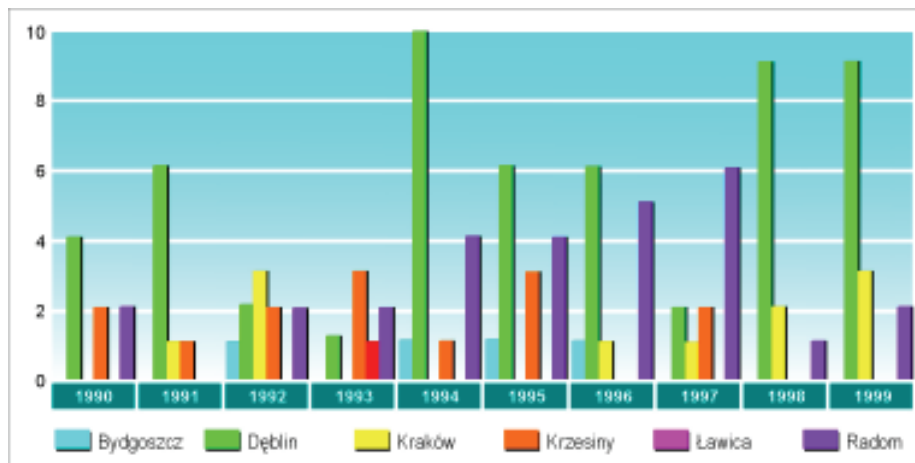


Fig. 1. The number of bird strike to aircraft at military airfields in Poland

In general in 1991-2000 in Polish Air Force 355 incidents were recorded (see diagram in Fig.1)[1]. It depicts that despite the fact that the number of flight hours in military aviation decreases and a lot of precaution methods is deployed, the number of bird collisions increases. The coefficient of collisions per 10 thousands of flight hours increased from 31,5 in 1991 to 56,55 in 2000.

2. PROJECT CHARACTERISTICS

The authors of the project have chosen the military airfield in Deblin as the main research area. It was chosen due to the fact that the number of bird collisions that happened in Deblin was significantly higher than on the other airfields in Poland. The main objective of the project is developing methods of aircraft and airfield protection against threats from breeding, non-breeding and migrating birds.

The following research hypotheses were established:

- the airfield surface in Deblin because the landscape and vegetation structure is very important breeding area for birds that constitutes direct threat to airships;
- biotope environment of the skirting parts of the airfield and its vicinities are very convenient for domiciling and breeding grounds establishing using this area as feeding and resting grounds during migration;
- there are few “key points” on the airfield and within its outskirts that “attract” birds increasing their number and species;

The executors of the project decided to perform the following researches:

1. Breeding preferences in scope of activity of birds at the airfield;

It will bring information about areas which are the most important for activity of certain species of birds. Special attention will be put on species that were identified during collisions. Researches will provide information about different forms of birds’ day activity (timing, feeding, rest etc.) on the airfield and its vicinities. The results will be analyzed and compared with vegetation map (Task 3.).

2. Breeding preferences in scope of birds activity in close (direct) vicinities of the airfield;

The inventory of “hot spots” in the radius of 5km out of airfield surface can be attractive for birds, for instance rookeries and other birds, water reservoirs, legal and illegal dumping grounds. The analyses described above will bring information on the attractiveness of environment for birds active at the airfield.

3. Development of vegetations map on the airfield and its vicinities area.

The accomplishment of this task will provide information on nest allocation preferences of birds.

4. Critical flight phases definition in the context of birds’ activity at the area of airfield, after takeoff.

The main purpose of this task is to define and point out the most dangerous phases of flight and analyze within the frame of birds’ activity map to develop the most efficient prevention methods to

be deployed by pilots and flight organizers. Moreover, there are ongoing researches on the status of knowledge of flight personnel on birds' behavior and different deterrence methods. There are some indications that this type of researches is necessary.

The authors foresee that the accomplishment of the project will allow to draw conclusions and recommendations how to manage the problem of vegetation coverage in the area of the airfield and its vicinities to restrict birds' activity and to develop prevention methods that can be a model for other airfields. At the same time this project should allow to develop prevention methodology and procedures for pilots and flights' organizers to minimize risk of bird strike to aircraft.

3. INITIAL RESEARCHES RESULTS

On the bases of prepared map and terrain researches, analysis of different elements of the airfield was carried out (few kilometers radius), to define spots of birds' activity and develop vegetation inventory in the examined area. After analysis, the airfield has been split into a few sectors and characteristics were assigned to each of them. Then one sector has been chosen to initiate researches.

Researches were carried out by two methods. One by transect and the other one by selected sector scanning. Different methods of the deployment were justified by the need of analysis of quantity dynamics and birds' distribution at the airfield, on the other hand, there was a need to recognize factors that influence birds' behavior in scope of airships activities in the examined area. Due to the fact that, researches initiation was planned for the beginning of the breeding time, in 2007 all researches were focused on the airfields' open area. There were no researches in residential area, buildings, parks and squares. Transect method consist of counting of birds (the ones that were seen or heard) on dislocating path. Besides birds, animals were found and the wisps of their activity hovels and molehills. The length of the transect was equal to 9.5-9.8km.

To meet the needs of the conducted behavioral research, a platform was raised on a birch tree in the eastern part of the airfield, near the approach zone in main landing direction. Observation sessions consisted of conducting telescopic scanning of a portion of a 120° sector at 6-minute intervals (10 scans per one hour of observation). Photographic documentation of the observation sessions was prepared at the same time.

The following events were noted during the scans:

- presence and behavior of all the birds in the field of scanning. All sighted birds, which behavior was defined, were classified as seen on or off the runway. The sightings were recorded regardless of the birds' species.
- presence and behavior of all the birds of prey and predatory mammals in the field of scanning. All sighted carnivorous animals, whose behavior was defined, were classified as seen on or off the runway. The sightings were recorded regardless of their species.

Prior knowledge of animal ecology points out to the fact that the presence of carnivorous animals limits the presence and population density of other animals. Therefore, during the scans, presence of all animals (birds and mammals) on the runway and the grass area of the airfield was recorded. The observations also concerned diurnal birds of prey of the order *Falconiformes* and predatory mammals, *Carnivora*, as well as animals such as shrikes, *Lanidae* which, although not regarded taxonomically as flesh-eating, evoke escape reactions in birds and aggressive interactions. The observations of diurnal birds of prey of the order *Falconiformes*, concerned such species as: Common buzzard *Buteo buteo*, Kestrel *Falco tinnunculus*, Marsh harrier *Circus aeruginosus*, Montagu's harrier *Circus pygarrus*. The representative of predatory mammals, *Carnivores* was the red fox, *Vulpes vulpes*. Therefore, using a specially trained dog with the aim of the examination of escape reactions in birds is also planned as one of the further directions of the presented research. As it turns out, this direction is in accordance with the world-wide trends. At some airports and airfields in Israel, the USA and Holland, *Border Collie* dogs are used for deterring birds.

In the studies conducted using the transect method in 2007 about 57 bird species were observed at the airfield in Deblin. The total number of individual birds was 4913 (Fig. 2), including (species which have a dominance of more than 5 per cent): European starling (blackbird) - 1496

(30.6 per cent), rook -1061 (21.6 per cent), Eurasian jackdaw – 754, (15.3 per cent), Lapwing - 286 (5.8 per cent).

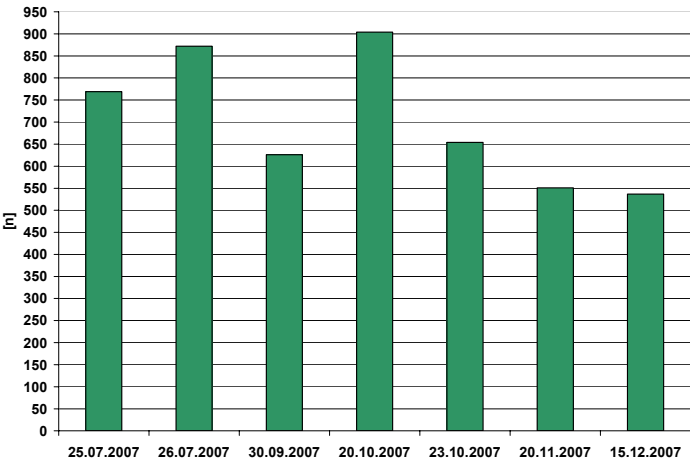


Fig.2. Bird population at Deblin airfield, found in individual observation sessions conducted using the transect method in 2007

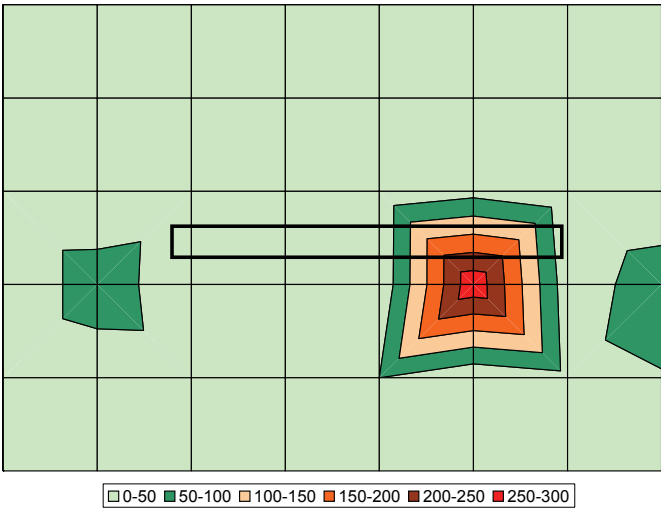


Fig. 3. Bird population density per 25 ha during the observation sessions in July 2007

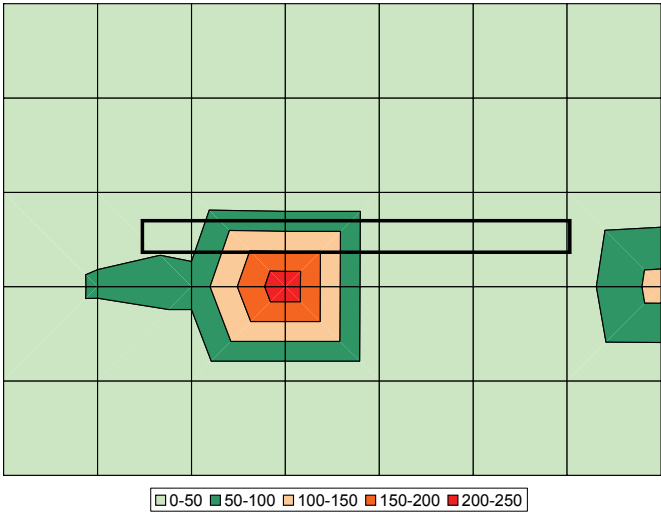


Fig. 4. Bird population density per 25 ha during the observation sessions in December 2007

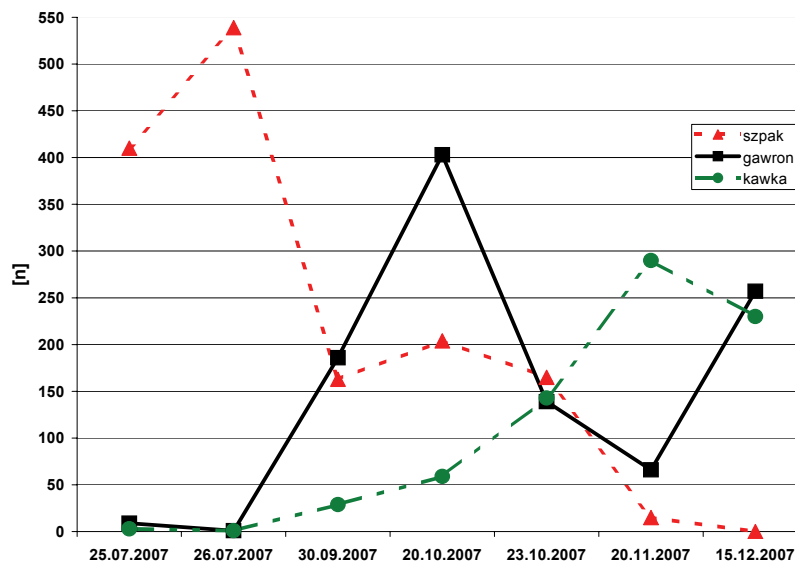


Fig. 5. Population changes of the European starling (blackbird) *Sturnus vulgaris* (n=1496), Rook *Corvus frugilegus* (n=1061) and Jackdaw *Corvus Monedula* (n=754) – dominant bird species

In fall-winter sessions, the highest bird concentrations were noted in the western and south-western portion of the runway, whereas in summer most birds were observed in its south-eastern portion (Fig. 3 and 4). The population changes of the most common species, i.e. Blackbird, Rook and Jackdaw were dynamic (Fig. 5).

European starling (blackbird) - The population of the European starling (blackbird) was the highest in July when, after the breeding season, large flocks gathered preparing to fly to the wintering sites. Then, the population of that species was found to be gradually diminishing and, in December, no starlings were sighted in the airfield.

Rook - With regard to that species, two peaks of population size may be observed. The first of them - higher - was reported in October, and the other - lower - in mid-December. The first peak of population size may have still included breeding birds, in preparation for the migration to the south of Europe, whereas the latter comprised the birds which had arrived for wintering from the east of Europe.

Eurasian jackdaw - The jackdaw population was increasing steadily, and reached its peak in late November and early December. It was probably the result of bird migration for wintering from the east of Europe. Every day 500 to 900 birds were present in the airfield all day and frequently on the runway or in its vicinity.

Despite the fact that observations were conducted for a relatively short period of time, interesting data were gathered from the scans. In the scanning field, 25 bird species and 4 mammal species were found, including individuals of 4 bird species which were found on the runway surface. The most numerous species was the kestrel, *Falco tinnunculus*, reported in almost 46 sessions. The maximum single sighting of that species in the scanning field comprised 4 individuals, and on average 1.51 individuals were sighted per session. That species does not seem to pose a serious threat, since it nests in the immediate vicinity of the airfield and undergoes very far-gone habituation process. What is more, the presence of that species even appears favorable, because of their attacks on some passerines (e.g. skylarks).

The three subsequent species which were observed most frequently were the barn swallow - 28 per cent, the great grey shrike - 19 per cent and the skylark - 18 per cent. Among the species that have already been mentioned, the barn swallow deserves special attention because its aggregations reached the maximum of 43 individuals, which could pose a threat to flight safety.

In the light of the behavioral research, the most serious threat to air traffic at the military airfield in Deblin could be posed by lapwings and blackbirds. This results from their high presence frequency in the scanning fields, which was 14.0 per cent and 10.5 per cent, respectively, as well as

high rate of their presence on the runway surface (especially lapwings) and forming large flocks, which for those species were observed to consist of the maximum of: 60 and 300 individuals respectively. The European white stork also used the airfield for feeding and was sighted on the runway surface in two observation sessions. Apart from those already mentioned, the birds representing 18 other species were sighted. However, their presence rate was lower than 7 per cent. No individual belonging to those species was sighted on the runway surface.

In the observation sessions, 4 species of mammals were detected, three of which on the runway surface. The presence of the red fox is a positive factor, since it evokes escape reactions in birds, whereas the presence of the European roe-deer poses as serious threat to flight safety as that of the bird flocks. The total of 45 escape reactions of individuals or bird flocks were observed. In 13 cases they resulted from the interaction with animals present at the airfield, and in 32 they were the reaction to anthropogenic factors (human presence and activity). Aircraft take-offs and landings caused 26 of the observed escape reactions in birds. From those escapes, 12 (46.1 per cent) concerned European starlings (blackbirds) and 11 (40.7 per cent) concerned lapwing flocks. Moreover, behavior observations shown that among 13 escape reactions of birds at the airfield, 46.1 per cent were evoked by a kestrel and 23 per cent resulted from the presence of a red fox. The above information ought to be taken into consideration in preventive activities. Firstly, red foxes, their burrows and feeding activities at the airfield should be tolerated. Hunting and frightening foxes away should be avoided. It is worth noting that the frequency of interactions involving a red fox was relatively high and that in all escape reactions evoked by a red fox, the affected animals did not return. Secondly, that fact proves that predatory animals (specially trained dogs) may be effective in frightening birds away and thus in reducing the bird strike risk.

CONCLUSIONS

As a result of the first phase of the research study, numerous conclusions may be drawn, concerning the diversity, presence frequency and activity level of the bird population at the Dęblin airfield.

In the conducted observation sessions 4913 birds were sighted, including (species which have a dominance of more than 5 per cent): European starling (Blackbird) - 1496 (30.6 per cent), Rook 1061 (21.6 per cent), Eurasian jackdaw – 754, (15.3 per cent), Lapwing - 286 (5.8 per cent). In the light of the behavioral research, it appears that the most serious threat to air traffic at the military airfield in Dęblin could be posed by Lapwings and European starlings. This results from their high presence frequency in the scanning fields, which was 14.0 per cent and 10.5 per cent, respectively, as well as from their high rate of presence frequency on the runway surface (especially lapwings) and forming large flocks, which for those species were observed to consist of up to 300 individuals. Furthermore, the frequency of interactions involving a red fox was relatively high and the fact that in all escape reactions evoked by a red fox the affected animals did not return proves that predatory animals (specially trained dogs) may be effective in frightening birds away from the runway area.

The observations also proved that available means of deterring the birds were not being used effectively. The above conclusions will be taken into consideration in subsequent research studies.

References

1. *Dzik T., Kiernicki A., Ptaki użytkownicy przestrzeni powietrznej (Avian Users Of The Air Space)*, PSP nr 8, Poznań 2005.
2. *Satheesan S.M., Satheesan M.* 2000. Serious vulture hits to aircraft the world. International Bird Strike Committee. IBSC 25/WP-SAL 67-87. Amsterdam, the Netherlands.
3. *Szymczak J., Zderzenia samolotów z ptakami (Bird strikes)*, PWLiOP nr 4, 1989.
4. Own materials of the authors.

A PREDICTION OF AIRCRAFT POSITION IN SATELLITE NAVIGATION RECEIVER FOR INSTRUMENT LANDING SYSTEM

In this paper theoretical grounds on prediction of a position in a satellite navigation receiver have been discussed in the circumstances of the inability of having other solutions, caused by various reasons.

INTRODUCTION

Numerous researches have proved that the main fault in the satellite navigation systems lies in having temporary breaks occurrence in a positioning sequence, caused by various reasons (interference, lack of reception of an adequate number of satellites by antennas, etc.). This leads to a temporary inadequate aircraft positioning and parameter calculations. In order to have GNSS system become the primary radio-navigation system used in aircraft for landing approach the enumerated restrictions should be eliminated.

The predictions forecast that one of possible solutions to this problem is to employ the concept of defining coordinates of an aircraft position in its approaching maneuver during temporary loss of information of its position by a GPS receiver. In this concept an aircraft is considered as a solid object having 6 degrees of latitude. The essence of the presented method is to assign aircraft position and its speed in three-dimension airspace.

It is predicted that this suggested solution should be used in new models of satellite receivers which would share the function of aircraft positioning with the help of satellite systems, and in case of information loss from the system, the receiver would calculate aircraft position on the basis of a ready-made mathematical model.

1. NAVIGATION WITH THE HELP OF POSITION POTENTIAL IN AIRSPACE

We shall use a new navigation filter, which will be mainly based on a segment of an aircraft / a vehicle position measurements, its velocity, and error position statistics (error position ellipsoid). When the segment is in motion it is assumed that its position and its corresponding error position statistics may be read by one or more navigation systems, such as: GPS or LORAN C. A navigation filter presently enables to determine the object's position and is able to detect at once its position in a given time in future.

In fact, the number of observed positions include all vital aircraft kinetic information. In the assumption to the program 'position potential' has been used aided with the data elaborated by the navigation services. According to Newton's gravitation law a free mass molecule is drawn by another mass. The molecule acceleration of a given mass is proportional to G gravitation constant and counter proportional to distance cube of the drawn mass. Analogically, we shall consider the areas of the most probable position (position error ellipsoid) as the 'power source', which should 'draw' a trajectory that passes through the above mentioned area. A potential field of a single molecule (of an aircraft) should reflect the observed position and expected pressure on a molecule, which should decrease steadily and proportionally to the molecule approach to the designated position.

When a molecule appears exactly in an ellipsoid error position it will be drawn by the force, which power is proportional to intensity of the potential. The potential decreases steadily along with the diminishing molecule distance from the designated position. Moreover, in order to let the molecule move after the designated position has appeared the potential of the drawing source will be in time dispersed ex-potentially. When choosing a density position function (position potential), which contains the index of dispersion α and the G parameter (the uncertainty of position assignment – the equivalent of the gravitation constant in Newton's theory of gravitation) we assume that the molecule trajectory will present the real route of the vehicle.

The attempt of creating a navigation filter based on this idea was firstly introduced by Inzinga i Vanicek [Vanicek; 2000]. Seeing, that the molecule motion equation is extremely difficult for an analytical solution, the following model of calculation was selected:

- selection of a position potential function
- formulating a temporary dispersing potential field
- description of a motion equation
- solving the motion equation
- defining the Alpha and G
- the navigation problem ultimate solution

As the first, we select an appropriate potential function. Using the chosen density position function we may determine the potential position field in different time for the assigned positions sequences. Then, we form a model of a molecule motion and solve the equation of its motion. In order to show a changing navigation environment, the potential function contains changing parameters. (Alpha and G). When the parameters Alpha and G and the initial environment are unknown, then there are unlimited possibilities of the molecules position. This means that further information is needed to determine an appropriate trajectory. Therefore, we establish for the filter the 'self-learning' procedure in order to determine the parameters and the environment from the previous observations. The parameters and the initial environment in the movement model relate to the previous observations through the 'motion equation.' At this stage we solve the motion equation having initial environment data. Next, we start determining the Alpha and G parameters. In order to optimize the above mentioned parameters we shall use the the method of the smallest squares. The estimation of the molecule position (aircraft) in a specified future (making a prediction) is possible due to the motion model with the determined parameters and on the basis of its present position. The estimation of error occurrence is possible in the moment of acquiring new information about the molecule position, due to the use of the magnitude of differences and real positions, through testing if the new position is found in the ellipsoid error position area.

1.1. Navigation model

Let's assume that the speed function (3) [Kącki 1975] for location of a three-dimensional random vector has a form:

$$\phi_{\mathbf{r}_0} = \frac{1}{K} \exp \left[-\frac{1}{2} (\mathbf{r} - \mathbf{r}_0)^T \mathbf{C}^{-1} (\mathbf{r} - \mathbf{r}_0) \right] \quad (1)$$

where:

$$\mathbf{r} = \begin{bmatrix} x \\ y \\ z \end{bmatrix}$$

- the vector situation of the particle at present moment „t”:

$$\mathbf{r}_0 = \begin{bmatrix} x_0 \\ y_0 \\ z_0 \end{bmatrix}$$

- the vector situation of the particle at established moment „t₀”

$$K = (2\pi)^{\frac{3}{2}} (\det \mathbf{C})^{\frac{1}{2}}$$

\mathbf{C} – covariance symmetrical matrix (4) [Plucińska 2000]

$$\mathbf{C} = \begin{bmatrix} c_{11} & c_{12} & c_{13} \\ c_{21} & c_{22} & c_{23} \\ c_{31} & c_{32} & c_{33} \end{bmatrix} = \begin{bmatrix} D^2 X & \text{cov}(X, Y) & \text{cov}(X, Z) \\ \text{cov}(Y, X) & D^2 Y & \text{cov}(Y, Z) \\ \text{cov}(Z, X) & \text{cov}(Z, Y) & D^2 Z \end{bmatrix}$$

Let's remind that the base of particle situation is potential of the particle U_i

$$U_i(t) = G(\mathbf{r} - \mathbf{r}_{oi})^T \mathbf{C}_i^{-1} (\mathbf{r} - \mathbf{r}_{oi}) e^{-\alpha(t-t_i)} \quad (2)$$

where:

$$(\mathbf{r} - \mathbf{r}_{0i})^T \mathbf{C}_i^{-1} (\mathbf{r} - \mathbf{r}_{0i})$$

is square shape which defining ellipsoid error site at moment “ t_i ”

czas $t \geq t_i$

time $t \geq t_i$.

\mathbf{C}_i is a covariance matrix i - tej particular positively define. However, positive parameters α & G (they are for determination) mean properly:

- parameter of dispersion

G - uncertainty of site assignment (equivalent of gravitation constant in Newton’s attracting)

In accordance with designation of potential (2), potential in changeable time “ t ” fabricated by “ n ” indicated sites of particular adopts form:

$$U = \sum_{i=1}^n U_i = G e^{-\alpha t} \sum_{i=1}^n (\mathbf{r} - \mathbf{r}_{0i})^T \mathbf{C}_i^{-1} (\mathbf{r} - \mathbf{r}_{0i}) e^{\alpha t_i} \quad (3)$$

where:

$t \geq t_n$.

Let us notice that the filter (the potential) keeps tempi to the kinematics of the particle (the plane). The ground of the potential in the variable time is brought to the fore by the new position of the small part for the purpose of inclusions as soon as possible the new information.

For the accepted definite potential with the equalization (3) we have to unknotting a following equation of the movement:

$$\ddot{\mathbf{r}} = - \frac{\partial U(t)}{\partial \mathbf{r}} \quad (4)$$

Let us accept following marks:

$$\mathbf{A} = 2 \sum_{i=1}^n e^{\alpha t_i} \mathbf{C}_i^{-1} \quad \text{the matrix (3x3)} \quad (5)$$

$$\mathbf{B} = 2 \sum_{i=1}^n e^{\alpha t_i} \mathbf{C}_i^{-1} \mathbf{r}_{0i} \quad \text{the vector} \quad (6)$$

the equation of the movement (4) will accept the figure

$$\ddot{\mathbf{r}}(t) = e^{-\alpha t} G (\mathbf{A} \mathbf{r} - \mathbf{B}); \quad t \geq t_n \quad (7)$$

There is this equation of the movement of the particle (the vehicle) in a field of the potential position in the variable time „ t ”, after the appearance „ n ” of appointed positions.

The equation of the movement (7) in coordinates will have a following figure:

$$\begin{aligned} \ddot{x}(t) &= -G(A_x x - B_x) e^{-\alpha t} \\ \ddot{y}(t) &= -G(A_y y - B_y) e^{-\alpha t} \\ \ddot{z}(t) &= -G(A_z z - B_z) e^{-\alpha t} \end{aligned} \quad t \geq t_n \quad (8)$$

For the purpose of solution of the system of ordinary differential equations of the second order we will use the substitution of the independent variable (the time- t)

$$s = \frac{2}{\alpha} e^{-\frac{\alpha}{2} t} \sqrt{G A_x}$$

We will receive differential equations Bessela whose solution will have a following figure:

$$\begin{cases} x(t) = \frac{B_x}{A_x} + a_1 J_0\left(\frac{2}{\alpha} e^{\frac{\alpha}{2}t} \sqrt{GA_x}\right) + a_2 N_0\left(\frac{2}{\alpha} e^{\frac{\alpha}{2}t} \sqrt{GA_x}\right) \\ y(t) = \frac{B_y}{A_y} + b_1 J_0\left(\frac{2}{\alpha} e^{\frac{\alpha}{2}t} \sqrt{GA_y}\right) + b_2 N_0\left(\frac{2}{\alpha} e^{\frac{\alpha}{2}t} \sqrt{GA_y}\right) \\ z(t) = \frac{B_z}{A_z} + c_1 J_0\left(\frac{2}{\alpha} e^{\frac{\alpha}{2}t} \sqrt{GA_z}\right) + c_2 N_0\left(\frac{2}{\alpha} e^{\frac{\alpha}{2}t} \sqrt{GA_z}\right) \end{cases} \quad (9)$$

Bessel' and (with functions cylindrical) the first and second kind about the indicator the zero. First elements in contained sums in solutions represent integrals special equation of heterogeneous, while elements with constants are general integrals of equation homogeneous.

To mark constants a_1 ; a_2 ; b_1 ; b_2 ; c_1 ; c_2 initial conditions should be used, i.e. to the system of equations (8) to add initial conditions (to formulate the problem Cauchyego).

For the purpose of the more easy delimitation the integration constant a_1 ; a_2 ; b_1 ; b_2 ; c_1 ; c_2 properties of the Bessels function should be used [Smirnow 1967], such as:

$$\begin{cases} \frac{dJ_0(t)}{dt} = -J_1(t) \\ \frac{dN_0(t)}{dt} = -N_1(t) \end{cases} \quad (10)$$

and

$$J_1(t)N_0(t) - J_0(t)N_1(t) = \frac{2}{\Pi t} \quad (11)$$

Calculated constants are defined by the following patterns:

$$\begin{cases} a_1 = -\frac{\Pi}{\alpha} \left[\left(x_n - \frac{B_x}{A_x} \right) \sqrt{GA_x} N_1\left(\frac{2}{\alpha} \sqrt{GA_x}\right) - \dot{x}_n N_0\left(\frac{2}{\alpha} \sqrt{GA_x}\right) \right] \\ a_2 = \frac{\Pi}{\alpha} \left[\left(x_n - \frac{B_x}{A_x} \right) \sqrt{GA_x} J_1\left(\frac{2}{\alpha} \sqrt{GA_x}\right) - \dot{x}_n J_0\left(\frac{2}{\alpha} \sqrt{GA_x}\right) \right] \\ b_1 = -\frac{\Pi}{\alpha} \left[\left(y_n - \frac{B_y}{A_y} \right) \sqrt{GA_y} N_1\left(\frac{2}{\alpha} \sqrt{GA_y}\right) - \dot{y}_n N_0\left(\frac{2}{\alpha} \sqrt{GA_y}\right) \right] \\ b_2 = \frac{\Pi}{\alpha} \left[\left(y_n - \frac{B_y}{A_y} \right) \sqrt{GA_y} J_1\left(\frac{2}{\alpha} \sqrt{GA_y}\right) - \dot{y}_n J_0\left(\frac{2}{\alpha} \sqrt{GA_y}\right) \right] \\ c_1 = -\frac{\Pi}{\alpha} \left[\left(z_n - \frac{B_z}{A_z} \right) \sqrt{GA_z} N_1\left(\frac{2}{\alpha} \sqrt{GA_z}\right) - \dot{z}_n N_0\left(\frac{2}{\alpha} \sqrt{GA_z}\right) \right] \\ c_2 = \frac{\Pi}{\alpha} \left[\left(z_n - \frac{B_z}{A_z} \right) \sqrt{GA_z} J_1\left(\frac{2}{\alpha} \sqrt{GA_z}\right) - \dot{z}_n J_0\left(\frac{2}{\alpha} \sqrt{GA_z}\right) \right] \end{cases} \quad (12)$$

Solutions (9) of the differential equation (8) contains unknown parameters

α [s^{-1}] parameter of dispersion

G [$m^2 s^{-2}$] – uncertainty of site assignment of the particle (the size of the potential U as in Newton's law is directly proportional to G)

1.2. The example of the optimization of α & G parameters

For the purpose of optimizing of parameters α and G let us consider the following problem consisting in solving of equation of the movement:

$$\begin{aligned}
\ddot{x}(t) &= -G(A_x x - B_x) e^{-\alpha t} \\
\ddot{y}(t) &= -G(A_y y - B_y) e^{-\alpha t} \\
\ddot{z}(t) &= -G(A_z z - B_z) e^{-\alpha t}
\end{aligned} \quad t \geq t_n \quad (13)$$

Lets consider case when the matrix of the covariance is a diagonal matrix , then:

$$\begin{aligned}
A_x &= 2 \sum_{i=1}^n e^{\alpha(t_i - t_n)} p_{xi} \\
A_y &= 2 \sum_{i=1}^n e^{\alpha(t_i - t_n)} p_{yi} \\
A_z &= 2 \sum_{i=1}^n e^{\alpha(t_i - t_n)} p_{zi}
\end{aligned} \quad (14)$$

and coordinates of the vector B express themselves as follows:

$$\begin{aligned}
B_x &= 2 \sum_{i=1}^n e^{\alpha(t_i - t_n)} p_{xi} x_{oi} \\
B_y &= 2 \sum_{i=1}^n e^{\alpha(t_i - t_n)} p_{yi} y_{oi} \\
B_z &= 2 \sum_{i=1}^n e^{\alpha(t_i - t_n)} p_{zi} z_{oi}
\end{aligned} \quad (15)$$

at given initial conditions for $t_n = 0$

$$\mathbf{r}(0) = \begin{bmatrix} x_n \\ y_n \\ z_n \end{bmatrix} \quad \dot{\mathbf{r}}(0) = \begin{bmatrix} \dot{x}_n \\ \dot{y}_n \\ \dot{z}_n \end{bmatrix} \quad (15)$$

The vector of the position of particles is definite by formulas

$$\begin{cases}
x(t) = \frac{B_x}{A_x} + a_1 J_0 \left(\frac{2}{\alpha} e^{-\frac{\alpha}{2} t} \sqrt{GA_x} \right) + a_2 N_0 \left(\frac{2}{\alpha} e^{-\frac{\alpha}{2} t} \sqrt{GA_x} \right) \\
y(t) = \frac{B_y}{A_y} + b_1 J_0 \left(\frac{2}{\alpha} e^{-\frac{\alpha}{2} t} \sqrt{GA_y} \right) + b_2 N_0 \left(\frac{2}{\alpha} e^{-\frac{\alpha}{2} t} \sqrt{GA_y} \right) \\
z(t) = \frac{B_z}{A_z} + c_1 J_0 \left(\frac{2}{\alpha} e^{-\frac{\alpha}{2} t} \sqrt{GA_z} \right) + c_2 N_0 \left(\frac{2}{\alpha} e^{-\frac{\alpha}{2} t} \sqrt{GA_z} \right)
\end{cases} \quad (16)$$

instead the vector of the speed qualify equations

$$\begin{cases}
\dot{x}(t) = \sqrt{GA_x} e^{-\frac{\alpha}{2} t} \left[a_1 J_1 \left(\frac{2}{\alpha} e^{-\frac{\alpha}{2} t} \sqrt{GA_x} \right) + a_2 N_1 \left(\frac{2}{\alpha} e^{-\frac{\alpha}{2} t} \sqrt{GA_x} \right) \right] \\
\dot{y}(t) = \sqrt{GA_y} e^{-\frac{\alpha}{2} t} \left[b_1 J_1 \left(\frac{2}{\alpha} e^{-\frac{\alpha}{2} t} \sqrt{GA_y} \right) + b_2 N_1 \left(\frac{2}{\alpha} e^{-\frac{\alpha}{2} t} \sqrt{GA_y} \right) \right] \\
\dot{z}(t) = \sqrt{GA_z} e^{-\frac{\alpha}{2} t} \left[c_1 J_1 \left(\frac{2}{\alpha} e^{-\frac{\alpha}{2} t} \sqrt{GA_z} \right) + c_2 N_1 \left(\frac{2}{\alpha} e^{-\frac{\alpha}{2} t} \sqrt{GA_z} \right) \right]
\end{cases} \quad (17)$$

and constants of integration by a relationship

$$\left. \begin{aligned} a_1 &= -\frac{\Pi}{\alpha} \left[\left(x_n - \frac{B_x}{A_x} \right) \sqrt{GA_x} N_1 \left(\frac{2}{\alpha} \sqrt{GA_x} \right) - \dot{x}_n N_0 \left(\frac{2}{\alpha} \sqrt{GA_x} \right) \right] \\ a_2 &= \frac{\Pi}{\alpha} \left[\left(x_n - \frac{B_x}{A_x} \right) \sqrt{GA_x} J_1 \left(\frac{2}{\alpha} \sqrt{GA_x} \right) - \dot{x}_n J_0 \left(\frac{2}{\alpha} \sqrt{GA_x} \right) \right] \\ b_1 &= -\frac{\Pi}{\alpha} \left[\left(y_n - \frac{B_y}{A_y} \right) \sqrt{GA_y} N_1 \left(\frac{2}{\alpha} \sqrt{GA_y} \right) - \dot{y}_n N_0 \left(\frac{2}{\alpha} \sqrt{GA_y} \right) \right] \\ b_2 &= \frac{\Pi}{\alpha} \left[\left(y_n - \frac{B_y}{A_y} \right) \sqrt{GA_y} J_1 \left(\frac{2}{\alpha} \sqrt{GA_y} \right) - \dot{y}_n J_0 \left(\frac{2}{\alpha} \sqrt{GA_y} \right) \right] \\ c_1 &= -\frac{\Pi}{\alpha} \left[\left(z_n - \frac{B_z}{A_z} \right) \sqrt{GA_z} N_1 \left(\frac{2}{\alpha} \sqrt{GA_z} \right) - \dot{z}_n N_0 \left(\frac{2}{\alpha} \sqrt{GA_z} \right) \right] \\ c_2 &= \frac{\Pi}{\alpha} \left[\left(z_n - \frac{B_z}{A_z} \right) \sqrt{GA_z} J_1 \left(\frac{2}{\alpha} \sqrt{GA_z} \right) - \dot{z}_n J_0 \left(\frac{2}{\alpha} \sqrt{GA_z} \right) \right] \end{aligned} \right\} \quad (18)$$

Let us consider case, when the parameter α is large and $t_i - t_{i-1} = 1$ [s] and $i = 1, 2, \dots, n$, then we have:

$$\begin{aligned} A_x &= 2 \left[e^{-n\alpha} p_{x_1} + \dots + e^{-1\alpha} p_{x_{n-1}} + e^{-0\alpha} p_{x_n} \right] \\ &= 2 \left[e^{-n\alpha} p_{x_1} + \dots + e^{-1\alpha} p_{x_{n-1}} \right] + 2p_{x_n} \leq \\ &\leq 2 \max_{1 \leq i \leq n-1} p_{x_i} \left[e^{-\alpha} + e^{-2\alpha} + \dots + e^{-n\alpha} \right] + 2p_{x_n} \\ &= 2e^{-\alpha} \frac{1 - (e^{-\alpha})^{n-1}}{1 - e^{-\alpha}} \max_{1 \leq i \leq n-1} p_{x_i} + 2p_{x_n} \approx 2p_{x_n} \end{aligned} \quad (19)$$

Leading the analogous reasoning we will receive:

$$\begin{cases} A_x = 2p_{x_n} \\ A_y = 2p_{y_n} \\ A_z = 2p_{z_n} \end{cases} \quad (20)$$

$$i \begin{cases} B_x = 2p_{x_n} x_{0n} \\ B_y = 2p_{y_n} y_{0n} \\ B_z = 2p_{z_n} z_{0n} \end{cases} \quad (21)$$

Our aim is optimizing by the method of smallest squares parameters α, G so that the function two variable

$$f(\alpha, G) = \sum_{i=1}^n [\tilde{r}(t_i) - \tilde{r}_{0i}]^2 = \text{the minimum}$$

or written in coordinates:

$$f(\alpha, G) = \sum_{i=1}^n \left\{ [x(t_i) - x_{0i}]^2 + [y(t_i) - y_{0i}]^2 + [z(t_i) - z_{0i}]^2 \right\} = \text{minimum} \quad (22)$$

where:

x_{0i}, y_{0i}, z_{0i} – the position of the particle (the plane) in the moment t_i (data given from the satellite)

$x(t_i), y(t_i), z(t_i)$ the position of the particle (the plane) in the moment t_i calculated with (16)

and

$x_{0n}, y_{0n}, z_{0n}, \dot{x}_{0n}, \dot{y}_{0n}, \dot{z}_{0n}$ – given positions and speeds of the particle received from the satellite calculated from examples (16) (17), after the earlier calculation of the value of the function Bessela (stabilized are).

2. INITIAL VERIFICATION OF MATHEMATICAL MODEL

The proposed algorithm of alternative navigation filter has been implemented due to the lack of mathematical solutions and the huge complexity of the problem. The resulting measurement data obtained on the basis of numerous experiments, the trajectory profiles, the number of factors influencing the degree of precision and the determined level of accuracy probability of the position allocation compels to develop a new method of data prediction (positions) in the situation when we lack them in the population of experimental data (measurement).

An elaboration based on the defined position potential function – calls for optimizing of this function in view of searching its minima, which, with the character implied, guarantees maximal approximation of estimated positions and a minimal error position in the 3D airspace. A special computer program elaborated by the author has been prepared to the analysis on searching the function minimum, the program based on the evolutionary algorithms theory [Ombach 2004]. Its employment became indispensable since the traditional methods of searching the global function extremes, such as:

- elementary method (fragmental derivatives);
- the linear programming method;
- the highest probability prediction method or the complex equation schemes solution method

did not guarantee the satisfactory results. In the connection with that the use of evolutionary logarithm became necessary as the mathematical apparatus applied in it proved to be indispensable to achieve the assumed aim. It became possible by implementing the concepts contained in the study on the employment of evolutionary algorithms, 'Theory of Evolutionary Algorithms', listed in this paragraph.

The presented model was used for computer analysis of flight data during the test flights to show results of used solutions. The optimization was carried out for digital time interval - s , $s+1$, $s+2$ as following :

- a potential s , $s+1$;
- a below function was examined for optimization;

$$f(\alpha, G) = \sum_{i=1}^n \{ [x(t_i) - x_{0i}]^2 + [y(t_i) - y_{0i}]^2 + [z(t_i) - z_{0i}]^2 \} \quad (23)$$

Conducted analysis of data of test flights show that proposed alternate navigation filter fulfill assumptions. The used model of navigation allows to include factors as following:

- covariance matrix showed in equation (2) i (3) do not have to be diagonal;
- potential of position will be used without limit presented in equation (19);
- optimization (22) of parameters α i G will be included both a three-dimensional vector and a speed vector.

Elimination of obstructions such as mentioned above (presented in paragraph concerning verification of navigation model too) allows to adjust calculated trajectory to real one.

References

1. Grzegorzewski M.: Navigating an aircraft by means of a position potential in three dimensional space – Annual of Navigation (2005);
2. Inzinga T. and Vaniček P. (1985). "A Two-Dimensional navigation Algorithm Using a Probabilistic Force Field." Presented at Third International Symposium on Intertial Tehnology for Surveying and Geodesy, Banff, Canada, 1985.
3. Kącki E., Siewierski L.: Wybrane działy matematyki wyższej z ćwiczeniami. Warszawa 1975. PWN.
4. Plucińska A., Pluciński E. Probabilistyka. Warszawa 2000. Wydawnictwo Naukowo-Techniczne.
5. Smirnow W.I., Matematyka Wyższa rozdz. V, I, II cz.2, W-wa, 1967, PWN.
6. Ombach J.: Some algorithms of global optimizations. Materiały pokonferencyjne. Uniwersytet Jagielloński. Kraków. 2004.

*Onder Turan, Asst. Prof. Dr., (Anadolu University, School of Civil Aviation), Turkey
T.Hikmet Karakoc, Prof. Dr., (Anadolu University, School of Civil Aviation), Turkey*

EXPERIMENTAL STUDY OF MICROTURBINE ENGINE FOR MAN AND UNMANNED AIRCRAFT

Abstract

In this study, experimental testing results of a small turbojet engine presented used initially in manned aircraft, remotely piloted vehicles (RPV) and starting systems for aircraft . Testing of microturbine engine has been done in engine test-cell. Thrust, specific fuel consumption and exhaust gas temperature performance charts versus number of revolution (RPM) of the experimental turbojet engine had been presented in this paper .

INTRODUCTION

Dating from the mid-1970s the microturbine engines is a small turbojet engine intended for the propulsion of manned and un-manned aircraft. This unit adopts a similar mechanical layout to the Auxiliary Power Units (APU). The engine adopts the classic reverse flow layout with the main shaft mounted on spring loaded angular contact bearings. This engine is arguably a distant relative of the Plessey Solent unit and bears many similarities. A beautifully built and straight forward gas turbine engine. Unfortunately a relatively rare engine but ideal for homebuilt aircraft projects and ground projects. One of only a few in its thrust class. Figure 1 shows the gas generator of the experimental turjet engine [1].



Figure 1. Gas generator of the experimental turbojet engine[1]

Table 1. Some model of APU engine[2]


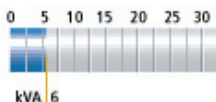
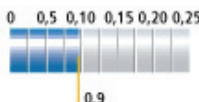

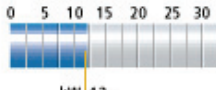
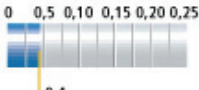

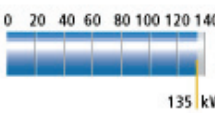
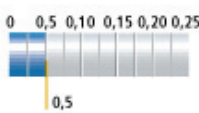

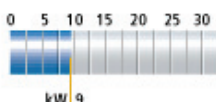
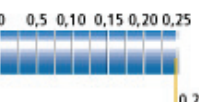

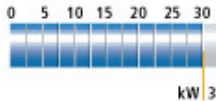
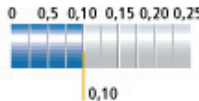


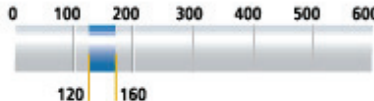



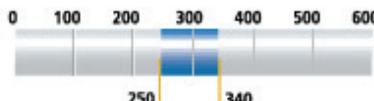



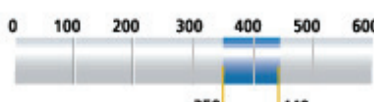



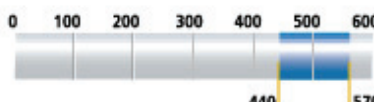

Model	Mechanical power (kW)	Electrical Power (kW, kVA)	Air Flow (kg/s)	Engine Starting	Application
 Rubis 305	Non applicable	 kVA 6	 0,9	M88 Snecma	Rafale C, M & D Dassault Aviation
 Saphir 10	Non applicable	 kW 12	 0,4	Adour Mk 871 Adour Mk 951 Turbomeca/Rolls-Royce	Hawk LIF Mk 127 & Hawk 200 Hawk LIF Mk 120,128 & 129 BAE Systems
 Saphir 100	 135 kW	Non applicable	 0,5	Non applicable	NH90 NHIndustries
 Saphir 4-2/4-5	Non applicable	 kW 9	 0,24	Electrical assistance	Falcon 20 Dassault Aviation
 Saphir 20/095	Non applicable	 kW 30	 0,10	Electrical assistance	EC725 Super Puma Eurocopter

Table 2. Some model of microturbojet engine[2]

Model	Architecture	Thrust (daN)	Main Application
 TRS 18-1	 Centrifugal Compressor	 120 to 160 daN / 270 to 360 lbt	 Mirach 100-5 Target drone - Galileo Avionica
 TRI 40	 4 stage-axial compressor	 250 to 340 daN / 560 to 750 lbt	 NSM anti-ship Missile - KDA / MBDA
 TRI 60-5	 3 stage-axial compressor	 350 to 440 daN / 800 to 1100 lbt	 MQM107 Target drone - Raytheon / BAE Systems / CEI
 TRI 60-20/-30	 4 stage-axial compressor	 440 to 570 daN / 1000 to 1250 lbt	 Storm Shadow/Scalp EG Cruise missile - MBDA

Experimental turbojet engines has specialized since 1960 in the design and manufacture for small gas turbine used initially in starting systems for aircraft. Further development of these gas turbines led to the production of a jet engine in the 100 daN (225 lbf) thrust class. For remotely piloted vehicles (RPV), thrust is increased to the engine life required and the utilization 115 daN (258lbf) and 150 daN (337 lbf) [3]. It can be shown easily that APU and turbojet application of microturbine engines in Table 1 and Table 2.

Experimental turbojet engine is a single shaft, through-flow engine of simple design. The rotating assembly comprises a single stage centrifugal compressor and single stage axial turbine mounted on a single shaft. Figure 2 shows the engine test-cell and Figure 3 shows the component of the experimental turbojet engine.



Figure 2. *Experimental turbojet engine test cell [4]*

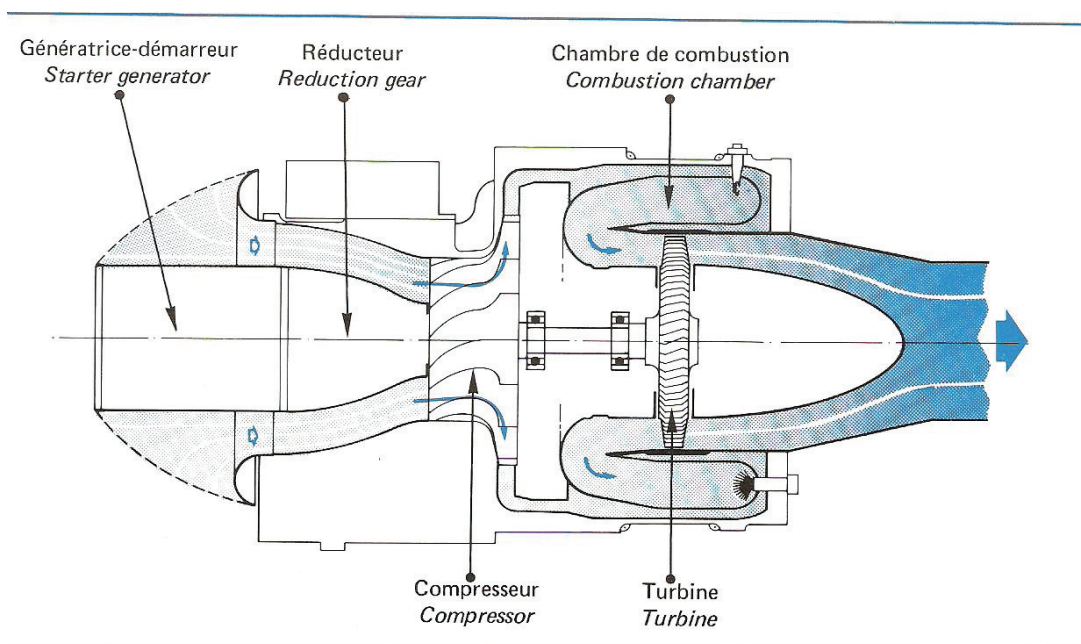


Figure 3. *Components of the experimental turbojet engine [5]*

There is no dilution of engine charge air. Start and governing are entirely automatic. Relight can be accomplished in flight by windmilling. Small size and low weight essential features. The rotor assembly comprises: a single-stage centrifugal compressor consisting of a cast steel inducer wheel and a light alloy impeller. A single-stage axial turbine cast in high-temperature steel. These are mounted on a single shaft carried on two inboard high speed ball bearings [6].

The core engine comprises: an air intake guard screen, an air intake casing, with integral oil reservoir and pump and a starter generator, a turbine casing containing the rotor assembly, an annular type combustor, a backplate with integral fuel manifold and ten spill type fuel burners, and exhaust cone, engine installed fuel and lubrication system accessories shown in Figure 4 and Figure 5.

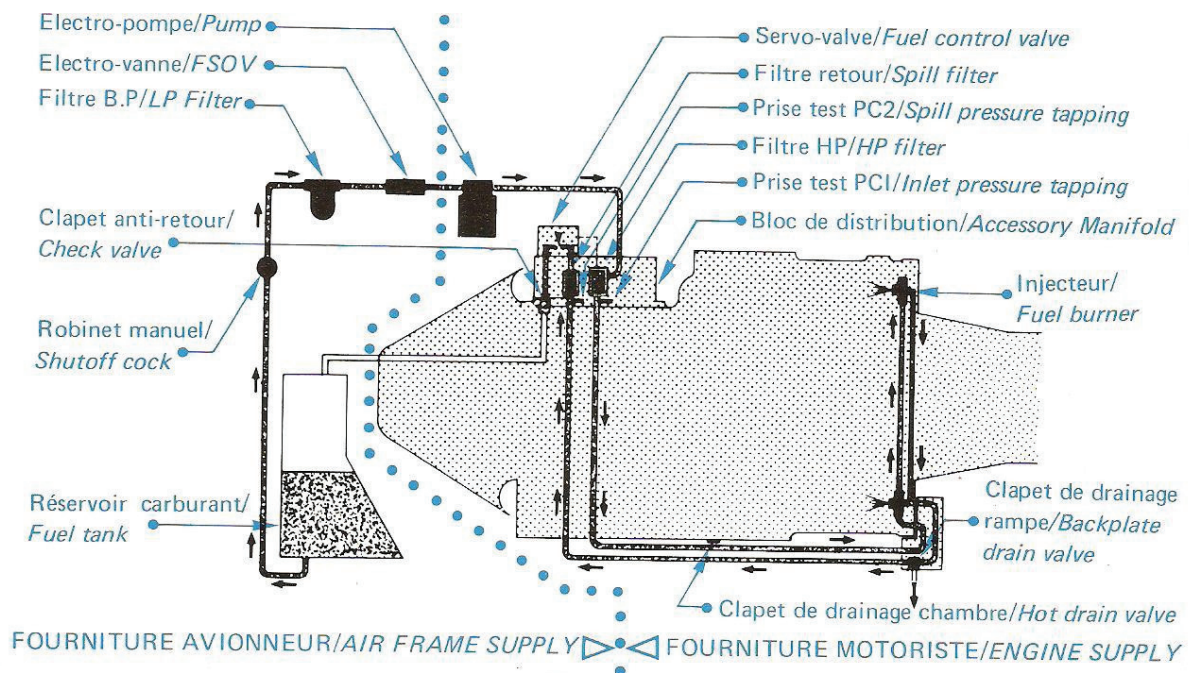


Figure 4. Fuel system of the experimental turbojet engine [5]

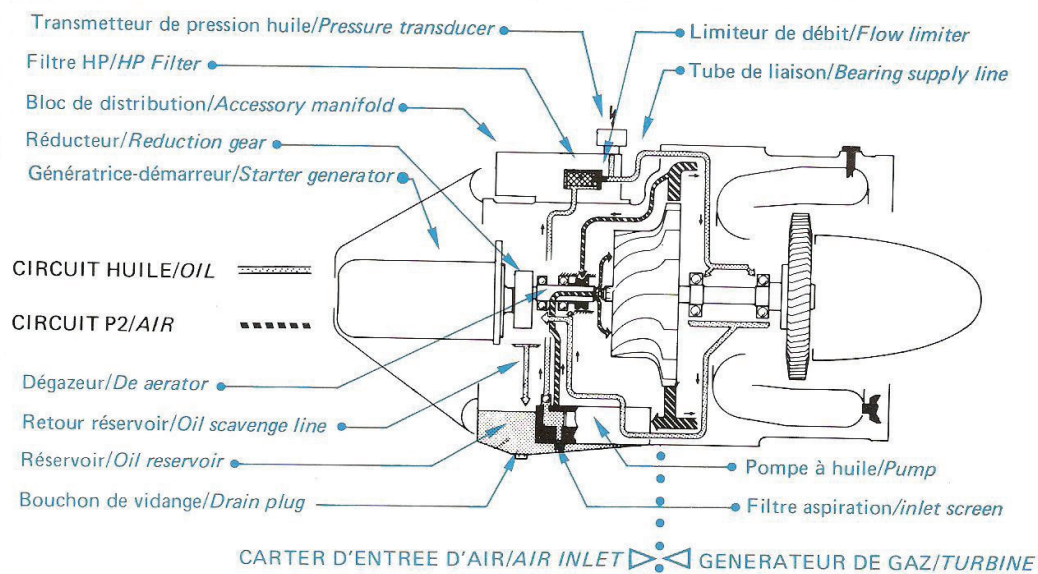


Figure 5. Lubrication system of the experimental turbojet engine [5]

An electrically driven fuel pump delivers fuel to the burners via a high pressure filter. The volume of fuel discharged by the burners into the combustion chamber is metered by a fuel control unit in function of ECU (Electronic Control Unit) commands. Fuel surplus to governing requirements is spilled back to the fuel tank.

Lubrication system is entirely contained within the engine. The pump, which is immersed in the oil sump through a wire mesh strainer and delivers it to the engine bearings. The return line from the bearings lubricates the reduction gears. Air from the emulsified oil is exhausted by a centrifugal deaerator.

MEASURED ENGINE PARAMETER IN ENGINE TEST-CELL

It can measured some data from engine test-cell such as [6]:

- Manifold outlet pressure (0-20 bar)
- Manifold inlet pressure (0-25bar)
- Total compressor outlet pressure (0-6 bar)
- Oil sump pressure (-1+1 bar)
- Starting air pressure (0-20 bar)
- Total air intake pressure (water column)
- Air intake bellmouth (water column)
- Total exhaust gaz temperature (8 digital indicators)
- Oil temperature (digital indicator)
- Vibration measurement channel
- Thrust measurement channel
- Fuel temperature sensor
- Fuel flowmeter
- -1+3 bar fuel pressure gage
- Pressure reducing valve
- Fuel shutoff valve
- Fuel inlet filter
- 0-9 bar pneumatic pressure gage
- Adjutment valve
- Filter

Engine leading particulars are as follows:

- Rated thrust: 150 daN
- Maximum continuous engine speed: 48250 RPM
- Idle: 30000 RPM
- Operating temperature range: 40⁰C to +50⁰C
- Maximum airspeed: 0.9 Mach
- Eelctrical power output: 1.5 kW
- Specific fuel consumption: <1.20 kg/daN.h
- Power supply for compressed air starting 0.0056 kg/s for 13 s.
- Power supply from generator at rated RPM: 53 A at 28.5 Vdc.
- Weight of engine with jet pipe: 42 kg
- Operating envelope: -500 and 1000m

CONCLUSION

In this study, introduction of the experimental turbojet engines and its test-cell in School of Civil Aviation in Anadolu University were presented. Propulsion department student can learn about starting engine, data acquisition some engine performance data such as thrust, pressure, temperature, specific fuel consumption, engine speed and vibration besides theoretic analysis of the turbojet engine in our school.

This turbojet engine can be converted to turboprop engine type for further study. Compressor and turbine map are easily drawn.

REFERENCES

- [1] <http://www.gasturbine.pwp.blueyonder.co.uk/TRS18.htm>
- [2] http://www.microturbo.fr/rubrique.php3?id_rubrique=11&lang=en
- [3] Microturbo Catalog, 1993.
- [4] Turbojet Engine Test-cell, Propulsion Department, School of Civil Aviation, Eskisehir, Turkey.
- [5] Small Turbojet Engine Test-Cell Operating Procedure, 1993.
- [6] Turbojet Engine Performance, Aircraft Propulsion Courses Notes, Turan O., 2008.

FUEL CONSUMPTION ESTIMATION OF COMMERCIAL TURBOFANS

Abstract

Steady state specific fuel consumption estimation of axial flow aircraft gas turbine engines used in middle and long-range aircraft has been investigated and parametric curves of the engine were drawn these purposes. In this study, nonafterburning and separate flow high bypass turbofan engine was selected as example on-design engine type and its ideal and real parametric specific fuel consumption was computed in this study.

INTRODUCTION

In this paper, on design analysis of high bypass turbofan engines with separate flow and no afterburning used in commercial aircraft were analysed and then effects of some design variables (e.g. compressor pressure ratio, fan pressure ratio, turbine inlet temperature, bypass ratio, cooling air ratio, nozzles pressure losses) and effects of different flight conditions (e.g. flight altitude and flight Mach number) on specific fuel consumption of the commercial engine in ideal and real cycles. A new software program had been developed for this purpose in visual and excel programming language. Values of specific fuel consumption were calculated and then performance curves were obtained in this software programs. In Figure 1, a typical turbofan engine component can be seen easily.

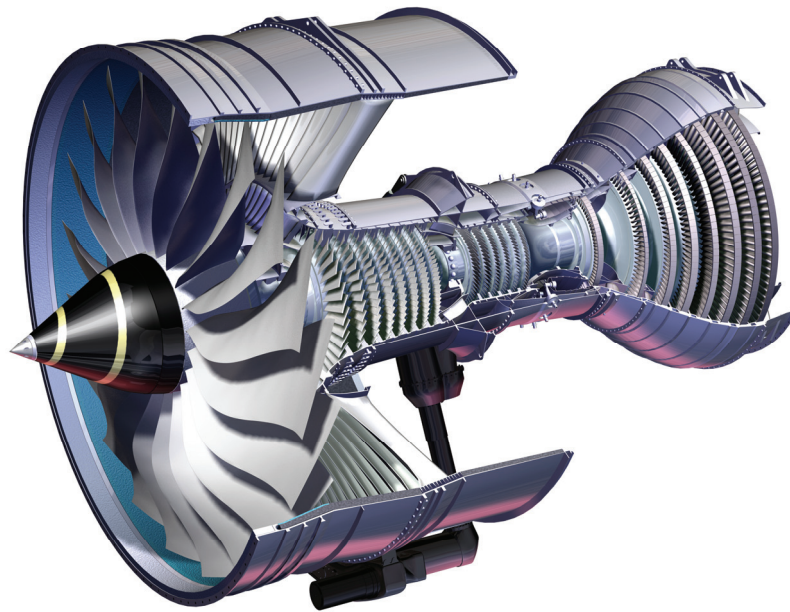


Figure 1. *High bypass turbofan engine[1]*

SPECIFIC FUEL CONSUMPTION CURVES IN IDEAL AND REAL CYCLE ANALYSIS

The object of cycle analysis is to obtain estimates of the performance parameters (primarily thrust and specific fuel consumption) in terms of design limitations (such as maximum allowable turbine temperature and attainable component efficiencies), the flight conditions (the ambient pressure, temperature, and Mach number), and design choices (such as compressor pressure ratio, fan pressure ratio, bypass ratio, as soon).

The engine design starts with the on-design (or design point) analysis, which presumes that all design choices are still under control, and that the size of the engine has yet to be chosen. In off-design performance analysis no component performances are available so that the component efficiencies as functions of operating conditions must be estimated. Final choice of an engine is based on its off-design performance over the entire aircraft mission [2-5]. On-design cycle analysis curves are very important for the cycle analysis of objective engine research. Because it is easy to see effect of the independent design parameters of the engine such as fan pressure ratio and bypass ratio on the dependent parameters such as the specific thrust and specific fuel consumption instead of numerical values. Figure 2 shows different engine specific fuel consumption values related to certificate date.

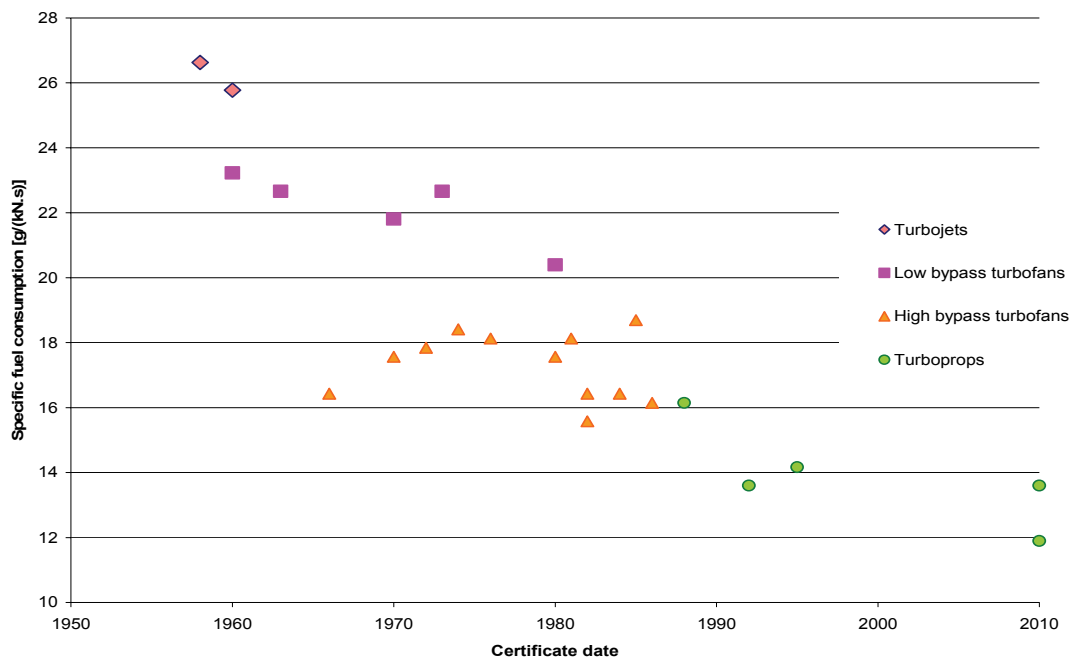


Figure 2. *Specific fuel consumption variation of each engine according to certificate date*

In Figure 3 through Figure 7 it is shown specific fuel consumption curves according to bypass ratio, compressor pressure ratio, fan pressure ratio and aircraft flight Mach number in ideal cycle analysis [6].

In Figure 8 through Figure 11 it is shown specific fuel consumption curves according to bypass ratio, compressor pressure ratio, fan pressure ratio and aircraft flight Mach number in real cycle analysis [7].

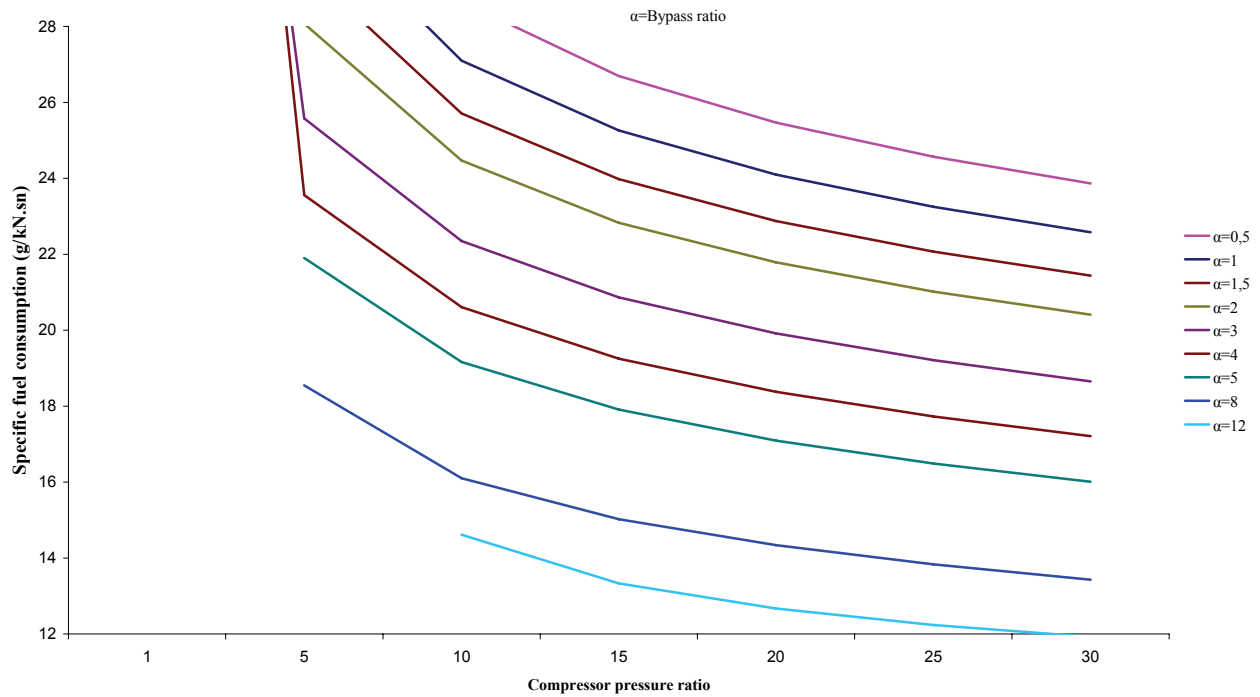


Figure 3. Compressor pressure ratio-specific fuel consumption curve for different bypass ratios of a high bypass turbofan engine at ideal cycle analysis[6]

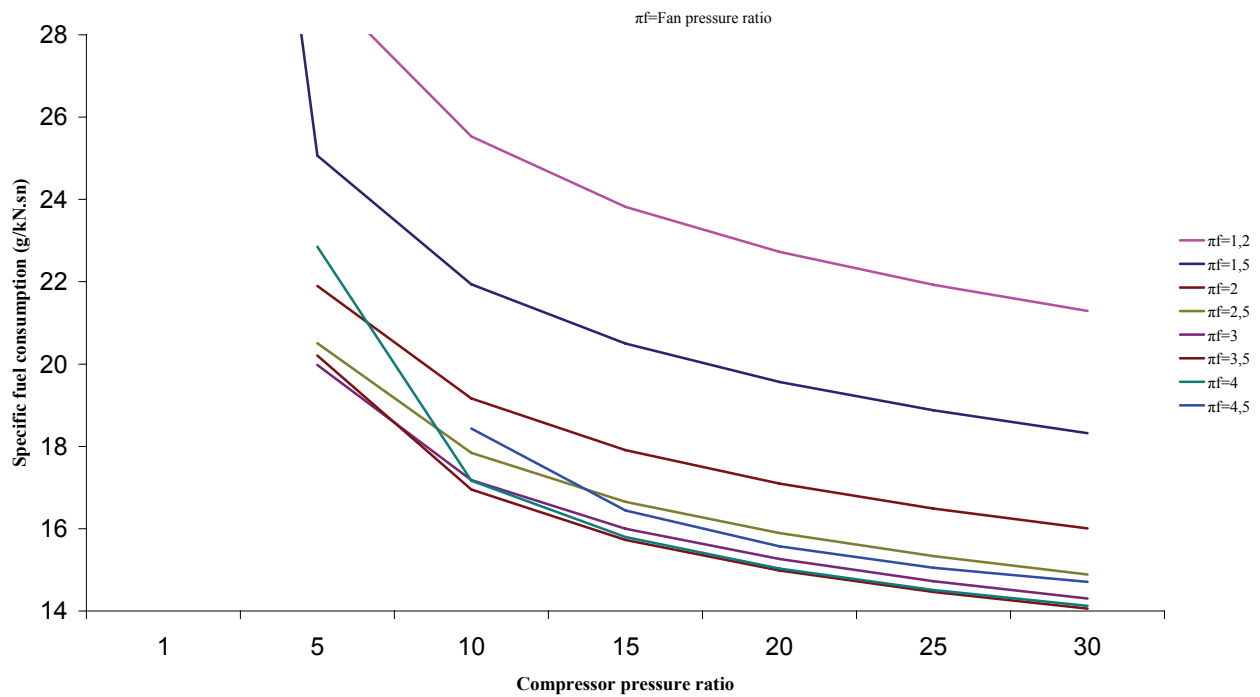


Figure 4. Compressor pressure ratio-specific fuel consumption curve for different fan pressure ratios of a high bypass turbofan engine at ideal cycle analysis[6]

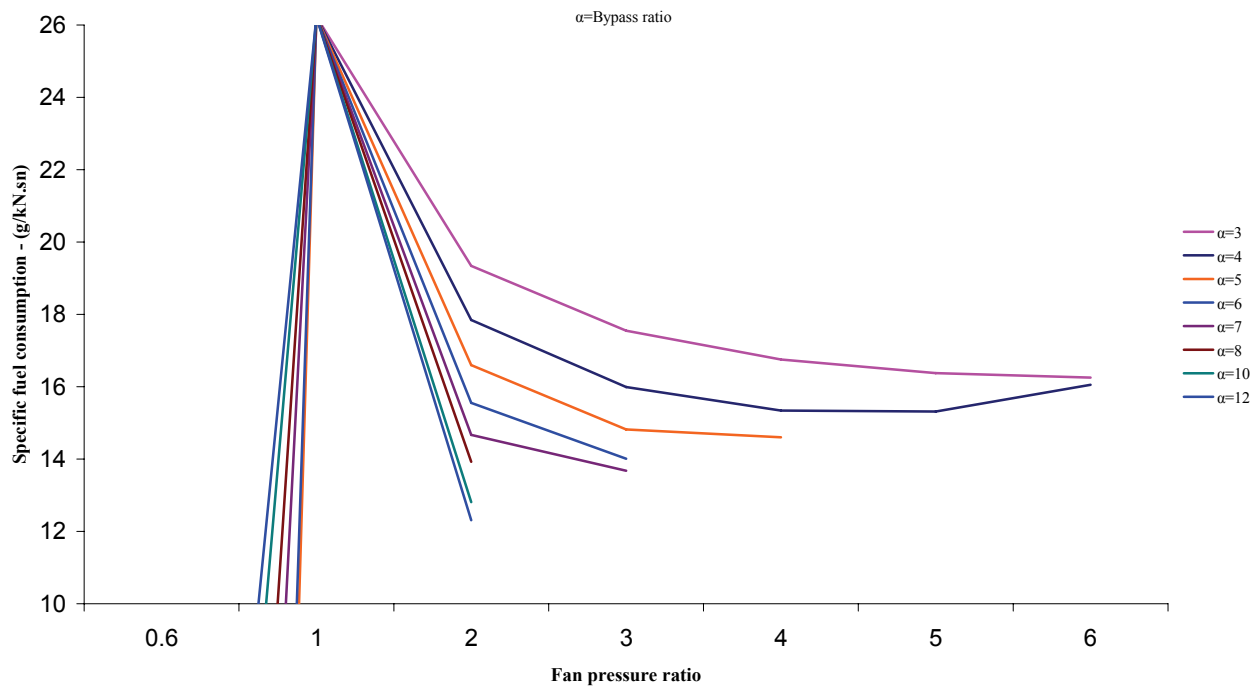


Figure 5. Fan pressure ratio-specific fuel consumption curve for different bypass ratios of a high bypass turbofan engine at ideal cycle analysis[6]

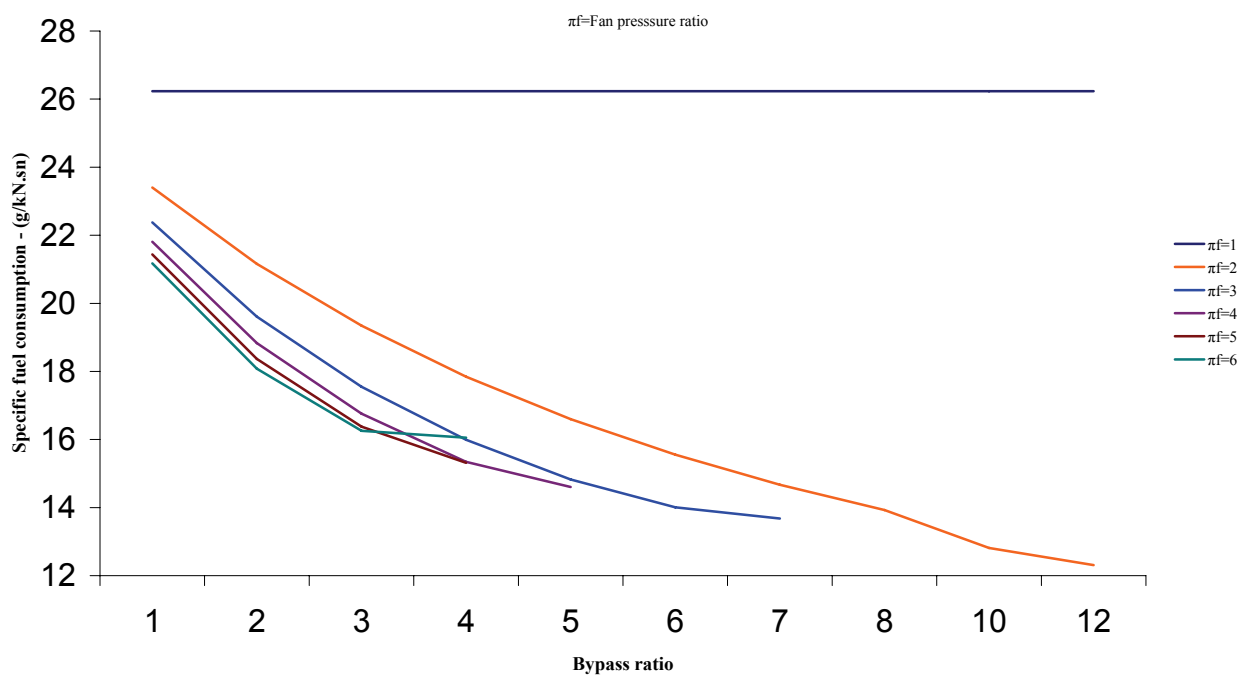


Figure 6. Bypass ratio-specific fuel consumption curve for different fan pressure ratios of a high bypass turbofan engine at ideal cycle analysis[6]

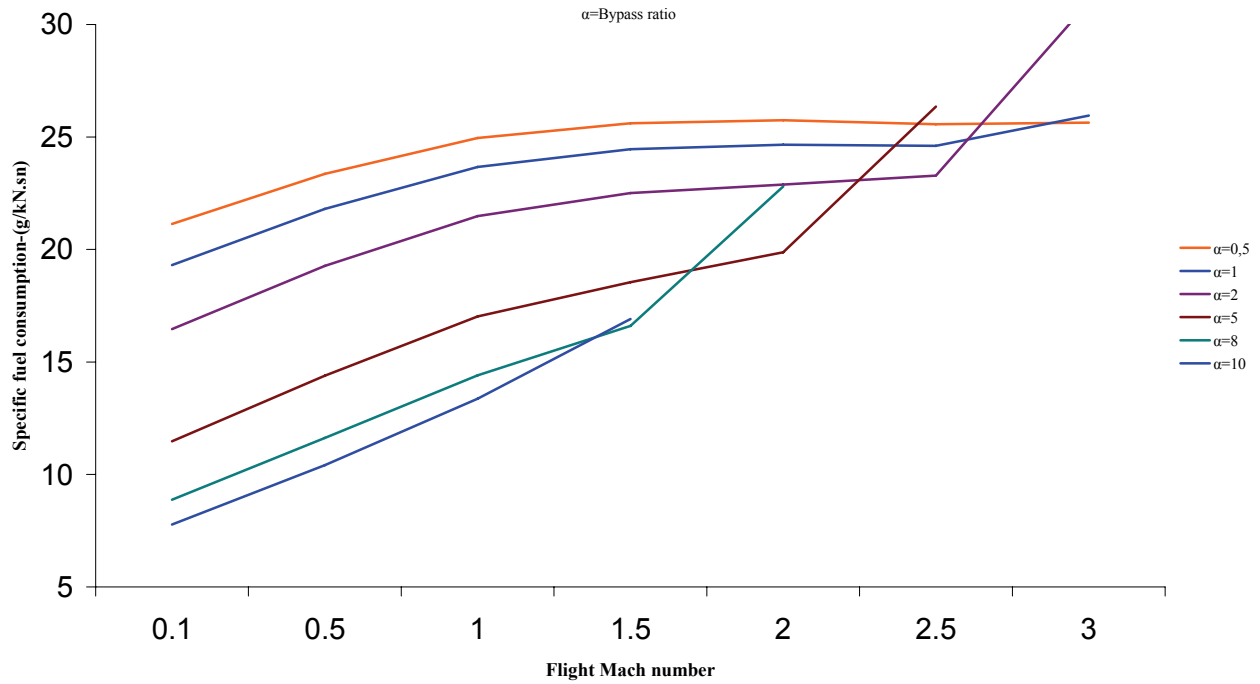


Figure 7. Flight Mach number-specific fuel consumption curve for different bypass ratios of a high bypass turbofan engine at ideal cycle analysis[6]

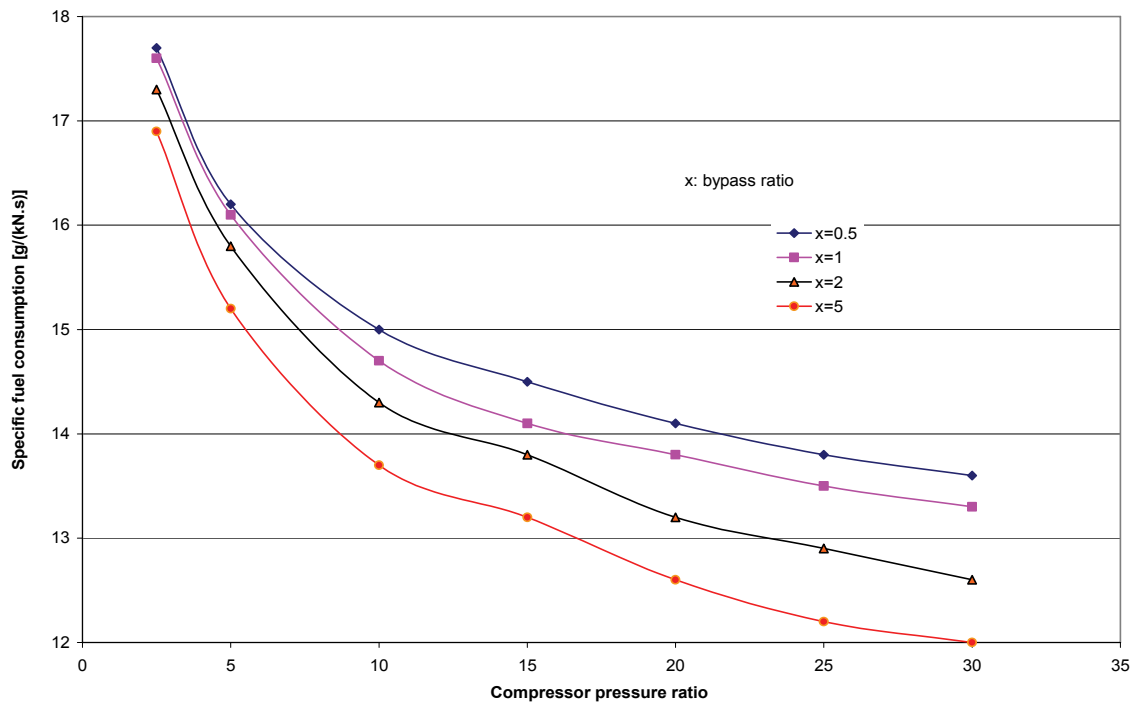


Figure 8. Compressor pressure ratio-specific fuel consumption curve for different bypass ratios of a high bypass turbofan engine at real cycle analysis[7]

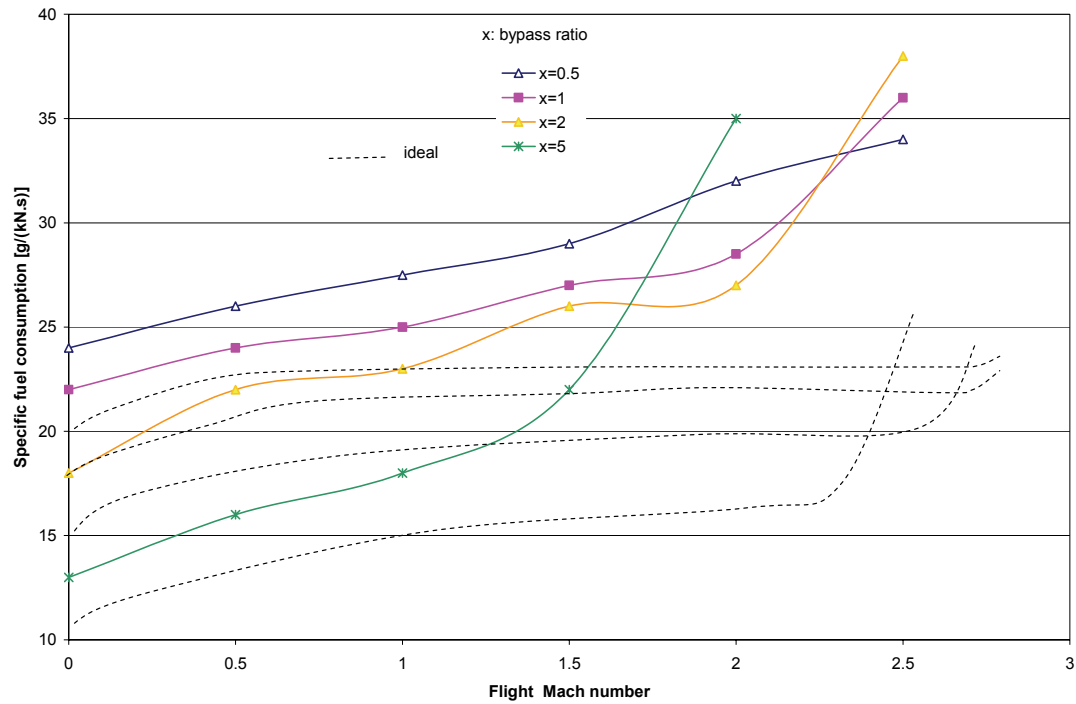


Figure 9. Flight Mach number-specific fuel consumption curve for different bypass ratios of a high bypass turbofan engine at real cycle analysis[7]

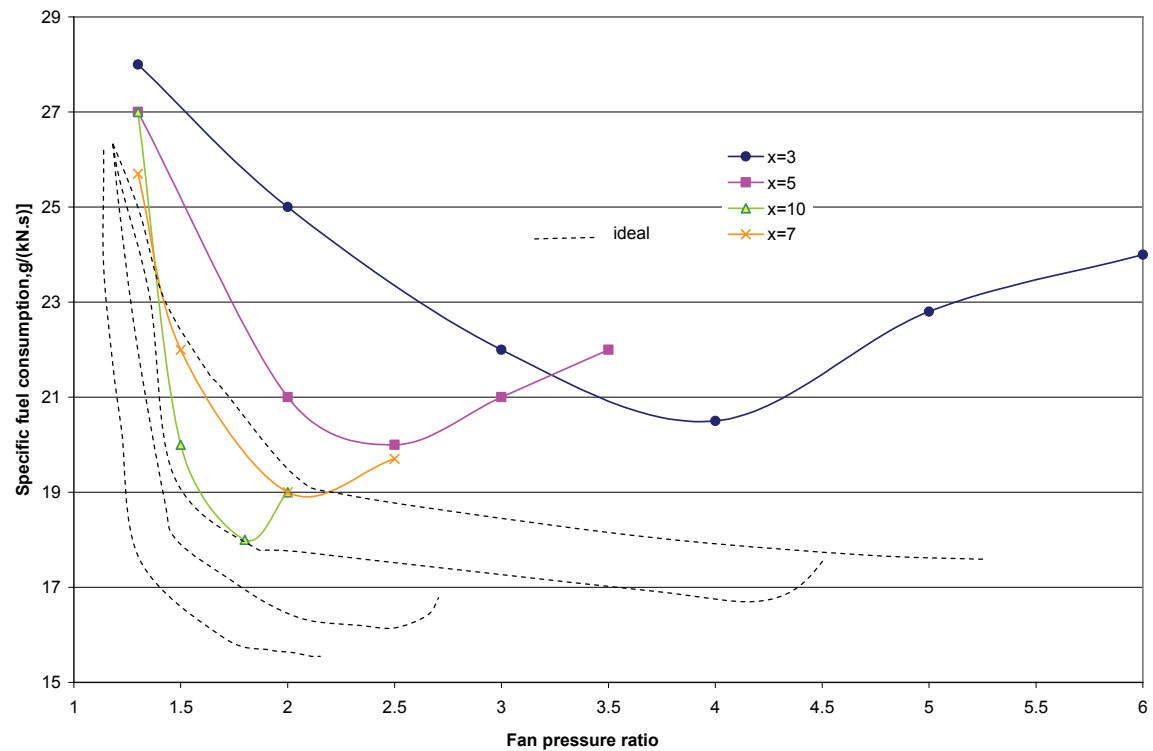


Figure 10. Fan pressure ratio-specific fuel consumption curve for different bypass ratios of a high bypass turbofan engine at real cycle analysis[7]

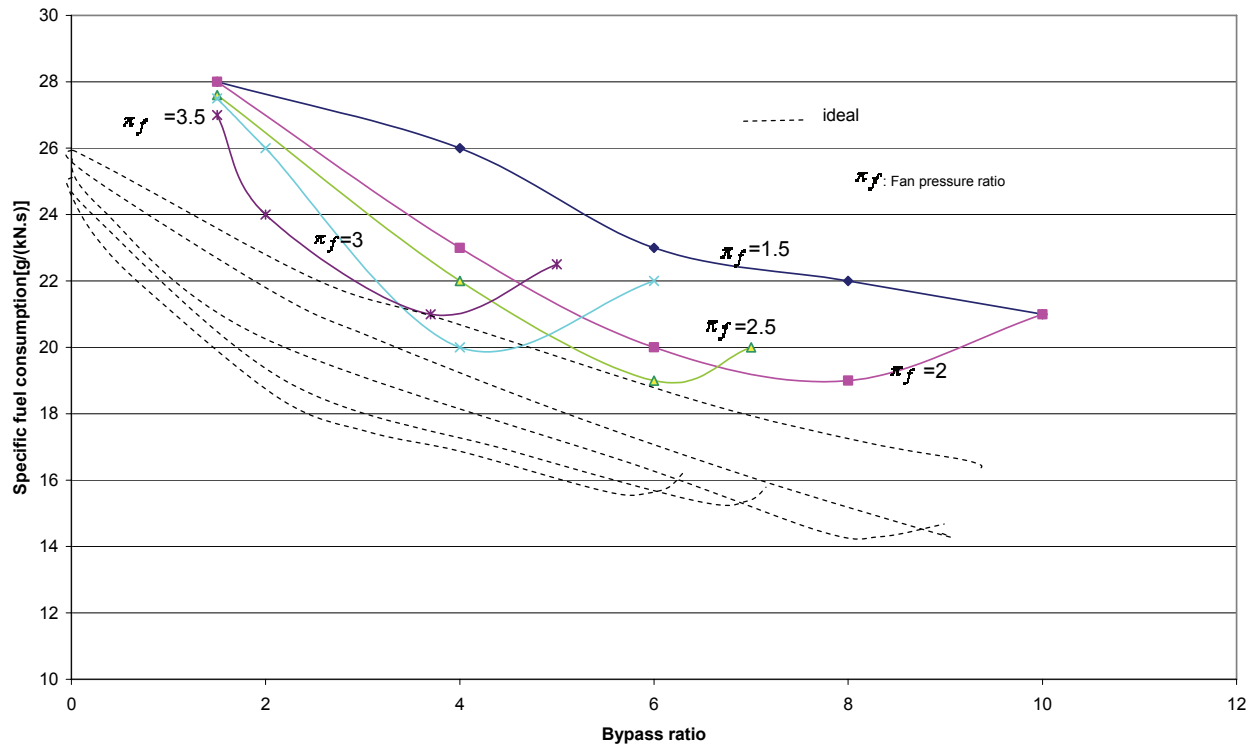


Figure 11. Bypass ratio-specific fuel consumption curve for different fan pressure ratios of a high bypass turbofan engine at real cycle analysis[7]

CONCLUSION

Steady state, ideal and real cycle specific fuel consumption estimation of axial flow aircraft gas turbine engines can be easily calculated with developing software program. In addition to on-design calculation, off-design performance analysis can also be performed using this method. With this programme we can analyse many different engine types. It is easy to access performance charts of several types of engine with program.

Designers can easily use it when they research new improvements and development of aircraft propulsion, because it is visual, easy to access and quick to compute. At the same time, more complex equations about propulsion technologies for further development can be solved and added to the programme in this manner.

REFERENCES

- [1] <http://www.investis.com/il/images/rrmedia>
- [2] **Aircraft Engine Design**, AIAA, 2002., Mattingly J., Heiser H., Daley H.,
- [3] **Analysis and Evaluation Programs of Gas Turbine Engines**, MSc Thesis, Anadolu University, Graduate School of Sciences, Civil Aviation Program, 2000., Turan O.
- [4] **Aerothermodynamics of Gas Turbine and Rocket Propulsion**, AIAA, 1997., Oates G.
- [5] **Performance analysis and evaluation program of gas turbine engines**, Anadolu University Journal of Science and Technology, 2002 (3), 351-360., Karakoc T.H., Turan O.
- [6] **Ideal parametric analysis of turbofan engines**, Mert M., Anadolu University School of Civil Aviation, BSc thesis, 2008.
- [7] **Optimization of turbofan engines with elitism-based genetic algorithm**, Turan O., PhD Thesis, Anadolu University School of Civil Aviation, 2007.

AERODYNAMIC CHARACTERISTICS OF AN ON THE GROUND MOUNTED VERTICAL AIR JET BEHIND THE DIRECTING VANES OF AERODYNAMIC PROPELLER

Annotation: The computer model of aerodynamic stand for the training of free flight in the vertical air jet of large diameter is developed. Submerged air jet is created by the rotating aviation screw (propeller), which is fixed on the vertical shaft of stationary engine. Propeller with the stator is located in the profiled ring. Method makes it possible to calculate the aerodynamic parameters of jet depending on the velocity of rotation of propeller, to optimize the geometry of propeller, ring and the form of the blades of stator, to analyze the ground effect and limiting walls. Mathematical model is described by nonstationary Navier-Stokes equations and numerically is solved by means of an adaptive movable mesh taking into account and with visualization of the process of rotation the propeller, and also taking in account the compressibility of medium, flow turbulence, appearance of separation zones and reverse flows. Method is proved by the development of the design of aerodynamic stand "Aerodium", prepared and installed in the town Sigulda (Latvia) in 2007.

INTRODUCTION

Main purpose of an aerodynamic stands of type like this is developing of base for the training of free flights, and also sport- entertaining amusement for the wide public in the place of organization of the sport shows (fig.1).

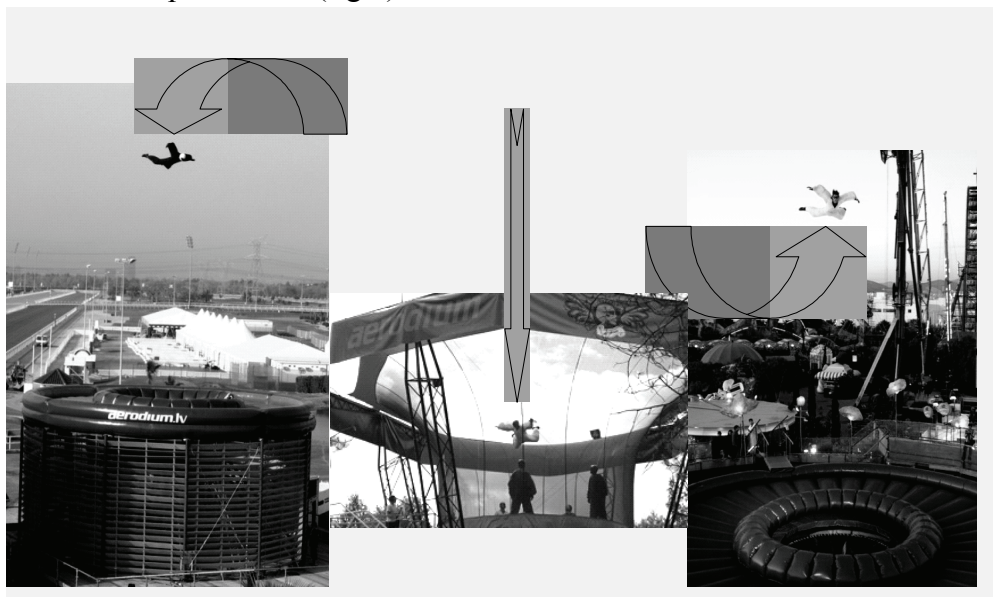


Fig.1 Flight (skydiving) of athlete in the air jet of aerodynamic installation "Aerodium", Latvia, town Sigulda.

Known aerodynamic equipment for training the athletes have the open (fig.1) or closed working zone with the maximum velocity of flow in the working zone 50-80 mps at the standard atmospheric conditions [1].

The main element of aerodynamic equipment with the free vertical submerged jet (fig.2) is the aerodynamic propeller of large diameter (approx. 3 – 4,5m), installed on the vertical shaft of immovable engine. Above the propeller is located the fixed directing vanes in form of ring with the profiled blades of counter vanes swirler, which is intended for eliminating the twist (spiral rotation) of jet in the working zone and decreasing of the speed drop near the axis of jet. The construction of directing vanes is significantly determined by the geometry of propeller and by its angular velocity

of rotation. The absence of directing vanes or the unsuccessful form of blades considerably worsen the flight conditions of athlete because of the appearance of a high velocity rotation of jet (twist) in respect to longitudinal axis, it decreases the long range of jet (reduction of the dimensions of working zone) and expansion (formation) of the zones of small or reverse velocities near the axis of jet (appearance of velocity drop). Presence or displacement of athlete in the working part of the jet also influences its characteristics and, therefore, conditions for free flight as well.

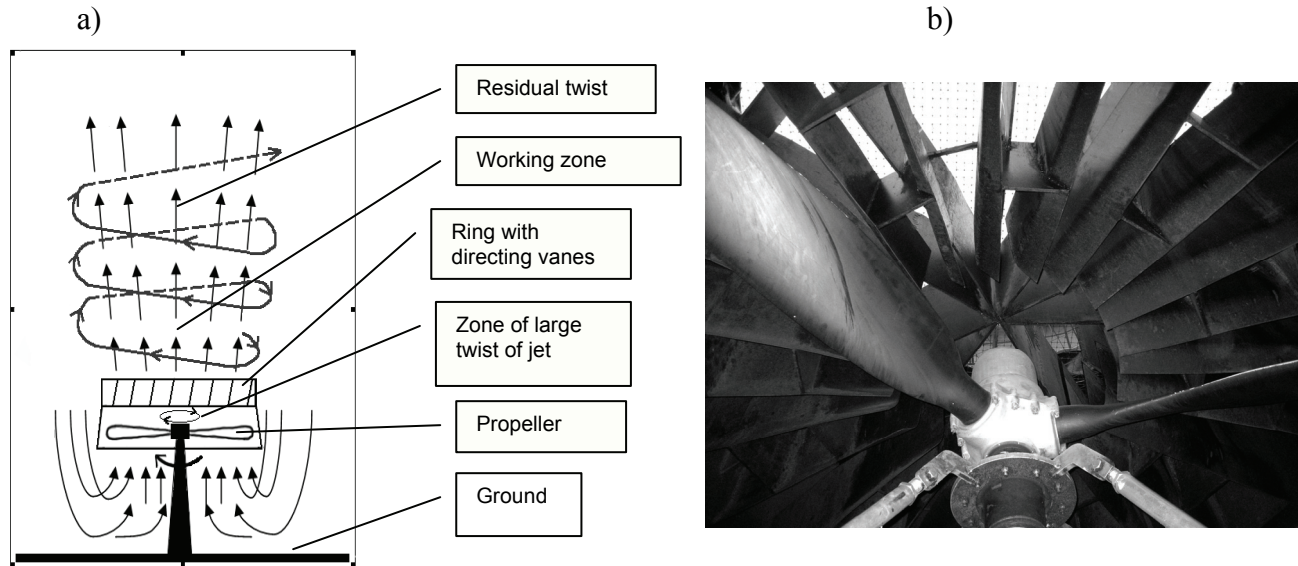


Fig. 2: a) - the diagram of flow in the jet behind the propeller and in the surrounding area;
b) - propeller and directing vanes (bottom view).

Purpose of this work: - to develop the method of the computer simulation of the aerodynamic parameters of the submerged vertical air jet, created by system “rotating propeller in the ring - directing vanes with the profiled blades”. Method must allow for the possibility of changing of the rotation the frequency of propeller, taking in account of the influence of the geometry of propeller, on the form of the blades of directing vanes, and to the influence of the geometry of other elements of device, limiting walls and ground on the parameters and the level of non-uniformity of the air flow in the working zone of jet as well. Aim of method is the optimization of the designing process of the system “ aerodynamic propeller - directing vanes”, the guarantee to defined velocity, twist and the uniformity of flow in the working area of jet.

METHOD

The special feature of this task consists in the necessity of calculating of formation process of submerged jet by the around fixed vertical axis rotating aerodynamic propeller. In addition to this it is necessary to consider the influence of the closely spaced solid or permeable surfaces, and also the formation of zones with the flow, induced by the submerged jet and area of reduced pressures before the propeller. (see the diagram of flow in fig.2). In the general case the flow in the jet is nonstationary and turbulent, while in the adjacencing to it the zones of the induced flows it can be transitional or laminar.

The mathematical model of the task, which makes it possible to consider a temperature and air density change, is described by Navier-Stokes equations and by equation of energy (First Law of Thermodynamics). For the turbulent, transitional and laminar flows after averaging by Reynolds method and use of $(k - \varepsilon)$ or *Low Re* $(k - \varepsilon)$ models of turbulence (k turbulent energy, ε - the speed of the dissipation of turbulent energy) the reference system of equations can be represented in the following form:

$$\frac{\partial \rho u_i}{\partial t} + \frac{\partial}{\partial x_j} (\rho u_i u_j - \tau_{ij}) + \frac{\partial P}{\partial x_i} = F_i \quad (1)$$

$$\frac{\partial \rho}{\partial t} + \frac{\partial}{\partial x_j} (\rho u_j) = 0; \quad (2)$$

$$\frac{\partial (\rho E)}{\partial t} + \frac{\partial}{\partial x_i} ((\rho E + P)u_i + q_i - \tau_{ij}u_j) = F_i u_i + Q_H; \quad (3)$$

$$\frac{\partial \rho k}{\partial t} + \frac{\partial}{\partial x_i} (\rho u_i k) = \frac{\partial}{\partial x_i} ((\mu_l + \frac{\mu_t}{\sigma_k}) \frac{\partial k}{\partial x_i}) + S_k; \quad (4)$$

$$\frac{\partial \rho \varepsilon}{\partial t} + \frac{\partial}{\partial x_i} (\rho u_i \varepsilon) = \frac{\partial}{\partial x_i} ((\mu_l + \frac{\mu_t}{\sigma_\varepsilon}) \frac{\partial \varepsilon}{\partial x_i}) + S_\varepsilon; \quad (5)$$

$$S_k = \tau_{ij}^R \frac{\partial u_i}{\partial x_j} - \rho \varepsilon + \mu_t P_B; \quad \rho = \frac{P}{RT}; \quad q_i = -(\frac{\mu_l}{Pr} + \frac{\mu_t}{\sigma_c}) c_p \frac{\partial T}{\partial x_i}; \quad (6)$$

$$S_\varepsilon = C_{\varepsilon 1} \frac{\varepsilon}{k} (f_1 \tau_{ij}^R \frac{\partial u_i}{\partial x_j} + \mu_t C_B P_B) - C_{\varepsilon 2} f_2 \frac{\rho \varepsilon^2}{k}; \quad P_B = -\frac{g_i}{\sigma_B} \frac{1}{\rho} \frac{\partial \rho}{\partial x_i}; \quad (7)$$

$$\tau_{ij} = \mu (\frac{\partial u_i}{\partial x_j} + \frac{\partial u_j}{\partial x_i} - \frac{2}{3} \frac{\partial u_l}{\partial x_l} \delta_{ij}) - \frac{2}{3} \rho k \delta_{ij}; \quad \mu = \mu_l + \mu_t; \quad (8)$$

$$E = h + \frac{u^2}{2}; \quad \tau_{ij}^R = \mu_t (\frac{\partial u_i}{\partial x_j} + \frac{\partial u_j}{\partial x_i} - \frac{2}{3} \frac{\partial u_l}{\partial x_l} \delta_{ij}) - \frac{2}{3} \rho k \delta_{ij}; \quad (9)$$

$$\mu_t = f_\mu \frac{C_\mu \rho k^2}{\varepsilon}; \quad f_\mu = [1 - \exp(-0.025 \frac{\rho \sqrt{k} y}{\mu_l})]^2 \cdot (1 + \frac{20.5 \mu_l \varepsilon}{\rho k^2}), \quad (10)$$

where u , P , ρ , T – fluid's velocity, pressure, density and temperature, R – gas constant, h – thermal enthalpy, t – time, F_i – mass-distributed external force per unit mass due to a porous media resistance, gravity and the coordinate system's rotation; Q_H – heat source on a volume unit, q_i – diffusive heat flux, δ_{ij} – Croncer symbol, τ_{ij} – viscous shear stress tensor, $\tau_{ij}^R \equiv -\overline{\rho u_i u_j}$ – stress tensor in Reynolds model, μ_l – dynamic viscosity coefficient, μ_t – turbulent viscosity coefficient, y – distance from the wall, g_i – components of gravitational acceleration in direction x_i ; $Pr = \mu c_p / \lambda$ – the Prandtl number, $\sigma_c, \sigma_B, \sigma_k, \sigma_\varepsilon, C_B, C_\mu, C_{\varepsilon 1}, C_{\varepsilon 2}$ – empirical constants; c_p – specific heat at constant pressure; λ – fluid thermal conductivity; for laminar flows parameters k, μ_t, ε are equal to zero summation is made on subscripts $i = x, y, z$; $j = x, y, z$.

Let us note that *Low Re* ($k - \varepsilon$) model is fitted for the solution of the problems, which contain zones both with the large and with the low velocities [2]. In particular, this model is convenient for the calculation of the high-velocity submerged jets, which flow into the large volume. Air jet interacts with the ambient air, implicating it into the induced movement, which ensures entering into the jet of air mass from the surrounding area. For the induced flows in the outlying zones are characteristic low Reynolds numbers $Re \sim 1500 \dots 5000$.

Navier-Stokes equations were solved numerically by the finite elements method with the use of an adaptive movable mesh, and also taking into account and visualization of the process of rotation of propeller. and compressibility of medium. For the solution of problems was used the CAD/CAE complex consisting from the SolidWorks/CFdesign software.

The designed three-dimensional geometric model of stand and its elements was created by the SolidWorks CAD software. Design model of the three-bladed propeller. with a diameter of 4 m with the rectangular form of blade is shown on fig. 3. The form of the blade sections profiles and

the law of variation of the twist of sections were calculated by the theory of N.E. Zhukovskiy [3,4]. For an improvement of the working conditions of propeller near the ground and to prevent the contraction of the jet it was installed into the profiled ring with the directing vanes (fig. 2).

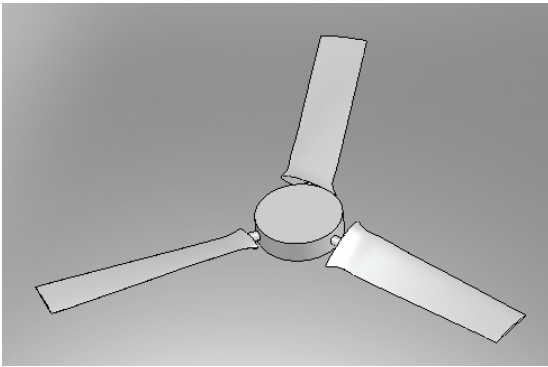


Fig. 3. Three - dimensional geometric model of three-bladed propeller with the rectangular blades.

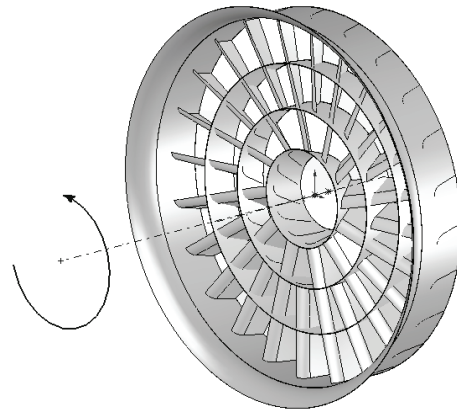


Fig 4. Calculation model of the directing vanes with 24 blades ($D=4m$).

Directing vanes (counter vanes swirler or honeycomb made from the sheet material) was installed on the exit of the ring coaxially with the propeller. The radial profiled blades of counter vanes swirler have geometric twist (geometric chords of sections are turned relative to the chord of root section, see. fig.4). Sectorial honeycomb is executed without the blade twist in two versions: with the radial profiled blades (fig.5 and b) and by the radial unprofiled blades (rectangular plates). Honeycomb is installed under the fixed angle of attack for decreasing of the losses on the inlet edge of blade (fig.5c). Both types of directing vanes are intended for eliminating the twist of jet, destruction of large vortexes and decrease of the nonuniformity of the profile of the longitudinal velocities near the axis in the working area of the jet. Calculation and layout of the profiled blades of directing vanes were made according to method of B.N. Yurev, based on the vortex theory and the considering special features of the velocity distribution in the sections of propeller blade.

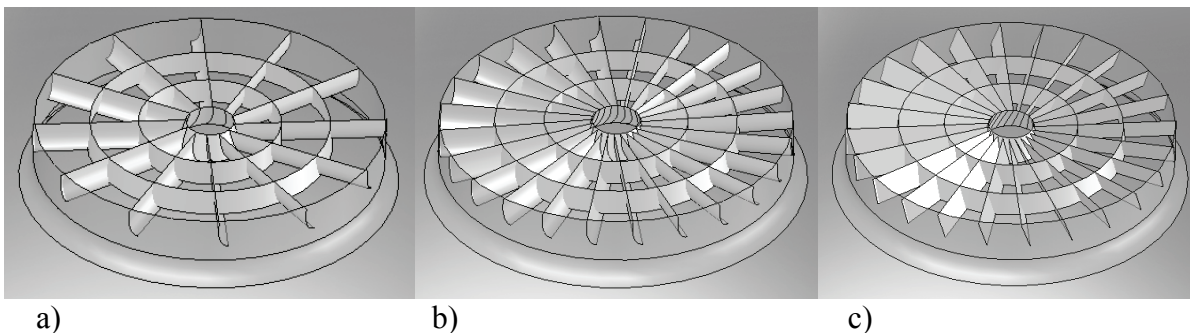


Fig.5. Modifications of the directing vanes: a) honeycomb with 12 profiled blades; b) honeycomb with 24 profiled blades; c) honeycomb with 24 rectangular blades without the twist.

Because of the constancy of the blade curvature the residual twist of flow and the nonuniformity of the profile of axial jet velocity in sectorial honeycomb is little more than curvature of counter vanes swirler, what is disadvantage. At the same time the blades of sectorial honeycomb are simpler both in the production and in the ring assembling process in comparison with the blades of counter vanes swirler.

The calculation of the parameters of the jet, created by the model of aerodynamic stand, was carried out by means of CAE software CFdesign [2]. For creating of the computational mesh of finite elements the electronic geometric model of aerodynamic stand (scale 1:1) was placed into the cylindrical computational region (domain). In practice the dimensions of domain is selected depending on the accuracy of calculation, possibilities of computer, its operational memory and permissible time of computation. For increasing of jet parameters calculation accuracy inside the main domain is coaxially placed the internal cylindrical domain of smaller diameter (see fig.6).

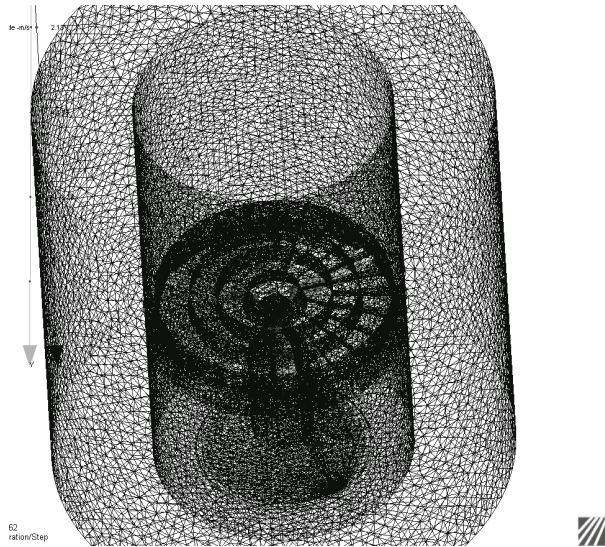


Fig. 6. Three-dimensional geometric model of aerodynamic stand with the computational mesh and the domains.

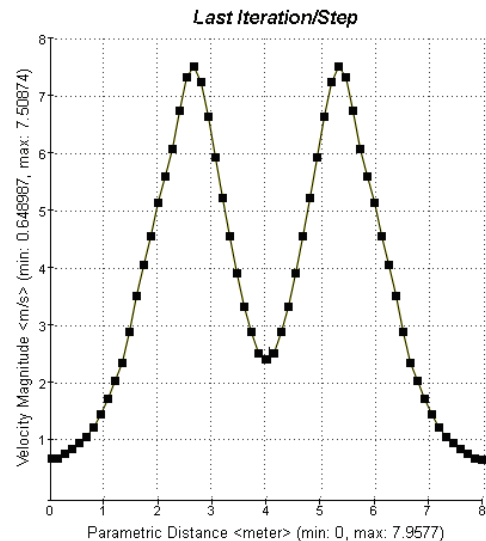


Fig.7. "Drop" of the longitudinal velocity near of the axis of jet.

The size of computational mesh in the internal domain is less than in the external. This makes it possible to significantly reduce the total number of computational cells, the time of computation and the required operational memory of computer. On all walls of external domain it is necessary to assign the appropriate boundary conditions. Adhesion conditions on the solid walls are assigned automatically. Because of the presence of the revolving propeller. all tasks are calculated as nonstationary.

For the calculating model with the full-scale geometric parameters and the cylindrical domain being investigated with the size of $\sim 8 \times 8.5$ m is required required $\sim (10^5 - 10^6)$ calculated mesh nodes and initial time step of the order of 4×10^{-4} s. In the case of three-bladed propeller with the number of revolutions $n_m = 1200$ rpm one revolution of the model of propeller occurs in 0,05s. The blades are fixed during the one time step Δt , and then they are turned to the angle of $\Delta \theta = 6n_m \Delta t$.

For the analysis of the influence of the twist of flow on the level of the velocity profile irregularity in the cross-section of jet and the value of velocity drop near the axis also was evaluated the simplified model of propeller in form of rotating disc with the infinite number of blades. Diameter, number of revolutions, the volumetric flow rate of air and the average degree "of the slippage of blades" relative to the air flow for the disc and propeller are equal. Disk is installed either before or inside the directing vanes. Because of the absence of the hub, which normally exists in the propeller, in this model do not appear the reverse flows, induced by flow separation on the rear side of the bushing.

The results of calculations for the propeller. with a diameter of $D = 4$ m are given below. Radius of the propeller hub 0.255 m, the chord of the rectangular blade $b_m = 0.3$ m, the number of revolutions of the screw $n_c = 1200 \text{ rpm} = 20 \text{ rps}$, the diameter of the ring $D_k = 4,1$ m, height of the ring $0,9$ m. Atmospheric conditions for the work of propeller - normal:

$$\rho_n = 1,225 \text{ kg} / \text{m}^3, P_n = 101300 \text{ N} / \text{m}^2.$$

RESULTS AND DISCUSSION

Twist significantly influence the level of non uniformity of longitudinal velocity in the working zone of the jet. It is shown that behind the propeller with the infinite number of blades which are installed inside the profiled ring without directing vanes, near the axis of jet is formed the zone with the intensive reverse flow, caused by the significant twist of flow and by the formation of rarefaction zone (fig.7).

Calculations confirmed the utility of installation of directing vanes in the form of counter vanes swirler or sectorial honeycomb behind the propeller, which it makes it possible to preclude not only the twist of jet, but also to significantly decrease the level of non-uniformity of the flow.

For an increase of velocity in the working part of the jet of the evaluated type of Aerodium of most efficient is the system “propeller, inside the profiled ring with the counter vanes swirler” [5], but not “the propeller, before the cylindrical ring with the counter vanes swirler”, which was previously realized on existing Aerodium (fig.8, curves 1, 5).

It is shown that the influence of engine block with the streamlined cover and the ground surface do not worsen, but in certain cases even improve the conditions for incoming flow into the ring (fig.9). In the case if the electromotor of propeller drive is also installed near the inlet into the ring, the radius of raised edge $r \geq 0.08D_k$ ensures the practical absence of separation zones. For the defined relative height of ring ($H_k/D_k \approx 0.22 \dots 0.25$.) it is useful to locate propeller, inside the ring before the cylindrical part at a distance approx. $0.1 D_k$ from the front edge of the ring.

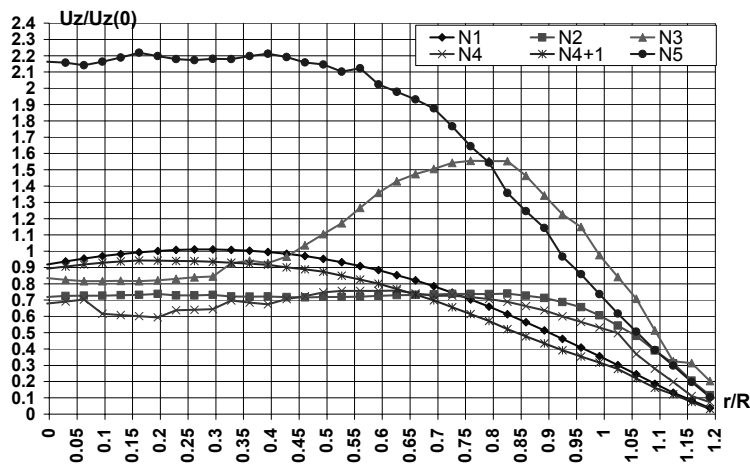


Fig.8. Plot of relative longitudinal speed in cross-section section of a jet $z=1\text{m}$ for variants of system the propeller - ring:

N₁ - basic version : propeller before the cylindrical ring without the counter vanes swirler.

N₂ - propeller inside the ring without the counter vanes swirler.

N₃ - propeller inside the profiled ring without the counter vanes swirler.

N₄ - propeller before the cylindrical ring with the counter vanes swirler

N₅ - propeller, inside the profiled ring with the counter vanes swirler.

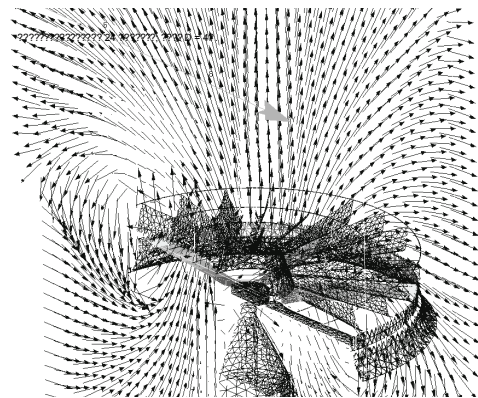


Fig.9. Improvement of the conditions for incoming flow into the ring and to the propeller at the installation of cone on the engine and consideration of ground effect.

It is proposed the construction of counter vanes swirler, which consists of 24 radial blades. For decreasing the excessive blocking up the center part by the blades are used two types of the blades: 12 long blades with are installed between the outer ring and the small cone, 12 short - between the outer ring and the internal cylinder. For decreasing of velocity drop behind the ring and increase of the strength of construction it is recommended to install inside the ring with directing vanes several coaxial truncated cones of different diameter with the expansion angle 10° to 12° . The diameter of the inlet base of the smallest cone, located opposite the propeller hub, must have the diameter more than diameter of the nonworking part of the propeller blades and be equal to $0.2D$ to $0.3D$. The small truncated cones increases efficiency of velocity drop smoothing in center part of jet near to inlet section of the ring.

The radial blades of counter vanes swirler should be performed from the sheet material with the along the blade variable curvature of the front section of profiles and longitudinally variable angles of blade setting profiles. The level of curvature, setting angles and blade-section chords depend on the geometric and aerodynamic characteristics of propeller and can be calculated according to the vortex theory of screw propeller.

The construction of sectorial honeycomb is differed from counter vanes swirler only with the fact, that its blades aren't twisted (angle of setting sections it does not change along the blade). Each section of the blade of honeycomb has the identical curvature, which is determined by some average geometric and aerodynamic characteristics of propeller blade. The curvature of the profile of the blade of the sectorial honeycomb can be approximately determined on the basis the analysis of velocity triangle on the outlet edge of the characteristic section of propeller. The width of the blades of counter vanes swirler and honeycomb is approximately equal to the length of the generatrix line of the cylindrical part of the ring, in which they are installed.

The nature of the influence of the directing vanes construction on the flow velocity in the working part at the identical propeller's working regime is possible to estimate on the basis of the comparisons of the relative longitudinal velocity profile in the fixed transverse section of jet (fig.8) It is evident that the best parameters have a counter vanes swirler with 24 profiled blades with the twist. Its main advantages:

- counter vanes swirler successfully liquidates the twist of the flow already at a distance of approximately 0.7 to 1.0 m from the outlet section of ring,
- satisfactorily smoothens velocity drop near the axis of jet at a distance approximately 1.0 m from the outlet section of ring, what makes it possible to install in this cross-section area of jet the shielding – trampoline.

In comparison with counter vanes swirler sectorial honeycomb less efficiently removes the twist of flow and smoothens velocity drop at the identical distances from the outlet section of ring (fig.8).

The developed method was used for the development of the design of aerodynamic installation "Aerodium" with the submerged free vertical air jet, which was prepared and installed in the town Sigulda (Latvia).

References

1. <http://www.verticalwind.com/>
2. CFdesign v.9, User's guide, Copyright (C) Blue Ridge Numerics, Inc. 1992-2006
3. *Barnes W. Mc Cormick*, Aerodynamics, Aeronautics and Flight mechanics, John Wiley & Sons.inc., 1995, 652 p.
4. *Александров В.Л.*, Воздушные винты, Москва, Оборонгиз, 1951, 475 стр.
5. *Куручкин Ф.П.*, Основы проектирования самолетов с вертикальным взлетом и посадкой, Москва, Машиностроение, 1970, 352 стр.

*S.I. Martynenko Can. Sc., A.A. Markov asp., M.S. Sharov asp., L.S. Yanovskiy Dr. Sc., Professor
Central Institute of Aviation Motors n.a. P.I. Baranov, Russia*

DEVELOPMENT OF NUMERICAL METHODS FOR SOLVING NAVIER-STOKES EQUATIONS IN PRIMITIVE VARIABLES FORMULATION

A new approach for reduction of computational cost of numerical algorithms for the Navier–Stokes equations in primitive variables formulation is proposed. The approach uses physical aspects of hydrodynamics for fast computation of “part” of pressure. For the given purpose, an auxiliary problem based on simplified Navier–Stokes equations and original pressure splitting is suggested. The paper represents detailed description of the algorithm and results of numerical experiments with benchmark and applied problems.

We begin with the 2D ($N = 2$) Navier–Stokes equations governing flow of a Newtonian, incompressible viscous fluid. Let $\Omega \in \mathbb{R}^N$ be a bounded, connected domain with a piecewise smooth boundary $\partial\Omega$. Given a boundary data, the problem is to find a velocity field and pressure such that

a) continuity equation

$$\frac{\partial u}{\partial x} + \frac{\partial v}{\partial y} = 0 \quad (1)$$

b) X-momentum

$$\frac{\partial u}{\partial t} + \frac{\partial(u^2)}{\partial x} + \frac{\partial(vu)}{\partial y} = -\frac{\partial p}{\partial x} + \frac{1}{Re} \left(\frac{\partial^2 u}{\partial x^2} + \frac{\partial^2 u}{\partial y^2} \right) \quad (2)$$

c) Y-momentum

$$\frac{\partial v}{\partial t} + \frac{\partial(uv)}{\partial x} + \frac{\partial(v^2)}{\partial y} = -\frac{\partial p}{\partial y} + \frac{1}{Re} \left(\frac{\partial^2 v}{\partial x^2} + \frac{\partial^2 v}{\partial y^2} \right) \quad (3)$$

Owing to the presence of the convection terms in the momentum equations, the Navier–Stokes system (1)–(3) is nonlinear. Linearization based on Picard’s or Newton iteration and discretization of (1)–(3) using finite differences or finite elements result in a generalized saddle point system

$$\begin{pmatrix} A & B^T \\ B & 0 \end{pmatrix} \begin{pmatrix} \alpha \\ \beta \end{pmatrix} = \begin{pmatrix} f \\ g \end{pmatrix} \quad (4)$$

in which α and β represent the discrete velocities and discrete pressure, respectively. Here nonsymmetric A is a block diagonal matrix, where each block corresponds to a discrete convection-diffusion operator with appropriate boundary conditions. The rectangular matrix B^T represents the discrete gradient operator while B represents its adjoint, the divergence operator.

It is clear that the system (4) cannot be solved by standard methods of linear algebra. Solution algorithms for the generalized saddle point problems can be subdivided into two categories, which we will call segregated (decoupled) and coupled methods. Segregated methods compute the two unknown vectors α and β , separately. This approach involves the solution of two linear systems of smaller size. Now method SIMPLE is the most popular algorithm for CFD problems [1]. Other popular algorithm is an artificial viscosity method [2]. Main advantages of the method are simplicity and absence of boundary conditions for pressure.

Survey of numerical methods for saddle point problems is given in [3]. In recent years there has been a surge of interest in saddle point problems, and numerous solution techniques have been proposed for this type of system. The methods have mathematical backgrounds.

In partial cases it is possible to obtain good approximation to solution of the Navier–Stokes equations based on physical aspects of hydrodynamics. As an example, we consider 2D flow between parallel plates. Assuming that the pressure is not changed across the flow ($p'_y = 0$), we obtain the simplified Navier–Stokes equations:

a) continuity equation

$$\frac{\partial u}{\partial x} + \frac{\partial v}{\partial y} = 0 \quad (5)$$

b) X-momentum

$$\frac{\partial u}{\partial t} + \frac{\partial(u^2)}{\partial x} + \frac{\partial(vu)}{\partial y} = -\frac{\partial p}{\partial x} + \frac{1}{Re} \left(\frac{\partial^2 u}{\partial x^2} + \frac{\partial^2 u}{\partial y^2} \right) \quad (6)$$

c) mass conservation equation

$$\int_0^1 u(x, y) dy = \int_0^1 u(0, y) dy \quad (7)$$

Since $p'_y = 0$, very efficient numerical methods for solving the simplified Navier–Stokes equations (5)–(7) have been proposed and developed [4, 5]. It should be noted that in this case pressure is computed in coupled manner by algebraic methods. Starting from solution of the simplified Navier–Stokes equations (5)–(7), we expect impressive reduction of computational efforts for solution of full Navier–Stokes equations (1)–(3) as compared with other starting guess. In follows, similar considerations will be used for convergence acceleration of numerical algorithms for the Navier–Stokes equations in primitive variables formulation.

First, consider 2D steady flow in driven cavity. Fig. 1 represents geometry of the problem.

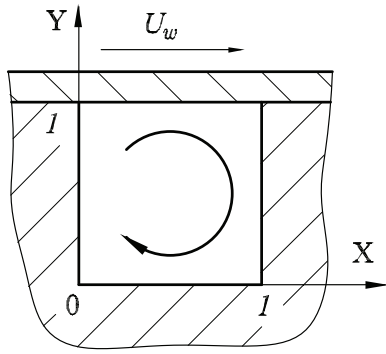


Fig. 1 Driven cavity

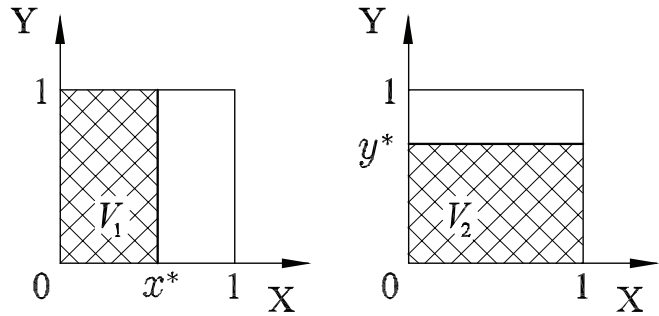


Fig. 2 Control volumes V_1 and V_2

Integration of the continuity equation (1) over the control volumes V_1 and V_2 shown on Fig. 2 gives two mass conservation equations

$$\int_0^1 u(x, y) dy = 0, \quad (8)$$

$$\int_0^1 v(x, y) dx = 0. \quad (9)$$

The mass conservation equations will be used as a priori information about the solution. In general, pressure can be splitting as

$$p(t, x, y, z) = p^x(t, x) + p^y(t, y) + p^z(t, z) + p^{xyz}(t, x, y, z), \quad (10)$$

where the superscripts x , y , z and xyz show dependence of the pressure “components” on spatial coordinates. “One-dimensional pressure components” $p^x(t, x)$, $p^y(t, y)$ and $p^z(t, z)$ can be computed by the same effective methods proposed for simplified Navier–Stokes equations (5)–(7). Domination of gradients of “one-dimensional pressure components” results in impressive reduction of the computational efforts. In this case amount of computations needed for solution of the full Navier–Stokes equations will be comparable with amount of work needed for the simplified Navier–Stokes equations. Maximum efficiency of the approach is expected at simulation of directed fluid flows.

According to the representation (10), the momentum equations have two pressure gradients. For example

$$\frac{\partial p}{\partial x} = \frac{\partial}{\partial x} (p^x(t, x) + p^y(t, y) + p^z(t, z) + p^{xyz}(t, x, y, z)) = \frac{\partial p^x}{\partial x} + \frac{\partial p^{xyz}}{\partial x}.$$

Instead of the continuity equation (1), the auxiliary problem uses the mass conservation equations for computation of the “one-dimensional pressure components”. In case of flow in a driven cavity, the auxiliary problem is formulated as

a) X momentum and mass conservation equation (8)

$$\begin{cases} \frac{\partial(u^2)}{\partial x} + \frac{\partial(\nu u)}{\partial y} = -\frac{dp^x}{dx} - \left[\frac{\partial p^{xy}}{\partial x} \right] + \frac{1}{Re} \left(\frac{\partial^2 u}{\partial x^2} + \frac{\partial^2 u}{\partial y^2} \right) \\ \int_0^1 u(x, y) dy = 0 \end{cases} \quad (11)$$

b) Y momentum and mass conservation equation (9)

$$\begin{cases} \frac{\partial(\nu u)}{\partial x} + \frac{\partial(\nu^2)}{\partial y} = -\frac{dp^y}{dy} - \left[\frac{\partial p^{xy}}{\partial y} \right] + \frac{1}{Re} \left(\frac{\partial^2 \nu}{\partial x^2} + \frac{\partial^2 \nu}{\partial y^2} \right) \\ \int_0^1 \nu(x, y) dx = 0 \end{cases} \quad (12)$$

where square brackets mean that the derivatives $(p^{xy})'_x$ and $(p^{xy})'_y$ are fixed and braces mean that the momentum and mass conservation equations are solved in coupled manner.

In follows, the pressure gradients $(p^x)'_x$ and $(p^y)'_y$ are fixed. Solution of the auxiliary problem (11) and (12) is considered to be a starting guess for the full Navier-Stokes equations. Taking into account the pressure splitting (10), the momentum equations are written as

$$\frac{\partial(u^2)}{\partial x} + \frac{\partial(\nu u)}{\partial y} = -\left[\frac{dp^x}{dx} \right] - \frac{\partial p^{xy}}{\partial x} + \frac{1}{Re} \left(\frac{\partial^2 u}{\partial x^2} + \frac{\partial^2 u}{\partial y^2} \right), \quad (13)$$

$$\frac{\partial(\nu u)}{\partial x} + \frac{\partial(\nu^2)}{\partial y} = -\left[\frac{dp^y}{dy} \right] - \frac{\partial p^{xy}}{\partial y} + \frac{1}{Re} \left(\frac{\partial^2 \nu}{\partial x^2} + \frac{\partial^2 \nu}{\partial y^2} \right). \quad (14)$$

Note that velocity components and “part” of the pressure (i.e. $p^x + p^y$) are computed in the coupled manner.

In numerical experiments “multidimensional pressure component” is computed in decoupled manner by the artificial viscosity method [2]. Convergence on pressure iterations (n_p) is estimated using the residual norm

$$R^{uv} = \max_{ij} \left| \frac{u_{i+1j} - u_{ij}}{h_x} + \frac{\nu_{ij+1} - \nu_{ij}}{h_y} \right|. \quad (15)$$

Fig. 3 represents the convergence acceleration in proposed algorithm ($Re=100$, staggered grid 101×101). Figs. 4 and 5 represent comparison of the solution of Navier-Stokes equations in primitive and “stream function – vortices” variables ($Re=1000$, staggered grid 301×301). Since the flow in the cavity has no preferential direction, the proposed algorithm has the least efficiency. Numerical experiments show reduction of execution time on $\sim 30...50\%$ as compared with traditional algorithms for similar problems.

The next benchmark problem is backward-facing step flow. Consider the flow over a backward-facing step, which is another well studied test case. Fig. 06 shows the geometry of the flow. The fact that the solution of the incompressible Navier-Stokes equations over a backward-facing step at $Re = 800$ is steady and stable has been confirmed in a number of recent works.

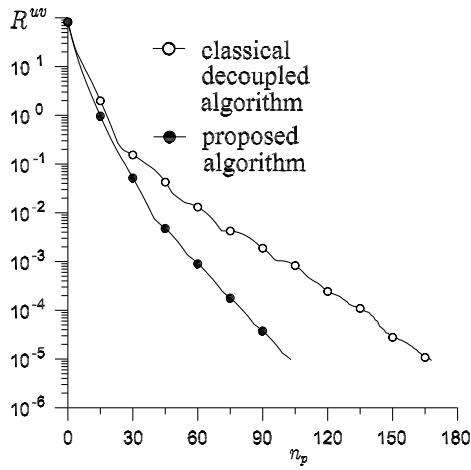


Fig. 3 Reduction of the residual norm R^{uv} (15)

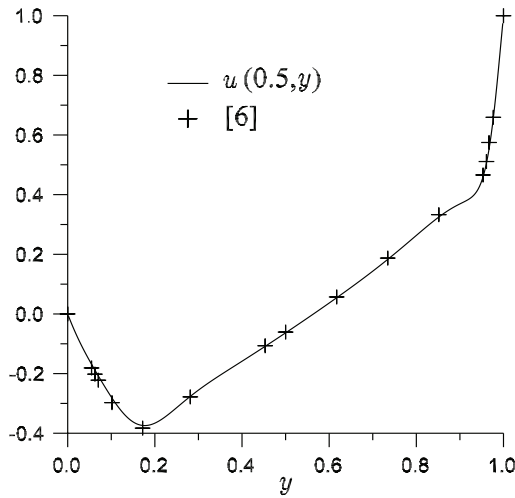


Fig. 4 X-direction velocity (u) in middle section

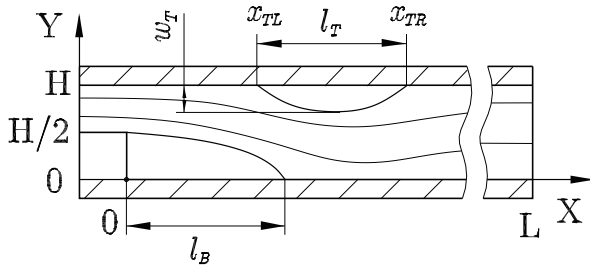


Fig. 6 Backward-facing step flow: geometry of problem

Numerical experiments show that execution time can be reduced in ~ 400 times for the given problem (staggered grid 101×1401). Fig. 7 explains the impressive reduction of the computational efforts. It is easy to see that pressure is changed in X-direction except small subdomain near attachment point of bottom eddy (i.e. $p \approx p(x)$). Therefore the proposed algorithm is very efficient for solving problems with directed fluid flows.

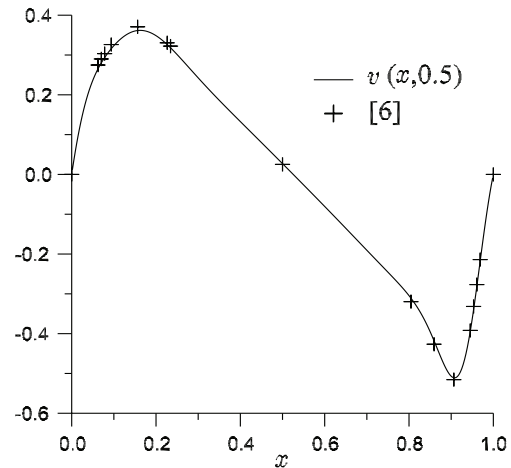


Fig. 5 Y-direction velocity (v) in middle section

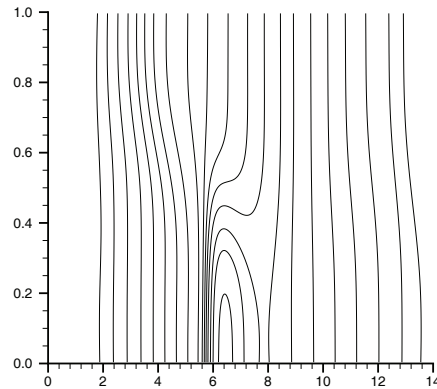


Fig. 7 Isobars ($Re = 800$)

References

- [1] S.V. Patankar, *Numerical Heat Transfer and Fluid Flows*. McGraw-Hill, New York, 1980.
- [2] A.J. Chorin, A numerical method for solving incompressible viscous flow problems, *J. Comput. Phys.*, V. 2, pp. 12–26, 1967.
- [3] M. Benzi, G.H. Golub, J. Liesen, Numerical solution of saddle point problems, *Acta Numerica*, pp.1–137, 2005.
- [4] W.R. Briley, Numerical method for predicting three-dimensional steady viscous flow in ducts, *J. Comp. Phys.*, V. 14, pp. 8–28, 1974.
- [5] C.A.J Fletcher, *Computational Techniques for Fluid Dynamics*, Vols 1,2, Springer, Berlin, 1988.
- [6] U. Ghia, K.N. Ghia, C.T. Shin, High-Re Solutions for Incompressible Flow Using the Navier-Stokes Equations and a Multigrid Method, *J. Comp. Phys.*, V. 48, pp. 387–411, 1982.

NUMERICAL INVESTIGATIONS OF TRANSSONIC AXIAL COMPRESSOR STAGE

There are results of numerical investigations of transonic axial compressor cascade with one-tier and tandem-blade impeller vane. There is recent numerical gas dynamics investigation methodic of compressor stage. The authors carried out some comparison of characteristic between one-tier and double vane stage.

Introduction

At present-day there is an aviation propulsion tendency to increase working condition (gas temperature in front of turbine, compressor pressure rate), weight and overall size decrease of power plant. For that it is necessary to develop of small-sized high-pressure compressor.

This problem may be realized by means decreasing of vane and stage numbers as well as rotor diameters. But using some of this way will lead to behavior increasing in every stage. It is possible at the expense of rotor operating speed, increasing flow gap in the compressor stage with increasing blade curvature and angle of attack.

The first of way is lead to supersonic streamline compressor vanes and initiation pressure races, that lead to flow separation and great efficiency decreasing. The second way is lead to swiftly wall boundary layer swelling and flow separation from vane back with great efficiency drop.

Hence one of the mane problems of modern compressor engineering is axis compressor stage effectiveness increasing and aerodynamic loading with usage of operation boundary layer mode.

As is obvious from investigations by Fikkert K, Chjen P., Bunimovich A., Svaytgorov A., Tereshchenko U., Bamert K. [1-7] and other, one of this way is usage tandem blade row in axis compressor stage.

The in axis compressor rotors is widely usage in compressor guide vane of aviation engines: Д-36, АИ-25, Д-30КУ, Д-30 КП, Д-30, АЛ-32Ф and other. In this case it was necessary to provide big angle flow rotate.

Statement or problem

From the point of view of the axis compressor rotor aerodynamic loading rise, the most appropriate is using rotors with. Widely known only a few works devoted to such researches. The least examined aria is the co-using of double blade row of rotor and guide vane in axis compressor stage.

The high-head transonic stage of axis compressor ОК-75 was chosen for the research. This stage contains of three parts: inlet guide vane, rotor, guide vane. This work contains its experimental characteristics and geometrical parameters. It's necessary to over profile in the ОК-75 stage the one-tier blade row for getting of axis compressor stage with tandem blade row.

Since the compressor stages characteristics in this work were examined by quantitative methods, for the correct comparison stage characteristics and one-tier and tandem blade impeller vane, we need to conduct numerous researches of stage ОК-75 characteristics by using viscous compressible flow model.

Thus, the aforesaid determined the conducting of research in the following sequence.

At the first stage we need to build the axis compressor stage ОК-75 calculated (rated) model, conduct quantitative calculation of its characteristics and compare with V.S. Svechnikov and A.B. Kirilov experimental researches results. This will let us to make the conclusion about the deviation of quantitative and experimental data.

At the next stage need to change the geometrical parameters of rotor and into equivalent double according to the existing recommendations [4, 9-11], conduct the quantitative calculation of stage characteristics with tandem blade rotor and guide vane blade row and compare with stage characteristics with one-tier vane row.

Research methodology

As investigation object it is apply axis compressor (OK-75) stage. Its blades profile was got by means BC-10 propeller profile scaling. The medial lines of all blade's profile are circle arcs. This stage designed for steady head along rotor blade and it contain inlet duct, rotor and guide vanes. There are modern numerical gas dynamics investigation

In process over profiling of rotor and guide vanes was used path of geometric parameters keeping namely: equality of double and one-tire blade row chord total value; equality of inlet and outlet structural angle of tandem blade and one-tire blade row; equality t/b . At slot canal profiling there are some constant value along blade height (at all area): canal ratio $F = f_a / f_b = 1.4$, relative blade thickness $\bar{c}_1 = \bar{c}_2 = \bar{c}$, blade front overlap $\bar{l}_s = l_s / b = 0.12$ (Figt. 1).

Relatively to recommendation [11] these parameters are provide maximal compressor grid efficacy. Minimum slot height f_b was changed along blade height by law [9, 10] (Fig. 2).

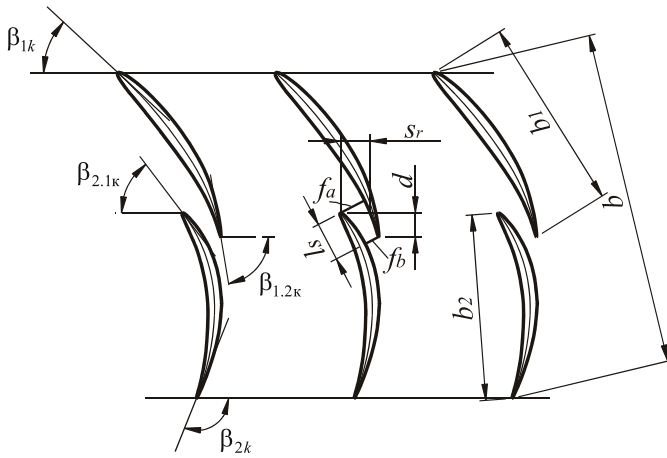


Fig. 1. Geometric parameters of tandem blade compressor grid.

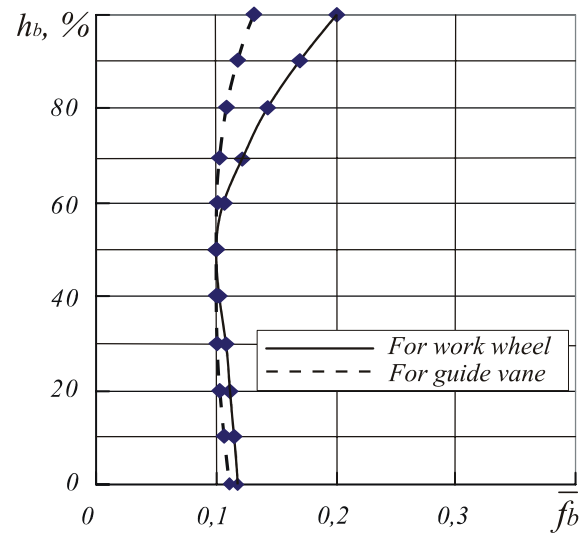


Fig. 2. Geometric parameter $\bar{f}_b = f_b / b$ distribution of tandem blade channel along blade

At investigations of axis compressor stages were defined: compressor stage pressure rate (1), adiabatic efficiency (2).

$$\pi_{st}^* = \frac{p_{3m}^*}{p_{0m}^*}, \quad (1)$$

where p_{0m}^* - mean value of total pressure at stage inlet; p_{3m}^* - mean value of total pressure at stage outlet.

$$p_{0m}^* = \frac{2\pi}{F_0} \int_{0.5}^1 \bar{r} p_0^*(\bar{r}) d\bar{r}, \quad p_{3m}^* = \frac{2\pi}{F_3} \int_{0.6}^1 \bar{r} p_3^*(\bar{r}) d\bar{r},$$

where F_0 , F_3 - ring area of setting at compressor inlet and outlet; $p_0^*(\bar{r})$, $p_3^*(\bar{r})$ - mean value of total pressure at interval compared to inlet duct and across beyond guide vane at adjusted radius.

$$p_0^*(\bar{r}) = \frac{1}{t(\bar{r})} \int_0^{t(\bar{r})} p_0^*(\bar{r}, t) dt, \quad p_3^*(\bar{r}) = \frac{1}{t(\bar{r})} \int_0^{t(\bar{r})} p_3^*(\bar{r}, t) dt.$$

$$\eta_{st}^* = \frac{T_{0st}^* (\pi_{st}^{*\frac{k}{k-1}} - 1)}{T_{3m}^* - T_{0m}^*}, \quad (2)$$

where T_{0m}^* , T_{3m}^* - mean value of total temperature at stage inlet and outlet.

$$T_{0m}^* = \frac{2\pi}{F_0} \int_{0.5}^1 \bar{r} T_0^*(\bar{r}) d\bar{r}, \quad T_{3m}^* = \frac{2\pi}{F_3} \int_{0.6}^1 \bar{r} T_3^*(\bar{r}) d\bar{r}$$

where $T_0^*(\bar{r})$, $T_3^*(\bar{r})$ - mean value of total temperature at interval compared to inlet duct and across beyond guide vane at adjusted radius.

Also it was defined total and static pressure, total and static temperature along blade height across beyond guide vane and rotor.

As calculation area it was choose periodic part of axis compressor stage. It contained one inlet duct, rotor and guide vane blade.

Since defining of stage characteristics carried out at two-dimensional area as calculation defining at two-dimensional area too (Fig. 3).

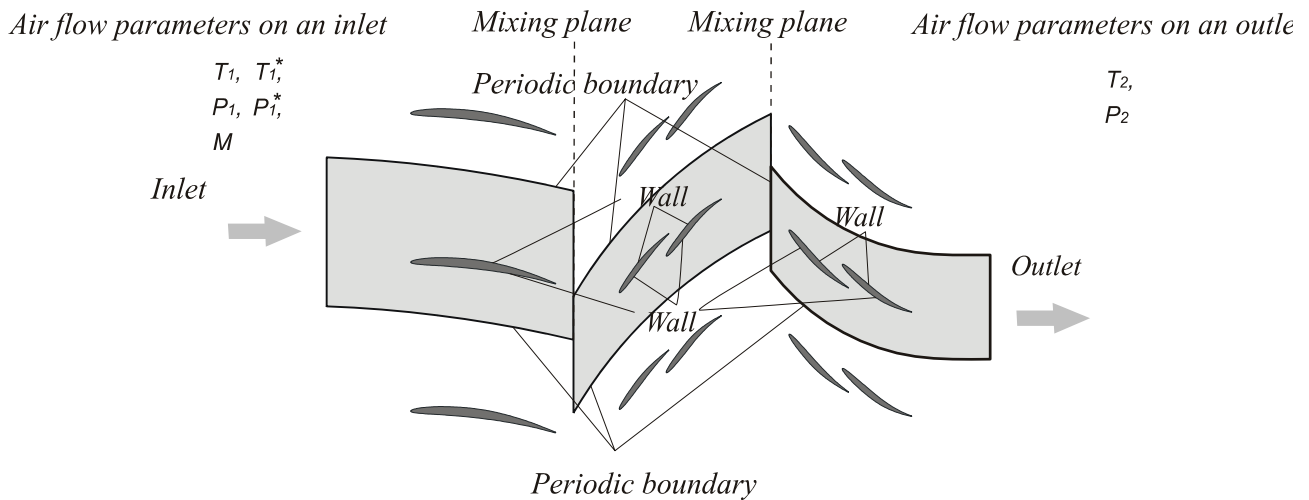


Fig. 3. Scheme of two-dimensional calculation area of axial compressor stage.

As mane stage geometry parameters with one-tired and tandem blade row are equal as defined areas are equal too. Stage characteristics were calculated at 11 two-dimensional area along height of blades. Computational grid was created with help program Gambit. It has unit-type structure and consist of structured grid with tetragonal elements of boundary layer at vane surface and non-structured grid with triangular elements at other defined area. General elements number for one-tired vane row was from 120000 to 140000, for double rotor and guide vane row was from 160000 to 185000 elements.

Spacing of vane surface by grid elements carried out 0.5. It was computational grid thickening at front and trailing edge of vane by bi-exponent low with thickening coefficient 0.7 [14]. At the bound of computational grid spacing was 1. On blade surface in boundary layer area the thickening was: first row height 0.01, growth factor 1.2, number of row 15.

Boundary conditions were defined on all surface calculated area and included inlet and outlet condition, periodic condition and condition on mixing frontier. Boundary conditions on hard walls (blade surface) were defined as adhesion condition to smooth adiabatic wall.

Inlet stage boundary conditions were total $T^*=300$ K, static pressure $p=101325$ Pa and adjusted flow velocity λ . On this one calculated Mach number, total temperature, total pressure. There are turbulent viscosity model $k-\omega$ (Menter's) used with standard constants $\alpha_\infty^*=1$, $\alpha_0=1/9$, $\alpha_1=0.31$, $\alpha_\infty=0.52$, $\beta_{i1}=0.075$, $\beta_\infty^*=0.09$, $\beta_{i2}=0.0828$, $\sigma_{k1}=1.176$, $\sigma_{k2}=1.0$, $\sigma_{\omega1}=2.0$, $R_\beta=8$, $R_k=6$, $\zeta^*=1.5$, $M_{i0}=0.25$ [15].

Outlet stage boundary conditions were sated with extrapolation of all flow parameters by inlet parameters (free inlet).

On periodic boundary of calculated area were defined periodic condition of interface between cheeks of calculated area.

In mixing zone aria of rotating and non- rotating used condition "mixing plane". In this zone occurred circular averaging of flow parameters in the line of turning of moving zone [16].

The calculations carried out on 4-th mode of compressor stage work, which sated by adjusted circular velocity Λ : 1,08; 0,910; 0,807; 0,638. For even calculated area the value of circular velocity recalculated according to value of area location radius.

$$\Lambda = u_R / a_*,$$

where u_R – circular velocity at rotor blade end, a_* – ultimate sonic speed.

$$a_* = 18.3\sqrt{T_0^*},$$

where T_0^* – total temperature at compressor stage inlet.

At two-dimensional compressor stage area calculating was applied matrix algorithm «coupled» with implicit solution of gas dynamic equation realized in program Fluent [17]. The gas viscosity simulated Svizerland's law [18].

Results

Quantitative calculation of stage characteristics axis compressor OK-75 with one-tire blade row showed that stage has maximum value pressure rate $\pi_{st}^* \approx 1,495$ by efficiency equal $\eta_{st}^* \approx 0,895$ on the mode $\Lambda = 1.08$, $\lambda_a = 0.56$ and maximum efficiency $\eta_{st}^* \approx 0,94$ by $\pi_{st}^* \approx 1,365$ on the mode $\Lambda = 0.910$, $\lambda_a = 0.44$ (Fig.4)

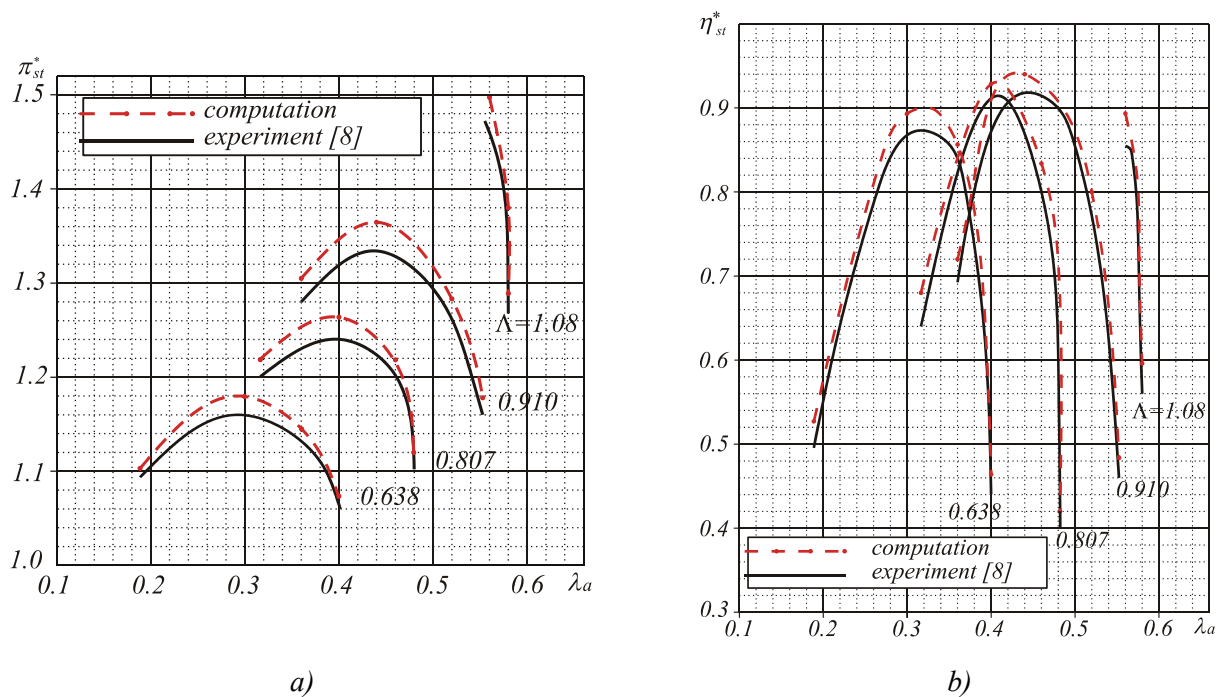


Fig. 4. Characteristics of axis compressor stage: a - π_{st}^* by adduced velocity λ_a ; b- efficiency relation by λ_a

Comparison of other authors' experimental stage characteristics with quantitative results of dissertation researches (of stage characteristics) showed some differences.

At the determination of π_{st}^* general mistake averaged 1,5% and 4,5% at the determination of η_{st}^* . This difference between quantitative and experimental researches results can be explained by calculation stage characteristics without taking into account three-dimensional gas flow effects.

By comparison stage characteristics compressor stages and compressor grids were used the following values: relative variable - $\delta\pi_{st}^* = (\frac{\pi_{m.st}^*}{\pi_{i.st}^*} - 1) * 100\%$; efficiency relative variable -

$$\delta\eta_{st}^* = (\frac{\eta_{m.st}^*}{\eta_{i.st}^*} - 1) * 100\%; \text{ gas dynamic stability relative variable } \delta\Delta K_{y.st} = (\Delta K_{y.m.st} / \Delta K_{y.i.st} - 1) * 100\%;$$

where indexes $m.st$ and $i.st$ mean modified and initial compressor stage.

Using tandem-blade row of rotor and guide vane in axis compressor OK -75 gave an opportunity to increase the stage of pressure rise and efficiency at off-design mode (Fig. 5).

On the border π_{st}^* increases approximately on $\delta\pi_{st}^* = 4 \div 7\%$ (near the stall border), and on $\delta\pi_{st}^* = 7 \div 10\%$ near the blocking border (Fig. 5 a). At simultaneously increasing efficiency stage accordingly on $\delta\eta_{st}^* = 20 \div 40\%$ and $\delta\eta_{st}^* = 60 \div 85\%$ (depends on mode of operation) (Fig. 5 b). Also should be mentioned that on the modes close to calculated (maximum efficiency) a small increase of π_{st}^* (approximately $\delta\pi_{st}^* = 1\%$) and efficiency decrease (on $\delta\eta_{st}^* = 2,2\% \div 4,3\%$) was noticed (depends on mode of operation (Λ)). As well the picture 5 shows that unlike the stage with one-tired blade row, stage with tandem-blade rows has more forcing flat curves. It indicates it's more constant work in all the variety of operation modes. It expresses in increase of compressor stage gas dynamic stability reserve approximately on $\delta\Delta K_{y.st} = 40 \div 50\%$ concerning to the stage with one-tired blade row.

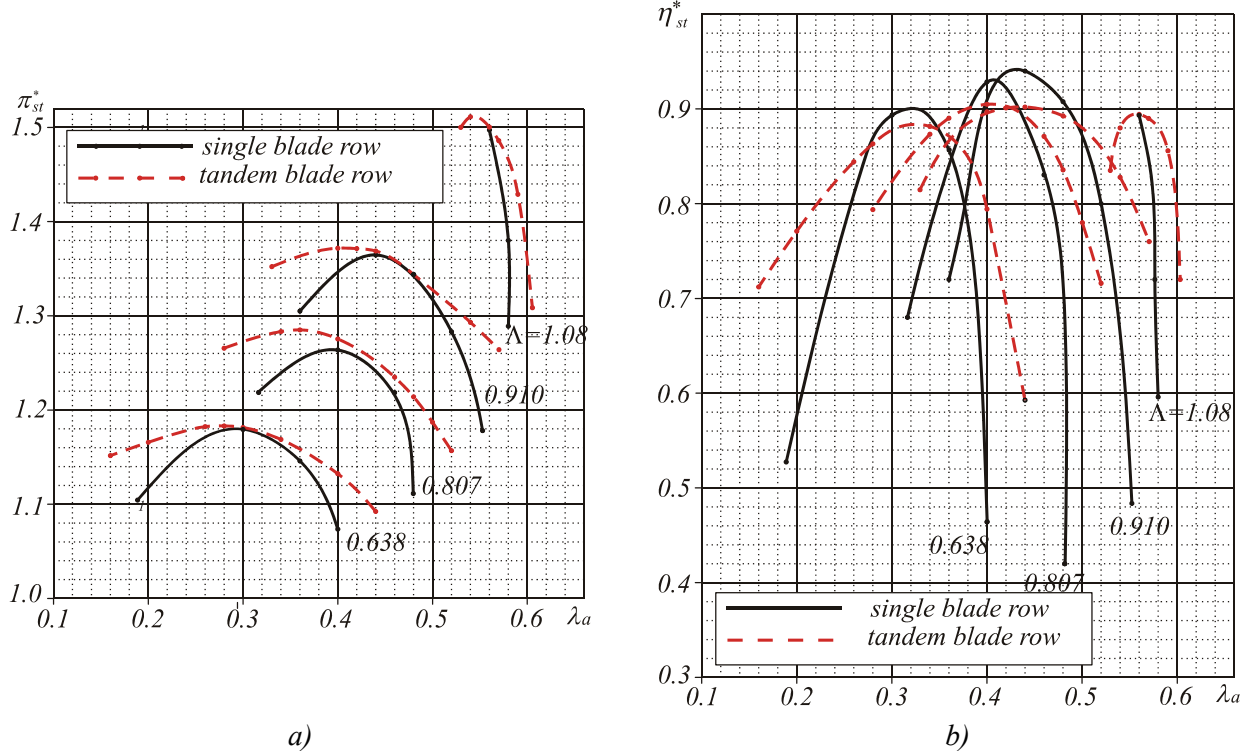


Fig. 5. Characteristics of axis compressor stage with tandem blade : a - π_{st}^* by adjoined velocity λ_a ;
b - η_{st}^* - efficiency relation by λ_a

Summary

The comparison of calculating and experimental data of OK-75 compressor stage is demonstrated at defining π_{st}^* common measure of inaccuracy 1,5%, at defining η_{st}^* – 4,5%. Measure of inaccuracy is not change at any mode of work. Thus, we can consequence that numerical calculus results sufficiently correlated with experimental data, program *Fluent* is useful for compressor flow calculation with compound tear-off events.

The research demonstrated better tolerance of stage on underexpanded modes and better parameters of operating process(π_{st}^* , η_{st}^*), however at the modes

Researching of axis compressor stage with rotor tandem-blade row shown necessity of it's development because at mode closed rated in tandem-blade row is distinguished some greater loss level (efficiency decreasing). Results of tandem-blade row compressor stage numerical calculus are good sort with research results by other authors.

Reference

1. **Фиккерт К.** Исследование диффузорных решёток с большим отклонением потока // Вопросы ракетной техники. – 1953. – №1. – С.57-67.
2. **Чжен П.К.** Управление отрывом потока. Пер. с. англ. М.: Наука, 1979. - 552 с.
3. **Бунимович А.И., Святогоров А.А.** Некоторые результаты экспериментального исследования плоских компрессорных решёток // Обтекание двухрядных компрессорных решёток при дозвуковых скоростях : – Труды ЦИАМ, 1955. -№ 307. – С. 16-30.
4. **Терещенко Ю.М.** Аэродинамическое совершенствование лопаточных аппаратов компрессоров. - М.: Машиностроение, 1988. – 168с.
5. **Терещенко Ю.М., Митрахович М.М.** Аэродинамика компрессоров с управлением отрывом потока. – К.: Институт математики НАНУ, 1996. - 250с.
6. **Bammert K. & Staude R.** Optimization for Rotor Blades of Tandem Design for Axial Flow Compressors // ASME paper, 1979. - № 79-GT-125. – 8 p.
7. **Bammert K. Beelte H.** Investigations of an Axial Flow Compressor with Tandem Cascades // Journal of Engineering Power. – 1980. - № 102. – P. 971 – 977.
8. **Свечников В.С., Кирилов А.Б.** Сборник аэродинамических характеристик ступеней осевого компрессора // Технический отчёт ЦАГИ. – 1958. - № 717. - 36 с.
9. **Sakai Y., Matsuoka A., Suga S.** Design and test of transonic compressor rotor with tandem cascade // International Gas Turbine Congress. – Tokyo, 2003. - № S-108. – 6 p.
10. **Hasegawa, H. Matsuoka, A., Suga, S.** Development of highly loaded fan with tandem cascade // AIAA Paper, 2003. -№ 2003-1065. – 8 p.
11. **Sanger N.L.** Analytical study of the effects of geometric changes on the flow characteristics of tandem-bladed compressor stators / NASA Technical memorandum, 1971. – № TN D-6264. – 60 p.
12. **Андерсон Д.** Вычислительная гидромеханика и теплообмен / Д.Андерсон, Дж.Таннехилл, Р.Плетчер. – М.: Мир, 1990. - 725 с.
13. Аэродинамический расчет и оптимальное проектирование проточной части турбомашин / Бойко А.В., Говорущенко Ю.Н., Ершов С.В., Русанов А.В., Северин С.Д. – Х.: НТУ “ХПИ”, 2002. – 356 с.
14. **Gambit 2.0 Modeling Guide. Chapter 3: Meshing the model.** - Fluent Inc., 2000. – 188 p.
15. **Fluent 6.2 User's Guide. Chapter 11: Modeling Turbulence.** - Fluent Inc., 2003. – 80 p.
16. **Fluent 6.2 User's Guide. Chapter 10: Modeling Flows in Moving and Deforming Zones.** - Fluent Inc., 2003. – 132 p.
17. **Fluent 6.2 User's Guide. Chapter 26: Using the Solver.** - Fluent Inc., 2003. – 110 p.
- Fluent 6.2 User's Guide. Chapter 8: Physical Properties.** - Fluent Inc., 2003. – 60 p.

THE MODELLING OF ACOUSTIC EMISSION RADIATION AT NORMAL WEAR

A model of the signal of acoustic emission resulting from the normal wear of friction pairs is considered. Its mathematical description is obtained. Modelling of acoustic emission signals at varying strained/deformed state and rotation speed of initial friction pairs is done. Experimental research of acoustic emission signals is performed and proved to be good when compared to the results of theoretical research.

Introduction

A significant amount of research has been performed on acoustic emission signals (AE) resulting from friction between the surface layer of different materials [1 - 6].

The results obtained show that, unlike static types of material loading, the processes of acoustic emission are registered as a continuous signal having a rather complicated structure. That is why the basic tendency of research lies in the search for the empirical dependence of varying parameters of AE signals on either loading characteristics or parameters of friction surface wear. At the same time, considerable difficulties in the description of signals, especially from the position of physical presentation of forming their processes, make it difficult not only to set up the experiments, but also to search for the parameters having the information about the processes flowing within the surface layers of friction units.

The approaches applied to static tests are usually used in the description of AE signals during dynamic loading. The basic one is the presentation of AE signal as a stochastic [7 - 16]. Not the physical process and the reasons for its appearance, but a signal when received by an exit signaller are meant. What is also meant is that the signal is the result of a great amount of some events occurring within the material and that each of the events occurs during a short period of time. In this case, the resulting signal is presented as the sum of the flow of instant impulse signals, which has the following appearance:

$$U(t) = \sum_i A_i F_i(t - t_i)$$

or $U(t) = \sum_i A_i F_i(t - t_i) + \sum_j G_j f_j(t - t_j^*) + S(t) + \lambda(t)$, here $u(t)$ is the sum of instant impulse signals in volts; A_i is the random amplitude of a single impulse that appears at a random moment of time t_i ; F_i - are characteristics of impulse form; G_j are the amplitude of the impulse noise component that appears at moment t_j^* ; f_j is the characteristic of the impulse noise component; $S(t)$ and $\lambda(t)$ are correspondingly sinusoidal and arbitrary constant noise components, $S(t) = S_0 \sin(\omega t)$, S_0 is amplitude; and ω is frequency. It is taken that the value of the signal form $F_i(t)$ is known. What is meant is that it looks like

$$F(t) = \sum_{k=1}^m e^{-t/\tau_k} \sin(2\pi f_k t), \text{ if } t \geq 0, \text{ and } 0, \text{ if } t < 0$$

here f_k is the frequency of the resonance signaller; τ_k are time shade characteristics and looks like $F(t) = \alpha_0 e^{-\beta t}$, here α_0 is initial amplitude; and β is shade coefficient [7, 11]. There are also other depictions of the signal shapes, the choice of which is based on the results of experiments [6, 16]. The impulse flow is considered to be described with the help of the poisson's law.

While the result signal processing a certain limit is introduced, it provides the transfer from the continuous signal to the impulse one. In this case the notion of the following parameters is used: density of amplitudes of probability a_i , length ($\tau_i = t_i - t_{i-1}$), average values $\bar{A}_i, \bar{A}_i^2, \bar{\tau}_i$, and either spectral densities or correlation functions. Moreover, AE information is characterized by amplitude distribution, entropy, summary number of signals, and other parameters. If one does not use the limit, then one may determine the density of the average amplitude values of probability and

correlation function of the resulting process. In fact, the stochastic approach supposes the determination of a certain amount of statistic parameters, altering the values of which may characterize change in the processes flowing within the materials. Approaches like that are attempts to *determine* the AE informative parameters. However, they do not allow one to establish or describe the regularity of its change depending on the mechanisms of the flowing processes and the conditions of their development.

The modelling and the basic regularities of parameters change determination of the AE signals will be held at the state of the normal wear.

Theoretical aspect

While considering the normal wear process of the friction pair surfaces at work [17] the signal AE models, emitting at the secondary structures of I and II types destruction, are developed.

The models were being formed for the tribosystem which has a kinematical scheme of the samples looking like the rollers. The surface of frictional contact is bounded by the surface s that looks like the thin line. It was considered that the contact surfaces are worked together. The material of the samples with the surface of contact interaction s is isotropic, excepting a small area s_m , which is not familiar and is located within the s area. the area of non-familiarity s_m is much less than s , $s_m \ll s$. Considering the destruction processes at the s_{mv} area, as well as the destruction of the secondary structures of the I and II kinds, allowed to obtain mathematical expressions for the resulting signals of AE in time in the following look. For the secondary structure of the ii kind (fragile distraction)

$$U_T(t) = U_0 \delta_0 \sigma_{0e}^3 e^{4zt} e^{-b\sigma_{0e} z t}, \quad (1)$$

here $U_0 = kN_0 cz$ is maximal possible displacement at the destruction without the dispersive surface layer of material S_T ; k is proportionality coefficient; N_0 is number of simple volumes in the area of non-familiarity S_T ; c, b are coefficients of distribution of elementary volumes taking strength as the parameter (depend on physical and mechanical characteristics of the material); σ_{0e} is initial equivalent of strain at the stage of normal wear; t is time; $z = E/\xi$; ξ is viscosity coefficient; E is

module of elasticity; $\delta_0 = \int_{t-\delta/2}^{t+\delta/2} a(\tau) d\tau$ is average continuity of amplitudes at the elementary volume destruction; $a(\tau)$ is function that determines the form of a single impulse of amplitudes (it is equal for all kinds of elementary volumes).

The equation is obtained considering the dependence of one-cycle amplitude on the value of elementary volume strength in the area s_m .

For the secondary system of the kind i (plastic deformation)

$$U_d(t) = U_{0d} \varepsilon_{0d} e^{rt} e^{-B\varepsilon_{0d} e^{rt}}, \quad (2)$$

here $U_{0d} = a_0 M \frac{v_d}{\ell_0} \delta_d$ is displacement amplitude that depends on physical and mechanical characteristics of the material; a_0 is amplitude of single impulse displacement at the dislocation movement (it is constant and doesn't depend on deformation); ℓ_0 is distance between two acts of emission of single dislocation; v_d is average speed of dislocation movement (is considered to be

constant); ε_{0d} is relative initial deformation; $\delta_d = \int_{t-\delta_1/2}^{t+\delta_1/2} a_1(\tau) d\tau$ is average continuity of the implying

impulse; $a_1(\tau)$ is function that determines the implying impulse form (is constant); M, B, r are the constants (depend on physical and mechanical characteristics of the materials).

Modelling of the AE signals according to the points (1) and (2) showed that with the increase of the initial level of the equivalent tension (σ_{0e}) a time decrease of the AE signal occurs as well as the increase of its amplitude.

The increase of the level of initial deformations (ε_{0d}) draws to the time decrease of the ae signal without changing its amplitude. The further modelling of the ae signals occurred under condition, that destruction of the secondary structures of the I and II orders can follow any way consequently with rather small periods of time. The obtained data showed that the resulting signal contained the amplitude drops along with consequent increase of its continuity.

The processes of forming the AE signals and modelling them occurred under the condition that the destruction of the secondary surfaces of the I and II kinds for the selected kinematical scheme occurs within one area of frictional contact interaction, which look like the area S as a line having some width. In the area it is considered that the secondary structures of the I and II kinds may exist together. And their destruction processes may occur either consequently, or with rather small (not sufficient) period of time between them. At an end of the given processes a finish AE signal occurs, which is shown in [17].

Under true conditions of the friction pair's work a consequent change of contact grounds occurs along the forming surface of the samples. In this case the destruction of the secondary structures of the I and II kinds occurs within consequently changing contact grounds. It is completely obvious that in this case at the result AE signal formation, a time of destruction processes appearance appears to be sufficient. The time will depend on the speed of change of friction pairs grounds, i.e. on the speed of the samples rotation taking into account the final width of the contact area. An obedient existence of the secondary structures of the I and II kinds being destroyed within the contact area, as well as the presence of dynamic load being replaced along with the contact areas in decreased time period, draws to the fact that the impulse AE signals will be covered not only within the contact area, but also at passing from a ground to a ground. In other words, with the decrease of time of destruction of the secondary structures of the I and II kinds appearance (with the increase of the destruction activity), a transfer from the resulting impulse process of the AE signals emission to the continuous one will take place.

All the considered above allows us represent the AE signal as the sum of signals appearing at random moments of time appearing at destruction of the secondary structures of the I and II kinds, i.e.

$$U'(t) = \sum_i U_T(t - t_i) + \sum_j U_d(t - t_j), \quad (3)$$

here t_i, t_j are random moments of AE signal appearance $U_T(t)$ and $U_d(t)$ at the destruction of the secondary structures of the I and II kinds correspondingly.

Keeping the (1) and (2) in mind the expression (3) will look like

$$U'(t) = \sum_i U_0 \delta_0 \sigma_{0e}^3 e^{4z(t-t_i)} e^{-b\sigma_{0e}} e^{z(t-t_i)} + \sum_j U_{0d} \varepsilon_{0d} e^{r(t-t_j)} e^{-B\varepsilon_{0d}} e^{r(t-t_j)}. \quad (4)$$

The (4) makes possible to see it under correct initial conditions (the given physical and mechanical characteristics of the materials of the friction pair at the constant contact area), that the resulting AE signal is determined by the initial strained and deformed state ($\sigma_{0e}, \varepsilon_{0d}$) and the time of the start of destruction of the secondary structures of the I and II kinds is (t_i, t_j). Basing on this, the modelling of the AE signals was held; it followed the (4), and had two stages. At the first stage at constant meanings of $\sigma_{0e}, \varepsilon_{0d}$ the change of resulting AE signal depending on the start point of the destruction of the secondary structures of the I and II kinds was researched. At the second stage at the constant time of the secondary structures of the I and II kinds the change of the resulting AE signal depending on change of $\sigma_{0e}, \varepsilon_{0d}$ was researched. The results of such a modelling looking like the graphs of change $\tilde{U}(t) = U'(t)/U_{\max}$ measured in relative values are depicted at fig. 1 and 2. At the graphs' construction the time is established to be enough for the action of the load over the friction couple, and it is equal to t_{\max} . The parameters $\sigma_{0e}, \varepsilon_{0d}, b$ and B are drawn to the non measured values.

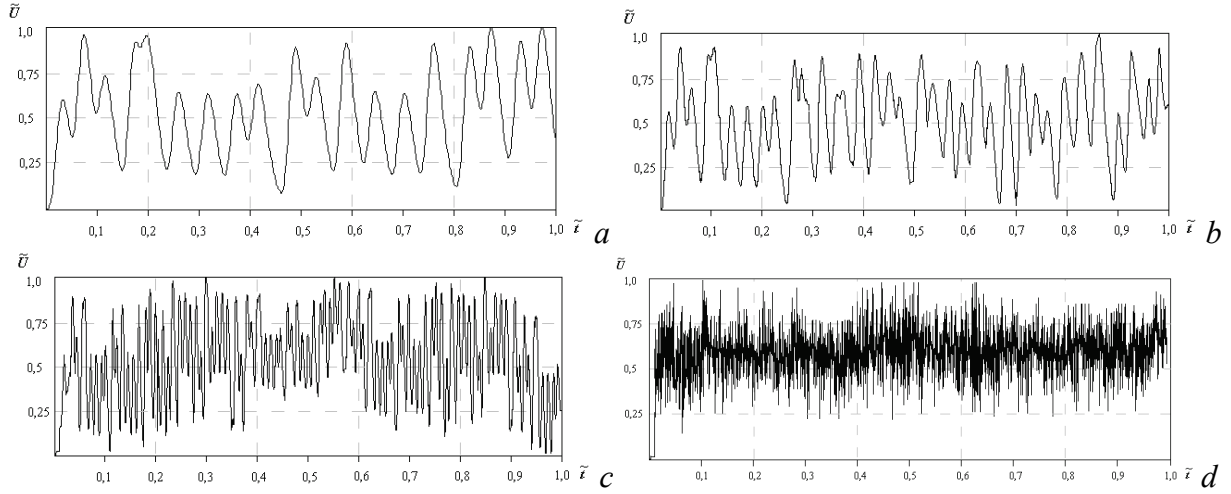


Fig 1. The forms of the AE signals at the stage of normal wear at various initial times of destruction of secondary structures of the I and II types: $\sigma_{0e}=17$; $\varepsilon_{0d}=17$; $b=B=10$. \tilde{U} is normal meaning for U_{\max} . \tilde{t} is the normal one for $t_{\max} = \text{const}$. The time step of destruction of every following structure of either I or II kinds in relative units: $a - 0,0007$; $b - 0,0004$; $c - 0,0001$; $d - 0,00001$

At the AE signals modelling at the first stage it was accepted that $\sigma_{0e}=17$, $\varepsilon_{0d}=17$, $b=B$, $b=B=10$. And the resulting signal, according to (4), has been formed at a consequent interchanging of the structures of I and II kinds according to a certain scheme, which did not change at the following stages of the modelling. A step occupies the time of start of destruction of the every following secondary structure of the I and II kinds varied from 0,0007 till 0,00001 relative units. And the time between the start of destruction of structures of I and II kinds did not change with the stage development.

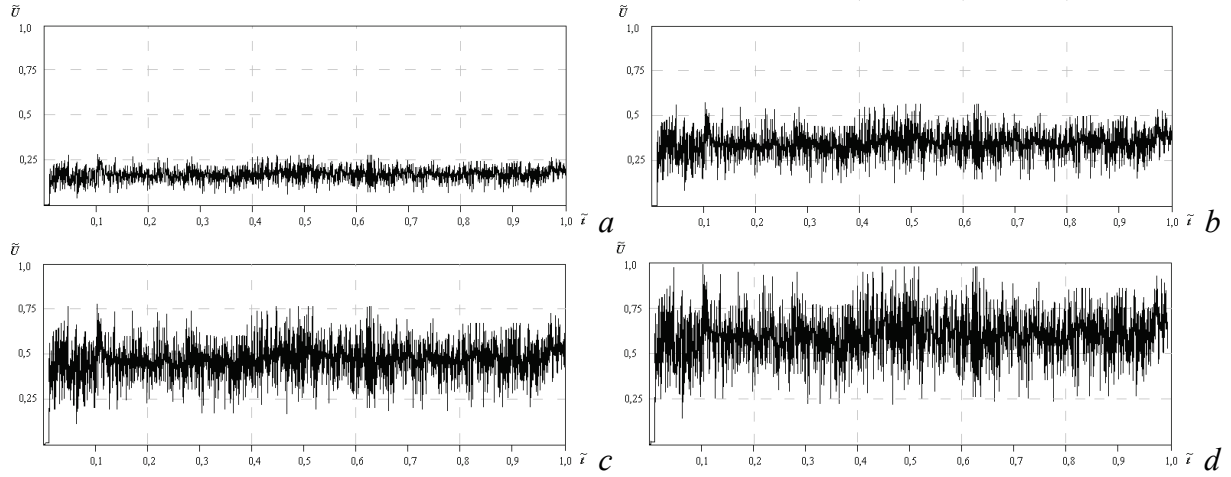


Fig 2. Forms of the AE signals at the stage of normal wear at the destruction of the secondary structures of the I and II kinds for various initial values of strains and deformations: $b=B=10$. The step of added start time of every following structure of either I or II kind is equal to 0,00001 in relative units. \tilde{U} is normal value for U_{\max} . \tilde{t} is normal value for $t_{\max} = \text{const}$. The values of the initial tensions and deformations are the following: $a - \sigma_{0e}=11$; $\varepsilon_{0d}=11$; $b - \sigma_{0e}=13$; $\varepsilon_{0d}=13$; $c - \sigma_{0e}=15$; $\varepsilon_{0d}=15$; $d - \sigma_{0e}=17$; $\varepsilon_{0d}=17$

At AE signals modelling at the second stage it has been accepted that $b=B=10$. The resulting signal according to (4), has been formed at the consequent interchange of destruction of the structures of the I and II kinds according to the certain specially selected scheme, that did not change at the following stages of modelling. The step of start time point of destruction each following structure of either I or II type did not change with the any following stage and was equal

to 0,00001 relative units. The values σ_{0e} and ε_{0d} changed from 11 to 17 with the additional step equal to 2.

From the obtained results one can see, that at the consequent destruction of the secondary structures of the I and II kinds with rather small time intervals the resulting AE signal looks like a continuous one (Figs 1, 2). In other words, the impulse AE signals formed under conditions of separate destruction of the structures of the I and II kinds, are transformed into a continuous AE signal that appears under the condition of consequent destruction of the secondary structures of the I and II kinds with arbitrary initial times [17]. Meanwhile, with the decrease of initial time of destruction of the secondary structures of the I and II kinds a compression of the signal in time and its form transformation occur (Fig 2), and it starts to look like a hilled signal with amplitude drops. At the give initial tensions and deformations, according to the research results, the amplitude of the impulse AE signal at the destruction of the secondary structure of the II kind exceeds the amplitude of the AE signal of the secondary kind of the I kind [17]. This makes obvious the fact that the amplitude drops will be determined by the destruction of the secondary structures of the second kind.

This is proved by the results obtained at the second stage of modelling when the initial tension and the deformation were changed (Fig 2). As far as we can see from the figure 2, at constant initial start time step of the destruction of the secondary structures of the I and II kinds with the given constant scheme, the increase of the initial tensions and deformations draws not only to the increase of the average amplitude level of the resulting AE signal, but also increase of arbitrary of the position along the amplitude (the difference between the maximal and the minimal values of the amplitude drops). Such a result can be explained in the following way. At the difference of the AE signals amplitude, the signals being formed in the process of destruction of the secondary surfaces of the I and II kinds, the upper layer of the resulting AE signal amplitude will be determined by the amplitude of the signal of the secondary structure of the II kind, and the lower one – by that of the I kind. At minimal initial tensions and deformations of AE signals amplitudes at the destruction of the secondary structures of the I and II kinds do not differ widely (on the order). At the result of imposing of an input of the signals at destruction of the secondary structures of the I kind into the resulting signal will be commensurable with the input of the signals appearing at the destruction of the structures of the II kind. Under the given conditions it is obvious that the amplitude dispersion of the resulting signal be minimal, which is observed in the modelling results (Fig 2, *a*). With the increase of the initial tensions and deformations the difference within the amplitude of AE signals for the structures of the I and II types increases, which has been shown in [17]. Under the conditions mentioned above the input into the resulting AE signal of the signal amplitude, and this signal having been appeared at the destruction of the secondary structure of the I kind, decreases. This, surely, must draw to the decrease of the lower layer of the resulting signal, and, as the result, to the increase of the medium level and the AE signal amplitude dispersion, which is observed in the results of the modelling (Fig 2).

Experimental research

Experimental research of the AE signals was held at the universal machine of CMT-1 type at the friction of the steel 12X2H4A examples. Along, a kinematical scheme “roller-roller” (“disc-disc”) has been realized. As for lubricant means the redactor lubricant Б-3В has been applied. The choice of the sample materials of the friction couples researched as well as the choice of the lubricating means is reasoned by their wide application in the transmissions of aviation gas-turbine engines (GTE).

In correspondence with the kinematical scheme selected, one of the samples of the friction couple has less rotation speed than another one which was rotating at a spindle of the CMT-1 machine (Fig 3, *a,b*). The regime of rolling friction was realized along, considering the 20 % sliding. Dimensions of the samples were the following: diameter $D = 25$ mm, thickness $h = 15$ mm. Rotation Speed of the friction machine's shaft was $V = 500$ rot/min. Its value was selected according to the maximum approach to the conditions of exploitation of the dots of friction begin

modelled. The working tensions of the contact interaction of the friction couple σ_p have been changed in the diapason of values within 400 MPa and 1000 MPa with the additional value of the step of value 200 MPa. The increase of the working tensions occurred at the stage of normal wear, i.e. after the finishing of friction pair's run-in.

The time of the initial addition of the friction couple was 20-25 minutes. The time of secondary addition after the increase of the working tensions was 4-5 minutes. The time of work of friction couple at each exploitation load was 5 hours.

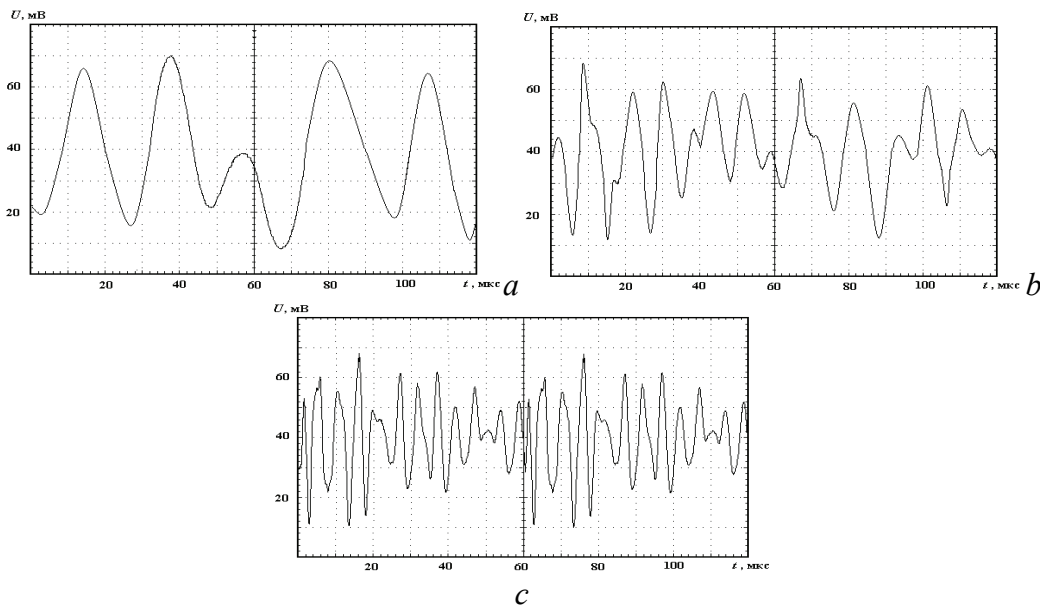


Fig 3. AE signals registered at the stage of normal wear at the constant working contact tension σ_p and at varying rotation speed of friction pair: *a* - $V=200$ rot/min; *b* - $V=500$ rot/min; *c* - $V=800$ rot/min. Working contact stress $\sigma_p=1000$ MPa

A piesoceramical signaler has been installed on the immovable sample of the frictional couple, this signaler being intended for the AE signals registration. The output signaler's signal was enforced the preliminary strengthener and was passed to AE diagnostic complex (AEDC). AEDC is the mobile computer with the program software, which allows to control the processor of measurements, and to process the AE signals parameters and present the analysis results as a table or a graph. AEDC allows processing the following AE signals parameters: averaged amplitude, energy, power; summary energy; gathered values of the parameters and the others. Moreover than that, graphic presentation of the initial AE signal and analyzing its parameters. The additional parameters researched include the friction moment, which was measured with the help of friction moment measurer.

Typical results of the AE signals registering at the change of frictional pair rotation speed and at constant value of the working contact tension σ_p at the stage of normal wear of friction pair are shown at the figure 3. The value σ_p was 1000 MPa. The figure 6 shows typical results of the AE signal registering at constant speed of the friction pair rotation and change of values of the working contact tensions σ_p at the stage of normal wear. The value of the rotation speed was equal to the 500 rpt/min.

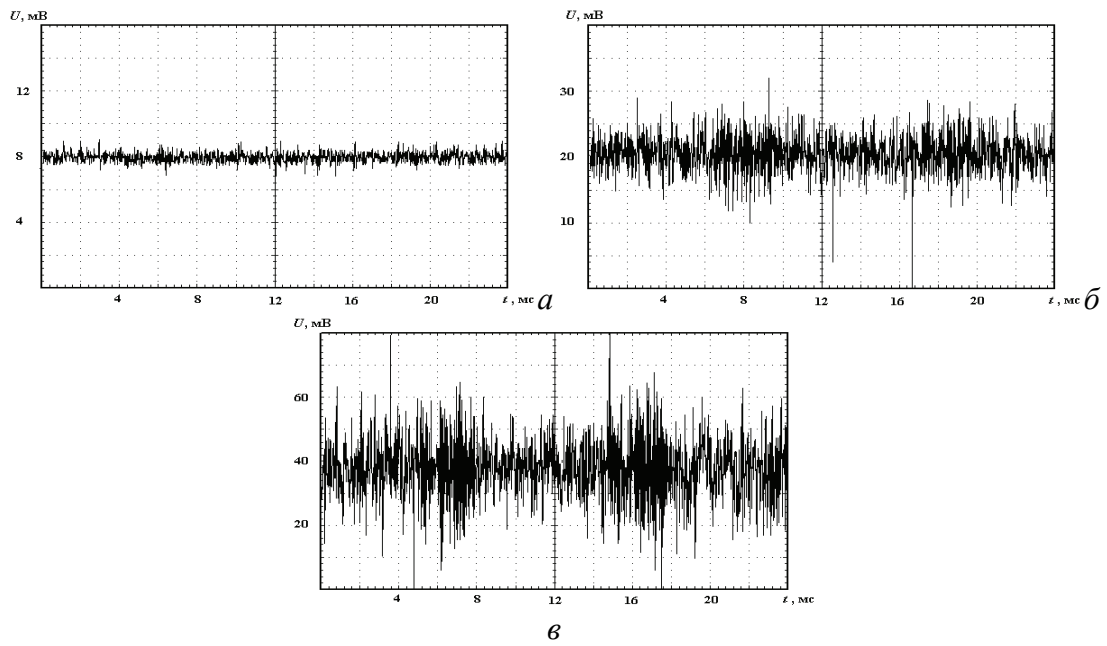


Fig 4. AE signals registered at increase of working contact tensions σ_p at the stage of normal wear of friction couple: *a* - $\sigma_p=400$ MPa; *b* - $\sigma_p=800$ MPa; *c* - $\sigma_p=1000$ MPa. The speed of rotation of friction pair $V=500$ rot/min

Figure 4 shows that the registered AE signals are the constant signals and have the complicated cut form. With the increase of the rotation speed of the movable sample of the friction couple from 200 rot/min till 800 rot/min and unchanging value of the working contact tension σ_p the transformation of the form of AE signal is observed as well as its time compression. Such a change AE signal character can be explained from the positions of the modelling held. Really the increase of the speed of frictional pair rotation corresponds to the decrease of time between the changes of contact grounds, and thus draws to the reduction of time between the consequent acts of destruction. According to the modelling held in figure 2, it must draw to the compression of the AE signal in time.

At the same time as it can be seen from the figure 4, when changing of working contact tensions σ_p and constant rotation speed of the movable friction pair couple sample, the AE registered signals have the complicated hilled form as well. Along with this, with the increase σ_p from 400 MPa to 800 MPa and 1000 MPa increase in not only average value of the AE signal amplitude is observed, but also the increase of the maximum and minimum values (dispersion) along the amplitude. Such a change of the parameters of the AE signals also accurately corresponds to the results of the modelling held (Fig 2).

Conclusion

At the result of the research held, a model of resulting AE signal is been developed, the AE signal is being formed at the stage of normal wear of friction pair. A model is built on the basis of already existing information of the normal wear process, connected with the destruction of the secondary structures of the I and II kinds. It is also shown that AE impulse signals formed under the condition of separate destruction of the structures of the I and II kinds are transformed into a continuous AE signal.

The resulting signal has the complicated form, change of view and transformation of which are reasoned by the differences in the parameters of the impulse AE signals, formed at the destruction of the structures of the I and the II kinds, as well as under the conditions of work of a friction pair. In accordance with the modelling held it was established that at constant values of initial stresses and deformations at the stage of normal wear, decreasing time between the start of distraction of the structures of the I and II kinds (increase of the speed of rotation of the friction

pair) draws to the AE signal compression in time and to its transformation into the signal of the hilled shape.

At the same time at constant speed of friction pair rotation the increase of the initial stress and deformation at the stage of normal wear draws to the increase of the average level of the resulting AE signal, as well as to increase in its amplitude dispersion.

References

1. Babak, V. P.; Filonenko, S. F.; Stadnychenko, V. N. 2006. Mechanism of transition of friction pairs to “quasiwearless” mode of operation. *Aviation*, 10(4): 8–13.
2. Babak, V. P.; Stadnychenko, V. N. 2004. Application of revitalisants for extension of resource and restoring of worn-out friction units of aviation axial-piston hydromachines. *Aviation*, 8(1): 8–12.
3. Bukhalo, O.; Klym, B.; Pochapsky, E. et al. 2000. An information-measuring system for an acoustic emission signal selection and processing. In *Proceedings of 15-th World Conf. On Non-Destr. Testing. (15-21 October 2000 in Rome)*, 78–82.
4. D’Attelis, C. E.; Pareiz, L. V. et al. 1992. A bank of Kalman filters for failure detection using acoustic emission signals. *Non-destructive testing*. Elsevier Pub., 29–33.
5. Harvey, T. J.; Wood, R. J. K.; Denuault, G. et al. 2002. Investigation of electrstatic charging mechanisms in oil lubricated tribo-Contacts. *Tribology Unternational*, 9(35): 605–614.
6. Houle, P. A.; Sethna, J. P. 1996. Acoustic emission from crumpling paper. *Physical review E*, 54(1): 278–283.
7. Lei, X.; Kusunose, K. 2000. Quasi-static fault growth and cracking in homogeneous brittle rock under triaxial compressing using acoustic emission monitoring. *Journal of Geoph. Research*, 105(3B): 6127–6139.
8. Lei, X.; Masuda, K.; Nishizawa, O. et al. 2004. Detailed analysis of acoustic emission activity during catastrophic fracture of faults in rock/ *Journal Of Structural Geology*. (26): 247–258.
10. Lypez Pumarega, M. I.; Piotrkowski, R.; Ruzzante, J. E. 1999. Discussion of log-normal distribution of amplitude in acoustic emission signals. *Journal of Acoustic Emission*, 17(1-2): 61–67.
11. Majeed, M. A.; Murthy, C. R. L. 2001. A model with nonzero rise time for AE signals. *Sādhanā*, 25(5): 465–474.
12. Minozzi, M.; Caldarelli, G.; Pietronero, L. et al. 2003. Dynamic fracture model for acoustic emission. *Eur. Phys. J. B.*, (36): 203–207.
13. Wang, L.; Wood, R.; Harvey, T. et al. 2003. Wear performance of oil lubricated silicon nitride sliding against various bearing steels. *Wear*, (255): 657–668.
14. Акустические и электрические методы в триботехнике. Под ред. В. А. Белого. Минск: Наука и техника, 280.
15. Бабак, В. П.; Філоненко, С. Ф.; Стадниченко, В. М. et al. 2007. Моделі сигналів акустичної емісії при руйнуванні поверхневих шарів матеріалів. *Проблеми тертя та зношування*, (47): 1–8.
16. Иванов, В. И.; Белов, В. М. 1981. *Акусто-эмиссионный контроль сварки и сварных соединений*. Москва: Машиностроение. 184 с.
17. Фадин, Ю. А. 1997. Динамика разрушения поверхности при сухом трении. *Письма в ЖТФ*, 23(15): 75–78.
18. Фадин, Ю. Ф.; Козирев, Ю. П.; Полевая, О. В. et al. 2001. Корреляционная связь акустической эмиссии с размерами частиц износа при сухом трении. *Заводская лаборатория. Диагностика материалов*, 67(3): 43–47.

ACOUSTO-EMISSION METHOD IN DIAGNOSTICS OF CONSTRUCTIONS' CONDITION

Results of cradle tests of an industrial building with application of acoustic emission method are considered. Change of radiation character and parameters of registered signals are shown. Kinetic laws of change of the accumulated energy of AE signals are obtained. Processing criteria estimations of the construction condition are carried out. Stages of loss of bearing ability of signals of acoustic emission are defined.

Introduction

Various methods of technical diagnostics among which methods of non-destructive control (ultrasonic and magnetic non-destructive testing, eddy current non-destructive testing and others) have the greatest distribution and are applied to carry out estimations of construction reliability [1-3]. The inspection of constructions and their elements with application of the given methods is carried out, as a rule, in static conditions. The control is directed to detecting the formed defects, defining their sizes and space orientation in material. Actually, by results of the control the static information on defects is obtained. Thus decision-making on further operation of the construction with detected defects is based on results of studying the destruction of materials by way of defect modeling (cuts, fatigue cracks and others) [4, 5]. However, the application of such approach does not allow estimating potential danger of the detected defects (their propensity to development), as concentrators of pressure, and their influence on bearing ability of constructions.

The destruction of construction does not occur instantly, and develops gradually. Thus development of processes of destruction is described by the general kinetic law [6] which is caused by gradual accumulation of damages prior full destruction of the construction. From the view-point of diagnostics of products the account of the given law, i.e. the account of danger of gradual accumulation of damages influencing bearing ability of the construction is important. One of the methods, allowing to obtain information on the internal processes occurring in materials at their loading, is the method of acoustic emission [7 - 10].

Many works are devoted to researching AE phenomenon. Basically, they are directed to searching laws of change of parameters of registered AE signals and working out criteria of estimating the condition. By their working out the approaches of non-destructive control (NDC) are accepted in traditional methods, i.e. an establishment of interrelation of the size of formed cracks with parameters of registered AE signals [11 - 15] is used. Therefore existing criteria estimations are accepted in many countries of the world [16, 17], and are directed to detecting cracks and tracking their propagation which is defined on increasing parameters of AE signals. However the interrelations applied are empirical and are suitable only for the investigated materials.

The theoretical analysis of AE signals [18 - 21] has allowed establishing the basic differences and laws of change of AE signal parameters, which emerge in crack formation and course of plastic deformations. Distinction of informative parameters of registered signals [22] that has allowed developing criterion of detecting AE signals from cracks [23] has been thus shown. At the same time, in detecting cracks it is not always possible to define degree of their potential danger, as these are the concentrators of the pressure inclined to development, and because interference of defects on bearing ability of designs takes place. It's necessary to say that the destruction of construction can occur at pressure of much less strength of a material.

It is known, that AE is the reflection of the internal processes occurring in a material at its loading, and its gradual development reflects kinetics of the processes. According to a kinetic principle of summation of separate destructions [6] in [24] AE criterion of destruction on the basis of similarity of avalanche character kinetics of destruction and kinetics of AE signals radiation is defined under the laws of change of parameters of AE signals [18 - 21] at change of the intense-deformed condition of a material. Thus the work [25] shows, that theoretical dependence of accumulation of energy of AE signals E_c from of enclosed pressure σ , taking into account dependence of energy on speed and self-acceleration of process of destruction, exponential function of the following kind is described:

$$E_c(\sigma) = E_{c_{\max}} e^{k(\sigma) - k(\sigma_{\max})}, \quad (1)$$

Where $E_{c\max}$ - the limiting accumulated energy which corresponds to the moment of full destruction; $k(\sigma)$ - the exponent, not linearly depends on pressure; σ_{\max} - limiting pressure of destruction.

However, the experimental results obtained in testing various samples of materials and products, have shown, that self-acceleration of destruction process results in considerable nonlinearity $k(\sigma)$. As dependence of change $k(\sigma)$ is a priori unknown (depends on a number of factors), it is difficult enough to use expression (1) for the data analysis. Therefore for approximation of experimental data the following function is used:

$$E_c = cH^d, \quad (2)$$

where E_c - accumulated energy of AE signals; c, d - constants for applied type of AE equipment, a material and conditions for carrying out tests; H - characteristic parameter for the given conditions of carrying out tests (loading - P , pressure - σ , deformation - ε or others).

Values E_c and H are normed, i.e. $E_c = E_T / E_{\max}$; $H = H_T / H_{\max}$ where $E_T, E_{\max}, H_T, H_{\max}$ - accordingly, current and maximum values of accumulated energy of AE signals and characteristic parameter.

It should be noted, that dependencies (2) are obtained when applying the joint analysis of data in time sections of processes of accumulation of energy of AE signals [25] for each value of characteristic parameter of H , for example, at the stage of construction loading on each degree of the enclosed loading. The results of tests of a cradle of an industrial building will be considered at its step loading in this work. The analysis of process of AE signal radiation will be carried out and stages of formation and development of cracks are defined. It will be shown, that dependence of accumulation of energy of AE signals on loading is described by sedate function and as loading where the beginning of loss of load-carrying capacity of the construction is fixed and defined.

Research technique

AE research is carried out in the tests of a cradle of an industrial building. Definition of load-carrying capacity of the construction, i.e. maximum loads at which the construction loses the load-carrying capacity was a main objective of tests. Thus, in the course of tests definition of deviation of real moving of the chosen control points in a plane of a cradle from settlement values was carried out.

The cradle of an industrial building represents the P-shaped design with length of flight 15m (fig.1). The cradle height in its central part made 6 m. It has been made of a steel of type St3. The loading cradles were subjected to the uniform dispersed loading which was placed on four points (P , fig. 1). They were placed at an identical distance from vertical cradle support. Cradle test was carried out under the program of step increase of loading and its endurance in time within 5 minutes (fig. 2.). Limiting value of loading on the cradle made calculation th 30,0 kN. In test the following levels of discrete loadings were used: 5,0 kN; 10,0 kN; 15,0 kN; 17,5 kN; 20,0 kN; 22,5 kN; 25,0 kN. The construction loading was carried out with use of hydraulic system. In process of the construction loading the measurements of pressure and deformations with use of 97 strain gauges were made. They have been established in knots of connections of elements of the cradle (the bottom and top parts of a vertical support, a joint of horizontal beams), as well as in the central part of horizontal beams (T , fig. 1). Measurements were carried out by means of multichannel digital strain-gauge instrumentation. By the results of measurements at each step of loading in control points (1, 2, 3, fig. 1) calculations and construction orthographic epures of vertical and horizontal movements were carried out. Typical orthographic epures of the construction moving at loading 20 kN are shown on fig. 2. Thus vertical movement is under construction in a cradle plane. Values of moving in fig. 2, result in relative units.

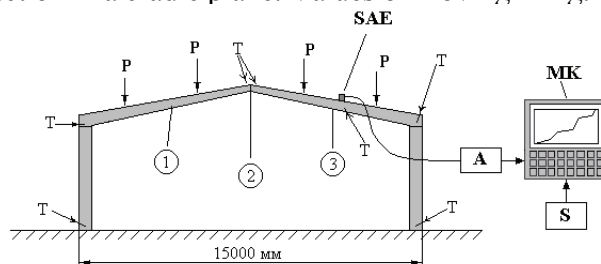


Figure 1. Scheme of carrying out tests of an industrial building cradle: P - points of the appendix of loading; T - locations of strain gauges; 1, 2, 3 - points of calculating movement to cradle planes; SAE - gauge of acoustic emission; A - amplifier; MK - mobile computer; S - software

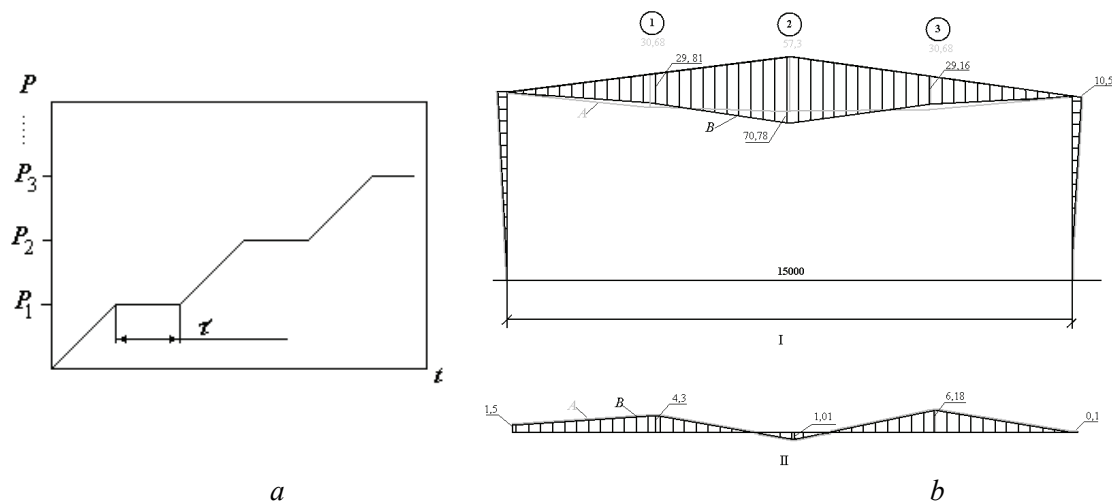


Figure 2. Scheme of loading of the industrial building cradle (a) and orthographic epures of its moving (b): P - loading; t - time; τ - endurance time under loading; I, II - accordingly, orthographic epures vertical and horizontal moving; 1, 2, 3 - points, according to fig. 1; A, B - accordingly, settlement and experimental curves. Values of moving are resulted in relative units

Measurements of pressure, deformations and calculations of moving were carried out by employees of the Test center of construction designs of the National University of construction and architecture. For research of AE signals a diagnostic complex “AKEM” was used. The AE complex consists of gauge AE, the mobile computer with program software (fig. 1). It is intended for registering pulse streams of AE signals, their processing, forming data files, conclusions and analysis results on the monitor screen. Processing of AE parameters is carried out on each registered signal (amplitude, duration, energy) and to their processes (accumulation of quantity of signals and energy). Processing of criteria estimations is held according [16, 17], as well as criterion of crack detection [23] and kinetic criterion of estimating danger of processes (2), which leads to loss of bearing ability of the construction [25]. To register AE signals a broadband piezoelectric transducer, installed on the top beam of a cradle of an industrial construction, was used (fig. 1).

Cradle tests were carried out as follows. Loading increase on a cradle with the controlled enclosed value on the indicator of the hydraulic pump was carried out. Achieving the level of loading the endurance of the construction was made for a number of steps under loading within 5 minutes. In the course of endurance registration and processing of AE signals was carried out. Upon termination of endurance strain-gauge measurements were made. By results of AE processing dependencies of parameter changes of registered signals within a certain period of time were under construction, the criterion of signal detection from cracks and parameters of kinetic dependence were analyzed, according to (2) were processed. By results strain-gauge measurement calculations were carried out and orthographic epures of moving of the top beams of a cradle to cradle planes, and their horizontal moving were under construction (fig. 2).

Experimental results

The analysis and processing of the AE information in the process of loading of an industrial construction cradle has shown, that process of AE signals radiation has a discrete character. Radiation of AE signals is registered, since loading on a cradle makes 15,0 kN. Intensity of radiation is low. The total of registered AE signals does not exceed 100. Thus amplitudes of AE signals have low level (fig.3a.). From fig. 3, a it is visible, that amplitudes of AE signals do not exceed size 0,22 V. This character of radiation and value of parameters of registered signals remain till loading on a cradle is 20,0 kN - intensity of radiation is low, amplitudes of signals do not exceed 0,27 V (fig. 3,b).

To further increase in level of the enclosed loading there is a change of character of radiation and parameters of registered signals of AE. So at loading 22,5 kN the sharp increase of intensity of radiation is observed. The total registered signals of AE exceed 1000. The increase in amplitude of signals (fig. 3,c) is thus observed. Increase of radiation intensity of AE signals and their parameters is fixed with the further increase of loading to 25,0 kN (fig. 3,d).

The analysis of process of radiation and parameters of AE registered signals at increase within time period of endurance of the cradle of the industrial building under loading has shown, that

gradual decrease of radiation intensity and parameters of registered signals of AE (fig. 4) eventually are observed. Similar change of character of radiation and parameters of AE signals, certainly, is connected with gradual redistribution and stabilization of the intense-deformed condition of the industrial building cradle, which is under loading.

Processing of criterion of detection of AE signals from cracks [23] which characterizes speed of energy change of AE registered signal, has shown, that formation and development of cracks is observed, since loading makes 20, 0 κN (fig. 5). When loading on the cradle of the industrial building makes 22,5 κN and 25,0 κN (fig. 5), AE signals from cracks are fixed. In fig. 5 each point corresponds to registered AE signal. Excess of numerical value criteria estimations of the size noted in fig. 5, shaped line corresponding to occurrence of AE signal from a crack.

The analysis of AE signals with processing criteria estimations of signals from cracks at endurance of a cradle under loading has shown the following. Since loading makes 22,5 κN and above in the course of endurance of the cradle of the industrial building under loading within time period development of cracks (fig.6) is also observed. Actually process of redistribution and gradual stabilization of pressure is accompanied by crack formation. Thus with loading increase the given process

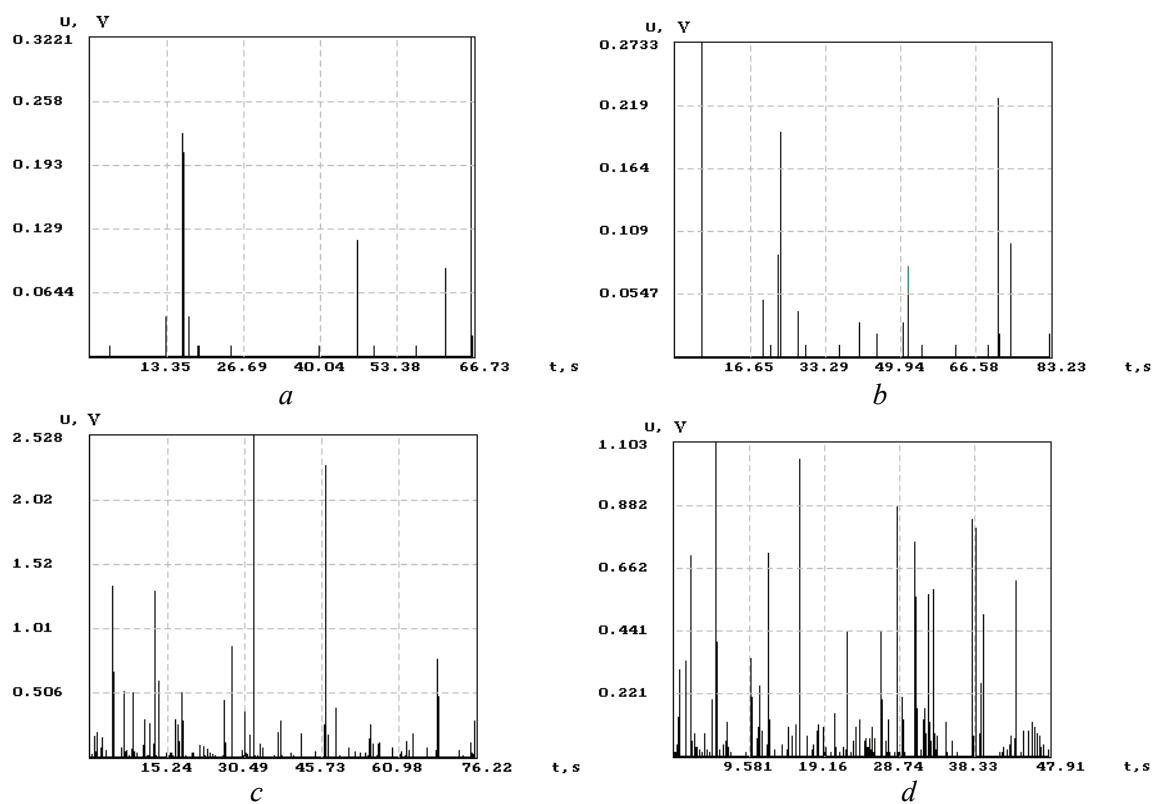


Figure 3. Dependencies of change of average amplitude of AE signals within time period. Loading on the cradle of the industrial building: *a* - 15,0 κN ; *b* - 20,0 κN ; *c*-22,5 κN ; *d* -25,0 κN proceeds more intensively. For some time the number of AE signals from cracks is not considerable. From the view-point of power AE fixed signals have low energy, their maximum value does not exceed $3,4 \cdot 10^3 \text{ mV}^2 \cdot \text{s}$. It testifies to development of processes of crack formation on micro level [9].

The joint analysis of the experimental data in time section of processes of accumulation of energy of signals on each degree of loading has shown, that from loading 15,0 κN and above, the

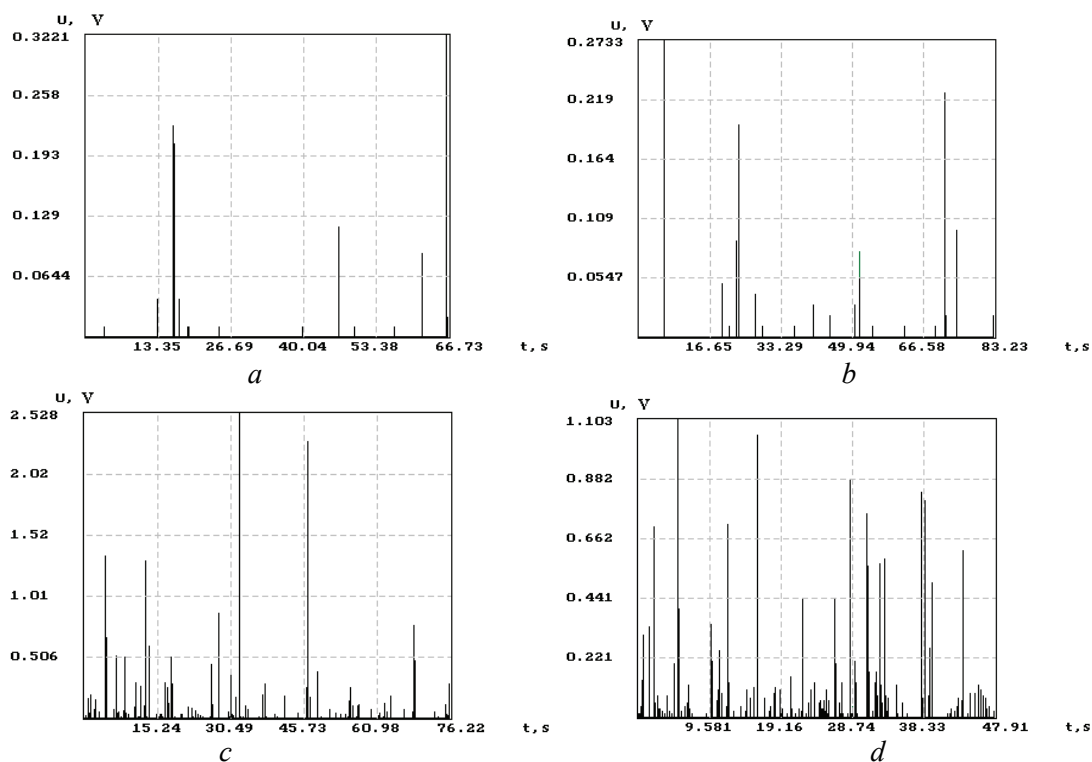


Figure 3. Dependencies of change of average amplitude of AE signals within time period. Loading on the cradle of the industrial building: *a* - 15,0 kN; *b* - 20,0 kN; *c*-22,5 kN; *d* -25,0 kN

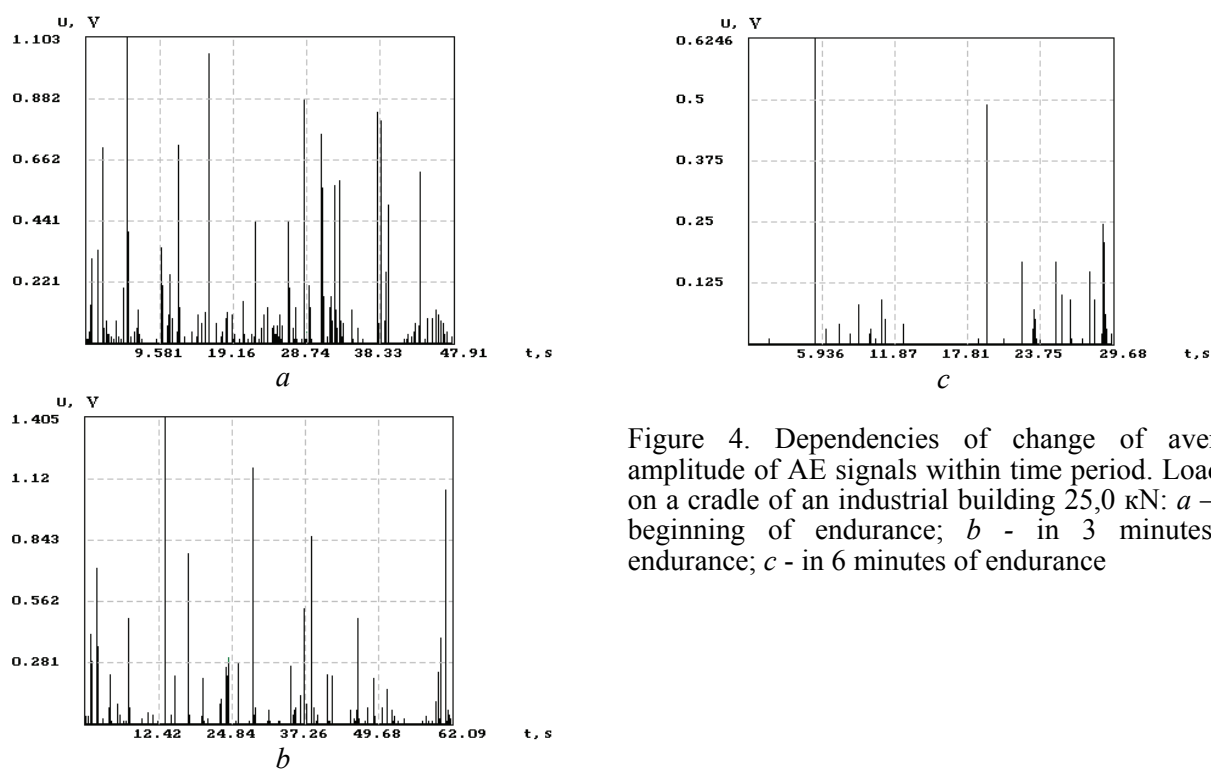


Figure 4. Dependencies of change of average amplitude of AE signals within time period. Loading on a cradle of an industrial building 25,0 kN: *a* – the beginning of endurance; *b* - in 3 minutes of endurance; *c* - in 6 minutes of endurance

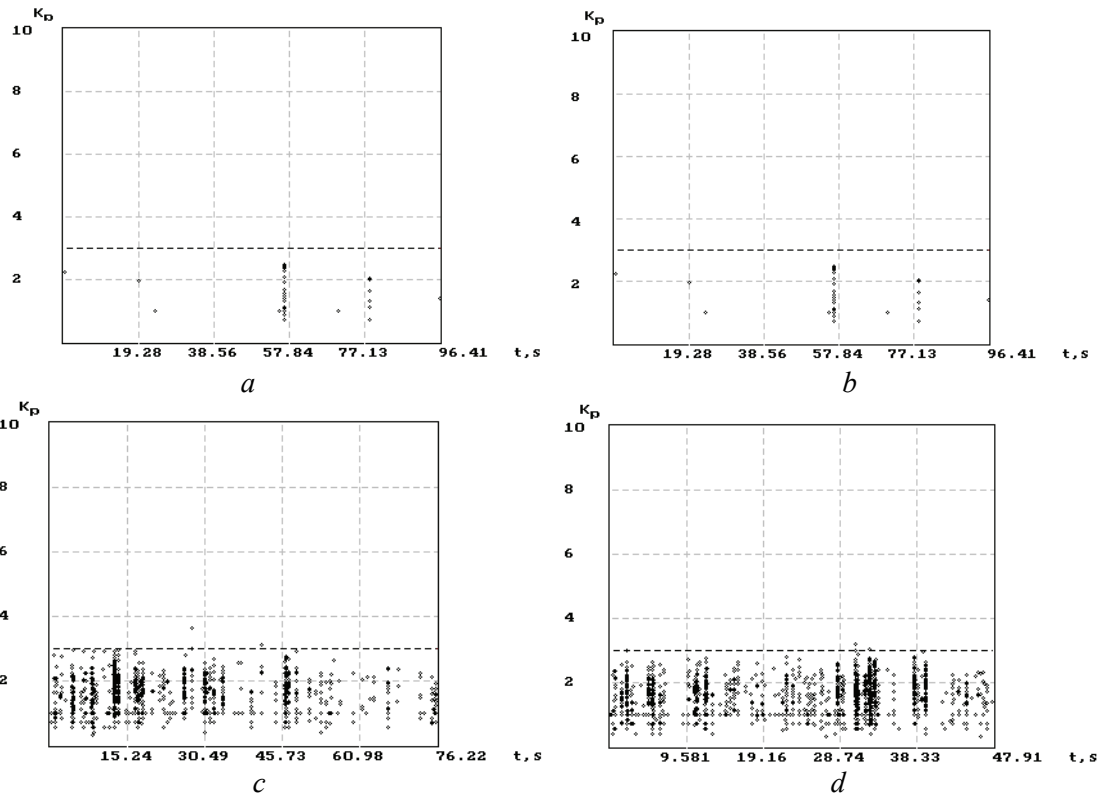


Figure 5. Dependencies of change of numerical value of criteria estimations of detection of AE signals from cracks within time period. Loading on a cradle of an industrial building: *a* - 15,0 κH; *b*-17,5 κH; *c* - 22,5 κH; *d*-25,0 κH

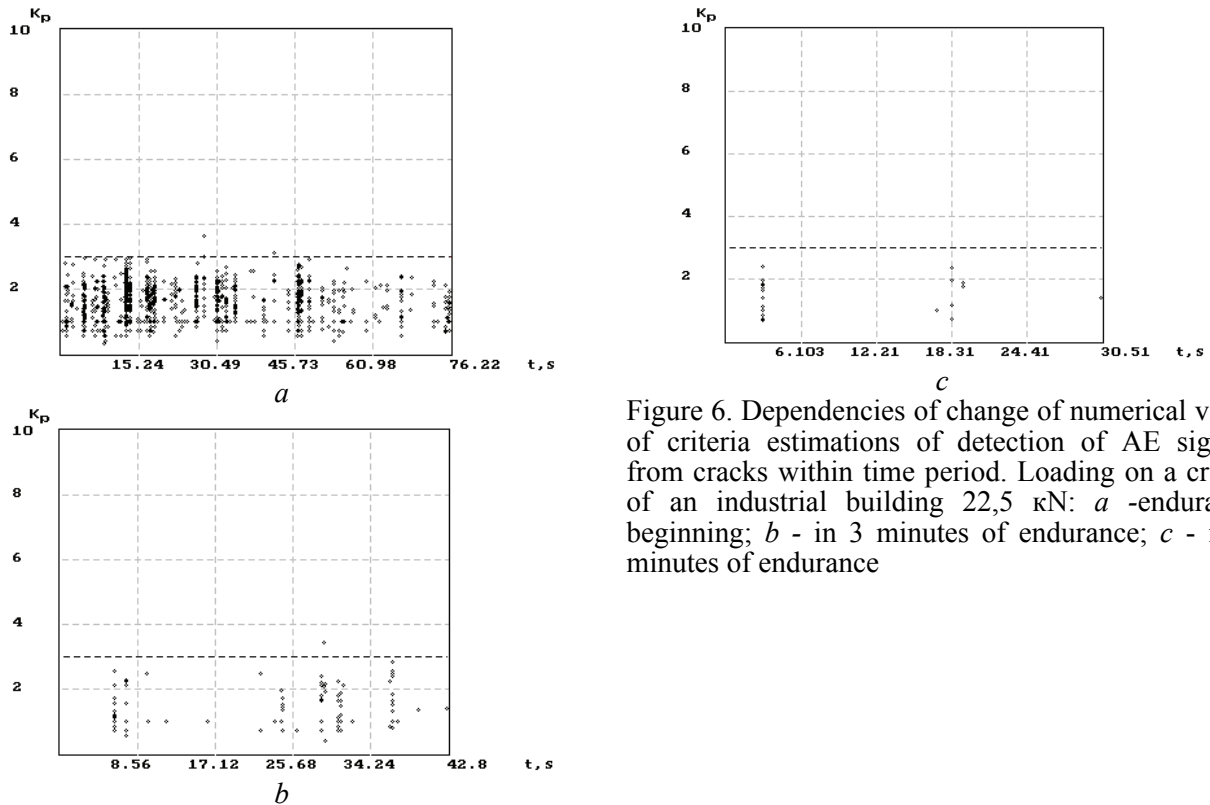


Figure 6. Dependencies of change of numerical value of criteria estimations of detection of AE signals from cracks within time period. Loading on a cradle of an industrial building 22,5 κN: *a* -endurance beginning; *b* - in 3 minutes of endurance; *c* - in 6 minutes of endurance

steady kinetic dependence (fig. 7) which is described by expression (2) is also observed. Characteristic parameter value of the loading enclosed into the cradle of the industrial building is used. Steady dependencies are observed during accumulation of energy of AE signals makes ≥ 6 s.

The dependencies obtained in fig. 7 are constructed in absolute values of energy in mV^2s , loading – in kN . Processing of the results obtained in relative units, according to (2), allows defining

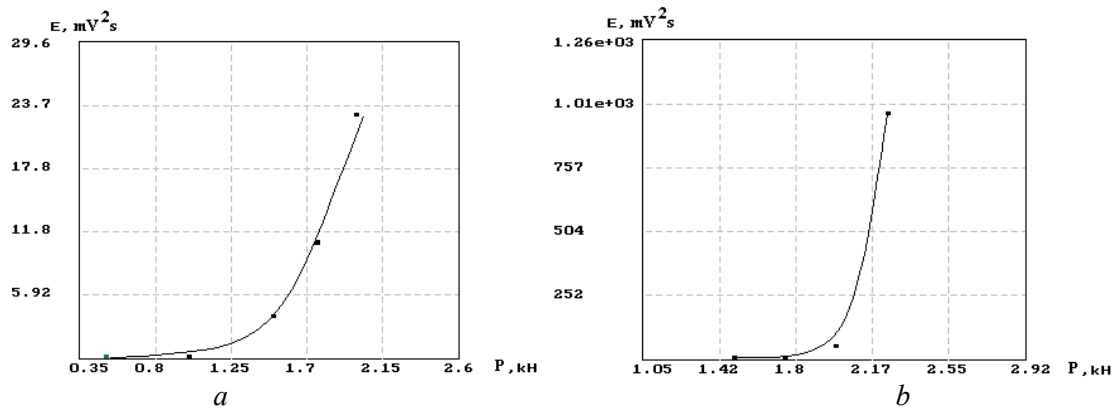


Figure 7. Dependencies of change of the saved up AE signal energy on loading in a cycle: *a* - at loading to 20,0 kN; *b* - at loading up to 22,5 kN. Time of energy accumulation for AE signals is 6 s

an exponent of the approximating expression characterizing stages of danger of processes which influence the bearing ability of the industrial building cradle. The values obtained are summed up in tab. 1. Criterion of approximating dependence choice is the minimum of a standard deviation (s^2).

AE data processing at each step of loading has allowed defining the development of dangerous and critical processes of stability loss [9]. It is observed, accordingly, at loading 17,5 kN and 20,0 kN, when value of an exponent makes $d \geq 10$ (tab. 1). At a step 25,0 kN at endurance of a cradle under loading within time period the continuous increase in deformations (moving) in a vertical plane of a cradle, continuous (critical loss) its stability is fixed. To prevent destruction of cradle test the emergency dump of loading is stopped and made. Results of calculating theoretical and actual vertical moving to cradle planes (by strain measurement data) for points 1, 2, 3 (fig. 1), executed by employees of the Test center of construction designs of the National university of construction and architecture, are summed up in tab. 2.

Table 1

Values of factors of approximating expression in the test of an industrial building cradle

Loading, kN	c	d	s^2
15,0	0,95	3,5	0,00752
17,5	0,93	8,26	0,022
20,0	1,1	10,2	0,00303
22,5	0,993	12,3	0,00136
25,0	0,999	13,4	0,00059

Table 2

Results of calculating vertical movement toward cradle planes

Loading, kN	<i>Diversion of actual and the theoretical moving</i>		
	%		
	Point 1	Point 2	Point 3
10,0	-12,26	-0,25	-13,89
15,0	-18,34	6,48	6,69
17,5	-3,65	6,26	-6,10
20,0	-2,84	23,53	-4,94
22,5	39,40	72,41	42,64

The obtained data (tab. 1, tab. 2) show, that at a stage of the beginning of critical loss of stability (20,0 kN) numerical value of an exponent b becomes more than 10, i.e. $b > 10$. Thus actual maximum vertical moving of a cradle exceeds theoretical by ~ 24 %. In subsequent increase of loading (22,5 kN) value of an exponent b increases ($b > 12$), and actual maximum vertical moving of a cradle exceeds the theoretical one already by ~ 73 %.

Conclusions

Thus, results of the researches have shown that AE method is an effective method of diagnostics and monitoring construction condition. Thus it is possible to estimate and define stages of danger of the processes influencing bearing ability of the construction. The given estimations are

carried out under kinetic law of processes of energy accumulation by AE signals at each loading stage. Thus formalized processing of the law allows defining an exponent of approximating law and change of its numerical value with increase in level of the enclosed loading. The application of the analysis of an exponent of approximating expression has allowed defining the beginning of loss of stability of the industrial building cradle and transition to a critical stage of stability loss. The results obtained have been confirmed by data of strain-gauge researches.

References

1. Крауткремер Й., Крауткремер Г. Ультразвуковой контроль материалов.-М: Металлургия, 1991.-752 с.
2. Ермолов И.Н., Останин Ю.Я. Методы и средства неразрушающего контроля качества.-М.: Высшая школа, 1988.-368 с.
3. Неразрушающий контроль металлов и изделий: Справочник /Под ред. Г.С.Самойловича.-М.: Машиностроение, 1976.-456 с.
4. Р.Б.Томпсон, Д.О.Томпсон. Применение ультразвука в неразрушающем контроле //ТИИЭР.-1985.-т.73.-№12.-С.23-67.
5. Неразрушающий контроль качества сварных конструкций / В.А.Троицкий, В.П. Радько, В.Г. Демидо и др..-Л: Техніка, 1986.- 155 с.
6. Регель В.Р., Слуцкер А.И., Томашевский Э.Е. Кинетическая природа прочности твердых тел.-М.: Наука, 1974.-560 с.
7. Иванов В.И., Белов В.М. Акусто-эмиссионный контроль сварки и сварных соединений.-М: Машиностроение, 1981.-184 с.
8. Андрейкив А.Е., Лысак Н.В. Метод акустической эмиссии в исследовании процессов разрушения.-К: Наукова думка, 1989.-176 с.
9. Филоненко С.Ф. Акустическая эмиссия. Измерение, контроль, диагностика.-К.:Издат-во КМУГА, 1999.-304 с.
10. Скальський В.Р., Коваль П.М. Акустична емісія під час руйнування матеріалів, виробів і конструкцій.-Львів:СПОЛІОМ, 2005.-396 с.
11. Болотин Ю.И., Маслов В.А., Полунин В.И. Установление корреляции между размером трещины и амплитудой импульсов акустической эмиссии // Дефектоскопия.-1975.-№ 4.- С.119-122.
12. Гусев О.В. Акустическая эмиссия при деформировании монокристаллов тугоплавких металлов.-М: Наука, 1982.-108 с.
13. Johnson M., Gudmundson P. Broad-band transient recording and characterization of acoustic emission events in composite laminates // Report 255, Department of solid mechanics, Royal institute of technology, Stockholm, Sweden, 1999.
14. Landy R.J., Ono K. Acoustic emission behavior of a low alloy steel. //J.of Acoust. Emiss.- 1982.-N1.-P.7-19.
15. Акусто-эмиссионная диагностика конструкций / А.Н.Серьезнов, Л.Н.Степанов, В.В.Муравьев и др.-М.: Радио и связь, 2000.-280 с.
16. ASME. "Acoustic emission for successive inspections. Section XI, Div.1", Case N-471, Supplement No 5,Cade cases 1989 Edition, Nuclear Components, Boiler and Pressure Vessels, Code Appruvel Date: 30 April 1990.
17. РД-03-131-97. Правила организации и проведения акусто-эмиссионного контроля сосудов, аппаратов, котлов и технологических трубопроводов.-М: Издательство стандартов, 1996, 40 С.
18. Бабак В.П., Филоненко С.Ф., Калита В.М. Модели формирования сигналов акустической эмиссии при деформировании и разрушении материалов //Технологические системы.-2002.-№1(12).-С.26-34.
19. Бабак В.П., Филоненко С.Ф., Калита В.М. Моделивання сигналів акустичної емісії при виникненні в матеріалі тріщин //Вісник НАУ.-2002.-№ 1.-С.5-10.
20. Бабак В.П., Филоненко С.Ф., Калита В.М. Моделирование сигналов акустической эмиссии при протекании в материале пластической деформации //Технологические системы, 2002.-№3(14).-С.77-81.
21. Филоненко С.Ф. Физические аспекты акустической эмиссии при протекании пластической деформации //Зб.наукових праць: Надтверді матеріали: створення та застосування /НАН України. ІНМ ім. В.М.Бакуля.-К.:2007.-С.131-138
22. Бабак В.П., Филоненко С.Ф., Калита В.М. Оценки информативности параметров сигналов акустической эмиссии //Технологические системы.-2003.-№ 3(19).-С.65-69.
23. Филоненко С.Ф. Анализ достоверности критериальной оценки выделения сигналов акустической эмиссии от трещин на источнике Су Нильсона //Автоматика, автоматизация, электротехнические комплексы и системы.-2001.-№2.-С.33-39
24. Бабак В.П., Байса Д.Ф., Різак В.М., Филоненко С.Ф. Конструкційні і функціональні матеріали:Основи фізики твердого тіла.Функціональні матеріали.-К:Техніка,2004.-368 с.
25. V. Babak , S.Filonenko. Technical diagnostics materials and elements of aviation designs dy the method of acoustic emission /Materials the World Congress "Aviation in the XXXI-st Century".-September 14-16, 2003, Kyiv, Ukraine.- P.2.1-2.7

VERACITY OF MEASUREMENTS IN HETEROGENEOUS AIR & SPACE COMPLEXES

The method and engineering technique of veracity definition of non equal on accuracy of measurement results in heterogeneous air and space complexes are offered. Index parameters of increase of veracity from integration information and measuring systems are entered. The estimation efficiency of the various integration systems is executed according to "CNS/ATM conception". Numerical examples and results of experimental researches of air & space complexes of different structure are given. Non equal on accuracy of measurement, space complexes, efficiency of integrating, optimum control of measurements, "CNS/ATM conception"

Introduction. Measurement as operation of a finding of value of physical value by practical consideration with the help of special means, provides direct connection between the theory and experiment, high veracity of scientific researches, optimum control of quality of manufacture and efficiency of the goods and services use [1,2]. Methods of metrology as sciences about measurements, methods and means of maintenance of their unity, ways of achievement of required accuracy and veracity, include methods of measuring transformations, direct and indirect measurements, the control and management of measurements, planning of experiment, maintenance of measurements unity, processing of measurements results, an estimation of accuracy and veracity of measurement, increase of measurements efficiency, decrease of expenses of resources on measurements and others.

Actual directions of metrology and adjacent sciences are creation of modern measuring systems and complexes for efficient control technological processes, improvement of the goods and services quality, the further increase of accuracy, veracity, speed, sensitivity, a degree of automation and convenience of use, expansion of a range and opportunities of measurements means, development of new methods and measurement techniques and others.

The problem of optimum control of non equal on accuracy of measurements naturally arises then when there unite in the measuring complexes of system constructed on various physical principles and in this connection having various on value errors of measurements. For example, according to "CNS/ATM conception" in system of global management of flying devices (planes, helicopters, rockets, satellites, space stations etc.) use ground, onboard and satellite systems of communication, navigation and supervision which use various principles in the physical essence. Therefore air & space complexes are diverse (heterogeneous) and on the agenda problems of the analysis, synthesis and optimization of accuracy and veracity of such complexes leave.

In our papers [3 - 6] the theoretical substantiation of optimum control by processing of signals in the integrated space navigating systems is given, parameters of efficiency of complexes non equal on accuracy of measurements are considered, problems of comparison of complexes among themselves and definitions of a degree of their affinity to complexes is equal exact measurements, numerical algorithms of the decision of a task in view with the help of introduction of characteristic number m_0 for heterogeneous complexes are given, the estimation of heterogeneous complexes errors by a method errors ranking of the systems forming complexes is executed. At the same time, problems of the veracity estimation non equal on accuracy of measurements remain are insufficiently investigated. And these problems are actual not only for the analysis and optimum synthesis of heterogeneous complexes, but also at a choice of measurements standards, at a substantiation of methods and techniques of complexes checking, at processing the non-uniform statistical data and in a number of other practically important cases [7,9].

The purpose of this paper is to create a method and an engineering technique of definition of results veracity of non equal on accuracy of measurements in heterogeneous air & space complexes.

For achievement of the purpose the following problems are put and solved: a substantiation of statement of primary goal, definition of the necessary initial data, a choice of a method of the decision of the problem adequate to its contents, forecasting of expected results, planning of

imitating experiment, processing of experiment results and their comparison with theoretical results, development of an engineering technique of definition of results veracity non equal on accuracy of measurements in heterogeneous air & space complexes.

Statement of a problem. Known initial given a decided problem serve probability characteristics of measuring physical values and accuracy of the systems forming a heterogeneous air & space complex. For manufacture of indirect measurements and optimum control of processing of results the method of results summation of indirect measurements with the optimum weight factors, offered by us in papers [3-5] is chosen. For realization of imitating experiment and data processing about veracity non equal on accuracy of measurements the system of scientific researches automation “Mathcad 14” is used. Veracity of measurements is estimated at a level of the given probabilities appropriate to fields of the admission, the value two, four, six of average square values for a measuring random variable.

Statement of the basic material. We shall solve a problem with use of the typical circuit of the heterogeneous optimum air & space complex [3,4] submitted on fig. 1. The circuit includes ground, onboard and space segments of indirect measurements, each of which contains two parts. One part carries out functions of processing of the initial data about measuring values, results of indirect measurements of object parameters of management and updating of errors. She is shown in the top part of figure. Other part carries out functions of transformation of physical values in electric signals, scaling of signals, calculation of minimal average square values measuring values, storing and display of results of measurement: estimations of measurement result, minimal average square values measuring values, values of a variation factor.

According to a method of summation of indirect measurements results with optimum weight factors the result of measurement represents optimum on a maximum of accuracy an estimation measuring values as:

$$X = \sum_{k=1}^m g_k \times Y_k, \quad (1)$$

where optimum value of weight factor g_i for i -th result Y_i of indirect measurements defines under the formula

$$g_k = 1/D_k \bigg/ \sum_{k=1}^m 1/D_k, \quad (2)$$

where D_i is a dispersion of an additive error i -th systems of a complex,
 m is the common number of systems in a complex.

The minimal value of a dispersion of an optimum estimation defines under the formula

$$D_{min}(X) = 1 \bigg/ \sum_{k=1}^m 1/D_k, \quad (3)$$

Hence, dispersions D_k , $k=1,m$, serve in the offered method in a role of the initial data, on them optimum weight factors g_k and the minimal value of a dispersion (3) expect. Optimum values of weight factors g_k use in the formula (1) for optimum processing results of indirect measurements Y_i .

Veracity of measurement is considered, as property of means of measurement to state a correct estimation of measuring values in the given conditions of measurement. As well as for systems of diagnosing in a role of the basic parameter of measurement veracity it is convenient to choose full probability of correct measurement, that is full probability of that measuring value will be in the given interval of values. As well as at diagnosing [10], in measurements it is convenient to use conditional and full probabilities of mistakes of the first and second kinds, and at additional distinction of correct and wrong measurements, also conditional and full probabilities of mistakes of the third and fourth kinds.

We use traditional parities for calculation of parameters of measurement veracity [10]. Full probability of a mistake of diagnosing is

$$Q(a, b, x) = \int_a^b f_1(x) \left[\int_{-\infty}^{\chi^{a-x}} f_2(\xi) d\xi + \int_{\chi^{b-x}}^{\infty} f_2(\xi) d\xi \right] dx + \\ + \int_{-\infty}^a f_1(x) \int_{\chi^{a-x}}^{\chi^{b-x}} f_2(\xi) d\xi dx + \int_b^{\infty} f_1(x) \int_{\chi^{a-x}}^{\chi^{b-x}} f_2(\xi) d\xi dx, \quad (4)$$

where a, b are the given borders of the tolerance band for measuring values,

$f_1(X), f_2(\xi)$ are densities of distribution measuring values and errors of measurement of its values,

χ - the factor of optimum expansion of the tolerance band, which choice minimizes a dispersion of an measuring value estimation according to the offered method and full probability of a mistake,

$$\chi(h) = h + 1/h, \quad (5)$$

where

$$h = \sigma_x^2 / \sigma_\xi^2 \quad (6)$$

the ratio of the signal / noise in measurements.

Measuring value Y_i at the moment of diagnosing t_i is received as value

$$Y(t_i) = X(t_i) + \xi(t_i) = Y_i. \quad (7)$$

Then it is defined, whether value has got $Y(t_i)$ in a field of the tolerance $[a, b]$. If $Y_i \in [a, b]$, it is made a decision that measurement value is in the given interval $[a, b]$.

Let's designate through $f_1(x), f_2(\xi)$, accordingly, distribution density of measurement signal and an additive error at the moment strobing t_i . Probability P of measurable signal staying in a field of the tolerance in this method is set to equal probability of performance of inequality $P(t_i) = P_i(a \leq X \leq b, t_i \text{ moment strobing})$

$$P = \int_a^b f_1(x) dx = P_i. \quad (8)$$

Parameters of veracity of the offered method non equal on accuracy optimum measurement is defined on known parities subject to features of a choice of a tolerance band and optimum estimation measurable values on strobe at the measurement moment.

Full probability of first sort measurement mistake (measurable value which is in the chosen field of the tolerance to recognize taking place outside the admission)

$$\alpha = \int_a^b f_1(x) \left[\int_{-\infty}^{\chi^{a-x}} f_2(\xi) d\xi \right] dx + \int_a^b f_1(x) \left[\int_{\chi^{b-x}}^{\infty} f_2(\xi) d\xi \right] dx. \quad (9)$$

Full probability second sort mistake (measurable value which is not in the given field of the tolerance to recognize taking place in a field of the admission)

$$\beta = \int_{-\infty}^a f_1(x) \left[\int_{\chi^{a-x}}^{\chi^{b-x}} f_2(\xi) d\xi \right] dx + \int_b^{\infty} f_1(x) \left[\int_{\chi^{a-x}}^{\chi^{b-x}} f_2(\xi) d\xi \right] dx. \quad (10)$$

Full minimal probability of measurement mistake

$$Q_{\min} = \alpha + \beta \quad (11)$$

Full probability of correct measurement

$$D = 1 - Q = 1 - \alpha - \beta \quad (12)$$

Conditional probability of first sort mistake measurements

$$P_\alpha = \alpha/P \quad (13)$$

Conditional probability of second sort mistake measurements

$$P_\beta = \beta/(1-P). \quad (14)$$

Probability parameters of measurement veracity are convenient for calculating, carrying out necessary linear transformations and using normalized dimensionless variables [10]

$$Z_1 = \frac{X(t) - m_x}{\sigma_x}; \quad Z_2 = \frac{\xi(t) - m_\xi}{\sigma_\xi}, \quad (15)$$

which for any moment of time have a zero mathematical expectation and unit dispersion. Having executed replacement of variables, we shall receive

$$P = \int_{-\eta}^{\eta} f_1(Z_1) dZ_1 \quad (16)$$

$$\alpha = \int_{-\eta}^{\eta} \sigma_x f_1(Z_1) \left[\int_{-\infty}^{\frac{\sigma_x(\chi\eta + Z_1)}{\sigma_\xi}} \sigma_\xi f_2(Z_2) dZ_2 \right] dZ_1 + \int_{-\eta}^{\eta} \sigma_x f_1(Z_1) \left[\int_{\frac{\sigma_x(\chi\eta + Z_1)}{\sigma_\xi}}^{\infty} \sigma_\xi f_2(Z_2) dZ_2 \right] dZ_1 \quad (17)$$

$$\beta = \int_{-\infty}^{-\eta} \sigma_x f_1(Z_1) \left[\int_{\frac{\sigma_x(\chi\eta - Z_1)}{\sigma_\xi}}^{\infty} \sigma_\xi f_2(Z_2) dZ_2 \right] dZ_1 + \int_{\eta}^{\infty} \sigma_x f_1(Z_1) \left[\int_{\frac{\sigma_x(\chi\eta - Z_1)}{\sigma_\xi}}^{\infty} \sigma_\xi f_2(Z_2) dZ_2 \right] dZ_1 \quad (18)$$

Where the absolute and normalized admissions is defined by parities

$$\delta = \frac{b-a}{2}; \quad \eta = \frac{b-a}{2\sigma_x} = \frac{\delta}{\sigma_x} \quad (19)$$

Earlier it was shown, that in diagnosing unitary strobing the normalized tolerance η , the absolute tolerance δ , mean-square value of a handicap σ_ξ , The attitude signal/noise $\Delta H = P_x/P_\xi$ And dynamic range ΔD of measurements are connected by parities:

$$\eta = \frac{\delta}{\sigma_\xi \sqrt{\Delta H}} = \frac{\delta}{\sigma_\xi \sqrt{P_x/P_\xi}} = \frac{\delta}{\sigma_\xi \sqrt{e^{\Delta D}}} = \frac{\delta/\sigma_\xi}{\sigma_x/\sigma_\xi} \quad (20)$$

From parities (20) follows that to operate measurement veracity with unitary strobing of measuring value under fixed σ_ξ is possible three ways: changing δ , ΔD or simultaneously δ and ΔD . Under the fixed value σ_ξ efficiency of diagnosing is defined with parities:

$$\eta \sqrt{e^{\Delta D}} = \frac{\delta}{\sigma_\xi}, \quad \sigma_\xi \eta = \delta / \sqrt{e^{\Delta D}}. \quad (21)$$

Parities (21) evidently show, how lack of a measurement dynamic range can "exchanges" for a width of tolerance band. Under the big signal dynamic range it is possible without fear to narrow a set tolerance band. The condition (20) is a condition of equivalence on mistake probability of three ways of control in volume of the measuring information under unitary strobing.

Efficiency of measurement unitary strobing can be connected with all parameters of volume of a measuring signal if to impose an additional condition that duration strobe should be multiple to an interval of digitization of a measuring signal according to Kotelnikov. Then capacity of a measuring signal in strobing time will define a parity

$$\sigma_x^2 = \frac{vk}{\Delta T} \int_{-\Delta T/2vk}^{\Delta T/2vk} X^2(t) dt = \frac{E(\Delta T, v, k)}{\Delta T} \quad (22)$$

Density of distribution measuring value and measurement errors are assumed normal and have a standard kind:

$$f_1(x) = \frac{1}{\sqrt{2\pi}\sigma_x} e^{-\frac{(m_x - x)^2}{2\sigma_x^2}} \quad f_2(\xi) = \frac{1}{\sqrt{2\pi}\sigma_\xi} e^{-\frac{(m_\xi - \xi)^2}{2\sigma_\xi^2}}$$

Where m_x and m_ξ - accordingly, population means measuring value and a regular error of measurement.

Basic feature of measurements estimation veracity in heterogeneous space complexes is using of the dispersion minimal value of measurements (3) in the attitude signal/noise (6) in measurements.

Let's consider a numerical example estimation veracity of measurements in heterogeneous space complexes. The initial data of an example have hypothetical character and this is intended to characterize a technique estimation veracity of measurements and the possible order of values.

The Example. We shall assume, that veracity of unitary measurement of a heterogeneous space complex "INS/GPS" (inertial navigation system/global position system) [8] in conditions of the established mode of flight at the altitude of circle $H = 1200 \text{ m}$ is estimated. We shall assume, that because of turbulence and other external factors the dispersion of altitude is equal $\sigma^2 = (60 \text{ m})^2$. We shall assume, that the inertial system has a dispersion of an additive error of measurement $\sigma_1^2 = (30 \text{ m})^2$, and satellite system - a dispersion of an additive error of measurement $\sigma_2^2 = (1.5 \text{ m})^2$.

It is required to estimate measurements veracity of inertial and satellite systems, and also the integrated heterogeneous complex formed from these two systems [8]. Except for it, it is necessary to calculate index parameters of efficiency of application of the integrated heterogeneous complex from the point of view of increase of measurements veracity at the given tolerance bands (2, 4, 6) at at probabilities of altitude presence in fields of the tolerance with probabilities, accordingly, $P1 = 0.6827$, $P2 = 0.9545$, $P3 = 0.9973$.

All imitating experiments and calculations are executed in system Mathcad 14. Results of calculations are submitted in tab. 1-3. For manufacture of calculations attitudes signal / noise in measurements, accordingly, for inertial and satellite systems, and also for a complex of a heterogeneous space complex "INS/GPS" were determined:

$$h_1 = \sigma^2 / \sigma_1^2, \quad h_2 = \sigma^2 / \sigma_2^2, \quad h_3 = \sigma^2 / \sigma_3^2, \quad (23)$$

where error mean square value of measurement for the complex was calculated by formula (3). As a result of calculations under the formula (23) the following values of attitudes signal / noise are received: $h1=4$, $h2=1600$, $h3=1604$.

For calculation of veracity parameters of measurement in heterogeneous space complexes the engineering technique of calculations which includes the following basic stages was developed:

1. Selection of the initial data: prospective value measuring a random variable m , its mean square value σ , mathematical expectation values mi and dispersions Di of measurements errors of systems which form a heterogeneous complex.

2. Calculate the dispersion minimal value of complex D_{min} under the formula (3) and the attitude signal / noise under the formula (23).

3. Calculate of optimum factor of a field of the tolerance under the formula (5).

The Note 1. The given accuracy of calculations under this formula and other formulas of indirect measurements provide with use of a command *float* Mathcad 14 systems.

4. Set probability of a presence of result of measurements in the tolerance band, and by it an tolerance band which is convenient for choosing on value σ for measuring values.

5. Define limits of changes for the measurements error for what use the minimal value

$$\sigma_{min} = \sqrt{1 / \sum_{k=1}^m 1 / D_k} \quad (25)$$

errors of measurement of a heterogeneous complex.

The Note 2. Thus it is necessary to provide implementation with the given accuracy of a condition of normalization for distribution of an error.

6. For implementation of integration in the chosen tolerance bands of set a sequence of change measuring values and measurement errors with required step for calculations accuracy providing.

7. Under formulas (4), (8) - (14) or (15) - (21) carry out calculations of parameters of veracity of measurement.

8. In case of insufficient measurements veracity take the measures to provide of the given veracity with use of the condition (21), and also take known ways of introduction of redundancy [3].

9. Make out results of calculations as the tables similar to tab. 1-3.

10. Formulate conclusions and practical recommendations by results of calculation.

In conformity with this technique calculations in an example are executed and tab. 1-3 are received.

Index parameters of veracity increase define under the following formulas:

$$I_\alpha = \alpha_i / \alpha_k, \quad I_\beta = \beta_i / \beta_k, \quad I_Q = Q_i / Q_k, \quad I_D = D_i / D_k, \quad (26)$$

For example, in the considered example increase of full probability of correct measurement at use GPS instead of INS at $P = 0,9545$ estimate so: $ID(0.9545) = 0.997584/0.04 = 24.94$. It speaks that application GPS in comparison with INS gives at 24.94 time higher veracity on full probability of correct measurement.

Application of a heterogeneous complex "INS/GPS" in comparison with use of one GPS provides $IQ(0.9545) = 2.4151 \times 10^{-3} / 2.41193 \times 10^{-3} = 1.00133$. From here follows, that high veracity of measurement in a heterogeneous complex "INS/GPS" is provided at the expense of application GPS.

By results of work and the carried out calculations it is possible to make the following conclusions.

1. At formation of structures of heterogeneous space complexes it is necessary to carry out calculations of measurements veracity of separate systems and a complex as a whole. Results of calculations allow to define "a weak part" complex and to take necessary measures for maintenance of required measurements veracity.

2. In the considered example a weak part is INS, veracity increase of a complex can be achieved as more often correction of measurements of this system by results of measurements GPS, and introduction in a complex of results of measurements of initial and secondary radars, increase of samples volume and others.

3. In considered example GPS can to play a part of the standard, therefore the method of replacement is quite acceptable. However, it is not always possible because of scope features of geographical regions satellite measurements.

4. The engineering technique offered in work of calculations veracity parameters of measurements of heterogeneous complexes can be applied as at early stages of creation of complexes according to "CNS/ATM conception" (outline, technical and design engineering), and in conditions of pilot experiment and use of complexes to destination. Thus the available aprioristic data on conditions of measurements regularly should be specified on апостериорным to results.

Table1 parameters of measurements veracity INS: $h_1=4$ $\sigma_1=30$

	P	α	P_t	β	P_m	Q	D
1	0,6827	0,6827	1,0	$3,981 \times 10^{-4}$	$1,255 \times 10^{-3}$	0,683087	0,316913
2	0,9545	0,95091	0,996	$9,087 \times 10^{-3}$	0,199721	0,959999	0,040001
3	0,9973	0,866874	0,8692	$1,3498 \times 10^{-3}$	0,499925	0,868223	0,131777

Table 2 parameters of measurements veracity GPS: $h_2=1600$ $\sigma_2=1,5$

	P	α	P_t	β	P_m	Q	D
1	0,6827	$5,359 \times 10^{-3}$	$7,8467 \times 10^{-3}$	$5,472 \times 10^{-3}$	$1,7241 \times 10^{-2}$	$1,0831 \times 10^{-2}$	0,9891687
2	0,9545	$1,18213 \times 10^{-3}$	$1,23848 \times 10^{-3}$	$1,23295 \times 10^{-3}$	$2,70972 \times 10^{-2}$ ₂	$2,4151 \times 10^{-3}$	0,997584
3	0,9973	$7,914 \times 10^{-5}$	$9,592 \times 10^{-5}$	$1,062 \times 10^{-4}$	0,0393	$1,854 \times 10^{-4}$	0,9998814

Table 3 parameters of measurements veracity INS/GPS: $h_3=1604$ $\sigma_3=1,49813$

	P	α	P_t	β	P_m	Q	D
1	0,6827	$5,351 \times 10^{-3}$	$7,834 \times 10^{-3}$	$5,472 \times 10^{-3}$	$1,72247 \times 10^{-2}$	$1,0815 \times 10^{-2}$	0,9891851
2	0,9545	$1,18065 \times 10^{-3}$	$1,23693 \times 10^{-3}$	$1,23295 \times 10^{-3}$	$2,70605 \times 10^{-2}$	$2,41193 \times 10^{-3}$ ₃	0,997582
3	0,9973	$7,901 \times 10^{-5}$	$9,577 \times 10^{-5}$	$1,061 \times 10^{-4}$	0,03928	$1,851 \times 10^{-4}$	0,9998021

References:

1. Игнатов В.А. Теория информации и передачи сигналов. М.: Радио и связь. – 1991. 2 – ое издание, перераб. и доп. – 280 с.
2. Орнатский П.П. Теоретические основы информационно-измерительной техники. К.: Вища школа, 1976. – 432 с.
3. Игнатов В.А., Боголюбов Н.В. Управление информационной избыточностью систем диагностирования и контроля //Контроль и управление техническим состоянием авиационного и радиоэлектронного оборудования воздушных судов гражданской авиации. Сборник научных трудов. Отв. редактор – В.А. Игнатов. – Киев: КИИГА, 1990. – С.3-13.
4. Теоретическое обоснование оптимального управления обработкой сигналов в интегрированных аэрокосмических навигационных комплексах. Игнатов В.О., Кудренко С.О., Нікулін В.І., Нориця М.І. Харьков.-НАКУ.- Авиационно-космическая техника и технология. 2007. № 3(39).- С.66-71.
- 5.Характеристические числа высокоточных структур структурно-избыточных информационно-измерительных комплексов из относительно неточных систем. Игнатов В.О., Кудренко С.О., Нікулін В.І., Нориця М.І. Харьков.-НАКУ.- Авиационно-космическая техника и технология. 2007. №1(37). - С.40-44.
6. Greenspan, R., L., “GPS/Inertial Overview”, Aerospace Navigation Systems, AGARD – AG – 331, Advisory Group for Aerospace Research and Development, Neuilly – sur – Seine, France, June 1995
7. Richard E. Phillips and George T. Schmidt “GPS/INS Integration”, System Implications and Innovative Applications of Satellite Navigation, AGARD – LS – 207, Advisory Group for Aerospace Research and Development, Neuilly – sur – Seine, France, June 1996.
8. Куршин В.В. Тестування GPS/WAAS/ГЛОНАСС алгоритмів. - <http://www.gssl.co.uk> (10.04.2003).
- 9.Игнатов В.А., Мачалин И.А. Оптимальное управление диагностированием изделий авиационной техники. Проблеми інформатизації та управління. К.: НАУ, 2006, Вип.17. С. 72-80.

COMPARATIVE ANALYSIS OF MODELING ADEQUACY OF THE NONSTATIONARY TRAFFIC IN TELECOMMUNICATION NETWORKS

In paper results of the comparative analysis of modeling adequacy of the nonstationary traffic in telecommunication networks are given. For optimum modeling dynamics of the traffic metrics of spaces Euclid and Hilbert are used. The algorithm and a technique of verification of optimum models are developed. It is shown, that modeling of the nonstationary traffic in space Hilbert is preferable as gives more exact models. Theoretical positions are illustrated by numerical examples and diagrams with use of system MathCAD.

Telecommunication networks, the nonstationary traffic, optimum modeling of the traffic, modeling adequacy of the traffic, the comparative analysis of models

Introduction. Problems of modeling, the analysis, synthesis of methods of optimum service of the traffic in telecommunication and computer networks become more and more actual in process of development of these networks, complication of their architecture, increase of number of levels in hierarchical structure of networks, transition to principles of construction of open information systems on the basis of seven levels reference model of standards OSI ISO, growth of a supply and demand in the market of methods of optimum synthesis of models of optimum service of the traffic at a transport level [1-3]. The hobby of some researchers models of the self-similar traffic [4] has resulted to that many real kinds of the periodic and nonstationary traffic remain outside of a field of vision, and, hence, behind frameworks of modeling and research. One of the main reasons of such state of affairs is complexity of the problems decision of modeling for nonstationary and nonlinear cases. In the known literature there are no results of the comparative analysis of models of the nonstationary traffic that in many respects is caused by weak development of mathematical methods of stochastic approximation of random nonstationary processes. The given work is directed on partial overcoming of the specified difficulties in the field of modeling and optimum service of the nonstationary traffic.

The purpose of work. The purpose of work is the comparative analysis of models of the nonstationary traffic in telecommunication and computer networks.

For achievement of the purpose the following tasks are put and solved: development of algorithm and a technique of the comparative analysis of adequacy of models of the non-stationary traffic in telecommunication and computer networks, a choice of the metrics of spaces of comparison of models and criteria of their optimality, a substantiation of reference models of the casual non-stationary traffic which the substantiation and a choice of criteria of an optimality of models of the non-stationary traffic, a substantiation of statement of a problem and construction of optimum models of the non-stationary traffic, the comparative analysis of adequacy of optimum models of the non-stationary traffic serve as base models of the comparative analysis of offered models of the real traffic, on the basis of the chosen parameters of adequacy, the decision of numerical examples, the formulation of conclusions by results of the comparative analysis of optimum models of the non-stationary traffic.

General statement of problems. In a role of the initial data are chosen initial polynomial representation of the reference non-stationary traffic with known Gaussian m dimension independent factors of decomposition. The basic methods of construction of the approached optimum models of the non-stationary traffic chooses a method of quantization of the traffic and Markovian approximations of casual process of change of conditions of the traffic, method РИТЦА and a method of the maximal plausibility. As results of the decision of a problem results of the comparative analysis of adequacy of models of the non-stationary traffic constructed on the basis of metrics of spaces Euclid and Hilbert, and also conclusions on results of the analysis serve.

The decision of a problem. We shall start with development of algorithm and a technique of

the comparative analysis of adequacy of models of the nonstationary traffic in telecommunication and computer networks. The logic analysis of a problem has shown that the operational basis of algorithm of the comparative analysis of adequacy of models of the nonstationary traffic should consist of 16 operations. Procedure of the comparative analysis of adequacy of models of the nonstationary traffic, as a matter of fact, is procedure of verification of models of the nonstationary traffic.

The general technique of verification of models of the nonstationary traffic offered by us is based on the following base algorithm of verification:

1. Normalization and reduction a dimensionless kind of a range of change of realizations the traffic envelope and its interval of the nonstationary. This operation allows to model "normalized dynamics of the traffic" in "a single square" with coordinates of tops: (0, 0), (0, 1), (1, 0), (1, 1).

2. A choice of the model dimension of n that is numbers of discrete conditions of the nonstationary traffic. This number shows, on how much quantum the individual square for step approximation of the nonstationary traffic shares and generally is the essential characteristic of the model dimension, and also its accuracy.

3. Definition of the dimensionless normalized intensities of changes of the traffic conditions. These of intensities are defined as intensities of crossing by the traffic of the given levels of quantization.

4. Construction of logical-mathematical model of dynamics of the traffic as the column as which tops conditions of the traffic serve, and the directed edges - arrows with the instruction of the directions changes of conditions the traffic.

5. Drawing up of differential equations Kolmogorov-Chepmen concerning the probabilities of the traffic conditions describing dynamics of the traffic, on logical-mathematical model of the traffic dynamics. B.V.Vasil'eva's known rule for drawing up of the differential equations on column [1] is used.

6. A choice of entry conditions system for the decision of problem Cauchy with the help of the made differential equations of dynamics of the traffic.

7. Direct transformation Laplace system of the differential equations in system of the algebraic equations concerning images of the conditions probabilities of the traffic at entry conditions of item 6.

8. The decision of the received system of the linear algebraic equations concerning images of the conditions probabilities of the traffic method Gauss or a method of a matrix system to a triangular kind in view of a normalization condition for unknown images.

9. Transformation by a method of uncertain factors of images to a kind of the sums of the simple rational fractions convenient for search of originals in return transformation Laplace.

10. Return transformation Laplace for the received images of probabilities.

11. Use of probabilities of conditions and quantized values of the traffic for definition of a population mean and a dispersion bending around nonstationary Gaussian the traffic.

By this technique with a required level of detailed elaboration of steps 1-16 algorithms in the further are solved the problems of the comparative analysis of models designated above and the reference traffic. For check of adequacy of models to the reference traffic dependences of parameters accuracy of modeling on parameters of models are used.

The basic features of a technique and base algorithm of a choice optimum quantized values we shall show for parallel consideration of two cases of modeling: discrete and continuous. These cases are different, as it was already marked, a choice of the metrics space comparison of reference and modeling characteristics (see item 12). In a discrete case the metrics space Euclid is used, in a continuous case the metrics space Hilbert is used.

Let's apply consistently base algorithm of the decision of problems of verification models at use of two conditions of the nonstationary traffic, we shall receive the following results.

1. Normalization and reduction a dimensionless kind of a range of change of realizations bending around the traffic and its interval nonstationary.

On fig. 1 " the individual square " for research of adequacy of modeling the first order

moments- population means nonstationary, growing on an interval nonstationary, Gaussian traffic is shown. The continuous line represents the normalized dimensionless population mean $m(t_k)$ the reference traffic submitted as normalized on normalized interval nonstationary $[0,1]$ parabola with casual independent Gaussian in factors:

$$m(t_k) = t_k \cdot (2 - t_k),$$

(1)

Where t_k – k -th moment of time from the dimensionless normalized interval $[0,1]$ times nonstationary. Stroke - dotted represent normalized dimensionless population means $M(t_k)$ the modeling traffic with optimized in space of Euclid quantized values of the traffic (fig. 1a) and with optimized in space of Hilbert quantized values of the traffic submitted in same normalized Hilbert space:

$$M(t_k) = Z_2 - (Z_2 - Z_1) \cdot P_{10} \cdot e^{-\eta_1 \cdot t_k},$$

(2)

Where Z_1, Z_2 - quantized values of the traffic, P_{10} - initial value of the first condition probability of the traffic, η_1 - intensity of change of the traffic for the first condition. Deeper sense of all parameters of expression (2) will be opened later at construction of model dynamics of the traffic.

2. A choice of dimension of model n , in other words, numbers of discrete conditions of the nonstationary traffic. For an illustration of a technique and the general algorithm the minimal dimension of model is chosen: $n = 2$. At $n = 2$ there are only two conditions of the traffic. They are defined by two quantum of traffic Δ_1, Δ_2 and three levels of quantization of the traffic: $z_0 = 0, z_1 = 0,5, z_2 = 1$. These values participate in definition of intensity of the traffic and optimum quantized values of traffic Z_1, Z_2 for two conditions. The elementary model is the least exact, reflects the worst case of modeling and gives pessimistic estimations.

When quantization of the traffic carry out the following nonlinear transformations of the traffic. All values of the traffic, which get in the first interval of quantization

$$\Delta_1 = z_1 - z_0,$$

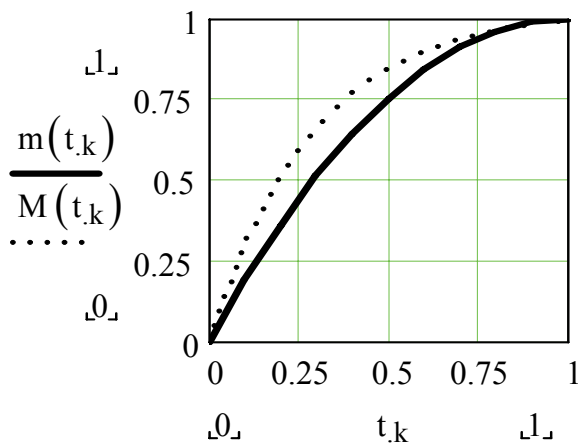
(3)

replace with one quantized value Z_1 . All values of the traffic, which get in the second interval of quantization

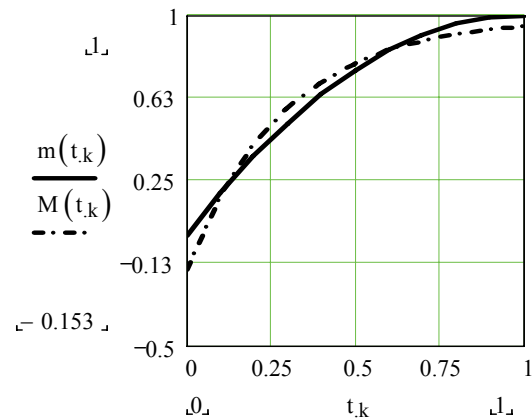
$$\Delta_2 = z_2 - z_1,$$

(4)

replace with one quantized value Z_2 .



a. A discrete case



б. A continuous case

Fig. 1. An illustration of normalization values of the traffic and an interval of time nonstationary

Thus, in the space quantization of continual changes of the traffic is replaced with discrete

space with final accounting number of conditions. In result continuous monotonous change of the nonstationary traffic is replaced with a step line which consists from quantized constant values of the traffic on intervals of quantization. In the further, quantized values of the traffic are considered as realization of the discrete traffic which take place with probabilities of discrete conditions of the traffic.

3. Definition dimensionless normalized intensities changes of conditions by the traffic.

At $n = 2$ there is only one change of the traffic intensity - intensity ηI transition of the traffic from the first condition to the second. By definition ηI there is a size, return to average time before crossing by a population mean of the reference traffic of the first level of quantization. More precisely the physical sense ηI can be defined as: intensity ηI changes of the traffic on the first interval is normalized on length of first interval ΔI speed v_I changes of the traffic:

$$\eta I = v_I / \Delta I = I / t_I$$

(5)

For definition ηI it is necessary to solve be relative t the equation

$$t \cdot (2 - t) = z_1 \quad \left| \begin{array}{l} \text{solve, } t \\ \text{float, 4} \end{array} \right. \rightarrow \begin{pmatrix} .2929 \\ 1.707 \end{pmatrix}$$

(6)

The decision of the equation (6), "with an accuracy of fourth mark after a point", is shown in system MathCAD for a case, when the first level of quantization $z_I = 0.5$. As the second root of a parabola does not belong to the normalized interval, as the decision the first root $t_I = 0.2929$ serves.

Hence, required dimensionless intensity for a case $z_I = 0.5$, $t_I = 0.2929$ is equal

$$\eta I = I / t_I = I / 0.2929 = 3.414.$$

4. Construction of logical-mathematical model of dynamics of the traffic as the column as which tops conditions of the traffic serve, and the directed edges - arrows with the instruction of directions of change of conditions traffic. At $n=2$ the most simple kind has form:

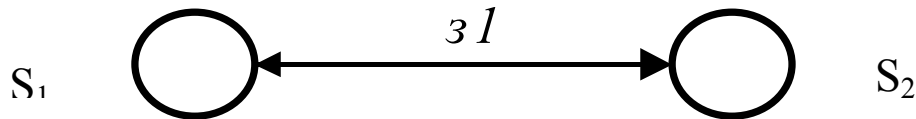


Fig. 2. Graf as logical-mathematical model of dynamics of the traffic

On fig. 2 the following designations are accepted: S_1, S_2 - the first and second conditions of the traffic, ηI - intensity transition of the traffic from the first condition to the second. Probabilities of a presence of the traffic at the moment of time t in conditions S_1, S_2 are designated through $P_1(t), P_2(t)$. After quantization of value of the traffic for these two conditions are equal, accordingly, to two quantized values Z_1, Z_2 which appear with probabilities $P_1(t), P_2(t)$. As events, which consist in hit of value of the traffic in this or that interval of quantization, form full group of events, for probabilities of conditions of the traffic fairly a condition normalization:

$$P_1(t) + P_2(t) = 1.$$

(7)

5. Drawing up of differential equations Kolmogorov-Chepmen concerning the probabilities of conditions of the traffic describing dynamics of the traffic, on logical-mathematical model of dynamics of the traffic.

We use Vasil'eva B.V.'s rule for drawing up of the differential equations on the column fig. 2. We shall receive:

$$\frac{dP_1(t)}{dt} = -\eta_1 P_1(t)$$

(8)

$$\frac{dP_2(t)}{dt} = \eta_1 P_1(t)$$

(9)

As probabilities of conditions are connected by conditions normalizations (7), it is necessary to solve system from two equations: the differential equation (8) and the algebraic equation (7):

$$\frac{dP_1(t)}{dt} = -\eta_1 P_1(t),$$
$$P_1(t) + P_2(t) = I.$$
(10)

6. A choice of system of entry conditions for the decision of problem Cauchy with the help of the made differential equations of dynamics of the traffic.

The assumption that at the initial moment of time t_0 value of the traffic can be in any interval is natural. General view entry conditions therefore are fair:

$$P_1(t_0) = P_{10}, \quad P_2(t_0) = P_{20}.$$

(11)

7. Direct transformation Laplace system of the differential equations in the system of the algebraic equations concerning images of probabilities of conditions traffic at entry conditions (11).

Applying to system (10) direct transformation Laplace by known rules [2], we shall receive

$$s P_1(s) - P_{10} = -\eta_1 P_1(s)$$

(12)

$$P_1(s) + P_2(s) = I/s$$

8. The decision of the received system of the algebraic equations concerning images of probabilities of conditions traffic method Gauss, a method of data of a matrix system to a triangular kind or a method of substitution in view of a condition normalization for unknown images.

Solving a system from two algebraic equations (12) concerning unknown images $P_1(s)$, $P_2(s)$ probabilities of conditions S_1 , S_2 a method of substitution in the second equation of the image of probability of the first condition, we shall find

$$P_1(s) = P_{10}/(s + \eta_1)$$

(13)

$$P_2(s) = \frac{1}{s} - \frac{P_{10}}{(s + \eta_1)}$$

(14)

9. Transformation by a method of uncertain factors of images to a kind of the sums of the rational fractions convenient for search of originals in return transformation Laplace.

Images (13), (14) in a considered simple case already represent the sums of simple rational fractions, therefore intermediate transformations it is not required.

10. Return transformation Laplace for the received images of probabilities.

Applying return transformation Laplace to images (13), (14) [2], we shall receive

$$P_1(t) = P_{10} e^{-\eta_1 t}$$

(15)

$$P_2(t) = 1 - P_{10} e^{-\eta_1 t}$$

(16)

11. Use of probabilities conditions and quantized values of the traffic for definition of a population mean and a dispersion bending around nonstationary Gaussian the traffic.

Let's use known formulas for a population mean and a dispersion of a discrete random variable and we shall take into account also that probabilities of conditions because of nonstationary the traffic depend on time. We shall receive

$$M(t) = \sum_{i=1}^2 Z_i P_i(t) = Z_2 + (Z_1 - Z_2) P_{10} e^{-\eta_1 t}$$
(17)

$$D(t) = \sum_{i=1}^2 Z_i^2 P_i(t) - M^2(t) \quad (18)$$

The formula (17) evidently shows, how quantization and Markov approximation result in models of a population mean of the nonstationary traffic as a linear combination an exhibitor. From the formula (17) follows, that in maintenance of adequacy of the modeling traffic to the reference traffic essential value has a correct choice quantized values. Further for optimization of a choice quantized values the method of maximal plausibility (MMP) which at normal multivariate distribution of the traffic results in use of a method of least squares (MLS) is used. Comparison (17) and (2) the reasons of modeling representation of the first initial moment of the nonstationary traffic as a linear combination the exhibitor completely opens.

Conclusions

1. Application of quantization and Markov approximations allows to build an adequate models of the nonstationary traffic submitted initial polynomial by decomposition with casual factors.
2. Use even the elementary model with two conditions of the traffic allows to approximate a population mean of the nonstationary traffic submitted as a normalized parabola with two casual parameters.
3. Offered the system of parameters and a technique of verification of models nonstationary traffic with various number of conditions of the traffic allow to carry out verification of models and to use quantitative estimations of a degree of adequacy of models to the real non-stationary traffic.

References

1. Ігнатов В.А., Жуков І.А., Гузій Н.Н. Даниліна Г.В. Моделювання перехідних режимів трафіку комп'ютерної мережі. Інформаційні технології і безпека. – Сборник научных трудов. – К.: Национальная академия наук Украины, Институт проблем регистрации информации, 2006. – Вып.9. – С. 84 – 87.
2. Гузій М.М., Даниліна Г.В., Ігнатов В.О., Милокум Я.В. Методи і алгоритми оптимального управління трафіком в обчислювальних мережах. Проблеми інформатизації та управління. – К.: НАУ, 2006. – Вип.17. – С. 32-37.
3. Гузій М.М., Даниліна Г.В., Ігнатов В.О. Мачалін І.О. Марковські рандомізовані моделі. Вісник Житомирського державного технологічного університету, Житомир 2006. – Вип. IV (39) – С. 179-184.
4. Koucheryavy Y., Harju J., A novel approach for self-similar traffic prediction// Proceedings of the St. Petersburg Regional International Teletraffic Seminar, St. Petersburg, Russia, January 29 - February 1, 2002, pp. 172 - 179.
5. Гузій М.М., Даниліна Г.В., Ігнатов В.О. Оцінювання ефективності використання ліній зв'язку в обчислювальних мережах. Проблеми інформатизації та управління. - К.: НАУ, 2006. – Вип.18. – С.54-59

*O.P. Martynova candidate of engineering sciences, associate professor
(National aviation university, Ukraine)*

MULTICRITERION ROUTING IN COMPUTER NETWORKS

The method of the multicriterion routing is offered in computer networks, which provides the set level of quality of service on a carrying capacity and reliability of passing information, and also takes into account the external affecting channels of information transfer.

Introduction

Presently computer networks find wide application in communication, navigation, supervision and organization of air motion networks. On the base of computer networks the intellectual air traffic control systems are developed. Continuous growth of complication of computer networks which are used for a supervision and organization of air motion is marked in this connection. Growth of complication of computer networks, the increase of volumes of the passed information is substantially increase requirement to the level of protected information from an unauthorized division to it. The task of increase of level of protected computer networks must be decided complexly jointly with the tasks of increase of efficiency of their functioning. Actuality of task of providing informative safety of users of computer networks is related also to the wide use in state and financial organizations, in industrial air enterprises and in organizations of defensive complex [1]. One of the directions of increase level of protected computer networks is related to perfection of methods routing of passing information in networks taking into account the risks of loss of information, its modification, and also influences of external factors on the channels of information transfer. The analysis of the last researches and publications [1-2] allows to draw conclusion that problem of estimation and increase of level of protected of computer networks is not enough full explored.

Perfection of methods routing in computer networks presently develops in the direction of providing the assured quality maintenance of users of computer networks on such criteria of quality as a carrying capacity, delay of communication of data, reliability of passing to information, load of knots of network and row other, which the quantitative estimations of level of protected of computer networks do not enter in the complement.

General statement of problem

The problem of development the method of the multicriterion routing in computer networks, which allows to take into account quality of service and informative safety of users of computer networks is set up.

The decision of a problem

The mathematical model of computer network will present a count the tops which are designed by knots-sources and knots-receivers of information. To the directed branches (to the ribs) of count we will confront the channels of passing to information between a knot-source and knot-receiver. Weight which characterizes quality of service and level of protected designed channel of passing information is appropriated the branches of count. With the purpose of quantitative estimation of scales of branches of count will make the system of private criteria of quality for the estimation of informative safety and quality of service. Under informative safety we will understand ability of technologies of informations to resist the threats of opponent. The threats of opponent will estimate by amount of attacks I_1 on the channel of information transfer, which is designed the branch of count. The risks of loss of information or its modification will take into account by the private criterion of quality I_2 . The next private criterion of quality I_3 will take into account the external affecting channel of information transfer. Under external influences atmospheric influences are understood (rain, floods and other). The transferred private criteria of

quality take into account affecting of opponent channels of information transfer, and also influencing on them of external indignations. We will enter in the system of criteria of quality of description of quality services, which are set as a set of parameters, providing the required level of service of service. In the system of criteria of quality of service we will enter the private criterion of quality I_4 , which characterizes speed of passing to information on a communication channel. Other important description of quality of service is reliability of passing to information on a communication channel. This description has connection with the level of protected channels of passing information from the different type of indignations and hindrances. Therefore in the system of criteria of quality of service we will enter the criterion of quality I_5^* , which takes into account reliability of passing to information on communication channels. Thus, the system of private criteria of quality is made, which takes into account threats and risks, caused an unauthorized division to information, external affecting quality of the past information, and also basic descriptions of quality of service. Further increase of amount of private criteria of quality beside the purpose, because in the case of far of criteria of quality substantially influence of every separate criterion of quality goes down on the choice of routes of passing to information. We will formulate the task of the multicriterion routing on a count model. For this reason we will bring all private criteria over of quality to the case of their minimization. We will enter the overhead estimation of maximally-legitimate value of reliability I_{5m} which is set technical descriptions of channel of passing information. In place of private criterion of quality I_5^* will enter the minimized criterion of quality $I_5 = I_{5m} - I_5^*$. Now we have the system of five minimized private criteria of quality I_1, I_2, I_3, I_4, I_5 . Disposing the estimations of resources of methods and facilities of unauthorized division to the channels of passing information we will enter the maximum-legitimate values of amount of attacks of opponent I_{1m} and maximum-possible risk I_{2m} of loss of information or its modification. On the basis of statistical information we will enter the maximum-legitimate value I_{3m} of estimation of the external affecting channel of information transfer, and on the basis of its technical descriptions we will set the maximum-legitimate value I_{4m} of speed of passing information on this channel. We will take advantage of overhead estimation of maximally-legitimate value of reliability I_{5m} of channel of passing information as a maximum-legitimate value of private criterion of quality I_5 . Taking into account that all included in the system of private criteria of size take on positive values or zero, the range of change of private criteria of quality can be set the system of limitations

$$0 \leq I_i \leq I_{im}, \quad i = 1, 2, 3, 4, 5. \quad (1)$$

For problem of the multicriterion routing definition on a count model it is necessary to carry out multicriterion optimization of scales of branches of count taking into account the system of limitations (1). It is suggested to set weight (length) of j branch a count on the basis of scalar packages of private criteria of quality on the nonlinear chart of compromises [3]:

$$J_j = \sum_{i=1}^5 \frac{1}{1 - \frac{I_{ij}}{I_{ijm}}}, \quad 0 \leq I_{ij} \leq I_{ijm}, \quad (2)$$

where I_{ij} – i the private criterion of quality of j column, I_{ijm} is a maximum-legitimate value of private criterion of quality I_{ij} .

Thus, appropriation the branches of count, designing a computer network, scales in obedience to expression (2) ground to set the problem of the multicriterion routing from a source to the receiver of information as a task about a short cut between a knot by a source and knot-receiver, if length vetvi a count proportional its weight. Case of unauthorized division, when attacks are on a computer network and the risks of loss of information or its modification increase in the process of

passing to information ensues from expression (2). The routes of passing information appear under influencing of methods and facilities of unauthorized division and multiply the length as compared to the routes of communication of data in which the attacks of opponent are absent. In the process of decision of task of routing accordant (2) routes, unsubject to the unauthorized division and attacks of opponent, will have less length, what routes of passing information under the action of attacks of opponent. Consequently, routes are not subject to the methods and facilities of unauthorized division will get out for passing to information in a computer network. Routes which are subject to the attacks of opponent, in the process of the multicriterion routing (2) will be eliminated from the routes of passing information. Thus, the multicriterion routing (2) reacts on the attacks of opponent and promotes the level of protected of users of computer network.

Conclusions

The offered method of the multicriterion routing allows taking into account the threats of opponent, risks of losing information or its modification, related to the unauthorized division to the channels of passing information. Informative safety of computer network rises without bringing in of additional programmatic and vehicles facilities of defense of information. Except for it, the multicriterion routing provides the set level of quality of service on a carrying capacity and reliability of passing information, and also takes into account the external affecting channels of information transfer.

Dignity of the offered method of the multicriterion routing is adaptation to the change of situations in which computer network functions.

References

1. *Вишневский В.М.* Теоретические основы проектирования компьютерных сетей. – М.: Техносфера, 2003. – 512 с.
2. *Чекатков А.А., Хорошко В.А.* Методы и средства защиты информации. – К.: Изд-во Юниор, 2003. – 504 с.
3. *Воронин А.Н.* Многокритериальный синтез динамических систем. – К.: Наук. думка, 1992. – 160 с.

WORKING OUT OF THE TECHNIQUE OF DEFINITION OF THE LAPSE OF PARAMETERS OF VIBRATIONAL DIAGNOSTIC OF GAS-TURBINE PLANTS

The new technique of definition of a lapse in the course of measurement, machining and spectral transformation of a vibrational signal is offered. The analysis of lapses of an estimation of spectra vibration velocities is carried out. It is displayed, that spectra are distorted in low-frequency area by stray components of a signal of the acceleration, the called low-frequency parasitic oscillations, noise of the amplifier and a transformation section.

Introduction. Magnification of the assigned resource of aviation gas-turbine engines, passage to maintenance of propellers on availability index of product cannot be realised without safe methods and the diagnostic aids allowing in time to determine originating imperfections, to size up extent of their danger to prolongation of maintenance GTE. Among such methods and means the important place is occupied by the vibrational diagnostic allowing by measurement and the analysis of broadband vibrational signals, to carry on a state estimation of the basic intense nodes and assemblies GTE.

Modern aviation GTE as installation of vibrational diagnostic, are complicated enough. Thin-walled constructions with a great many of resonance zones, nonlinear effects, impossibility to approach sensing transducers to troubleshoot nodes, for example bearings, lead often to impossibility of application of well proved techniques of vibrational diagnostic on aviation gas-turbine engines.

For made now aviation GTE, monitoring of a common level of vibrations in a strip of rotor frequencies, as is regularly provided at conducting of trials at a factory the manufacturer, and in maintenance. It is explicitly not enough used monitoring of vibrations, as cost of repair of propellers after their maintenance at heightened vibrations is very high.

At the same time, development of gauges and the analysis of vibrations, development of computer production engineering of machining of vibrational signals, support of databases allow to build the developed system of vibrational diagnostic embracing full life cycle of the propeller, from its manufacture and trials, in maintenance, after repair. The most effective hardware components of diagnostic, both stationary, and portable, are under construction on the basis of computer technics and production engineering. These means allow to use all possibilities of such perspectiv methods of deriving of the information, as emission analysis, the analysis enveloping and statistical discernment of statuses.

The analysis of last publications and researches. Modern production engineering of digital machining of signals allows to develop on the basis of the analysis of vibrational signals methods of a discernment of imperfections of various nodes and assemblies of propellers at an early stage of their development.

There are two groups of methods of measurement of parametres of vibrations: contact, implying mechanical link of the sensing transducer with a prototype system, and noncontact, i.e. not linked with installation mechanical link.

The system approach is necessary for implementation of advantage of use of modern methods of vibrational diagnostic with reference to GTE to the analysis of lapses of an estimation of spectra of signals of acceleration, velocities and migrations on which foundation sampling of devices organising system vibration diagnostics is made. How the sensing transducers, which provided in a propeller construction, have the restricted frequency range containing components only with a rotational speed of curls GTE. Hence, the most informative high-frequency range containing components with frequencies of vanes of compressors and turbines and frequencies of remating of teeth of sprockets of steps of the drive of assemblies is not used.

Problem solutions on detection of imperfections GTE at an early stage of their evolution the land control are carried on in following directions:

- In application of a noncontact method of measurement of vibration of the working propeller with use of the laser converter of the vibration allowing for a short time to remove from the big number of points a trustworthy information about a status of the basic nodes of the propeller and other assemblies. For the first time about perspectivity of use of this method for diagnostic GTE it was noted in V.I.Ljulko's dissertational operation. [1];
- In sampling of the optimal from the point of view of a problem of a discernment of status GTE of regimes of start [3];
- In application of advanced processing methods of the signals which are not demanding knowledge of standard levels of vibrations suitable GTE and allowing to determine originating imperfections on a modification of such relative parametres, as depth peak and an index angular modulations of spectral characteristics [2,3].
- In raise of an exactitude of measurements at vibration diagnostic and the systems analysis of lapses of an estimation of a spectrum at each stage of transformation of a signal vibration accelerations and derivings of a primary estimation of a spectrum [4].

Statement of problem. To carry out the analysis of lapses of an estimation of spectra of acceleration, a velocity and the migration, gained by means of sweeping Fourier transforms (FFT), for a justification of sampling of metrology performances of devices organising system vibration diagnostics.

The problem solution. We will consider, that the acceleration analogue signal in a time domain admits representation in the form of a reconversion of the Fourier

$$A(t) = \frac{1}{2\pi} \int_{-\infty}^{\infty} S(\omega) \exp(j\omega t) d\omega = \frac{1}{2\pi} \int_{-\omega_m}^{\omega_m} S(\omega) \exp(j\omega t) d\omega, \quad (1)$$

Where $A(t)$ - an acceleration signal, $S(\omega)$ - a spectrum of a signal of acceleration.

Primary estimations of a spectrum of acceleration, velocity and migration after, numbering and discrete Fourier transform (ДПФ)

$$\begin{aligned} \tilde{S}_A(\omega_i) &= \sum_{n=0}^{N-1} A(t_n) \Delta t \exp(j\omega_i t_n), \quad \tilde{S}_V(\omega_i) = \sum_{n=0}^{N-1} V(t_n) \Delta t \exp(j\omega_i t_n), \\ \tilde{S}_X(\omega_i) &= \sum_{n=0}^{N-1} X(t_n) \Delta t \exp(j\omega_i t_n), \end{aligned} \quad (2)$$

Where $V(t_n)$ - a velocity, $X(t_n)$ - migration, $t_n = n\Delta t$ - a discrete time, Δt - a pitch of a digitization of a signal on a time, $\omega_i = i\Delta\omega$ - a grid of frequencies, $\Delta\omega = 2\pi/T$ - the permission on frequency, T - duration of implementation of a signal of acceleration.

For the analysis of spectra of accelerations, velocities and the migrations gained by a FFT, we use integral representation of discrete expressions (2)

$$\tilde{S}_{A,V,X}(\omega_i) = \frac{\Delta t}{2\pi} \int_{-\infty}^{\infty} S_{A,V,X}(\omega) K_N(\omega - \omega_i) d\omega, \quad \text{where} \quad (3)$$

$$K_N(\omega - \omega_i) = \frac{\exp(j(\omega - \omega_i)N\Delta t) - 1}{\exp(j(\omega - \omega_i)\Delta t) - 1}, \quad (4)$$

$$K_N(\pm\omega_i) = 0, \quad K_N(0) = N, \quad K_N(\omega \pm \omega_d) = K_N(\omega)$$

- Function of the basic spectral window at a FFT, a defining exactitude of a primary estimation of a spectrum by means of a FFT and its limiting properties, N - a sample size, equal to extent of number two, $S_{V,X}(\omega)$ - spectra of analogue signals of velocities and migrations at ideal integration of a signal of acceleration.

Lapses of an estimation of velocity spectra and migrations at integration of acceleration by the analogue integrator with private performance $H(\omega)$

$$\Pi = \max_i \left| \tilde{S}_{H,V,X}(\omega_i) - S_{V,X,T}(\omega_i) \right|, \quad S_{V,X,T}(\omega) = \int_0^T S_{V,X}(\varepsilon) K(\omega - \varepsilon) d\varepsilon, \quad (5)$$

Where $\tilde{S}_{H,V,X}(\omega)$ - estimations of spectra of signals of velocities and the migrations, gained according to (3), but thus in (3) $S_V(\omega) = H(\omega)S(\omega)$, $S_X(\omega) = H^2(\omega)S(\omega)$, $K(\omega) = (1 - \exp(j\omega T)) / j\omega$ - the basic spectral window.

Using an inequality Cauchy-Bunyakovsky and (5), estimations of relative errors of definition of velocity spectra and migrations are gained, at integration of acceleration by the analogue integrator,

$$\gamma_{S1} \leq \frac{2P}{N} \max_i \sqrt{\int_{-P\Delta\omega}^{P\Delta\omega} |((\varepsilon + \omega_i)H_0(\varepsilon + \omega_i) - 1)|^2 \frac{d\varepsilon}{2P\Delta\omega}} \leq \sqrt{\frac{4}{3}} \frac{P^2 \Delta\omega}{N\omega_a}, \quad (6)$$

$$\gamma_{S2} \leq \frac{2P^2 \Delta\omega}{N\omega_a^2} \sqrt{(P\Delta\omega)^2 / 5 + P\Delta\omega / 2 + 4\omega_a^2 / 3}, \quad (7)$$

Where parametre $P=1,2,3,4$. It is defined by number of side lobes of function $K_N(\omega)$ which are necessary for considering at an estimation of reference of a spectrum, $H_o(\omega)$ - AЧХ the analogue integrator about null.

On the basis of the analysis of expressions for a lapse it is gained following two demands for correct definition of spectra of acceleration, a velocity and migration

$$\begin{aligned} P\Delta\omega << \omega_{0A}, \omega_{0A} + 2P\Delta\omega < \omega_n, \\ P\Delta\omega << \omega_{0I}, \omega_{0I} + 2P\Delta\omega < \omega_n, \quad 2\omega_m < \omega_D \end{aligned} \quad (8)$$

Where $\omega_{0A} \leq \omega_{0I}$ - the lower frequency of shearing АЧХ of the amplifier of a charge, ω_n - the least frequency of a spectrum of a signal of acceleration, ω_{0I} - the lower frequency of shearing АЧХ of the integrator.

The velocity and the migration gained by single-valued and repeated digital integration of acceleration, admit discrete and integral representation

$$\begin{aligned} V_n &= \sum_{k=0}^n g_k A_k \Delta t, V_n = \frac{1}{2\pi} \int_{-\infty}^{\infty} S(\omega) \sum_{k=0}^n g_k \exp(j\omega t_k) d\omega, \\ X_n &= \sum_{k=0}^n g_k V_k \Delta t, 0 = \frac{1}{2\pi} \int_{-\infty}^{\infty} S_V(\omega) \sum_{k=0}^n g_k \exp(j\omega t_k) d\omega, \leq n \leq N-1, \end{aligned} \quad (9)$$

Where g_k - the weight numbers defined by algorithm of integration $\forall k \in [0, N]$.

Let's observe lapses of an estimation of spectra at analogue both digital integration and numbering of a signal of an analogue-digital converter with a transformation nonlinear response. Let signal numbering is carried out with an analogue-digital converter having an integral nonlinear response of transformation which is approximated by aspect expression

$$U_{\text{blx}}(t_n) = u(t_i) + \text{INL} \left(1 - \frac{u^2(t_n)}{u_m^2} \right), \quad (10)$$

Where INL - the integral nonlinearity of an analogue-digital converter measured in units of a low significant digit, u_m - the maximum arrival signal of an analogue-digital converter, $u(t_n) \leq u_m$ - a signal on an analogue-digital converter entry. Expression for an estimation of a spectrum of a signal of acceleration at numbering of an analogue-digital converter with a nonlinear response of transformation (10).

Spectrum of a complex sinusoidal test signal

$$\begin{aligned}\tilde{S}(\omega_i) = & \frac{\Delta t}{2\pi} \int_{-\infty}^{\infty} S(\omega) K_N(\omega - \omega_i) d\omega + INL \Delta t K_N(-\omega_k) - \\ & - \frac{INL \Delta t}{(2\pi)^2} \int_{-\infty}^{\infty} \int_{-\infty}^{\infty} \frac{S(\omega_1)}{u_m} \frac{S_{ex}(\omega_2)}{u_m} K_N(\omega_1 + \omega_2 - \omega_i) d\omega_1 d\omega_2.\end{aligned}\quad (11)$$

Let the arrival signal is a complex sinusoidal signal with an exact binding of a phase of start of an analogue-digital converter. The spectrum of such signal is defined by expression $S(\omega) = 2\pi A \delta(\omega - \Omega)$, where A - amplitude, Ω - the circular frequency varying over the range $-\omega_m \leq \Omega \leq \omega_m$. For analysis simplification we will observe further a spectrum of a complex sinusoidal test signal which according to (11) is equal

$$\tilde{S}(\omega_k) = \Delta t A K_N(\Omega - \omega_k) + INL \Delta t A K_N(-\omega_k) - INL \Delta t \frac{A^2}{u_m^2} K_N(2\Omega - \omega_k). \quad (12)$$

Distortions of harmonics in a spectrum gained by means of a FFT after numbering of a signal of an analogue-digital converter with nonlinearity equally

$$H_{2\Gamma} = \frac{INL}{u_m} \frac{A}{u_m} = \frac{INL}{2^{M-1}} \frac{A}{u_m}, \quad (13)$$

Where M - digit capacity of an analogue-digital converter, INL^* - the integral nonlinearity of an analogue-digital converter measured in quanta. For an analogue-digital converter with $M=12$, $INL^* = 2$, an analogue-digital converter with $M=14$, $INL^* = 3$ and analogue-digital converter $M=16$, $INL^* = 2$ maximum lapse is equal 0,1 %, 0.036 % and 0,003 % accordingly. Hence, for signal numbering at вибродиагностике it is necessary to use an analogue-digital converter with digit capacity not less than 12 and INL^* no more than 2.

Let's carry out the analysis of agency of differential nonlinearity of an analogue-digital converter on an exactitude of an estimation of spectra of acceleration, a velocity and migration. Let signal numbering is carried out to the real analogue-digital converters having final piecewise linear performance of transformation of an aspect

$$\begin{aligned}U(t) = & \int_{-u_m}^{u(t)} g(v) dv - u_m, g(u(t)) = \sum_{i=1}^M \Delta \delta(u(t) - u_i), u_i = i\Delta + q_i - u_m, \\ 2u_m = & \Delta M,\end{aligned}\quad (14)$$

Where q_i - differential nonlinearity (DNL) an analogue-digital converter, measured in shares of a low significant digit, Δ - an average quantum of an arrival signal on amplitude, M - number of levels of quantization, u_m - the maximum arrival signal of an analogue-digital converter, $u(t)$ - a signal on an analogue-digital converter entry, $\delta(u)$ - a delta function of the Dirac, $U(t_n)$ - an analogue-digital converter starting signal in discrete instants. Expression for a lapse of an estimation of a spectrum of a sinusoidal signal of acceleration

$$\Pi_A \leq \frac{A_\Omega T}{\pi \Delta \omega} \left[\sum_{i=P_A}^{Q_A} \frac{\Delta}{A_\Omega} \sqrt{1 - \left(\frac{i\Delta - u_m}{A_\Omega}\right)^2} - \frac{\pi}{2} + \left| \sum_{i=P_A}^{Q_A} \frac{\Delta^2}{A_\Omega^2} \left[1 - \left(\frac{i\Delta - u_m}{A_\Omega}\right)^2 \right]^{-1/2} \frac{q}{\Delta} \right| \right]. \quad (15)$$

At magnification of digit capacity and number of levels of quantization of analogue-digital converters recut by a signal, the first item in (15) disappears, and the augend has the order of magnitude $8q\sqrt{\Delta/A_\Omega}/3\Delta\omega$, where q - magnitude DNL passported for the given analogue-digital converter. It is visible, that a lapse of an estimation of the spectrum, called DNL, it will be maximum for small high-frequency components of a signal, for example, for higher harmonics, and will increase at permission magnification on frequency at a FFT.

Exactitude of definition of amplitude of a complex sinusoidal signal with an exact binding of a phase of start of an analogue-digital converter by means of algorithm of a FFT at conducting of metrology certification of system vibration diagnostics. Expression for a spectrum and an amplitude spectrum maxima

$$\begin{aligned}\tilde{S}_A(\omega_i) &= A\Delta t K_N(\Omega - \omega_i), \\ \max_i |\tilde{S}_A(\omega_i)| &= A \left| [\exp(j\alpha\Delta\omega T) - 1] / (j\alpha\Delta\omega) \right| = AT \left| \sin \pi\alpha / (\pi\alpha) \right|,\end{aligned}\quad (16)$$

Where α - a fractional part of a ratio of frequency of a sinusoidal signal to magnitude of quantum of the permission on frequency $\Delta\omega$. At $\alpha=0$ $\max |\tilde{S}_A(\omega_i)| = AT$ and the amplitude of an initial signal is sized up precisely, and at $\alpha=0,5$ lapse of definition of amplitude is maximum and equal $(1-2/\pi)$ 100 % $\approx 36,3$ %. Knowing the permission on frequency and parametre α it is possible to eliminate a lapse of definition of amplitude of a sinusoidal signal by means of a FFT.

Leading-outs:

- The analysis of lapses of an estimation of velocity spectra and migrations has displayed, that spectra are distorted in low-frequency area by stray components of a signal of the acceleration, the called low-frequency parasitic oscillations and noise of the amplifier which frequencies lay below frequency ω_H .
- For elimination of distortion of spectra of a velocity and migration to realise a digital filtering of an initial signal of acceleration by the order filter not below the fourth shearing with frequency equal $0,5\omega_H$ and to integrate the centered magnitudes of acceleration and a velocity.
- It is necessary to size up spectra of a velocity and migration on a FFT from the centered rates of speed and migration.

References:

1. V.I.Ljulko. Working out of the theoretical fundamentals and practical recommendations for the purpose of maintenance of aircraft engines of air courts of a commercial aviation on availability index of product and perfecting of processes of their diagnosing. M:STBOOK, 2004.
2. And. V.Barkov, N.A.Barkova, A.J.Azovtsev Monitoring and diagnostic of rotor cars on vibration. St.-Petersburg.: Изд. SPSEU, 2000. 158 with.
3. With. V.Tvaradze, And. P.Ushakov. Problems of operative detection of imperfections of propulsion systems of trasport facilities. Commercial aviation academy, the Interuniversity subject collector of proceedings «Problems of maintenance and perfecting of transport systems». Thom X, 2005. p.174-181.
4. V.P.Maksimov, And. V.Egorov, V.A.Karasev. Measurement, machining and the analysis быстросменных processes in cars. M: Engineering industry, 1987. 206 p.
5. M.K.Sidorenko. Vibrational measurements gas-turbine engines. M: Engineering industry 1973. 224 with.
6. Lenkov S.V., Koljasev V. A, Molinas S.M.analys of agency of analogue and digital integration of a signal of acceleration and nonlinearity of an analogue-digital converter on an exactitude of an estimation of velocity spectra and migrations at вибродиагностике space technics//Bulletin ПГТУ. Space technics, N 13. 2002, Perm. - p. 55-60.

DESIGNING LOCAL AREA NETWORKS THAT HAS A VOICE-VIDEO-TEXT TRAFFIC

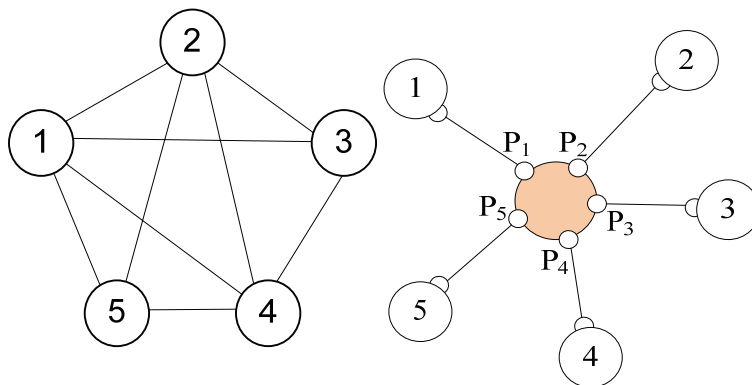
Is described the algorithm of designing and calculating local network (LAN) with the multimedia traffic. The concrete example of calculation is given. Is in detail examined the construction of the information-geometric model of network, the construction of the model of ideal switch, the realization of ideal switch in the assigning class of industrial switches, the setup of the parameters of industrial switch

The principal stages of projection and calculation LAN. M Possible it recommended several good sources [1-3] for the acquaintance with the principles of the design of local networks on the basis of switches. However, the algorithm of designing and an example of calculation you here will not find.

The analysis of technologies of designing of separate firms shows, that the algorithm of designing LAN can be broken on three consecutive parts:

- designing and the calculation of active equipment, i.e., the apparatus configuration of the transport and final nodes of the of the network;
- designing and the calculation of passive equipment, including the calculation of topology and characteristics of communication channels;
- the determination of the setups of the nodes of network (switches, computers, operating systems, applications).

The formal description of information and computer networks in the form graphs and matrices. Topology of networks. In the general case the projected network possible it represented by the set of graphs and matrices. The apexes of graphs indicate the nodes of network (sources, the users of information), and the connections between the apexes indicate the information or physical connections between the nodes. The configuration of graph is called topology. Figure 1 shows two types of the configurations: full-connected and star.



Apexes of the graph: $n=1, 2, \dots, N$

Sides of the graph: $\mathbf{A} = \| a_{ij} \|$, где $i, j = 1, 2, \dots, N$. (1)

Figure 1. Representation of network by the graph

Initial data for the designing networks. Applications. In the first approximation, the model of network possible was considered the following set of graphs and matrices:

$$\mathbf{A}^0, \mathbf{A}^1, \dots, \mathbf{A}^m, \dots, \mathbf{A}^M, \quad m=0, 1, 2, \dots, M \quad (2)$$

где: A^0 - geometric line pattern (matrix of the distances between the nodes of network),

A^1, \dots, A^M - the configuration of applications.

The configuration of applications is the functional-informational model of network. This model it is reflected the distribution of applications over the nodes of network, and also the intensity of the individual flows between servers and clients of the applications of network. By examples of applications they can it served: WWW, FTP, VoIP, NC (server for administration of network) and others.

Intensities of applications - function of time. However, in the majority of the cases for calculating the network possible it limited to the average values of the intensities of traffic for the specific time intervals.

Let for the certainty the network consist of $N=34$ nodes, among which there are the servers: VoIP ($n=1$), Video ($n=2$), WWW ($n=3$), FTP ($n=4$), and also working stations (RS) with the client parts of applications ($n=5, \dots, 34$).

As a result the model of network wakes represented by the matrix of the distances between the nodes of network A^0 and by the matrices of the intensities of the traffic: VoIP (A^1), Video (A^2), WWW (A^3), FTP (A^4).

Transformation of the model of a network of the type "full-connected" into the model of a network of the type "star" by the help of ideal switch. In the network of the type "full-connected" for connection N of nodes it is required $N(N-1)/2$ physical duplex communications, i.e., quadratic dependence on the number of nodes occurs. Furthermore, each computer in the network must it had the large quantity of communication ports, sufficient for the connection with each of the remaining computers in the network. Both these factors neutralize the key advantage of these networks - their logical simplicity.

In practice they minimize a quantity of physical connections of network. It is reached this via the binding of the nodes through the switch. As a result the type of network "full-connected" will change into the type "star" (Fig.1).

It easily saw that a quantity of ports in the switch coincides with the number of nodes of network, and the traffic, passing through each port of switch and respectively through connected with this port node of network, coincide.

In other words, the intensities of the traffic through the ports of switch are also described by the set of the matrices: A^1, \dots, A^M

Importantly and necessarily it noted that the ideal switch must it was for the network transparent, i.e., by no means it did not influence the passing through the switch information bit flows.

The calculated distribution of traffic of applications according to the ports of the ideal switch. If it summed up the intensities of traffic ($a^m_{i,j}$) of any concrete application m ($m=1, 2, \dots, M$), which take place through each (i) port of switch, then it was received the total intensity of traffic of this concrete application for this (i) port of switch, i.e.:

$$b_i^m = \sum_{j=1}^{j=N} a^m_{i,j} \quad (3)$$

In our example by the values of matrices A^1, A^2, A^3, A^4 it is determined the total intensities of traffic of applications in the ports of switch - this:

B^1 (traffic VoIP), B^2 (traffic Video), B^3 (www- traffic), B^4 (ftp- traffic).

The short-cut calculation of the distribution of traffic of applications according to the ports of ideal switch. The distribution of traffic of the applications (\mathbf{B}^m) on ports of the ideal switch can be established by more simple way. Let's consider an example.

On a first step we shall construct the table $\| a_{ij}^1 \|$ by dimension 34x34, which each element of a matrix will be equal 0 or 1::

$\| a_{ij}^1 \| = 1$, if connection on the IP-telephone is possible between the nodes (i,j) of switch,
 $\| a_{ij}^1 \| = 0$, otherwise.

\mathbf{B}_0^1 (смотреть табл.1).

For the second step we shall calculate quantity of possible sessions of negotiation on the IP-telephone for all ports of the switch - matrix \mathbf{B}_0^1 (To look the table 1).

At the third step let us determine a quantity of simultaneous negotiations according to IP-telephone (simultaneous sessions of application VoIP) through each port of switch. It is obvious, that in ports of the switchboard connected to workstations, the number of simultaneous sessions will be equal 1, and through port-1 30 sessions simultaneously can be established. In result we shall receive one more line - matrix \mathbf{B}_1^1 .

On the fourth step we shall specify for each session quantity of duplex connections and bit speed of transfer of a vote (in view of the chosen standard of coding). In our case one session will need two duplex communication lines with bit speed 64 Kbit/s (at election of the standard of coding PCM). In result we shall receive the next matrix - line \mathbf{B}^1 .

Similarly for the video- application we shall calculate a matrix - line \mathbf{B}^2 . Here unique difference will be in speed of the video-traffic. For definiteness let it will be the compressed video signal with bit speed 1,024 Mbit/s.

For definiteness also we shall set any meanings of intensity of WWW-traffic (\mathbf{B}^3) and intensity of FTP-traffic (\mathbf{B}^4).

The table 1. An example of account of productivity of ports of the switch

	1	2	3	4	5	6	7-33	34	Sum
	VoIP - gate	Video - gate	www-server	ftp-server	PC-1	PC-2	PC (3-29)	PC-30	
\mathbf{B}_0^1	30				30	30	30	30	
\mathbf{B}_1^1	30				1	1	1	1	
\mathbf{B}^1	3,840				0,128	0,128	3,46	0,128	8
\mathbf{B}^2		61,440			2,048	2,048	55,296	2,048	123
\mathbf{B}^3			570,00		19,00	19,00	513,00	19,00	1140
\mathbf{B}^4				750,00	25,00	25,00	675,00	25,00	1500
\mathbf{T}^0			570,00	750,00	44,00	44,00	1188,00	44,00	2640
\mathbf{H}^{Vo}	3,84	61,44	0,00	0,00	2,18	2,18	58,75	2,18	131
\mathbf{H}^{Be}	0,00	0,00	570,00	750,00	44,00	44,00	1188,00	44,00	2640
\mathbf{V}	19	307	633	833	51	51	1385	51	3332

Accounting of distribution of classes of traffic on ports of the ideal switch.

One of overall objectives of designing of a local network, in which the traffic consists of a mix of a vote, images and text, is to prevent damage of each of these traffic.

For the decision of this task according to the recommendations of the standard 802.1D-1998 all traffic of local networks is divided into eight classes (table 2). It allows to transform matrixes of

distribution of traffic of the application on ports of the switch \mathbf{B}^m to eight matrixes of classes of traffic:

$$\{\mathbf{B}^1, ..., \mathbf{B}^m, ..., \mathbf{B}^M\} \Rightarrow \{\mathbf{T}^7, ..., \mathbf{T}^0\}. \quad (4)$$

The table 2. Types of the traffic in a local network

Priority	A designation	A type of the traffic
1	BK	The background traffic
2	—	The economical traffic
0 (by default)	BE	The traffic transmitted with the maximal efforts
3	EE	The priority traffic
4	CL	The controllable traffic
5	VI	Video (delay and the jitter less than 100 ms)
6	VO	Vote (delay and the jitter less than 10 ms)
7	NC	The control of a network

In our example:

$\mathbf{T}^6 = \mathbf{B}^1$ (The traffic VoIP is referred to a class VO),

$\mathbf{T}^5 = \mathbf{B}^2$ (Traffic of the Video-application is referred to a class VI),

$\mathbf{T}^0 = \mathbf{B}^3 + \mathbf{B}^4$

As it is visible, WWW- and the FTP-traffic are referred to one class (matrix - line \mathbf{T}^0 in the table 1).

Simplification of model of the ideal switch by merge of classes of the traffic.

The switch, which supports function QoS, can use several queues for various processing of classes of the traffic. The switch usually supports some maximum quantity of queues, which can appear less, than required number of classes of the traffic. In this situation some classes will be served by one queue, that is actually will merge in one class. The standard 802.1D-1998 recommends what classes of the traffic it is necessary to realize in a network in conditions of the limited quantity of queues in switch.

With the existence only of one queue in the network there is only one class of the traffic — BE (Best Effort).

Two queues give possibility it divided traffic into two classes — BE и VO (Voice). In this case to class VO wakes it related any sensitive to delay traffic, i.e., not only voice, but also video, or traffic of control of network.

Further increase in the quantity of queues allows it more differently attended traffic, up to the recommended eight classes.

For definition of two basic classes of traffic in the ideal switch (VO and BE) possible it used the formula:

$$\mathbf{H}^{VO} = \mathbf{T}^7 + \mathbf{T}^6 + \mathbf{T}^5, \quad (5)$$

$$\mathbf{H}^{BE} = \mathbf{T}^4 + \mathbf{T}^3 + \mathbf{T}^2 + \mathbf{T}^1 + \mathbf{T}^0.$$

In a considered example: $\mathbf{T}^7 = \mathbf{T}^4 = \mathbf{T}^3 = \mathbf{T}^2 = \mathbf{T}^1 = 0$,

$$\mathbf{H}^{VO} = \mathbf{T}^6 + \mathbf{T}^5 = \mathbf{B}^1 + \mathbf{B}^2 \text{ (traffic VoIP and Video are poured into one class),}$$

$$\mathbf{H}^{BE} = \mathbf{T}^4 + \mathbf{T}^3 + \mathbf{T}^2 + \mathbf{T}^1 + \mathbf{T}^0 = \mathbf{B}^3 + \mathbf{B}^4 \text{ (in one class the traffic WWW, FTP).}$$

Reservation of throughput of ports of the ideal switch. It is known, that the basic idea underlying all methods of maintenance of the characteristics QoS, consists in the following: the common productivity of each resource should be shared between different classes of the traffic non-uniformly. In that specific case productivity of ports of the switch also should be shared between different classes of the traffic non-uniformly.

It is known, that a primary factor influencing size of delays of packages in the switch, so, and on quality of service, is operating ratio of a resource. Therefore for maintenance of the certain quality of service it is important, that operating ratio of port of the switch did not exceed the certain size.

So, for simplification of a task all flows are shared into two classes - sensitive to delays (traffic of real time, for example voice) and elastic, admitting the large delay, but sensitive to losses of the data.

Agrees [2] dependence of delays of packages on operating ratio of a resource the function $W=W(\rho)$ in a fig. 2. Here W_s - delay of the traffic, sensitive to delays, and W_e - delay of the elastic traffic.

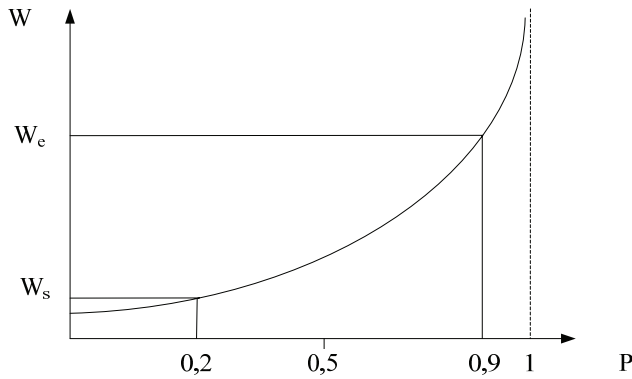


Figure 2.

As it is visible, the limiting loading of port of the switch by the sensitive traffic should not exceed 0.2, and the limiting common loading of port by the sensitive and elastic traffic should not exceed 0.9.

In view of the accepted designations and named restrictions it is possible to define throughput of ports of the switch ($v_{i=1,\dots,N}$) for two classes of the traffic H^{VO} and H^{BE} by the following formula:

$$v_i = \max ((h^{VO}_i + h^{BE}_i) / 0.9, h^{VO}_i / 0.2) \quad (6)$$

The result of account of throughput of all ports of the switch (matrix-line \mathbf{V}) is given in table 1.

The reservation of throughput of ports of the switch under the formula (6) is based on two classes of service. But this formula is easy for modifying for more than two classes of service, and so that each class worked on the part of a curve of delays.

Calculation of parameters of a configuration of the ideal switch. On the basis of table 1 it is possible to determine parameters of a configuration of the ideal switch (tab. 3). Here common productivity of the switch is equal to the double sum productivity of all ports of the switch.

The table 3. A configuration of the ideal switch

№	The name of parameter	Meaning
1	Common productivity of the switch	6,7 Gbit/s
2	Quantity of ports	34
3	Productivity of ports:	
	Productivity of port - 1	19 Mbit/s
	Productivity of port - 2	307 Mbit/s
	...	
	Productivity of port - 34	51 Mbit/s
4	Quantity of priority queues in ports	2

Algorithm of realization of the ideal switch. Definition of criteria of a choice. The elementary algorithm of realization of the ideal switch can be shown to search of such industrial model of the switch, which configuration covers and is closest to a configuration of the ideal switch is, first. And, secondly, it is necessary, that the parameters of industrial model could change by the manager of a network so that after the appropriate adjustment the industrial switch was identical to the ideal switch.

Let's determine a sequence of parameters of industrial model, which should be taken into account. Certainly, first of all, industrial model should have parameters not worse what are displayed in the table 3. In the second turn it is necessary to take into account in the priority order the following parameters: the number of levels of management, opportunity of aggregation of ports, opportunity of the shaping of ports, opportunity of maintenance of parameters of quality of service of the traffic (QoS, CoS), is desirable presence of the Web-interface for adjustment, firm - manufacturer, price.

Having chosen parameter "L3" (number of levels of management), we narrow search of required industrial model in a class of switches of 3-rd level, which are intended for division of large local networks on sub-networks.

The step-by-step comparison of parameters of a configuration of the ideal switch (tab. 3) with parameters of a configuration of firm switch of a class "L3" of firm "D-link" shows, that the parameters of model DES-3852 (tab. 4) coincide or not worse than parameters of the ideal switch.

Setup of the parameters of industrial switch and nodes of the network. The model of the switch DES-3852 has a powerful set of functions (protocols) and teams of adjustment, which allow:

- Port and link Aggregation,
- Support 802.1p priority queuing Quality of Service,
- To create virtual networks.

Port and link Aggregation. Port trunk groups are used to combine a number of ports together to make a single high-bandwidth data pipeline. The Switch treats all ports in a trunk group as a single port. Data transmitted to a specific host (destination address) will always be transmitted over the same port in a trunk group. This allows packets in a data stream to arrive in the same order

they were sent. Link aggregation allows several ports to be grouped together and to act as a single link. This gives a bandwidth that is a multiple of a single link's bandwidth.

Link aggregation is most commonly used to link a bandwidth intensive network device or devices, such as a server, to the backbone of a network. The Switch allows the creation of up to 32 link aggregation groups, each group consisting of 2 to 8 links (ports). All of the ports in the group must be members of the same VLAN, and their STP status, static multicast, traffic control, traffic segmentation and 802.1p default priority configurations must be identical. Port locking, port mirroring and 802.1X must not be enabled on the trunk group. Further, the aggregated links must all be of the same speed and should be configured as full-duplex.

The Master Port of the group is to be configured by the user, and all configuration options, including the VLAN configuration that can be applied to the Master Port, are applied to the entire link aggregation group. Load balancing is automatically applied to the ports in the aggregated group, and a link failure within the group causes the network traffic to be directed to the remaining links in the group.

The Spanning Tree Protocol will treat a link aggregation group as a single link, on the switch level. On the port level, the STP will use the port parameters of the Master Port in the calculation of port cost and in determining the state of the link aggregation group. If two redundant link aggregation groups are configured on the Switch, STP will block one entire group, in the same way STP will block a single port that has a redundant link.

The table 4. Structure of parameters of model of the switch DES-3852

№	Name of the parameter	The value
1	Productivity	15,7 Gbit/s
2	Quantity of ports 10/100/1000/STP	2
3	Quantity of ports 10/100/1000	2
4	Quantity of ports 10/100	48
5	Quantity of priority turns	8
6	Number of levels of management	L3
7	802.3ad Link Aggregation: 32 groups, 8 ports per group	+
8	Management of a passband: a step for each port 64 Kb/s	+
9	QoS/CoS	+
10	The price (\$)	1030

Support 802.1p priority queuing Quality of Service. QoS is an implementation of the IEEE 802.1p standard that allows network administrators a method of reserving bandwidth for important functions that require a large bandwidth or have a high priority, such as VoIP (voice-over Internet Protocol), web browsing applications, file server applications or video conferencing. Not only can a larger bandwidth be created, but other less critical traffic can be limited, so excessive bandwidth can be saved. The Switch has separate hardware queues on every physical port to which packets from various applications can be mapped to, and, in turn prioritized.

The Switch has eight priority classes of service and the bandwidth control settings are used to place a ceiling on the transmitting and receiving data rates for any selected port.

For strict priority-based scheduling, any packets residing in the higher priority classes of service are transmitted first. Multiple strict priority classes of service are emptied based on their priority tags. Only when these classes are empty, are packets of lower priority transmitted.

For weighted round-robin queuing, the number of packets sent from each priority queue depends upon the assigned weight.

For weighted round-robin queuing, if each CoS queue has the same weight value, then each CoS queue has an equal opportunity to send packets just like round-robin queuing.

For weighted round-robin queuing, if the weight for a CoS is set to 0, then it will continue processing the packets from this CoS until there are no more packets for this CoS. The other CoS queues that have been given a nonzero value, and depending upon the weight, will follow a common weighted round-robin scheme.

QoS can be customized by changing the output scheduling used for the hardware classes of service in the Switch. As with any changes to QoS implementation, careful consideration should be given to how network traffic in lower priority classes of service is affected. Changes in scheduling may result in unacceptable levels of packet loss or significant transmission delay. If choosing to customize this setting, it is important to monitor network performance, especially during peak demand, as bottlenecks can quickly develop if the QoS settings are not suitable.

Utilizing the **QoS Output Scheduling Configuration** window (for xStack DGS/DXS-3300 Series) can implement a combination queue for forwarding packets. This combination queue allows for a combination of strict and weight-fair (weighted round-robin “**WRR**”) scheduling for emptying given classes of service.

Conclusion. Is described the algorithm of designing and calculating local network (LAN) with the multimedia traffic. The concrete example of calculation is given.

Is in detail examined the construction of the information-geometric model of network, the construction of the model of ideal switch, the realization of ideal switch in the assigning class of industrial switches, the setup of the parameters of industrial switch.

The author hopes, that the concept, stated in work, of designing of local networks with the multimedia traffic will be useful to the students, post-graduate students and technical experts in the field of telecommunications.

The algorithm, developed and described by the author, is used in 2008 by the students – graduates (Малиновский С.В., Ляхно А.Н., Матвиюк М.Н.) in their degree works.

References:

1. Система для автоматизированного проектирования локальных вычислительных сетей. - <http://www.netwizard.ru>. – 2008.
2. Олифер В.Г., Олифер Н.А. Локальные сети на основе коммутаторов: Информационно-аналитические материалы. - <http://www.citforum.ru> -2008.
3. Олифер В.Г., Олифер Н.А. Компьютерные сети. Принципы, технологии, протоколы: Учебник для вузов. 3-е изд.- СПб.: Питер, 2007. - 958 с.

THE INFORMATION-MEASURING MONITORING SYSTEM OF WATER-BLACK OIL EMULSIONS BURNING PROCESS

The opportunity of creation is appreciated and the block diagram of the information measuring monitoring system of burning water-fuel oil emulsion process of through definition of optimum dispersity is offered, is considered concrete means on the basis of which the given system can be constructed..

Statement of a problem

Necessary conditions for reliable work of boiler units and furnaces are stability of torches and conformity their physical parameters to optimum conditions of heat exchange in fire-chamber device. Completeness of combustion of fuel appreciably depends on average shallowness and uniformity of dispersion by atomizers. Except for constructive characteristics of atomizers, on shallowness dispersions viscosity and density of liquid fuel influences. Proceeding from this, in technological processes of burning high-viscosity fuel (black oil) it is accepted to warm up the last before direct its submission on an atomizer [1, 2].

Any fluctuation of humidity in fuel which moves in fire-chamber, attracts corresponding simultaneous change of the combustible weight charge and factor of air surplus which inevitably influences fire-chamber work through sharp deterioration of burning process stabilization conditions, down to full failure of a flame. Even at burning black oil with conditioned contents of water (5 %) the average factor of surplus of air appears the supreme of optimum on 5,5 % and average efficiency thermal device (the boiler, the furnace) falls on 0, 5-1,1 %.

The analysis of researches

One of directions of an effective utilization achievement of watered liquid black oil is their burning under condition of uniform distribution of water on all volume, i.e. as water-black oil emulsion (WBOE) [1, 3]. The given technology known it is enough for a long time and it is used presently rather widely in various combinations and applications (fuel - water, fuel - gas, fuel - water-gas emulsion-suspension structures) in engines of internal combustion, turbine engines, furnace units of the various enterprises. Except for substantial increase of ecological effect, use water-fuel emulsions justifies itself from the economic point of view: the increase in efficiency of the boiler at some percent, owing to more full combustion of fuel and reduction of air surplus factor (due to effect of "microexplosion" fine-dyspersated drops of water in sprayed drops of black oil), also occurs economy of fuel up to 12 % [1].

As well as any another, technology of burning water-fuel emulsions in thermal devices the industrial enterprises is not deprived the characteristic problems. One of the major is definitions of viscosity emulsion as key parameter which influences efficiency of dispersion and, accordingly, combustions of fuel. As well as in technology of burning "dry" dehydrated black oil, necessary which value of viscosity is provided of heating before submission on atomizers, by preparation emulsion it too warm up to the necessary temperature. But in this case viscosity of the emulsion influences also a volumetric part of a phase of water.

According to [1], viscosity WBOE submits to the equation which is received by research way:

$$\nu_{em} = \nu_n (1 + aW + bW_s) \quad (1)$$

where ν_{em} and ν_n - kinematic viscosity accordingly emulsion and fuel; W_s - concentration of a disperse phase (water); a , b - empirical factors which depend on mark of black oil and a way of

preparation WBOE. In turn, from dispersiveness and uniformity of distribution of a disperse phase depends on mark and a kind of liquid fuel and a way of preparation emulsion. I.e. factors *a* also *b* should take into account these rather important factors.

Reduction of the disperse phase particle size at its identical concentration results in increase in viscosity of system, but to the certain level (0,1 - 0,8 microns [1]); nonlinearity of this connection proves to be true also its indulgence in process of increase in the particle size [4]. Here [4] it is established, that at diameters of particles than 100 microns influence of their size on viscosity of system it there are more becomes so small, that they can disdain, and at the sizes about 10 microns - influence rather essential. Precise analytical dependences of an estimation of this influence it is not found.

Homogenized in cavity mixer with the big specific cavitation energy water-black oil emulsion has appreciably smaller viscosity than pure black oil [5], but, in this case, extremely small particles of water will not provide the necessary effect of "microexplosion" due to which additional crushing drops of fuel after their dispersion in a zone of burning, and as consequence, achievement of the most effective combustion of fuel is carried out. The maximal effect from "microexplosions" for water-black oil emulsion is reached at average value of diameter disperse water particles about 5-15 microns (about 0,1 from diameter of an emulsion drop, sprayed by an atomizer in fire-chamber) [1]. And generally the size disperse particles waters for effective "microexplosions" is determined by a complex of a thermalphysic parameters of the disperse environment such, as viscosity, a superficial tension, etc.

So, from the point of view of the phenomenon of "microexplosion" (and, accordingly, increase of efficiency of combustion of fuel) for everyone water-fuel emulsion is such optimum value of dispersiveness at which the maximal effect of process its burning and which rather essentially influences viscosity emulsion is reached.

The purpose of work

The task of the given research is studying an opportunity of creation of information-measuring system (IMS) for definition of optimum dispersiveness water-black oil emulsion with the purpose of maintenance of its most effective burning.

To physicomechanical parameters WBOE, which actual for specified IMS, concern:

- Temperature WBOE, as key parameter which influences its viscosity;
- Kinematic viscosity WBOE that influences on shallowness dispersions and the form of a torch;
- Humidity WBOE, i.e. a volumetric ratio of water and fuel in emulsion;
- Dispersiveness WBOE on which depends efficiency of burning process.

Viscosity WBOE as one of key parameters which influence an overall performance of boiler units and furnaces, can characterize not only macroscopical parameters of a stream of substance, but also microscopic features of molecular structure emulsions on the basis of mineral oil. In works [6, 7] revealing of internal structure emulsion through use of the majority of structural - sensitive methods is shown, that, it is possible only in liquids which are in a rest condition. Measurement rheological parameters represents an opportunity of an estimation of internal structure emulsions directly in streams. Thus, viscosimeter can be used for the analysis not only viscosity, but also emulsions dispersiveness.

Results of researches

For the decision of a task of the emulsion physicomechanical parameters automatic control in a stream there can be used bridge throttle converter (BTC) as the measuring converter of kinematic viscosity. The principle of action BTC is rather thoroughly described in works [8-12]. As an emulsion viscosity will considerably depend on its temperature, in a zone of measurement it is necessary to lead heatset to exclude influence of the given parameter.

Block diagram IMS which carries out a complex estimation of physicomechanical parameters WBOE and carries out regulation of its dispersiveness for increase of efficiency burning is represented on fig. 1.

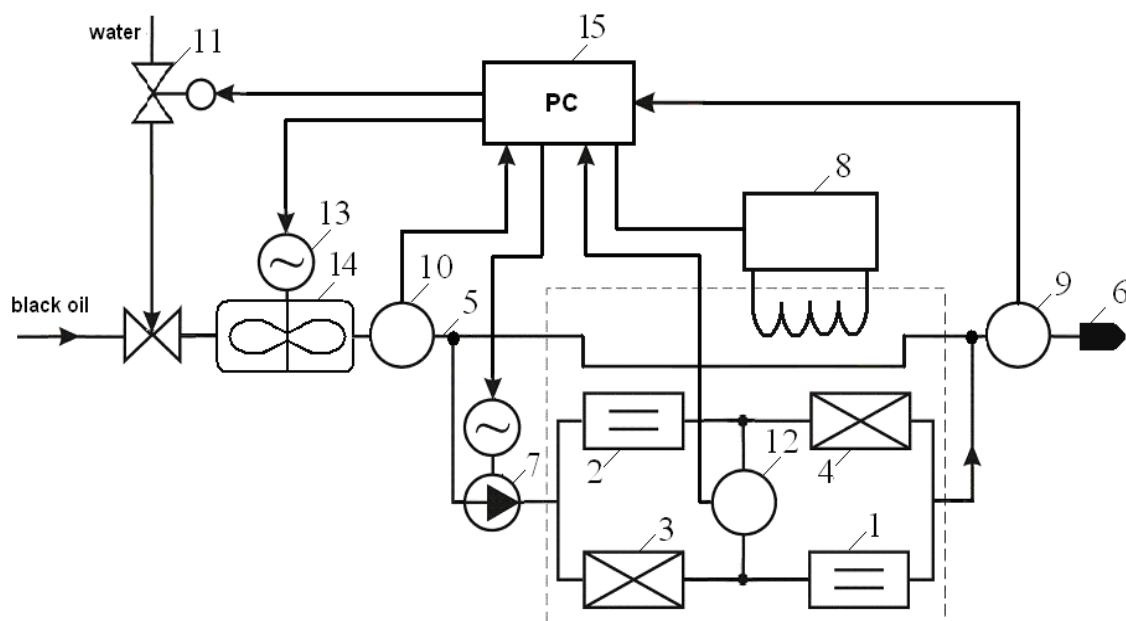


Fig. 1. The block diagram of information-measuring system of physicochemical parameters WBOE: 1, 2 - laminar a throttle, 3, 4 - turbulent a throttle, 5 - fuel pipe, 6 - an atomizer, 7 - gear pump, 8 - a heater, 9 - the gauge of temperature, 10 - the main gauge of black oil humidity, 11 - the regulating valve, 12 - pressure-gauge, 13 - the electric drive, 14 - cavity mixer, 15 - a personal computer.

Given IMS it is created on the basis of the bridge throttle converter constructed on two laminar 1 and 2 (long capillaries) and two turbulent (diaphragms) throttles 3 and 4, connected in the bridge hydraulic measuring circuit. From a fuel pipe 5, that submits WBOE on atomizers 6, selection emulsion to the converter for the express train - analysis of its physicochemical properties is carried out. At known constant value of a volumetric expense through BTC, that is created by the pump 7 at the moment of balance of the bridge it is possible to define kinematic viscosity of a liquid.

For heating and heatset of an emulsion the heater 8 and the gauge of temperature 9 is used. Constant value of a ratio of components WBOE is provided with a contour of regulation of water delivery which structure includes the gauge of humidity of black oil 10 and the regulating valve 11.

At such configuration of system the initial signal pressure-gauge 12 will enable to judge dispersiveness WBOE. Leaning on these data, it is possible to supervise over frequency of rotation of the electric motor 13, that actuates a cavity mixer rotor 14 and by that to change dispersiveness of water fraction of emulsion.

The experimental research of efficiency of burning will enable to find optimum value of dispersiveness for process of burning on concrete object and by that to raise its economic parameters. According to researches of burning water-black oil emulsion in fire-chamber device at heat-electric power station described in [13, 14], efficiency without optimization on dispersiveness of a water phase emulsion is shown in increase of efficiency on 1,6-1,7 % and economy of 5-10 % of fuel.

Processing of the measuring information in given IMS is carried out by a personal computer 15 with the special software. Signals about the current condition of system from sensitive elements act on the specialized payment of an input / conclusion of a personal computer. According to programm realized algorithm and an operating mode, there is a processing of entrance signals and definition of basic physicochemical parameters WBOE. Formation of the certain signal of management on change of viscosity and dispersiveness for optimization of process of burning occurs automatically, according to the received information and an operating mode of system.

At a choice of means IMS it is necessary to take advantage, basically, the standard normalized devices. The bridge throttle converter which is a non-standard element of system, works

at rather small expenses, therefore for submission of a liquid in a diagonal of a power it is possible to use gear pump which has the linear static characteristic which is solving at a choice of the pump. Calculation of the geometrical sizes of laminar and turbulent throttles of BTC for the chosen range of measurement of kinematic viscosity and density of mineral oil is carried out in view of technical opportunities of regulation of size of a volumetric expense through the converter.

Conclusions

The analysis of references and publications of results of experimental researches on a theme is carried out.

The opportunity of creation an IMS for definition of optimum dispersiveness water-black oil emulsion is appreciated with the purpose of maintenance the most effective its burning.

Block diagram IMS of the burning water-black oil emulsion process control which allows by stabilization of percentage contents of water in black oil is offered, and also due to change of cavity mixer transfer energy, to create water-black oil emulsion with the set dispersiveness and to reach high technical and economic parameters of burning process.

References

1. Volikov A.N. Burning of gas and liquid fuel in boilers of low power. - L.: Bowels, 1989. - 160 p.
2. Beloselskij B.S., Soliakov V.K. Power fuel. - M.: Energy, 1980. - 168 p.
3. Krivonogov B.M. Increase of efficiency of gas burning and preservation of the environment. - L.: Bowels, 1986. - 280 p.
4. V.P. Promyshlennaja's Thrones preparation of oil. - Kazan: 2000. - 414 p.
5. <<http://www.nwmtc.ac.ru>> - The Centre of science of nonlinear wave mechanics and technology of the Russian academy of sciences.
6. Evdokimov I.N., Eliseev N.Yu., Akhmetov B.R. Initial stages of asphaltene aggregation in dilute crude oil solutions: studies of viscosity and NMR relaxation. Fuel. V.82. №7.2003, P.817-823.
7. Evdokimov I.N., Eliseev D.Yu., Eliseev N.Yu. Rheological evidence of structural phase transitions in asphaltene-containing petroleum fluids. Journal of Petroleum Science and Engineering, V.30, 2001. - №3/4. - P.199-211.
8. Drevetskij V.V., Jatsuk A.P., Kos V.M., Measurement of kinematic viscosity of liquids by the counterbalanced throttle bridge converter // „Bulletin of the Lvov polytechnical institute”. - Lvov. - 1976. - № 100. - p. 28-32.
9. Drevetskij V.V., Gorejko A. S., Jatsuk A.P. Use of the information in viscosity liquid fuel for increase of technical and economic parameters heat engineering installations // Problems of power and heat technology: Bulletin sc. works - M.: MEI, 1983. - p. 78-84.
10. Drevetskij V.V., Tsibulskij B.V., Jatsuk A.P., Tkacheva L.M. "Automatic measurement of viscosity of mineral oil ". - M.: CNIITE oil refining and petrochemical industry, 1987. - 64 p.
11. Drevetskij V.V., Jatsuk A.P., Gorejko A. S., Kuzmin S.T., Tsibulskij B.V. Analyzer of kinematic viscosity. - Rovno. 1988.
12. Drevetskij V.V. Information-measuring system of mineral oil kinematic viscosity // Methods and devices of quality assurance. - 2005. - №15. - p. 116-119.
13. Presnov G.V., Bublej P.V., etc. Use non-polluting cavitation technologies on branches of joint-stock company MOSENERGO. The ecological bulletin of the Moscow region №2.2001, - p. 45-50.
14. Bulgakov A.B., Presnov G.V., etc. Improvement of liquid fuels properties from hydromechanical processing in a cavitation field // Energetik. - 2002. - №7. - p. 29-34.

N.A. Vinogradov, Doctor of Science (Techn.) (National Aviation University, Ukraine)

I. A. Zhukov, Doctor of Science (Techn.) (National Aviation University, Ukraine)

N.N. Guziy, Candidate of Science (Techn.) (National Aviation University, Ukraine)

MANAGEMENT OF DATA FLOWS AND CONTROL OF OVERLOAD IN AERONAUTICAL TELECOMMUNICATION NETWORKS

The problems of quality of service in the aeronautical telecommunication networks are researched. The method of control of networks based on partitioned estimation and control as unified framework for adaptive real-time systems is developed. Considering of delays of control data and compensating of delays due to prediction of traffic parameters in advance we decrease negative impact of these delays. The results of calculations of improvement of network performance are represented.

Aeronautical telecommunication network (ATN) has such specific features. Firstly, it is the system of critical application, which is characterized by great spread in values of necessary calculating resources for optimum and extreme cases. All telecommunication services must be represented in real time-scale under any conditions of implementation. Secondly, it is heterogeneous system having huge number of network and terminal equipment with large range of technical parameters, application interfaces and protocols. It's clear that capacity, quality of service (QoS), reliability and other characteristics of network in general are limited by corresponding characteristics of the most poor chain link. Thirdly, the requirements to QoS, especially to reliability of data transfer, have to be very high since aviation safety depends from unbreakable work of communications directly.

Besides, ATN as any complex and distributed system is system with delayed response. The sources of delays are fundamental limitations on speed of propagation of signals through any physical media and communication and processing nodes, such as switches, routers etc. We may consider these limitations on the stages of projecting and technical exploitation of networks.

Another serious sources of delays, losses and forced retransmissions of data are overloads and congestions of critical parts of network. The most efficient way of loss control is continuous analysis and optimal control of network functioning including routing and redirection of data flows.

A number of different control mechanisms have been proposed to solve these problems. Algorithms of traffic policing and shaping such as leaky and token buckets are ones of the methods widely used in the network access control field and they can dynamically allocate bandwidth and efficiently minimize packet losses. Additionally, different control strategies were proposed to manage traffic flow into the backbone network. The results showed that the feedback control laws can improve network performance by improving throughput, reducing packet losses, and relaxing congestion. On the other hand, in [1], it was observed that the system performance was highly degraded in the presence of feedback delay (arising from communications). Due to the time delay, what we capture in real time is the lagged or delayed traffic information. Control based on delayed information leads to excessive degradation of network performance. Thus, in practice, its impact cannot be ignored and must be taken into consideration and compensated for.

Traffic prediction methods have been widely used in network management. By use of prediction techniques, that is, forecasting the future behavior of the traffic, one can effectively prevent traffic jams, traffic congestion, and network crashes. Inspired by these ideas, we have applied prediction techniques [2,3] to solve the problems encountered in [1].

For this purpose, we propose a real-time feedback control mechanism based on the predicted state and traffic. The traffic and state information are predicted for different values of prediction times based on their past history (the traffic history measured online). An accurate prediction for the future traffic and state (short-term prediction) is able to provide better control compensating for time delay. Thus the impact of time delay can be minimized and the system performance improved.

In this work an online predictor based on the principle of the least mean square error (LMSE) is developed. It is one of the simplest methods. It was noted in [4], that LMSE can achieve better accuracy compared to those complex long-memory predictors for online measurements. Without the requirement of complex computation, it can be implemented at a high speed. As a result of traffic prediction, the system performance degradation due to delay is reduced by use of proper control actions. According to our results, it is possible to optimize the system performance and minimize the cost function by implementing the new method.

In order to understand and solve the performance-related problems in computer communication network, it is critical to build a dynamic model of the information flow through the system (Fig.1). Further, the basic statistical properties of measured trace data must be known.

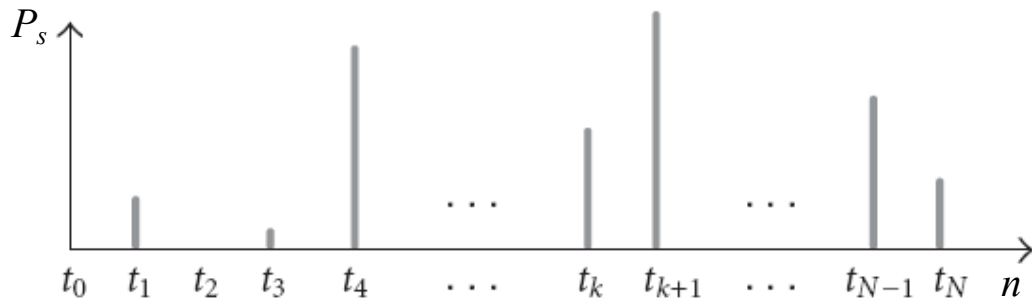


Fig. 1. General model of network traffic. P_s – packet size (bytes).

Traditional characterization of the Internet traffic is based on the Poisson process (which exhibits short-range dependence), Bernoulli process, or more generally doubly stochastic Poisson process (DSPP).

A recent study [5] shows that network traffic has self-similarity characteristics and long-range dependence. Self-similarity means that a certain property of traffic behavior is preserved over space and/or time scales, and long-range dependence is said to exhibit long-term correlations which decay at rates slower than exponential ones. On the other hand, the correlation functions of traditional traffic models decay exponentially or faster. In this paper, a general model is constructed to simulate the incoming traffic illustrated in Fig. 2.1, which is similar to those in [6].

To simulate a network, we construct a mathematical model comprised of N individual users (traffic streams), served by N corresponding, all of which are coupled to a multiplexor connected to an outgoing link having (bandwidth) capacity C .

Each token bucket implements its algorithm to police the arriving packet. The nonconforming traffic streams are dropped while all the conforming traffic are multiplexed and queued up for entering the multiplexor. As a matter of fact, not all conforming traffic from token buckets will be accepted because of the size limitation of the multiplexor (buffer size Q) and the link capacity (speed) of the accessing node. If the sum of these traffics exceeds the multiplexor size, some part of the conforming traffic maybe dropped. The discarded traffic is defined as the traffic loss at the multiplexor $L(t_k)$.

In general, the traffic loss at the token buckets during the k_{th} time interval is given by

$$L_T(t_k) = \sum_{i=1}^N r_i(t_k) = \sum_{i=1}^N [V_i(t_k) - g_i(t_k)],$$

where $V(t_k)$ – packet size of the arriving traffic; $r(t_k)$ – conforming traffic; $g(t_k)$ – non-conforming traffic, while the multiplexor loss during the same time interval is given by

$$L_M(t_k) = \sum_{i=1}^N g_i(t_k) - \sum_{i=1}^N g_i(t_k) \wedge [\mathcal{Q} - ([q(t_k) - C * \tau] \vee 0)]$$

In addition to these losses, it is also important to include a penalty for the waiting time or time spent on the queue before being served. For simplicity we assume that it is unambiguous function of queue length.

Adding all these, we obtain the cost functional. Since the incoming source (or user demand) is a random process, we must compute the average cost as being the expected value of the sum of all the costs described above. This is given by

$$J(u) = E \left\{ \sum_{k=0}^K \alpha(t_k) L_M(t_k) + \sum_{k=0}^K \beta(t_k) L_T(t_k) + \sum_{k=0}^K \gamma(t_k) q(t_k) \right\}, \quad (1)$$

where u is the control law which determines the state of the system and hence the individual losses and finally the total cost. The functions α, β, γ represent the weights or relative importance given to each of the three distinct losses.

Since the exact stochastic characterization of our traffic is not available or is unknown, the Monte Carlo method is employed to compute the expected values of the performance measures. For applying the Monte Carlo technique [7], we let N_s denote the number of samples used and let $\Omega = \{\omega_j, j = 1, 2, 3, \dots, N_s\}$ denote the elementary events or sample paths with finite cardinality N_s . The objective functional (1) is then given by

$$J(u) \cong \frac{1}{N_s} \sum_{j=1}^{N_s} \left\{ \sum_{k=0}^K \alpha(t_k) L_M(t_k, \omega_j) + \sum_{k=0}^K \beta(t_k) L_T(t_k, \omega_j) + \sum_{k=0}^K \gamma(t_k) q(t_k, \omega_j) \right\}.$$

The first term of the expression gives the average weighted loss at the multiplexor, the second gives that for token buckets, and the last one is the penalty assigned to the average waiting time in the multiplexor.

To illustrate the dependence of estimation error on the observation window size W_s and the prediction time T_a , we use the statistical modeling technique to compute the expected value of the (estimation) error given by where w_j denotes the j -th sample path and N_s denotes the number of sample paths used. The inverse of the signal-to-noise ratio (E_{SNR}) is used as another measure to evaluate the quality of prediction results:

$$E_{SNR} = (SNR)^{-1} = \frac{\sum e^2}{\sum (V(t_k))^2} = \frac{\left((1/N_s) \sum_{j=1}^{N_s} \left(\hat{V}(t_k, w_j) - V(t_k, w_j) \right) \right)^2}{\sum (V(t_k))^2}.$$

For any fixed window size, E_{SNR} increases with the increase of prediction time and appears to reach a plateau. As expected, E_{SNR} is smaller for larger Hurst parameters due to increasing of long-range dependence of parameters of random process. This is further illustrated in Fig. 2.

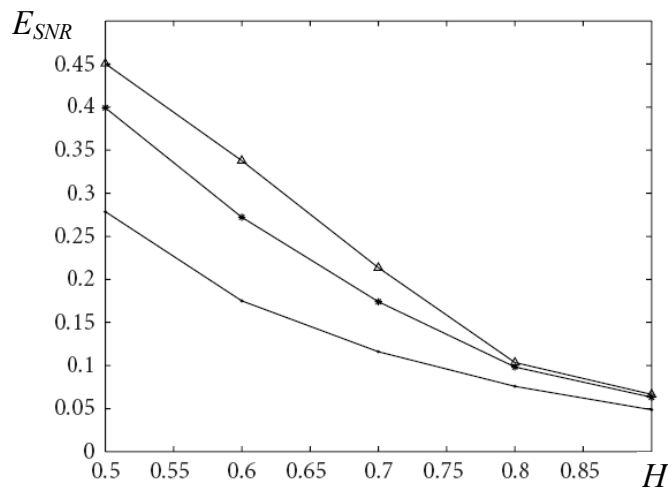


Fig. 2. Prediction errors versus Hurst parameter under constant delay time T_d :

- △— $T_d = 1\tau$
- $T_d = 3\tau$
- $T_d = 5\tau$

Conclusion

It is possible to compensate the impact of communication delay causing performance degradation using the method of prediction of traffic variations and expected network overload. The method of LMSE presented in this paper improves the overall system performance and prevents network losses. The numerical simulation results presented have shown the effectiveness of the proposed predictive feedback control law. It was found that processes with larger Hurst parameter have better prediction performance. This result is expectable in considering long-range dependence of self-similar traffic characteristics. The results of this work also lead to a better understanding of the impact of Hurst parameters on network performance. In summary, this work provides a useful tool for design and optimization of future networks using predictive feedback control law thereby avoiding transfer instability.

References

1. Андрусяк А.И., Дем'янчук В.С., Юр'єв Ю.М. *Мережа авіаційного електрозв'язку*. К.: НАУ, 2001. – 448 с.
2. Марпл мл. С.Л. *Цифровой спектральный анализ и его приложения*. – М.: Мир, 1990. – 584 с.
3. Макхол. *Линейное предсказание. Обзор* // Труды института инженеров по электротехнике и радиоэлектронике, т. 63, № 4. – 1975. – С. 20 – 44.
4. Рабинер Л.Р., Шафер Р.В. *Цифровая обработка речевых сигналов*. – М.: Радио и связь, 1981. – 496 с.
5. Столлингс В. *Современные компьютерные сети*. 2-е изд. – СПб.: Питер, 2003. – 783 с.
6. Виноградов Н.А. *Анализ потенциальных характеристик устройств коммутации и управления сетями новых поколений* // Зв'язок. К.: – 2004. – №4. – с. 10 – 17.
7. Гнеденко Б.В., Коваленко И.Н. *Введение в теорию массового обслуживания*. – М.: Наука, 1987. – 336 с.

*N. Shibitskaya, Ph.D, associate Professor
G. Timofeeva, postgraduate student
(National Aviation University of Ukraine),*

PILOT'S SKILLS PREDICTING SYSTEMS FOR FLIGHT SAFETY

The objective of a given paper is to proposed mathematical model of psycho physiological operator's parameters identification, described by ordinary differential equations with unknown coefficients. Developed method allows, after solving the system of equations, to obtain unknown parameters with any given accuracy. Results will be useful in predicting of pilot's skills and abilities for Flight Safety

Introduction

Characteristic property of scientific and technological advance is not only the increasing rate of development and use of new technologies and systems but also the increasing rate of dominant role of a person as the main unit of a man-machine symbiosis. As a consequence of this an individual discharges more and more leading functions. At the same time psychological impact on a person's mind has risen sharply; a person has to estimate and forecast operating efficiency of equipment and other people. Accordingly one of the major aims is the search of methods of impartial evaluation and prediction of a human-operator's functional condition as an object of ergotic system.

Functional effectiveness of ergotic system is greatly caused by the level of personnel training. It is known that one of the main culprits of accidents is not engineering but a person (1). According to the statistics the main part of accidents for example in aviation is connected with human element (60-70% and in Ukraine and countries of Commonwealth of Independent States about 90%). At the same time in most cases deviation in activities of aviation personnel is the main cause of accidents in aviation. And combinations of pilot's, flying control officer's and other flying operators' errors are repeated. According to the observational data of Intergovernmental aircraft committee the reason of the majority of incidents is insufficient level of vocational training of crewmen and flying control officers. Nearly all events were the result of combinations of flight crews' and flying control officers errors. In that way improving training of flight crews and quality control of level of knowledge is a top-priority aim. Since at the modern stage of aviation development the information technologies participate more and more in vocational training of crewmen and flying control officers, namely flight mathematic models, it is necessary to work out new analysis techniques and prediction of standard of education.

Analysis of articles

Last time the problems of modeling of perception and preservation processes of knowledge by the ergotic systems operators are very popular. The best known are the studies devoted to the processes of preservation of didactic material in short-term memory (2). But the basic information is preserved in long-term memory so the process of diagnostics and forecast of level of knowledge stimulates scientific interest with time.

The investigations of processes of memory by H. Ebbinghaus, P. Radossalievich, A. Pieron are the best known. But the results of these researches characterize the process of forgetting of ultimate discrete informational body, and the elements of this informational body have no logic connection. So they cannot show the common law of preservation and forgetting any information.

Target setting

There is an absolute necessity of prediction the capacity for work of ergotic systems' operators because of increasing concentration of guided power in hand of a person. For integrated diagnostics of an operator's condition they need quantitative and qualitative evaluation of human resources for a performance of every task that an operator fulfils. They use for that mathematical description of the processes of informational retrieval, information processing and decision making. These processes are basic functions of memory. Therefore the task of quantitative evaluation of

these functions is the receiving of mathematical values which determine the dependence of the entrance information's characteristic (its volume, speed of receiving) and the accuracy of its reproduction, time of preservation and so forth.

Hence the researches of mathematic model of ergotic system operator's memory (by the example of an aircraft operator) for the determination of capacity for work and namely the prediction of levels of knowledge is of interest.

Mathematic model

The process of training of a flight crew is the process of compound object's control, where the operator of the aircraft is the control object and the training system is the control item. So methodology of control is transferred to the process of training that allows to use the methods of management theory for adaptive system of personnel training. (Fig.1)

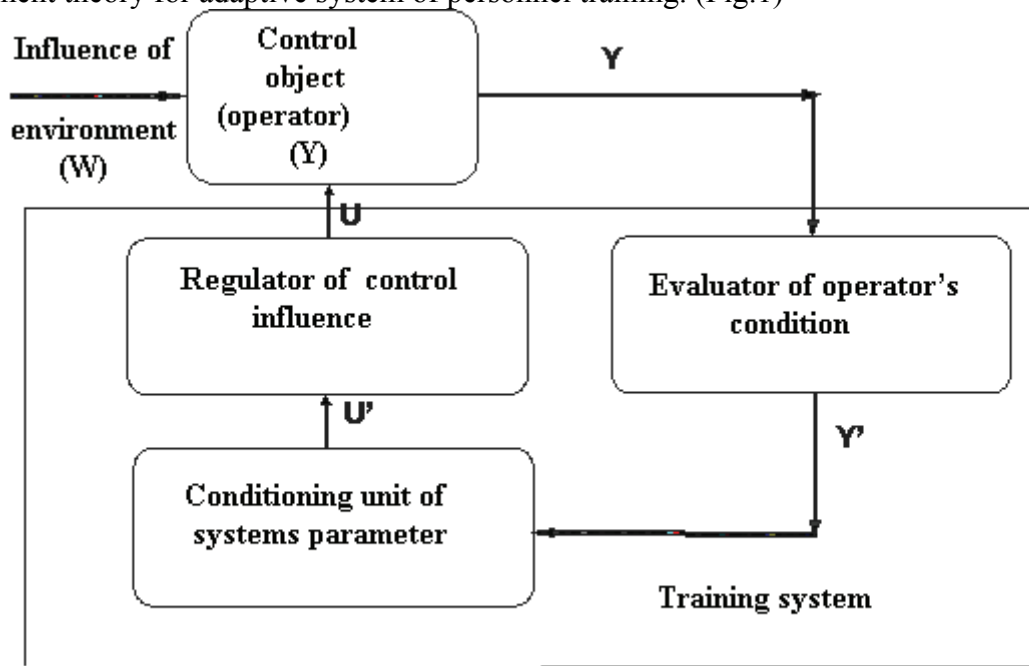


Fig.1 General arrangement of training system's control

The influence of environment on a person and other factors in general can be described by the function $W = W(w_1, \dots, w_m, \Omega)$ where w_1, \dots, w_m - factors of environment (temperature and the like) Ω - psychological condition of a person. Y' - the results of evaluation of operator's condition, which are received at the regulator of control influence. It generates executive instructions U' . The regulator of control influence works them over to change the condition of input signal U .

The process of vocational training of any person and particularly operators of aircrafts consists of periods of accumulation and preservation of knowledge. Timing data of the system determine speed and duration of accumulation and forgetting information in long-term memory.

Prediction of level of knowledge of ergotic systems' operator is only possible by input data and output data, which were received as a result of an experiment so the process of preservation of information in memory is poorly formalized area as long as a priori information about the system's operation factors and its physical environment is not given or incomplete.

Let's examine the time $[0, T]$ of experimental observations of an operator's condition. They put into practice the testing for determination of the degree of learning in different time: t_0 - before learning, t_1 - at the moment of training effect ending, t_2 - after some period of time. The mathematic model of the law of preservation of knowledge in operator's memory looks like:

$$f(t) = \begin{cases} f_1(t) & \text{для } 0 \leq t < t_1; \\ f_2(t) & \text{для } t_1 < t < t_2, \end{cases} \quad (1)$$

where $f_1(t)$ - law of conservation in the range $[0, t_1]$; $f_2(t)$ - the law of preservation of information for $t > t_1$.

It was proved that the process of identification of operation factors of an ergotic system's operator and the prediction of his condition eventually looks like differential equation of the second order:

$$k_2 \frac{d^2 f(t)}{dt^2} + k_1 \frac{df(t)}{dt} + k_0 f(t) = k u_{ex}(t), \quad (2)$$

where $y(t)$ – measurand output quantity (level of operators' knowledge); $u_{ex}(t) = u(t) + \frac{du(t)}{dt}$ - incoming informational flow at that $u(t)$ – given entrance value (test signal), that is element of knowledge; $\frac{du(t)}{dt}$ - speed of presenting information; k_i ($i = 0, 1 \dots n$) operation factors of an operator's condition, which are caused by psychophysiological characteristics; k – coefficient characterizing the complication of informational flow.

Let incoming informational flow $u_{ex}(t)$ which can be determined by the function (3) look like (Fig.2),

$$u(t) = \begin{cases} a \cdot t + b, & \text{для } 0 < t \leq t_1; \\ 0, & \text{для } t_1 < t \leq \infty, \end{cases} \quad (3)$$

where $a = \frac{1-b}{t_1}$, b - level of basic knowledge.

Let's form the algebraic linear systems equations (ALSE) for identification of the operation factors. It characterizes the parametric model of an operator in mathematical form based on experimental researches in boundary points of subruns $y(t_0)$, $y(t_1)$, $y(t_2)$:

$$Y * K = k(U + U') \quad (4)$$

where Y – matrix of operator's condition; U - input stream of information; U' - velocity vector of information presenting in boundary points of subruns.

It is known that roots of ALSE (4) discharge the next functions: k_2 characterizes the response time of thinking, k_1 is a generalized parameter of the process of adoption of information, k_0 determines the ability of prolonged preservation of information in the long-term memory of an operator.

Let's form the law of adoption and preservation of information (1) at the interval $[0, T]$. Let's find a solution of the linear equation (2) with constant coefficient for the intervals $[0, t_1]$ and $[t_1, T]$ using operational calculus, and namely Laplas' transformation (4).

$$f(t) = \begin{cases} \frac{ak}{k_0} \cdot \frac{1}{p_2 p_3} \left(t + \frac{b}{a} + \frac{1}{k} + \frac{p_1 + p_2}{p_1 p_2} \right) + \frac{1}{p_1 - p_2} \left(\frac{ak}{k_0} \cdot \frac{1}{p_1^2} + f_1(0)p_1 + \frac{kb+a}{k_0} \cdot \frac{1}{p_1} + v + \frac{k_1 f_1(0)}{k_0} \right) \cdot e^{p_1 t} + \\ + \frac{1}{p_2 - p_1} \left(\frac{ak}{k_0} \cdot \frac{1}{p_2^2} + f_1(0)p_2 + \frac{kb+a}{k_0} \cdot \frac{1}{p_2} + v + \frac{k_1 f_1(0)}{k_0} \right) \cdot e^{p_2 t} & \text{для } 0 \leq t < t_1 \\ \frac{1}{p_1 - p_2} \left(f_2(0)p_1 + v + \frac{k_1 f_2(0)}{k_0} \right) \cdot e^{p_1 t} + \frac{1}{p_2 - p_1} \left(f_2(0)p_2 + v + \frac{k_1 f_2(0)}{k_0} \right) \cdot e^{p_2 t} & \text{для } t_1 < t < t_2 \end{cases} \quad (5)$$

Examine by the example the processes of adoption and preservation of information in operator's memory. For the calculation of the system's operation factors let's fix the value of function $y(t)$ and its derivatives in limit points $t_0 = 0$, $t_1 = 10$, $t_2 = 100$. Let's form entrance information flow $u_{ex}(t_n)$ for the complexity $k = 0,7$, which was determined by means of expert evaluation. As a result of experimental dimensions in the points of subruns $y(t_0) = 0,3$, $y(t_1) = 0,65$, $y(t_2) = 0,45$.

Form ALSE (4), where $y'(t_0) = \frac{y(t_1) - y(t_0)}{t_1 - t_0}$, $y''(t_0) = \frac{y'(t_1) - y'(t_0)}{t_2 - t_1}$.

As far as the point t_1 is the extreme point then $y'(t_1) = 0$, and $y''(t_1) = -y''(t_0)$. Similarly to t_0 find $y'(t_2)$, $y''(t_2)$. So ALSE looks like:

$$\begin{bmatrix} 0,0035 & 0,035 & 0,3 \\ -0,0035 & 0 & 0,65 \\ -2.4691e-005 & -0,0022222 & 0,45 \end{bmatrix} * \begin{bmatrix} k_0 \\ k_1 \\ k_2 \end{bmatrix} = \begin{bmatrix} 0,34 \\ 0,7 \\ 0 \end{bmatrix} \quad (6)$$

Solving (6) we can find the value of vector $[k_0, k_1, k_2]$. Using the roots of ALSE let's make the mathematic model in the form of equation (5), which allows to define the duration of preservation and the level of total knowledge with time (Pic.3)

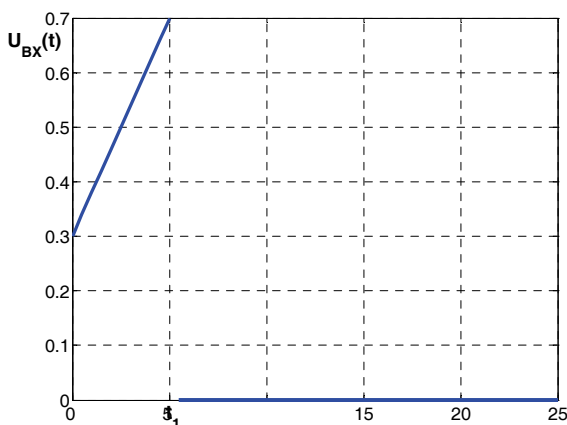


Fig. 2 Triangular insert training pulse

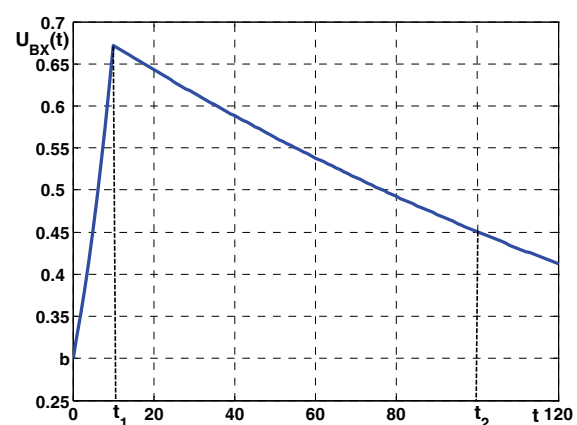


Fig.3 Graph of adoption and preservation of information in operator's memory

Resume

So diagnostics of the condition of a human-operator permits to provide operating efficiency of ergotic systems. It includes not only monitoring, evaluation of knowledge and skills but also data systematization for processing, analysis and for possibility of reliable prognosis of the level of knowledge and skills with time. It gives the possibility of appropriate simulation of the process of retraining and raising the level of air crew's skills.

Elaborated model of the system of prediction of aircraft operators' skills according to the form of conception of entrance information flow permits to find mathematical dependence between the characteristics of entrance information (form, size) and the characteristics of an operator.

Simulation of the process of preservation of information in the memory of an operator permits to perfect the coordination of control system and an operator in the process of training, to forecast the level of training and keeping operator's skills with time and to fulfill individual approach to everybody, what means for its turn the raising of level of flights safety.

References

1. Безпека авіації Бабак В.П., Харченко В.П., Максимов В.О. та ін. – К.: Техніка, 2004. — 584 с.
2. Присняков В.Ф., Приснякова Л.М. Математическое моделирование переработки информации оператором человека-машинных систем – М.: Машиностроение, 1990.-248 с.
3. Шибицкая Н.Н. Метод идентификации объектов в эргатической системе управления процессом обучения // Кибернетика и вычислительная техника.–Вып. 121.– К., 1999. – С. 52–58.
4. Мартыненко В.С. Операционное исчисление.-К.:Вища школа, 1973. – 268 с.

METHOD OF MANAGEMENT OF PRODUCTIVITY OF THE EQUIPMENT FOR THE AUTOMATED SYSTEMS OF INDUSTRIAL PURPOSE

The method of management is offered by productivity of the equipment of the automated systems at an estimation and start in manufacture of the concrete order

Introduction

Efficiency of use of industrial resources in conditions of modern competitive market attitudes is one of key conditions of development of the domestic enterprises. Process of decision-making on terms of performance, costs and the main thing of efficiency of industrial orders is still intuitive and based on experience, knowledge and the given concrete experts of the enterprise. Unfortunately, this process is far from optimum and practically is not automated by modern information systems of type ERP used at the enterprise, CRM, PDM, etc [1].

Statement of a problem

Development of a subsystem is preceded with problems of formalization and algorithmization of the industrial and design-technological information which are considered in the material presented by the author.

Results of researches

At an estimation of orders traditionally use concept of capacity of the enterprise (shop, a site). In a general view capacity is defined, how the greatest possible output during the corresponding period of time under concrete conditions of use of the equipment and industrial resources (the areas, energy, raw material of a manpower). The leading factor influencing capacity and defining its name, the equipment, that is means of change of a material component of production is. Ability of manufacture to let out the set quantity of production is defined by excess of size of free capacity over quantity of production under the given contract [2].

At an estimation of the resources corresponding parameters of a product, it is necessary to estimate an opportunity of release of the set quantity of production. Specificity of this problem consists in necessity of adjustment not all parameters of technological process, but only in an estimation of security of manufacture of products of the set quantity and the nomenclature, incorporated in projects and resources available on manufacture (time, the personnel, park of machine tools, materials, the tool). Thus, the problem of an estimation of industrial resources in their effective utilization in concrete conditions consists of three components:

1. The estimation of conformity of parameters of a product to resources available at the enterprise;
2. The estimation of an opportunity of release of the set quantity of production (i.e. an estimation of productivity and loading of the equipment);
3. The estimation of variable costs (cost of raw material and materials, labour expenses, power consumption).

The parameters of technological process necessary for an estimation of loading of the equipment (an expense of materials, norm of time), depend on mark of the equipment. The model of structure of technological process is necessary for an estimation of presence of resources on manufacturing the given product and its conformity to the resources necessary for performance of each operation.

For an estimation of a technical opportunity it is offered to define total capacity of all kinds of the equipment, for performance of the given operation.

Productivity of the equipment is characterized by a maximum quantity of products C_j which can be made with use of various variants of the equipment (on separate operation):

$$C_j = \sum_{i=1}^n C_j^i \quad (1)$$

where n - quantity of variants of the equipment.

The quantity of products which can be made on the chosen equipment defined as follows:

$$C_j^i = \frac{Rf_i - Tz_i}{Nt_j^i}$$

(2)

where Rf_i – regime fund of time;

Tz_i – loading of the equipment (time necessary for production, included in the plan of manufacture for the set period);

Nt_j – norm of time.

As, designing and planning of manufacture of new products is carried out in conditions of the existing volume of orders at the certain capacities it is necessary to consider planned loading of the equipment according to the production program:

$$Tz_i = \sum Nt_l \times Pp_l \times Kl_l, \quad (3)$$

where Pp_l – the production program on the given technological operation;

Kl_l – the factor considering waste and losses.

For an estimation of an opportunity of release of the set quantity of products it is necessary to define quantity (weight, volume) production, a work in progress, on each operation of technological process. Thus according to a design procedure of normative cards the quantity of production on an output is set and quantitative characteristics by a work in progress of production at each stage of technological process in view of waste and losses are defined.

$$NP = \{np_1, np_2 \dots np_k\}, \quad (4)$$

where np_k – settlement quantity a work in progress of production on each technological operation;

κ – quantity of technological operations.

Hence, in view of (2-4) technical opportunity DP of release of the set quantity of products can be certain under the formula:

$$DP = (c_1 \geq np_1) \wedge (c_2 \geq np_2) \wedge \dots (c_k \geq np_k), \quad (5)$$

The author develops a subsystem of information support of decision-making according to acting orders, updating operatively-planned schedules in view of optimum loading the industrial equipment and structures of routing technological processes. The subsystem is realized by tool means of PDM-system ENOVIA-SmarTeam V5R18, and can be used by means of the APT-interface ERP and CRM by systems, and also the automated systems of technical training of manufacture. In a basis of a subsystem the method of automated management is put by productivity of the equipment of the industrial enterprise at an estimation and start in manufacture of the concrete order.

The method allows to solve following problems:

1. Parametrical adjustment of routing technological process at a level of operations and transitions;
2. Formation of variants of the applied equipment for each industrial order;
3. Calculation of material specifications according to a method of calculation of normative cards;

4. Definition of total quantity of production which can be let out in view of optimum loading the equipment;

5. In case of excess of regime fund above settlement for manufacturing the set quantity of production granting of an opportunity to experts of the enterprise a choice of variants of the process equipment with a necessary quantitative estimation of their realization and maintenance of necessary information support. Otherwise - granting to the technologist of the information on absence of release of the set quantity of production and the reasons of absence those (absence of the equipment with the set characteristics, congestion of the equipment, shortage of regime fund of time, etc.).

6. Definition of quantitative characteristics of need for raw material and materials, and also needs for a manpower according to the chosen variants of performance of industrial orders.

7. Automated management by productivity of the equipment by preparation and start of concrete orders.

Advantage of the given method consists in information integration of process of designing and manufacture that allows to define more precisely a technical opportunity of production, and also to make design decisions in view of economic consequences. In case of absence of such technical opportunity the method allows to define the reasons and possible variants of the decision.

Conclusions

The offered method provides following advantages:

1. Gives a practical opportunity to operate productivity of the equipment proceeding from requirements of the customer to characteristics planned to output;

2. Provides information support on decision-making on a choice of the concrete equipment according to size of variable costs, cost of industrial equipment and a level of complexity of adjustment of the equipment.

References

1. Павленко П.М. Автоматизовані системи технологічної підготовки розширених виробництв. Методи побудови та управління: Монографія.— К.: Книжкове вид-во НАУ, 2005.— 280 с.

2. Норенков И.П., Кузьмик П.К. Информационная поддержка наукоёмких изделий. CALS- технологии. — М.: Изд – во МГТУ им. Н.Э. Баумана, 2002. — 320 с.

Cherednikov I. (post graduate students, National Aviation University, Ukraine)
Borisov A. (Chernigov State Technological University, Ukraine)

The synthesis of the measuring systems of deviations from cylinderstics

Theoretical researches of measuring cylinderstics enable to carry out the choice of chart and planning of measuring device. That provides the possibility of improvement charts of measuring and the increase of the control productivity in production terms. The influence of sensor's motion trajectory on the exactness and control productivity is determined. The use of 3-d design is necessary at determination and estimation of spatial form errors.

Introduction

The modern tendencies of industry development require the increase of labour productivity and the control of let-out production. The specified problems depend on metrological maintenance of manufacture. The introduction of the automated manufacture equipped with robotechnical complexes, flexible readjusted modules and co-ordinate measuring machines demands another methodological approach and new scientific generalisations to define and estimate the parametres of product quality.

The considerable attention is paid to the definition of the criteria which estimate technical, organizational and economic levels of informative -measuring systems. The analysis of literary and patent data has shown that the synthesis and estimation of informative measuring systems efficiency can't be easily decided. It has induced to the choice of the criteria and the definition of their importance. At the same time the statistical estimation of measuring results allows to define an absolute and relative error of the chosen methods without economic indicators. These indicators are not always determining as the basic criterion is the exactness and time of measuring . The estimation of measuring exactness includes such constituents as repetition and reproduction. The decision of a problem of manufacture metrological maintenance is directed to the quality improvement and the decrease of the let-out production cost price. To maintain the quality of let-out products in machine-building manufacture the question of improvement device quality its accuracy, durability and universality is urgent.

Tasks and working hypothesis

It is not possible to carry out the synthesis of the measuring systems of deviations from cylinderstics without efficiency criterion. The attempts to decide the estimation problem of informative processes and systems efficiency by mechanical transference of computer and network technologies have no result. Because the reliability of the initial data is substantially defined by the chosen scheme of measurement and its physical realisation taking into account a considerable quantity of operating factors [1-3]. The objective of the research is to work out the synthesis of the measuring systems of deviations from cylinderstics as a complex indicator of the form errors. It should be done by taking into account the efficiency of information processes of measurement and influence of sensor's motion trajectory on the basis of the system approach.

The tasks of the research are as following:

- to choose the factors which influence the efficiency of the informative -measuring systems;
- to investigate the informative systems hierarchical structure, comparison of structures and their classification;
- to minimize the amount of the criteria of the measuring systems efficiency;
- to develop the formalized method of choice of the sensor's motion trajectory taking into account the authenticity of information and 3d model adequacy of the measuring object.

Research methods

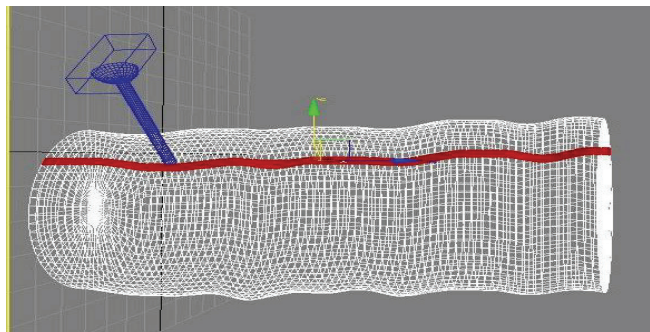
Methodological basis of the research is the system approach to the study of kinematics of motions taking into account the limits on the exactness and authenticity of finding extreme points of the subject measuring surface. The basic scientific positions of theoretical mechanics, the basing theory, theory of probability and the mathematical statistics give the grounds for a theoretical substantiation. Also they provide the possibility of practical use of the formalized indicators of informative-measuring systems efficiency.

The object of the research is the informative-measuring system under conditions of its use to all the spectrum of cylinder surfaces geometrical parametres. Using the method of the system analysis the area of existence of optimum indicators of a management efficiency is defined by the production. To get rid of any errors and raise the accuracy of measuring the transference of the control functions to computer is necessary. The target data will be visualised by means of the computer interface and the work of the operator (editing, construction of schedules and tables) will be convenient and simple. Such schemes of the control cylinderstics are considered:

- On forming
- On a spiral
- On sections
- Multisensor method

It is possible to use the scheme of the forward motion of the circle on a straight line at the measuring the deviations from cylinderstics [2]. The sensor will circle measuring the surface and carry out the movement in a step along an axis.

The quality monitoring cylinderstics on the forming means that the sensor measures the parametres only with one section in parallel to the axis of a detail (drawing 1).

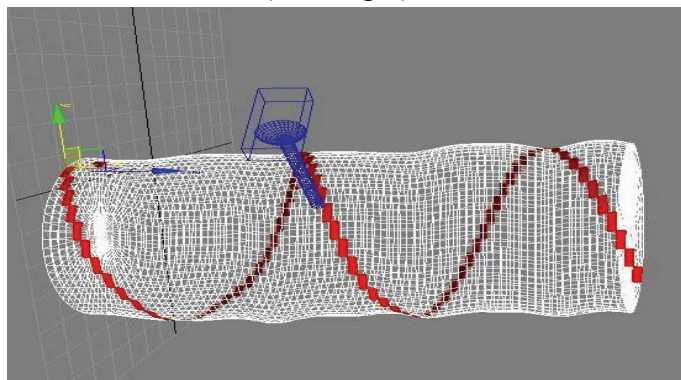


Drawing 1 - the scheme cylinderstics control on forming.

The advantage of the scheme: simplicity of realisation.

The disadvantage: rather low accuracy as the surface only in one section is supervised.

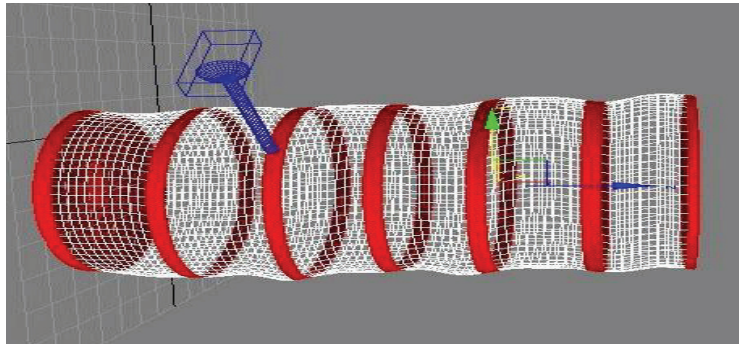
At the cylinderstics control under the second considered scheme the sensor moves along a spiral trajectory on the controllable surface (drawing 2).



Drawing 2 - the control Scheme of cylinderstics on spiral.

The scheme provides high accuracy, but technically it is difficult to be realized as a rectilinear and rotary motion should be provided. The cylinderstics control on sections consists in the measuring the roundness in group of cross-section of a detail. Having made a circle the sensor displaces along the axis of a detail on a step and repeats actions again (drawing 3).

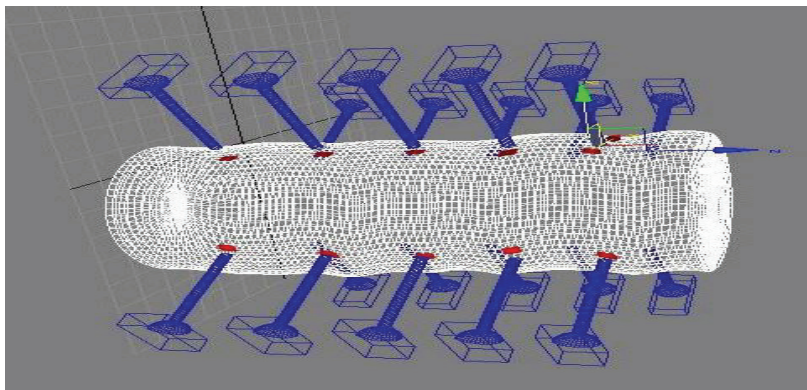
The scheme of sensor circular motions is used in the cases of exemplary rotation of details in different kinds of roundness measuring and in co-ordinate - measuring machines when the contact sensor is motionless or moves on a circular trajectory. In this case sufficiency of the measuring information will depend on an h step between measurements. The less it is the more measurements at length L will be made and the accuracy of deviations estimation from cylinderstics will be higher. The variant when step h between measurements of the sensor is the least provides the full picture of a surface condition.



Drawing 3 - the control scheme of cylinderstics on sections

The scheme provides high accuracy, technically it is easily to be realized. The realization of the scheme is possible by the modifying of existing devices for the roundness control or by the designing of a new one on its basis.

The most perspective method is multisensor method. It is realised through the group of sensors (drawing 4).



Drawing 4 - the control scheme of cylinderstics by multisensor method

The scheme provides high accuracy and speed. Technically it is easily realised but demands the considerable quantity of expensive compact sensors. The result of each schemes measurement is the file of values. Compiling this file is possible to judge the deviations from cylinderstics.

Conclusions

The results of computer modelling prove the accepted hypotheses and practical data. That provides the possibility of improvement charts of measuring and the increase of the control productivity in production terms. Form deviations should be regulated by complex indicators. And also they should be characterized by gamma factors that describe the complex deviations which are controlled during the production. The factors allow to set the demands of the accuracy taking into account the operation demands to the detail (the differentiated and complex factors of form deviations).

The theoretical importance of the research is as following: the investigated theoretical positions give the grounds for the judgement of complex system of efficiency factors of informative measuring systems. These factors are the necessary components for the further improvement of metrological systems, increase of measurements accuracy, decisions of modernisation tasks, successful new technologies introduction. The methodology and mathematical formalisation of kinematic control transition calculations allow to define the ways of increasing the productivity of cylinderstics measurements. And it promotes the achievement of the necessary accuracy, sufficiency and reliability of the measuring information as a whole.

References

1. Верхотуров Б.Я., Кузьмин Б.И. Трехточечный разностный метод измерения отклонений от круглости // Вестник машиностроения. – 1982. – № 11.
2. Патент №2134404. Накладной кругломер Пат. №2158895. Способ измерения геометрической формы номинально круглой цилиндрической детали и устройство для его реализации .
3. ГОСТ 24642-81 (СТ СЭВ 301-76). Допуски формы и расположения поверхностей. Основные термины и определения
4. ГОСТ 17353-89. Приборы для измерений отклонений формы и расположения поверхностей вращения. Типы, общие технические требования
5. Квасніков В.П. Теорія вимірювання об'єктів із складною просторовою поверхнею // Прогресивні технології та системи машинобудування: Збірник наукових праць Донецького державного технічного університету – Донецьк: Донату, 2002. – № 4. – С.19-21.
6. ISO 4292-1985E. Methods for the assessment of departure from roundness. – Measurement by two- and three-point methods.

METHODS OF DATA PROCESSING BY SENSORS OF TRAFFIC MONITORING VIDEOSYSTEM

The methods of data processing developed by the author are considered by sensor controls of traffic monitoring videosystem that allow to improve functionality of such sensor controls and to lower requirements to computational capability of hardware realising these methods. The considered methods of processing of the video data can be applied in the automated systems of video safety and robot sight.

Introduction

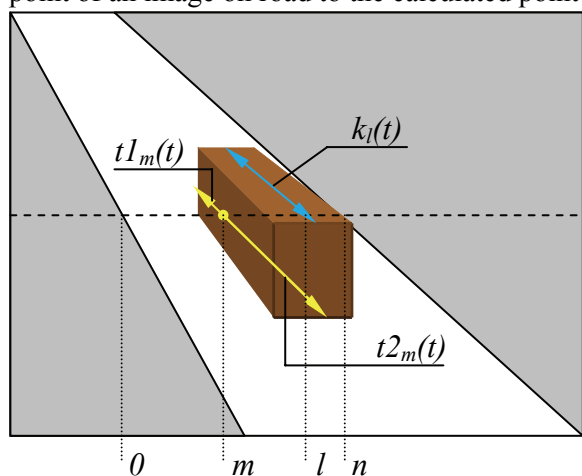
For vehicles detecting and their subsequent support it is necessary to spend difficult, behind quantity of calculations, operation of video deformation an image that allows to compensate optical and perspective distortions of road. On the deformed video image the road looks like not a trapeze, and a rectangle. Further, knowing road borders, algorithms of detecting and support of mobile objects considerably become simpler.

Task setting

It is necessary to develop methods of video stream processing that will allow to reduce quantity of computing operations in the course of the map preparation a frame for the subsequent revealing and classification of sliding images.

Decision of the task

The Brezenhem method is used in the computer drawing for a straight line conclusion. Use of a Brezenhem method for achievement of the return purpose is offered. Scanning in a piece of an image allows to exclude completely operations of deformation of a shot and to receive the same result at processing, as with them. As at adjustment of a sensor control of system video capture borders are established, the system has the information on co-ordinates of a road image trapeze. It gives the chance to define trapeze-filter co-ordinates. The gauge onetime performs operation of point calculation of a straight lines intersection of the drawn through lateral sides of a road trapeze. In the subsequent scanning of a video image is spent from a point of an image on road to the calculated point of intersection.



On Fig. 1 the example of image scanning along road is resulted. In the course of scanning there are arrays $D1(t)$, $D2(t)$ containing quantity of the pixels belonging to the vehicles on lines of scanning along allowed band of scanning (road) upwards and downwards in each cell to an appropriate point of road through which there is a scanning. Array $K(t)$ contains in each cell quantity nonseparable (the small error is admitted) pixels on scanning lines are lengthways expensive, to belonging roofs of vehicles.

Fig. 1. Sliding objects scanning

PASSING VEHICLES QUANTITY CALCULATION

The sum of appropriate units of arrays $D1$, $D2$ specifies length of the HARDWARE the given point of road in the area of scanning. At vehicles capture/loss occurs sum races $d1i+d2i$. On Fig. 2 the schedule showing change of $D1$, $D2$ arrays cells values is resulted at vehicles passing through a scanning line.

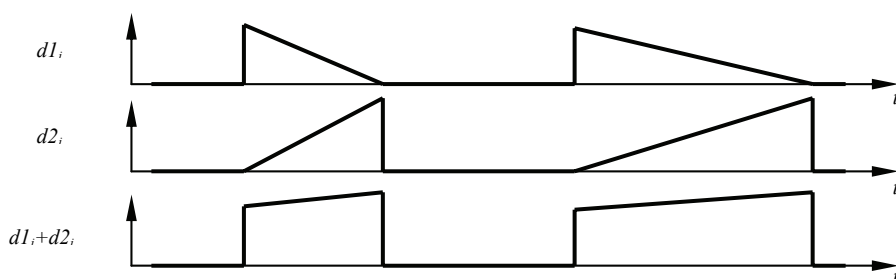


Fig. 2. Changing of arrays cells values at vehicles passing

Apparently about Fig. 2, at crossing by image of a vehicle of a scanning line, there is its capture and support. Intensity of reduction or $d1i$, $d2i$ values increase it is proportional to speed of the vehicle movement. Smooth reduction of values $d1i$ testifies to movement of the vehicles from the top part of a shot to bottom, increase – on the contrary. Values $d2i$ similar to $d1i$ also are a little increased in connection with perspective distortions.

On Fig. 3 the schedule of the sum change of all $D1$, $D2$ arrays cells in a current of time of journey through a line of vehicles scanning is resulted.

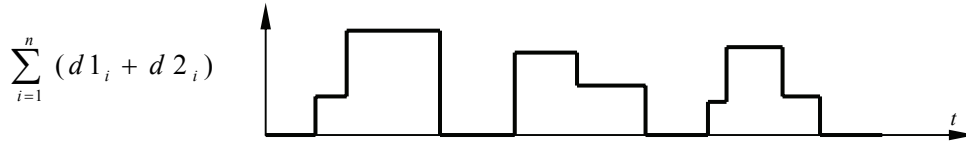


Fig. 3. the sum $D1$, $D2$ arrays changing during passing of vehicles through a scanning line

On Fig. 3, n – dimension of $D1$, $D2$ arrays. The situation, when is considered: 2 vehicles serially enters into a zone of detecting and leave simultaneously; 2 vehicles simultaneously enter and leave by turns; one vehicle enters, the second vehicle enters, then the first, then the second. The formula is more low resulted, allowing to calculate in connection with this law quantity of the passing vehicles.

$$m(t) = \begin{cases} m(t-1) + 1, (\sum_{i=1}^n (d1_i(t) + d2_i(t)) - \sum_{i=1}^n (d1_i(t-1) + d2_i(t-1))) \geq k \\ m(t-1), (\sum_{i=1}^n (d1_i(t) + d2_i(t)) - \sum_{i=1}^n (d1_i(t-1) + d2_i(t-1))) < k \end{cases}, (1)$$

$$u(t) = \begin{cases} u(t-1) + 1, (\sum_{i=1}^n (d1_i(t-1) + d2_i(t-1)) - \sum_{i=1}^n (d1_i(t) + d2_i(t))) \geq k \\ u(t-1), (\sum_{i=1}^n (d1_i(t-1) + d2_i(t-1)) - \sum_{i=1}^n (d1_i(t) + d2_i(t))) < k \end{cases}, (2)$$

$$c(t) = \begin{cases} \max \{m(t), u(t)\}, \sum_{i=1}^n (d1_i(t) + d2_i(t)) = 0 \\ c(t-1), \sum_{i=1}^n (d1_i(t) + d2_i(t)) \neq 0 \end{cases}, (3)$$

where $d1_i(t)$, $d2_i(t)$ - values of cells of arrays $D1$, $D2$ in an instant t ; k – a threshold of detecting of an input (output) of the vehicle in scanning allowed band; $m(t)$ – quantity of the vehicles that have entered into detecting allowed band; $u(t)$ – quantity of the vehicles that have quitted detecting allowed band; $c(t)$ – quantity of the last vehicles. Formulas (1) and (2) make count entering and exiting of allowed band of scanning of the vehicles. At the moment of absence of sliding (3) objects in scanning allowed band there is a choice of maximum value from $m(t)$ and $u(t)$. This value is resulting.

DEFINITION OF VEHICLES MOVEMENT SPEED

Speed of sliding objects is defined in each point of allowed band of scanning. At the moment of object occurrence in scanning allowed band value $d1i$ is fixed – is long the vehicle (4) on projections cameras photomatrixes in pixels. As occurrence time in allowed band of scanning (6) is fixed. At an output of the vehicle from scanning allowed band return operations (5, 7) are made.

For a difference of time of passing of allowed band of scanning of the vehicle passes the distance equal to length. The sum $d1i$ and $d2i$ is equal double vehicle length (before and after scanning allowed band). The formulas describing process of calculation of vehicle speed in each point of allowed band of scanning are more low resulted.

$$\lambda 1_i(t) = \begin{cases} d1_i(t), (d1_i(t) - 2 \cdot d1_i(t-1)) > 0 \\ \lambda 1_i(t-1), (d1_i(t) - 2 \cdot d1_i(t-1)) \leq 0 \end{cases} \quad (4)$$

$$\lambda 2_i(t) = \begin{cases} d2_i(t), (d2_i(t) - 2 \cdot d2_i(t-1)) > 0 \\ \lambda 2_i(t-1), (d2_i(t) - 2 \cdot d2_i(t-1)) \leq 0 \end{cases} \quad (5)$$

$$\tau 1_i(t) = \begin{cases} t, (\lambda 1_i(t) - 2 \cdot \lambda 1_i(t-1)) > 0 \\ \tau 1_i(t-1), (\lambda 1_i(t) - 2 \cdot \lambda 1_i(t-1)) \leq 0 \end{cases} \quad (6)$$

$$\tau 2_i(t) = \begin{cases} t, (\lambda 2_i(t) - 2 \cdot \lambda 2_i(t-1)) > 0 \\ \tau 2_i(t-1), (\lambda 2_i(t) - 2 \cdot \lambda 2_i(t-1)) \leq 0 \end{cases} \quad (7)$$

$$v_i(t) = \begin{cases} \frac{\lambda 1_i + \lambda 2_i}{2 \cdot (\tau 1_i - \tau 2_i)}, (d1_i(t) + d2_i(t)) = 0 \\ v_i(t-1), (d1_i(t) + d2_i(t)) \neq 0 \end{cases} \quad (8)$$

where $\lambda 1_i(t)$, $\lambda 2_i(t)$ – is object length in the pixels, fixed at the moment of occurrence and its exit from a scanning zone in a point i scanning zones; $\tau 1_i(t)$, $\tau 2_i(t)$ – fixed time of occurrence and object output; $v_i(t)$ – the object speed which has passed a point of a zone of scanning i , fixed at the moment of its exit from a scanning zone.

At the moment when in a point of a line of scanning there are no sliding objects, there is a count of speed of movement of the object which has passed through this point (8).

On Fig. 4 the change example values $v_i(t)$ is resulted at vehicle passage.

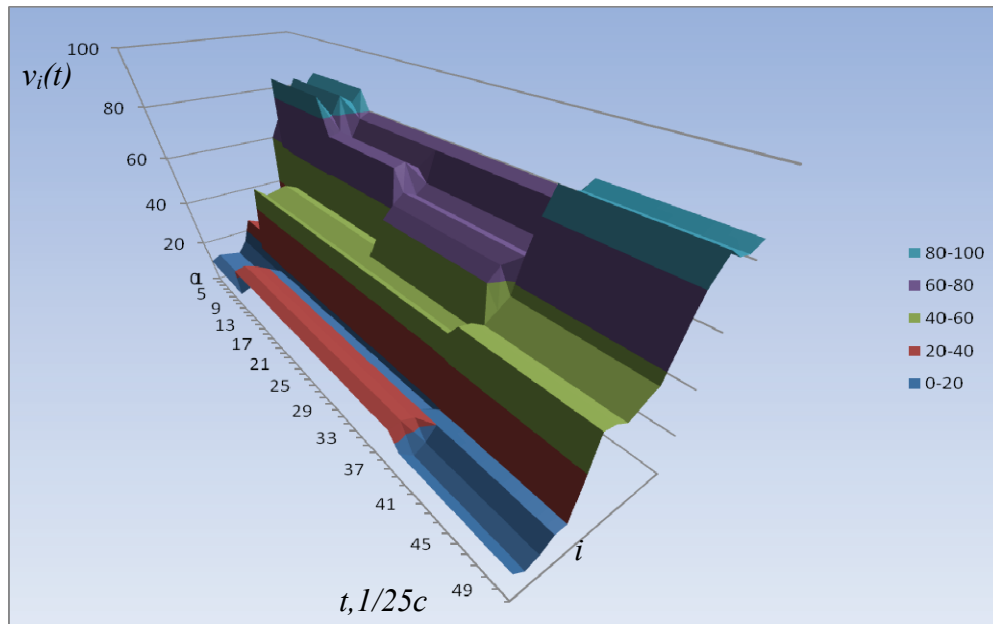


Fig. 4 Measurement of objects speed in points of allowed band of scanning eventually

THE LARGE-SIZED VEHICLE DETECTING

As a result of passing of the large-sized vehicle to $D1$, $D2$ arrays there are big numerical values. Because of complexity of the form and big are long, the large-sized vehicles can provoke malfunctionings at count of quantity of vehicles by the resulted formulas (1-3). In this connection to detect the large-sized vehicle it is necessary irrespective of vehicles quantity count procedure for this purpose what more precisely to detect the large-sized vehicles and to adjust result of accounting of the last vehicle. For detecting of the large-sized vehicles there is array F .

$$f_i(t) = \begin{cases} 0, d1_i(t) + d2_i(t) < l \\ 1, d1_i(t) + d2_i(t) > l \end{cases} \quad (9)$$

where $f_i(t)$ – array cells F ; l – the long vehicle detecting threshold.

Further calculation of the vehicle large-sized occurs similarly to formulas (1-3) and operations of vehicles quantity calculation are made in parallel.

$$q(t) = \begin{cases} q(t-1) + 1, (\sum_{i=1}^n f_i(t) - \sum_{i=1}^n f_i(t-1)) \geq j \\ q(t-1), (\sum_{i=1}^n f_i(t) - \sum_{i=1}^n f_i(t-1)) < j \end{cases}, \quad (10)$$

$$w(t) = \begin{cases} w(t-1) + 1, (\sum_{i=1}^n f_i(t-1) - \sum_{i=1}^n f_i(t)) \geq j \\ w(t-1), (\sum_{i=1}^n f_i(t-1) - \sum_{i=1}^n f_i(t)) < j \end{cases}, \quad (11)$$

$$m(t) = \begin{cases} m(t-1), \sum_{i=1}^n f_i(t) \neq 0 \\ \max\{q(t), w(t)\}, \sum_{i=1}^n f_i(t) = 0 \end{cases}, \quad (12)$$

where $f_i(t)$ - current video frame cell value of array F ; j - operation threshold; $q(t)$ - quantity of the large-sized vehicles that have entered into detecting allowed band; $w(t)$ - quantity of the large-sized vehicles that left a detecting zone; $m(t)$ - quantity of the passed large-sized vehicles.

CONCLUSION

Use of the resulted methods of video stream processing in traffic monitoring systems gives possibility considerably to reduce quantity of the calculations spent by the intellectual gauge. The spent experimental researches have shown reduction of time of calculations and references to memory by 26 %. It gives possibility to lower power consumption and requirements to the processor of the gauge or to increase functionality of system.

References

1. Витязев В.В. Цифровая обработка сигналов; ретроспектива и современное состояние // Электросвязь. — 1997. — №6. — С.10-11
2. Голд Б., Рэйдер Ч. Цифровая обработка сигналов / Под ред. М. Трахтмана. — М.: Сов. радио, 1973. — 367 с.
3. Goodman G.C., Sin K.S. Adaptive filtering, prediction and control. Englewood Cliffs. Prentice-Hall, 1984. — 552p.
4. Dudek, C.L., and C.J. Messer. Incident detection on urban freeways. Transpn Res. Rec 495, 1974, P.12-24.
5. Kuhne, R.D. Freeway control and incident detection using a stochastic continuum theory of traffic flow. Proc. 1st Int. Conf. 'Applications of Advanced Technologies in Transportation Engineering' (San Diego, California, February 1989), P.287-292.
6. J. Versavel et al, "Camera and Computer Aided Traffic Sensor", IEE Second International Conference on Road Traffic Monitoring, London, 1989.



CONGRESS SECRETARIAT

National Aviation University 1, Kosmonavta
Komarova ave., Kyiv, 03680, Ukraine



Tel: +38044 406-7212

Fax: +38044 406-7212



e-mail: aviacon@nau.edu.ua

Congress homepage:

<http://congress.nau.edu.ua>